Exploration of World

Launch and Flight in Space without Rockets
(v.2)
Alexander A. Bolonkin
Dr.Sci., professor of Russian and American Universities
Former Senior Researcher of NASA,
USA Air Force and Russian Space Industry

USA, Lulu, 2011

Title **Launch and Flight in Outer Space without Rockets**
Author: Alexander Bolonkin
ISBN **978-1-365-81382-5**

   In the past years the author and other scientists have published a series of new methods which promise to revolutionize space launching and flight. These include the cable accelerator, circle launcher and space keeper, space elevator transport system, space towers, kinetic towers, the gas-tube method, sling rotary method, asteroid employment, electromagnetic accelerator, tether system, Sun and magnetic sails, solar wind sail, radioisotope sail, electrostatic space sail, laser beam, kinetic anti-gravitator (repulsitor), Earth–Moon or Earth–Mars non-rocket transport system, multi-reflective beam propulsion system, electrostatic levitation, etc.
   There are new ideas in aviation which can be useful for flights in planet atmosphere. Some of these have the potential to decrease launch costs thousands of times, other allow the speed and direction of space apparatus to be changed without the spending of fuel.
   The author summarizes some revolutionary methods for scientists, engineers, students, and the public. He seeks attention from the public, engineers, inventors, scientists for these innovations and he hopes the media, government and the large aerospace companies will increase research and development activity in these areas.

Contents

Abstract

At present, rockets are used for launches and flights into space. They have been intensively developed since World War II when the German engineer F. Von Braun designed the first long distance rocket FAU-2. In the subsequent 60 years liquid and solid rockets reached the peak of their development. Their main shortcomings are (1) very high cost of space launching $20,000 – 50,000/kg; (2) large fuel consumption; (3) fuel storage problems because the oxidizer and fuel (for example; oxygen and hydrogen) require cryogenic temperatures, or they are poisonous substances (for example; nitric acid, N_2O_3).

In the past years the author and other scientists have published a series of new methods which promise to revolutionize space launching and flight. These include the cable accelerator, circle launcher and space keeper, space elevator transport system, space towers, kinetic towers, the gas-tube method, sling rotary method, asteroid employment, electromagnetic accelerator, tether system, Sun and magnetic sails, solar wind sail, radioisotope sail, electrostatic space sail, laser beam, kinetic anti-gravitator (repulsitor), Earth–Moon or Earth–Mars non-rocket transport system, multi-reflective beam propulsion system, electrostatic levitation, etc.

There are new ideas in aviation which can be useful for flights in planet atmosphere. Some of these have the potential to decrease launch costs thousands of times, other allow the speed and direction of space apparatus to be changed without the spending of fuel.

The author summarizes some revolutionary methods for scientists, engineers, students, and the public. He seeks attention from the public, engineers, inventors, scientists for these innovations and he hopes the media, government and the large aerospace companies will increase research and development activity in these areas.

Preface

The new methods are only proposals. There are a lot of problems that must be researched, modeled, and tested before these ideas can be developed, designed, built, and explored. Most of ideas are described in the following way: there is a brief explanation of the idea including its advantages and short comings, then methods estimation and computations of the main system parameters, and a brief description of projects, including estimations of the main parameters.

  The first and third parts are in a popular form accessible to the wider public, the second part is requires some mathematical and scientific knowledge of technical graduate students. The book gives the main physical data and technical equations in attachment which will help researchers, engineers, students and readers make estimations for their projects. Also inventors will find the extensive field an inventions and innovations in this book.

  The author has published a lot of new ideas and articles about non-rocket launches and flights in recent years (see General References at the end of the book). That is, the way he seeks to draw more attention to new ideas than the old ideas that are covered in many publications and are well-known to scientist and the public.

  The book mainly contains material from the author's articles published in the last few years.

About the Author

Bolonkin, Alexander Alexandrovich (1933-)

Alexander A. Bolonkin was born in the former USSR. He holds doctoral degree in aviation engineering from Moscow Aviation Institute and a post-doctoral degree in aerospace engineering from Leningrad Polytechnic University. He has held the positions of senior engineer in the Antonov Aircraft Design Company and Chairman of the Reliability Department in the Clushko Rocket Design Company. He has also lectured at the Moscow Aviation Universities. Following his arrival in the United States in 1988, he lectured at the New Jersey Institute of Technology and worked as a Senior Researcher at NASA and the US Air Force Research Laboratories.

Bolonkin is the author of more than 180 scientific articles and books and has 17 inventions to his credit. His most notable books include The Development of Soviet Rocket Engines (Delphic Ass., Inc., Washington , 1991); Non-Rocket Space Launch and Flight (Elsevier, 2006); New Concepts, Ideas, Innovation in Aerospace, Technology and Human Life (NOVA, 2007); Macro-Projects: Environment and Technology (NOVA, 2008); Human Immortality and Electronic Civilization, 3-rd Edition, (Lulu, 2007; Publish America, 2010).

Chapter 1
Space Elevator, Transport System for Space Elevator, and Tether System

Summary

The chapter brings together research on the space elevator and a new transportation system for it. This transportation system uses mechanical energy transfer and requires only minimal energy so that it provides a "Free Trip" into space. It uses the rotary energy of planets. The chapter contains the theory and results of computations for the following projects: 1. Transport System for Space Elevator. The low cost project will accommodate 100,000 tourists annually. 2. Delivery System for Free Round Trip to Mars (for 2000 people annually). 3 Free Trips to the Moon (for 10,000 tourists annually).

The projects use artificial material like nanotubes and whiskers that have a ratio of strength to density equal to 4 million meters. At present scientific laboratories receive nanotubes that have this ratio equal to 20 million meters.

Brief History

The concept of the space elevator first appeared in 1895 when a Russian scientist, Konstantin Tsiolkovsky, considered a tower that reached a geosynchronous orbit. The tower was to be built from the ground up to an altitude of 35,800 kilometers (geostationary orbit). Comments from Nikola Tesla suggest that he may have also conceived such a tower. His notes were sent behind the Iron Curtain after his death.

Tsiolkovsky's tower would be able to launch objects into orbit without a rocket. Since the elevator would attain orbital velocity as it rode up the cable, an object released at the tower's top would also have the orbital velocity necessary to remain in geosynchronous orbit.

Building from the ground up, however, proved an impossible task; there was no material in existence with enough compressive strength to support its own weight under such conditions. It took until 1957 for another Russian scientist, Yuri N. Artsutanov, to conceive of a more feasible scheme for building a space tower. Artsutanov suggested using a geosynchronous satellite as the base from which to construct the tower. By using a counterweight, a cable would be lowered from geosynchronous orbit to the surface of Earth while the counterweight was extended from the satellite away from Earth, keeping the center of mass of the cable motionless relative to Earth. Artsutanov published his idea in the Sunday supplement of *Komsomolskaya Pravda* in 1960. He also proposed tapering the cable thickness so that the tension in the cable was constant–this gives a thin cable at ground level, thickening up towards GEO (http://www.liftport.com/files/Artsutanov_Pravda_SE.pdf). An American scientist, Jerome Pearson, designed a tapered cross section that would be better suited to building the tower. The weight of the material needed to build the tower would have been thousands of tons.

In 1975b Arthur C. Clarke introduced the concept of a space elevator to a broader audience in his 1978 novel, *The Fountains of Paradise*.

David Smitherman of NASA/Marshall's Advanced Projects Office has compiled plans for an elevator. His publication, "Space Elevators: An Advanced Earth-Space Infrastructure for the New Millennium" (http://flightprojects.msfc.nasa.gov/fd02_elev.html), is based on findings from a space infrastructure conference held at the Marshall Space Flight Center in 1999.

Space elevator proponents are planning competitions for space elevator technologies (http://msnbc.msn.com/id/5792719/), similar to the Ansari X Prize. Elevator: 2010 (http://www.elevator2010.org/) will organize annual competitions for climbers, ribbons and power-beaming systems. The Robolympics Space Elevator Ribbon Climbing (http://robolympics.net/rules/climbing.shtml) organizes climber-robot building competitions.

Short Description

The space elevator is a cable installation which connects the Earth's surface to a geostationary Earth orbit (GEO) above the Earth 37.786 km in altitude (fig.1.1)
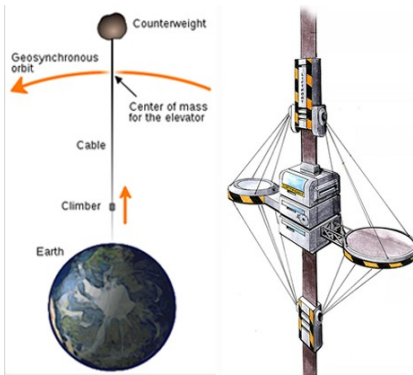.

Fig. 1.1. Space elevator.

The GEO is a 24-hour orbit and stays over the same point above the equator as the Earth rotates on its axis. The installation center of mass is at or above this altitude. The space elevator has a counterweight, which allows it to have its center of gravity at or above GEO, and climbers. Once sent far enough, climbers would be accelerated further by the planet's rotation. A space elevator, also known as a space bridge, is one of the technology concepts that are aimed at improving access to space. Also called a geosynchronous orbital tether, it is one kind of **skyhook**.
  The evator would have to be built of a material that could endure tremendous stress while also being light-weight, cost-effective, and manufacturable. A considerable number of other novel engineering problems would also have to be solved to make a space elevator practical. Today's technology does not meet these requirements.
  There are a variety of space elevator designs. Almost every design includes a base station, a cable, climbers, and a counterweight. The base station designs typically fall into two categories: mobile and stationary. Mobile stations are typically large oceangoing vessels (fig. 1.2). Stationary platforms are generally positiored in high-altitude locations.

Fig. 1.2. Sea space elevator.

The building of a space elevator has two main problems: tire need for material with a very high tensile stress/specific density ratio, and the very large cost of installation. But a space elevator could be made relatively economically if a cable with a density similar to graphite, with a tensile strength of around 65–120 <u>GPa</u> could be produced in bulk at a reasonable price.

By comparison, the strongest steels are no more than 5 GPa (1 GPa = 100 kg/mm^2 = 0.1 ton/mm^2), but steel is heavy. The much lighter material <u>kevlar</u> has a tensile strength of 2.6 – 4.1 GPa, while <u>quartz</u> fiber can reach upwards of 20 GPa; the tensile strength of <u>diamond</u> filaments would theoretically be minimally higher.

Carbon nanotubes have a theoretical tensile strength and density that lie well within the desired range for space elevator structures, but the technology to manufacture bulk quantities and fabricate them into a cable has not yet been developed. Theoretically carbon nanotubes can have tensile strengths beyond 120 GPa. Even the strongest fiber made of nanotubes is likely to have notably less strength than its components (30–60 GPa). Further research on purity and different types of nanotubes will hopefully improve this value.

Note that at present (March 2004), carbon nanotubes have an approximate cost of $100/gram, and 20 million grams would be necessary to form even a seed elevator. This price is decreasing rapidly, and large-scale production would reduce it further.

Climbers cover a wide range of designs. On elevator designs whose cables are planar ribbons, some have proposed to use pairs of rollers to hold the cable with friction. Other climber designs involve magnetic levitation (unlikely due to the bulky track required on the cable).

Power is a significant obstacle for climbers. Some solutions have involved nucler power, <u>laser</u> or <u>microwave</u> <u>power beaming</u>. They are very complex, or expensive, or have very low efficiency. The primary power methods (laser and microwave power beaming) have significant problems with both efficiency and heat dissipation on both sides. Below the author offeres a cable transport system which is more realistic at the present time.

There have been two methods proposed for dealing with the counterweight needed: a heavy object, such as a captured asteroid, positioned just beyond geosynchronous orbit; and extending the cable itself well beyond geosynchronous orbit. The latter idea has gained more support, it is simpler and the long cable located out of GEO (up to 144,000 km) may be used for launching payload to other planets.

A space elevator could also be constructed on some of the other planets, asteroids and moons (Mars, Moon). A Mars space elevator could be much shorter than one on Earth. Exotic materials might not be required to construct such an elevator. A lunar tather would need to be very long—more than twice the length of an Earth elevator. It could also be made of existing engineering materials.

There are a lot of problems in the development and design of a space elevator: corrosion of cable cable, meteroids, micrometeorites and space debris, Earth's weather, Earth's satellites, failure modes and safety issues, sabotage, vibrational harmonics, the event of failure, breaking of the cable, elevator pods, Van Allen Belts (radiation region), political issues, economics problems, etc.

The building of a space elevator involves lifting the entire mass of the elevator into geosynchronous orbit. One cable is lowered downwards towards the Earth's surface while another cable is simultaneously deployed upwards. This method requires lifting hundreds or even thousands of tons on conventional rockets, which would be very expensive. The other way of building an elevator from the Earth's surface is offered by the author and presented in this book (see chapter 5, Kinetic space towers).

Transport System for the Space Elevator*

This section proposes a new method and transportation system to fly into space, to the Moon, Mars, and other planets. This transportation system uses a mechanical energy transfer and requires only minimal energy so that it provides a "Free Trip" into space. It uses the rotary and kinetic energy of planets, asteroids, meteorites, comet heads, moons, satellites and other natural space bodies.

This chapter contains the theory and results of computations for three projects. The projects use artificial materials like nanotubes and whiskers that have a ratio of tensile strength to density equal to 4 million meters. In the future, nanotubes will be produced that can reach a specific stress up 100 million meters and will significantly improve the parameters of suggested projects.

The author is prepared to discuss the problems with serious organizations that want to research and develop these innovations.

Nomenclature (metric system):

a – relative cross-section area of cable (cable);
a_m – relative cross-section area of Moon cable (cable);
A – cross-section area of cable [m^2];
A_o – initial (near planet) cross-section area of cable [m^2];
C – cost of delivery 1 kg;
C_i – primary cost of installation [$];
D - distance from Earth to Moon [m], D_{min} = 356,400 km, D_{max} = 406,700 km;
D - specific density of the cable [kg/m^3];
E – delivery energy of 1 kg load mass [j];
g – gravity [m/s^2];

g_o - gravitation at the R_0 [m/s^2]; for Earth g_o = 9.81 m/s^2 ;
g_m - gravitation on Moon surface [m/s^2];
F – force [n];
H – altitude [m];
H - cable tensile stress [n/m^2];
H_p – perigee altitude [m];
$k = \sigma/\gamma$ – ratio of cable tensile stress to density [nm/kg];
$K = k/10^7$ – coefficient [million meters];
L – annual load [kg];
n – overload;
n – number of working days;
N_eS_e – annual employee salary [$];
$m = m_2/m_1$ – relative apparatus mass. Here are m_2 is mass of apparatus, m_1 is mass of asteroid [kg];
M – equalizer mass [kg];
M_a – annual maintenance of installation [$];
M_e – final mass of an Installation [kg];
M_o – load mass delivered in one day;
r – variable;
R - radius [m];
R_o - radius of planet [m];
R_g - radius of geosynchronous orbit [m];
R_m - radius of Moon [m];
T - orbit period [hours].
v - volume of a cable [m^3];
V - speed of space ship around asteroid [m/s];
V_a - initial speed of asteroid around space ship [m/s];
V_d – delivery speed [km/s];
V_r – maximum admitted cable speed [m/s];
V_1 - circulate speed [m/s];
V_2 - escape speed [m/s];
ΔV - ship additional speed received from asteroid [m/s];
W - mass of a cable [kg];
W_r - relative mass of cable (ratio of cable mass to ship mass W_s);
T - orbit period [hours];
Y – live time [years];
σ - tensile strength [N/m^2];
ω - angle speed of a planet [rad/s];
ω_m - angle speed of the Moon [rad/s].
γ - density of cable [kg/m^3];

Introduction

At present, rockets are used to deliver payloads into space and to change the trajectory of space ships and probes. This method is very expensive in the requirement of fuel, which limits the feasibility of space stations, interplanetary space ships, and probes. Since 1997 the author has proposed a new revolutionary transport system for (1) delivering payloads and people into space, (2) accelerating a space ship for interplanetary flight, and (3) changing the trajectory of space probes. This method uses a mechanical energy transfer, energy of moved down loads, and the kinetic energy of planets, of natural planet satellites, of asteroids, of meteorites and other space bodies. The author has not found an analog

for this space mechanical energy transfer or similar facilities for transporting a payload into space in the literature and patents.

The present method does not require geosynchronous orbit (which is absent from most planets, moons, and asteroids which have weak gravitation) and instead, uses the kinetic and rotational energy of the space body to modify the trajectory and impart additional speed to the artificial space apparatus. The installation has a cable transport system and counterbalance, which is used for balancing the moving load. For this proposal, the cable, which is used for launching or modifying the speed or direction of a space vehicle or for connecting to an asteroid, is spooled after use and may be used again.

Brief history. There are many articles that develop a tether method for a trajectory change of space vehicles[1,2] and there is an older idea of a space elevator (see reviews[3,4]). In the tether method two <u>artificial</u> bodies are connected by cable. The main problem with this method, which requires energy for increasing the rotation of the tether system (motorized tether[2]) is how to rotate it with a flexible cable and what to do with momentum after launch if the tether system is used again, etc. If this system is used only one time, it is worse than a conventional rocket because it loses the second body and requires a large source of energy.

In the suggested method, the space vehicle is connected to a <u>natural</u> body (planet, asteroid, moon, meteorite). The ship gets energy from the natural body and does not have to deal with the natural body in the future.

In the older idea, a space elevator is connected between a geosynchronous space station and the Earth by a cable[4]. This cable is used to deliver a payload to the station. The main problems are the very large cable weight and delivery of the energy for movement of the load container.

In this suggested transport system the load engine is located on the Earth and transfers energy to the load container and the space station using a very simple method (see Project 1, capability is 100,000 tourists per year). The author also found and solved the differential equations of the cable for an equal stress for a complex Earth–Moon gravitation field which allows the cable weight to be decreased by several times.

The main difference in the offered method is the transport system for the space elevator and the use of the planet rotational energy for a free trip to another planet, for example, Mars (see project 2, capability is 2000 people annually).

In project 3 wit in a capability of 10,000 tourists per year, the author suggests the idea of connecting the Moon and the Earth's pole by a load cable. He solves the problem of transfering the energy to the load container, finds the cable of equal stress, and shows a possibility of this project in the near future.

There are some millions of asteroids in the Sun system. In project 4 the author suggests a way of increasing the maneuverability of space apparatus by some millions of times by using asteroid energy. The author's other non-rocket methods are presented in publications listed in the References[12–22].

Brief Description, Theory, and Computation of Innovations

The objective of these innovations is to: a) provide an inexpensive means to travel to outer space and other planets, b) simplify space transportation technology, and c) eliminate complex hardware. This goal is obtained by new space energy transfer for long distance, by using engines located on a planet (e.g. the Earth), the rotational energy of a planet (e.g. the Earth, the Mars, etc.), or the kinetic and rotational energy of the natural space bodies (e.g. asteroids, meteorites, comets, planet moons, etc.). Below is the theory and research for four projects, which can be completed in the near future.

1. Free trip to Space (Project 1)

Description

 A proposed centrifugal space launcher with a cable transport system is shown in Fig. 1.3. The system includes an equalizer (balance mass) located in geosynchronous orbit, an engine located on Earth, and the cable transport system having three cables: a main (central) cable of equal stress, and two transport cables, which include a set of mobile cable chains connected sequentially one to an other by the rollers. One end of this set is connected to the equalizer, the other end is connected to the planet. Such a separation is necessary to decrease the weight of the transport cables, since the stress is variable along the cable. This transport system design requires a minimum weight because at every local distance the required amount of cable is only that of the diameter for the local force. The load containers are also connected to the chain. When containers come up to the rollers, they move past the rollers and continue their motion up the cable. The entire transport system is driven by any conventional motor **located on the planet**. When payloads are not being delivered into space, the system may be used to transfer mechanical energy to the equalizer (load cabin, the space station). This mechanical energy may also be converted to any other sort energy.
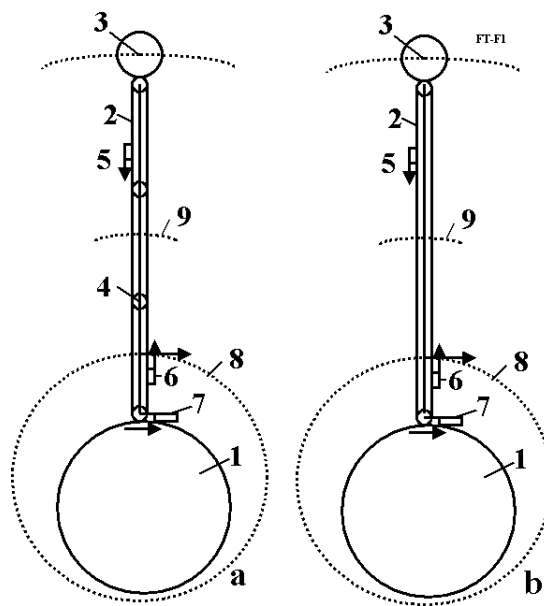

Fig. 1.3a,b. The suggested Space Transport System. Notations: 1 – Rotary planet (for example, the Earth); 2 - suggested Space Transport System ; 3 - equalizer (counterweight); 4 - roller of Transport System; 5 - launch space ship; 6 - a return ship after flight ; 7 – engine of Transport System; 8 – elliptic orbit of tourist vehicles; 9 - Geosynchronous orbit. a – System for low coefficient k, b – System for high coefficient k (without rollers 4).

   The space satellites released below geosynchronous orbit will have elliptic orbits and may be connected back to the transport system after some revolutions when the space ship and cable are in the same position (Fig. 1.3). If low earth orbit satellites use a brake parachute, they can have their orbit closed to a circle.

   The space probes released higher than geosynchronous orbit will have a hyperbolic orbit, fly to other planets, and then can connect back to the transport system when the ship returns.

   Most space payloads, like tourists, must be returned to Earth. When one container is moved up, then another container is moved down. The work of lifting equals the work of descent, except for a small loss in the upper and lower rollers. The suggested transport system lets us fly into space without expending enormous energy. This is the reason why the method and system are named a "Free Trip".

Devices shown on fig. 1.4 are used to change the cable length (or chain length). The middle roller is shown in fig. 1.5.
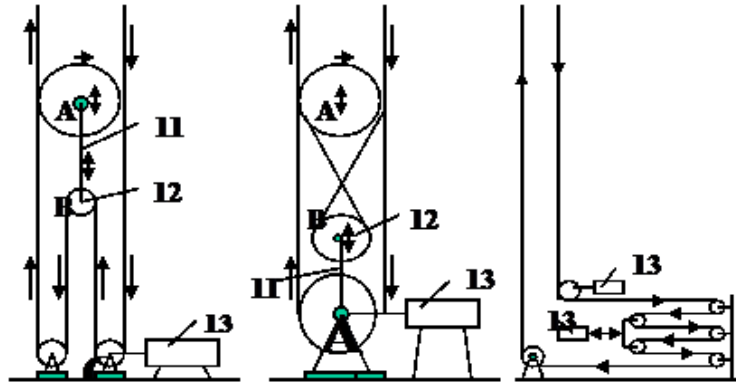

Fig. 1.4. Two mechanisms for changing the rope length in the Transport System (They are same for the space station). Notations: 11 - the rope which is connected axis A,B. This rope can change its length (the distance AB); 12 - additional rollers.
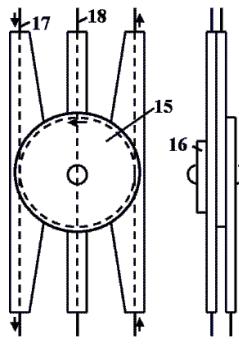

Fig. 1.5. Roller of Space Transport System. Notations: 15 – roller, 16 – control; 17 – transport system cable; 18 – main cable.

If the cable material has a very high ratio of safe (admissible) stress/density there may be one chain (Fig. 1.3b). The transport system then has only one main cable. Old design (fig. 1.1) has many problems, for example, in the transfer of large amounts of energy to the load cabin.

Theory and Computation
(in metric system)

1. The cable of equal stress for the planet. The force active in the cable is:

$$F = \sigma A = F_0 + \int_{R_0}^{R} dW = F_0 + \int_{R_0}^{R} \gamma A dR \qquad (1.1)$$

where

$$\gamma = \gamma_0 g_0 \left[\left(\frac{R_0}{R} \right)^2 - \frac{\omega^2 R}{g_0} \right] . \qquad (1.2)$$

If we substitute (1.2) in (1.1) and find the difference to the variable upper integral limit, we obtain the differential equations

$$\frac{1}{A}dA = \frac{\gamma_0 g_0}{\sigma}\left[\left(\frac{R_0}{R}\right)^2 - \frac{\omega^2 R}{g_0}\right]dR .$$
(1.3)

Solution to equation (1.3) is

$$a(R) = \frac{A}{A_0} = \exp\left[\frac{\gamma_0 g_0 B(R)}{\sigma}\right]$$
(1.4)

$$B(r) = R_0^2\left\{\left(\frac{1}{R_0} - \frac{1}{R}\right) - \frac{\omega^2}{2g_0}\left[\left(\frac{R}{R_0}\right)^2 - 1\right]\right\} ,$$

where a is the relative cable area, $B(r)$ is the work of lifting 1 kg mass.

The computation for different $K = \sigma/\gamma_0/10^7$ is presented in Figs. 1.6, 1.7.
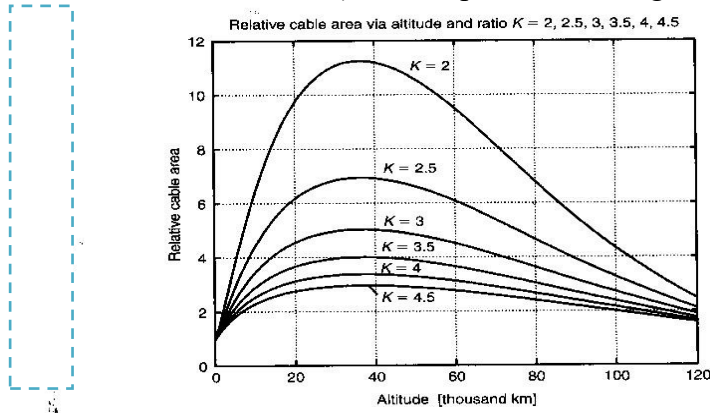
Fig. 1.6.   Relative cable area via altitude [thousand km] for coefficient $K = 2$–4.5.
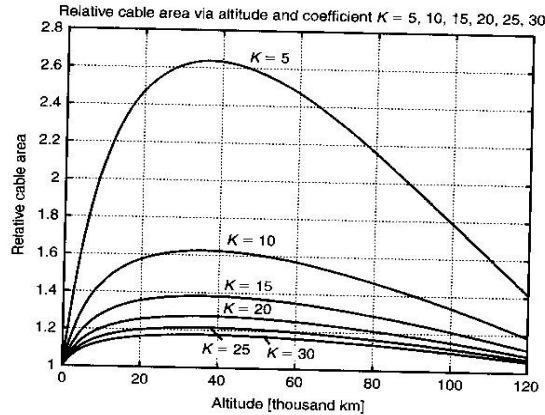
Fig. 1.7.   Relative cable area via altitude [thousand km] for coefficient $K = 5$–30.

As you see for $K = 2$ the cable area changes by 11 times, but for very high $K = 30$ only by 1.19 times.

2.   The mass of the cable W and a volume v can be calculated by equations

$$v = A_0\int_{R_0}^{R} adR = \frac{F_0}{g_0}\int_{R_0}^{R} adR , \quad W(R) = \gamma_0 v = \frac{F_0}{g_0}\int_{R_0}^{R}\exp\left(\frac{\gamma g_0 B}{\sigma}\right)dR .$$
(1.5)

The results of the computation of the cable mass for the load mass of 3000 kg (force 30000 N) and cable density of 1800 kg/m³ is presented in Figs. 1.8, 1.9.

Earth cable mass via K; cable density = 1800 kg/m³; force = 30,000 N

Fig. 1.8. Cable mass [tons] via counterweight altitude for Earth's surface force of 3 ton, cable density 1800 kg/m³, and K = 2–4.5.

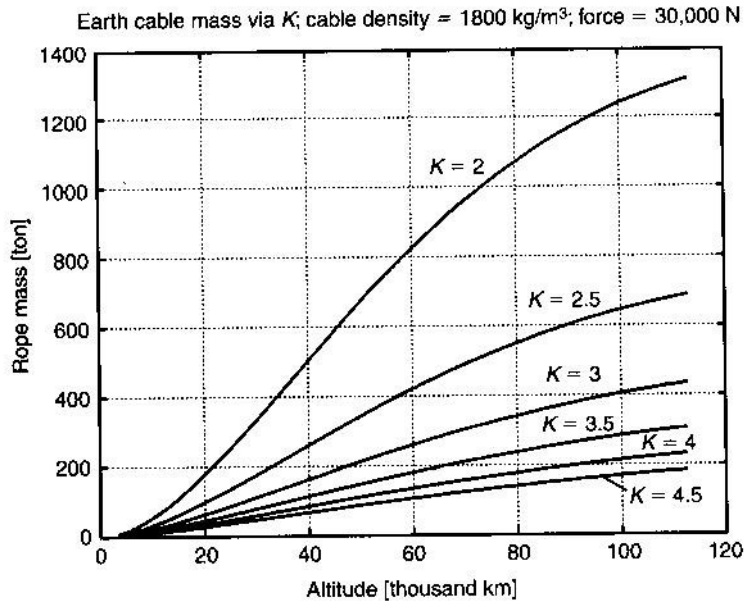**Earth cable mass via K; cable density = 1800 kg/m³; force = 30,000 N**
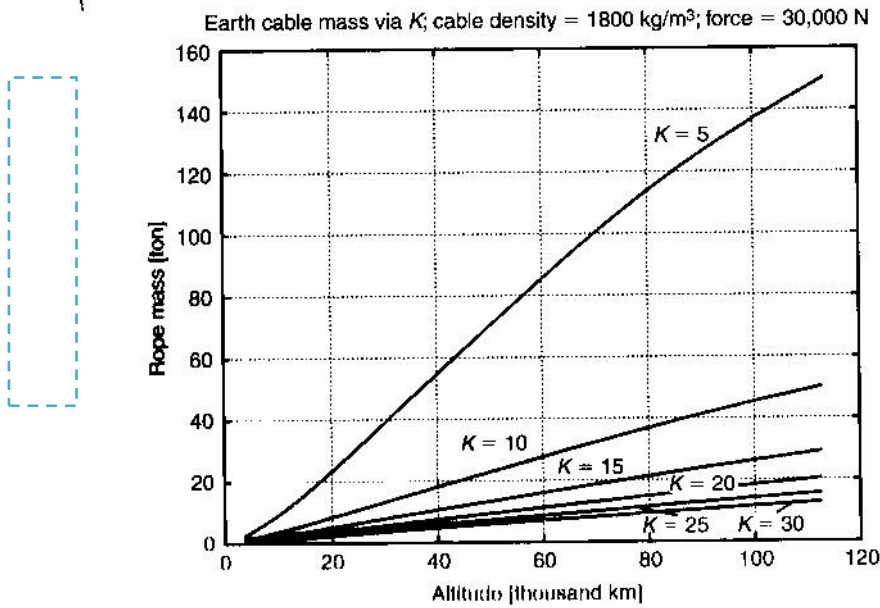

Fig. 1.9. Cable mass [tons] via counterweight altitude for Earth's surface force of 1 ton, cable density 1800 kg/m³, and K = 5–30.

3. The lift force of a mass of 1 kg, which is located over geosynchronous orbit and has speed $V > V_1$ is

$$\Delta F = \frac{\omega^2 R}{g_0} - \left(\frac{R_0}{R}\right)^2 \qquad [\text{kgf/kgm}]. \qquad (1.6)$$

The result of this computation is presented in Fig. 1.10. Every 100 kg of a mass of the equalizer gives 5 kgf of lift force at the altitude 100,000 km.
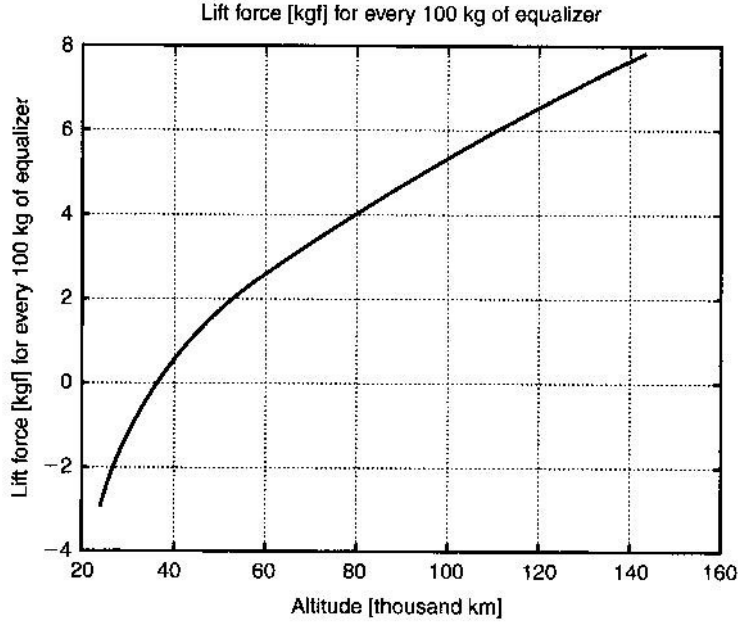
Lift force [kgf] for every 100 kg of equalizer

Fig. 1.10. Lift force [kgf] via altitude {thousand km] for every 100 kg of a counterweight (equalizer).

4. The equalizer mass (counterweight) M for different radius (altitudes) R and K may be computed from the equilibrium equation and (1.6):

$$F_0 a(R) + F_0 = M \left[\frac{\omega^2 R}{g_0} - \left(\frac{R_0}{R}\right)^2 \right],$$

$$M = \frac{F_0 [a(R) + 1]}{\dfrac{\omega^2 R}{g_0} - \left(\dfrac{R_0}{R}\right)^2} . \qquad (1.7)$$

Results of this computation are presented on Fig. 1.11–1.14. For a lift force of 10 tons at Earth (payload of 3000 kg), the equalizer mass is 570 tons for $K = 4$ and about 435 tons for $K = 10$ at the altitude 100,000 km.

5. If the balance cabin (load) to be moved down is absent, then the delivery work of 1 kg mass may be computed by the equation

$$E(R) = R_0^2 \left\{ \left(\frac{1}{R_0} - \frac{1}{R} \right) - \frac{\omega^2}{2g_0} \left[\left(\frac{R}{R_0}\right)^2 - 1 \right] \right\} . \qquad (1.8)$$

The result of this computation presented in Fig. 1.15.

Equalizer (counterweight) mass [ton] for force $F = 100$ kgf
and coefficient $K = 2, 2.5, 3, 3.5, 4, 4.5$

Fig. 1.11. Counterweight (equalizer mass) [tons] via altitude [thousand km] for ground force 100 kgf (at Earth's surface) for $K = 2$–4.5. (It is centrifugal force without additional force, which supports the cable of equal stress.)

Balance mass [ton] for load $F = 100$ kg and
ratio $K = 5, 10, 15, 20, 25, 30$

Fig. 1.12. Counterweight [tons] via altitude [thousand km] for ground force 100 kgf (at Earth's surface) for $K = 5$–30. (It is centrifugal force without additional force, which supports the cable of equal stress.)

6.

Equalizer mass for load F = 100 kgf, altitude H = 120,000 km

Fig. 1.13. Counterweight [tons] via altitude [thousand km] for ground force 100 kgf (at Earth's surface) for K = 2–4.5. (It is centrifugal force without additional force, which supports the cable of equal stress.)

Equalizer mass for load F = 100 kgf, altitude H = 100,000 km
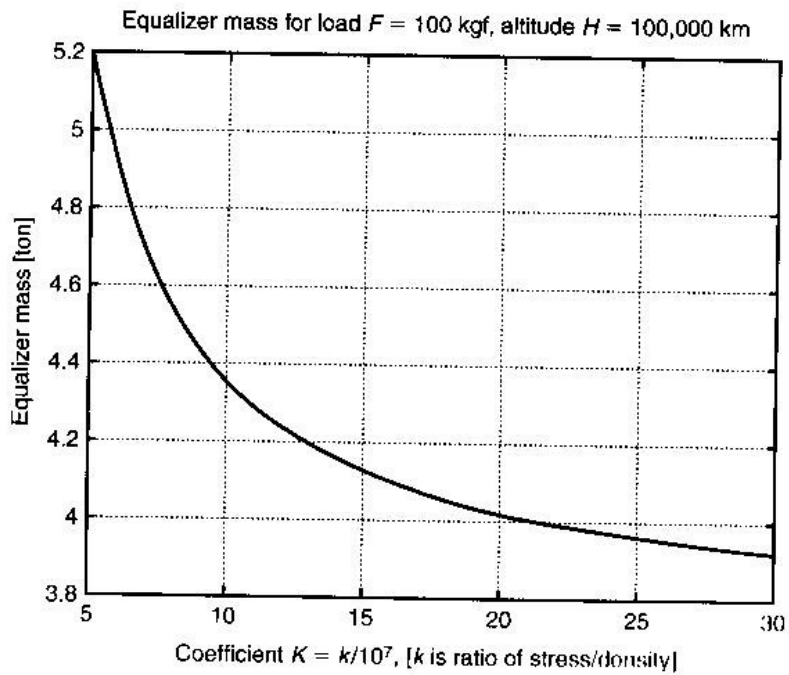
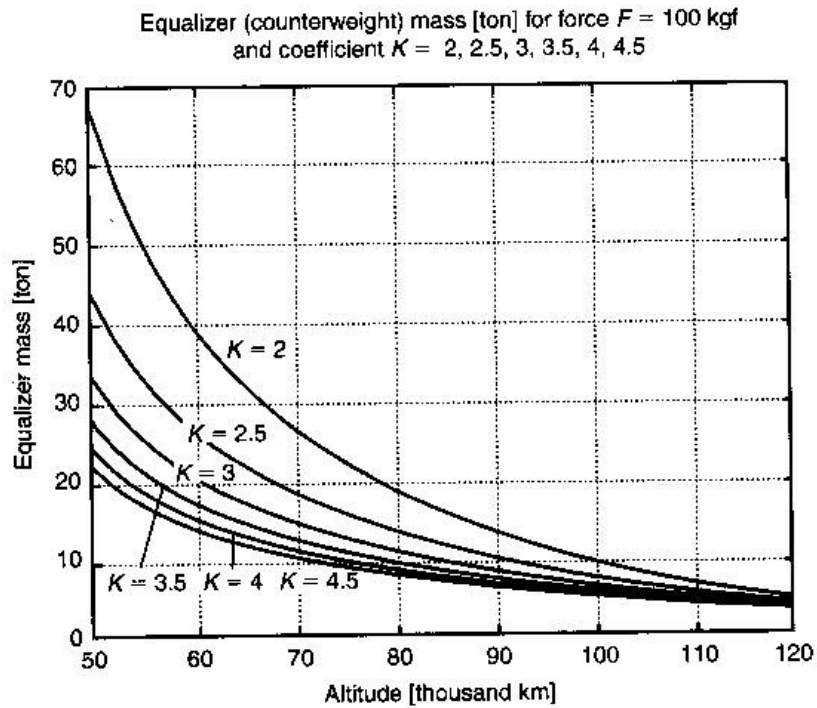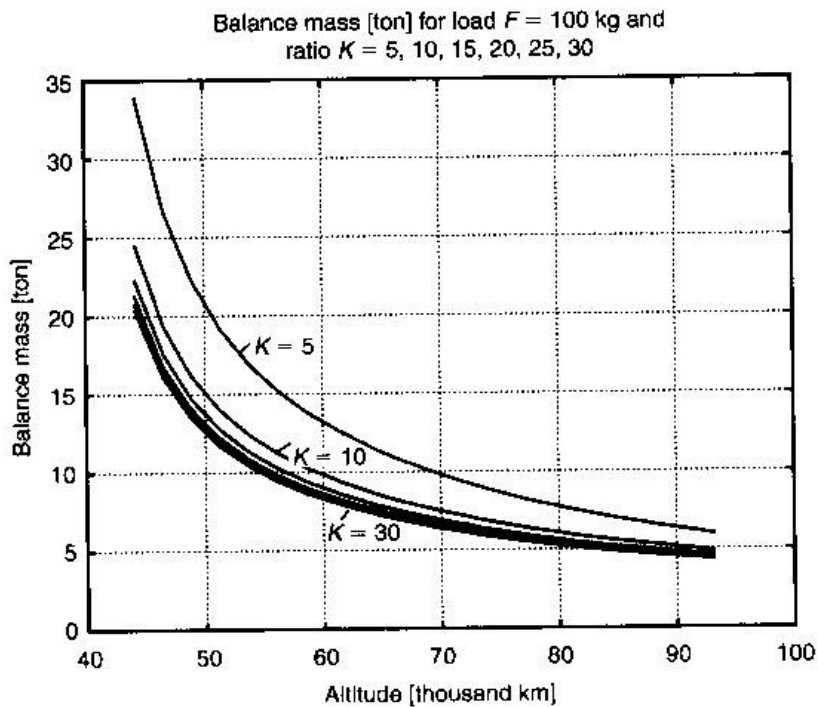**Fig. 1.14.** Counterweight [tons] via altitude [thousand km] for ground force 100 kgf (at Earth's surface) for K = 5–30. (It is centrifugal force without additional force, which supports the cable of equal stress.)
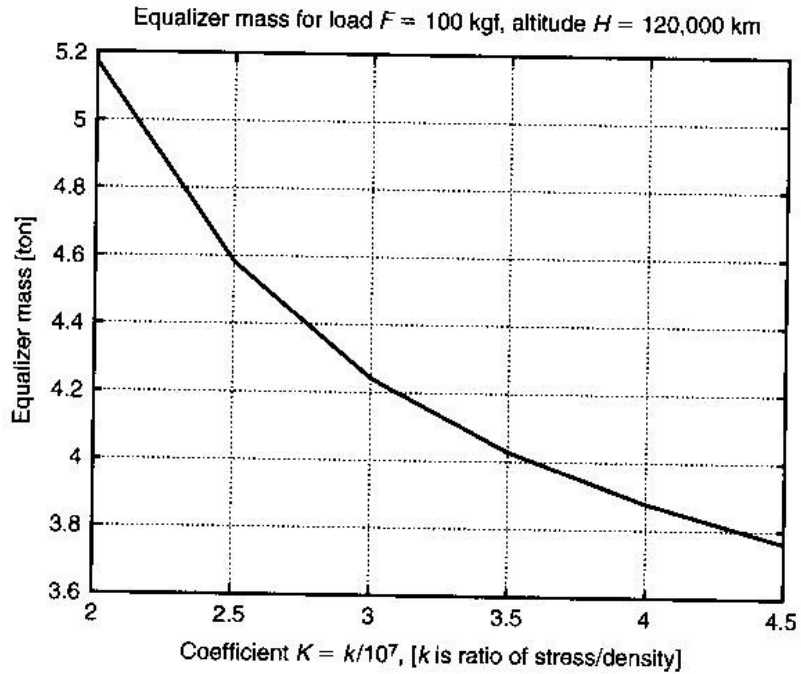
Earth delivery work of 1-kg load via altitude
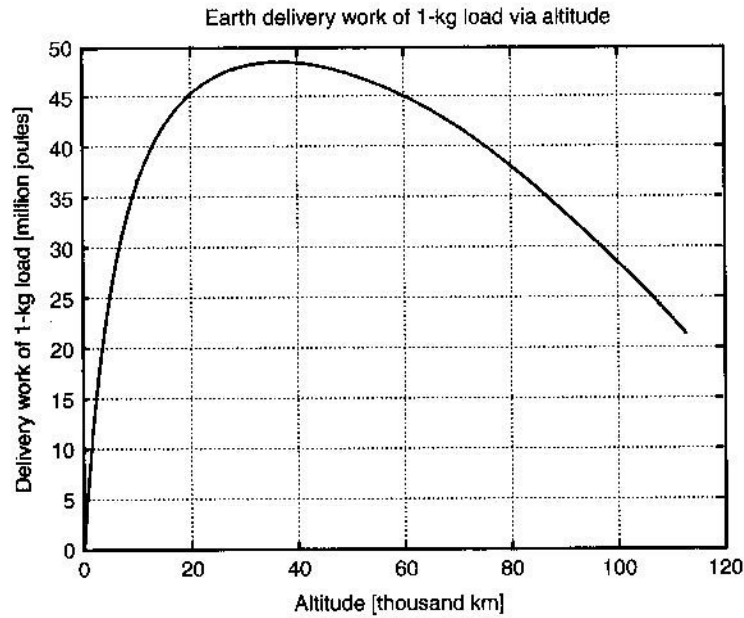
Fig. 1.15. Earth delivery work [million joules] of 1 kg load via altitude [thousand km].

6. When a space vehicle (satellite) is disconnected from the transport system before reaching geosynchronous orbit then an orbit perigee r (perigee altitude H) and period time T can be computed by the equations

$$H = r - R_0 \, , \quad r = \frac{uR}{2-u} \, , \quad T = \frac{\pi(r+R)^{3/2}}{3600\sqrt{2c}} \, , \tag{1.9}$$

where $u = \omega^2 R^3/c, \ c = 3.986 \times 10^{14}$.

The result of this computation is presented in Fig. 1.16, 1.17. When this space vehicle is in a suitable position (after the return flight), it can be connected back to the transport system.
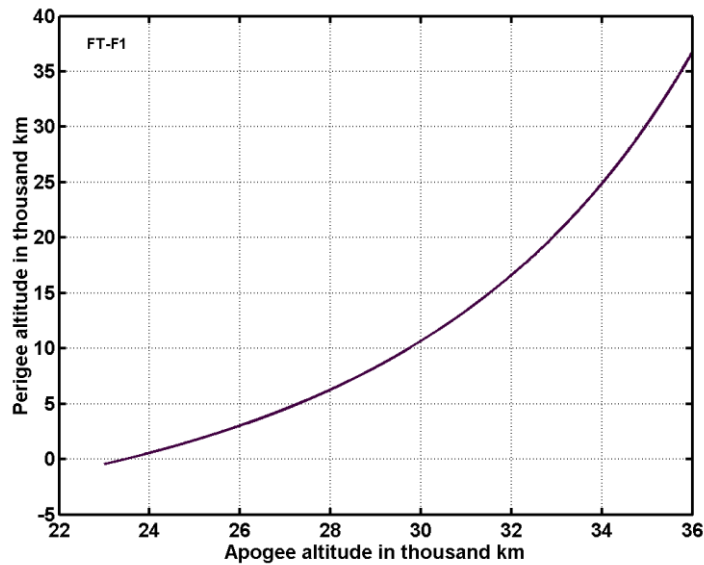
Fig. 1.16. Perigee altitude (in thousand km) via disconnected (apogee) altitude of a space ship.
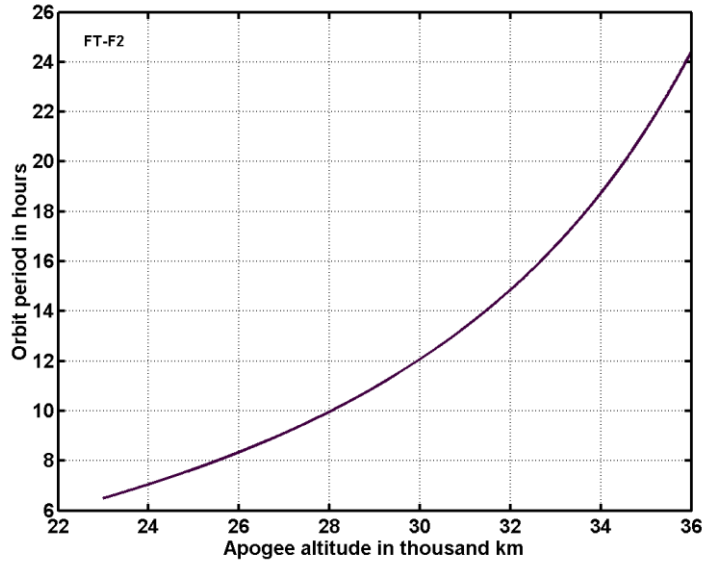
Fig. 1.17. Orbit period (in hours) via apogee altitude (in thousand km).

7. When the space vehicle is disconnected from the transport system higher than the geosynchronous orbit, then the vehicle speed V, the first space speed V_1, and the second (escape) space speed V_2 can be computed by formulas

$$V = \omega R , \quad V_1 = \frac{19.976 \cdot 10^6}{\sqrt{R}} , \quad V_2 = 1.414 V_1 . \qquad (1.10)$$

Then the result of computation are given in Fig. 1.18. Above an altitude of 50,000 km the space vehicle can go into interplanetary orbit. The necessary speed and direction can be set by a choice of the disconnect point and position system in space. Additional speed over the escape velocity may reach 6 km/sec. This is more then enough for a flight to the far planets. When the space vehicle returns it can also choose a point in the transport system for connection.
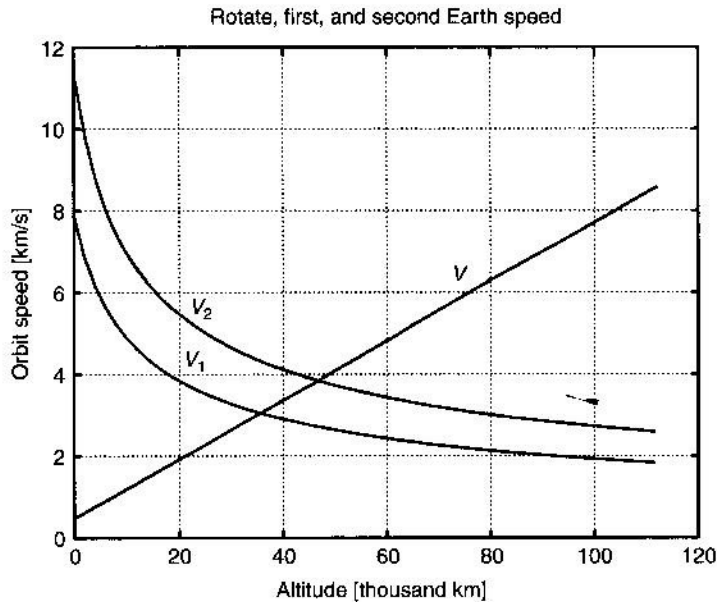
Fig. 1.18. Rotate, first, and second Earth speed [km/s] via altitude [thousand km].

8. Let us take a small part of a rotary circle and write it equilibrium

$$\frac{2AR\alpha\gamma V^2}{R} = 2A\sigma\sin\alpha .$$

The maximum safe cable speed of chains is

$$V_r = \sqrt{\frac{\sigma}{\gamma}} = \sqrt{10^7 K} \qquad [\text{m/s}] . \qquad (1.11)$$

Results of this computation are presented in Fig. 1.19.

9. The delivery cost of 1 kg load is (Fig. 1.20)

$$C = \left(\frac{C_i}{Y} + N_e S_e + M_a\right)\frac{1}{3V_d} . \qquad (1.12)$$

10. The increase of the space installation mass is a geometric progression

$$n = 1 + \frac{\ln(M_e / M_0)}{\ln\left[(M_0 + M_g)/M_0\right]} , \qquad (1.13)$$

where n – number of working days (Fig. 1.21).

11. The planetary parameters used for computations in all projects are as shown in Table 1.1.

Table 1.1

Planet	Radios R_0 10^6 m	Gravitation g_0 m/s^2	Angle speed ω 10^{-6}[rad/s]	Geosynchr. R_g 10^6 m
Earth	6.378	9.81	72.685	42.2
Mars	3.39	3.72	71.06	20.38
Moon	1.737	1.62	2.662	88.55

Transport system for Space Elevator (Project 1)

That is an example of an inexpensive transport system for cheap annual delivery of 100,000 tourists, or 12,000 tons of payload into Earth orbits, or the delivery up to 2,000 tourists to Mars, or the launching of up to 2,500 tons of payload to other planets.

Main results of computation

The suggested space transport system can be used for delivery of tourists and payloads to an orbit around the Earth, or to space stations serving as a tourist hotel, scientific laboratory, or industrial factory, or for the delivery of people and payloads to other planets.

Technical parameters: Let us take the safe cable stress 7200 kg/mm^2 and cable density 1800 kg/m^3. This is equal to $K = 4$. This is not so great since by the year 2000 many laboratories had made experimental nanotubes with a tensile stress of 200 Giga–Pascals (20,000 kg/mm^2) and a density of 1800 kg/m^3. The theory of nanotubes predicts 100 ton/mm^2 with Young's modulus of up to 5 Tera Pascal's (currently it is 1 Tera Pascal) and a density of 800 kg/m^3 for SWNTs nanotubes. This means that the coefficient K used in our equations and graphs can be up to 125.

Assume a maximum equalizer lift force of 9 tons at the Earth's surface and divide this force between three cables: one main and two transport cables. Then it follows from Fig. 1.11, that the mass of the equalizer (or the space station) creates a lift force of 9 tons at the Earth's surface, which equals 518 tons for $K = 4$ (this is close to the current International Space Station weight of 450 tons). The equalizer is located over a geosynchronous orbit at an altitude of 100,000 km. Full centrifugal lift force of the equalizer (Fig. 1.10) is 34.6 tons, but 24.6 tons of the equalizer are used in support of the cables.

Safe cable speed [km/s]
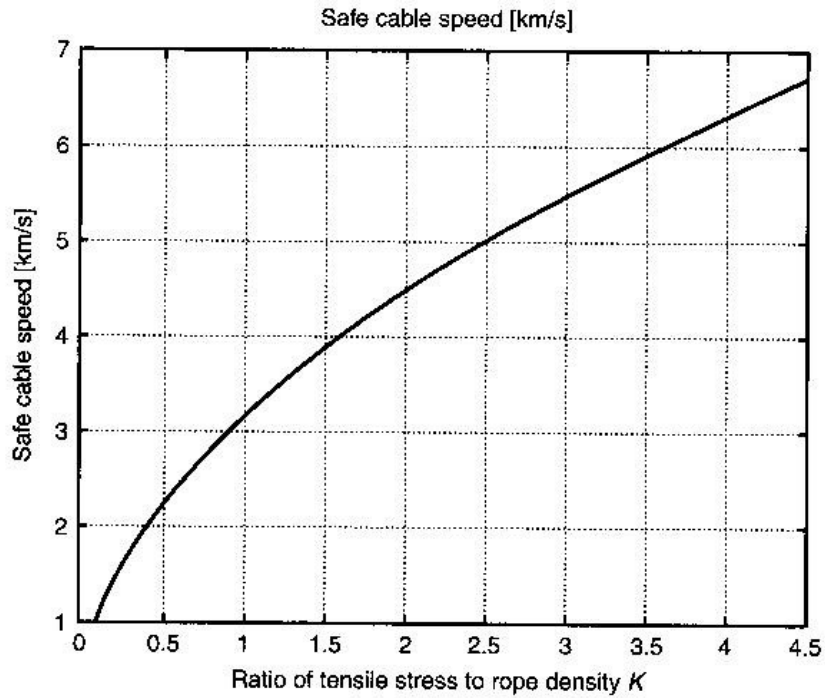
Fig. 1.19. Safe cable speed [km/s] via the ratio of tensile stress to cable density (coefficient K).

Delivery cost of 1 kg load in $, installation lifetime Y = 20 years,
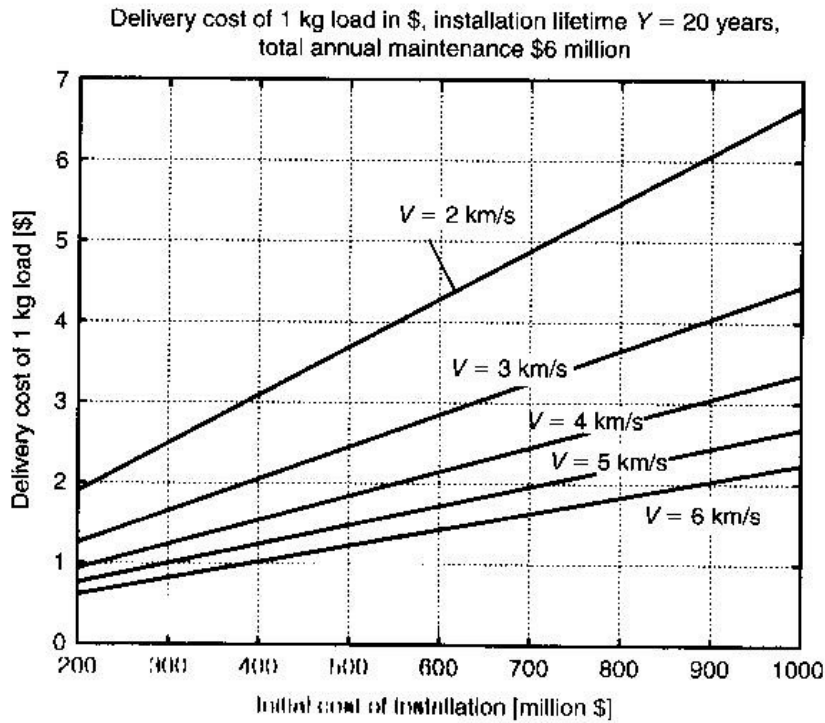total annual maintenance $6 million

Fig. 1.20. Delivery cost of 1 kg of load [$] via initial cost of installation [million dollars] for delivery speed of 1 .... km/s, for live time 20 years, total annual salary $ million, maintenance 1 million [US dollars].

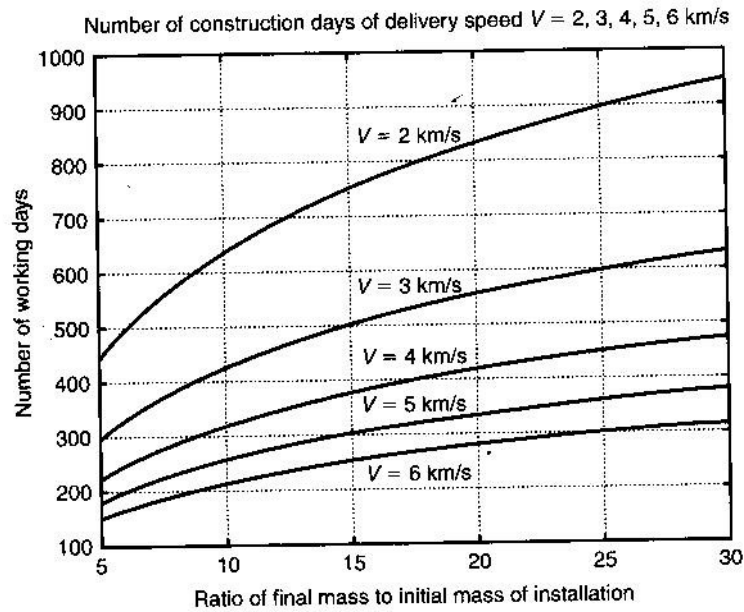Number of construction days of delivery speed V = 2, 3, 4, 5, 6 km/s

Fig. 1.21. Number of working days via the ratio of final mass to initial mass of the installation for delivery speed V = 2–6 km/s.

The transport system has three cables: one main and two in the transport system. Each cable can support a force (load) of 3000 kgf. The main cable has a cross-sectional area of equal stress. Then the cable cross-section area is (see Fig. 1.6) A = 0.42 mm^2 (diameter D = 0.73 mm) at the Earth's surface, maximum 1.4 mm^2 in the middle section (D = 1.33 mm, altitude 37,000 km), and A = 0.82 mm^2 (D = 1 mm) at the equalizer. The mass of main cable is 205 tons (see Fig. 1.8). The chains of the two transport cable loops have gross section areas to equal the tensile stress of the main cable at given altitude, and the capabilities are the same as the main cable. Each of them can carry 3 tons force. The total mass of the cable is about 620 tons. The three cables increase the safety of the passengers. If any one of the cables breaks down, then the other two will allow a safe return of the space vehicle to Earth and the repair of the transport system.

If the container cable is broken, the pilot uses the main cable for delivering people back to Earth. If the main cable is broken, then the load container cable will be used for delivering a new main cable to the equalizer. For lifting non-balance loads (for example, satellites or parts of new space stations, transport installations, interplanetary ships), the energy must be spent in any delivery method. This energy can be calculated from equation (1.8)(Fig. 1.15). When the transport system in Fig. 1.3 is used, the engine is located on the Earth and does not have an energy limitation[11]. Moreover, the transport system in Fig. 1.3 can transfer a power of up to 90,000 kW to the space station for a cable speed of 3 km/s. At the present time, the International Space Station has only 60 kW of power.

Delivery capabilities. For tourist transportation the suggested system works in the following manner. The passenger space vehicle has the full mass of 3 tons (6667 pounds) to carry 25 passengers and two pilots. One ship moves up, the other ship, which is returning, moves down; then the lift and descent energies are approximately equal. If the average speed is 3 km/s then the first ship reaches the altitude of 21.5 – 23 thousands km in 2 hours (acceleration 1.9 m/s^2). At this altitude the ship is separated from the cable to fly in an elliptical orbit with minimum altitude 200 km and period approximately 6 hours (Figs. 1.16, 1.17). After one day the ship makes four revolutions around the Earth while the cable system makes one revolution, and the ship and cable will be in the same place with the same speed. The ship is connected back to the transport system, moves down the cable and lifts the next ship. The orbit may be also 3 revolutions (period 8 hours) or 2 revolutions (period 12 hours). In one day the

transport system can accommodate 12 space ships (300 tourists) in both directions. This means more then 100,000 tourists annually into space.

The system can launch payloads into space, and if the altitude of disconnection is changed then the orbit is changed (see Fig. 1.17). If a satellite needs a low orbit, then it can use the brike parachute when it flies through the top of the atmosphere and it will achieve a near circular orbit. The annual payload capability of the suggested space transport system is about 12,600 tons into a geosynchronous orbit.

If instead of the equalizer the system has a space station of the same mass at an altitude of 100,000 km and the system can has space stations along cable and above geosynchronous orbit then these stations decrease the mass of the equalizer and may serve as tourist hotels, scientific laboratories, or industrial factories.

If the space station is located at an altitude of 100,000 km, then the time of delivery will be 9.36 hours for an average delivery speed of 3 km/s. This means 60 passengers per day or 21,000 people annually in space.

Let us assume that every person needs 400 kg of food for a one–year round trip to Mars, and Mars has the same transport installation (see next project). This means we can send about 2000 people to Mars annually at suitable positions of Earth relative to Mars.

Estimations of installation cost and production cost of delivery

Cost of suggested space transport installation[5,6]. The current International Space Station has cost many billions of dollars, but the suggested space transport system can cost a lot less. Moreover, the suggested transport system allows us to create other transport systems in a geometric progression [see equation (1.13)]. Let us examine an example of the transport system.

Initially we create the transport system to lift only 50 kg of load mass to an altitude of 100,000 km. Using the Figs. 1.6 to 1.14 we have found that the equalizer mass is 8.5 tons, the cable mass is 10.25 tons and the total mass is about 19 tons. Let us assume that the delivery cost of 1 kg mass is $10,000. The construction of the system will then have a cost of $190 million. Let us assume that 1 ton of cable with $K = 4$ from whiskers or nanotubes costs $0.1 million then the system costs $1.25 million. Let us put the research and development (R&D) cost of installation at $29 million. Then the total cost of initial installation will be $220 million. About 90% of this sum is the cost of initial rocket delivery.

After construction, this initial installation begins to deliver the cable and equalizer or parts of the space station into space. The cable and equalizer capability increase in a geometric progression. The installation can use part of the time for delivery of payload (satellites) and self-financing of this project. After 765 working days the total mass of equalizer and cables reaches the amount above (1133 tons) and the installation can work full time as a tourist launcher or continue to create new installations. In the last case this installation and its derivative installations can build 100 additional installations (1133 tons) in only 30 months [see equation (1.13) and Fig. 1.21] with a total capability of 10 million tourists per year. The new installations will be separated from the mother installations and moved to other positions around the Earth. The result of these installations allows the delivery of passengers and payloads from one continent to another across space with low expenditure of energy.

Let us estimate the cost of the initial installation. The installation needs 620 tons of cable. Let us take the cost of cable as $0.1 million per ton. The cable cost will be $62 million. Assume the space station cost $20 million. The construction time is 140 days [equation (1.13)]. The cost of using of the mother installation without profit is $5 millions/year. In this case the new installation will cost $87 million. In reality the new installation can soon after construction begin to launch payloads and become self-financing.

Cost of delivery

The cost of delivery is the most important parameter in the space industry. Let us estimate it for the full initial installation above.

   As we calculated earlier the cost of the initial installation is $220 millions (further construction is made by self-financing). Assume that installation is used for 20 years, served by 100 officers with an average annual salary of $50,000 and maintenance is $1 million in year. If we deliver 100,000 tourists annually, the production delivery cost will be $160/person or $1.27/kg of payload. Some 70% of this sum is the cost of installation, but the delivery cost of the new installations will be cheaper.

   If the price of a space trip is $1990, then the profit will be $183 million annually. If the payload delivery price is $15/kg then the profit will $189 millions annually.

   The cable speed for $K = 4$ is 6.32 km/s [equation (1.11), Fig. 1.19]. If average cable speed equals 6 km/s, then all performance factors are improved by a factor of two times.

   If the reader does not agree with this estimation, then equations (1.1) to (1.13) and Figs. 1.6 to 1.21 are able calculation of the delivery cost for other parameters. In any case the delivery cost will be hundreds of times less than the current rocket powered method.

Delivery System for Free Round Trip to Mars (Project 2)

   A method and similar installation (Figs.1.3 to 1.5) can be used for inexpensive travel to other planets, for example, from the Earth to Mars or the Moon and back (Fig. 1.22). A Mars space station would be similar to an Earth space station, but the Mars station would weigh less due to the decreased gravitation on Mars. This method uses the rotary energy of the planets. For this method, two facilities are required, one on Earth and the other on another planet (e.g. Mars). The Earth accelerates the space ship to the required speed and direction and then disconnects the ship. The space ship flies in space along the defined trajectory to Mars (Fig. 1.22). On reaching Mars the space ship connects to the cable of the Mars space transport system, then it moves down to Mars using the transport system.

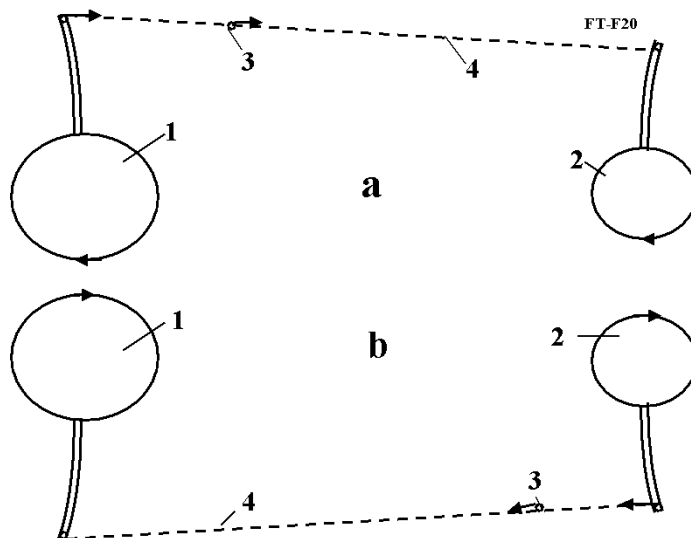**Fig. 1.22**. Using the suggested transport system for space flight to Mars and back. Notation: 1 – Earth, 2 – Mars, 3 – space ship, 4 – trajectory of space ship to Mars (a) and back (b).

   The inverse of the process is used for the return trip. If two ships are used for descent and lifting payloads (Fig. 1.2), energy will only be required to overcome the small amount of friction losses in the

lift transmission. The way back is the same. The Mars space ship chooses a cable disconnect point with a suitable speed and direction or a connect–disconnect in a special arrival–departure port.

Technical parameters of Mars transport system.

Equations (1.1)–(1.13) may be used for estimation main parameters of mars transport system. These computations are presented in Figs. (1.23) to (1.29). If we want to accept Earth space ships of 3 tons mass, then the parameters of the Mars transport system will be $K = 4$, three cables, and an equalizer altitude of 50,000 km.

Equalizer mass is 94.7 tons. The total cable mass is 51 tons. Cross-section area of one cable is 0.158 mm^2 (diameter $D = 0.45$ mm) at Mars surface, $D = 0.5$ mm at altitude 20,000 km, and $D = 0.47$ mm at altitude 50,000 km.

For construction on Mars we need to deliver only the cables. The equalizer can be made from local Mars material, for example, stones. Delivery capability is about 1000 tons, or 2000 people annually.
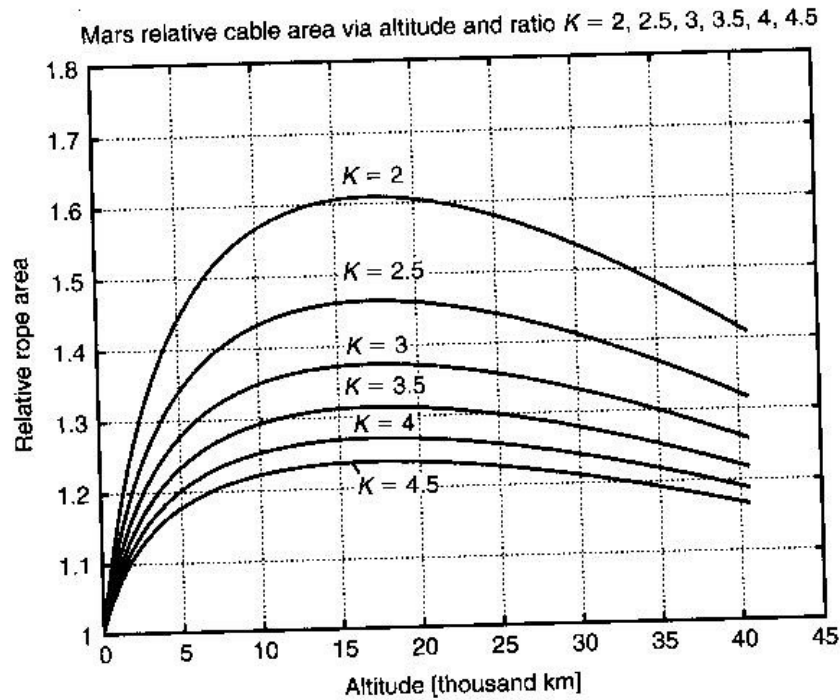
Fig. 1.23. Mars relative cable area via altitude and coefficient $K = 2$–4.5.

Mars cable mass via altitude and $K = 2-4.5$,
cable density $= 1800$ kg/m^3, force $= 11376$ N, and load mass $= 3$ ton
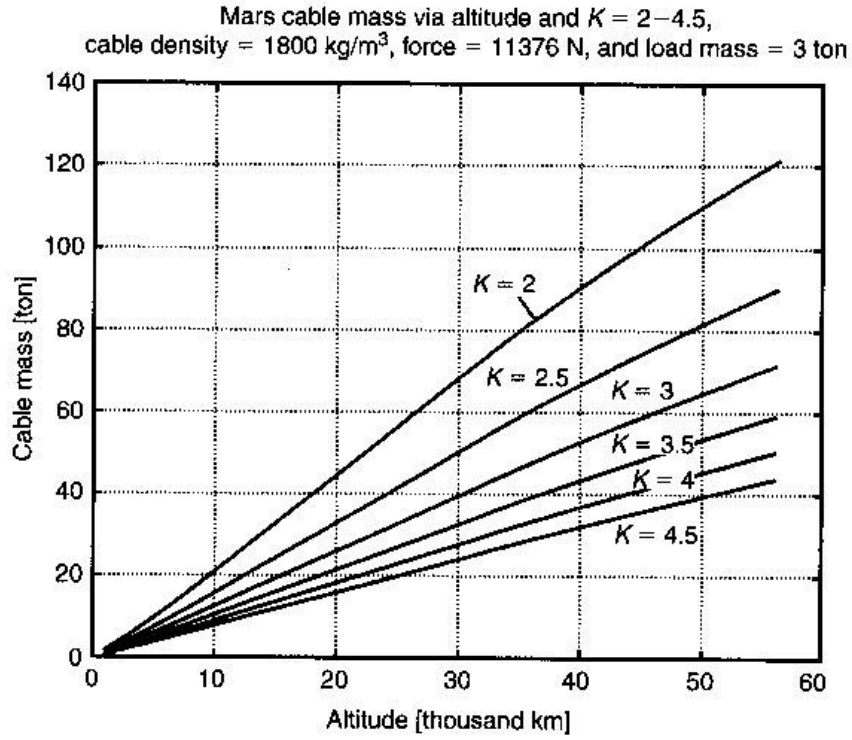
Fig. 1.24. Mars cable mass via altitude [thousand km], a cable density 1800 kg/m^3 and a load mass of 3 ton.

Lift force [kgf] for every 100 kg of mars counterweight mass
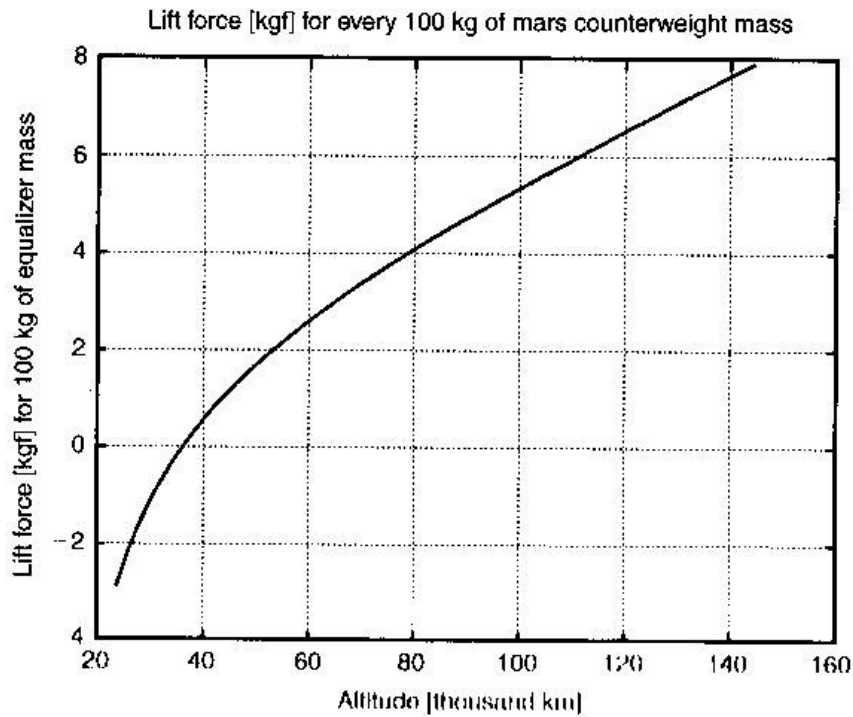
Fig. 1.25. Lift force [kgf] via altitude [thousand km] for every 100 kg of Mars equalizer mass.

Equalizer mass [ton] for force $F = 100$ kgf
and $K = 2, 2.5, 3, 3.5, 4, 4.5$
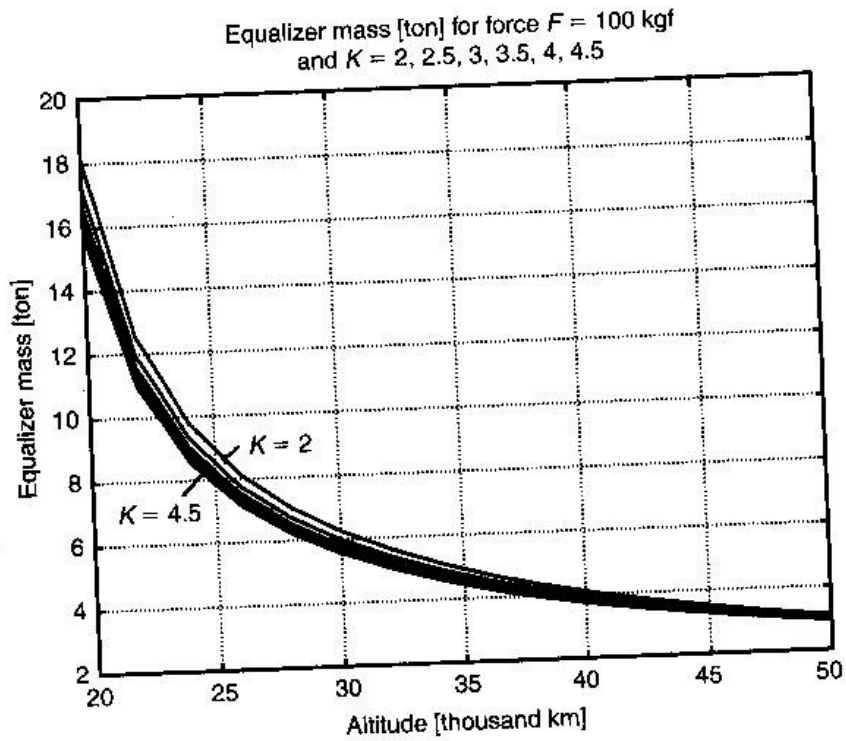
Fig. 1.26. Mars counterweight (equalizer) mass [tons] via altitude [thousand km] for the force 100 kgf and the coefficient $K = 2$–4.5.

Equalizer mass for load $F = 100$ kgf, altitude $H = 50,000$ km
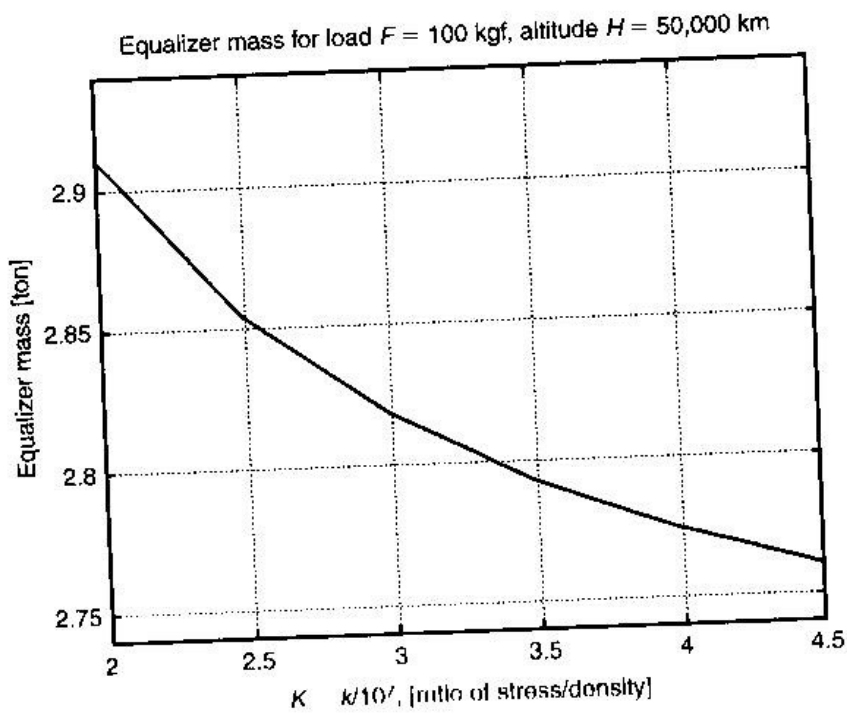
Fig. 1.27. Mars counterweight mass [tons] via the coefficient $K = 2$–4.5 for altitude 50,000 km and the force 100 kgf.

Rotate, first and second Mars speed
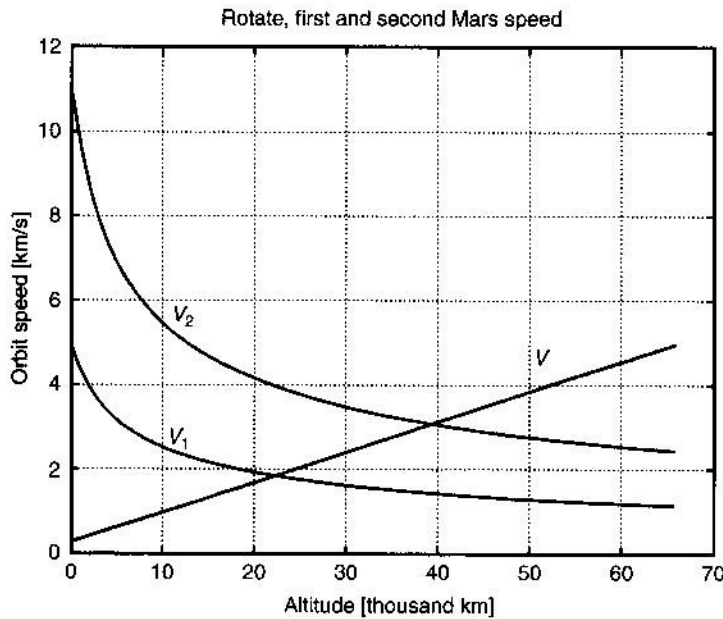
¡. **1.28.** Rotate, first, and second Mars speed via altitude [thousand km].

Mars delivery work of 1 kg load via altitude
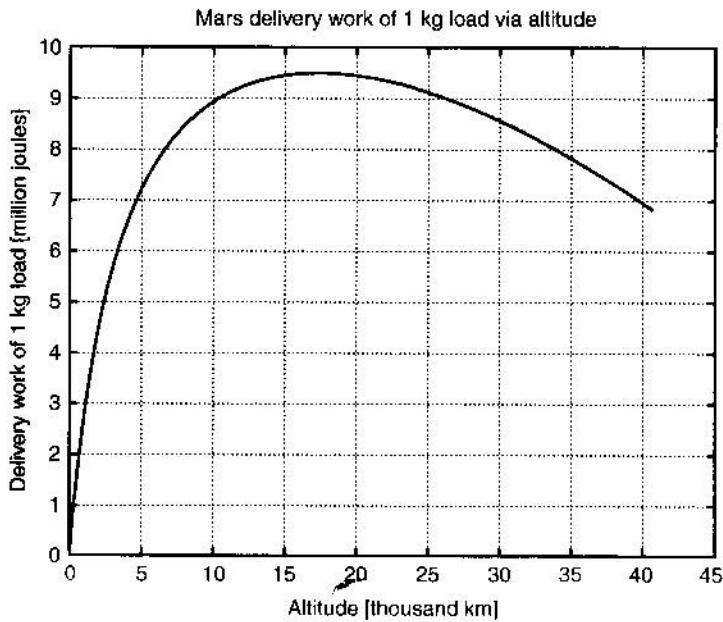
. **1.29.** Mars delivery work [million joules] of 1 kg of a load via altitude [thousand km].

Free Trip to Moon (Project 3)

This method may be used for an inexpensive trip to a planet's moon, if the moon's angular speed is equal to the planet's angular speed, for example, from the Earth to the Moon and back (Fig. 1.30 to 1.32). The upper end of the cable is connected to the planet's moon. The lower end of the cable is connected to an aircraft (or buoy), which flies (i.e. glides or slides) along the planet's surface. The

lower end may be also connected to an Earth pole. The aircraft (or Earth polar station, or Moon) has a device which allows the length of cable to be changed. This device would consist of a spool, motor, brake, transmission, and controller. The facility could have devices for delivering people and payloads to the Moon and back using the suggested transport system. The delivery devices include: containers, cables, motors, brakes, and controllers. If the aircraft is small and the cable is strong then the motion of the Moon can be used to move the airplane. For example, if the airplane weighs 15 tons and has an aerodynamic ratio (the lift force to the drag force) equal to 5, a thrust of 3000 kg would be enough for the aircraft to fly for infinity without requiring any fuel. The aircraft could use a small engine for maneuverability and temporary landing. If the planet has an atmosphere (as the Earth) the engine could be a turbine engine. If the planet does not have an atmosphere, a rocket engine may be used.

   If the suggested transport system is used only for free thrust (9 tons), the system can thrust the three named supersonic aircraft or produce up to 40 millions watts of energy.

   A different facility could use a transitional space station located at the zero gravity point between the planet and the planet's moon. Fig. 1.31 shows a sketch of the temporary landing of an airplane on the planet surface. The aircraft increases the length of the cable, flies ahead of the cable, and lands on a planet surface. While the planet makes an angle turn ($\alpha + \beta = 30°$, see Fig. 1.31) the aircraft can be on a planet surface. This time equals about 2 hours for the Earth, which would be long enough to load payload on the aircraft
.
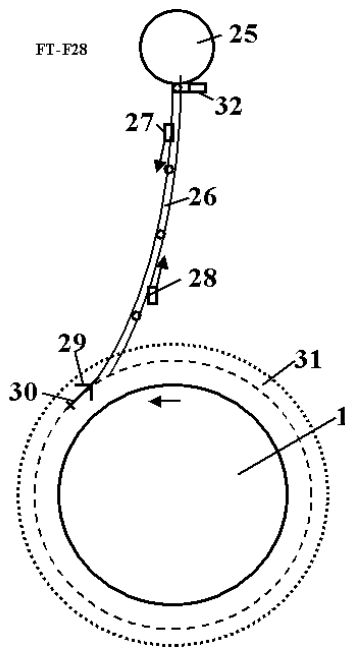
Fig. 1.30. The suggested transport system for the Moon. Notations: 1 – Earth, 25 - Moon, 26 – suggested Moon transport system, 27, 28 – load cabins, 29 – aircraft, 30 – cable control, 32 – engine.

   The Moon's trajectory has an eccentricity (Fig. 1.32). If the main cable is strong enough, the moon may used to pull a payload (space ship, manned cabin), by trajectory to an altitude of about 60,000 kilometers every 27 days. For this case, the length of the main cable from the Moon to the container does not change and when the Moon increases its distance from the Earth, the Moon lifts the space ship. The payload could land back on the planet at any time if it is allowed to slide along the cable. The Moon's energy can be used also for an inexpensive trip around the Earth (Figs. 1.30 and 1.32) by

having the moon "drag" an aircraft around the planet (using the Moon as a free thrust engine). The Moon tows the aircraft by the cable at supersonic speed, about 440 m/s (Mach number is 1.5).
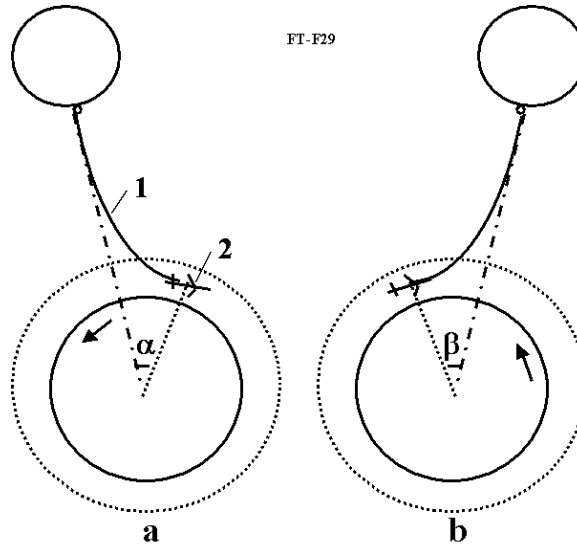
Fig. 1.31. Temporary landing of the Moon aircraft on the Earth's surface for loading. **a**– landing, **b**– take-off.
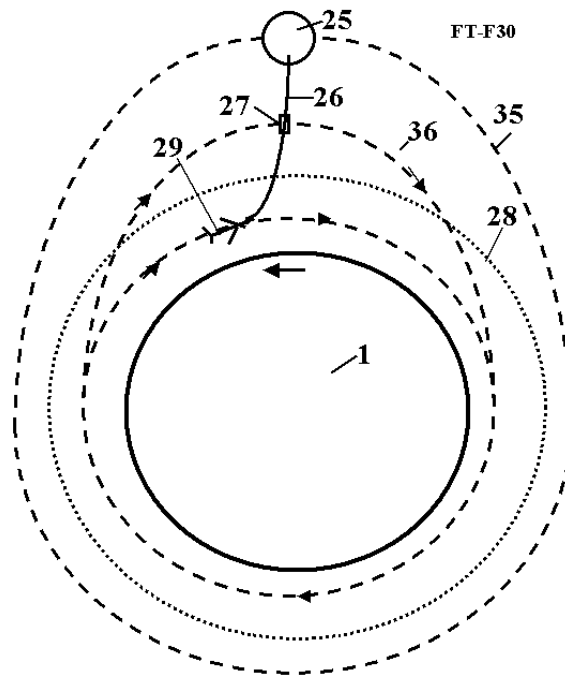
Figs. 1.32. Using the Moon's elliptical orbit for a free trip in space of up to 71,000 km. Notations: 1 – Earth, 25 – Moon, 26 – cable from Earth to Moon, 27 – Space Vehicle, 28 – limit of Earth atmosphere, 35 – Moon orbit, 36 – elliptical orbit of a Moon vehicle.

The other more simple design (without aircraft) is shown in Fig. 7.1, chapter 7. The cable is connected to on Earth pole, to a special polar station which allows to change a length of cable. Near the pole the cable is supported in the atmosphere by air balloons and wings.

Technical parameters

The following are some data for estimating the main transport system parameters for connecting to the Moon to provide inexpensive payload transfer between the Earth and the Moon. The system has three cables, each of which can keep the force at 3 tons. Material of the cable has $K=4$. All cables would have cross-sectional areas of equal stress. The cable has a minimal cross-sectional area A_0 of 0.42 mm^2 (diameter $d = 0.73$ mm) and maximum cross-sectional area A_m of 1.9 mm^2 ($d = 1.56$ mm). The mass of the main cable would be 1300 tons (Fig. 1.36). The total mass of the main cable plus the two container cables (for delivering a mass of 3000 kg) equals 3900 tons for the delivery transport system in Figs. 1.30 to 1.33. An inexpensive means of payload delivery between the Earth and the Moon could thus be developed. The elapsed time for the Moon trip at a speed of 6 km/s would be about 18.5 hours and the annual delivery capability would be 1320 tons in both directions.

Discussion
Cable Problems

Most engineers and scientists think it is impossible to develop an inexpensive means to orbit to another planet. Twenty years ago, the mass of the required cable would not allow this proposal to be possible for an additional speed of more 2,000 m/s from one asteroid. However, today's industry widely produces artificial fibers that have a tensile strength 3–5 times more than steel and a density 4–5 times less than steel. There are also experimental fibers which have a tensile strength 30–60 times more than steel and a density 2 to 4 times less than steel. For example, in the book *Advanced Fibers and Composites* is p. 158, there is a fiber C_D with a tensile strength of $\sigma = 8000$ kg/mm^2 and density (specific gravity) $\gamma = 3.5$ g/cm^3. If we take an admitted strength of 7000 kg/mm^2 ($\sigma = 7\times10^{10}$ N/m^2, $\gamma = 3500$ kg/m^3) then the ratio, $\sigma/\gamma = 0.05\times10^{-6}$ or $\sigma/\gamma = 20\times10^6$ ($K = 2$). Although (in 1976) the graphite fibers are strong ($\sigma/\gamma =10\times10^6$), they are at best still ten times weaker than theory predicts.

Steel fiber has tensile strengths of 5,000 MPA (500 kg/mm^2), but the theoretic value is 22,000 MPa (1987). Polyethylene fiber has a tensile strength of 20,000 MPa and the theoretical value is 35,000 MPa (1987).

The mechanical behavior of nanotubes also has provided excitement because nanotubes are seen as the ultimate carbon fiber, which can be used as reinforcements in advanced composite technology. Early theoretical work and recent experiments on individual nanotubes (mostly MWNTs) have confirmed that nanotubes are one of the stiffest materials ever made. Whereas carbon–carbon covalent bonds are one of the strongest in nature, a structure based on a perfect arrangement of these bonds oriented along the axis of nanotubes would produce an exceedingly strong material. Traditional carbon fibers show high strength and stiffness, but fall far short of the theoretical in-plane strength of graphite layers (an order of magnitude lower). Nanotubes come close to being the best fiber that can be made from graphite structure.

For example, whiskers made from carbon nanotubes (CNT) have a tensile strength of 200 Giga-Pascals and Young's modulus of over 1 Tera Pascal (1999). The theory predicts 1 Tera Pascal and Young modulus 1–5 Tera Pascals. The hollow structure of nanotubes makes them very light (specific density varies from 0.8 g/cc for SWNTs up to 1.8 g/cc for MWNTs, compared to 2.26 g/cc for graphite or 7.8 g/cc for steel).

Specific strength (strength/density) is important in the design of our transportation system and space elevator; nanotubes have this value at least 2 orders of magnitude greater than steel. Traditional carbon fibers have a specific strength 40 times greater than steel. Where nanotubes are made of graphite carbon, they have good resistance to chemical attack and have high terminal stability. Oxidation studies

have shown that the onset of oxidation shifts by about 100 $^{\circ}$C higher temperatures in nanotubes compared to high modulus graphite fibers. In vacuums or reducing atmospheres, nanotubes structures will be stable at any practical service temperature. Nanotubes have excellent conductivity like copper.

The price for the SiC whiskers produced by Carborundun Co. with σ = 20,690 MPa, γ = 3.22 g/cc was \$440/kg in 1989. Medicine, the environment, space, aviation, machine-building, and the computer industry need cheap nanotubes. Some American companies plan to produce nanotubes in 2–3 years.

Below the author provides a brief overview of the annual research information (2000) regarding the proposed experimental test fibers.

Data that can be used for computation

Let us consider the following experimental and industrial fibers, whiskers, and nanotubes:
1. Experimental nanotubes CNT (carbon nanotubes) have a tensile strength of 200 Giga-Pascals (20,000 kg/mm^2), Young's modulus is over 1 Tera Pascal, specific density γ=1800 kg/m^3 (1.8 g/cc) (year 2000).
   For safety factor n = 2.4, σ = 8300 kg/mm^2 = 8.3×10^{10} N/m^2, γ=1800 kg/m^3, (σ/γ)=46×10^6, K = 4.6. The SWNTs nanotubes have a density of 0.8 g/cc, and MWNTs have a density of 1.8 g/cc. Unfortunately, the nanotubes are very expensive at the present time (1994).
2. For whiskers C_D σ = 8000 kg/mm^2, γ = 3500 kg/m^3 (1989) [p.158][7].
3. For industrial fibers σ = 500 – 600 kg/mm^2, γ = 1800 kg/m^3, σ/γ = 2,78×10^6, K = 0.278 – 0.333,
   Figures for some other experimental whiskers and industrial fibers are give in Table 1.2.

Table 1.2

Material	Tensile strength	Density	Fibers	MPa	Density
Whiskers	kg/mm^2	g/cc			g/cc
AlB$_{12}$	2650	2.6	QC-8805	6200	1.95
B	2500	2.3	TM9	6000	1.79
B$_4$C	2800	2.5	Thorael	5650	1.81
TiB$_2$	3370	4.5	Allien 1	5800	1.56
SiC	1380–4140	3.22	Allien 2	3000	0.97

See References [7, 8, 9, 10].

Conclusions

The new materials make the suggested transport system and projects highly realistic for a free trip to outer space without expention of energy. The same idea was used in the research and calculation of other revolutionary innovations such as launches into space without rockets (not space elevator, not gun); cheap delivery of loads from one continent to another across space; cheap delivery of fuel gas over long distances without steel tubes and damage to the environment; low cost delivery of large load flows across sea streams and mountains without bridges or underwater tunnels [Gibraltar, English Channel, Bering Stream (USA–Russia), Russia–Sakhalin–Japan, etc.]; new economical transportation systems; obtaining inexpensive energy from air streams at high altitudes; etc. some of these are in reference[12–21].

The author has developed innovations, estimations, and computations for the above mentioned problems. Even though these projects seem impossible for the current technology, the author is prepared to discuss the project details with serious organizations that have similar research and development goals.

Patent Applications are 09/789,959 of 02/23/01; 09/873,985 of 6/4/01; 09/893,060 of 6/28/01; 09/946,497 of 9/6/01; 09/974,670 of 10/11/01; 09/978,507 of 10/18/01, USA.

Tether system

In a tether system two artificial bodies are connected by a cable. The system rotates around its common axis and the Earth. This section contains a brief description of the idea of a tether system. The reader can find details in the Tethers in Space Handbook[1] and special researches made in this area.

   Short description. A space tether is a long cable used to couple masses to each other or to other spacecraft, such as a spent booster rocket of a space station (Fig. 1.33). Space tethers are usually made of strong cable. The tether can provide a mechanical connection between two space objects that enables the transfer of energy and momentum from one object to the other. They can be used to provide space propulsion without consuming propellant. Conductive space tethers can interact with the Earth's magnetic field and ionospheric plasma to generate thrust or drag forces without expending rocket fuel.

   Tether propulsion uses long, strong strings (known as tethers) to change the orbits of **spacecraft**.
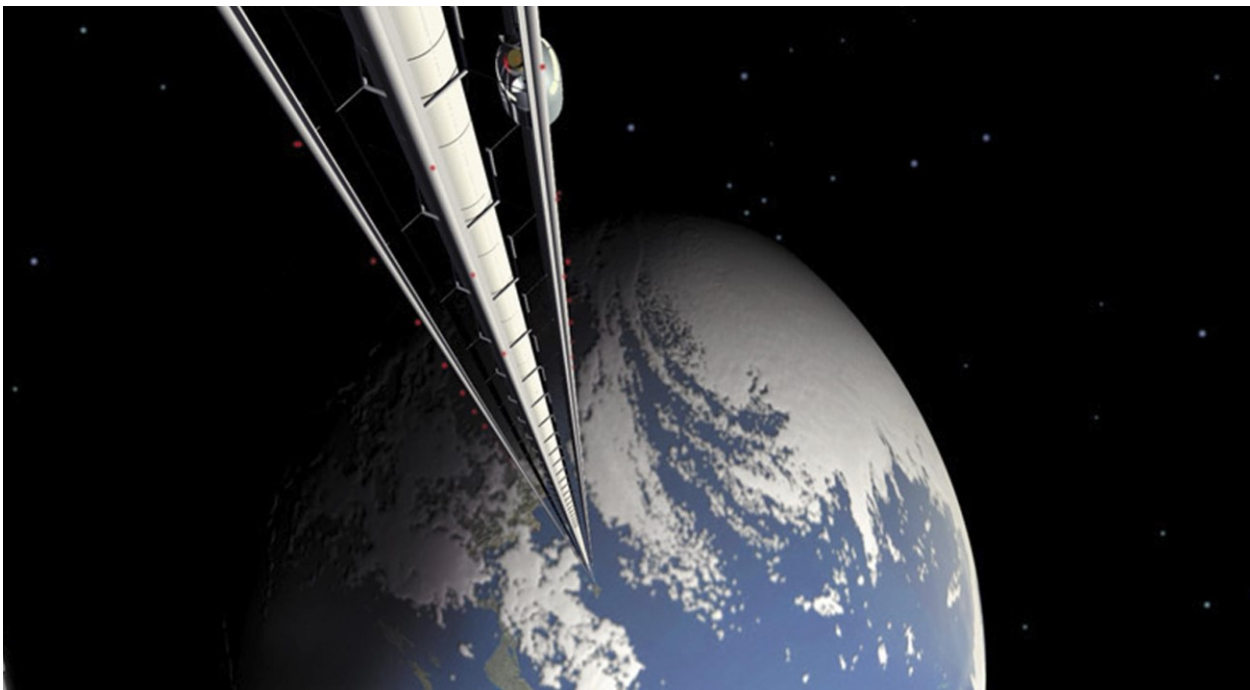
Fig. 1.33. Tether system.

Space tethers can also provide the applications as then allow momentum and energy to be transferred between objects in space. For example, the tether system enables spacecraft to be thrown from one orbit to another. Electrodynamic tethers interact with the Earth's magnetosphere to generate power or propulsion without consuming propellant.

   Most current tether designs use crystalline plastics such as Spectra. A possible future material would be carbon nanotubes, which have theoretical strengths up to 100 GPa.

   There are four potential ways to use tethers for propulsion.

   1. Tidal stabilization for altitude control. The tether has a small mass on one end, and a satellite on the other. Tidal forces stretch the tether between the two masses, stabilizing the satellite. Its long dimension is always oriented towards the planet. Some of the earliest satellites were stabilized this

way, or used mass distribution to achieve tidal stabilization. This is a simple form of stabilization that uses no electronics, rockets or fuel. A small bottle of fluid must be mounted in the spacecraft to damp vibrations.

2. Electrodynamic tethers. An electrodynamic tether conducts current in order to act against a planetary magnetic field. It's a simplified, very low-budget magnetic sail. The tether inducts the Earth's magnetic field electric force to use as power and produce substantial work. When a conductive tether is trailed in a planetary or solar magnetosphere (magnetic field), it generates a current, and thereby slows the spacecraft into a lower orbit. The tether's end can be left bare. This is sufficient to make contact with the ionosphere and allow a current to flow. A circuit in electrodynamic tethers can be used as a phantom loop, with a cathode tubes placed at the ends of the tethers. A double-ended cathode tube tether will allow alternating currents.

A similar concept was used in the **wireless transmission of energy**.

Electrodynamic tethers build up vibrations from variations in magnetic and electric fields. One plan to control these is to vary the tether current to oppose the vibrations. In simulations, this keeps the tether together. By channelling direct current through a tether, the spaceship can be moved into a higher orbit.

3. Rotovators. A rotovator is a rotating tether. A spacecraft in one orbit ajigns with the end of the tether, latching onto it and being accelerated by its rotation. This is not free; the tether's angular momentum changes. They separate later, when the spacecraft's velocity has been changed by the rotovator. Rotovators could theoretically open up inexpensive transportation throughout the solar system, as long as the net mass flow was toward the Sun. On airless planets (such as the Moon), a rotovator in a polar orbit would provide cheap surface transport as well.

A rotovator can be an electrodynamic tether in a planetary magnetic field. Its angular momentum can be charged electrically from solar or nuclear power, by running current through a wire that goes the length of the tether. When the tether turns over, the direction of current must reverse to act against the magnetic field. Ultimately, such a tether pushes agains the angular momentum of the planet.

Rotovators can also be charged by momentum exchange. Momentum charging uses the rotavator to move mass from a place that's higher in the gravity well to a place that is lower in the gravity well. The energy from the falling weight speeds up the rotation of the rotavator. For example, it is possible to use a system of two or three rotovators to implement trade between the Moon and Earth. The rotovators are charged by lunar mass (dirt, if imports are not available) dumped on Earth, and use the momentum so gained to boost Earth goods back to the Moon.

A rotavator can pick up a moving vehicle and sling it into orbit. For example, a rotavator could pick up a Mach-12 aircraft from the upper atmosphere of the Earth, and move it into orbit without using rockets. It could likewise catch such aircraft, and lower them into atmospheric flight. An important practical modification of a rotovator would be to add several latch points, to achieve different momentum transfers. This is a very valuable option, given that such performance otherwise requires extremely exotic spacecraft propulsion systems.

4. Space elevators (beanstalks) may be considered as a special case when the tether system is a rotovator powered by the spin of a planet. For example, on Earth, a beanstalk would go from the equator to geosynchronous orbit.

5. Problems. Simple tethers are quickly cut by micrometeoroids. The lifetime of a one-strand tether in space is on the order of 5 hours for a length of 10 km. Several systems have been proposed to correct this. The U.S. Naval Research Lab has successfully flown a longterm tether that used very fluffy yarn. This is reported to remain uncut several years after deployment. Another proposal is to use tape or

cloth.

Rotovators are currently limited by the strengths of available materials. The ultra-high strength plastic fibers (Kevlar and Spectra) permit rotovators to pluck masses from the surface of the Moon and Mars. Rotovators made from these materials cannot lift masses from the surface of the Earth.   Tethers have many modes of vibration, and these can build to cause stresses so high that the tether breaks. Mechanical tether-handling equipment is often surprisingly heavy, with complex controls to damp vibrations. Electrodynamic tethers can be stabilized by reducing their current when it would feed the oscillations, and increasing it when it opposes oscillations.

Unexpected electrostatic discharges have cut tethers, damaged electronics, and welded tether–handling machinery.

References for Chapter 1:

1. Edited by Cosmo M.L. and Lorenzini E.C.. *Tethers in Space Handbook*. 3rd Edition. Smithsonian Astrophysical   Observatory. December, 1997.
2. Ziegler S.W.and Cartmell M.P., "Using Motorized Tethers for Payload Orbital Transfer", *Journal of Spacecraft and Rockets,* Vol.38, No 6, 2001.
3. Edwards, Bradley C., "Design and Deployment of Space Elevator". *Acta Astronautica*, Vol. 47, No. 10, pp. 735–744, 2000.
4. Smitherman D.V. Jr., "Space Elevators", NASA/CP-2000-210429.
5. Palmer M.R., "A revolution in Access to Space Through Spinoffs of SDI Technology", *IEEE Transactions on Magnetics*, Vol. 27, No. 1, January 1991, pp.11–20.
6. Palmer M.R., "Economics and Technology Issues for Gun Launch to Space", *Space Technology*, 1996, part 3,   pp. 697–702.
7. Galasso F.S., *Advanced Fibers and Composite*, Gordon and Branch Science Publisher, 1989.
8. *Carbon and High Performance Fibers, Directory,* 1995.
9. *Concise Encyclopedia of Polymer Science and Engineering*, Ed. J.I. Kroschwitz, 1990.
10. Dresselhous M.S., *Carbon Nanotubes*, Springer, 2000.
11. Anderson, J.D., *Hypersonic and High Temperature Gas Dynamics*, McCrow-Hill Book Co., 1989.
12. Bolonkin, A.A., Hypersonic Gas-Rocket Launch System., AIAA-2002-3927, 38th AIAA/ASME/SAE/ASEE Joint Propulsion Conference and Exhibit, 7-10 July 2002. Indianapolis, IN, USA.
13. Bolonkin, A.A. Inexpensive Cable Space Launcher of High Capability, IAC-02-V.P.07, 53rd International Astronautical Congress, The World Space Congress – 2002, 10–19 Oct 2002. Houston, Texas, USA.
14. Bolonkin, A.A, "Non-Rocket Missile Rope Launcher", IAC-02-IAA.S.P.14, 53rd International Astronautical Congress, The World Space Congress – 2002, 10–19 Oct 2002. Houston, Texas.
15. Bolonkin, A.A., "Hypersonic Launch System of Capability up 500 tons per day and Delivery Cost $1 per lb". IAC-02-S.P.15, 53rd International Astronautical Congress, The World Space Congress – 2002, 10–19 Oct 2002. Houston, Texas.
16. Bolonkin, A.A., "Employment Asteroids for Movement of Space Ship and Probes". IAC-02-S.6.04, 53rd International Astronautical Congress, The World Space Congress – 2002, 10–19 Oct 2002. Houston, Texas.
17. Bolonkin, A.A., "Non-Rocket Space Rope Launcher for People", IAC-02-V.P.06, 53rd International Astronautical Congress, The World Space Congress – 2002, 10–19 Oct 2002, Houston, Texas.

18. Bolonkin, A.A., "Optimal Inflatable Space Towers of High Height". COSPAR 02-A-02228, 34th Scientific Assembly of the Committee on Space Research (COSPAR), The World Space Congress – 2002, 10–19 Oct 2002. Houston, Texas.

19. Bolonkin, A.A., "Non-Rocket Earth-Moon Transport System", COSPAR-02 B0.3-F3.3-0032-02, 02-A-02226, 34th Scientific Assembly of the Committee on Space Research (COSPAR). The World Space Congress – 2002, 10–19 Oct 2002. Houston, Texas.

20, Bolonkin, A.A., "Non-Rocket Earth-Mars Transport System", COSPAR 02-A-02224, 34th Scientific Assembly of the Committee on Space Research (COSPAR). The World Space Congress – 2002, 10–19 Oct 2002. Houston, Texas.

21. Bolonkin, A.A., "Transport System for delivery Tourists at Altitude 140 km". IAC-02-IAA.1.3.03, 53rd International Astronautical Congress. The World Space Congress – 2002, 10–19 Oct 2002. Houston, Texas.

22. Bolonkin, A.A., Non-Rocket Transport System for Space Travel, *JBIS*, Vol. 56, No. 7/8, 2003, pp. 231–249.

Chapter 2
Cable Space Accelerator*

Summary

A method and facilities for delivering payload and people into outer space are presented. This method uses, in general, engines and a cable located on a planetary surface. The installation consists of a space apparatus, power drive stations located along the trajectory of the apparatus, the cable connected to the apparatus and to the power stations, and a system for suspending the cable. The drive stations accelerate the apparatus up to hypersonic speed.

   The estimations and computations show the possibility of making these projects a reality in a short period of time (two project examples are given: a launcher for tourists and a launcher for payloads). The launch will be very cheap at a projected cost of $1–$5 per pound. The cable is made from cheap artificial fiber widely produced by modern industry.

----

1. Introduction

   At present, rockets are used to carry people and payloads into space, or to deliver bombs over long distances. This method is very expensive, and requires a well-developed industry, high technology, expensive fuel, and complex devices[1].

   Other than rockets, methods to reach the space velocities are the space elevator[2], the hypersonic tube air rocket[3] and the electromagnetic system[4]. Several new non-rockets methods were also proposed by author at the World Space Congress-2002, Houston, USA, 10–19 October 2002.

   The space elevator requires very strong nanotubes, as well as rockets and high technology for the initial development. The tube air rocket and non-rocket systems require more detailed research. The electromagnetic transport system, suggested by Minovich, is not realistic at the present time. It requires a vacuum underground tunnel 1530 kilometers long located at a depth of 40 kilometers. The project requires a power cooling system (because the temperature is very high at this depth), a complex power electromagnetic system, and a huge impulse of energy which is greater than the energy of all the electric generating stations on Earth.

   This chapter suggests a very simple and inexpensive method and installation for launching into space.

   This is a new revolutionary space launcher system for delivering hypersonic speeds. This method uses the straight cable launcher, intermediate power (drive) stations, any conventional engines (mechanical, electrical, gas turbines), and flywheels (as storage energy) located on the ground. After completing an exhaustive literature and patent search, the author cannot find the same space method or similar facilities mentioned elsewhere.

   The distinguishing features of the given research in comparison with that previously described[5] is the installation design (single cable and short distance between drive stations) that allows the use of the cheap artificial fiber widely produced by current industry.

2. Description of Suggested Launcher

Brief Description. The installation includes (see notations in Fig. 2.1): a cable; power drive stations; winged space apparatus (space ship, missile, probe, projectile and so on); conventional engines and flywheels; and a launching area (airdrome). Between drive stations the cable is supported by columns. The columns can also hold additional cables for future launches and a delivery system for used cable.
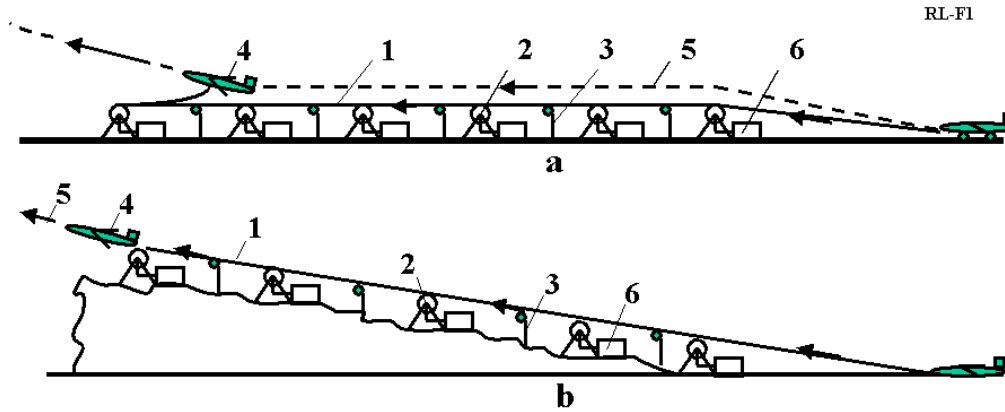

Fig. 2.1. a. Launcher for a crewed space ship with single cable. Notation: 1 – cable contains 3 parts: main part, outlet part, and directive part; 2 – power drive station; 3 – cable support columns; 4 – winged space apparatus (space ship, missile, probe, projectile and so on); 5 – trajectory of space apparatus; 6 – engine. b. A fixed slope small launcher for projectiles.

   The installation works in the following way. All drive station start to run. The first power station pulls the cable, 1, connected to the winged space apparatus. The apparatus takes off from the start area and flies with acceleration along trajectory 5. When the apparatus reaches the first drive station, this drive station disconnects from the cable and the next drive station continues the apparatus acceleration, and so on. At the end of the distance, the winged apparatus has reached hypersonic speed, disconnects from the cable, changes the horizontal acceleration into vertical acceleration (while it is flying in the atmosphere) and leaves the Earth's atmosphere.
. The power stations contains the engines. The engine can be any type, for example, gas turbines, or electrical or mechanical motors. The power drive station has also an energy storage system (flywheel accumulator of energy), a type transmission and a clutch. The installation can also have a slope and launch a projectile at an angle to horizon (Fig. 2.1b).
   The cable includes three parts (Fig. 2.2): directive part, inlet part, and main (pull) part. The lengths of the inlet and main parts equal the distance between drive stations, the directive part controls only itself. It directs the inlet part to the drive stations. Its length equals the full acceleration distance minus the inlet and pull parts. This design allows the use the current fibers and minimizes the cable mass and energy.
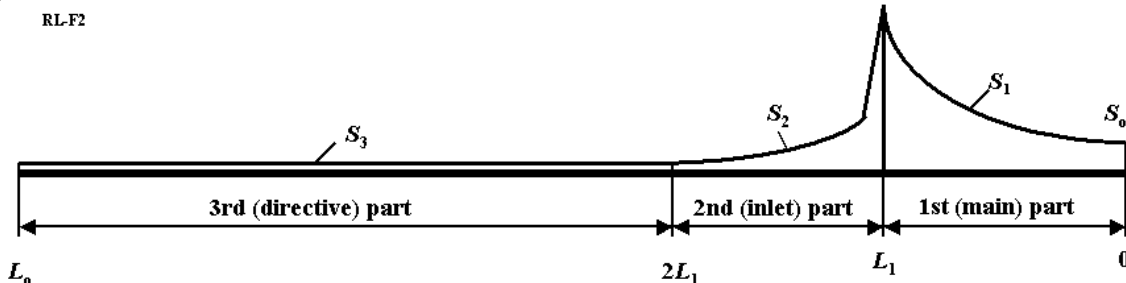

Fig. 2.2. Optimal cable cross-sectional area along the launch distance.

The cables are made from light strong material such as artificial fibers, filaments, whiskers, and nanotubes. The better the cable properties the less the installation requires in terms of the drive stations, cable mass and energy.

The rollers are made from strong matter such as a composite material.

Advantages. The suggested launch cable system has big advances in comparison with current rocket systems:

1. The cable launcher is cheaper by several times than the modern rocket launch system. No expensive rockets are needed.
2. The cable launcher decreases the delivery cost by some thousand times (up to $1–$2 per pound).
3. The cable launcher can be made in one year. Modern rocket launch systems requires some years for development, design, and building.
4. The cable launcher does not require high technology and can be made by any non-industrial country.
5. Rocket fuel is expensive. The cable launcher can use the cheapest sources of energy such as wind, water, or nuclear power, or the cheapest fuels such as gas, coal, peat, etc., because the engine is located on the Earth's surface. The flywheels may be used as an accumulator of energy.
6. It is not necessary to have highly qualified personnel such as rocket specialists with high salaries.
7. The fare for the space tourists is small.
8. There is no pollution of the atmosphere from toxic rocket gas.
9. Thousands of tons of useful loads can be launched annually.
1. **Cable discussing.** The reader can find the cable discussing in Chapter 1 and cable characteristics in References[5–9]. In our projects we use only cheap artificial fibers widely produced by present industry.

3. Theory of the Cable Launcher
Formulas for Estimation and Computation (in metric system)

Below are a well-known formula from physics and formulas developed by the author. These formulas can be used for calculation of the different variants.

1. **Relative cross-section area**, $\overline{S}$, and weight of an optimal cable of an equal (constant) stress can be found as a solution of the differential equation of local balance of inertia force, F, and cable stress force.

a) For the main part of the cable the relative cross-section area is

$$dF_1 = ngdm_1 = ng\gamma S_1 dL = \sigma dS_1 , \quad \frac{dS_1}{S_1} = \frac{ng\gamma}{\sigma} dL , \quad \ln S_1 \Big|_{S_0}^{S_1} = \frac{ng\gamma}{\sigma} \Big|_0^L , \quad W = \int_0^L \gamma S_1 dL ,$$

$$or \quad \overline{S}_1 = \frac{S_1}{S_0} = \exp\frac{ng\gamma L}{\sigma} , \quad S_0 = \frac{ngm}{\sigma} , \quad W = m\left[\exp\left(\frac{ng\gamma L}{\sigma}\right) - 1\right], \quad K = 10^{-7}\frac{\sigma}{\gamma} ,$$

(2.1)

where S_1 is the cross-section cable area of main part [m²]; S_o is the cross-section area of cable near the ship [m²]; n is the overload; $g = 9.81$ m/s² is gravity; σ is the tensile stress [N/m²]; γ is the specific density [kg/m³]; L is the distance between power stations [m]; m is the mass of apparatus [kg]; m_1 is the mass of the main cable part [kg]; W is the cable weight [kg]; K is the stress coefficient. The result of the computation is shown in Figs. 2.3 to 2.7.

K = 0.1 0.2 0.3 0.4 0.5, overload n=3 "g"

Fig. 2.3. Relative cable cross-sectional area versus the distance between drive stations for stress coefficient $K = 0.1$–0.5 ($K = 10^{-7}\sigma/\gamma$) and overload 3g.

K = 0.1 0.2 0.3 0.4 0.5, overload n=3 "g", ship mass M = 15000 kg

Fig. 2.4. Cable mass versus distance between drive stations for $K = 0.1$–0.5, overload 3g, space ship mass 15 tons.

K = 1 1.5 2 2.5 3, overload n = 3g

Alex40-F5

K = 1

K = 1.5

K = 2

K = 2.5

K = 3

Relative cross-section cable area

Distance between drive stations, km
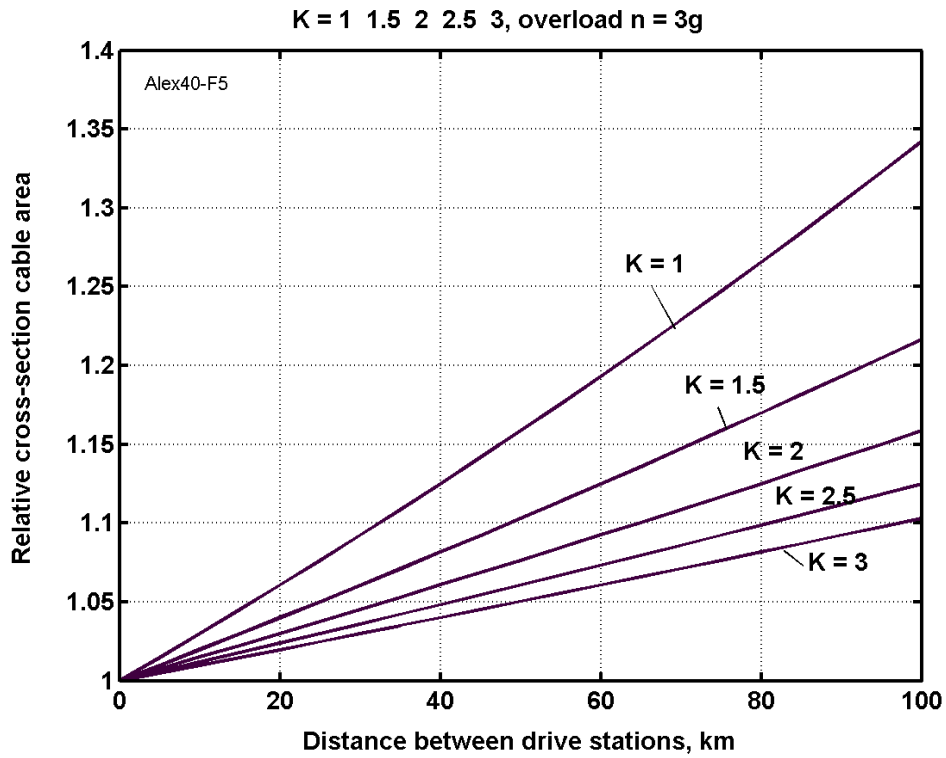
Fig. 2.5. Relative cable cross-sectional area versus distance between drive station for K = 1–5, overload 3g. A high stress coefficient allows a decrease in the drive station distance (compare with Fig. 2.3).

K = 0.1 0.2 0.3 0.4 0.5, overload n = 267g, projectile mass M = 100 kg.

Alex40a-F6

K = 0.1

K = 0.2

K = 0.3

K = 0.4

K = 0.5

Relative cross-section cable area

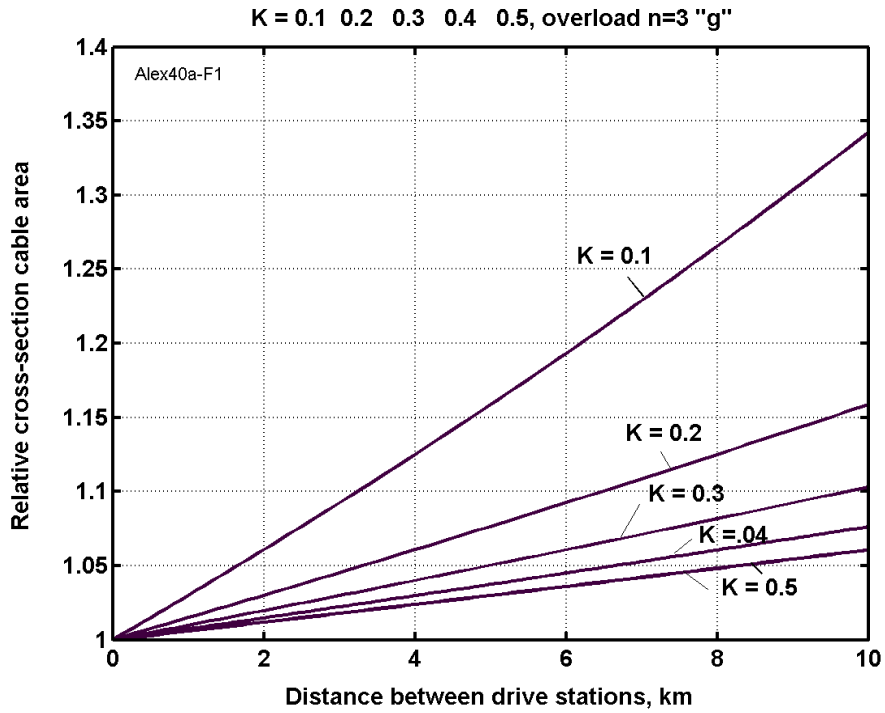Distance between drive stations, km

Fig. 2.6. Relative cable cross-sectional area versus the distance between drive stations for stress coefficient K = 0.1–0.5 (K = $10^{-7}\sigma/\gamma$) and overload 267g, projectile mass 100 kg.
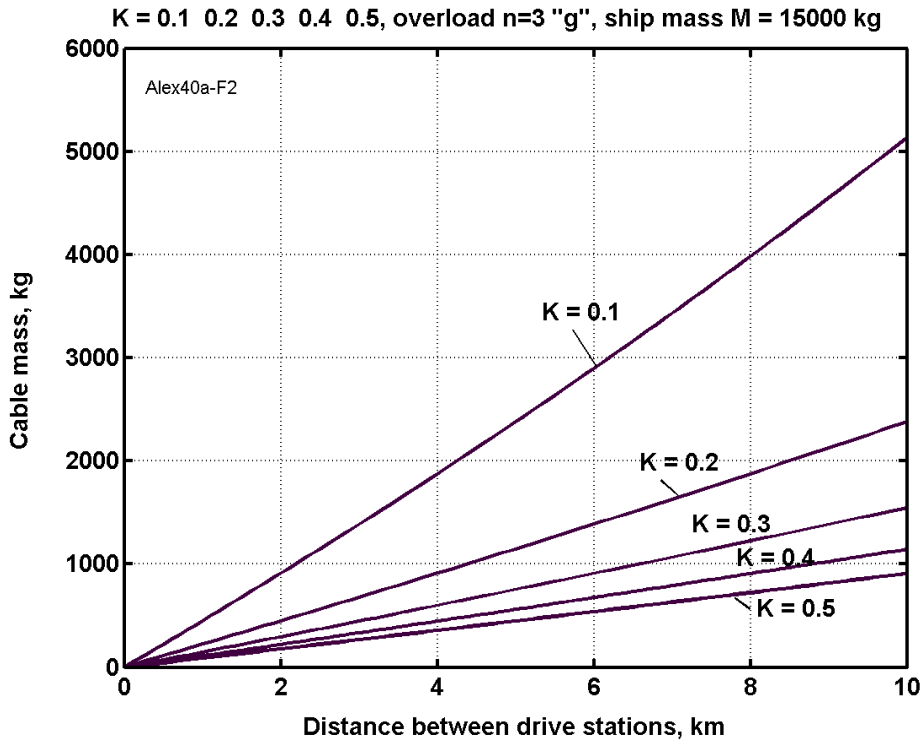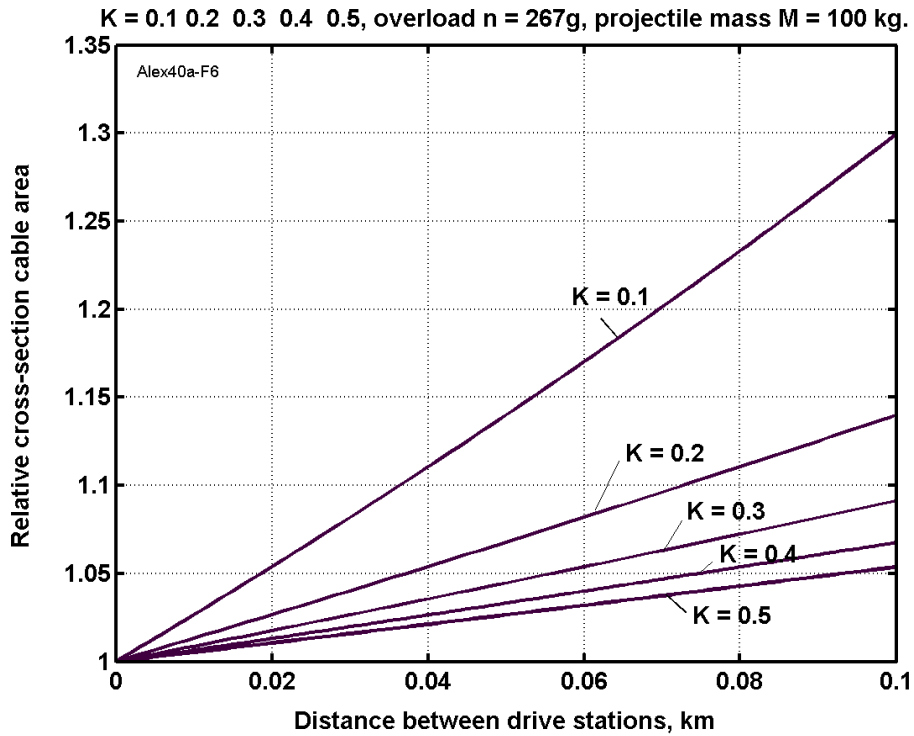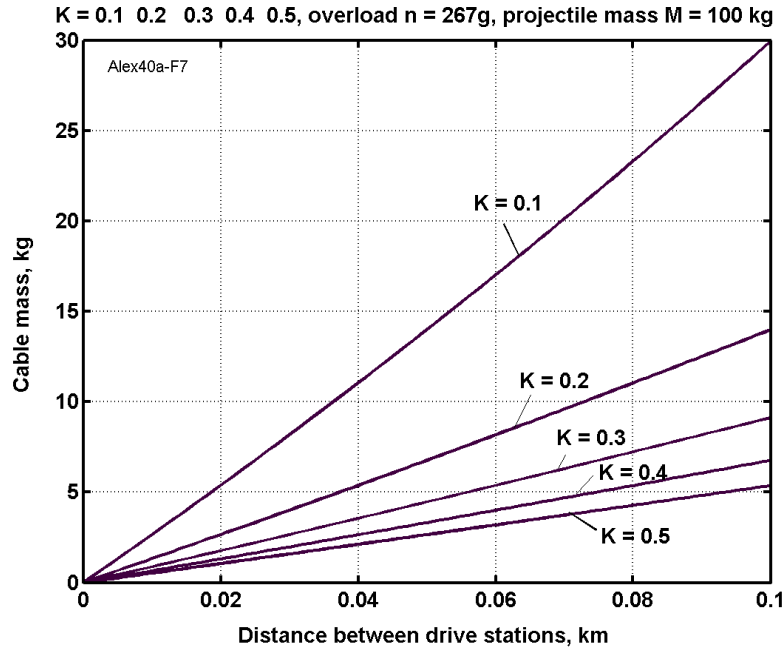
Fig. 2. 7. Cable mass versus distance between drive stations for $K = 0.1$–0.3, overload 267g, and apparatus mass 100 kg.

b) For the inlet part of the cable the noted values are

$$dF_2 = ngdm_2 = ng\gamma S_0 \exp\left[\frac{ng\gamma}{\sigma}(L_1 - L)\right]dL, \quad F_2 = ngm\exp\left[\frac{ng\gamma}{\sigma}L_1\right]\left(1 - \exp\left[-\frac{ng\gamma}{\sigma}L\right]\right),$$

$$S_0 = \frac{ngm}{\sigma}, \quad S_2 = \frac{F_2}{\sigma}, \quad W = \int_0^{L_1} \gamma S_2 dL, \quad or$$

$$\overline{S}_2 = \frac{S_2}{S_0} = \exp\frac{ng\gamma L_1}{\sigma}\left[1 - \exp\left(-\frac{ng\gamma}{\sigma}\right)\right], \quad W = \gamma S_0 \exp\frac{ng\gamma L_1}{\sigma}\left[L_1 + \frac{\sigma}{ng\gamma}\left(\exp\left(-\frac{ng\gamma L_1}{\sigma}\right) - 1\right)\right]$$

(2.1a)

where L_1 is the distance between drive stations [m]. F_2 is the force in the inlet cable part [N], and m_2 is the mass of the inlet cable part. The inlet part introduces the main part to an inlet of the drive station.

c) The directive part directs the inlet part to an inlet of the drive station and supports only itself. This part can be thin and has a constant cross-section.

The optimal cable cross section area is shown in fig.2.2.

2. **Safety cable speed**. Let us take a small part of the rotary circle and write the balance

$$\frac{2SR\alpha\gamma V^2}{R} = 2S\sigma\sin\alpha,$$

where V is the rotary cable speed [m/s], R is the circle radius [m], and α is the angle between the ends of the circle part [rad]. If $\alpha \to 0$ the relationship between maximum rotational speed V and tensile stress of the closed loop (curve) cable is

$$V = \sqrt{\frac{\sigma}{\gamma}}.$$

(2.2)

3. **Energy**, E, storage by the rotary flywheel per 1 kg cable [joules/kg] can be found from the known equation of the kinetic energy and equation (2.2)

$$E = \frac{V^2}{2} = \frac{1}{2}\frac{\sigma}{\gamma} . \tag{2.3}$$

4. **The maximum distance** L [km] between supports of the suspension system (without wings) for $h \ll R$ where $R = 6{,}378$ km, the radius of the Earth, can be found from geometry. That is

$$L \cong 2\sqrt{(R+h)^2 - R^2} \approx 2\sqrt{2Rh} = 226\sqrt{h} , \tag{2.4}$$

where h [km] is the altitude of support.

5. **The amound of sag ΔH of the cable** (from its weight and the curvature of the Earth) can be found from the balance between weight and stress. The cable has a parabolic form under its weight: $y = ax^2 - b$, $a > 0$, $y' = 2ax$, $a = \mathrm{tg}\alpha/2x = \mathrm{tg}\alpha/L$. If $x = 0$, then $b = H_2$. If $y = 0$, then $x = \pm L/2$. We also have the balance equation $W = 2T\sin\alpha$ or $\sin\alpha = W/2T$. We substitute these equations and put $\mathrm{tg}\alpha \cong \sin\alpha \cong \alpha$. The cable sag, H_2, under its weight is the as

$$H_2 = \frac{\tan\alpha}{L}\left(\frac{L}{2}\right)^2 = \frac{\alpha L}{4} = \frac{WL}{8T} = \frac{SL\gamma L}{8T} = \frac{S\gamma L^2}{8T}$$

The sag from the Earth's curvature is $H_1 = L^2/8R$ from equation (2.4), and the total sag is

$$\Delta H = H_1 + H_2 \approx \frac{L^2}{8}\left(\frac{S\gamma}{T} + \frac{1}{R}\right) = \frac{L^2}{8}\left(\frac{\gamma}{g\sigma} + \frac{1}{R}\right) , \tag{2.5}$$

where ΔH is the sag of the cable [m]; L is the distance between supports [m]; T is the tension of the cable [kg], S is the cross-section cable area [m^2], R is the Earth's radius [m], W is the cable weight [kg].

6. The estimation of maximum horizon **flight range**, r, of the winged projectile in the atmosphere is found from the kinetic energy

$$Dr = \frac{m}{2}\left(V_2^2 - V_1^2\right), \quad D = gm/k_3 , \quad or \quad r = \frac{k_3}{2g}\left(V_2^2 - V_1^2\right) , \tag{2.6}$$

where: k_3 is the projectile ratio of lift/drag ($k_3 = 3$–6); V_2 is the initial speed of the projectile [m/s]; and V_1 is the final speed of projectile [m/s].

7. The equation for the estimation of **wave drag** D of an edge ship cable for supersonic velocity can be given from aerodynamic equations

$$dD = C_D\frac{\rho(H)V^2}{2}dA, \quad D = C_D\frac{\rho V^2}{2}A, \quad C_D = \frac{4c^2}{\sqrt{M^2-1}}, \quad V = aM, \quad A = wH/\sin\theta,$$

$$c = \frac{h_1}{w}\sin\theta, \quad \rho = \rho_0 e^{bH}, \quad for\ M > 3 \quad \frac{M}{\sqrt{M^2-1}} \approx 1. \tag{2.7}$$

where D is the air drag [N], M is the Mach number, $a = \mathrm{const}$ – the speed of sound [m/s], C_D is the drag coefficient, A is the specific area [m^2], V is the cable speed [m/s], $c = h_1/w$ is the ratio a thickness, h_1, to width, w, of an edge type cable, ρ [kg/m^3] is the air density at altitude H [m], $\theta = \mathrm{const}$ – the angle of the cable to the horizon, $b \cong -1.3115.10^{-4}$ – the coefficient of change of air density with altitude, $\rho_0 = 1.225$ – the air density at $H = 0$.

Let us substitute equations (2.7) in the first equation for D given above and integrate this for the interval of altitude from H_0 to H:

$$D = 2c^2 Vwa\sin\theta \int_{H_0}^{H}\rho(H)dH = \frac{2\rho_0 aVc^2 w\sin\theta}{b}(e^{bH} - e^{bH_0}) = \frac{2\rho_0 aVc^{1.5}S^{0.5}\sin\theta}{b}(e^{bH} - e^{bH_0}),$$

$$\tag{2.8}$$

where $S = wh_1$ [m^2] is the cable cross-section area.

8. **Loss** ΔV [m/s] **of speed**, when a projectile passes through the atmosphere with a trajectory angle θ = const, can be found from the energy equation

$$E = \int_{H_0}^{H} \frac{D}{\sin\theta} dH, \quad D = C_D \frac{\rho V^2}{2} F, \quad E = \frac{2c_1^2 a V A F}{\sin\theta} \int_{H_0}^{H} \rho_0 e^{bH} dH = \frac{2c_1^2 a V A F \rho_0}{b\sin\theta}(e^{bH} - e^{bH_0}).$$

For other cases the amount of energy lost, E, is

$$E = \frac{m}{2}(V^2 - V_1^2), \quad V_1 = \sqrt{V^2 - \frac{2E}{m}}, \quad V_1 = V - \Delta V,$$

or

$$\Delta V = V - \sqrt{V^2 - \frac{2E}{m}}, \quad E = \frac{2c^2 a V F \rho_0}{b\sin\theta}(e^{bH} - e^{bH_0}), \quad (2.9)$$

where V is the initial speed of the projectile [m/s]; m is the mass of the projectile [kg]; $a = 300$ m/s – the speed of sound; F is the specific area of the projectile [m²]; c_1 is the semi-angle of the projectile edge in radians; θ is the angle of the trajectory to the horizon; H is the altitude at which the projectile disconnects from the cable [m]; $\rho_0 = 1.225$ kg/m³ – air density at altitude $H = 0$. The result of this computation (for $c_1 = 0.1$, $F = 0.01$ m², $a = 300$ m/s, $H_0 = 3$ km, $H = 50$ km) is presented in Fig. 2.8. This loss is small.

   Many people know about the "Shuttle" heating up in the atmosphere and think that a hypersonic space projectile will have a large amount of heat when it crosses the atmosphere. This is wrong. The purposes of the "Shuttle" and a hypersonic space projectile are opposed. A space ship, when it re-enters into the atmosphere, has a huge kinetic energy and must decrease its hypersonic speed (energy) to subsonic speed. The Shuttle has a special spherical body nose and pointless wing edge to increase the air drag by tens to hundreds of times. This means a lot of heating takes place. The Shuttle also has a long horizontal trajectory along the Earth's surface. The purpose of a projectile is to save speed and energy. The projectile has a sharp body bow, and wing edge. The required head protection of launch rockets is tens of time less then re-entry apparatus.

9. Estimation of **cable friction** due to the air. This estimation is very difficult because there are no experimental data for air friction of an infinitely very thin cable (especially at hypersonic speeds). A computational method for plates at hypersonic speed as described by Anderson[10], p. 287 was used. The computation is made for two cases: a laminar and a turbulent boundary layer.

   The results of this comparison are very different. Turbulent flow has maximum friction. About 80% of the friction drag occurs in the troposphere (from 0 to 12 km). If cable end is located on a mountain at 4 km altitude the maximum air friction will be decreased by 30%.

   It is postulated that half of the cable surface will have a laminar boundary layer because a small wind or trajectory angle will blow away the turbulent layer and restore the laminar flow. The blowing away of the turbulent boundary layer is studied in aviation and is used to restore laminar flow and decrease air friction. The laminar flow decreases the friction in hypersonic flow about by 280 times! If half of the cable surface has a laminar layer, it means that we must decrease the air drag calculated for full turbulent layer a minimum of two times.

   Below, the equations from Anderson for computation of the local air friction for a two-sided plate are given.

$(T^*/T) = 1 + 0.032M^2 + 0.58(T_w/T - 1); \quad \mu^* = 1.458 \times 10^{-6} T^{*1.5}/(T^* + 110.4);$

$\rho^* = \rho T/T^*; \quad R_e^* = \rho^* V x/\mu^*; \quad C_{f,l} = 0.664/(R_e^*)^{0.5}; \quad C_{f,t} = 0.0592/(R_e^*)^{0.2}; \quad (2.10)$

$\rho^* D_L = 0.5 C_{f,l} \rho^* V^2 S; \quad D_T = 0.5 C_{f,t} \rho^* V^2 S, \quad S = \pi d.$

Where T^*, Re^*, ρ^*, μ^* are reference (evaluated) temperature, Reynolds number, air density, and air viscosity respectively. M is Mach number, V is speed, x is length of plate (distance from the beginning of the cable), T is flow temperature, T_w is body temperature, $C_{f.l}$ is a local skin friction coefficient for laminar flow, $C_{f.t}$ is a local skin friction coefficient for turbulent flow. S is area of skin [m^2] of both plate sides (this means for the cable we must take $0.5S$); and D is air drag (friction) [N]. It may be shown that the general air drag for the cable equals $D_g = 0.5D_T + 0.5D_L$, where D_T is turbulent drag and D_L is laminar drag.

From equation (2.10) we can derive the following equations for turbulent and laminar flows of a horizontal cable

$$D_T = 0.0465 \rho^{*0.8} \mu^{*0.2} \, V^{1.8} L^{0.8} d , \qquad (2.11)$$
$$D_L = 0.521 \rho^{*0.5} \mu^{*0.5} \, V^{1.5} L^{0.5} d . \qquad (2.12)$$

Where d is the diameter of the cable [m]. The laminar drag is less than the turbulent drag by 200–300 times and can be neglected.

Let us note: if L_o is the full acceleration distance (initial length of cable) [m], L_1 is the distance between drive stations [m], and L is the variable length of cable [m], we can write the following equations for turbulent drag of the different cable parts:

1) Main cable part
   a) If $0 < L < (L_0 - L_1)$, then $D_1 = B \cdot L_1^{0.8} d_1$,
      where $B = 0.5 \times 0.0465 \rho^{*0.8} \mu^{*0.2} V^{1.8}$, $V = (2ngL)^{0.5}$.
   b) If $(L_0 - L_1) < L < L_0$, then $D_1 = B \cdot (L_0 - L)^{0.8} d_1$.
2) Inlet cable part
   a) If $0 < L < (L_0 - 2L_1)$, then $D_2 = B \cdot L_1^{0.8} d_2$.
   b) If $(L_0 - 2L_1) < L < (L_0 - L_1)$, then $D_2 = B \cdot (L_0 - L)^{0.8} d_2$.
   c) If $0 < L < (L_0 - 2L_1)$, then $D_2 = 0$.
3) Directive part
   a) If $0 < L < (L_0 - 2L_1)$, then $D_3 = B \cdot (L_0 - L)^{0.8} d_3$.
   b) If $(L_0 - 2L_1) < L < L_0$, then $D_3 = 0$.

Here d_1 , d_2, d_3 are average cable diameters of the main, inlet, and directive parts respectively [m]. Full cable drag is thus

$$D = D_1 + D_2 + D_3 . \qquad (2.13)$$

10. **Mass of cable** is

$$M = M_1 + M_2 + M_3 = \frac{\pi}{4} \gamma [d_1^2 L_1 + d_2^2 L_1 + d_3^2 (L_0 - 2L_1)] . \qquad (2.14)$$

The accelerated cable mass is

$$M_a \approx M_1 + M_2 + 0.125 M_3 , \qquad (2.15)$$

where the coefficient 0.125 is the product of an average length (0.5) and an average speed (0.5^2) of the directive cable part.

11. The **energy** required by the cable air drag is

$$E = \int_0^{L_0} D dL . \qquad (2.16)$$

The results of computations of equations (2.13) to (2.15) are presented in Fig. 2.9 to 2.14 for two projects (see below) and different initial cable diameters.
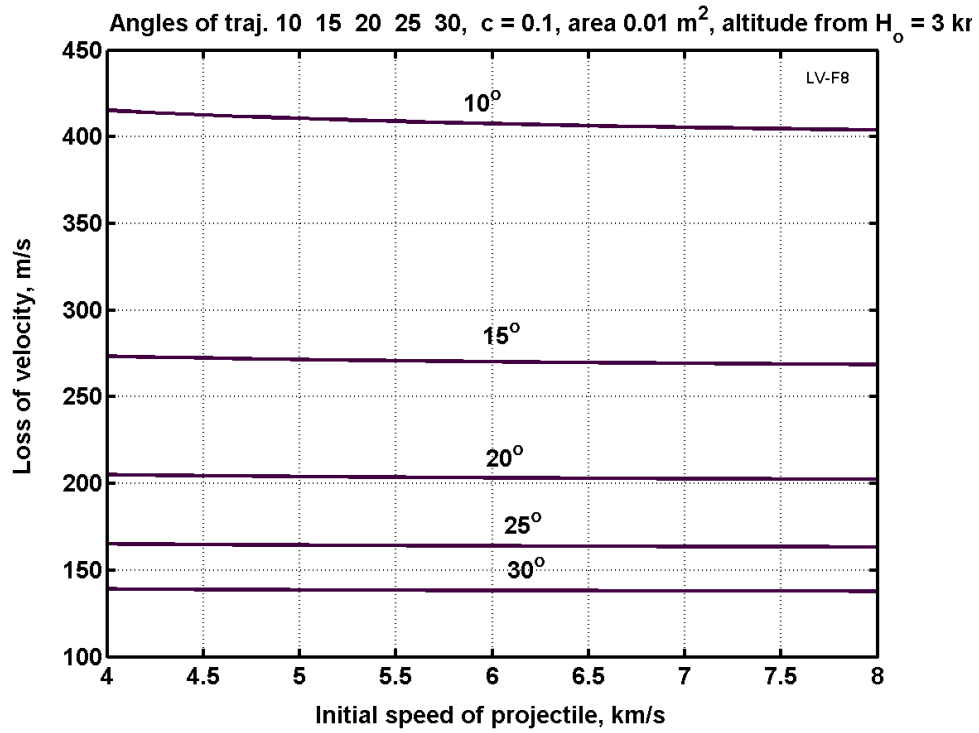
Angles of traj. 10 15 20 25 30, c = 0.1, area 0.01 m^2, altitude from H$_o$ = 3 kr

LV-F8

10°

15°

20°

25°

30°

Fig. 2.8. Estimation of velocity lost by a projectile in the atmosphere versus initial speed of projectile, for the different trajectory angles $10° \div 30°$ to the horizon, relative thickness $c = 0.1$, cross-section area 0.01 m^2, at altitude $H_0 = 3$ km

D= 10 km, d = 10 15 20 25, d$_3$ = 1 mm, overload n = 3g, altitude H$_o$ = 2 km

DVC3-F1

d = 25 mm

d = 20 mm

d = 15 mm

d = 10 mm

Fig. 2.9. Cable drag along the acceleration distance for initial cable diameter at ship $d_o = 10$–25 mm, cable diameter of part 3 $d_3 = 1$ mm, overload 3g, at altitude 2 km.

D = 10 km, overload n=3g, d$_3$ = 1 mm, average altitude H$_o$ = 2 km

DVC3-F2

Full cable mass

Accelerated cable mass

Y-axis: Accelerated cable and total mass, tons

Fig. 2.10. Cable mass versus the initial cable diameter at ship 10–25 mm, for distance between drive stations $L_1 = 10$ km, overload $n = 3$g, $d_3 = 1$ mm, average altitude $H = 2$ km

D=10, km, overload n = 3g, d$_3$ = 1 mm, altitude H$_o$ = 2 km, V$_m$ = 7.9 km/s

DVC3-F3

Y-axis: Energy, giga joules

X-axis: Cable diameter at vehicle, mm

Fig. 2.11. Cable air drag energy versus the initial cable diameter at ship 10–25 mm, for distance between drive stations $L_1 = 10$ km, overload $n = 3$g, $d_3 = 1$ mm, average altitude $H = 2$ km, V_{max} = 7.936 km/s.

D=0.1 km, d = 10 15 20 25, d_3 = 1 mm, overload n = 267g, altitude H_o = 2 km

DVC3-F12

d = 25 mm
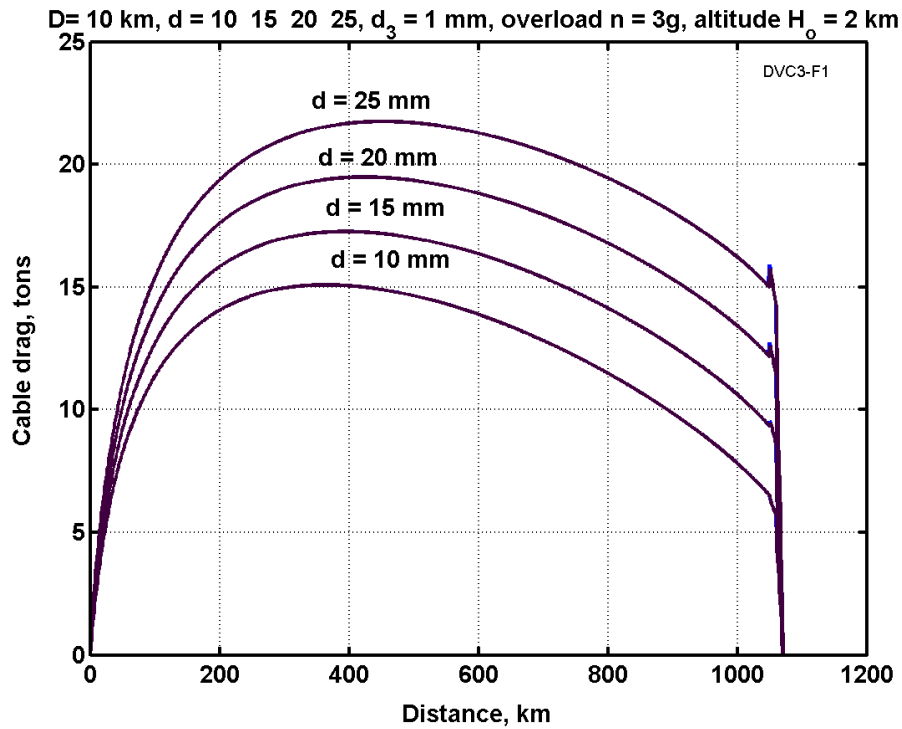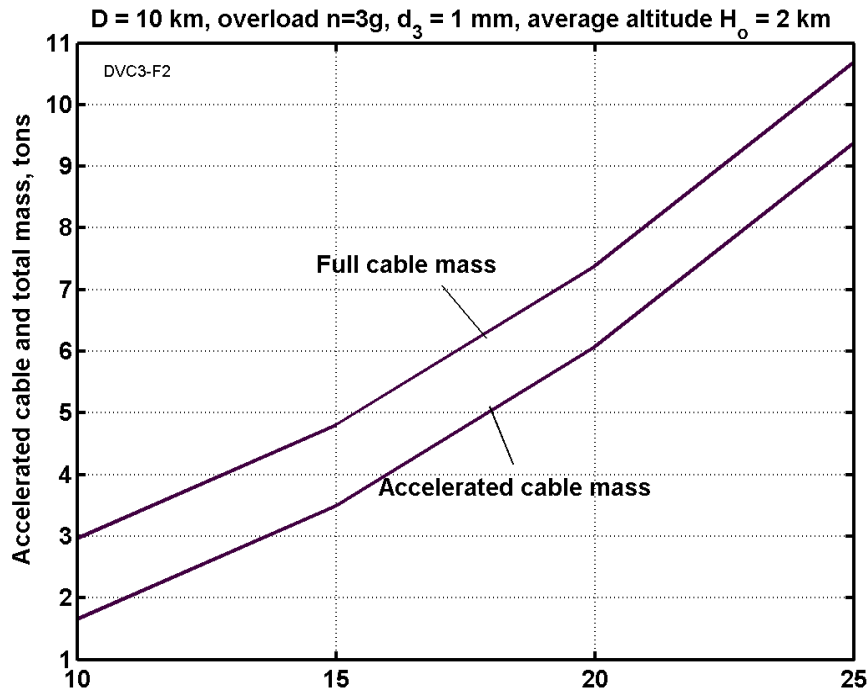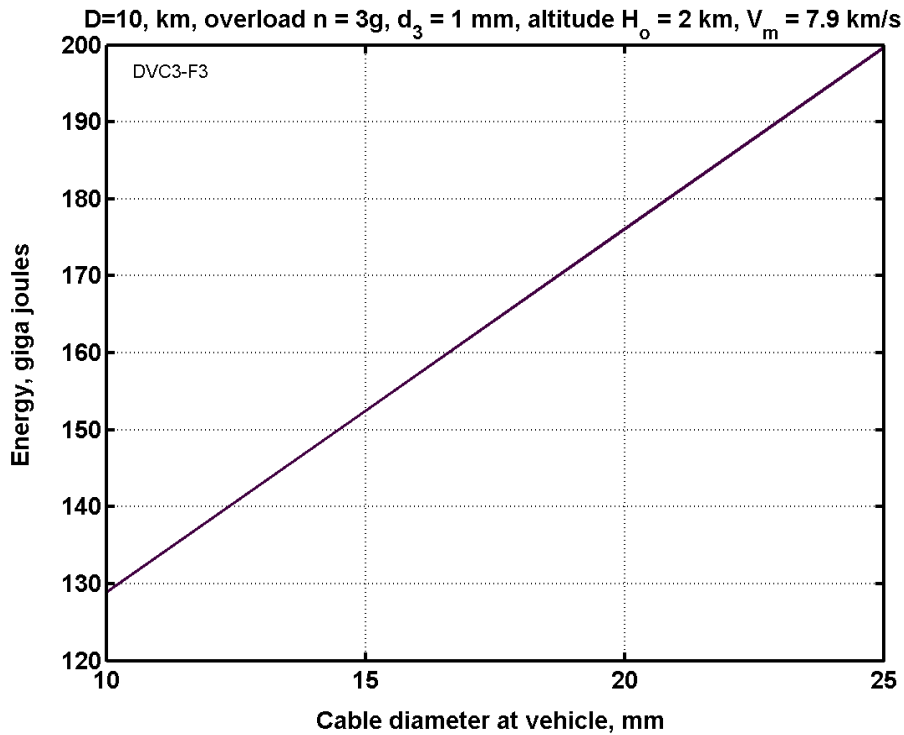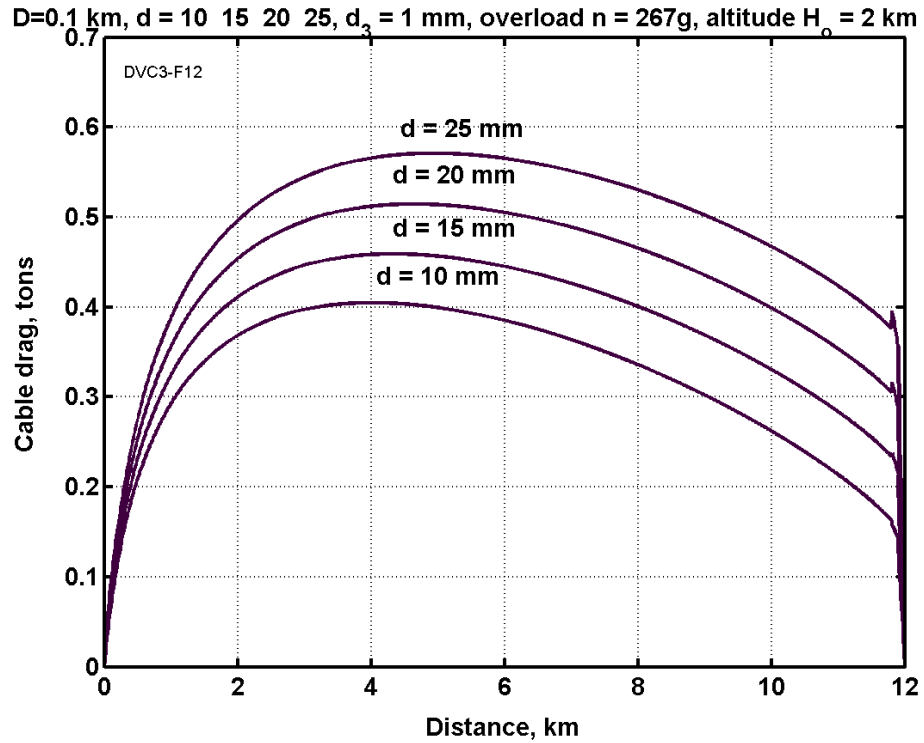
d = 20 mm

d = 15 mm

d = 10 mm

Cable drag, tons

Distance, km

Fig. 2.12. Cable drag along the acceleration distance for initial cable diameter at ship d_o = 10–25 mm, cable diameter of part 3 d_3 = 1 mm, overload n = 267g, at altitude 2 km.

D = 0.1 km, overload n = 267g, d_3 = 1 mm, average altitude H_o = 2 km

DVC3-F13

Full cable mass

Accelerated cable mass

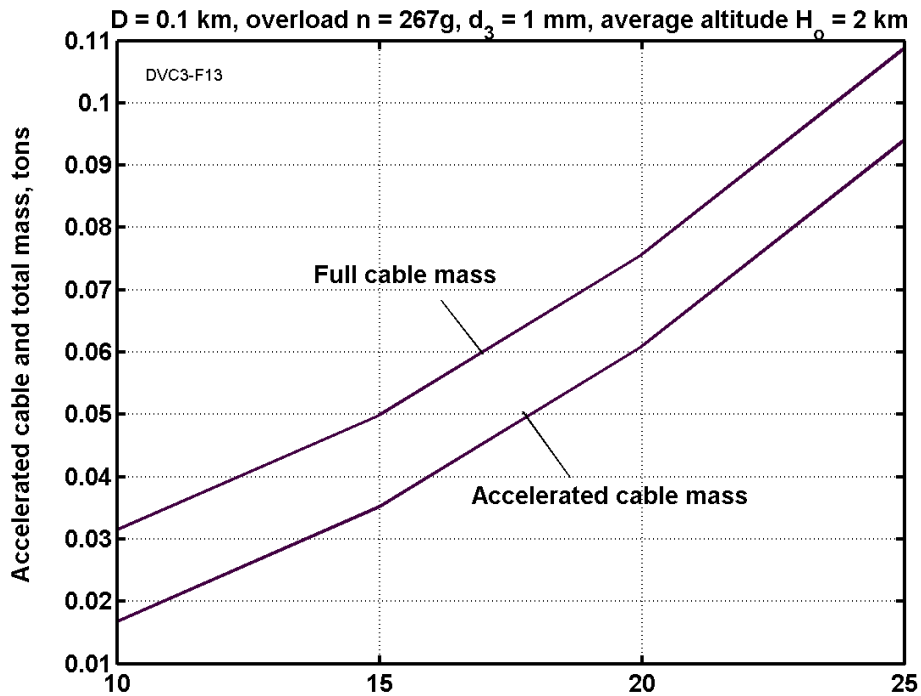Accelerated cable and total mass, tons

Fig. 2.13. Cable mass versus the initial cable diameter at ship 10–25 mm, for distance between drive stations L_1 = 0.1 km, overload n = 267g, d_3 = 1 mm, altitude H = 2 km.

Fig. 2.14. Cable air drag energy versus the initial cable diameter at ship 10–25 mm, for distance between drive stations $L_1 = 0.1$ km, overload $n = 267$g, $d_3 = 1$ mm, altitude $H = 2$ km, $V_{max} = 8$ km/sec.
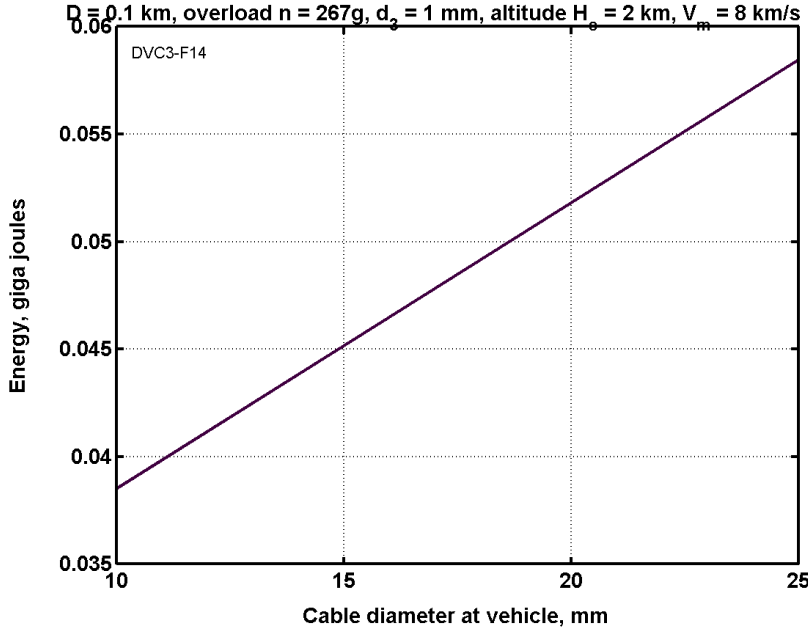
12. For subsonic speed the formulas (2.11) to (2.12) are the same, but conventional ρ and μ must be inserted.

13. The last drive station can be located on a mountain top. The final ship trajectory will have an angle to the horizon. After disconnection from the launcher the winged ship can increase this angle while flying in the atmosphere. This additional angle, lost velocity, and time can be estimated in the following way. First write the standard ship equations of air movement.

$$\dot{H} = V \sin \theta, \quad \dot{V} = -\frac{D}{m} - g \sin \theta, \quad \dot{\theta} = \frac{L}{mV} - \frac{g}{V} \cos \theta + \frac{V \cos \theta}{R}.$$

where H is the altitude, V is the speed, θ is the trajectory angle [rad], D is the drag, L is the lift force, m is the ship's mass, R is the Earth's radius.

If parameter changes in θ angle and time t, are small, and the speed is close to 8 km/s, we have

$$\sin \theta \approx \theta, \quad \cos \theta \approx 1, \quad \theta_a = 0.5(\theta + \theta_0), \quad D = ngm / k, \quad L = ngm, \quad \frac{g}{V} - \frac{V}{R} \approx 0,$$

$$t = \frac{\Delta H}{V \sin \theta_a}, \quad \Delta V = -\left(\frac{ngm}{mk} + g \sin \theta_a\right) t, \quad \theta - \theta_0 = \frac{ngm}{kmV} t, \quad k = \frac{L}{D},$$

or equations for estimation

$$\theta \approx \left(\theta_0^2 + \frac{2ng\Delta H}{V^2}\right)^{0.5}, \quad \Delta V \approx -\frac{g\Delta H}{V}\left(1 + \frac{n}{k\theta_a}\right), \quad t \approx \frac{\Delta H}{V \sin \theta_a}. \tag{2.17}$$

where n is the overload, ΔH is the altitude change [m], ΔV is the speed change (speed lost)[m/s], $k = L/D$ – average ratio of lift/drag of the ship ($k = 3$–7), θ_0 is the initial trajectory angle [radians], t is time [seconds].

The results of the computation are presented in Fig. 2.15 to 2.16.

n = 3 4 5 6g, initial angle 0°, thickness of atmosphere 40 km
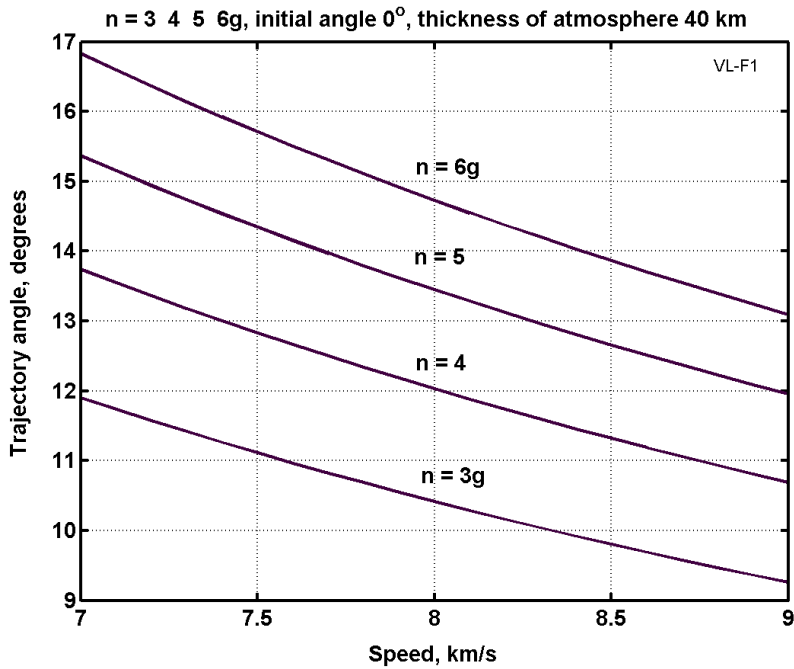
Figs. 2.15. Final trajectory angle versus speed for overload $n = 3 - 6$ g, initial trajectory angle 0°, thickness atmosphere 40 km.

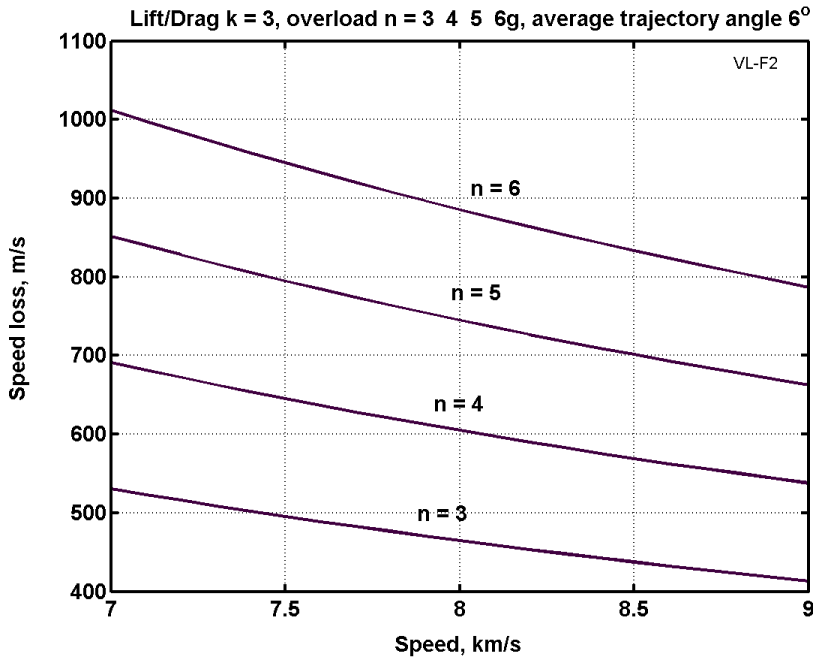**Lift/Drag k = 3, overload n = 3 4 5 6g, average trajectory angle 6°**

Fig. 2.16. Speed loss (method 2) versus speed for the ratio lift/drag $k = 3$, overload $n = 3 - 6$ g, and average trajectory angle $\theta_a = 6° = 0.1$ radian.

4. *Projects*

Below are estimations for two projects: (1) tourists with low acceleration (3g); and (2) payloads (projectiles) with high acceleration (270g).

Project 1
The Launch of Tourists into Space (Fig. 2.1a, Single Cable Version)

Assume the mass of the space vehicle is m = 15 tons (100 tourists and 4 members of crew); overload is n = 3 "g", the acceleration is $a = 3g \cong 30$ m/s ($g = 9.81 \cong 10$ m/s^2)(this acceleration is safe for conventional purposes); the final speed is 8 km/s.

The required distance of acceleration is $L = V^2/2a \cong 1070$ km. The time of horizontal acceleration is $t = V/a \cong 4$ min 27 sec. (If trained cosmonauts are launched the safe acceleration can be taken as $8g$ and the required launch distance will be 400 km and the time 1 min 40 sec.). The time of vertical acceleration ($3g$) in the atmosphere (after disconnection) is about 50 seconds. The final angle is about $\theta = 12°$.

Assume we use the artificial cheap fiber widely produced by current industry. Safe tensile strength of the vehicle cable is σ = 180 kg/mm^2 (safety factor is n_1 = 600/180 = 3.33), density γ = 1800 kg/m^3 (K = 180/1800 = 0.1). Then the cross-section area of the vehicle cable about the vehicle will be $S_0 = nmg/\sigma$ = 250 mm^2, diameter $d_o = 2(S/\pi)^{0.5}$ = 17.8 mm, average diameter is about $d_{o,a}$ = 19 mm.

Let us assume that the drive stations are located every L_1 = 10 km. We need 107 drive stations. The final drive station is located at altitude H_0 = 4 km. Mass of the cable is M = 7 tons, accelerated cable mass is M_a = 5.6 tons (Fig. 2.10). A variable cross-section areas of main and inlet cables are included in the average diameter.

The energy required for accelerating the ship and cable is $E = (m+M_a)V^2/2 = 659×10^9$ J (659 Gigajoules) if V = 8 km/s. The energy of air drag of the cable is 172 Gigajoules (see Fig. 2.11). The average drag of the ship is about $D = m/k = 15/3 = 5$ tons (here k is the ratio of the lift force to the drag of the ship). This is $E = DL = 5×10^4×1070,000 = 53.5$ Gigajoules. The total energy required for one launch is E_T = 884.5 GigaJoules. If the launches are made every hour the engines must have a total power of about $P = E_T/t = 884×10^9/60/60 = 246,000$ kW distributed between 107 drive station (that is 2300 kW each). If the engine efficiency is η = 0.3 the fuel consumption will be $F = 884×10^9/\varepsilon/0.3 = 70$ tons per each flight. Here $\varepsilon = 42×10^6$ [J/kg] is the energy capability of Diesel fuel. This means that 700 liters of fuel is used for each tourist. If the safe tensile strength is 180 kg/mm^2, then the total mass of the flywheels (as energy of storage) will be about $M_w = 2E/k = 2×884×10^9/10^6 = 1768$ tons or 1768/107 = 16.5 tons for each drive station.

Economic efficiency

Assume a cost of 500 millions dollars for the installation[11], a life time of 10 years, and an annual maintenance cost of 5 million dollars. If 100 tourists are launched on every flight, and there is one flight every hour for 350 days a year, then 840,000 passengers will be launched per year. The launch cost for one passenger is 55,000,000/840,000 = $65.5 plus fuel cost. If 700 liters of fuel are used for 1 passenger and the fuel price is $0.25 per liter, then the fuel cost is $175 dollars per passenger. The total production cost will then be $241 per person. If the ticket is sold for $349, then the profit will be about 90 million dollars per year.

Any reader who does not agree with this estimation can recalculate for other data. In any case, the cost of delivery will be hundreds of times less than delivery by rockets. Critics must remember that the main content of this chapter is not economical estimations, but the new idea for the launch of space apparatus.

Project 2
The Launcher for Payload (Projectile) with High Acceleration (267g)(Fig. 2.1b)

We can use the equations from Project 1 for the estimation of Project 2. Assume the mass of the space apparatus is 100 kg (222 lb); the escape velocity is 8 km/s, the distance of acceleration is 12 km, the height of a mountain is 3 km (a slope is about 15º) and the acceleration stations are located every 0.1 km. The acceleration will be

$$a = V^2/2L = 8000^2/2 \cdot 12000 = 2666 \text{ m/s} = 267g.$$

Assume a fiber tensile strength of σ =180 kg/mm² for all cable parts. The cross-section area of the cable is 148 mm², and the average diameter 15 mm. The total mass of the cables is 50 kg. The required energy for one launch is about 5 Gigajoules. If the engine efficiency is $\eta = 0.3$ then the required amount of fuel is 397 kg for one launch. If the frequency of launching is 0.5 hours then the required total power is 2800 kW or 2800/120 ≅ 23.3 kW for every drive station. The total mass of flywheels is about 10 tons or 84.3 kg in every station. The loss of velocity is 275 m/s when the projectile crosses the atmosphere at an angle 15º (Fig. 2.8).

Economic efficiency

Assume the cost of installation is 20 million dollars, the life time is 10 years, and the maintenance cost is $1 million per year, with a frequency of launching of 30 minutes.

We can launch 4.8 tons per day or 4.8 × 350 = 1680 tons per year. The production cost will be 3,000,000/1,680,000 = $1.78 /kg plus fuel cost.

We take the fuel consumption as 4 kg per 1 kg payload and the price as $0.25 per kg. The fuel cost is $1 . The total cost is 1.78 + 1 = $2.78 per kg.

General discussion

Science laboratories have whiskers and nanotubes that have high tensile strength. The theory shows that these values are only one tenth of the theoretical level. We must study how to produce a thin cable, such as the strings or threads we produce from cotton or wool, from whiskers and nanotubes.

The fiber industry produces fibers which are used for the author's projects at the present time. However the whiskers and especially nanotubes strongly improve the possibility of this method. They decrease the requires number of drive stations, the cable mass and drag (energy). These projects are unusual (strange) for specialists and people now, but they have huge advantages, and they have a big future.

References for Chapter 2.

1. Space Technology and Application. International Forum (STAIF) , Aalbuquerque, MN, USA, 1996-1997.

2. D.V. Smitherman, Jr., "Space Elevators", NASA/CP-2000-210429, 2000.

3. A.A. Bolonkin, Earth Accelerator for Space Ships and Missiles, *JBIS*, Vol. 56, No. 11/12, 2003, pp. 394–404.

4. M. Minovich, "Electromagnetic Transportation system for manned Space travel", US Patent #4,795,113, January 3 1989.

5. A.A. Bolonkin, "Space Cable Launchers", Paper No. 8057 presented at the Symposium "The Next 100 years", Dayton, OH, USA, 14-17 July, 2003.

6. F.S. Galasso, *Advanced Fibers and Composites*, Gordon and Branch Scientific Publisher, 1989.

7. *Carbon and High Performance Fibers, Directory*, 1995.

8. *Concise Encyclopedia of Polymer Science and Engineering*, Ed. J.I. Kroschwitz, 1990.

9. M.S. Dresselhous, *Carbon Nanotubes*, Springer, 2000.

10. J.D. Anderson, *Hypersonic and High Temperature Gas Dynamics*. McCraw-Hill Book Co.,1989.

11. D.E. Koell, *Handbook of Cost Engineering*, TCS, Germany, 2000.

Chapter 3
Circle Launcher and Space Keeper*

Summary

In this chapter proposes a new method and installation for flight in space. This method uses the centrifugal force of a rotating circular cable that provides a means to launch a load into outer space and to keep the stations fixed in space at altitudes at up to 200 km. The proposed installation may be used as a propulsion system for space ships and/or probes. This system uses the material of any space body for acceleration and changes to the space vehicle trajectory. The suggested system may also be used as a high capacity energy accumulator.

   The article contains the theory of estimation and computation of suggested installations and four projects. Calculations include: a maximum speed given the tensile strength and specific density of a material, the maximum lift force of an installation, the specific lift force in planet's gravitation field, the admissible (safe) local load, the angle and local deformation of material in different cases, the accessible maximum altitudes of space cabins, the speed than a space ship can obtain from the installation, power of the installation, passenger elevator, etc. The projects utilize fibers, whiskers, and nanotubes produced by industry or in scientific laboratories.

Nomenclature

a – acceleration, m/s,

$C_{f,l}$ – local skin friction coefficient of a two-sided plate for laminar flow,

$C_{f,t}$ – local skin friction coefficient of a two-sided plate for turbulent flow,

$C_{c,l} = 0.5 C_{f,l}$ – local skin friction coefficient of cable for laminar flow,

$C_{c,t} = 0.5 C_{f,t}$ – local skin friction coefficient of cable for turbulent flow,

D – air drag (friction) [N].

D_T – turbulent drag [N],

D_L – laminar drag [N],

d – cable diameter [m],

E – Young's modulus,

E_s – energy stored by rotary circle per 1 kg of the cable [J/kg],

F – air friction [N],

g – specific gravity of the planet, m/s^2 (for the Earth $g = 9.81$ m/s^2 at an altitude $H = 0$),

G – local load [kg],

H – altitude [m] or [km].

H_{max} – maximam altitude of a circle top [m] or [km]

ΔH – decrement of an altitude [m] or [km],

$k = \delta/\gamma$ – ratio of tensile stress to cable density,

$K = k/10^7$ – strength coefficient,

L – length of a cable [m],

M – Mach number,

m – throwing mass [kg],

m_{ss} – mass of a space ship [kg],

n – safety factor,

N – power [J/s].

p – internal pressure on the cable circle [N/m^2],

P – maximum vertical lift force of the vertical cable circle in the constant gravity field of a planet [N],

P_1 – specific lift force of 1 kg of cable mass in a planet's gravity field [N],

P_L – specific lift force of 1 m of cable in a planet's gravity field [N],

P_a – full lift force of a closed-loop cable circle rotated around a planet [N],

$P_{a,1}$ – specific lift force of a 1 kg closed-loop cable circle rotated around a planet [N],

$P_{a,L}$ – specific lift force of a 1 m closed-loop cable circle rotated around a planet, when $g = 0$ [N],

P_{max} – maximum lift force of the rotary closed-loop cable circle when gravity $g = 0$ [N],

r – radius of cable cross-section area or half of cable width [m],

R – cable (circular) radius [m],

R_{max} – maximum cable radius [m],

R_o – radius of planet [m],

R_v – radius of observation [m],

$Re*$ – reference Reynolds number,

S – cross-section area of cable [m^2],

S_c – cable surface [m^2],

S_s – area of skin [m^2] of both plate sides, which means for cable we must take $S_c = 0.5 S_s$,

T – air temperature [^{o}C],

$T*$ – reference (evaluated) air temperature [^{o}C],

T_w – temperature of wall (cable) [^{o}C],

T_e – temperature of flow [^{o}C],

T_{max} – maximum cable thrust [kg],

t – time [seconds],

V – rotary cable speed [m/s],

V_a – maximum speed of a closed-loop circle around a planet [m/s],

V_{min} – minimum speed of a closed-loop circle [m/s],

V_c – mass speed [m/s],

V_f – speed of falling from an altitude H [m/s],

W – weight (mass) of cable [kg] or [ton],

w – thickness of a boundary layer [m], for cable $w \approx 5r$,

x – length of plate (distance from the beginning of the cable) [m],

Δh – cable deformation about a local load [m],

Δh_o – cable deformation about a local load for the cable circle around a planet [m],

ΔR – increase in cable radius from internal pressure [m],

ΔV – additional speed which a space ship obtains from a cable propulsion system [m/s].

α – angle of cable section [rad],

α_h – cable angle to the horizon about a local load [rad],

γ – cable density [kg/m^3],

μ – air viscosity; for standard conditions $\mu = 1.72 \cdot 10^{-5}$,

$\mu*$ – reference air viscosity [kg/m·s],

ρ – air density; for standard condition $\rho = 1.225$ kg/m^3

$\rho*$ – reference air density [kg/m^3],

σ – cable tensile stress [N/m^2],

ω – planet angle speed [rad/seconds].

Introduction

   The author proposes a revolutionary new method and launch device for: (1) delivering payloads and people into space, (2) accelerating space ships and probes for space flight, (3) changing the trajectory of space probes, (4) landing and launching of space ships on space bodies with small gravity, and (5) accelerating other space apparatus. The system may be used as a space propulsion system by utilizing the material of space bodies for propelling space apparatus, as well as for storing energy. This method utilizes the centrifugal force of a closed-loop cable circle (hoop, semi-circle, double circle). The cable circle rotates at high speed and has the properties of an elastic body.

   The current proposal is a unique transport system for delivering loads and energy from Earth to the space station and back. The major difficulties of the space elevator[1,2] are in delivering the energy to the transport gondola of a space elevator and the fact that electric wire weighs a lot more than a load bearing cable. The currently proposed space transportation system solves this problem by locating a motor on the Earth and using conventional energy to provide the power to move the gondola to the space station. Moreover the present transportation system can transfer large amounts of mechanical energy from the Earth to the space station on the order of 3 to 10 million watts.

Description of Circle Launcher

The installation includes (Fig. 3.1): a closed-loop cable made from light, strong material (such as artificial fibers, whiskers, filaments, nanotubes, composite material) and a main engine, which rotates the cable at a fast speed in a vertical plane. The centrifugal force makes the closed-loop cable a circle. The cable circle is supported by two pairs (or more) of guide cables, which connect at one end to the cable circle by a sliding connection and at the other end to the planet's surface. The installation has a transport (delivery) system comprising the closed-loop load cables (chains), two end rollers at the top and bottom that can have medium rollers, a load engine and a load. The top end of the transport system is connected to the cable circle by a sliding connection; the lower end is connected to a load motor. The load is connected to the load cable by a sliding control connection.
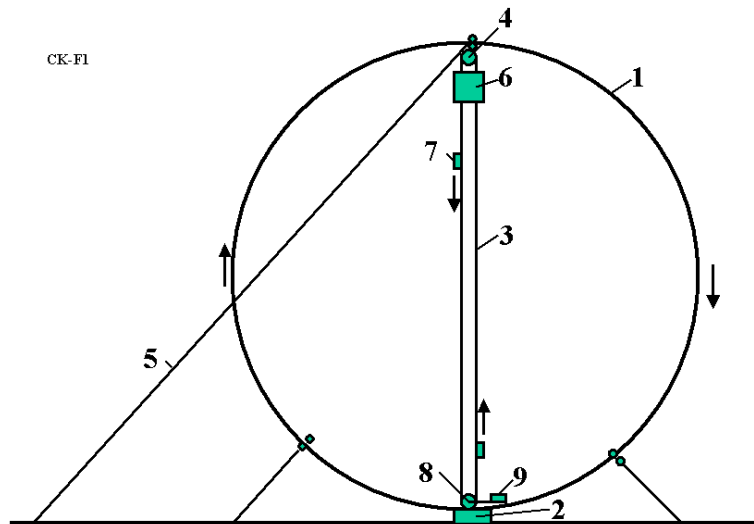

Fig. 3.1. Circle launcher (space station keeper) and space transport system. Notations are: 1 – cable circle, 2 – main engine, 3 – transport system, 4 – top roller, 5 – additional cable, 6 – the load (space station), 7 – mobile cabin, 8 – lower roller, 9 – engine of the transport system.

The installation can have an additional cables to increase the stability of the main circle, and the transport system can have an additional cable in case the load cable is damaged.

The installation works in the following way. The main engine rotates the cable circle in the vertical plane at a sufficiently high speed so the centrifugal force becomes large enough to it lifts the cable and transport system. After this, the transport system lifts the space station into space.

The first modification of the installation is shown in Fig. 3.2. There are two main rollers 20, 21. These rollers change the direction of the cable by 90 degrees so that the cable travels along the diameter of the circle, thus creating the form of a semi-circle. It can also have two engines. The other parts are same.
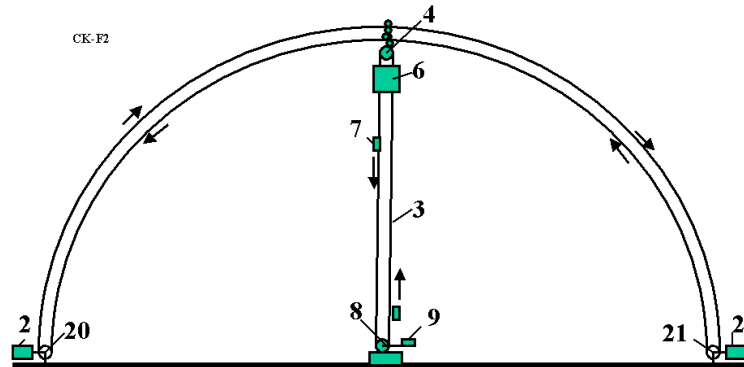

Fig. 3.2. Semi-circle launcher (space station keeper) and transport system. Notation is the same with Fig. 3.1 with the edditional 20 and 21 – rollers. The semi-circle is the same (see right side of Fig. 3.4).

The installation can be used for the launch of a payload to outer space (Fig. 3.3). The load is connected to the cable circle by a sliding bearing through a brake. The load is accelerated by the cable circle, lifted to a high altitude, and disconnected at the top of the circle (semi-circle).

The installation may also be used as transport system for delivery of people and payloads from one place to another through space (Fig. 3.4).
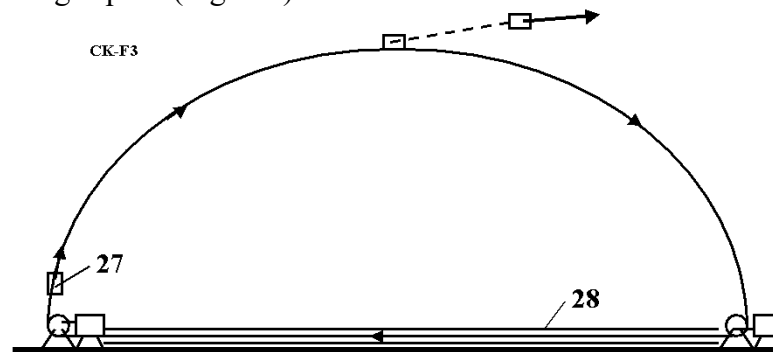

Fig. 3.3. Launching the space ship (probe) into space using cable semi-circle. 27 – load, 28 – vacuum tube (option).
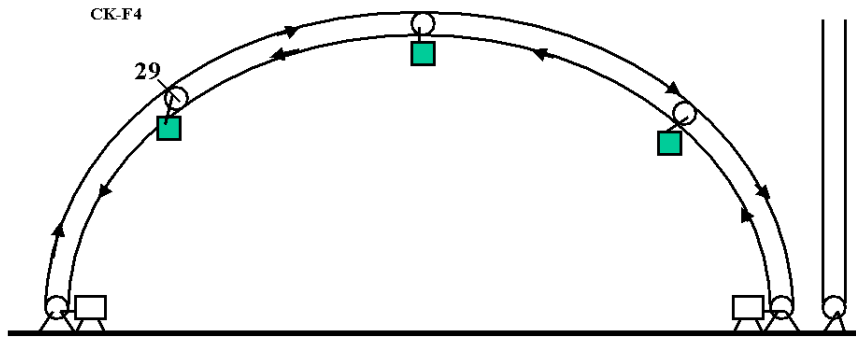
CK-F4

Fig. 3.4. Double semi-circle with opposed speeds for delivery of load to another semi-circle end. 29 -Roller.

The double cable can be used as an excellent launch system, which generates a maximum speed three times the speed of the cable. The launch system has a space probe (Fig. 3.5) connected to the semi-circular cable and to a launch cable. The launch cable is connected through a roller (block) to the main cable. A tackle block is used in which the maximum speed is three times more then the cable speed.

The maximum cable speed depends on the tensile strengths of the cable material. Speeds of 4–6 km/s can be achieved using modern fibers, whiskers, and nanotubes (see attached projects).

For stability, the installation can have guide cables connected to the top of the cable circle by a sliding connection and to the ground (Fig. 3.6).
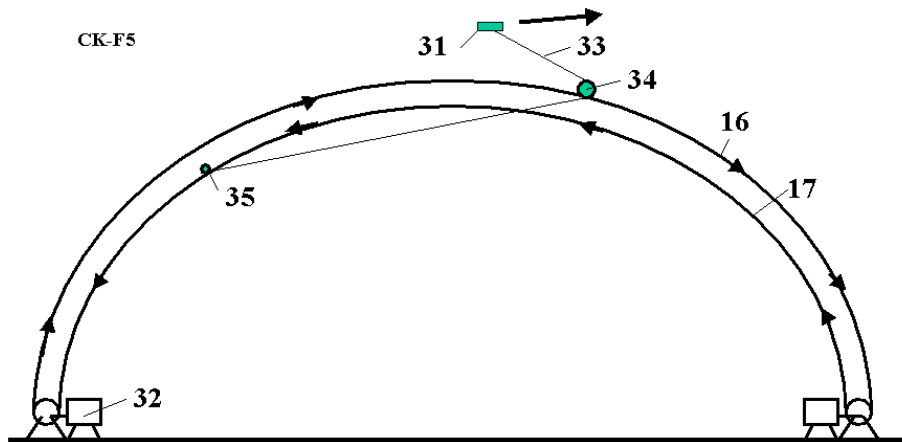
CK-F5

Fig. 3.5. Launching a load into space with a triple circle rope speed using the double semi-circle. Notations are: 31 – space probe, 32 – engine, 33 – launch cable, 34 – roller, 35 – connection point of the launch cable, 16, 17 – semicircle.
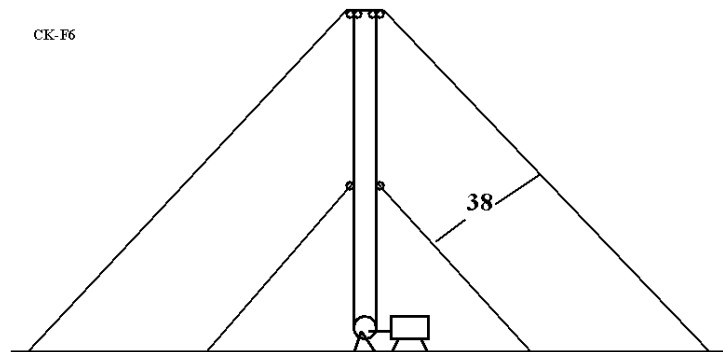
CK-F6

Fig. 3.6. Supporting the semi-circle in vertical position (for stability). 38 – guide cable.

The ship installation may be used as a system for vertical landing on or taking-off (launch) from a planet or asteroid because the cable circle can work like a spring.

The cable circle of the space ship can be used as a propulsion system (Fig. 3.7). The propulsion system works in the following way. Material from asteroids or meteorites, or garbage from the ship, is packed in small packets. A packet is connected to the cable circle. then circle engine turns on and rotates at high speed. At the desired point the pack is disconnected from the circle and, as the ejected mass flies off with a velocity, the space ship gets an impulse in the required direction.

The suggested cable circle or double cable circle can be made around a planet or space body (Fig. 3.8). This system can be used for suspended objects such as space stations, tourist cabins, scientific laboratories, observatories, or relay station for TV and radio stations.
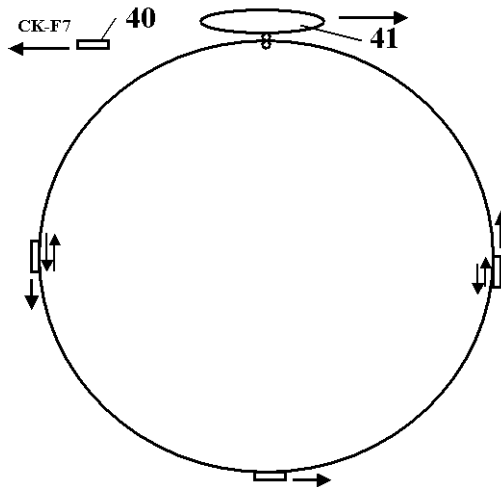
Fig. 3.7. Using the rope circle as a propulsion system. Notations are: 40 – garbage, 41 – space ship.
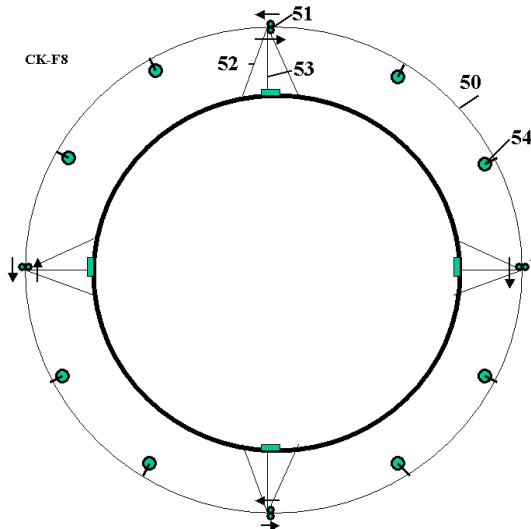
Fig. 3.8. Cable circle around the Earth for 8–10 space objects. Notations are: 50 – double circle, 51 – drive stations, 52 – guide cable, 53 – energy transport system, 54 – space station.

This system works in the following way. The installation has two cable circles, which move in the opposite directions at the same speed. The space stations are connected to the cable circle through the sliding connection. They can move along the circle in any direction when they are connected to one of

the cable circles through a friction clutch, transmission, gearbox, brake, and engine, and can use the transport system in Figs. 3.1 and 3.2 for climbing to or descending from the station. Because energy can be lost through friction in the connections, the energy transport system and drive rollers transfer energy to the cable circle from the planet surface. The cable circles are supported at a given position by the guide cables (see Project 2). No towers for supporting the circle cable are needed.

The system can have only one cable (Figs. 3.1, 3.3).

The installation can have a system for changing the radius of the cable circle (Fig. 3.9). When an operator moves the tackle block, the length of the cable circle is changed and the radius of the circle is also changed.
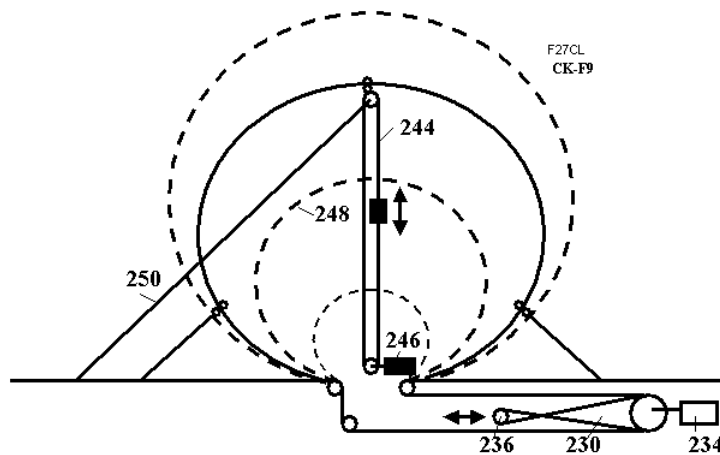

Fig. 3.9. System for changing the radius of the circle circle. Notations are: 230 – system for radius control, 234 – engine, 236 – mobile tackle block, 244 – transport system, 246 – engine, 248 – circle, 250 – guide cable.

With the radius system the problem of creating the cable circle is solved very easily. Expensive rockets are not necessary. The operator starts with a small radius near the planet surface and increases it until the desired radius is achieved. This method may be used for making a semi-circle or double semi-circle system.

The small installation may be used as a crane for construction engineering, developing building, bridges, in the logging industry, and so on.

The main advantage of the proposed launch system is its very low cost for the amount of payload delivered into space and over long distances. Expensive fuels, complex control systems, expensive rockets, computers, and complex devices are not required. The cost of payload delivery into space would drop by a factor of a thousand. In addition, large amounts of payloads could be launched into space (in the order of a thousand tons a year) using a single launch system. This launch system is simple and does not require high-technology equipment. The payloads could be delivered into space at production costs of 2–10 dollars per kg (see computations in the attached projects).

Cable problem (see in chapters 1,2).

Theory of Circle Launcher

The equations developed and used for estimation and computation are provided below. All equations are in the metric system. The nomenclature was given in special section at the beginning of the chapter.

Take a small part of a rotary circle and write the equilibrium

$$2SR\alpha\gamma V^2/R = 2S\sigma\sin\alpha .$$

When $\alpha \to 0$, the relationship between maximum rotary speed and tensile strength of a closed-loop circle cable is

$$V = (\sigma/\gamma)^{1/2} = k^{1/2}. \qquad (3.1)$$

Results of this computation are presented in Fig. 3.10.

Maximum lift force P_{max} of the rotary closed-loop circle cable when the gravity $g = 0$ equals the cable tensile force is:

$$P_{max} = 2V^2\gamma S = 2\sigma S . \qquad (3.2)$$

The maximum vertical lift force P of the vertical cable circle in the constant gravity field of a planet equals the lift force in equation (3.2) minus the cable weight

$$P = 2S(\sigma - \pi R\gamma g) . \qquad (3.3)$$

The maximum lift force P of the double semi-circle cable in the gravity field of a planet is

$$P = 4S(\sigma - 0.5\pi R\gamma g) . \qquad (3.3a)$$

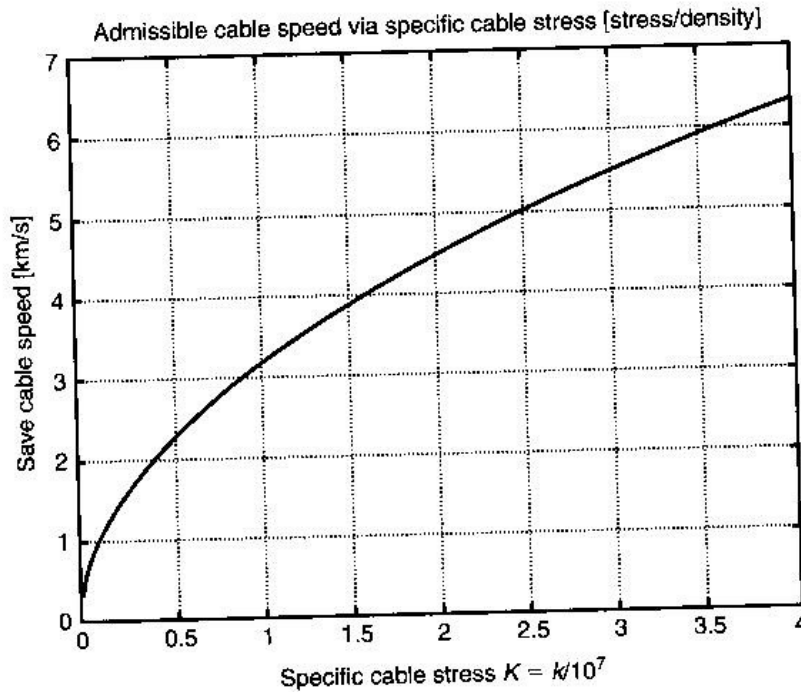Approximately one quarter of this force can be used. The results of computation are presented in Fig. 3.11.

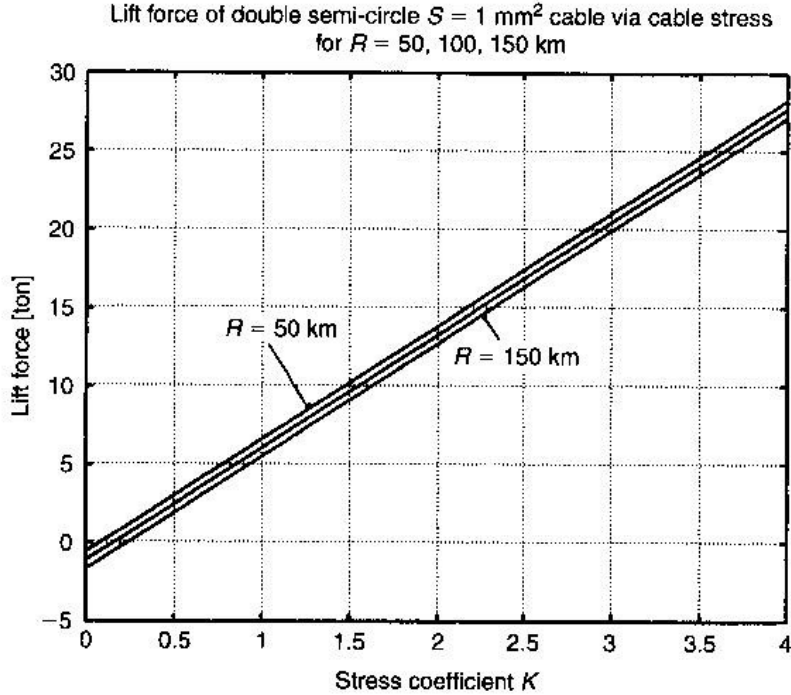**Fig. 3.10.** Maximum cable speed versus safe specific cable stress.

Lift force of double semi-circle $S = 1 \ mm^2$ cable via cable stress
for $R = 50, 100, 150$ km

Fig. 3.11. Maximum lift force of cable $S = 1 \ mm^2$ versus stress.

The minimum speed of the cable circle can be found from equations (3.3) and (3.1) for $P = 0$

$$V_{min} = \sqrt{\pi R g} \quad . \tag{3.4}$$

Example: For $R = 0.15$ m, the minimum speed is 2.15 m/s; for $R = 50$ km, the minimum speed is 1241 m/s.

The minimum speed of the double semi-circle can be found from equations (3.3a) and (3.1) for $P = 0$

$$V_{min} = \sqrt{0.5 \pi R g} \ . \tag{3.4a}$$

The specific lift force of one kg of cable mass P_1 in a planet's gravity field equals the lift force in equation (3.3) divided by the cable weight $2\pi R S \gamma$. For a conventional circle

$$P_1 = (\sigma / \pi \gamma R) - g \tag{3.5}$$

while for a double semi-circle

$$P_1 = (2\sigma / \pi \gamma R) - g \ . \tag{3.5a}$$

The specific lift force P_L of one meter of cable in a planet's gravity field equals the lift force in (3.3) and (3.3a) divided by the cable length, respectively

$$P_L = S[(\sigma / \pi R) - \gamma g] \ , \quad P_L = 2S[(\sigma / \pi R) - 0.5 \gamma g] \quad . \tag{3.6},(3.6a)$$

The length of a cable L, which supports the given local load G is

$$L = G / P_L . \tag{3.7}$$

The cable angle, α_h, to the horizon about a local load equals (from a local equilibrium)

$$\alpha_h = \arg\sin(G / 2 \sigma S) \ . \tag{3.8}$$

Cable deformation about a local load (decrease in altitude) for a cable semi-circle in a planet gravity's field can be found approximately:

$$\Delta h \cong GL / 12 \sigma S \ . \tag{3.9}$$

Cable deformation about a local load for the double cable circle around a planet in space is

$$\Delta h_0 \approx \frac{\pi(R_0 + H)}{24}\left(\frac{G}{\sigma S}\right)^2 .$$ (3.10)

The internal pressure on the cable circle can be derived from the equilibrium condition. The result is

$$p = \pi r \sigma/2R .$$ (3.11)

The increase in cable radius under an internal pressure is

$$\Delta R = \gamma V^2 R/E .$$ (3.12)

The maximum cable radius (maximal cable top) in a constant gravity field can derived from the equilibrium of the lift force and a cable weight:

a) Full circle (from (3.3))

$$R_{max} = \sigma/\pi\gamma g , \qquad H_{max} = 2R_{max} .$$ (3.13)

b) Semi-circle (from (3.3a))

$$R_{max} = 2\sigma/\pi\gamma g , \qquad H_{max} = R_{max} .$$ (3.13a)

The results of this computation are presented in Fig. 3.12.

Maximum radius of Earth cable semi-circle [km]

Specific cable stress (stress/density) $K = k/10^7$, $k[N/m^2]$
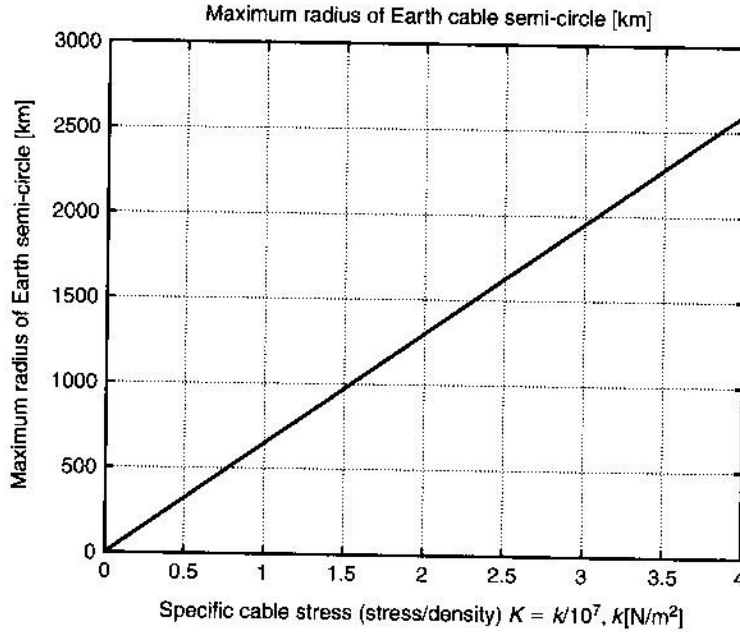
radius of Earth semi-circle versus specific cable stress.

Fig. 3.12. Maximum radios of the Earth semi-circle versus specific cable stress
The maximum cable radius in a variable gravity field of a rotating planet can be found from the

equation of a circle located on a flat equator

$$R\left[\frac{1 + R/R_0}{(1 + 3R/R_0)^{3/2}} - \omega^2(R_0 + R)\right] = \frac{\sigma}{\pi\gamma g} .$$ (3.14)

The maximum speed of a closed-loop circle rotated around a planet (Fig. 3.8) can be found from the equilibrium between centrifugal and gravity forces

$$V_a = [(\sigma/\gamma) + Rg]^{1/2} .$$ (3.15)

The results of computation are presented in Fig. 3.13. The minimum value $V_a = (Rg)^{1/2}$ occurs when $k = \sigma/\gamma = 0$.
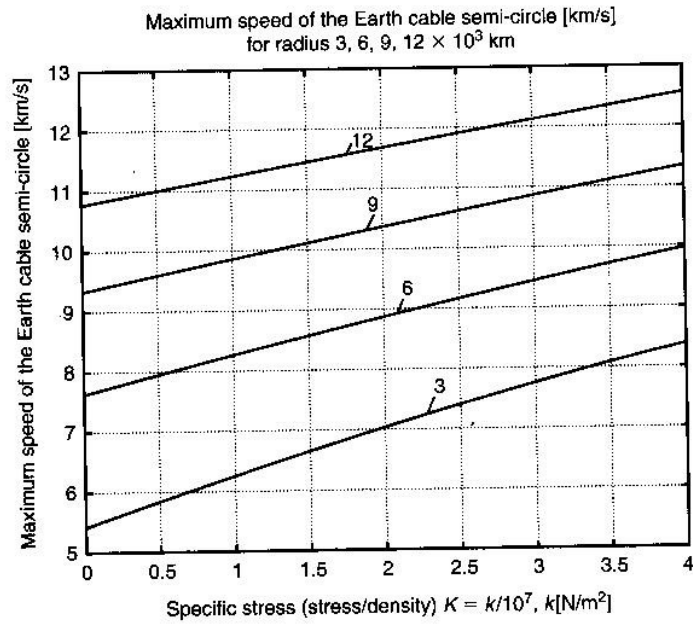
Fig. 3.13. Maximum speed of a closed-loop circle around a planet.

The lift force P_a of a double closed-loop cable circle rotated around a planet can be found from equilibrium of a small circle element

$$P_a = 4\pi S\gamma\,(V_s^2 - k - Rg).\qquad(3.16)$$

The full lift force of a double closed-loop cable circle rotated around a planet is found by multipling p from equation (3.11) by a cable area $4\pi Rr$, or

$$P_a = 2\pi\sigma S\ .\qquad(3.16a)$$

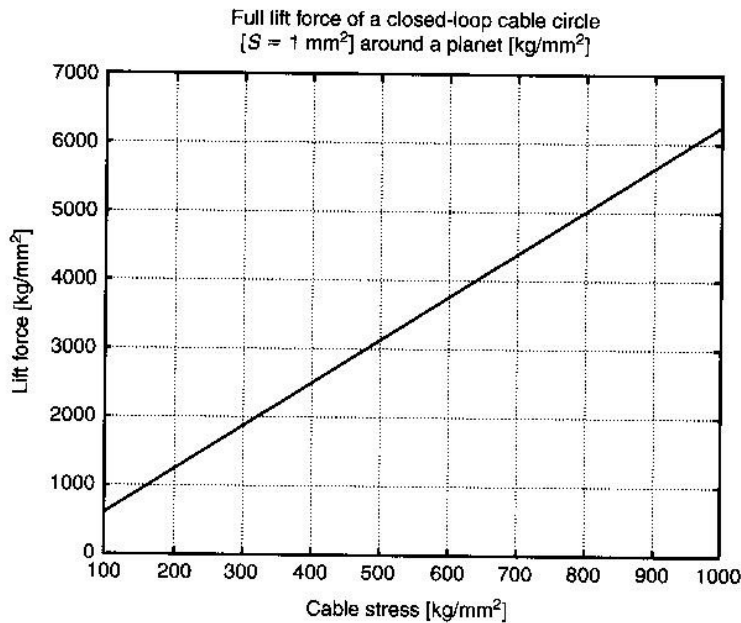The results of computation are presented in Fig. 3.14.

Fig. 3.14. Full lift force of the closed-loop cable circle rotated around a planet.

The specific lift force of a one kg closed-loop cable circle rotated around a planet can be found from equation (3.16), by dividing by cable weight

$$P_{a,1} = \sigma/\gamma R \ . \tag{3.17}$$

The specific lift force of a one meter closed-loop circle around a planet in space, when $g = 0$, can also be found from equation (3.16), if it is divided by the cable length

$$P_{a,L} = S\sigma/R \ . \tag{3.18}$$

We can derive from momentum theory an additional speed, ΔV, which a space ship (Fig.3.7) gets from a cable propulsion system

$$\Delta V = V_c m/(m_{ss} - m) \quad . \tag{3.19}$$

The results of computation are presented in Fig. 3.15.

The speed of falling from an altitude H is given by

$$V_f = (2gH)^{0.5} \ . \tag{3.20}$$

The energy, E_s , stored by a rotary circle per 1 kg of the cable mass can be derived from the known equation of kinetic energy. The equation is

$$E_s = \sigma/2\gamma \quad . \tag{3.21}$$

The results of computation are presented in Fig. 3.16.

The radius of observation versus altitude H [km] over the Earth is approximately

$$R_r = (2R_oH + H^2)^{0.5} \quad [\text{km}] \quad , \tag{3.22}$$

where Earth radius $R_o = 6378$ km. If $H = 150$ km, then $R_r = 1391$ km.

Estimation of Cable Friction Due to the Air

This estimation is very difficult because there are no experimental data for air friction of an infinitely very thin cable (especially at hypersonic speeds). A computational method for plates at hypersonic speed was used, see reference[4] p.287. The computation is made for two cases: a laminar and a turbulent boundary layer.

The results are very different. The maximum friction is for turbulent flow. About 80% of the friction drag occurs in the troposphere (from 0 to 12 km). If we locate the cable end on a mountain at an altitude of 4 km the maximum air friction decreases by 30%. So the drag is calculated for three cases: when the cable end is located on the ground $H = 0.1$ km above sea level, $H = 1$ km and when it is located on the mountain at $H = 4$ km (2200 ft).

The major part of cable will have the laminar boundary layer because a small wind will blow away the turbulent layer and restore the laminar flow. The blowing away of the turbulent boundary layer is studied in aviation and is used to restore laminar flow and decrease air friction. The laminar flow decreases the friction in hypersonic flow by 280 times! If half the cable surface has a laminar layer it means that we must decrease the air drag calculated for the full turbulent layer by a minimum of two times.

Below the equations from Anderson[4] for computation of local air friction for a two-sided plate are given.

$$\frac{T^*}{T} = 1 + 0.032M^2 + 0.58\left(\frac{T_w}{T} - 1\right), \quad M = \frac{V}{a}, \quad \mu^* = 1.458 \times 10^6 \frac{T^{*1.5}}{T^* + 110.4},$$

$$\rho^* = \frac{\rho T}{T^*}, \quad R_e^* = \frac{\rho^* V x}{T^*}, \quad C_{f,L} = \frac{0.664}{(R_e^*)^{0.5}}, \quad C_{f,T} = \frac{0.0592}{(R_e^*)^{0.2}}, \quad C_{c,l} = 0.5C_{f,l}, \quad C_{c,t} = 0.5C_{f,t},$$

$$D_L = 0.5C_{f,l}\rho^* V^2 S, \quad D_T = 0.5C_{f,t}\rho^* V^2 S. \quad D = 0.5(D_T + D_L). \tag{3.23}$$

To apply the above theory to the double semi-circle case we can approximate the atmosphere density by the exponential equation

$$\rho = \rho_0 e^{bh} \ ,$$ (3.24)

where $\rho_0 = 1.225$ kg/m^3, $b = -0.00014$, h is the altitude [m]. Then the air friction drag is

$$D_{T,L} = \pi d V^2 \int_{H_0}^{H} C_{c,t,l}(h)\rho^*(h)dh/\cos\alpha_1 \quad , \quad \alpha_1 = \arg\sin\frac{h-H_0}{H_m-H_0},$$ (3.25)

where $D_{T,L}$ and $C_{c,l,t}$ are the turbulent and laminar drag and drag coefficient respectively, α_1 is the angle of the cable element to the horizon. The full drag is $D = 0.5(D_T+D_L)$. The results of computation are presented in Fig. 3.17.

The simplest formula for air friction F is

$$F = \mu V S_c / w \ .$$ (3.26)

The required power, N, is

$$N = DV \ .$$ (3.27)

The results of computations using equation (3.27) are presented in Fig. 3.18.

4. Case Studies

Data on artificial fiber, whiskers, and nanotubes in Chapter 1.

Project 1

Space Station for Tourists or a Scientific Laboratory at an Altitude of 140 km (Figs. 3.1 to 3.6)
The closed-loop cable is a semi-circle. The radius of the circle is 150 km. The space station is a cabin with a weight of 4 tons (9000 lb) at an altitude of 150 km (94 miles). This altitude is 140 km under load.

The results of computations for three versions (different cable strengths) of this project are in Table 3.1.

Table 3.1. Results of computation Project 1.

Variant	σ, kg/mm^2	γ, kg/m^3	$K = \sigma/\gamma /10^7$	V_{max}, km/s	H_{max}, km	S, mm^2
1	2	3	4	5	6	7
1	8300	1800	4.6	6.8	2945	1
2	7000	3500	2.0	4.47	1300	1
3	500	1800	0.28	1.67	180	100

P_{max}[tons]	G, kg	Lift force, kg/m	Loc. Load, kg	L, km	α^0	ΔH, km
8	9	10	11	12	13	14
30	1696	0.0634	4000	63	13.9	5.0
12.5	3282	0.0265	4000	151	16.6	7.2
30.4	170x10^3	0.0645	4000	62	4.6	0.83

Cable Thrust T_{max}, kg,	Cable drag $H = 0$ km, kg	Cable drag $H = 4$ km, kg	Power MW $H = 0$ km	PowerMW $H = 4$ km	Max.Tourists men/day
15	16	17	18	19	20
8300	2150	1500	146	102	800
7000	1700	1100	76	49	400
50000	7000	5000	117	83.5	800

The column numbers are: 1) the number of the variant; 2) the permitted maximum tensile strength [kg/mm^2];

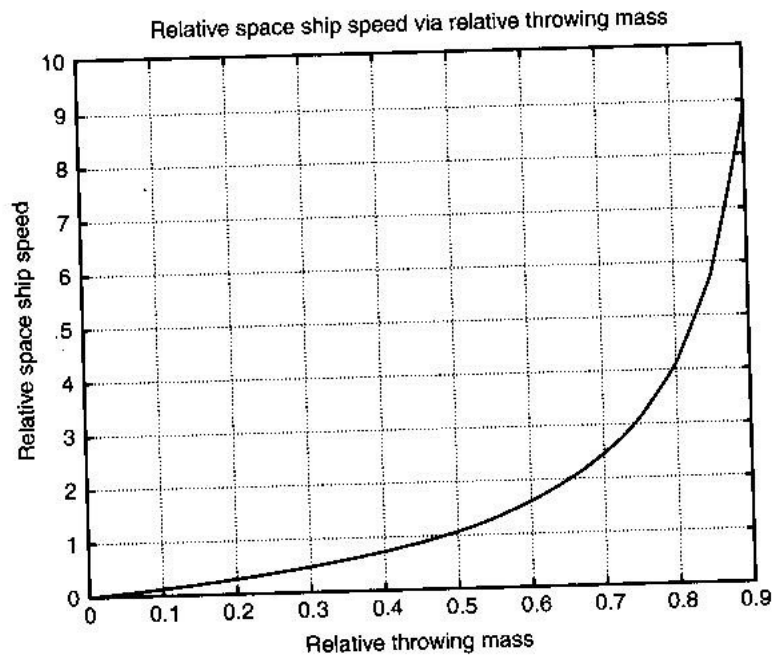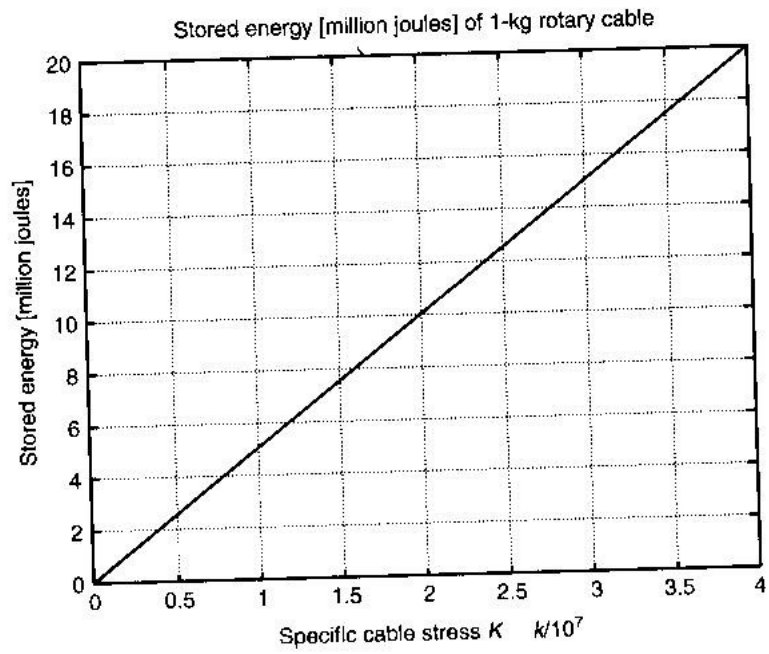### Relative space ship speed via relative throwing mass

Fig. 3.15. Relative speed of space ship versus relative throwing mass.

Stored energy [million joules] of 1-kg rotary cable

Fig. 3.16. Storage energy of 1 kg of the cable

Drag via speed for cable diameter d = 1 mm, altitude from H_0 = 0.1, 1, 2, 3, 4, 5 km to H = 70 km

H_0 = 0.1 km
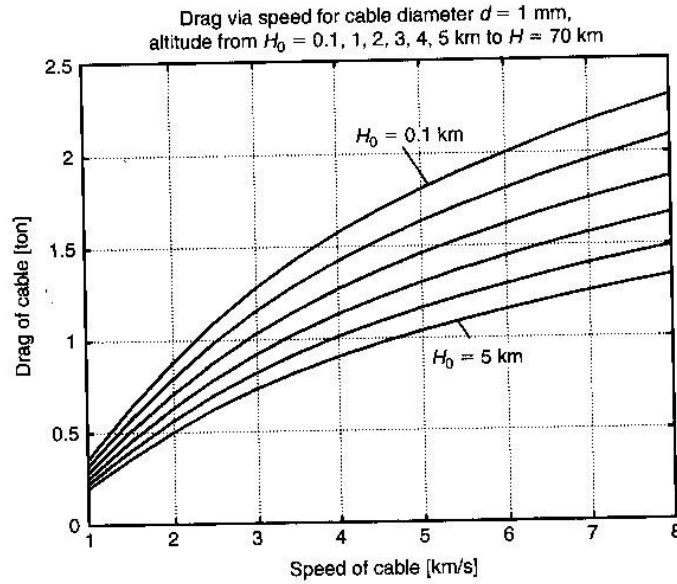
H_0 = 5 km

Drag of cable [ton]

Speed of cable [km/s]

Fig. 3.17. Estimation of the friction air drag [ton] versus cable speed [km/s] and initial altitude [km] for a double semi-circle keeper.

Power [kW] via speed for cable diameter d = 1 mm, altitude from H_0 = 0.1, 1, 2, 3, 4, 5 to H = 70 km

$\times 10^5$

H_0 = 0.1 km

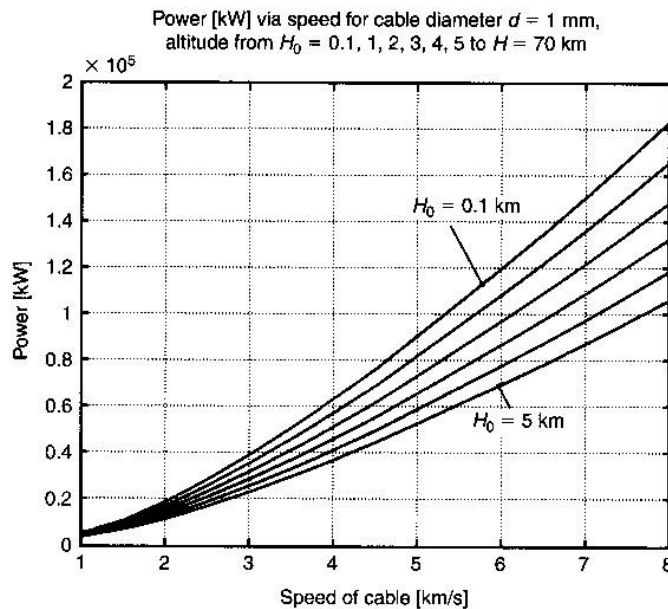H_0 = 5 km

Power [kW]

Speed of cable [km/s]

Fig. 3.18. Estimation of the drive power [kW] versus cable speed [km/s] and initial altitude [km] for a double semi-circle keeper.

3) the cable density [kg/m^3]; 4) the ratio $K = \sigma/\gamma \, 10^{-7}$; 5) the maximum cable speed [km/s] for a given tensile strength; 6) the maximum altitude [km] for a given tensile strength; 7) the cross-sectional area of the cable [mm^2]; 8) the maximum lift force of one semi-circle [ton]; 9) the weight of the two semi-circle cable [kg]; 10) the lift force of one meter of cable [kg/m]; 11) the local load (4 tons or 8889 lb); 12) the length of the cable required to support the given (4 tons) load [km]; 13) the cable angle to the horizon near the local load [degrees]; 14) the change of altitude near the local load; 15) the maximum cable thrust [kg]; 16) the air drag on one semi-circle cable if the driving (motor) station is located on the ground (at altitude $H = 0$) for a half turbulent boundary layer; 17) the air drag of the cable if the drive station is located on a mountain at $H = 4$ km; 18) the power of the drive stations [MW] (two semi-circles) if located at $H = 0$; 19) the power of the drive stations

[MW] if located at $H = 4$ km; 20) the number of tourists (tourist capacity) per day (0.35 hour in station) for double semi-circles.

Economic Estimations of these projects for Space Tourisms.

Take the weight (mass) of the tourist cabin as 2 tons (it may be up to 4 tons), and the useful payload as 1.3 tons (16 tourists plus one operator). Acceleration (braking) is $0.5g$ ($a = 5$ m/s). Then the time to climb and descend will be about 8 minutes ($H = 0.5at^2$) and 20 minutes for observation at an altitude 150 km. The common flight time will be 30 minutes. The passenger capability will be about 800 tourists per day.

Let us use the following equation to estimate the delivery cost, C :

$$C = \frac{I/n_1 + M + Ntc/q\eta}{n_2 n_3} ,$$ (3.26)

where: I = installation cost, $; n_1 = installation life time, years; M = yearly maintenance, $; $N = DV$ – engine power, J/s; t – year time ($t = 3600 \cdot 24 \cdot 365$), seconds; c = fuel cost, $/kg; q = fuel heat capability, J/kg (for benzene $q = 43 \cdot 10^6$, J/kg, for coal $q = 20 \cdot 10^6$; for natural gas $q = 45 \cdot 10^6$); η = engine efficiency, $\eta = 0.2$–0.3; n_2 = number of tourist per day, people/day; n_3 = number of working days in year.

Let us take for variant 3: $I = \$100$ million; $n_1 = 10$ years; $M = \$2$ million in year; $N = DV$ – engine power, J/s, where $D = 50,000$ N, $V = 1670$ m/s; $t = 3600 \cdot 24 \cdot 365 = 31.5 \cdot 10^6$ s; $c = 0.25$, $/kg; $q = 43 \cdot 10^6$, J/kg; $\eta = 0.25$; $n_2 = 400$ people; $n_3 = 360$. Results of computations are presented in Fig. 3.19.
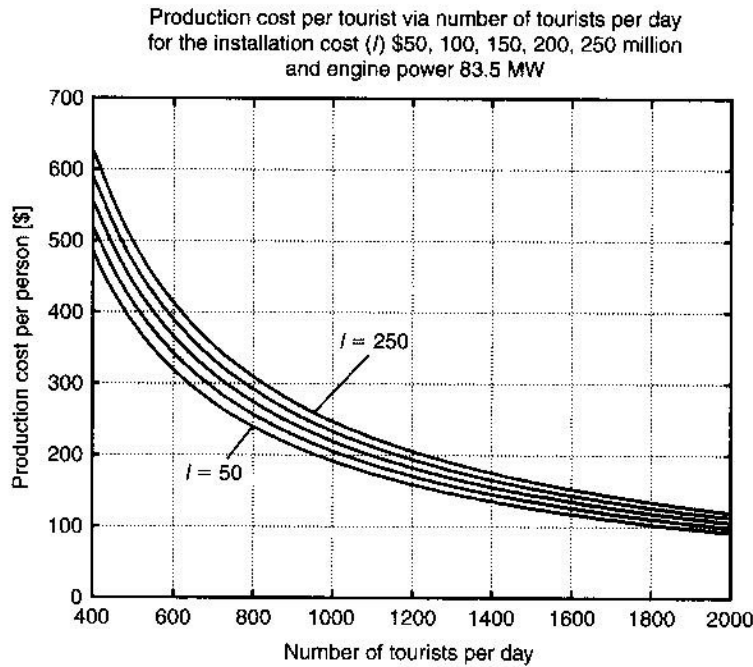
Fig. 3.19. Estimation of the production cost per tourist versus number of tourists per day for the installation cost US $ (in million): 50, 100, 150, 200, and 250 and engine power 83.5 MW.

Then the production cost of a space trip for one tourist will be equal to $508 (about 84% of this cost is the cost of benzene). This cost is $363 for variant 2. If the cost of the trip ticket is $100 more than the production cost, the installation will give a profit of about $14–49 million per year. This profit may be larger if we design the installation especially for tourism. If our engines use natural gas (not benzene), the production cost decreases by the ratio of the cost of gas to benzene.

Discussion of Project 1.

1) The first variant has a cable diameter of 1.13 mm (0.045 inches) and a general cable weight of 1696 kg (3658 lb). It needs a power (engine) station to provide from 102 to a maximum of 146 MW (the maximum amount is needed for additional research).
2) The second variant needs the engine power from 49 to 76 MW.
3) The third variant uses a cable with tensile strength near that of current fibers. The cable has a diameter of 11.3 mm (0.45 inches) and a weight of 170 tons. It needs an engine to provide from 83.5 to 117 MW.

The systems may be used for launching (up to 1 ton daily) satellites and interplanetary probes. The installation may be used as a relay station for TV, radio, and telephones.

Project 2
Semi-circle of a Radius 1000 km (625 miles) for Delivering Passengers to a Distance of 2000 km (1250 miles) through Space (Fig. 3.4)

The two closed-loop cable is a semi-circle. The radius is 1000 km. The space cabin has a weight of 4 tons (9000 lb). The maximum altitude is 1000 km. The results of computation for two versions are given in Table 3.2.

Table 3.2. Result of computations for Project 2

σ, kg/mm^2	γ, kg/m^3	V, km/s	S, mm^2	W, tons	P_{max}, tons	P_{us}, kg	Men/day	Time[min]
1	2	3	4	5	6	7	8	9
8300	1800	4.6	1	11.3	11	3000	2000	27
7000	3500	2.0	1	20.2	3	750	500	27

The columns number are: 1) Tensile strength [kg/mm^2]; 2) Density [kg/m^3]; 3) Cable speed [km/s]; 4) Cross sectional cable area [mm^2]; 5) Cable weight of two semi-circles [tons]; 6) Maximum cable lift force [tons]; 7) Useful local load [kg]; 8) Maximum passenger capability in both directions [people/day]; 9) Time of flight in one direction.

Estimation of economic efficiency

Let us take the cost of installation and service as the same as the previous project. Then the delivery cost of one passenger will be same (see Fig. 3.19). If a ticket is marked up by 50 dollars more (from $130 to $180 if there are 2000 passengers), then the profit will be about 18 million dollars per year.

Discussion of Project 2

Version 1 has a cable diameter of 1.13 mm (0.047 inches), and a cable weight of 11.3 tons, and has a passenger capacity of 2000 people per day in two directions. The distance is 2000 km (1250 miles) and delivery time 27 minutes.

These transport systems may be used for launching (weight up to 1 ton) satellites. Such a system may also be the optimum way to travel between two countries that are separated by a third country which does not have an air corridor for conventional airplanes, or is an enemy country. The suggested project goes into outer space ($H = 1000$ km) and out of the atmosphere of the third country.

Project 3
Circle Around the Earth at an Altitude of 200 km (125 miles) for 8–10 Scientific Laboratories (Fig. 3.8)

The closed-loop cable is the circle around the Earth at an altitude H of 200 km (125 miles). The radius is 6578 km. The space stations are 8–10 cabins with a weight of 1 ton (2222 lb).

Results of computation for three versions are given in Table 3.3.

Table 3.3. Result of computations for Project 3.

No	σ, kg/mm^2	γ, kg/m^3	V, km/s	S, mm^2	P_{max}, tons	Weight, tons	Lift force, kg/km	Angle α, degree	Δh_o, km
1	2	3	4	5	6	7	8	9	10
1	8300	1800	10.53	1	52.1	74.4	1.26	3.45	12.5
2	7000	3500	9.19	1	44	145	1.06	4.1	17.2
3	500	1800	8.06	10	31.4	744	0.76	5.74	35

The numbers are: 1) The variant; 2) Tensile strength [kg/mm^2]; 3) Cable density [kg/m^3]; 4) Cable speed [km/s]; 5) Cross sectional cable area [mm^2]; 6) Maximum cable lift force [tons]; 7) Cable weight [tons]; 8) Lift force of 1 km of cable [kg/km]; 9) Cable angle to the horizon near a local load [degrees]; 10) Change (decrease) in altitude under a local load of 1 ton [km].

Discussion of Project 3

The variant 3 using current fibers (σ = 500 kg/mm^2; 5000 MPa) has a cable diameter of 3.6 mm (0.15 inches), a cable weight of 744 tons, and can keep 10 space stations with useful loads (200–500 kg) for each station at an altitude of 180 km (112 miles). This may also be used for launching small (up to a weight 200 kg) satellites.

Project 4
Using the Cable Circle as a Propulsion System and Energy Storage System
(Fig. 3.7)

As presented in the main text the suggested system may be used as a space ship launch system, as a landing system for space ships on planets and asteroids, or as a delivery system for people and payloads from a space ship to the planet or asteroid's surface and back without landing the ship.

Below we consider an application of this system as a propulsion system using *any* mass (for example, a meteorites, asteroid material, ship garbage, etc.) to create the ship's thrust. The offered system may be used also for storing energy.

Let us suggest that a space ship has a nuclear energy station. The ship has a lot of energy. However, the ship can not use this energy efficiently for thrust because known ion thrusters (electric rocket engines) produce only small amounts of thrust (from grams to kg). Consequently any trip would take a long time (years). Rocket engines require a lot of expensive fuel (for example, liquid hydrogen for a nuclear engine) and oxidizer (for example, liquid oxygen), which greatly increases launch costs, the ship mass, requirements for low temperatures and difficulties for storage.

The suggested system allows any material (mass) to be used for imparting speed to a ship. For example, let the space ship have the cable system made from carbon nanotubes (tensile strength 8300 kg/mm^2 and density 1800 kg/m^3). This means [equation (3.1)] the cable system can have a maximum speed of 6800 m/s (Table 3.2, column 5). The system can throw off mass at this speed in any direction and provide thrust for the space ship. The specific impulse of the cable system, 6800 m/s, is better than the specific impulse of any modern rocket engine. For example, current rocket engines have impulses 2000–2500 m/s (solid fuel), 3000–3200 m/s (liquid kerosene–oxygen fuel), and up to 4200 m/s (hydrogen–oxygen fuel). If the ship takes 50% of its mass in asteroid material, it can achive an additional speed of 6800 m/s [see equation (3.19)]. The space ship can also use any of the ship's garbage to produce thrust.

As an energy storage system the suggested cable system allows 23 MW of energy to be stored per every kilogram of a cable [see equation (3.21)]. Tis is more than any current kg of a conventional fuel (fuel and oxidizer).

Discussing, Summary, and Conclusions

The offered method and installations promise to decrease launch costs by a factor of thousands. They are very simple and inexpensive. As with any new system, the suggested method requires further detailed theoretical research, modeling, and development.

Science laboratories have whiskers and nanotubes that have high tensile strength.

The fiber industry produces fibers that can be used for some of the author's projects at the present time. These projects are unusual (strange) for specialists and people now, but they have huge advantages, and they have a big future. The government shoul support scientific laboratories and companies who can produce a cable with the given performances for a reasonable price, and who research and develop prospective methods.

References for Chapter 3

1. *Space technology & Application. International Forum*, 1996–1997, Albuquerque, MN, USA, parts 1–3.
2. D.V. Smitherman, Jr, "Space Elevators", NASA/CP-2000-210429, 2000.
3. F.S. Galasso, *Advanced Fibers and Composite*, Gordon and Branch Scientific Publisher, 1989.
4. J.D. Anderson, *Hypersonic and High Temperature Gas Dynamics*, McGraw-Hill Book Co., 1989.
5. *Carbon and High Performance Fibers*, Directory, 1995.
6. J.I. Kroschwitz (ed.), *Concise Encyclopedia of Polymer Science and Engineering*, 1990.
7. M.S. Dresselhous, *Carbon Nanotubes*, Springer, 2000.
8. A.A. Bolonkin, "Centrifugal Keeper for Space Stations and Satellites", *JBIS*, Vol.56, No. 9/10, 2003, pp. 314-327.

Chapter 4.
Optimal Inflatable Space Towers*

Summary

In this Chapter the author provides theory and computations for building inflatable space towers up to 100 kilometers in height. These towers can be used for tourism, scientific observation of space, the Earth's surface, weather and the top atmosphere; as well as for radio, television, and communication transmissions. These towers can also be used to launch space ships and Earth satellites.

These projects are not expensive and do not require rockets. They require thin strong films composed of artificial fibers and fabricated by current industry. They can be built using present technology. Towers can be used (for tourism, communication, etc.) during the construction process and provide self-financing for further construction. The tower design does not require work at high altitudes; all construction can be done at the Earth's surface.

The transport system for a tower consists of a small engine (used only for friction compensation) located at the Earth's surface. The tower is separated into sections and has special protection mechanisms in case of damage.

Problems involving security, control, repair, and stability of the proposed towers will be addressed in other publications. The author is prepared to discuss these and other problems with serious organizations desiring to research and develop these projects.

----

1. Introduction

Brief History. The idea of building a tower high above the Earth into the heavens is very old[1]. The writings of Moses, about 1450 BC, in Genesis, Chapter 11, refer to an early civilization that in about 2100 BC tried to build a tower to heaven out of brick and tar. This construction was called the Tower of Babel, and was reported to be located in Babylon in ancient Mesopotamia. Later in chapter 28, about 1900 BC, Jacob had a dream about a staircase or ladder built to heaven. This construction was called Jacob's Ladder. More contemporary writings on the subject date back to K.E. Tsiolkovski in his manuscript "Speculation about Earth and Sky and on Vesta," published in 1895[2]. This idea inspired Sir Arthur Clarke to write his novel, The Fountains of Paradise[3], about a space tower (elevator) located on a fictionalized Sri Lanka, which brought the concept to the attention of the entire world.

Today, the world's tallest construction is a television transmitting tower near Fargo, North Dakota, USA. It stands 629 m high and was build in 1963 for KTHI-TV. The CNN Tower in Toronto, Ontario, Canada is the world's tallest building. It is 553 m in height, was build from 1973 to 1975, and has the world's highest observation desk at 447 m. The tower structure is concrete up to the observation deck level. Above is a steel structure supporting radio, television, and communication antennas. The total weight of the tower is 3,000,000 tons.

The Ostankin Tower in Moscow is 540 m in height and has an observation desk at 370 m. The world's tallest office building is the Petronas Towers in Kuala Lumpur, Malasia. The twin towers are 452 m in height. They are 10 m taller than the Sears Tower in Chicago, Illinois, USA.

Current materials make it possible even today to construct towers many kilometers in height. However, conventional towers are very expensive, costing tens of billions of dollars. When considering how high a tower can be built, it is important to remember that it can be built to any height if the base is large enough. Theoretically, you could build a tower to geosynchronous Earth orbit (GEO) out of bubble gum, but the base would likely cover half the surface of the Earth.

The proposed inflatable towers are cheaper by factors of hundreds. They can be built on the Earth's surface and their height can be increased as necessary. Their base is not large. The main innovations in this project are the application of helium, hydrogen, or warm air for filling inflatable structures at high altitude and the solution of a stability problem for tall (thin) inflatable columns, and utilization of new artificial materials[4–7].

The tower applications. The inflatable high towers (3–100 km) have numerous applications for government and commercial purposes:
- Entertainment and observation platform.
- Entertainment and observation desk for tourists. Tourists could see over a huge area, including the darkness of space and the curvature of the Earth's horizon.
- Drop tower: tourists could experience several minutes of free-fall time. The drop tower could provide a facility for experiments.
- A permanent observatory on a tall tower would be competitive with airborne and orbital platforms for Earth and space observations.
- Communication boost: A tower tens of kilometers in height near metropolitan areas could provide much higher signal strength than orbital satellites.
- Solar power receivers: Receivers located on tall towers for future space solar power systems would permit use of higher frequency, wireless, power transmission systems (e.g. lasers).
- Low Earth orbit (LEO) communication satellite replacement: Approximately six to ten 100-km-tall towers could provide the coverage of a LEO satellite constellation with higher power, permanence, and easy upgrade capabilities.

Further methods proposed by the author for access to space are given in the references[8–16].

Description of Innovation and Problem

Tower structure. The simplest tourist tower includes (Fig. 4.1): Inflatable column, top observation desk, elevator, expansions, and control stability. The tower is separated into sections by horizontal and vertical partitions (Fig. 4.2) and contains entry and exit air lines and control devices.

2.2. Filling gas. The compressed air filling the inflatable tower provides the weight. Its density decreases at high altitude and it cannot to support a top tower load. The author suggests filling the towers with a light gas, for example, helium, hydrogen, or warm air. The computations for changing pressure of air, helium, and hydrogen are presented in Fig. 4.3 [see equation (4.1)]. If all the gases have the same pressure (1.1 atm) at Earth's surface, their columns have very different pressures at 100 km altitude. Air has 0 atm, hydrogen 0.4 atm, and helium 0.15 atm. A pressure of 0.4 atm means that every square meter of a tower top can support 4 tons of useful load. Helium can support only 1.5 tons. Fig. 4.3.

Unfortunately, hydrogen is dangerous as it can burn. The catastrophes involving dirigibles are sufficient illustration of this. Hydrogen can be used only above an altitude of 13–15 km, where the atmospheric pressure decreases by 10 times and the probability of hydrogen burning is small.

The average temperature of the atmosphere in the interval from 0 to 100 km is about 240 °K. If a tower is made from dark material, the temperature inside the tower will be higher than the temperature of the atmosphere at a given altitude in day time, so that the tower support capability will be greater [equation (4.1)].
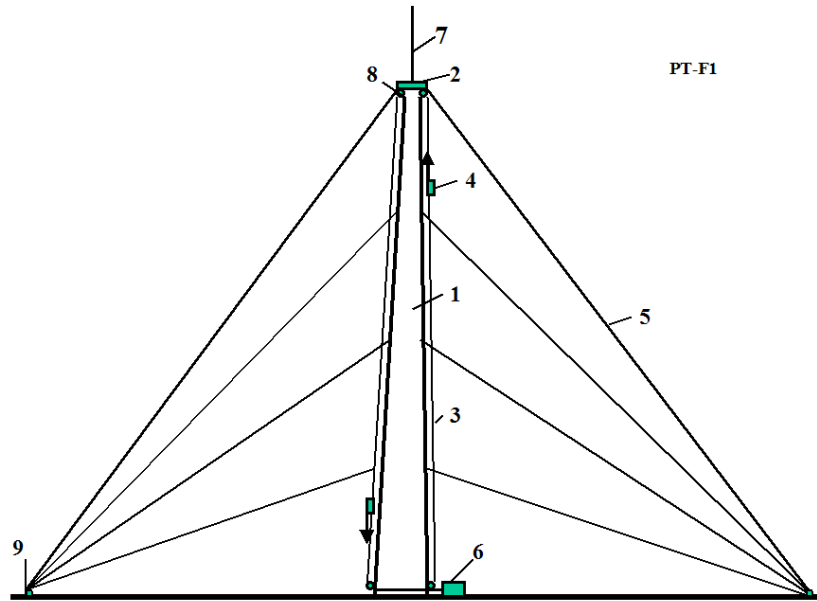
PT-F1

Fig. 4.1. Inflatable tower of height 3 km (10,000 ft). Notations: 1 – Inflatable column of radius 5 m; 2 – observation desk; 3 – load cable elevators; 4 – passenger cabin; 5 – expansions; 6 – engine; 7 – radio and TV antenna; 8 – rollers of cable transport system; 9 – stability control.
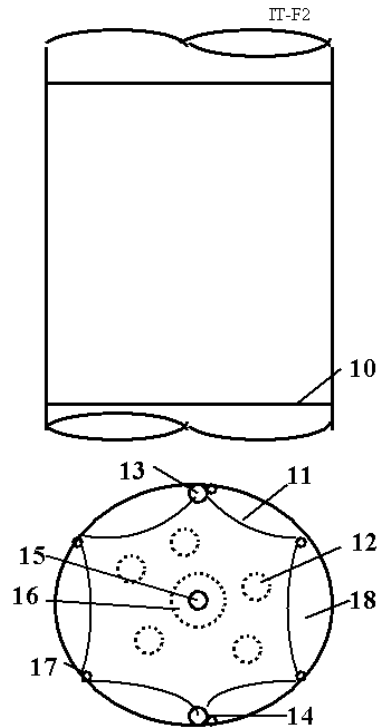
IT-F2

Fig. 4.2. Section of inflatable tower. Notations: 10 – horizontal film partitions; 11 – light second film (internal cover); 12 – air balls; 13 – entrance line of compression air and pressure control; 14 – exit line of air and control; 15 – control laser beam; 16 – sensors of laser beam location; 17 – control cables and devices; 18 – section volume.

The observation radius versus altitude is presented in Figs. 4.4–4.5 [equation (4.23)].
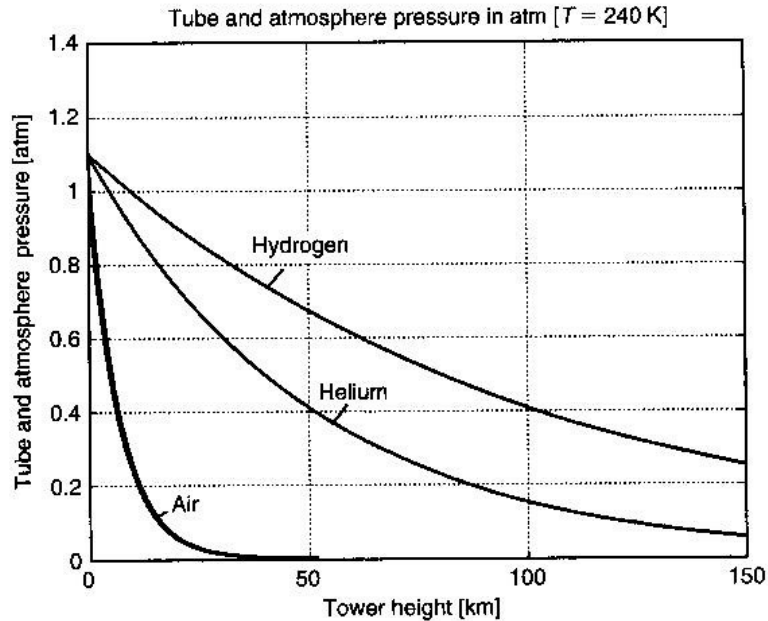

Fig. 4.3. Change in hydrogen, helium, and air pressure for intervals of 0–150 km of altit
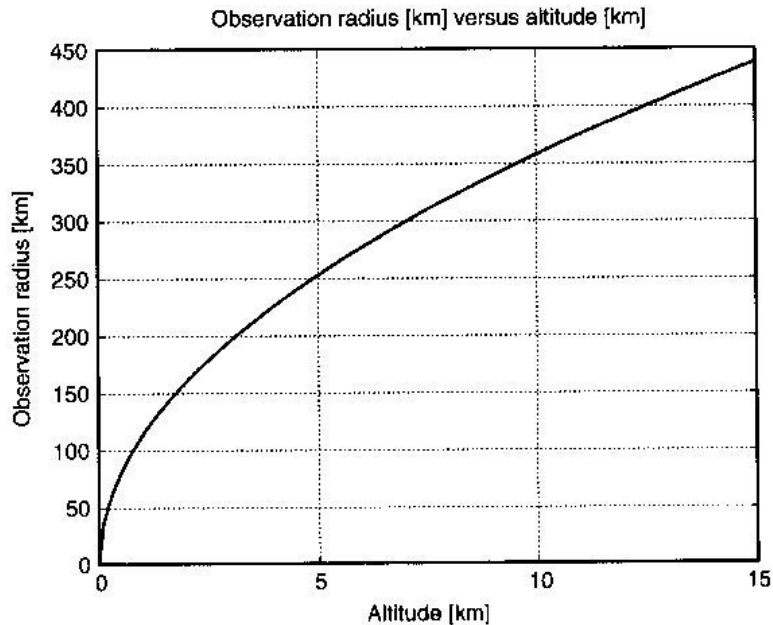

Fig. 4.4. Observation radius for altitudes up to 15 km

Tower material. The author has found only old (1973) information about textile fiber for inflatable structures[4]. This refers to DuPont textile Fiber **B** and Fiber **PRD-49** for tire cord. They are six times as strong as steel (psi is 400,000 or 312 kg/mm^2) with a specific gravity of only 1.5. Minimum available yarn size (denier) is 200, tensile modulus is 8.8×10^6 (**B**) and 20×10^6 (**PRD-49**), and ultimate elongation (percent) is 4 (**B**) and 1.8 (**PRD-49**).

The tower parameters vary depending on the strength of the textile material (film), specifically the ratio of the safe tensile stress σ to specific density γ. Current industry widely produces artificial

fibers that have tensile stress $\sigma = 500–620$ kg/mm^2 and density $\gamma = 1800$ kg/m^3. Their ratio is $K = \sigma/\gamma$ $= 0.28–0.34$. There are whiskers (in industry) and nanotubes (in scientific laboratories) with $K = 1–2$ (whisker) and $K=5–11$ (nanotubes). Theory predicts fiber, whisker and nanotubes could have K values ten times greater[5–7].
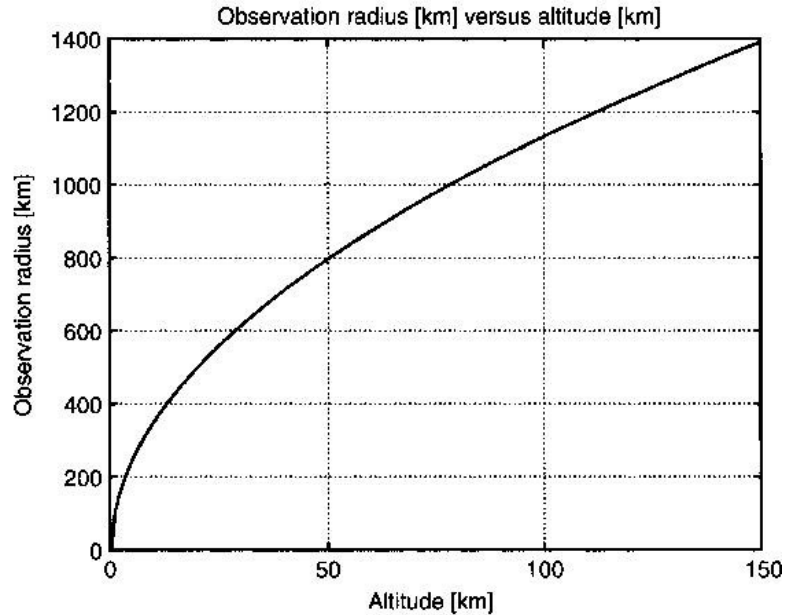

Fig. 4.5. Observation radius for altitudes up to 150 km.

The tower parameters have been computed for $K = 0.05 – 0.3$, with a recommended value of $K = 0.1$. The reader can estimate tower parameters for other strength ratios.

Tower safety. Many people think that inflatable construction is dangerous, on the basis that a small hole (damage) could deflate the tower. However that assumption is incorrect. The tower will have multiple vertical and horizontal sections, double walls (covers), and special devices (e.g. air balls) which will temporarily seal a hole. If a tower section sustains major damage, the tower height is only decreased by one section. This modularity is similar to combat vehicles – bullets many damage its tires, but the vehicle continues to operate.

Tower stability. Stability is provided by expansions (tensile elements). The verticality of the tower can be checked by laser beam and sensors monitoring beam location (Fig. 4.2). If a section deviates from vertical control cables, control devices, and pressure changes restore the tower position.

Tower construction. The tower building will not have conventional construction problems such as lifting building material to high altitude. All sections are identifiable. New sections are put in at the bottom of the tower, the new section is inflated, and the entire tower is lifted. It is estimated the building may be constructed in 2–3 months. A small tower (up to 3 km) can be located in a city.

Tower cost. The inflatable tower does not require high cost building materials. The tower will be a hundred times cheaper than conventional solid towers 400–600 m tall.

Theory of Inflatable Towers
(all equations in metric system)
Equations developed and used by author for estimations and computation are provided below.

1. **The pressure of any gas in a column versus altitude.**
   The given molecular weight, μ, temperature, T, of an atmospheric gas mixture, gravity, g, of planet, and atmospheric pressure, P, versus altitude, H, may be calculated using the equation

   $$P = P_o \exp(-\mu g H/RT) \quad \text{or} \quad P_r = P/P_o = \exp(-aH), \quad (4.1)$$

   where P_o is the pressure at the planet surface (for the Earth $P_o \approx 10^5$ [N/m^2]), $R = 8314$ is gas constant. For air: $\mu = 28.96$, for hydrogen: $\mu = 2$, for helium $\mu = 4$; $a = \mu g/(RT)$.

2. **Optimal cover thickness and tower radius.**
   Let us consider a small horizontal cross-section of tower element. Using the known formulas for mass and stress, we write

   $$Pds = gdm, \quad dm = 2r\gamma\delta dH, \quad s = \pi(R^2 - r^2), \quad R = r + dr, \quad ds = 2\pi r dr, \quad (4.2)$$

   where m – cover mass [kg], γ – cover specific weight [kg/m^3], σ – cover tensile stress [N/m^2], d – sign of differential, s – tower cross-section area which supports a tower cover [m^2], $g = 9.81$ [m/s^2] gravity, R, r – radius of tower [m], $\pi = 3.14$, P is surplus internal gas pressure over outside atmosphere pressure [N/m^2].
   Substituting the above formulas in the first equation, we get

   $$pdr = g\gamma\delta dH . \quad (4.3)$$

   From equations for stress we find the cover thickness

   $$2RPdH = 2\delta\sigma dH \quad \text{or} \quad \delta = RP/\sigma . \quad (4.4)$$

   If we substitute (4.4) in (4.3) and integrate, we find

   $$R = R_o \exp(-gH/k) \quad \text{or} \quad R_r = R/R_o = \exp(-gH/k), \quad (4.5)$$

   where R_r is relative radius, R_o is base tower radius [m], $k = \sigma/\gamma$.

3. **Tower lift force F**

   $$F = PS, \quad S = S_r S_o, \quad S_r = \pi(R_r R_o)^2/S_o, \quad S = S_o R_r^2, \quad (4.6)$$

   $$F = PS_o R_r^2 , \quad (4.7)$$

   where $S_o = \pi R_o^2$ is a cross-section tower area at $H = 0$, $S_r = S/S_o$ is the relative cross-section pf the tower area.
   If we substitute (4.1), (4.5) in (4.7) we find

   $$F = P_o S_o \exp[-(a+2\pi g/k)H] \quad \text{or} \quad F_r = F/P_o S_o = \exp[-(a+2\pi g/k)H], \quad (4.8)$$

   where F_r is the relative force.

4. **Base area for a given top load W [kg].** The required base area S_o (and radius R_o) for given top load W may be found from (4.8) if $F = gW$.

   $$P_o S_o = gW/F_r(H_{max}) \quad \text{and} \quad R_o = (S_o/\pi)^{1/2} . \quad (4.9)$$

5. **Mass of cover.** From (4.2)

   $$dm = 2\pi R\gamma\delta dH . \quad (4.10)$$

   If we substitute (4.1),(4.4) and (4.5) in (4.10) we find

   $$dm = (2\pi/k)P_o S_o\{\exp[-(a+2\pi/k)H]\}dH . \quad (4.11)$$

   Integrate this relation from H_1 to H_2, we get

   $$M = [2\pi P_1 S_1/k(a+2\pi g/k)][F_r(H_1) - F_r(H_2)] , \quad (4.12)$$

   or relative mass (for $H = 0$) is

   $$M_r = M/(P_o S_o) = [2\pi/k(a+2\pi g/k)](1 - F_r) . \quad (4.13)$$

6. **The thickness of a tower cover** may be found from equations (4.4),(4.5) and (4.1)

$$\delta = (\pi/\gamma k)P_oR_o\{\exp[-(a+\pi g/k)H]\} \ . \tag{4.14}$$

Relative thickness is

$$\delta_r = \delta/P_oR_o = (\pi/\gamma k)\{\exp[-(a+\pi g/k)H]\} \ . \tag{4.15}$$

7. **Maximum safety bending moment** (example, from wind) [see (4.8) and (4.5)]
$$M_b = FR = R_oP_oS_oR_rF_r \tag{4.16}$$

or relative bending moment is

$$M_{b,r} = M_b/(R_oP_oS_o) = R_rF_r \ . \tag{4.17}$$

8. **Gas mass M into tower**. Let us write the gas mass as a small volume and integrate this expression

for altitude:
$$dm_g = \rho dV, \quad dV = \pi R^2 dH, \quad \rho = \mu P / RT = \rho_0 P_r, \tag{4.18}$$

where V is volume, ρ is gas density, ρ_1 is gas density at altitude H_1. If we substitute P_r from (4.1), integrate, and substitute F_r from (4.8), we have
$$M_g = [\pi\rho_1 R_1{}^2/(a+2\pi g/k)][F_r(H_1) - F_r(H_2)] \ , \tag{4.19}$$

where lower index "$_1$" means values for lower end and "$_2$" means values for top end.,,
Relative gas mass is
$$M_{g,r} = M_g / \rho_1 R_1^2 = [\pi /(a + 2\pi g / k)][F_r(H_1) - F_r(H_2)]. \tag{4.20}$$

9. **Base tower radius.** We get from (4.8) for $F = gW$.
$$R_1 = (gW/\pi P_1 R_r)^{1/2} \ , \tag{4.21}$$

where W is the top load [kg].

10. **Tower mass M [kg] is**
$$M = \pi R_1{}^2 P_1 \ . \tag{4.22}$$

Distance L of Earth view from a high tower
$$L \approx (2R_eH + H^2)^{0.5} \ ,$$

(4.23)
where $R_e = 6,378$ km is the Earth's radius. Results of computations are presented in Figs. 4.4 to 4.5.

Project 1. A simple air tower of 3 km height
(Base radius 5 m, 15 ft, $K = 0.1$)

This inexpensive project provides experience in design and construction of a tall inflatable tower, and of its stability. The project also provides funds from tourism, radio and television. The inflatable tower has a height of 3 km (10,000 ft). Tourists will not need a special suit or breathing device at this altitude. They can enjoy an Earth panorama of a radius of up 200 km. The bravest of them could experience 20 seconds of free-fall time followed by 2g overload.

 Results of computations. Assume the additional air pressure is 0.1 atm, air temperature is 288 ºK (15 ºC, 60 ºF), base radius of tower is 5 m, $K = 0.05 – 0.3$. Take $K = 0.1$, computations of radius are presented in Fig. 4.6. If the tower cone is optimal, the tower top radius must be 4.55 m. (Fig. 4.6). The maximum useful tower top lift is 46 tons (Fig. 4.7). The cover thickness is 0.087 mm at the base and 0.057 mm at the top (Fig. 4.8). The outer cover mass is only 11.5 tons (Fig. 4.9). If we add light internal partitions, the total cover weight will be about 16 – 18 tons (compared to 3 million tons for the 553 m tower in Toronto). Maximum safe bending moment versus altitude (as presented in Fig. 4.10) ranges from 390 ton×meter (at the base) to 210 ton×meter at the tower top.

Economic efficiency. Assume the cost of the tower is $5 million, its life time is 10 years, annual

maintenance $1 million, the number of tourists at the tower top is 200 (15 tons), time at the top is 0.5 hour, and the tower is open 12 hours per day. Then 4800 tourists will visit the tower per day, or 1.7 million per year. The unit cost of one tourist is (0.5 + 1)/1.7 = 1 $/person. If a ticket costs $9, the profit is 1.7×8 = $13.6 million per year. If a for drop from the tower (in a special cabin, for a free-fall (weightlessness) time of 20 seconds, followed by a overload of 2g) costs $5 and 20% of tourists take it, the additional profit will be $1.7 million
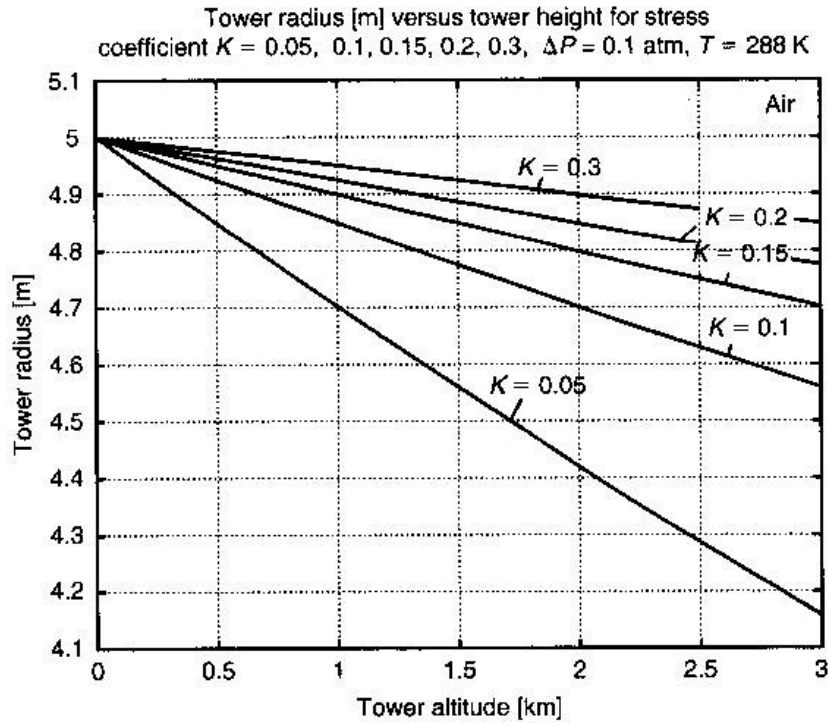

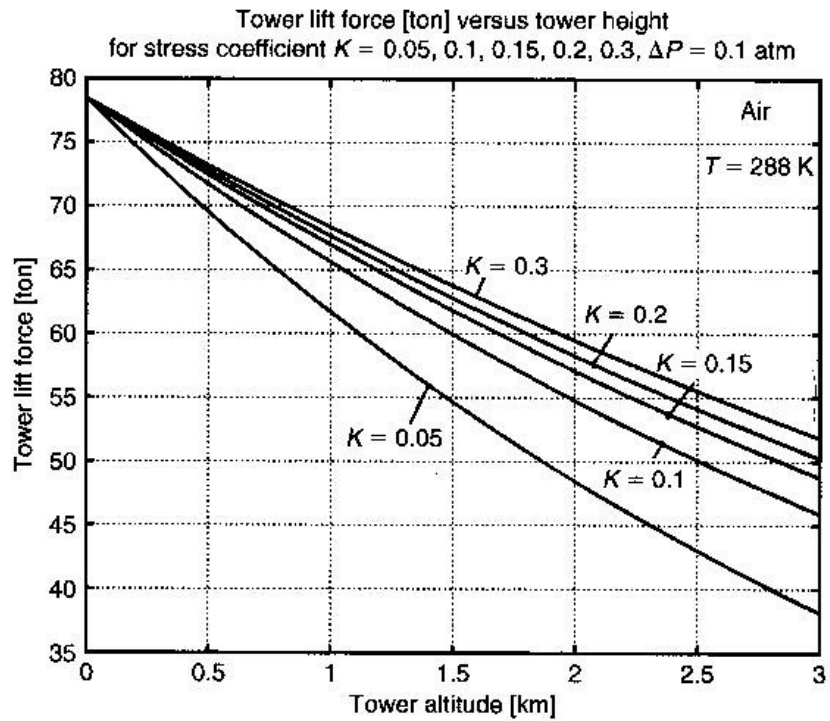**Fig. 4.6.** Tower radius versus tower height for the 3-km air tower.
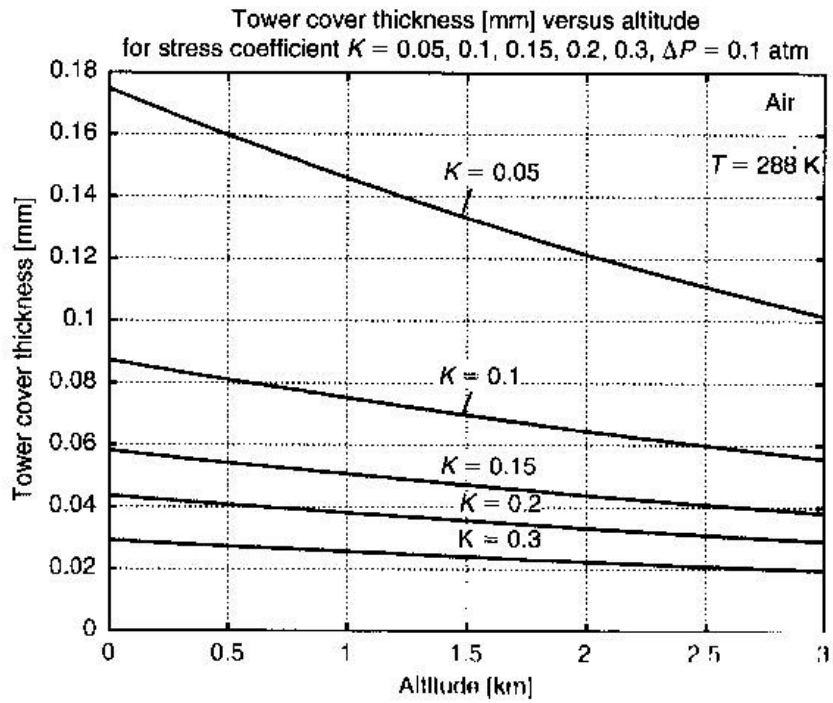
Tower lift force [ton] versus tower height
for stress coefficient K = 0.05, 0.1, 0.15, 0.2, 0.3, ΔP = 0.1 atm

Air

T = 288 K

K = 0.3

K = 0.2

K = 0.15

K = 0.05

K = 0.1

Tower altitude [km]

Tower lift force [ton]

Fig. 4.7. Tower lift force versus tower height for the 3-km air tower.

Tower cover thickness [mm] versus altitude
for stress coefficient K = 0.05, 0.1, 0.15, 0.2, 0.3, ΔP = 0.1 atm

Air

T = 288 K

K = 0.05

K = 0.1

K = 0.15

K = 0.2

K = 0.3

Altitude [km]

Tower cover thickness [mm]

Fig. 4.8. Tower cover thickness for the 3-km air tower.

Cover mass [ton] versus stress coefficient K
for base radius 5 m, altitude 3 km, cover density = 1800 kg/m^3,
temperature 288 K, ΔP = 0.1 atm, gas is air (μ = 28.96)
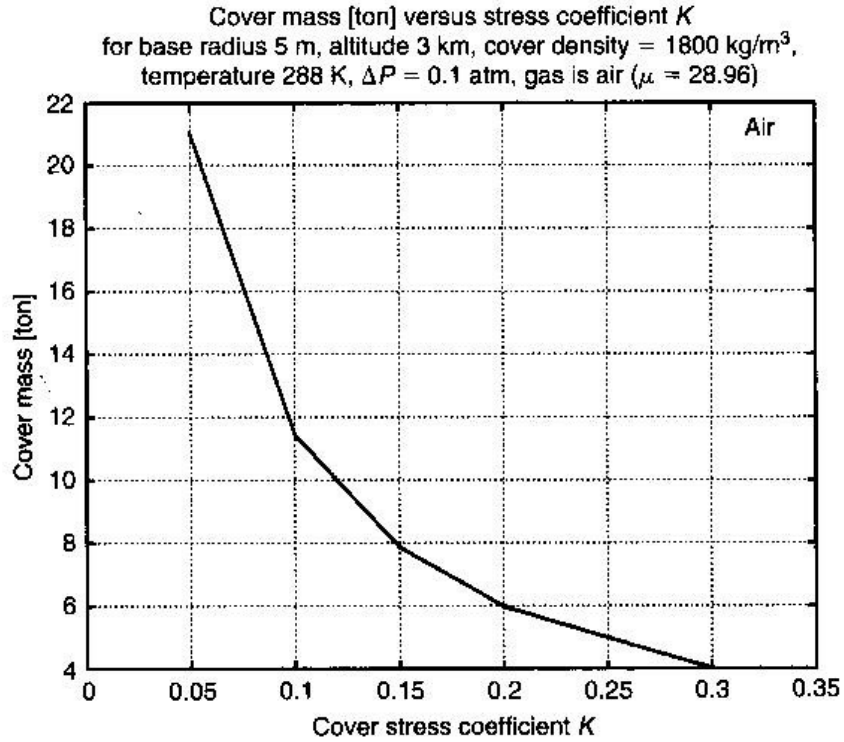
Fig. 4.9.   Cover mass of the 3-km air tower versus stress coefficient.

Maximum safe bending moment [ton m] versus altitude
and stress coefficient K = 0.05, 0.1, 0.15, 0.2, 0.3,
P = 0.1 atm, base radius 5 m, ΔP = 0.1 atm
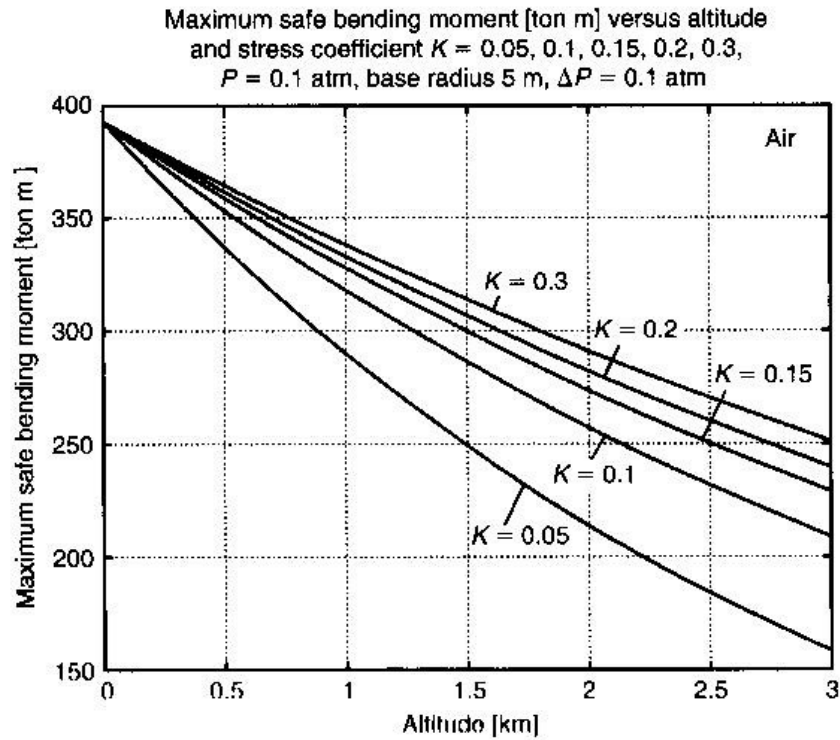

Fig. 4.10. Maximum safe bending moment

Project 2. Helium tower 30 km
(Base radius is 5 m, 15 ft, $K = 0.1$)

   Results of computation. Let us take the additional pressure over atmospheric pressure as 0.1 atm. The change of air and helium pressure versus altitude are presented in Figs. 4.3 and 4.4. The change of radius versus altitude is presented in Fig. 4.11. For $K = 0.1$ the radius is 2 m at an altitude of 30 km.   The useful lift force is presented in Figs. 4.12 and 4.15. For $K = 0.1$ it is about 75 tons at an altitude of 30 km, thus it is a factor of two times greater than the 3 km air tower. It is not surprising, because the helium is lighter than air and it provides a lift force. The cover thickness is presented in Fig. 4.13. It changes from 0.08 mm (at the base) to 0.42 mm at an altitude of 9 km and decreases to 0.2 mm at 30 km. The outer cover mass is about 370 (Fig. 4.14) tons. Required helium mass is 190 tons (Fig. 4.16).
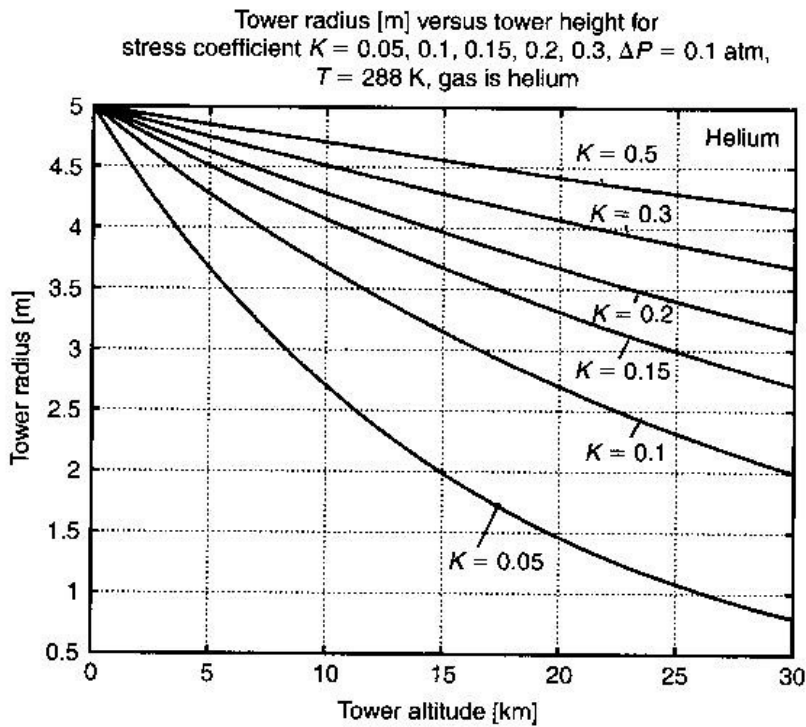

Fig. 4.11.   Tower radius versus tower height for the 30-km helium tower.

Tower lift force [ton] versus tower height for base radius 5 m,
stress coefficient K = 0.05, 0.1, 0.15, 0.2, 0.3, ΔP = 0.1 atm,
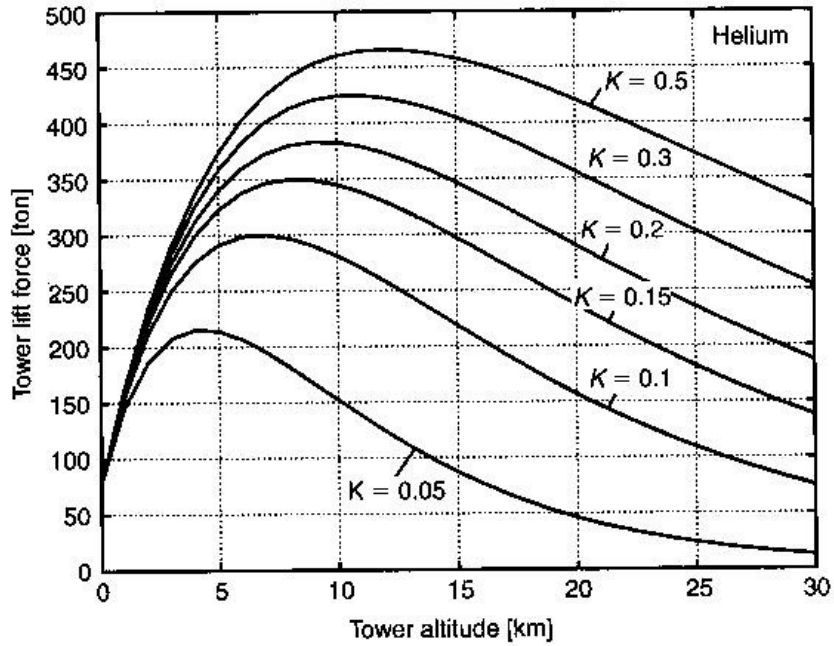T = 288 K, gas is helium

Fig. 4.12. Tower lift force versus tower height for the 30-km helium tower.

Tower cover thickness [mm] versus altitude
for stress coefficient K = 0.05, 0.1, 0.15, 0.2, 0.3, ΔP = 0.1 atm,
base radius 5 m, T = 240 K, gas is helium

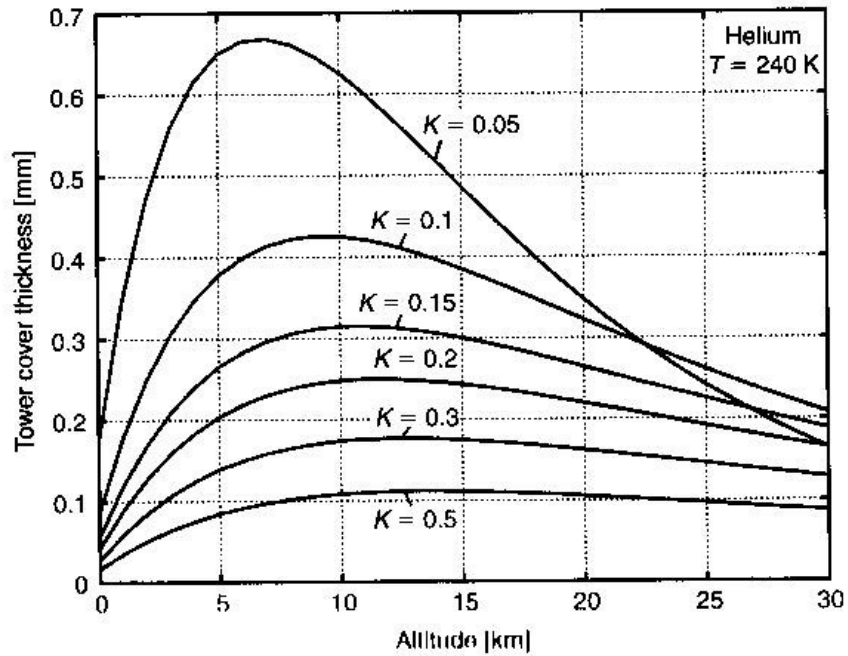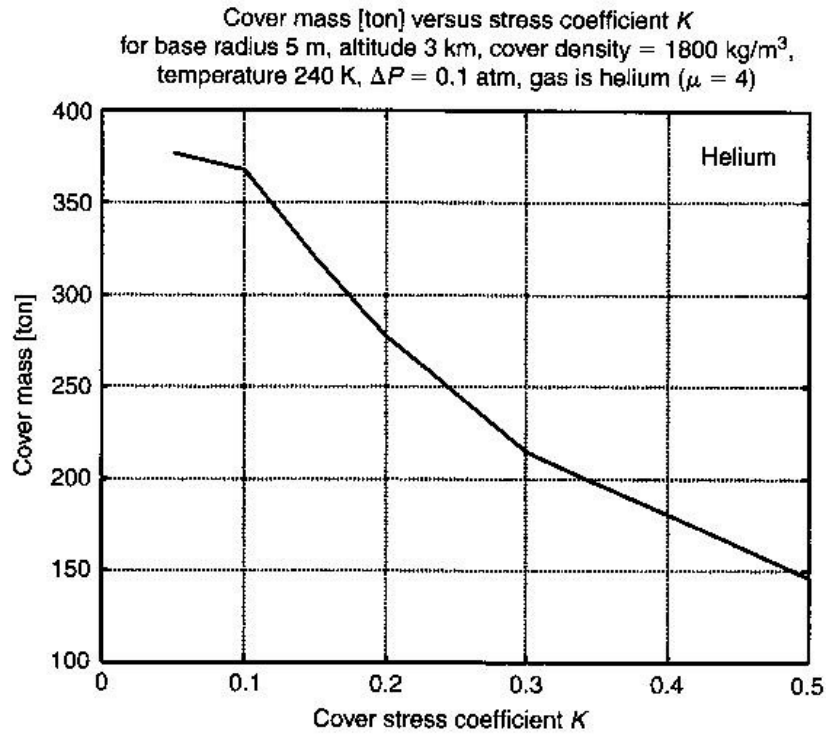**Fig. 4.13.** Tower cover thickness versus tower height for the 30-km helium tower.

Cover mass [ton] versus stress coefficient K
for base radius 5 m, altitude 3 km, cover density = 1800 kg/m³,
temperature 240 K, ΔP = 0.1 atm, gas is helium (μ = 4)

Fig. 4.14. Cover mass versus stress coefficient for the 30-km helium tower.

Top tube lift forces[ton] versus stress coefficient K,
for base radius 5 m, altitude 30 km, T = 240 K, cover
density = 1800 kg/m³, ΔP = 0.1 atm
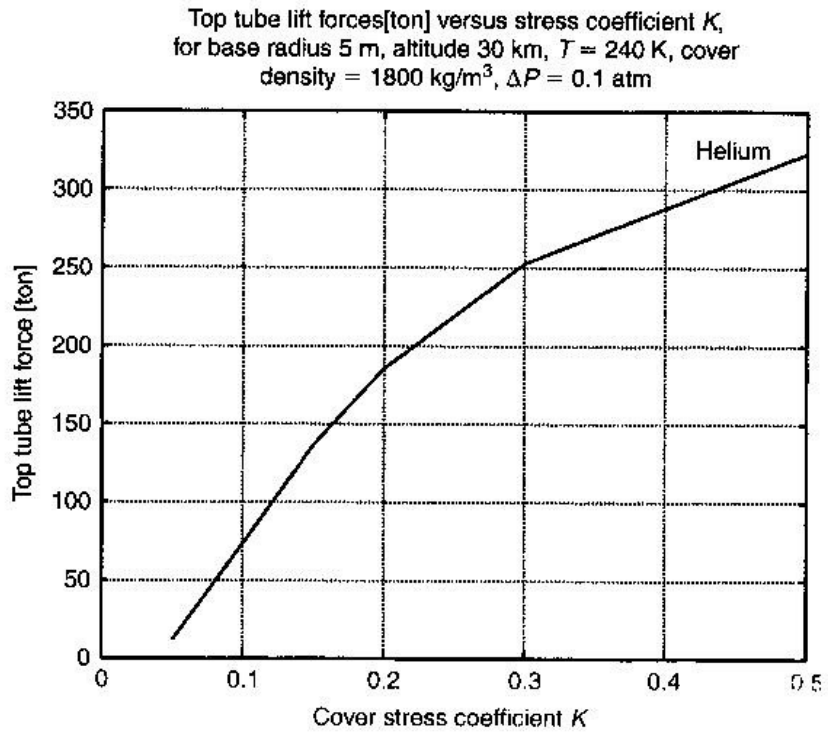
Fig. 4.15. Top lift force for the 30-km helium tower.

Helium mass into tube [ton] versus stress coefficient K, for base radius 5 m, altitude 30 km, T = 240 K, cover density = 1800 kg/m³, ΔP = 0.1 atm
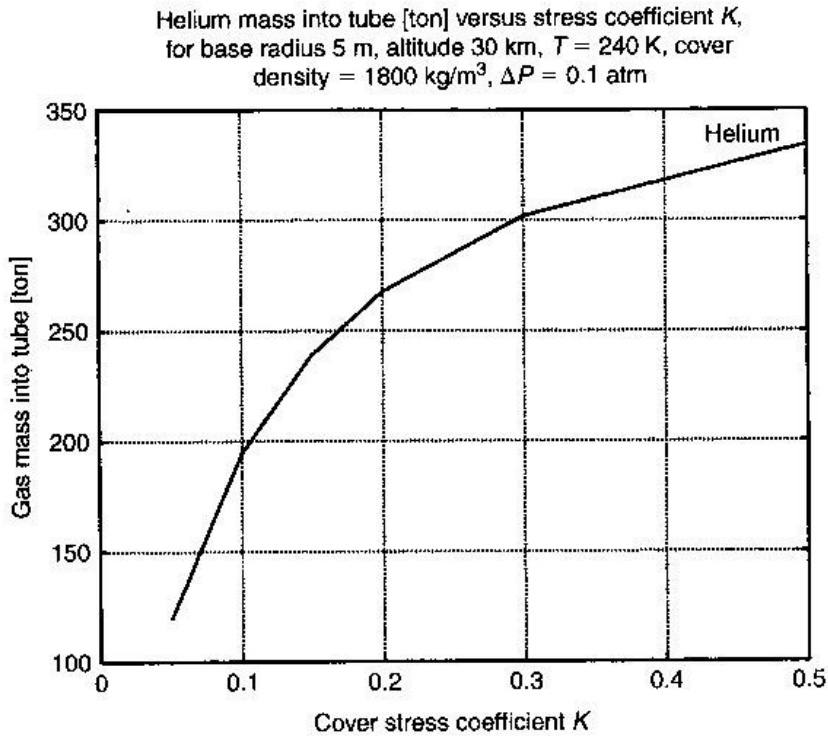
Fig. 4.16. Helium mass for the 30-km tower.

The tourist capability of this tower is twice than of the 3 km tower, but all tourists must stay in cabins.

Project 3. Air-hydrogen tower 100 km
(Base radius of air part is 35 m, the hydrogen part has base radius 5 m)

This tower is in two parts. The lower part (0–15 km) is filled with air. The top part (15–100 km) is filled with hydrogen. It makes this tower safer, because the low atmospheric pressure at high altitude decreases the probability of fire. Both parts may be used for tourists.

Air part, 0–15 km. The base radius is 25 m, the additional pressure is 0.1 atm, average temperature is 240 °K, and the stress coefficient $K = 0.1$. Change of radius is presented in Fig. 4.17, the useful tower lift force in Fig. 4.21, and the tower outer tower cover thickness is in Fig. 4.18, maximum safe bending moment is in Fig. 4.19, the cover mass in Fig. 4.20. This tower can be used for tourism and as an astronomy observatory. For $K = 0.1$, the lower (0–15 km) part of the project requires 570 tons of outer cover (Fig. 4.20) and provides 90 tons of useful top lift force (Fig. 4.21).
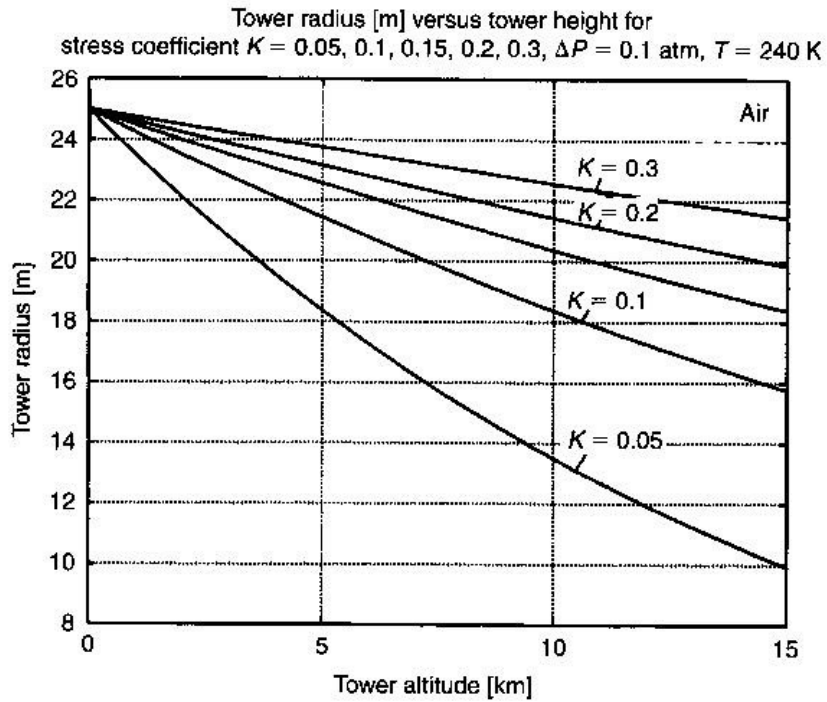
Tower radius [m] versus tower height for
stress coefficient K = 0.05, 0.1, 0.15, 0.2, 0.3, ΔP = 0.1 atm, T = 240 K

Fig. 4.17. Air lower part of 100-km tower. Tower radius versus altitude.

Tower cover thickness [mm] versus altitude for
stress coefficient K = 0.05, 0.1, 0.15, 0.2, 0.3, ΔP = 0.1 atm,
base radius 25 m, T = 240 K, gas is air
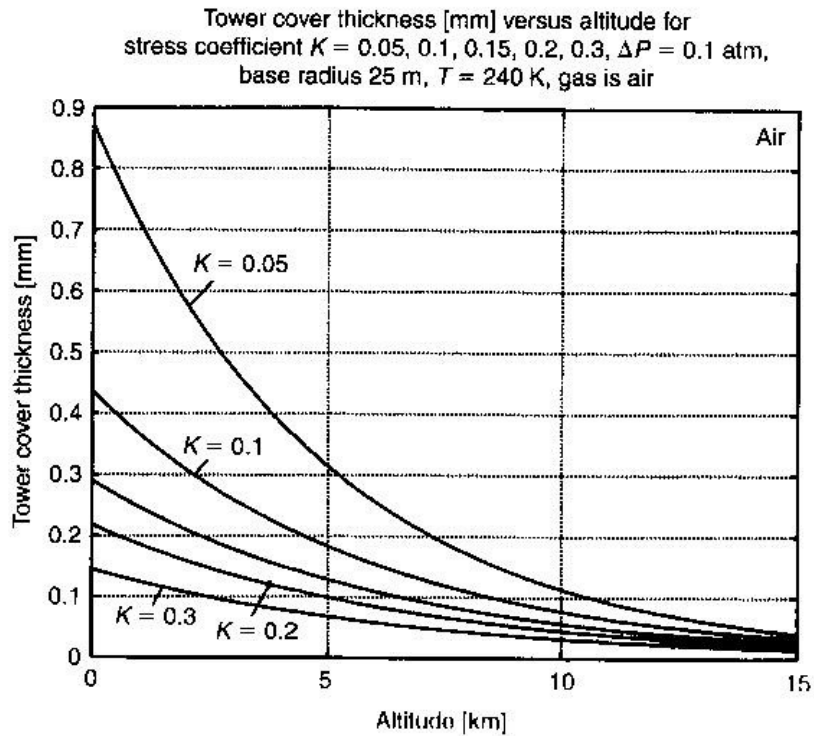
Fig. 4.18. Air lower part of 100-km tower. Tower cover thickness versus altitude.

Maximum safe bending moment [ton m] versus altitude
and stress coefficient $K = 0.05, 0.1, 0.15, 0.2, 0.3$, $P = 0.1$ atm,
base radius 25 m, $\Delta P = 0.1$ atm, $T = 240$ K, gas is air
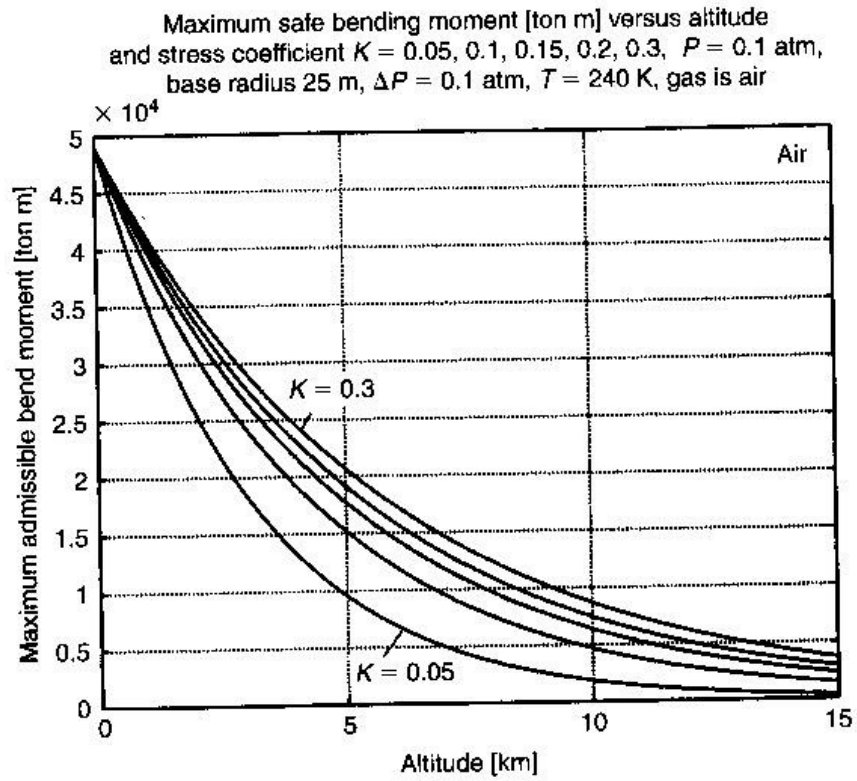
Fig. 4.19. Air lower part of 100-km tower. Maximum safe bending moment.

Cover mass [ton] versus stress coefficient K
for base radius 25 m, altitude 15 km, cover density = 1800 kg/m^3,
temperature 240 K, $\Delta P = 0.1$ atm, gas is air ($\mu = 28.96$)
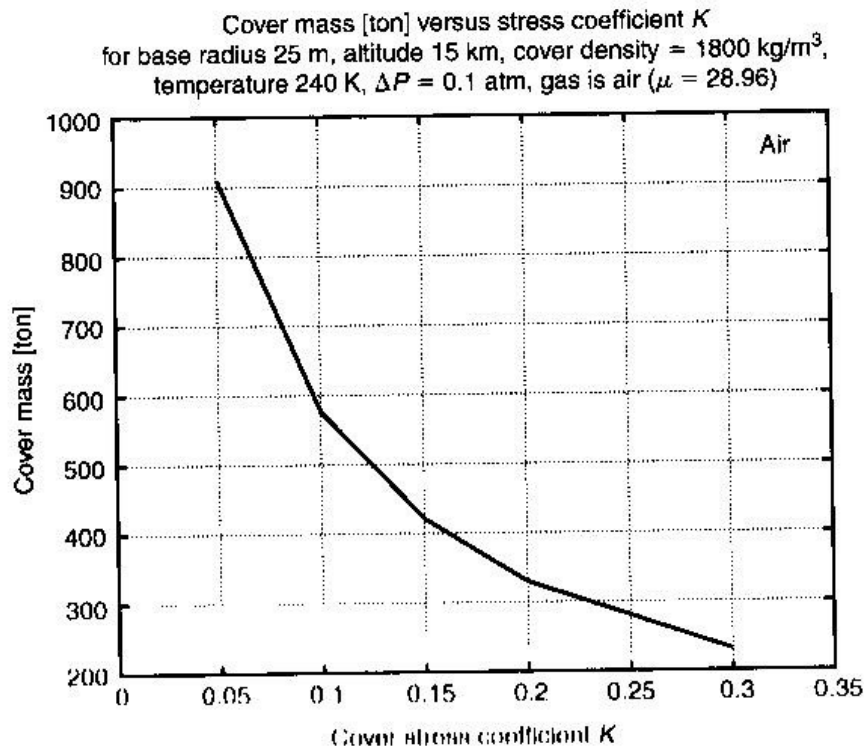
Fig. 4.20. Air lower part of 100-km tower. Cover mass.

Top tube lift forces [ton] versus stress coefficient K,
for base radius 25 m, altitude 15 km, $T = 240$ K,
cover density $= 1800$ kg/m^3, $\Delta P = 0.1$ atm, gas is air
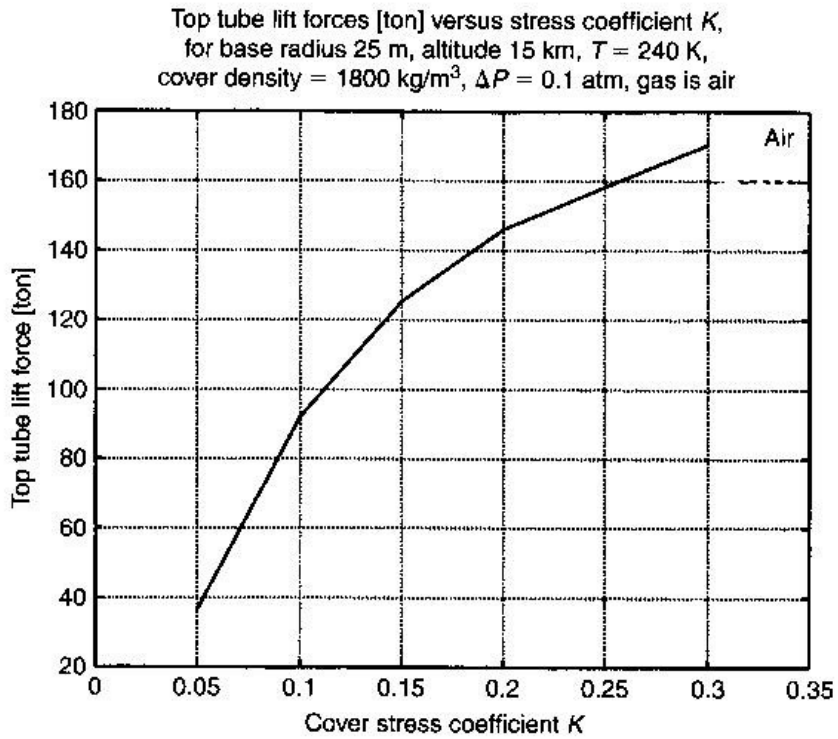
Fig. 4.21. Air lower part of 100-km tower. Top lift force.

Tower radius [m] versus tower height
for stress coefficient $K = 0.05, 0.1, 0.15, 0.2, 0.3$, $\Delta P = 0.1$ atm,
$T = 240$ K, gas is hydrogen
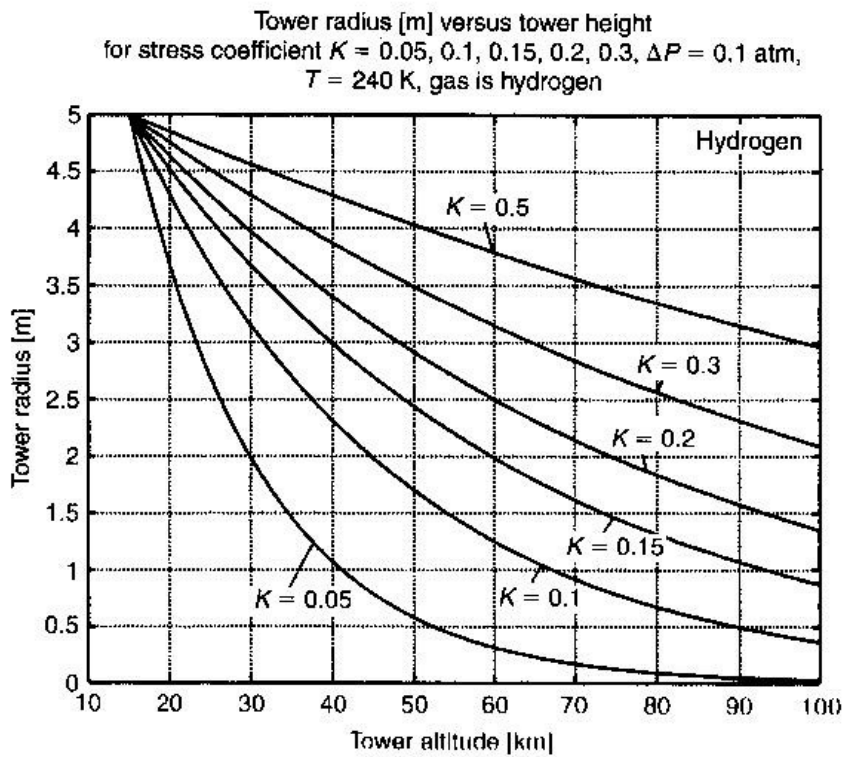
Fig. 4.22. Hydrogen top part of 100-km tower. Tower radius versus altitude.

Tower lift force [ton] versus tower height for base radius 5 m,
stress coefficient K = 0.05, 0.1, 0.15, 0.2, 0.3, ΔP = 0.1 atm,
T = 240 K, gas is hydrogen
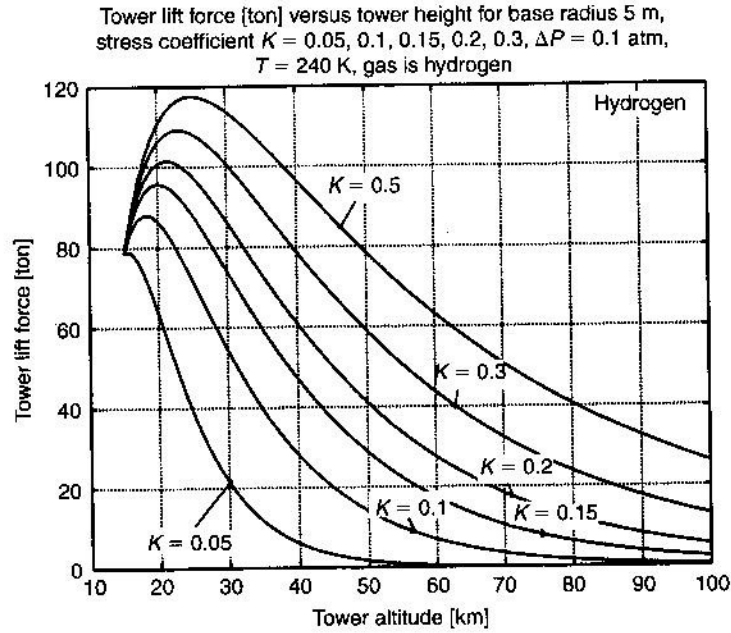
Fig. 4.23. Hydrogen top part of 100-km tower. Tower lift force versus altitude.

Tower cover thickness [mm] versus altitude
for stress coefficient K = 0.05, 0.1, 0.15, 0.2, 0.3, 0.5 ΔP = 0.1 atm,
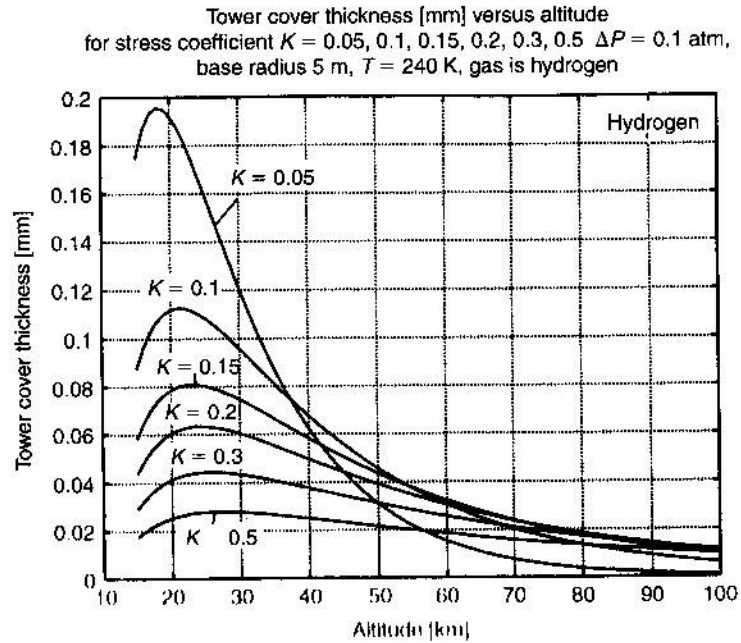base radius 5 m, T = 240 K, gas is hydrogen

Fig. 4.24 Hydrogen top part of 100-km tower. Tower cover thickness.

Hydrogen part, 15–100 km. This part has base radius 5 m, additional gas pressure 0.1 atm, and requires a stronger cover, with $K = 0.2$.

The results of computation are presented in the following figures: the change of air and hydrogen pressure versus altitude are in Fig. 4.3; the tower radius versus altitude is in Fig. 4.22; the tower lift force versus altitude is in Fig. 4.23; the tower thickness is in Fig. 4.24; the cover mass is in Fig. 4.25; the lift force is in Fig. 4.26; hydrogen mass is in Fig. 4.27.
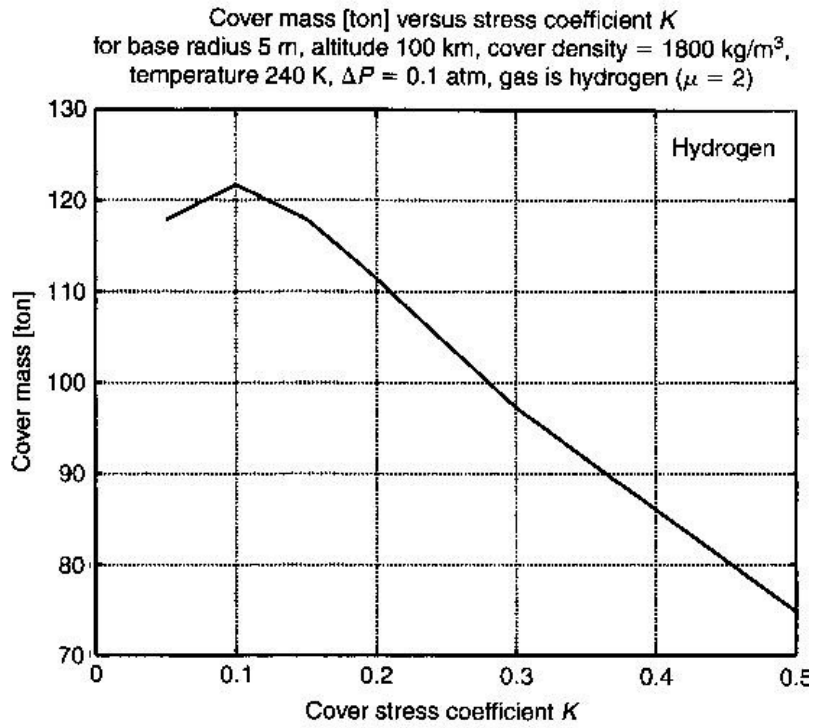
Cover mass [ton] versus stress coefficient K
for base radius 5 m, altitude 100 km, cover density = 1800 kg/m^3,
temperature 240 K, $\Delta P = 0.1$ atm, gas is hydrogen ($\mu = 2$)

Fig. 4.25. Hydrogen top part of 100-km tower. Cover mass.

Top tube lift forces [ton] versus stress coefficient K,
for base radius 5 m, altitude 100 km, $T = 240$ K,
cover density =1800 kg/m^3, $\Delta P = 0.1$ atm, gas is hydrogen ($\mu = 2$)
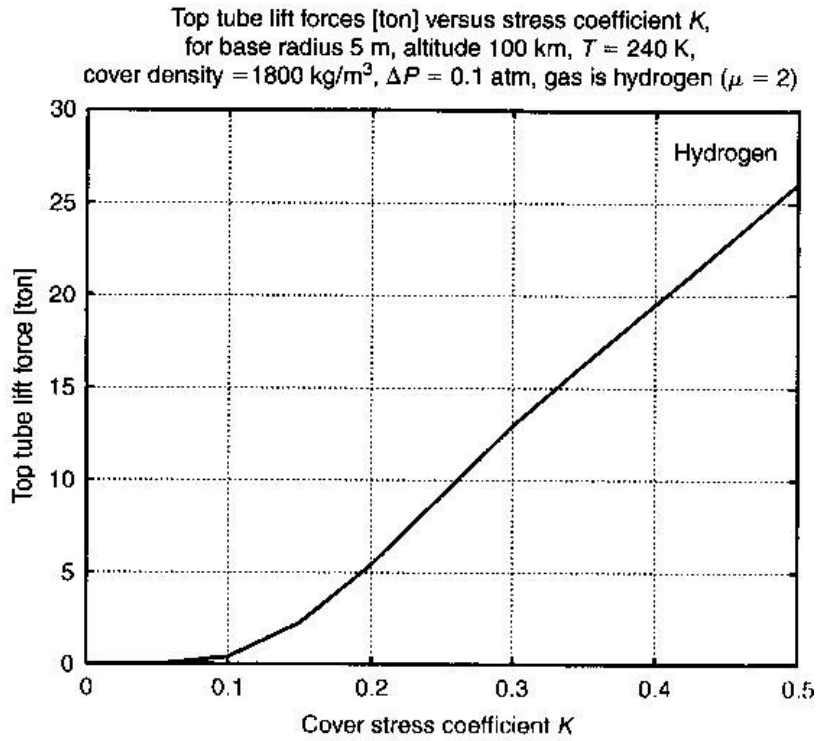
Fig. 4.26. Hydrogen top part of 100-km tower. Tower top lift force.

Hydrogen mass into tube [ton] versus stress coefficient K,
for base radius 5 m, altitude 100 km, $T = 240$ K,
cover density $= 1800$ kg/m^3, $\Delta P = 0.1$ atm
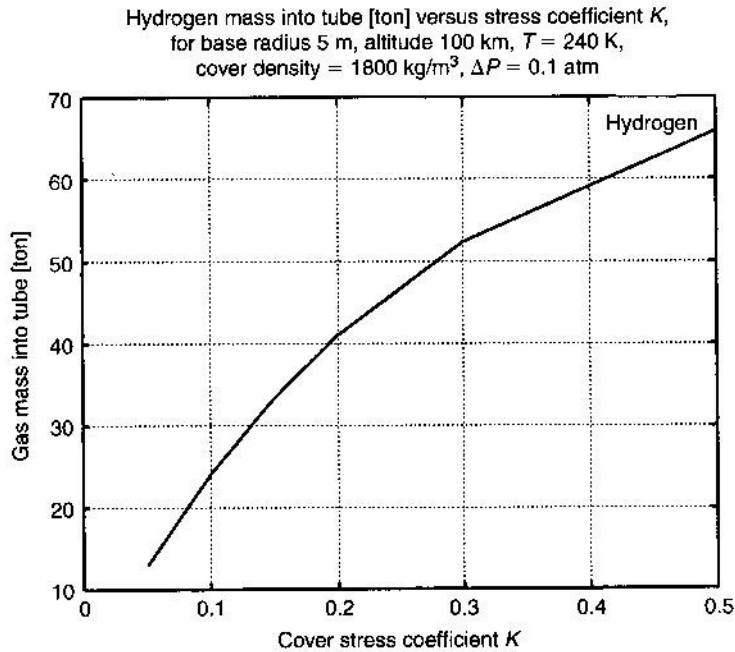

Fig. 4.27. Hydrogen top part of 100-km tower. Required hydrogen mass.

The useful top tower load can be about 5 tons, maximum, for $K = 0.2$. The cover mass is 112 tons (Fig. 4.25), the hydrogen lift force is 37 tons. The top tower will press on the lower part with a force of only $112 - 37 + 5 = 80$ tons. The lower part can support 90 tons.

Readers can easily calculate any variant by using the presented figures.

The proposed projects use the optimal change of radius, but designers must find the optimal combination of the air and gas parts.

Conclusion

The presented theory and computation show that an inexpensive tall tower can be designed and constructed and can be useful for industry, government and science.

The author has developed the innovation, estimation, and computations for the above mentioned problems. Even though these projects may seem impossible using current technology, the author is prepared to discuss the details with serious organizations that want to develop these projects.

References for Chapter 4

1. D.V. Smitherman, Jr., "Space Elevators", NASA/CP-2000-210429.
2. K.E. Tsiolkovski:"Speculations Abot Earth and Sky on Vesta", Moscow, Izd-vo AN SSSR, 1959; Grezi o zemle i nebe (in Russian), Academy of Sciences, USSR., Moscow, p. 35, 1999.
3. A.C. Clarke: *Fountains of Paradise*, Harcourt Brace Jovanovich, New York, 1978.
4. J.T. Harris, *Advanced Material and Assembly Methods for Inflatable Structures*. AIAA, Paper No. 73-448 (1973).
5. F.S. Galasso, *Advanced Fibers and Composite*, Gordon and Branch Science Publisher, 1989.
6. *Carbon and High Performance Fibers*, Directory, 1995.
7. M.S. Dresselhous, *Carbon Nanotubes*, Springer, 2000.
8. A.A. Bolonkin, "Optimal Inflatable Space Towers with 3-100 km Height", *JBIS*, Vol. 56, pp. 87–97, 2003.
9. Geoffrey A. Landis, Craig Cafarelli, The Tsiolkovski Tower Re-Examined, *JBIS*, Vol. 32, p. 176–180, 1999.

Chapter 5
Kinetic Space Towers*
Summary

This chapter discusses a revolutionary new method to access outer space. A cable stands up vertically and pulls up its payload into space with a maximum force determined by its strength. From the ground the cable is allowed to rise up to the required altitude. After this, one can climb to an altitude using this cable or deliver a payload at altitude. The author shows how this is possible without infringing the law of gravity.

  The chapter contains the theory of the method and the computations for four projects for towers that are 4, 75, 225 and 160,000 km in height. The first three projects use the conventional artificial fiber widely produced by current industry, while the fourth project use nanotubes made in scientific laboratories. The chapter also shows in a fifth project how this idea can be used to launch a load at high altitude.

Introduction

Lyrical note. Many people have seen films showing trick by Indian magician. The magician arrives at an Indian village, calls the residents, and shows them the trick. He shows a flexible rope to the people, then he takes this rope, says the magic words, flips the rope, and it stands up vertically. A boy climbs up to the top of the rope and descends. The magician again says the magic words and the rope fall down.

  I have asked a lot of scientists: what is the scientific explanation of this trick. This is hypnosis. However, you can hypnotize people, but you cannot hypnotize a camcorder.

 Current access to outer space is described in references[1–12].

  This chapter suggests a very simple and inexpensive method and installation for lifting and launching into space. This method is different from the centrifugal method[6] in which a cable circle or semi-circle and a centrifugal force are used, which keeps the space station at high altitude. In the offered method there is a straight line vertical cable connecting the space station to the Earth's surface. The space station is held in place by reflected cable and cable kinetic (shot) energy. The offered method expends more than twice as little energy in air drag because the cable length is twice as short as in the semi-circle and has a shorter distance (vertical beeline) than a full circle.

  This is a new method and transport system for delivering payloads and people into space. This method uses a cable and any conventional engine (mechanical, electrical, gas turbines) located on the ground. After completing an exhaustive literature and patent search, the author cannot find the same space method or similar facilities.

Description of Suggested Launcher

Brief Description of innovation

  The installation includes (see notations in Fig. 5.1a,b and others): a strong closed-loop cable, two rollers, any conventional engine, a space station, a load elevator, and support stabilization ropes.

The installation works in the following way. The engine rotates the bottom roller and permanently sends up the closed-loop cable at high speed. The cable reaches a top roller at high altitude, turns back and moves to the bottom roller. When cable turns back it creates a reflected (centrifugal) force. This force can easily be calculated using centrifugal theory, or as reflected mass using a reflection theory. The force keeps the space station suspended at the top roller; and the cable (or special elevator) allows the delivery of a load to the space station. The station has a parachute that saves people if the cable or engine fails.
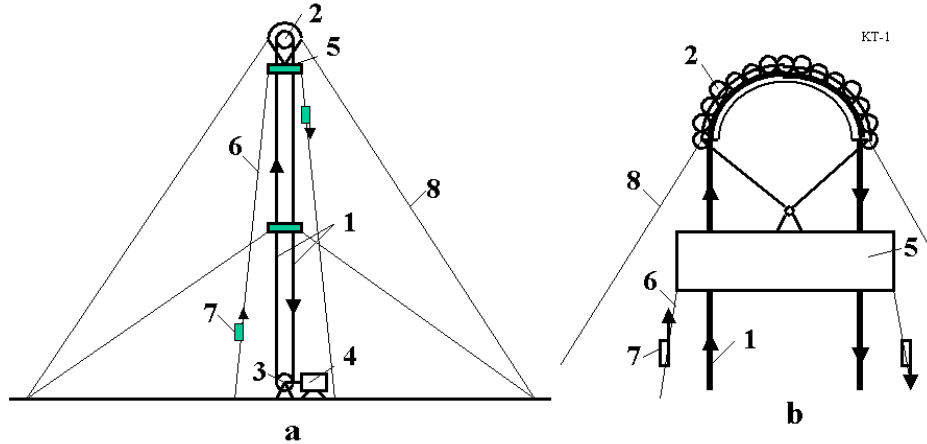

Fig. 5.1. a. Offered kinetic tower: 1 – mobile closed loop cable, 2 – top roller of the tower, 3 – bottom roller of the tower, 4 – engine, 5 – space station, 6 – elevator, 7 – load cabin, 8 – tensile element (stabilizing rope).   **b**. Design of top roller.

The theory shows, that current widely produced artificial fibers (see References[4–6] for cable properties) allow the cable to reach altitudes up to 100 km (see Projects 1 and 2). If more altitude is required a multi-stage tower must be used (Fig. 5.2, see also Project 3). If a very high altitude is needed (geosynchronous orbit or more), a very strong cable made from nanotubes must be used (see Project 4).

  The offered tower may be used for a horizon launch of the space apparatus (Fig. 5.3). The vertical kinetic towers support horizontal closed-loop cables rotated by the vertical cables. The space apparatus is lifted by the vertical cable, connected to horizontal cable and accelerated to the required velocity.

  The closed-loop cable can have variable length. This allows the system to start from zero altitude, and goves the ability to increase the station altitude to a required value, and to spool the cable for repair. The device for this action is shown in Fig. 5.4. The offered spool can reel in the left and right branches of the cable at different speeds and can change the length of the cable.

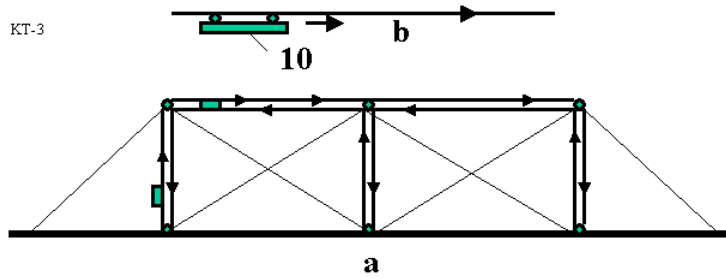**Fig. 5.2**. Multi-stage kinetic tower. Notations are same in Fig.5.1.

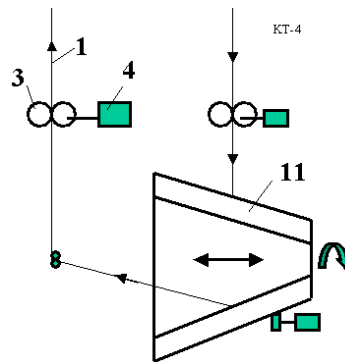**Fig. 5.3a.** Kinetic space installation with horizontally accelerated parts. **b**. 10 – accelerated missile.

Fig. 5.4. Variable cable spool. Notations: 1 – cable, 3 – rollers, 4 – engines, 11 – cable spool.

Advantages. The suggested towers and launch system have made big advances in comparison with the currently avalible towers and rocket systems:

They allow a very high altitude (up to geosynchronous orbit and more) to be reached, which is impossible for solid towers.

They are cheaper by some thousands at times than the current low towers. No expensive rockets are required.

The kinetic towers may be used for tourism, power, TV and radio signal relay a wide over very area, as a radio locator, are as a space launcher.

The offered towers and space launcher decrease the delivery cost by some thousand times (up to $1–$4 per lb weight).

The offered space tower launcher can be made in a few months, whereas the modern rocket launch system requires some years for development, design, and building.

The offered cable towers and space launcher do not require high technology and can be made by any non-industrial country from current artificial fibers.

Rocket fuel is expensive. The offered cable towers and space launcher can use the cheapest sources of energy such as wind, water or nuclear power, or the cheapest fuels such as gaseous gas, coal, peat, etc., because the engine is located on the Earth's surface. The flywheels may be used as an accumulator of energy.

There is no necessary to have highly qualified personnel such as rocket specialists with high salaries.

We can launch thousands of tons of useful loads annually.

The advantages of the offered method are the same as for the centrifugal launcher[6] (see also Chapter 3). The suggested method is approximately half the cost of the semi-circle launcher[6] because it uses only one double vertical cable. It also has approximately half the delivery cost (up to $2–4 per kg), because it has half the air drag and fuel consumption.

Cable discussing. The reader can find detail of the cable discussion in Chapter 1 and cable characteristics in References[5–6]. In the projects 1–3 we use only cheap artificial fibers widely produced by current industry.

Theory of the Kinetic Tower and Launcher

1. **Lift force of the kinetic tower**.

a) To find the lift force of the kinetic support device from centrifugal theory, take a small part of the rotary circle and write the equilibrium

$$\frac{2SR\alpha\gamma V^2}{R} = 2S\sigma \sin \alpha , \qquad (5.1)$$

where V is rotary cable speed [m/s], R is circle radius [m], α is angle of circle part [rad]. S is cross-section of cable areas [m^2], σ is cable stress [n/m^2], γ is cable density [kg/m^3].
When $\alpha \to 0$ the relationship between the maximum rotary speed V and the tensile stress of the closed loop (curve) cable is

$$V = \sqrt{\frac{\sigma}{\gamma}} = \sqrt{k} , \quad F = 2\sigma S , \qquad (5.2)$$

b) where F is the lift force [n], $k = \sigma/\gamma$ is the relative cable stress [m^2/s^2]. The computations of the first equation for intervals 0–1K, 1K–10K ($K = k/10^7$) are presented in Figs. 5.5 – 5.6.
We can find the lift force of the offered installation from theoretical mechanics. Writing the momentum of the reflected mass in one second we find

$$F = mV - (-mV) = 2mV, \quad m = \gamma SV, \quad or \quad F = 2\gamma SV^2 , \qquad (5.3)$$

where m is the cable mass reflected in one second [kg/s].
If we substitute equation (5.2) in (5.3), the expression for lift force $F = 2\sigma S$ will be the same. The computation of equation (5.2) for intervals 0–1K, 1K–10K ($K = k/10^7$) is presented in Figs. 5.5 and 5. 6.

2. **Lift force in a constant gravity field**. In a constant gravity field without air drag, the lift force of the offered device equals the centrifugal force F minus the cable weight W

$$F_g = F - W = F - 2\gamma gSH = 2\gamma S(V^2 - gH) = 2S(\sigma - \gamma gH) = 2S\gamma(k - gH), \qquad (5.4)$$

where H is the altitude of the kinetic tower [m].

3. **Maximum tower height or minimum cable speed in a constant gravity field** are (from equation (5.4)):

$$H_{max} = \frac{\sigma}{g\gamma} = \frac{k}{g} , \quad V_{min} = \sqrt{gH} . \qquad (5.5)$$

Computations for $K = 0$–1 are presented in Figs. 5.7 and 5.8. In this case the installation does not produce a useful lift force and will support only itself.
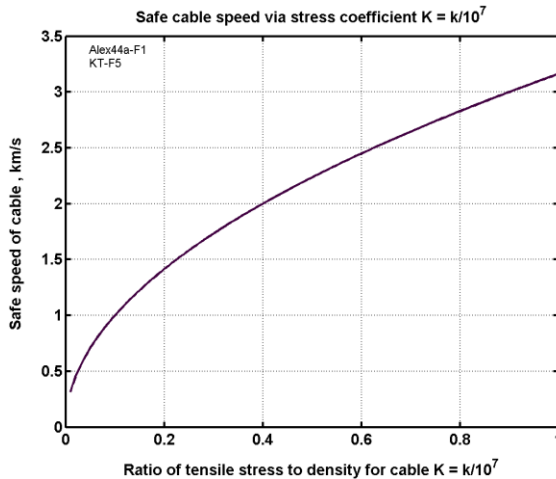

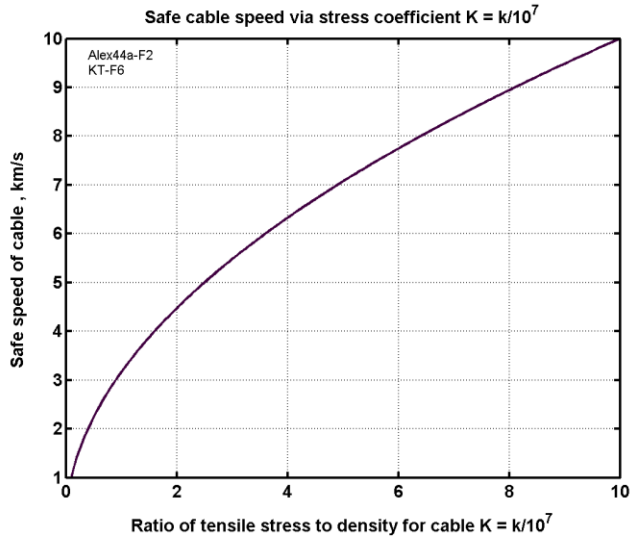**Fig. 5.5**. Safe cable speed via stress coefficient $K = 0$–1.

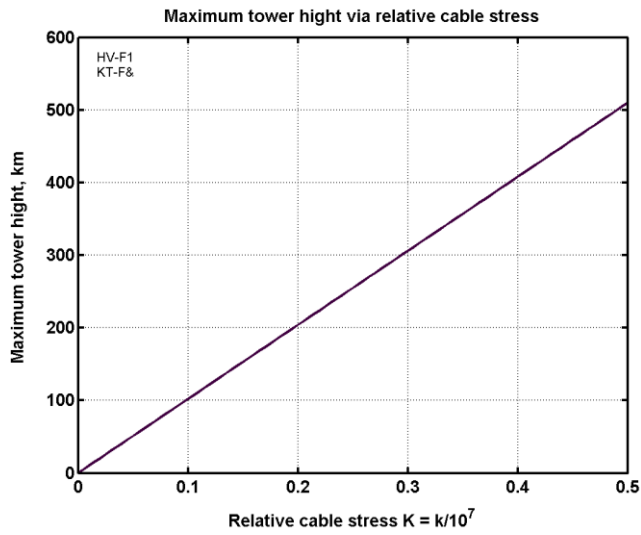**Fig. 5.6**. Safe cable speed via relative stress coefficient K = 1–10.

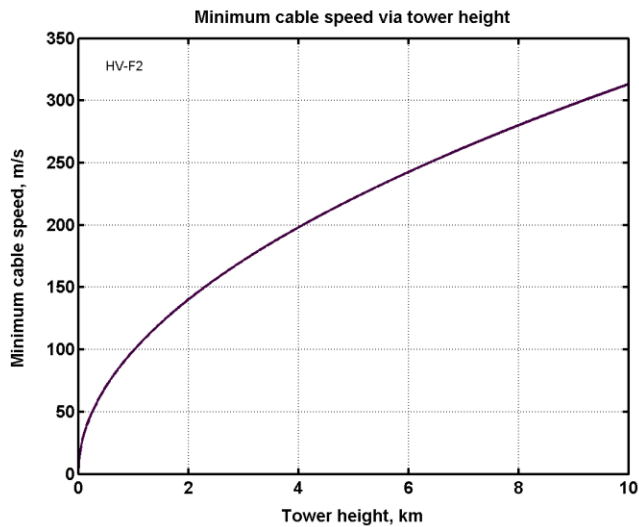**Fig. 5.7.** Maximum tower height via relative cable stress.

Fig. 5.8. Minimum cable speed via tower height.

4. Kinetic lift force in a variable gravity field and for the rotary Earth.

$$dP = \left(g - \frac{V^2}{R}\right)dm, \quad g = g_0\left(\frac{R_0}{R}\right)^2, \quad \frac{V^2}{R} = \omega^2 R, \quad dm = \gamma S dR, \quad R = R_0 + H,$$

$$P = \int_{R_0}^{R}\left[g_0\left(\frac{R_0}{R}\right)^2 - \omega^2 R\right]\gamma S dR = g_0\left(R_0 - \frac{R_0^2}{R}\right) - \frac{\omega^2}{2}\left(R^2 - R_0^2\right), \quad or \tag{5.6}$$

$$F = 2\sigma S - 2P = 2\gamma S k - 2P = 2\gamma S\left[k - g_0\left(R_0 - \frac{R_0^2}{R}\right) + \frac{\omega^2}{2}\left(R^2 - R_0^2\right)\right], \quad k = \frac{\sigma}{\gamma} = V^2,$$

where k is the relative cable stress. We will use a more convenient value for graphs of $K = 10^{-7}k$.
Minimum cable stress or minimum cable speed of a variable rotary planet equals

$$k_{min} = g_0\left(R_0 - \frac{R_0^2}{R}\right) - \frac{\omega^2}{2}\left(R^2 - R_0^2\right), \quad V_{min}^2 = g_0\left(R_0 - \frac{R_0^2}{R}\right) - \frac{\omega^2}{2}\left(R^2 - R_0^2\right). \tag{5.7}$$

Computation of these equations for Earth is presented in Figs. 5.9 and 5.10. If $K > 5$ the height of the kinetic tower may be beyond the Earth's geosynchronous orbit. For Mars this is $K > 1$, and for the Moon it is $K > 0.3$. One point to note from Fig. 5.9 the offered tower of a height of 145,000 km can be maintance without a cable rotation, and if the tower height is more 145,000 km, the tower has a useful lift force that allows a payload to be lifted using an immobile cable.
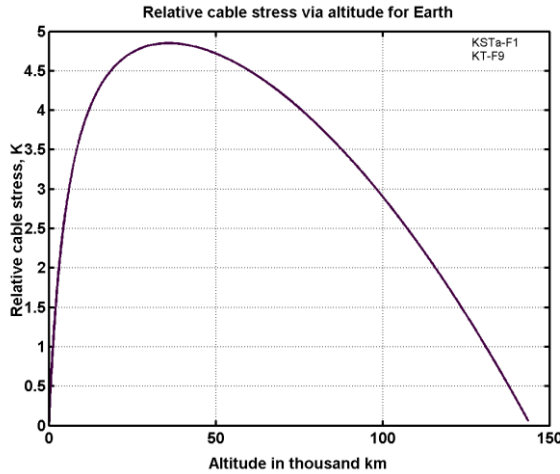

Fig. 5.9. Relative cable stress via altitude for rotary Earth with variable gravity.
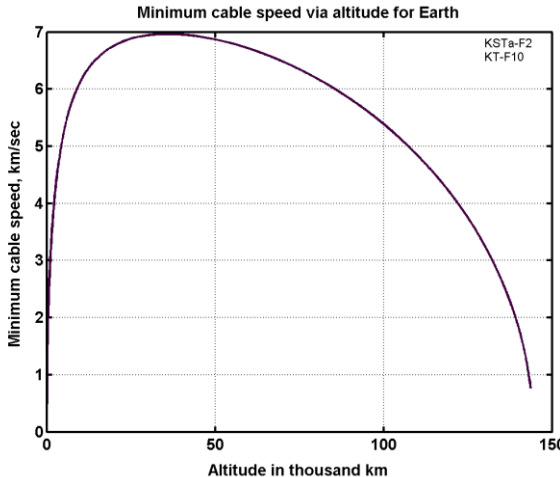

Fig. 5.10. Minimum cable speed via altitude for rotary Earth with variable gravity.

4. Estimation of cable friction in the air.

This estimation is very difficult because there are no experimental data for air friction of an infinitely thin cable (especially at hypersonic speeds). A computational method for plates at hypersonic speed described in the book *Hypersonic and High Temperature Gas Dynamics* by J.D. Anderson, p. 287[7], was used. The computation is made for two cases: laminar and turbulent boundary layers.

The results of this comparison are very different. Turbulent friction is greater than laminar friction by hundreds of times. About 80% of the friction drag occurs in the troposphere (from 0 to 12 km). If the cable end is located on the mountain at 4 km altitude the maximum air friction will be decreased by 30%.

It is postulated that half of the cable surface will have the laminar boundary layer because a small wind or trajectory angle will blow away the turbulent layer and restore the laminar flow. The blowing away of the turbulent boundary layer is studied in aviation and is used to restore laminar flow and decrease air friction. The laminar flow decreases the friction in hypersonic flow about by 280 times! If half of the cable surface has a laminar layer, it means that we must decrease the air drag calculated for full turbulent layer by a minimum of two times.

Below, the equation from Anderson[7] for computation of local air friction for a two-sided plate is given.

$$\frac{T^*}{T} = 1 + 0.032M^2 + 0.58\left(\frac{T_w}{T} - 1\right), \quad M = \frac{V}{a}, \quad \mu^* = 1.458 \times 10^6 \frac{T^{*1.5}}{T^* + 110.4},$$

$$\rho^* = \frac{\rho T}{T^*}, \quad R_e^* = \frac{\rho^* V x}{T^*}, \quad C_{f,L} = \frac{0.664}{(R_e^*)^{0.5}}, \quad C_{f,T} = \frac{0.0592}{(R_e^*)^{0.2}}$$

$$D_L = 0.5C_{f,l}\rho^*V^2S; \quad D_T = 0.5C_{f,t}\rho^*V^2S. \tag{5.8}$$

where: T^*, Re^*, ρ^*, μ^* are the reference (evaluated) temperature, Reynolds number, air density, and air viscosity respectively. M is the Mach number, a is the speed of sound, V is speed, x is the length of the plate (distance from the beginning of the cable), T is flow temperature, T_w is body temperature, $C_{f,l}$ is a local skin friction coefficient for laminar flow, $C_{f,t}$ is a local skin friction coefficient for turbulent flow. S is the area of skin [m²] of both plate sides, so this means for the cable we must take 0.5S; D is air drag (friction) [N]. It can be shown that the general air drag for the cable is $D_g = 0.5D_T + 0.5D_L$, where D_T is the turbulent drag and D_L is the laminar drag.

From equation (5.8) we can derive the following equations for turbulent and laminar flows of the vertical cable

$$D_T = \frac{0.0592\pi d}{4}\rho_0^{0.8}\left(\frac{T}{T^*}\right)^{0.8}\mu^{0.2}V^{1.8}\int_{H_0}^{H}h^{-0.2}e^{0.8bh}dh = 0.0547d\left(\frac{T}{T^*}\right)^{0.8}\mu^{0.2}V^{1.8}\int_{H_0}^{H}h^{-0.2}e^{0.8bh}dh,$$

$$\tag{5.9}$$

$$D_L = \frac{0.664\pi d}{4}\rho_0^{0.5}\left(\frac{T}{T^*}\right)^{0.5}\mu^{0.5}V^{1.5}\int_{H_0}^{H}h^{-0.5}e^{0.5bh}dh = 0.5766d\left(\frac{T}{T^*}\right)^{0.5}\mu^{0.5}V^{1.5}\int_{H_0}^{H}h^{-0.5}e^{0.5bh}dh,$$

where d is the diameter of the cable [m], $\rho_0 = 1.225$ is air density at $H = 0$. The laminar drag is less than the turbulent drag by 200–300 times and we can ignore it.

Engine power and additional cable stress can be computed by conventional equations:

$$P = 2DV, \quad \sigma = \pm\frac{D}{S} = \pm\frac{4D}{\pi d}, \tag{5.10}$$

where P is engine power [j, w]. The factor of 2 is because we have two branches of the cable: one moves up and the vother moves down. The drag does not decrease the lift force because in the different branches the drag is in opposite directions.

Computations are presented in Figs. 5.11 and 5.12 for low cable speed and relative cable stress $K = 0$–2, in Fig. 5.13 and 5.14 for high cable speed and the stress $K = 0$–10.
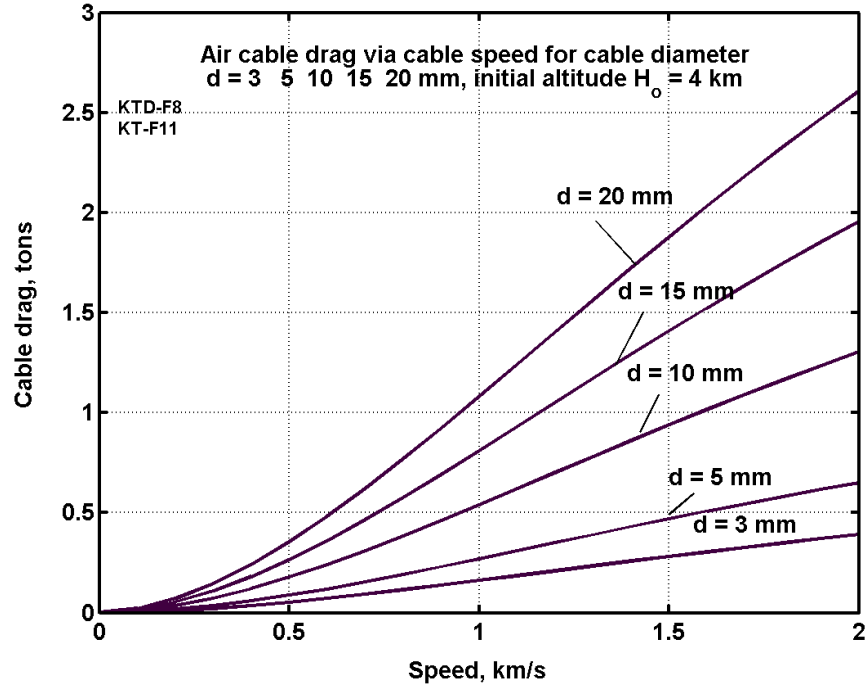
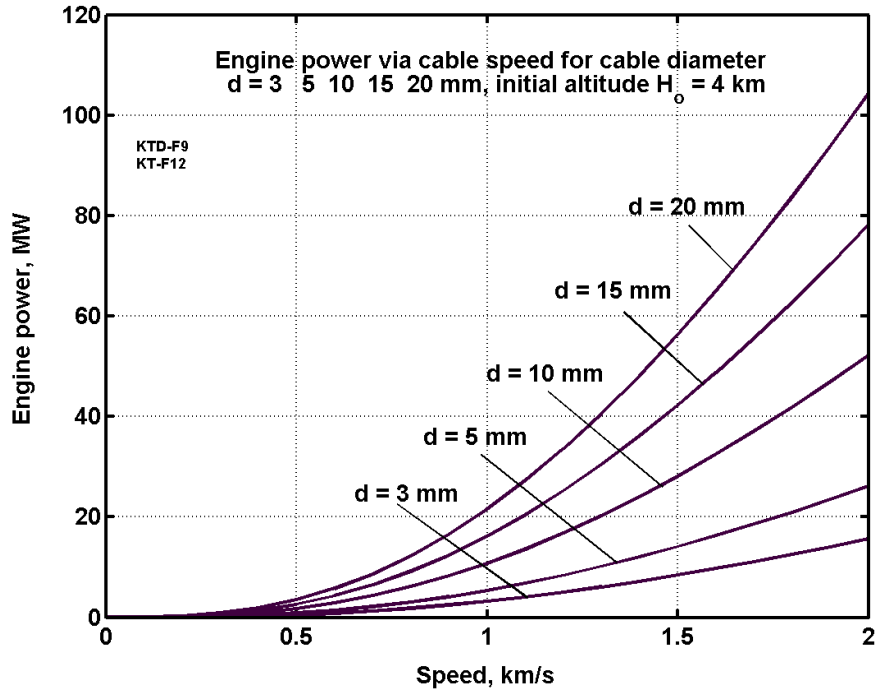**Fig. 5.11.** Air cable drag via cable speed 0–2 km/s for different cable diameter.

Fig. 5.12. Engine power via cable speed 0–2 km/s for different cable diameter.
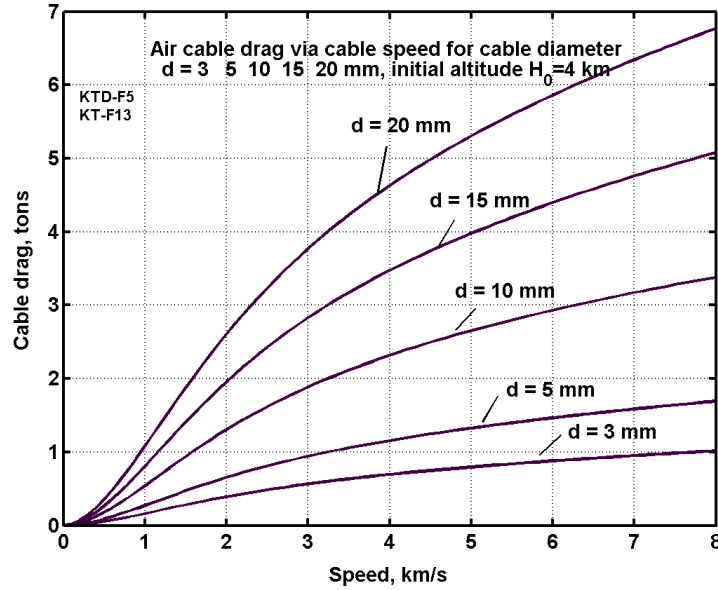
Fig. 5.13. Air cable drag via cable speed 2–8 km/s for different cable diameter.
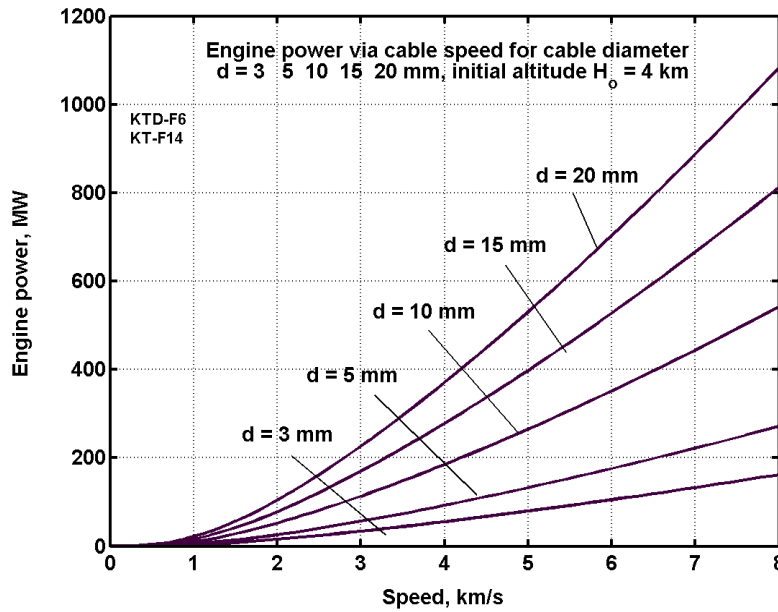
Fig. 5.14. Engine power via cable speed 2–8 km/s for different cable diameter.

6. People security. If the cable is damaged, the people can be rescued using a parachute with variable area. Below the reader will find equations and computations of the possibility of saving people on the tower. The parachute area is changed so that overload does not go belyod a given value ($N < 5g$).

$$\frac{dH}{dV} = -V, \quad \frac{dV}{dt} = g - \frac{D}{m}, \quad \frac{D}{m} = C_D \frac{\rho a V}{2p}, \quad p = \frac{0.5 C_D \rho a V}{gN}, \quad p \geq 0, \quad \frac{D}{mg} \leq N, \tag{5.11}$$

$$for \quad H = 0 - 10 km \quad \rho = 1.225 e^{-H/9218}, \quad for \quad H = 10 - \infty \quad \rho = 0.414 e^{-(H-10000)/6719}$$

where H is altitude [m], V is speed [m/s], t is time [seconds], m is mass [kg], D is drag [n], $g = 9.81$ m/s^2 is gravity, C_D is the drag coefficient, ρ is air density [kg/m^3], a is speed of sound [m/s], p is the parachutes specific load [kg/m^2], N is overload [g].

Computations are presented in Figs. 5.15 to 5.17. The conventional people (tourists) can be rescued from altitudes up to 250–300 km. The cosmonauts can outstay an overload up 8g and may be rescued from greater altitudes.

Fig. 5.15. Speed via altitude for variable parachute area. (See hard copy)

Fig. 5.16. Overload via altitude for variable parachute area.

Fig. 5.17. Parachute load via altitude.

Projects

Project #1. Kinetic Tower of Height 4 km

For this we can take a conventional artificial fiber widely produced by industry with the following cable performances: safe stress is $\sigma = 180$ kg/mm^2 (maximum $\sigma = 600$ kg/mm^2, safety coefficient $n = 600/180 = 3.33$), density is $\gamma = 1800$ kg/m^3, cable diameter $d = 10$ mm.

The special stress is $k = \sigma/\gamma = 10^6$ N/m^2 ($K = k/10^7 = 0.1$), safe cable speed is $V = k^{0.5} = 1000$ m/s, the cable cross-section area is $S = \pi d^2/4 = 78.5$ mm^2, useful lift force is $F = 2S\gamma(k-gH)=27.13$ tons. Requested engine power is $P = 16$ MW (equation (5.10)), cable mass is $M = 2S\gamma H = 2\cdot78.5\cdot10^{-6}\cdot1800\cdot4000 = 1130$ kg.

Assume that the tower is used for tourism with a payload of 20 tons. This means 20000/75 = 267 tourists may be in the station at same time. We take 200 tourists every 30 minutes, i.e. 200 × 48 = 9600 people/day. Let's say 9000 tourists/day which corresponds to 9000×350 = 3.15 million/year.

Assume the cost of installation is \$15 million[8] the life time is 10 years, and the maintenance cost is \$1 million per year. The cost of an installation to service a single tourist is 2.5/3.15 = \$0.8 per person.

The required fuel $G = Pt/\varepsilon\eta = 16\times10^6\times350\times24\times60\times60/(42\times10^6\times0.3) = 38.4\cdot10^6$ kg. If the fuel cost is \$0.25 per kg, the annual fuel cost is \$9.6 millions, or 9.6/3.15 = \$3.05 per person. Here t is annual time [s], ε is fuel heat capability [J/kg], and η is the engine efficiency coefficient.

The total production cost is 0.8 + 3.05 = \$3.85 per tourist. If a trip costs \$9, the annual profit is (9–3.85)×3.15 = 16.22 million of US dollars. If readers do not agree with this estimation, calculations can be made with other data.

Project 2. Kinetic Tower of Height 75 km

For this tower take the safe cable stress $K = 0.1$, the cross-section area $S = 90$ mm^2 ($d = 10.7$ mm), the cable density $\gamma = 1800$ kg/m^3. Then the lift force is $F = 2S\gamma(k-gH) = 7$ tons. The required engine power is $P = 11$ MW (equation (5.10), Fig. 5.12), cable mass is $M = 2S\gamma H = 2\times 90\times10^{-6}\times100\times75000 = 24.3$ tons, the cable speed is 1000 m/s.

Project 3. Multi-Stages Kinetic Tower of Height 225 km

Current industry widely produces only a cheap artificial fiber with maximum stress $\sigma= 500$–620 kg/mm^2 and density $\gamma = 1800$ kg/m^3. We take an safe stress $\sigma = 180$ kg/mm^2 (safety coefficient is $n = 600/180 = 3.33$), $\gamma = 1800$ kg/m^3. Then $k = \sigma/\gamma = 1000000$ N/m^2 or $K = k/10^7 = 0.1$. From this cable one can design a one-stage kinetic tower with a maximum height 100 km (payload = 0). Assume we want to design a tower height is 225 km high using the current material. We can design then 3- stage tower with each stage at height $H = 75$ km and useful load capability $M_{3,p} = 3$ tons at the tower top.

In this case the 3rd (top) stage (150–225 km) must have a cross-section area $S_3 = M_{3,p}/[2\gamma(k-gH)] = 33.3$ mm^2 ($d = 6.5$ mm), and the cable mass of the 3rd stage is $M_{3,c} = 2S_3\gamma H = 9$ tons. Total mass of third stage is $M_3 = 9 + 3 = 12$ tons.

The 2nd stage (75–150 km) must have a cross-section area $S_2 = M_3/[2\gamma(k–gH)] = 133$ mm^2 ($d = 13$ mm), and the cable mass of 2rd stage is $M_{2,c} = 2S_2\gamma H = 36$ tons. Total mass of third + second stages is $M_2 = 12 + 36 = 48$ tons.

The 1st stage (0–75 km) must have cross-section area $S_1 = M_2/[2\gamma(k–gH)] = 533$ mm^2 $(d = 26$ mm), and the cable mass of the 1rd stage is $M_{1,c} = 2S_2\gamma H = 144$ tons. Total mass of third + second+ first stages is $M_0 = 48 + 144 = 192$ tons.

Project 4. Kinetic Tower with Height 160,000 km

Assume that nanotube cable is used, with $K = 6$ (for this height K must be more than 5, see Fig. 5.8). This means the safe stress is $\sigma = 6,000$ kg/mm^2 and the cable density is $\gamma = 1000$ kg/m^3. At the present time (2000) scientific laboratories produce nanotubes with $\sigma = 20,000$ kg/mm^2 and density $\gamma = 0.8$–1.8 kg/m^3. Theory predicts $\sigma = 100,000$ kg/mm^2. Unfortunately, there are no widely produced industrial nanotubes and the laboratory samples are very expensive.

Take a cross-section cable area of 1 mm^2. The required speed is $V = (k)^{0.5} = (6 \cdot 10^7)^{0.5} = 7.75$ km/s, the mass of cable is $M = S\gamma H = 320$ tons, and the engine power (only in an installation launch) is $P = 50$ kW (equation (5.10)). When full altitude is reached the engine can be turned off and the centrifugal force of the Earth's rotation will support the cable. Moreover, the installation has a lift force of about 1000 kg, so a useful load can be connected to the cable, the engine can be turned on or slow speed and the load can be delivered into space.

Project 5. Kinetic Tower as Space Launcher

The suggested installation of Fig. 5.3 can be used as a space launcher. The space apparatus is lifted to high altitude by the left kinetic tower, connected to the horizon line and accelerated. The required acceleration distance depends on the safe acceleration. For a projectile it may be 10–50 km ($N = 64$–320g), for cosmonauts it may be 400 km ($N = 8$g), for tourists it may be 1100 km ($N = 3$g).

Discussion

The proposed method offers a new, simpler, cheaper, more realistic method for space launches than many others. It is impossible to demand immediately solutions to all problems. This is only the start of much research and development of the associated problems. The purpose here is to offer a new idea and show that it has good prospects, but it needs further research.

It is thought that this method has a big future. It does not need expensive rockets as current methods do, or rockets to launch a counterbalance into space and thousands of tons of nanotube cable as the space elevator does. It only needs conventional cable and a conventional engine located on a planet. It is very important not to dismiss new ideas when they are first contained.

References

1. Space Technology & Application. International Forum, parts 1-3, Albuquerque, MN, 1996–1997.

2. D.V. Smitherman Jr., "Space Elevators", NASA/CP-2000-210429.

3. A.A. Bolonkin, "Hypersonic Gas-Rocket Launch System.", AIAA-2002-3927, 38th AIAA/ASME/SAE/ASEE Joint Propulsion Conference and Exhibition, 7–10 July, 2002. Indianapolis, IN, USA; IAC-02-S.P.15, World Space Congress-2002/Oct. 10–19, Houston, USA; Journal *Actual problems of aviation and aerospace systems*, No.1, V.8, 2003, pp. 45–58, Kazan, Daytona Beach.

5. A.A. Bolonkin, "Asteroids as Propulsion Systems of Space Ships", *JBIS*, Vol. 58, 3–4, pp. 98–107.

6. A.A. Bolonkin, "Space Cable Launchers", Paper 8057 at Symposium "The Next 100 years", 14–17 July 2003, Dayton, Ohio, USA.

6. A.A. Bolonkin, "Centrifugal Keeper for Space Stations and Satellites", *JBIS*, Vol 56, pp. 314-322, Sept–Oct 2003.

7. J.D. Anderson, *Hypersonic and High Temperature Gas Dynamics*. McGraw-Hill Book Co.,1989.

8. D.E. Koell, *Handbook of Cost Engineering*, TCS, Germany, 2000.

9. A.A. Bolonkin, "Kinetic Space Towers and Launchers", *JBIS*, Vol. 57, Nos 1/2, 2004, pp.33–39.

Chapter 6
Gas Tube Hypersonic Launcher*

Summary
The present chapter describes a hypersonic gas rocket, which uses tube walls as a moving compressed air container. Suggested burn programs (fuel injection) enable use of the internal tube components as a rocket. A long tube (up to 0.4–0.8 km) provides mobility and can be aimed in water. Relatively inexpensive oxidizer and fuel are used (compressed air or gaseous oxygen and kerosene). When a projectile crosses the Earth's atmosphere at an angle more then 15°, loss of speed and the weight of the required thermal protection system are small. The research shows that the launcher can give a projectile a speed of up to 5–8 km/s. The proposed launcher can deliver up to 85,000 tons of payloads to space annually at a cost of one to two dollars per pound of payload. The launcher can also deliver about 500 tons of mail or express parcels per day over continental distances and may be used as an energy station and accumulator. During war, this launch system could deliver military munitions to targets thousands to tens of thousands of kilometers away from the launch site.

Main Nomenclature (metric system):

C_p – heat capability at constant pressure $C_p = 1.115$ [kJ/kg·°K] for air, $C_p = 1.069$ for oxygen,
C_v – heat capability at constant volume,
G_p – mass of the projectile (payload)[kg],
$K = C_p/C_v$ – coefficient, $k = 1.34$ for air; $k = 1.2$ for rocket gas,
L – length of launch tube [m],
L_r – length of rocket air column [m],
M – mass of rocket [N],
M_k – rocket mass at end of acceleration [N],
M_o – rocket mass at beginning of acceleration [N],
V – speed of rocket [m/s],
V_o – speed of the rocket after initial acceleration [m/s],
V_p – projectile speed after being shot at sea level [m/s],
ΔV – increment of rocket velocity [m/s],
w – speed of gas after nozzle [m/s],
P – pressure of gas from nozzle [atm],
P_o – initial pressure of gas in tube,
Q – amount of heat [J],
R – gas low constant, $R = 287$ for air, $R = 325$ for rocket gas,
t – time [seconds],
T – absolute temperature, °K,
θ – trajectory angle to a horizon [degrees].
β – fuel rate [kg/s],

$\mu = M_k/M_o$ – relative mass of rocket.

Introduction

Unfortunately, most specialists, when they see projectiles in tubes, think of a gun (cannon). They know very well that a gun cannot give a projectile speed of more than 1–2 km/sec [1–5]. They also know that a gas gun using hydrogen can give a speed of up to 3–4 km/s, which however is still not enough for space flight.

 A high-speed ground-based gun is very large, complex and expensive, and can shoot only from one point on the Earth or in Space[6–12], therefore they do not want to read or hear about a new revolutionary method.–

 As is shown in the Reference[12] the offered installation is a gas rocket in a tube. It looks like the solid traveling charge gun[13–14], but the offered tube rocket uses air and kerosene as fuel (not powder as in the traveling charge gun).

 Short history of the high speed gun. The first high-speed gun was the Krupp gun in World War 1. After World War II research into a big high-speed gun was made in project HARP[11].

 The cannon had a caliber of 16.4 inches (417 mm), with a barrel length at 45–126 calipers (18.8–52.5 m), and the weight of the gunpowder was 780 lbs (351 kg). Maximum pressure reached 340 MPa (3400 atm). The projectile weighing 38 lbs (17 kg) had speeds up to 6000–6135 ft/s (2 km/s). Iraq made the most recent attempt to create a big cannon, which was destroyed by the UN.

 A gun with a solid traveling charge was studied by the Ballistic Research Laboratory[13, 14]. They used solid gunpowder as rocket fuel and a small bore (5/8 inch)(9.5 mm). The traveling charge gun was initiated at the Ballistic Research Laboratories, Aberdeen Proving Group, Maryland. The objective of their paper [13] is to show that it is possible to build a device capable of accelerating small projectiles (weight range of 1 to 5 grams) to velocities in excess of 20,000 ft/s (6 km/s) without subjecting the projectile to severe acceleration force. Their result is as follows.

 In theory there is no upper limit to the velocity that can be attained. All that is required is more propellant and a longer barrel. However the shot time is about 4 ms and the required fast burning rate of 2000 inches/second is three orders of magnitude greater than the burning rate of solid gun propellants. This problem could not be solved by using a porous (grains) propellant (gunpowder). It was noted that it could be possible for the propellant to detonate. Some experiments with ball powder in a long tube (analogous to a long grain of porous propellant) have indicated that rapid burning of the propellant may change over a detonation.

 The suggested method and installation[15,16] uses conventional compressed air (as oxidizer) and conventional kerosene (as fuel). The barrel is long (up to 0.4–1 km) and the time of the shot is long (up to 0.5–1.2 s). The injection fuel program keeps constant pressure in the rocket (constant thrust) and avoids detonation. Other differences and advantages are shown later.

Description

 Fig. 6.1a shows a design of the tube of the suggested hypersonic gas-rocket system. The system is made up of a tube, a piston with a fuel tank and payload, and nozzle connected to the piston, and valves.

 The tube rocket engine can be made without a special nozzle (Fig. 6.1b). In this case, the fuel efficiency of the gas-rocket engine will decrease but its construction becomes simpler.

 The tube may be placed into a frame (Fig. 6.1c). The frame is placed into water and connected to a ship for mobility and aiming.
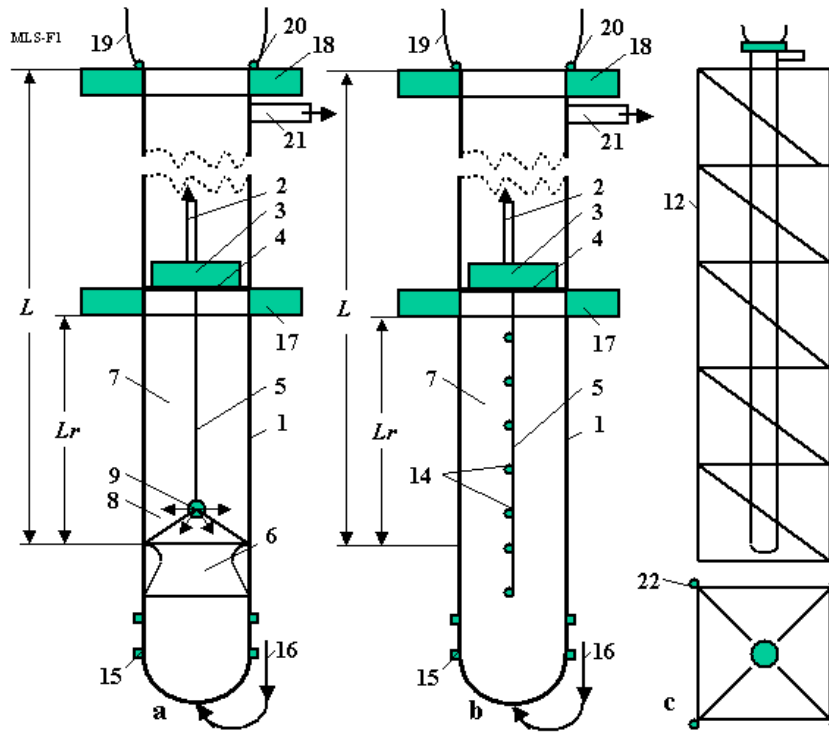
Fig. 6.1.   a - Space launcher with the gas rocket and rocket nozzle in the tube. The system comprises the
        following: 1 – tube, 2 – payload (projectile), 3 – fuel tank, 4 – piston , 5 – fuel pipeline, 6 – nozzle
        connected to piston, 7 – rocket air column, 8 – combustion chamber, 9 – injectors of the combustion
        chamber, 12 – tube frame, 14 – additional injectors, 15 – lower tube injectors, 16 – air pipeline, 17 –
        lower valve, 18 – upper valve, 19 – top valve, 20 – air lock, 21– gas pipe, 22 – electric engines.
         b - Space launcher with the gas rocket and no the rocket nozzle. c – Launcher in frame.

   The launch sequence is as follows. First the movable piston with the fuel tank (containing liquid fuel),
and payload are loaded into the tube. The piston is held in place by the fasteners or closed valve 17 (Fig.
6.1). The direction and angle of the launch tube are set.
   Valve 19 (Fig. 6.1) is closed and a vacuum (about 0.005 atm) is created in the launch tube space above
the payload/piston to reduce the drag imparted to the payload/piston as it moves along the launch tube.
The tube, of a length of 630 m and a diameter of 10 m, contains 61 tons of air at atmospheric pressure. If
this air is not removed, the payload must be decreased by the same value. If air pressure is decreased
down to 0.005 atm, the parasitic air mass is decreased to 300 kg. This is an acceptable parasitic load.
   Valve 17 is closed and an oxidizer (air, oxygen, or a mixture) is pumped into the space below the
payload/piston.

   Liquid fuel (benzene, kerosene) is injected into the space below nozzle 6 through the launch tube
injectors (item 15, Fig. 6.1) and ignited. Valve 17 (Fig. 6.1) is opened. The hot combustion gas expands
and pushes the payload/piston system along the launch tube together with the air column (item 7)
between the piston and nozzle.

   When the piston reaches the maximum gun speed (about 1 km/s), the compressed air column begins
to work as a rocket engine using one of the special injection fuel programs (see Reference[12]).
   As the payload/piston approaches the end of the launch tube, valve 19 is opened and the airlock (item
20) begins to operate. After the payload/piston has left the launch tube, valve 18 closes the end of the

launch tube and re-directs the hot combustion gases down the bypass tube (item 21) to various turbo-machines preparing compressed air for the next shot and electricity for customers.

If a high launch frequency is required, then internal tube water injectors are used to quickly cool the launch tube.

After the payload/piston system leaves the launch tube, the payload (projectile) separates from the piston and the empty fuel tank. The payload continues to fly along a ballistic trajectory. At apogee, the payload may use a small rocket engine to reach orbit or to fly to any point on Earth.

The method by which the fuel is injected and ignited within the launch tube is critical to high-speed (hypersonic) acceleration of the payload. The author has developed the five fuel injection programs for the launch system[12].

In these programs the thrust (force) is constant at all times, which means that pressure and all parameters in the rocket engine are constant. Parts of the programs have two steps. In the first step the fuel is injected into compressed air at the lower part of the tube to support a constant pressure and provide the initial acceleration of the rocket (together with air column L_r) to the velocity V_o. In the second step the rocket engine begins to thrust and support the constant pressure and temperature in the rocket combustion chamber. The result is that the thrust force of the gas-rocket engine remains constant. In the reference article the author considered only a simplified model (Fig. 6.1b) when a rocket nozzle is absent.

Methods of Estimation and Results of Computation

Estimation of missile velocity

Take the well-known rocket equation

$$M \frac{dV}{dt} = \beta w + P \qquad . \tag{6.1}$$

and its solution

$$\Delta V = -\left(w + \frac{P}{\beta}\right) \ln \mu, \tag{6.2}$$

where ΔV = increment of speed [m/s], $\mu = M_k/M_o$ = relative mass of rocket; M_k = rocket mass at the end of acceleration [kg]; M_o = rocket mass at the beginning of acceleration [kg]; β = fuel (gas consumption) rate [kg/s] (constant); w = speed of gas at nozzle exit [m/s] (constant), P = force of pressure at nozzle exit [N] (constant).

From the theory of nozzle expansion the following relations are known

$$P = 10^4 g P_n S_n, \quad \beta = \rho_c w_c S_c, \quad p_c = p_0 \left(\frac{2}{k+1}\right)^{\frac{k}{k-1}}, \quad \rho_c = \frac{10^4 g P_0}{RT} \left(\frac{2}{k+1}\right)^{\frac{1}{k-1}}, \quad w_c = \sqrt{\frac{2kRT}{k+1}}$$

where subscript "$_c$" denotes parameters in a critical (most narrow) nozzle area; subscript "$_o$" denotes the gas parameters in tube rocket before combustion; subscript "$_n$" denotes parameters in the nozzle exit, S is the cross-section area of the tube [m²], T is the gas temperature in the combustion chamber [°K], p is the gas pressure in the rocket [kg/cm²], k, R are gas constants, g = 9.81 m/s² is gravity.

In this chapter the computations are given only for the simplest case: the rocket a without special nozzle (the tube is used as a nozzle of constant cross-section area), where: $S = S_n = S_c$, $w = w_c$, $P_n = P_c$.

Let us substitute the above expressions into (6.2):

$$w = \sqrt{\frac{2kRT}{k+1}}, \quad \frac{P}{\beta} = \sqrt{\frac{2RT}{k(k+1)}}, \quad w + \frac{P}{\beta} = \sqrt{\frac{2(k+1)RT}{k}}, \quad \rho_c = \rho_0\left(\frac{2}{k+1}\right)^{\frac{1}{k-1}},$$

$$\rho_0 = \frac{10^4 g p_0}{RT}, \quad T_c = \frac{2}{k+1}T, \quad \Delta V = -\sqrt{\frac{2(k+1)}{k}}\sqrt{RT}\ln\mu, \quad V = V_0 + \Delta V. \tag{6.3}$$

where $k = 1.4$, $R = 287$ for air and $k = 1.2$, $R = 325$ for rocket gas, V_o is the initial speed [m/s]. Substituting $k = 1.4$, $R = 287$ for air into the above expressions, we obtain the following equations:

$$\Delta V = -31.68\sqrt{T}\ln\mu, \quad w_c = 18.13(T)^{0.5}, \quad (w_c + P/\beta) = 31.68(T)^{0.5},$$

$$\rho_c = 0.634\rho_0, \quad p_c = 0.565p_0, \quad T_c = 0.833T. \tag{6.4}$$

If we substitute $k = 1.2$, $R = 325$ for rocket gas

$$\Delta V = -34.5\sqrt{T}\ln\mu, \tag{6.5}$$

The conditional temperature T in the combustion chamber without molecular dissociation and with a constant coefficient of heat capacity at constant pressure C_p, may be calculated by the equation (for kerosene):

$$\Delta T = \frac{Q}{C_p} = \frac{2.95\cdot 10^3\left(\dfrac{n}{21}\right)}{1.115\left[1+0.067\left(\dfrac{n}{21}\right)\right]}, \quad T = 288° + \Delta T, \tag{6.6}$$

where n = percentage of oxygen in the air ($n = 21\%$–100%). $Q = 0.067\varepsilon = 2.95\cdot 10^3$ is the amount of heat [joules] when 0.067 kg kerosene is fully combusted in 1 kg of air containing 21% oxygen, $\varepsilon = 44\cdot 10^6$ [J/kg] is the heat capacity of kerosene, $1.115 = C_p$ is the heat capacity of gas at a constant pressure.

The computation gives: $n = 21\%$ (conventional atmosphere air), $T = 2768$ °K; $n = 40\%$, $T = 4750$ °K, $n = 60\%$, $T = 6600$ °K; $n = 100\%$, $T \cong 9850$ °K.

In this linear model the top temperatures are higher than the temperatures of molecular dissociation, however the high pressure retards this dissociation. For example, the dissociation of water vapor at atmospheric pressure starts at temperature of 2500 °K and finishes of 4500 °K. If the pressure is 100 atm, the water vapor dissociation begins at 3500 °K and finishes at 6500 °K. We use the pressure from 300 to 1200 atm (and more) where dissociation is not so much. We can also use this because in the rocket nozzle, when the gas expands and the temperature decreases, the molecules recombine and the energy of the dissociation returns (comes back) to the gas. We have the same situation in conventional internal combustion engines, rocket engines, and guns.

The initial velocity of the tube rocket is taken as 1 km/s. It requires approximately 1/3 additional length of the compressed air rocket column $L_r = 30$ m.

Fig. 6.2 shows an estimate of the hypersonic velocity V via a given initial (under piston) pressure p_o and ratio n of oxygen in the air [equation (6.5)], with a cargo (piston plus payload) weight of $M_k = 20$ tons (44,000 lb), a tube diameter of 10 m (15 ft) ($S = 78.5$ m^2) and rocket air column length $L_r = 15$ m. As one can see, the speed of the projectile reaches 7.2 km/s when $P = 500$ atm for conventional air (oxygen 21%) and reaches 8.2 km/s for 30% gaseous oxygen. For $P = 800$ atm the speed is $V = 7.5$ and 8.8 km/s, respectively. In a conventional tank gun the pressure reaches up to 4500 atm and the temperature up to 4500 °C.
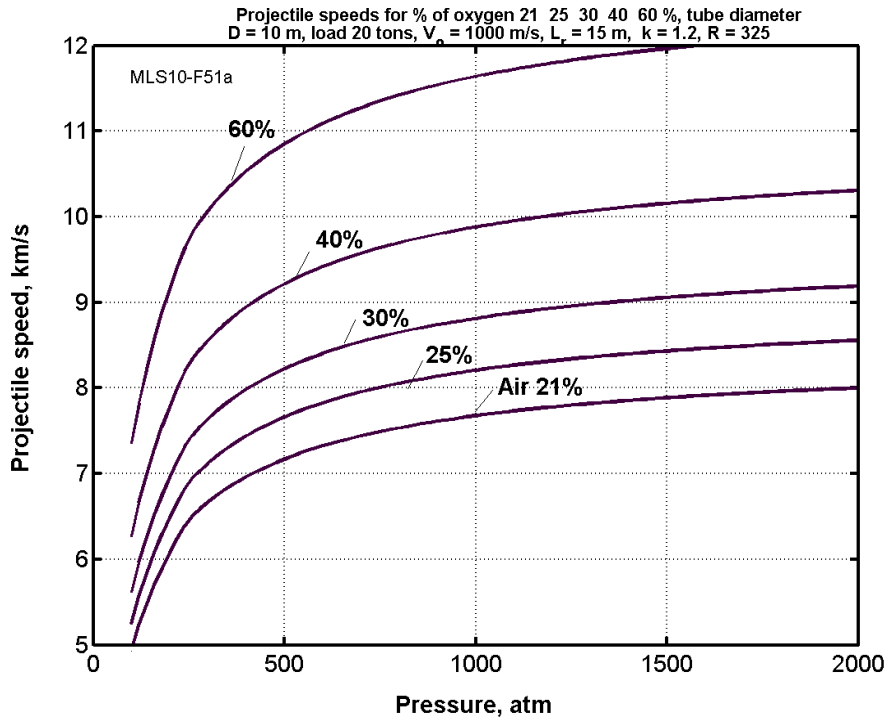
Fig. 6.2. Projectile speed for a load of 20 tons, tube diameter 10 m, rocket air column 15 m and percentage oxygen in air 21–60%.
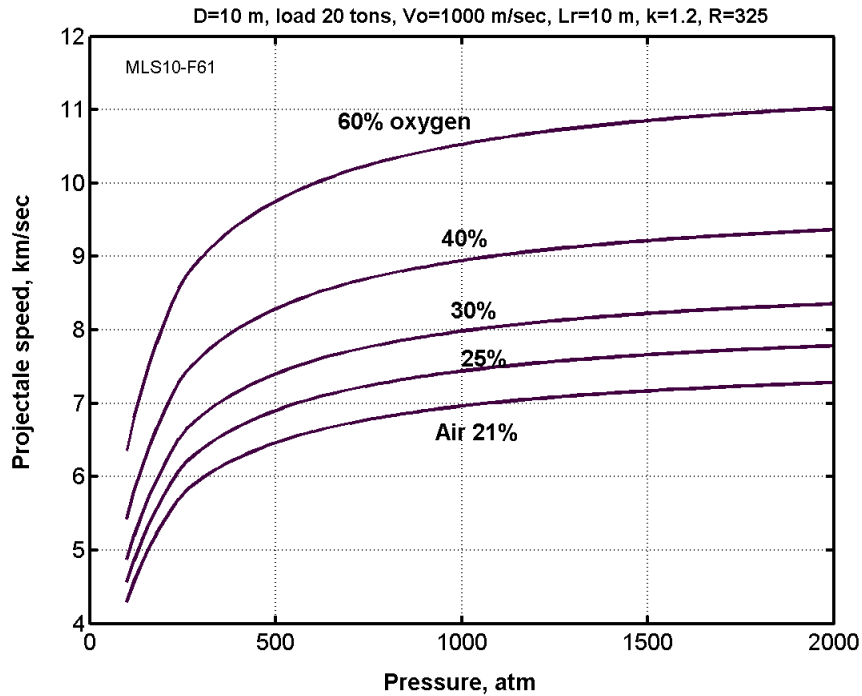
Fig. 6.3. Projectile speed for a load of 20 tons, tube diameter 10 m, rocket air column 10 m and percentage oxygen in air 21–60%.

The high speed of the projectile is not a surprise because we can get a very high mass ratio $M_o/M_k = 1/\mu$ in this launcher. For example, this ratio reaches 30 for $P = 500$ atm, while it only equals maximum 8–10 for a one-stage conventional rocket. The specific impulse is 181 seconds for air and 280 seconds for

60% oxygen. Increasing the diameter and the rocket air column increase the charge and projectile speed. Decreasing the air column from 15 to 10 m decreases the projectile speed from 7.2 to 6.5 km/s (Fig. 6.3).

The rocket nozzle reduces the required fuel (increases efficiency), but this nozzle requires more tube length. Unfortunately, the brevity of this chapter does not allow the presentation of the many computations (see the note at the end of the chapter).

Estimation of tube length

Calculating acceleration requires two assessments: acceleration of the load together with the rocket air column from 0 to speed $V_o = 1$ km/sec (the tube is used as a gun) and the rocket acceleration of the load from V_o to exit V by the rocket air column 7.

a) Length for the initial acceleration from 0 through $V_o = 1$ km/s (tube is used as a gun) (unmarked equations show the process of arriving at the estimation):

$$L_1 = V_o^2/2a \; ; \quad t_1 = V_o/a \; ; \quad a = F/M_o \; ; \quad F = 10^4 g p_o S \; ; \quad M_o = M_k + M_f + M_a \; , \quad M_a = 1.225 \cdot S p_o L_r/q \; ,$$

$$M_f = 0.067 \frac{n}{21} M_a \; , \quad q = \begin{cases} 1 & if \; p < 250 \, atm \\ 1 + 0.001332(p - 250) & if \; p > 250 \end{cases}, \quad t_1 = \frac{V_0 M_0}{10^4 g p_0 S} \; , \quad L_1 = \frac{V_0 t_1}{2} \; , \quad (6.7)$$

where p_o = pressure of gas in the tube [kg/cm²], L_r = length of the rocket air column [m], a = acceleration [m/s²], F = moving force [N], M_a = mass of the air column [kg], 1.225 [kg/m³] = air density in a pressure of 1 atm, M_f = mass of fuel [kg], M_k is mass of the load (piston + payload) [kg], M_o = full mass of the rocket [kg], q is the correction of air compressibility for $P_o > 250$ atm (for $P_o <$ 250 atm $q = 1$), t_1 = acceleration time [seconds] for distance L_1 [m] when the installation works as a gun.

b) The length of acceleration as a rocket after substituting equation (6.3) into (6.4) and with the numerical data (k, R for air) is:

$$L_2 = \int_0^{t_2} V dt, \qquad L_2 = \int_0^{t_2} \left[V_0 - \left(w + \frac{P}{\beta} \right) \ln \left(1 - \frac{\beta t}{M_0} \right) \right] dt = V_0 t_2 + \left(w + \frac{P}{\beta} \right) \left(\frac{M_0}{\beta} \right) \left[\mu (\ln \mu - 1) + 1 \right] \quad (6.8)$$

where

$$t_2 = (M_a + M_f)/\beta \; ; \quad \beta = \rho_c w S \; ; \quad \mu = M_k/M_o \; ; \quad w + \frac{P}{\beta} = \sqrt{\frac{2(k+1)RT}{k}} \; , \quad \rho_c = \frac{10^4 g p_0}{RT} \left(\frac{2}{k+1} \right)^{\frac{1}{k-1}} .$$

Here t_2 = time of acceleration for the distance L_2 , ρ_c = gas density in the nozzle, $M_o = M_k + M_a + M_f$ = initial mass of rocket, M_k = mass of shot [load (projectile or payload) + piston], $M_k = 20{,}000$ kg, M_a = mass of air in the rocket, M_f = mass of fuel in the rocket [see equation (6.7)].

c) The full length of the launch tube and the acceleration times are:

$$L = L_1 + L_2 + L_3 \; , \qquad t = t_1 + t_2 \; , \qquad\qquad (6.9)$$

where $L_3 = 1.3 L_r$ – length of air column plus air column for initial acceleration (30% from L_r).

Fig. 6.4 represents the barrel length required for the speeds in Fig. 6.2. At a pressure of 500 atm, the tube length equals $L = 650$ m for conventional atmosphere air ($V = 7.2$ km/s) and $L = 1400$ m for 39% additional oxygen (total oxygen is 60%) ($V = 10.9$ km/s). This is no surprise, because we use the SAME pressure in the shot for air and oxygen. If the tube length is less then the required length for a given air pressure, the use of oxygen (for a given program and the same pressure) does not give an increase in speed but only increases the load (two or more times). The oxygen allows the combustion time to increase (length of tube) and the exit projectile speed to increase. For a pressure of $P_o = 1000$ atm using 40% gaseous oxygen we can reach a shot velocity of about 10 km/s for a tube length of 700 m (Fig.

6.4). This length is acceptable if we place the tube in water. We can considerably decrease the tube length if we decrease the rocket air column, but the projectile speed is then also decreased. For example, if at 500 atm we decrease the air column from 15 to 10 m, the tube length decreases from 650 to 430 m (Fig. 6.5), and speed from 7.2 to 6.45 km/s (Fig. 6.3).
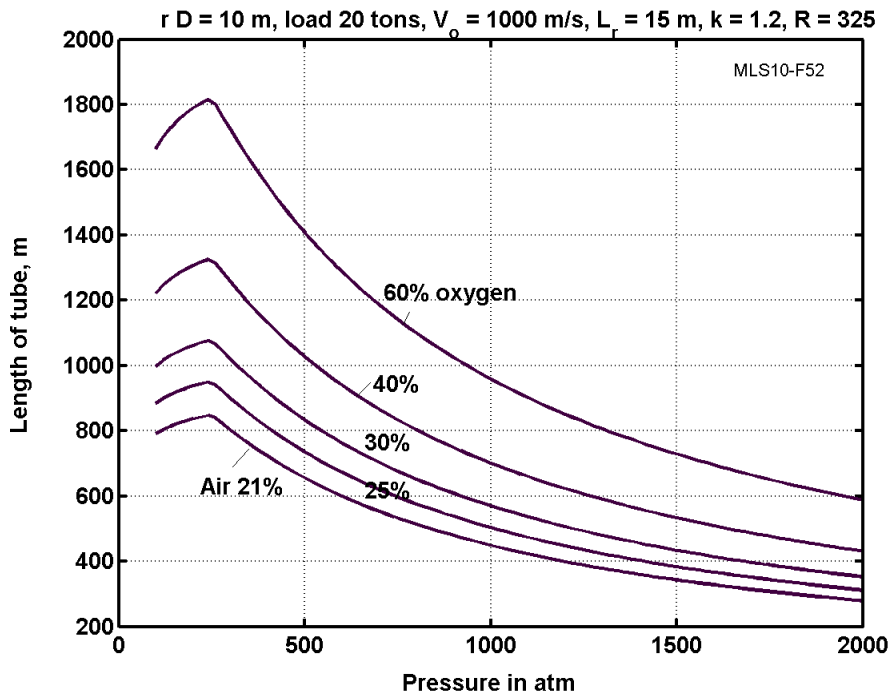

Fig. 6.4. Required tube length for a load of 20 tons, tube diameter 10 m, rocket air column 15 m and percentage oxygen in air 21–60%.
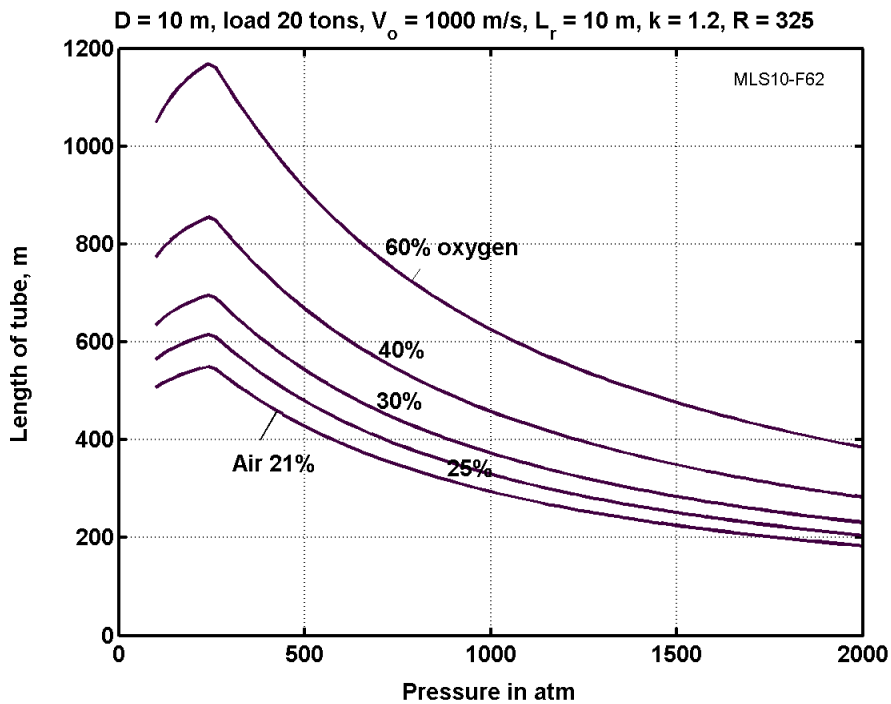

Fig. 6.5. Required tube length for a load of 20 tons, tube diameter 10 m, rocket air column 10 m and percentage oxygen in air 21–60%.

Loss of velocity in the atmosphere

The loss of velocity of the projectile in air is small if the projectile is properly shaped and its trajectory is more then 15 degrees to the horizon. For an exponential density of the atmosphere, at a constant speed of sound ($a = 300$ m/s), we arrive at the following equation as an estimation of the decrement of speed (unmarked equations show the process of computation):

$$M_p V_p^2/2 = A, \quad A = \int_0^H \frac{D}{\sin\theta}dh, \quad \rho = \rho_0 \int_0^\infty e^{bh}dh = \frac{\rho_0}{b}, \quad D = 2\alpha^2\rho_0 a V_p S_p/b,$$

$$A/M_p = 2\alpha^2\rho_0 a V_p S_p/M_p\sin\theta, \qquad \Delta V_a = V_p - \sqrt{V_p^2 - \frac{2A}{M_p}}, \tag{6.10}$$

where V_p = initial projectile speed after shot [m/s], S_p = specific projectile area (m^2), α = relative thickness (0.1), θ = angle of trajectory to the horizon, $\rho = \rho(h)$ density of atmosphere (h – altitude), ρ_o = 1.225 kg/m^3 – atmosphere density at sea level, M_p = mass of projectile [kg], A = work of passing [J], D = wave drag of projectile (90% of total drag). The drag of the projectile depends linearly on speed for large Mach numbers.

  It is shown, that the loss of energy in an exponential Earth atmosphere equals the loss of energy in an atmosphere with constant density $\rho_o = 1.225$ kg/m^3 and altitude $h = 8900$ m.

  The results of the computation for different M_p/S_p [ton/m^2] are shown in Fig. 6.6. The loss does not depend on speed because the more the speed then the less the time of braking. It is about 30–100 m/s.
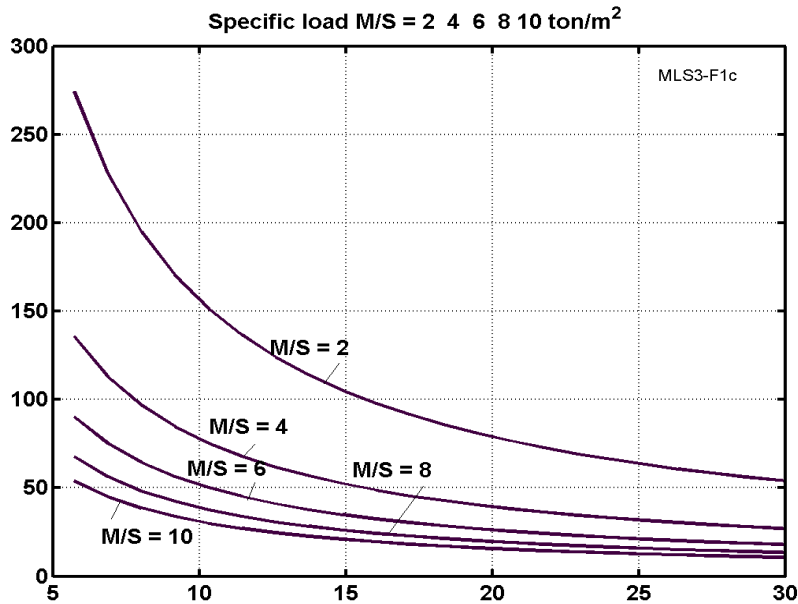
Fig. 6.6. Loss of velocity ΔV_a [m/s] of a projectile via angle θ [degrees] in the atmosphere versus shot angle for specific load 2, 4, 6, 8 ton/m^2.

  Some people think that passing through the atmosphere makes a projectile heat up consideration. They know that the space "Shuttle" needs a lot of heat protection for re-entry into the Earth's atmosphere. However, the Shuttle has to decrease its speed $V_1 = 8$ km/s to $V_2 = 0.3$ km/s. For a mass $m = 20$ tons that equals energy $E = m(V_1^2 - V_2^2)/2 = 6.4\times10^{11}$ J. All this energy is converted into a heat. In our case the speed decreases from $V_1 = 8$ km/s to $V_2 = 7.9$ km/s, which for a mass $m = 20$ tons equals energy $E = m(V_1^2 - V_2^2)/2 = 0.16^.10^{11}$ J. Hence this 40 times less.

The same problem exists in electromagnetic launcher. Research mentioned in the References[17] p. 395 show that a sharp nose five ton projectile needs only 0.9 kg a lithium refrigerant for protection projectile head when crossing the atmosphere at an angle of 15°.

Load delivered to orbit

The load delivered to orbit can be computed by the following equations:

$$\vartheta = \frac{V^2}{V_c^2}, \quad V_c = \frac{19.976 \cdot 10^6}{\sqrt{R_0}}, \quad p = \vartheta r \cos^2 \theta, \quad e = \sqrt{1 - \vartheta(2 - \vartheta)\cos^2 \theta}, \quad r_a = \frac{p}{1 - e},$$

$$r_a = R_0 + H, \quad V_a = \frac{Vr\cos\theta}{r_a}, \quad V_d = V_{c,H} - V_a, \quad \frac{M_k}{M_0} = \exp\left(-\frac{V_d}{w}\right), \quad R_0 = 6378 \; km. \tag{6.11}$$

where ϑ – ratio of speed V to circular speed V_c at a given point [m/s], R_0 – Earth radius [m], p – parameter of elliptical orbit, e – eccentricity of elliptical orbit, r_a – radius apogee [m], H – altitude [m], V_a – speed at apogee [m/s], θ – trajectory angle to horizon, V_d – required additional speed at apogee [m/s], $V_{c,H}$ – required circular speed [m/s], M_k/M_0 – ratio of final (useful) mass to initial mass, w – speed of rocket exhaust gas [m/s].

Results of computation for a rocket engine with impulse $w = 2000$ m/s are presented in Figs. 6.7 and 6.8.
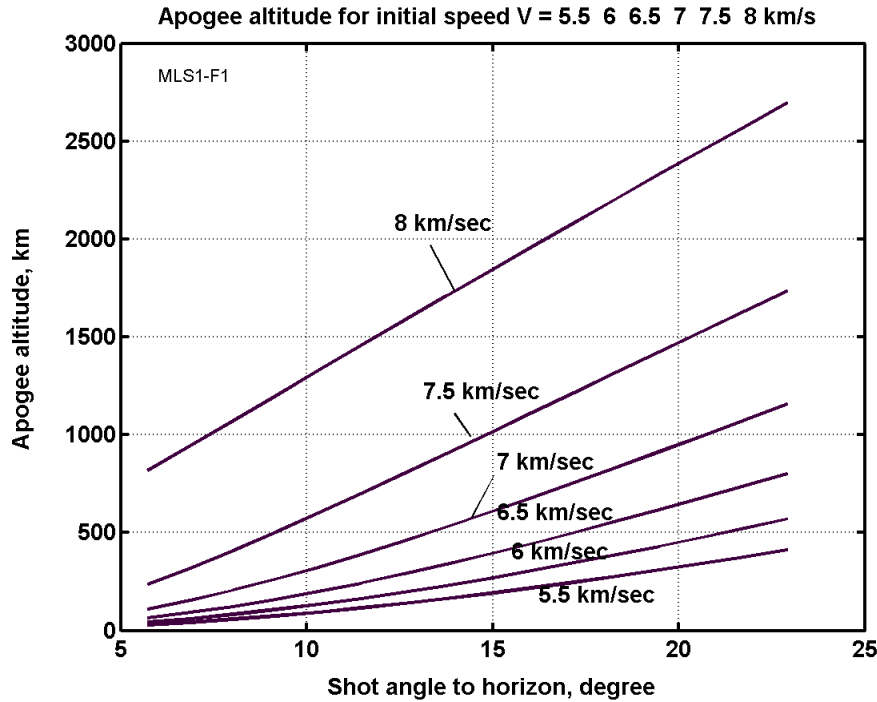
Fig. 6.7. Apogee altitude versus shot angle for initial projectile speed.

Example of use. If we have a tube diameter of 10 m², a load of 20 tons and tube pressure of 500 atm, from Fig. 6.2 and air we find that for air the shot speed is 7.2 km/s, and from Fig. 6.4 the required tube length is 650 m. From Fig. 6.6 the loss of velocity in the atmosphere for a shot angle of 18° and $M/A = 4$ ton/m² is 45 m/s. From Fig. 6.7 we find the apogee of orbit altitude is $H = 1000$ km for the shot angle of 18° and speed 7155 m/s.

Assume that in 20 tons of load a piston weight equals 5 tons and 15 tons is the orbit load. From Fig. 6.8 for $V = 7.155$ km/s and the shot angle of 18° we find that the useful part of the orbit load is 47% or

about 7 tons. The eigth tons is rocket fuel for increasing the apogee speed to circular speed at a given altitude.
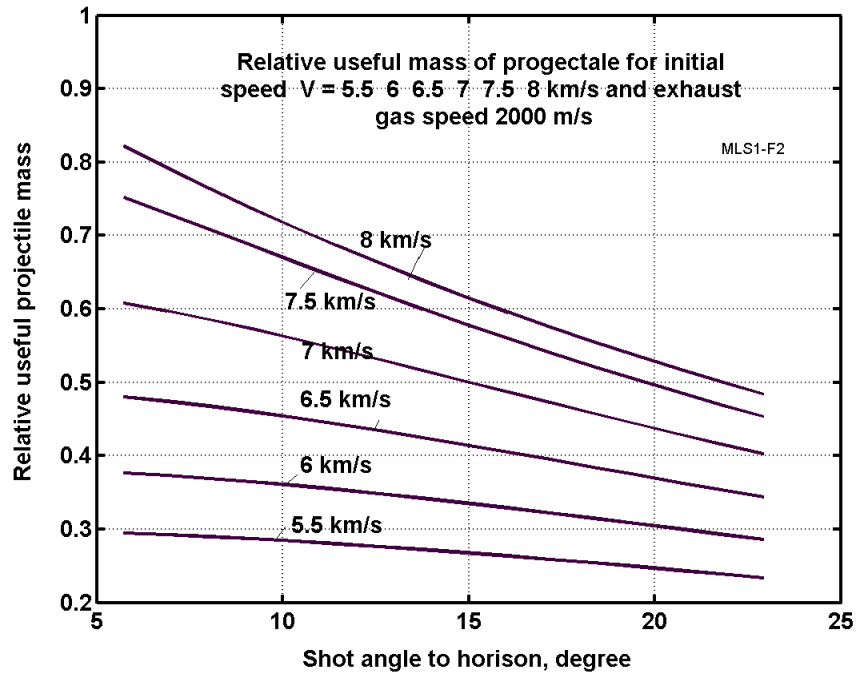
Fig. 6.8. Relative useful mass of projectile for initial speed 5.5–8 km/s and specific impulse 2000 m/s.

Production cost of delivery

The production cost of delivery is the most important feature of the suggested launcher. In "Hypersonic Launcher"[12, 19] Fig.18 shows computations of delivery cost versus annual payload in thousand tons and an initial cost of the installation. The following data were used: life time of the installation 20 years, cost of fuel (kerosene) $0.25 per liter, requested time for preparing of a shot 0.5 hours, 10 people working with average salary of $20 per hour, payload of one launch 5 tons (11,000 lb) (25% from 20 tons of piston-projectile system). The load (20 tons) is: payload – 5 tons, a solid engine for generating additional speed of 3 km/s at apogee – 10 tons, piston - 5 tons. Maximum capability is 86,400 tons per year. The resulting computations are presented in Fig. 6.9.

Fig. 6.9. Delivery cost of payload versus annual payload for installation cost of $200–1000 million, life time 20 years, annual maintenance $10 millions per year, kerosene cost $0.25 per kg.

As one can see, the production delivery cost may be about $1–2 per kg if the payload is approximately 50–80 thousand tons per year. About 70% of this cost is fuel (kerosene or gasoline).

Excess of energy

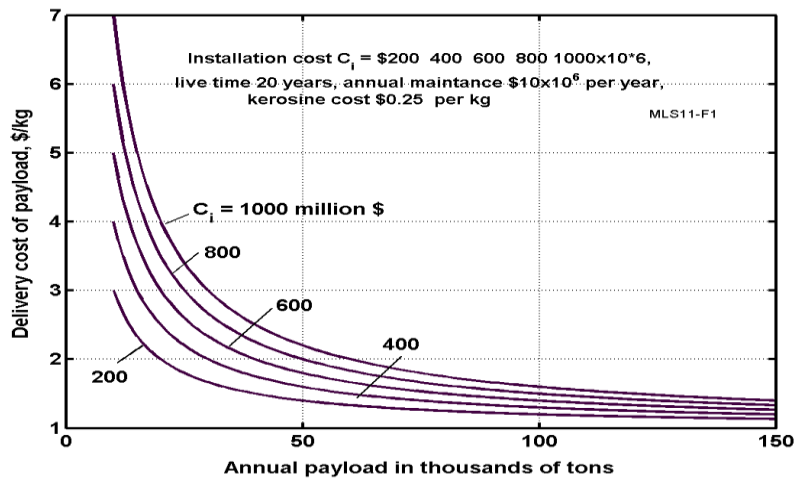The hypersonic launcher uses a very high compression ratio, which means that its efficiency coefficient is very high at about 85–95%. Such efficiency is higher than other head engines. Part of this energy is uses in a load acceleration, and part is lost in non-useful gas expansion. However, the hypersonic launcher has a huge excess of shot energy over gas compression energy. If the launcher has a top valve, this energy can be used for the production of compressed air, electricity, oxygen, etc.

Let us estimate this energy. After the shot is fired the valve closes the tube. The pressure in the tube and the possible work of one kg of gas can be computed as follows (Fig. 6.10):

$$T_3 = T_2 + \Delta T , \quad L_3 = 1.3 L_r \frac{T_3}{T_1} , \quad T_4 = T_3 \left(\frac{L_3}{L} \right)^{k-1} , \quad P_4 = P_3 \left(\frac{L_3}{L} \right)^{k} , \quad T_5 = \frac{T_3}{P_3^{\frac{k-1}{k}}} , \quad T_2 = T_1 ,$$

$$(6.12)$$

$$W_{4-5} = \frac{RT_5}{k-1} \left[1 - \left(\frac{P_4}{P_5} \right)^{\frac{k-1}{k}} \right] , \quad W_{T,1-2} RT_1 \ln \frac{P_2}{P_1} , \quad W_{A,1-2} = NRT_1 \frac{k}{k-1} \left(1 - \varepsilon^{\frac{k-1}{k}} \right) , \quad \varepsilon = \sqrt[N]{P_2} .$$

where T is temperature at marked points, °K, $T_1 = 288$ °K; ΔT is increase in temperature from fuel: it equals 2480 °C for air, 4660 °C for adding 20% oxygen, 6614 °C for adding 40% oxygen; P is pressure at marked (sup index) points, atm; W is work at marked lengths [J]; W_T is isothermal work, W_A is adiabatic work; $R = 287$ is the thermodynamic coefficient; $k = 1.4$ is the thermodynamic coefficient; L is tube length [m]; L_3 is tube length where the pressure can be constant [m]; N is the number of cooling radiators in the compression process.
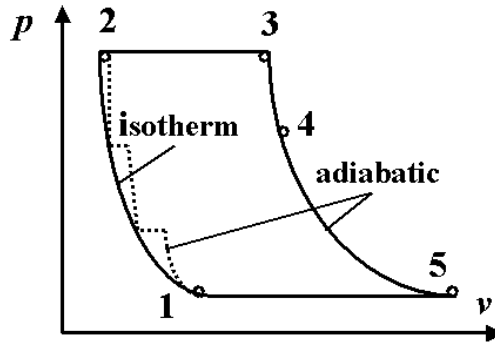
Fig. 6.10. Thermodynamic diagram of launcher. 1– point of atmospheric pressure; 2 – point of common air columns volume and tube pressure; 3 – point after fuel combustion; 4 – point of tube volume; 5 – point after gas exhaust.

The result of computation are presented in Fig. 6.11. A 1 kg of gas for $N = 4$, $p = 500$ atm has an excess of energy of about 2535 kJ. Our launcher for $p = 500$ atm has about $M = \rho V/q =$ 1.225·500·78.5·20/1.72 = 559 tons of compressed air, which means, after the shot and compressing the air for next shot we have $E_a = 2535·559 = 1417065$ MJ $= 1.4·10^{12}$ J of excess energy.

The required fuel for a shot is $M_f = 0.067·559 = 37.45$ tons. This has an energy $E = M_f \varepsilon =$ 37.45·10³·44.10⁶ = 1.65·10¹² J. The energy of the projectile is $E_p = mV^2/2 = 20000·7200^2/2 =$ 0.144·10¹². The excess energy (which can be used) is $E_a = 1.4·10^{12}$ J . The total efficiency (without loss of compressed gas to the atmosphere) is $(E_p + E_a)/E = (1.4+0.144)/1.65 = 0.93$. This is more than any

current heat machine because we use a very high compression ratio of $p = 500$ atm. The exhaust gas has a temperature $T = 980$ °K ($p = 500$ atm). Utilization of this high level of heat can give additional energy.

M =1 kg, N = 2 4 6 8, Charge = 20 m, tube length = 650 m, k = 1.2, R = 325.

Fig. 6.11. Adiabatic expansion (after shot) and compression work of 1 kg gas for cooling radiators $N = 2$–8, charge length 20 m, tube length 650 m.

Launcher as an accumulator of energy

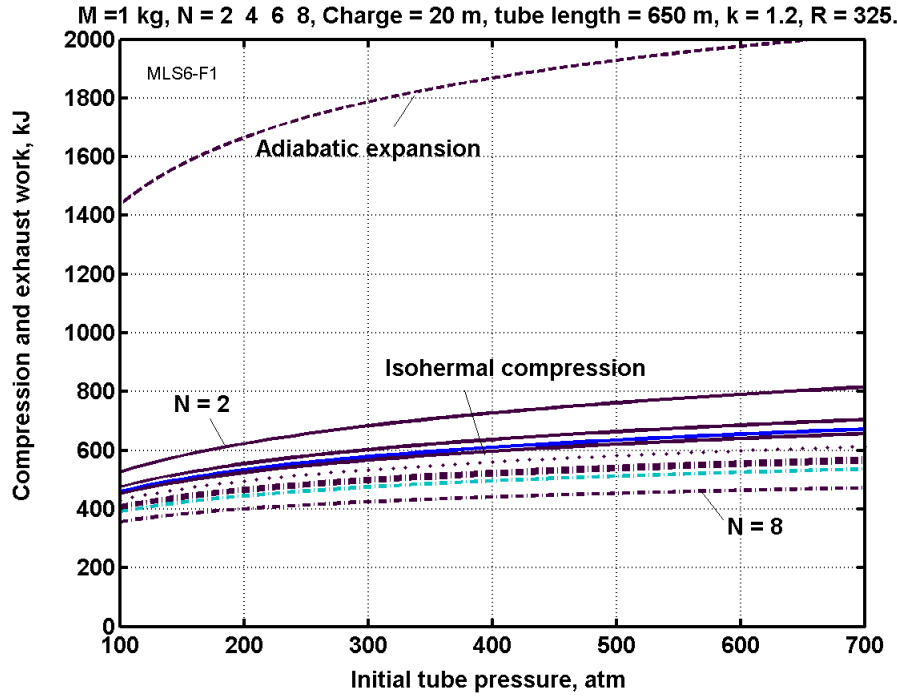There is a big problem in the electric energy industry. Power stations have high efficiency when they work in a constant regime. This means they produce excess energy at night and lack energy during the day. To balance their energy the electricity industry builds special hydro-accumulator stations. These stations pump water into a compensation (balancing) reservoir when they generate excess energy and produce additional energy when it is insufficient.

  We have a gigantic reservoir for highly compressed air. When the launcher does not have work to do, it can be used as an accumulator of energy. The launcher draws energy from electricity stations, and pumps compressed air into the tube. When there is lack of energy, the launcher produces energy from the compressed air and send it is to customers. If it uses sea water for cooling the air during compression and heating the air during expansion, the efficiency of this method may be high (80–90%), especially if we use cool deap-sea ($T_1 = 7$ °C) water for cooling and warm ($T_2 = 20$–25 °C) surface water for heating. The equation for heating is

$$W_1 = RT_1 N \frac{k}{k-1}\left(1 - \varepsilon^{\frac{k-1}{k}}\right), \quad \varepsilon = \sqrt[N]{p_2} \quad W_2 = RT_2 N \frac{k}{k-1}\left(1 - \frac{1}{\varepsilon^{\frac{k-1}{k}}}\right), \quad \eta = 1 - \frac{W_1 - W_2}{R\dfrac{T_1 + T_2}{2}\ln\dfrac{p_2}{p_1}}.$$

$$(6.13),$$

where W_1 = work in compression, W_2 = work expansion, p_2 = tube pressure, η = efficiency coefficient, N = number of cooling radiators.

  Results of computation are presented in Fig. 6.12. At 500 atm 1 kg air gives 580 kJ when it is isotherm expending. In the tube $V = SL = 78.5 \cdot 650 = 51025$ m^3 under pressure $p = 500$ atm we have $M = \rho p V =$

$1.225 \cdot 500 \cdot 5.1 \cdot 10^4/q = 30.6 \cdot 10^6$ kg compressed air. This contains $E = 580 \cdot 30.6 \cdot 10^6 = 17.748 \cdot 10^9$ kJ of energy. The installation can work as a 100 MW electric power station in during $17.748 \cdot 10^9/3600/10^5 = 49.3$ hours and $\eta = 0.88$ if $N = 8$, $T_1 = T_2$.
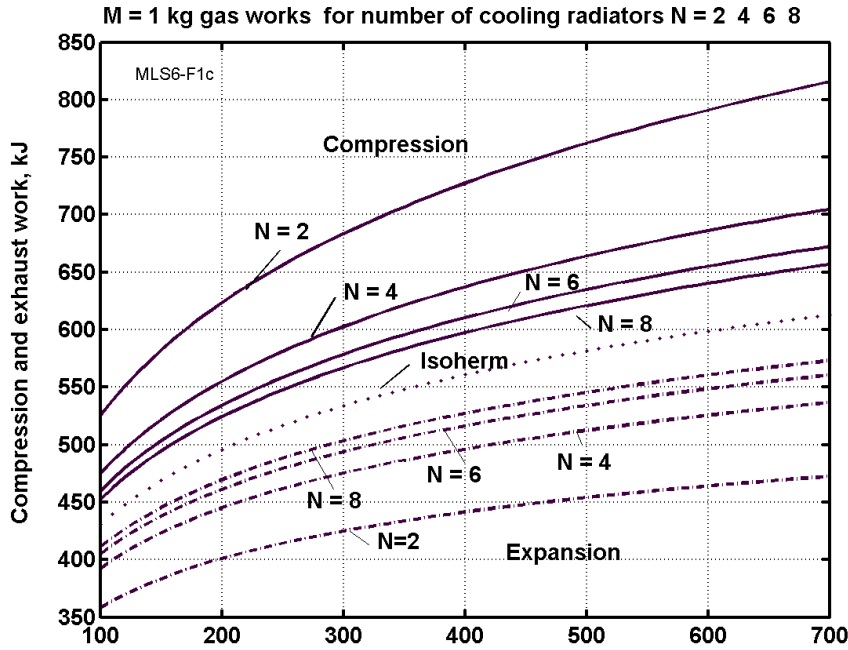
M = 1 kg gas works for number of cooling radiators N = 2 4 6 8

Fig. 6.12. Compression and expansion work versus gas pressure (atm) of 1 kg gas for cooling radiators $N = 2$–8.

Gun Recoil

The recoil of the launcher can be computed by the theoretical mechanics equation

$$m_1 V_1 = m_2 V_2, \qquad (6.14)$$

where m_1, m_2 are mass and V_1, V_2 are speed of the projectile and installation respectively.

For example, if the projectile mass equals 20 tons and its speed is 8 km/s; the water inside the installation frame $15 \times 15 \times 650$ m^3 is $14.6 \cdot 10^4$ tons, the installation speed after the shot will be $V_2 = 20 \cdot 8000/14.6 \cdot 10^4 = 1.1$ m/s.

Tube curvature

Tube straightness is checked using a laser beam and the tube supported by engines located along it. The maximum force from the tube curvature can be calculated using the equation

$$n = \frac{V^2}{gR}, \quad R = \frac{L^2}{8h}, \quad n = \frac{8hV^2}{gL^2}, \qquad (6.15)$$

where n is centrifugal overload [g]; V is projectile speed [m/s]; $g = 9.81$ m/s is Earth's gravity; R is the radius of curvature [m]; L is length of the tube [m]; h is deviation of the tube from a straight line [m].

For example: if the middle of the tube has a deviation of 0.1 m, its length is 1000 m and the projectile speed in the middle of the tube is $V = 5000$ m/s, the centrifugal overload will be $n = 2g$. This is a very small force in comparison with acceleration along tube which equals about 1000g.

Wall thickness

The tube wall thickness can be estimated in the following way. Take the tube length $L = 1$ cm. The tensile force equals $F = PDL$, where P is pressure, atm [kg/cm^2], D is a tube internal diameter [cm], F is

tensile force [kg]. The cross-section area [cm^2] of the tube walls is $s = F/\sigma$, where σ is safe tensile stress [kg/cm^2]. The wall thickness is $s/2$.

For example, if the pressure is $P = 500$ atm, the tube diameter is $D = 10$ m $= 1000$ cm, $L = 1$cm, then the force is $F = PDL = 500$ tons. If the tube is made from a composite material with maximum $\sigma = 500$ kg/mm^2, coefficient (margin) of safety 5, and safe tensile stress $\sigma = 100$ kg/mm^2, then the wall thickness will be 25 cm.

If the tube is made from steel with maximum $\sigma = 250$ kg/mm^2, margin of safety 5, and admissible (safe) tensile stress $\sigma = 50$ kg/mm^2, then the wall thickness will be 50 cm for a tube diameter 10 m.

Gas friction

Let us estimate gas friction around the wall. We use the method described by Reference[5].

Below, the equation from Anderson for computation of local air friction for a plate is given

$$\frac{T^*}{T} = 1 + 0.032M^2 + 0.58\left(\frac{T_w}{T} - 1\right), \quad M = \frac{V}{a}, \quad \mu^* = 1.458\times10^6 \frac{T^{*1.5}}{T^* + 110.4},$$

$$\rho^* = \frac{\rho T}{T^*}, \quad R_e^* = \frac{\rho^* Vx}{T^*}, \quad C_{f,l} = \frac{0.664}{(R_e^*)^{0.5}}, \quad C_{f,t} = \frac{0.0592}{(R_e^*)^{0.2}},$$

$$D_L = 0.5C_{f,l}\rho^*V^2S, \quad D_T = 0.5C_{f,t}\rho^*V^2S, \quad x \approx L_r/3, \tag{6.16}$$

Where: T^*, Re^*, ρ^*, μ^* are reference (evaluated) temperature, Reynolds number, air density, and air viscosity respectively. M is Mach mumber, V is speed, x is the length of plate (distance from the beginning of the cable), T is flow temperature, T_w is body temperature, $C_{f,l}$ is a local skin friction coefficient for laminar flow, $C_{f,t}$ is a local skin friction coefficient for turbulent flow, S is the area of skin [m^2] of both plate sides, which means for the cable we must take $0.5S$, D is air drag (friction) [N]. Our gas column is moved with acceleration which means (from aerodynamics), that we have the laminar layer.

The results of computation of laminar friction are presented in Fig. 6.13. The average friction is about 0.4 ton/m^2. The friction area decreases with increasing speed. If the average area is $S = \pi D L_r/2 = 3.14\times10\times15/2 = 235.5$ m^2, the average wall drag is 94 tons. This is a small value in comparison with the drive force of $20\times10^{4\cdot}0.5 = 10^5$ tons.
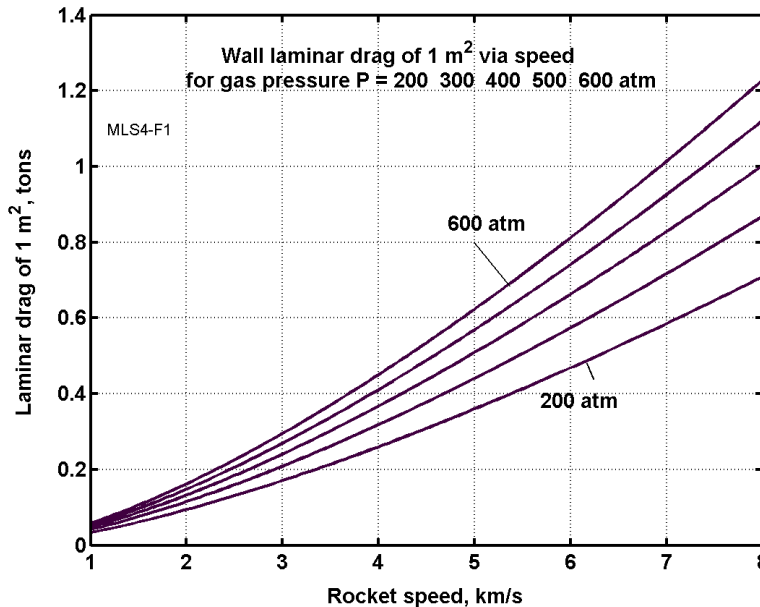

Fig. 6.13. Wall laminar drag of 1 m^2 versus speed for gas pressure 200–600 atm.

Advantages of the proposed space launcher

One advantage of this launch system over existing fixed "gun" systems is that of placing the launch system in water. The installation becomes mobile and can be aimed (by adjusting the azimuth) at any point in space or on Earth. The launch tube may be integrated into a watertight enclosed frame (Fig. 6.1c). Water can then be forced into and out of the frame to control the position of the launch tube like a submarine. Electric motors may be attached to the frame for maneuverability and to maintain the frame in a desired location. The launch tube is fixed inside the frame by control cables. The azimuth of the launch tube, hence the "aim," is obtained by sinking one end of the launch tube/frame. The launch tube is brought into a horizontal position to transport the system to another location or to conduct maintenance on the system.

Additional advantages, each of which is an important innovation, that this launch system has over a conventional fixed "gun" system are listed as follows:

1)   In a conventional "gun" system, powdered fuel is ignited all at once to move the projectile. The velocity of the projectile cannot exceed the velocity of the combustion gases, which is usually the speed of sound (at most 1 to 2 km/s). In the proposed launch system, the mass of gas in the launch tube is pushed along with the payload/piston, which later works as a rocket engine. This "rocket engine" is different from conventional rocket engines since the proposed "engine":

a) does not have to move heavy tanks of compressed oxidizers;

b) is not limited by the speed of sound;

c) is allowed to reach a very high ratio of fuel mass (compressed air + fuel) to payload mass (up to 30 and more);

d) allows the payload to reach hypersonic speeds (up 7 to 10 km/s).

2) The vacuum (less 0.01 atm) above the payload/piston eliminates a significant amount of air resistance, which could prevent the payload from reaching high velocities when the launch tube is very long.

3) The launch tube can be long (0.4 to 2 km), which is not conducive in ordinary "gun" systems. In addition, by placing the launch system in water, the payload can be aimed at any point in space or on the Earth. A fixed conventional "gun" system cannot be moved or aimed. The use of water also allows the launch system to be hidden below the surface and in the event of an accident, the high pressures under the water can help contain the explosive materials and avoid injuring people.

4) Conventional fuels and oxidizers (such as air or gaseous oxygen) can be used with the proposed launch system. In regular rockets for example, gaseous oxygen can not be used since the fuel tank weights would be too high and liquid oxygen requires special equipment for storage and transportation.

The main advantage of the proposed launch system is a very low cost for payload delivery into space and over long distances. Expensive fuels, complex control system, expensive rockets, computers, and complex devices are not required. The cost of payload delivery to space would drop by a factor of a thousand. In addition, large payloads could be launched into space (in the order of thousands of tons a year) using a single launch system. This launch system is simple and does not require high-technology equipment. The launch system could easily be developed by any non-industrialized country and the cost of this launch system is ten times lower than that of contemporary rocket systems.

Computations show that if the launch tube is designed to a diameter of 2–7 m, a length of 1–4 km, and gas pressure of 200–800 atmospheres, then 3–20 tons of payload per launch could be delivered into Earth orbit. If the launch frequency is every 30 minutes, then 15–45,000 tons of payloads could be delivered to space per year at production costs of $2–10 per kg.

During peace time, this launch system can be also used for the delivery of mail or express parcels over long distances (for example, from one continent to another) and give a profit of $5–10 millions per day. The installation can be also used for energy storage. However, during war, this launch system could deliver munitions to targets thousands to tens of thousands of kilometers away. It is known that 90% of loads delivered into orbit are items that can endure high acceleration.

In this chapter I wanted to show the feasibility of the suggested method. The parameters of the launcher are not optimized. Selection of the tube diameter, rocket nozzle, and length of the rocket air column could possibly increase the projectile speed and weight, and decrease the tube length and fuel consumption. The hot gas after the shot may be used for electricity production or as an energy accumulator.

The author has more detailed research on this concept and innovations which solve problems that could appear in development and design of the suggested Launcher. The author is prepared to submit his research and to discuss the problems with serious organizations wanting to research and develop this project.

Discussion

The computations in this chapter are not exact but only estimations to show that the suggested simple gas tube rocket can reach a hypersonic speed of 4–8 km/s. Hypersonic speeds depend only on the right gas tube rocket design and the right fuel injection program. The estimates are made with the conventional technical accuracy of 5–10%, except perhaps temperatures (and projectile speed) with a high level of oxygen (more then 40%) when the temperature exceeds the conventional combustion chamber temperature of 4000 °K and the gas dissociation decreases the temperature. However, the velocity of 5.5–7 km/s (Fig. 6.2), which is reached before this temperature, is hypersonic. A more exact computation is complex and would need financial support. There are some factors which allow the increase in temperature in the combustion chamber and utilization it in the tube nozzle: (1) the heat is not spent on evaporation and heating of the liquid oxygen from 90 °K to 288 °K (we use gaseous oxygen); (2) we use very high pressure, which decreases the temperature dissociation by approximately 500 °K per every 100 atm pressure; (3) with the tube nozzle the recombination time is fast enough (0.5–1 seconds). In a conventional short rocket nozzle the gas flows out into the vacuum space and recombination time is not long enough (0.001 seconds). Also, ionization for the given temperature is small.

There are also good margins for increasing the efficiency of the gas tube rocket. Some metals (Be, Li, B, Mg, Al, Si) have a heat capability 1.5–2 time more then kerosene. However their application is limited because in the high expansion nozzle used in a conventional rocket these metals condense from gas to liquid and decrease efficiency of a nozzle. In our case we have a nozzle that has a small expansion (or use the rocket without a nozzle, as in this chapter). This means we can use a liquid fuel with a high concentration of the metal powder and achieve the high efficiency (projectile speed).

The author has many detailed computations for different gas tube rocket designs and programs for fuel injection. Organizations interested in these projects can contact to the author (http://Bolonkin.narod.ru).   Patent applications: 09/013,008 of 01/216/98; 09/344,235; 10/051,013.

References

1. *Gun propulsion technology*, 1998, AIAA.
2. *Development of High-Speed Vehicle Propulsion Systems*, AIAA, 1996.
3. 12th Symposium Propulsion System, AIAA,1995.
4. Space Technology & Application. International Forum,1996–1997, Albuquerque, MN, part 1-3.
5. Anderson, J.D., *Hypersonic and High Temperature Gas Dynamics*, NY, 1989.

6. Henderson B.W., "Livermore Proposes Light Gas Gun For Launch of Small Payloads", *Aviation Week & Space Technology*, July 23, 1990, pgs. 98–99.

7. Henderson, B.W., "World's Largest Light Gas Gun", *Aviation Week & Space Technology*, August 10, 1992, pgs. 57–59.

8. Wolkomir, R., "Shooting right for the stars with one gargantuan gas gun". Smithsontan, Vol. 6, No. 10, p. 84–91, January, 1996.

9. Tuler, V.M., "Gun barrel launching", *Space/Aeronautics*, February 1959, p. 52–54.

10. Seigel, Arnold E., "Theory of High-Muzzle-Velocity Guns", AIAA,1978, p. 40.

11. Bull, G.V., Murphy, C.H., Paris Kanoneu – the Paris Guns and Project HARP, 1988.

12. Bolonkin A.A., "Hypersonic Space Launcher", *Actual Problem of Aviation and Aerospace*, KAI, No. 1, 2003, pp. 45-69.

13. Baer, P.G., "The Traveling Charge Gun as a Hypervelocity Launching Device", Ballistic Research Laboratories, Maryland, 1960.

14. Vest, D.C., "An Experimental Traveling Charge Gun", Ballistic Research Laboratory report No. 773 (1951).

15. Bolonkin A.A., "Hypersonic Gas-Rocket Launcher of High Capacity", *IBIS*, Vol. 57, No. 5/6, 2003, pp. 162–172.

16. Bolonkin A.A. , "Hypersonic Launch System of Capacity up 500 tons per day and Delivery Cost $1 per lb", IAC-02-S.P.15, 53rd International Asronautical Congress. The World Space Congress-2002, 10–19 Oct. 2002, Houston. Texas, USA.

Chapter 7
Earth–Moon Cable Transport System*

Summary

This chapter proposes a new transportation system for travel between Earth and the Moon. This transportation system uses mechanical energy transfer and requires only minimal energy, using an engine located on Earth. A cable directly connects a pole of the Earth through a drive station to the lunar surface. The equation for an optimal equal stress cable for the complex gravitational field of the Earth–Moon has been derived that allows significantly lower cable masses. The required strength could be provided by cables constructed of carbon nanotubes or carbon whiskers. Some of the constraints on such a system are discussed.

Introduction

The author offers a revolutionary new transportation system for delivering payloads and people from the Earth to the Moon[1–4]. This method uses mechanical energy transfer, with an engine located on the Earth and energy recovery by simultaneously moving one cabin upward and another cabin downward. The author has not found an analog for this space mechanical energy transfer (transmission to space) or similar facilities for transporting a payload into space in the technical literature or patents. The offered system may also used as a space elevator between Earth and a geosynchronous station, as a satellite launcher, for traveling to Mars, and for launching or modifying the speed or direction of a space vehicle.

Brief history

There are many articles that develop tether methods for trajectory change of space vehicles[5] and concepts exist for a space elevator[3]. In the tether method two artificial bodies are connected by cable and the system is rotated in space around their common gravitational system center. For example, a two-tether system for Moon travel is described in the current literature[6], (p. 69) and works as follows. The first tether is located near the Earth, the second is located near the Moon. High speed aircraft

(which do not exist at the present time) deliver loads to an altitude of 80─100 km. Here the first tether system connects to the load, increases its speed (how?), and sends it in the Moon's direction. After its flight through space, the second (Moon) tether system must catch this load, decrease its speed, and drop it onto Moon's surface. The main problem with this method is that it requires energy for increasing the rotation of the tether system (motorized tether). The problems are how to rotate it with a flexible cable and what to do with momentum after launch if the tether system is to be used again. If this system is used only one time, it is worse than conventional rockets because it loses the second body and requires a large space source of energy.

In the space elevator concept, a cable is connected between a geosynchronous space station and the Earth's equator[3]. This cable is used to deliver a payload to the station. The main problems are the very large cable weight and delivery of the energy to move the load container (climber).

The proposed system differs from a conventional tether system because it connects two natural bodies, the Earth and the Moon. It may be compared with an aerial ropeway in the mountains. It is different also from a space elevator, in that it is connected to the Earth's pole, whereas a space elevator must be connected to the Earth's equator.

The proposed system differs from previous concepts in that it has a relatively simple mechanical system for transferring energy from a mechanical engine located on Earth to a load cabin located in space through a series of cable links. Also new is the idea of separating the transport cable into sub-sections, which dramatically decreases the total system weight.

Brief Description, Theory, and Computation of Innovations

The objectives of the proposed system are to provide an inexpensive means of travel between the Earth and the Moon, to simplify space transportation technology, and to eliminate complex hardware. The proposed Earth–Moon cable transport system is shown in Fig. 7.1. The system consists of three cables: a main (central) cable, which supports the weight of the entire system, and two closed-loop transport cables, which include a set (5–10) of cable chain links connected sequentially to one other by rollers [3,4] (see Fig.1.3a). The system is connected at the Earth's pole and to any position on the Moon's surface that continually faces Earth. An engine located on a planet (e.g. the Earth, but it could be the Moon) drives the cable transport system. On the Earth, the cable is supported in the atmosphere by a winged device, which also counteracts the rotation of the Earth. The transfer cable system transfers energy between load cabins moved up and down, which requires the engine moving the cable system to overcome only frictional forces.

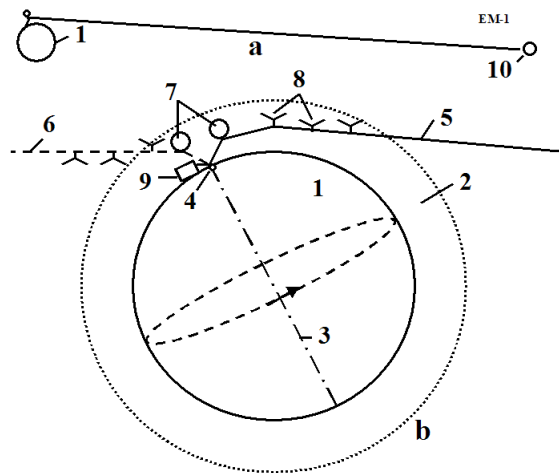**Fig. 7.1**. A conceptual Earth–Moon transportation system. One end is connected to the Earth's pole. the second end is connected to the Moon. Notation: 1 – the Earth; 2 – Earth's atmosphere; 3 – axis of Earth rotation; 4 – Earth Pole; 5 – Earth–Moon cable transport system in right position (one extreme of the Moon's position); 6 – Earth–Moon system in left position; 7 – air balloons; 8 – support wings; 9 – drive station; 10 – Moon.

An optimal (minimum mass, equal stress) variable diameter cable is defined for the main tether. The main cable has a relatively large but variable cross-section area (diameter) because it has to support the total system weight, which is several hundred times the load weight. In an optimal main cable the cross-section area increases (for $K = 2$, about 20 times) in the altitude range 0–150,000 km, is approximately constant in the range 150,000–380,000 km, and decreases near the Moon's surface, from 20,000 km to the surface.

The mass of the main cable is minimized because its diameter is variable along the distance (see the next section for calculation of the main cable cross-section areas and mass). The transport cables pull (move) the load cabins (one up, the other down) along the main cable. As these are moveable parts, they must have constant diameter. If they had to carry a load the full distance to the Moon, their mass would be very large. My concept separates the full distance into sub-distances (5–10), with closed-loop links for every sub-distance connected by rollers. These rollers transfer the transport cable movement from one link to another. In this case, the mass of the transport cables is minimized because at every local length (sub-distance) the cable diameter is determined by the local force. Total mass of the transport cable should be close to double the mass of the main cable.

The load containers are connected to the transport cable. When containers come up to the rollers, they pass the rollers, connect to the next link and continue their motion along the main cable. The load (cabin) has special clamps to allow this transfer between the different diameter cables in each link[1]. Most space payloads, like tourists, must be returned to Earth. When one container is moved up, another container is moved down. The work of lifting equals the work of descent, except for a small friction loss in the rollers. The transport system may be driven by a conventional motor located at the Earth drive station, on a space station, or on the Moon. When payloads are not being delivered into space, the system may be used to transfer mechanical energy to the Moon. For example, the Earth drive station can rotate an electric generator on the Moon.

The cable is supported in the Earth's atmosphere by air balloons (around the pole) and winged devices (far from the pole). The maximum speed of the system in the atmosphere is about 190 m/sec at the maximum distance of 2700 km in the right-hand position of Fig. 7.1. When the cable is located in the left-hand position, some wings may be out of the atmosphere and not so effective.

The Moon's orbit has eccentricity. Every 29 days the Moon's distance from Earth changes by about 50,000 km. Devices shown in Fig. 5.4 (in Chapter 5) must be used to change the length (or link length) of the transport cables as the Earth–Moon distance changes. They may be located at the Earth drive station, on a space station, in space, and/or on the Moon. The average speed of a cable length change is about 40 m/s. As the Moon pulls the transport system, it may be used to produce mechanical energy. If the cables can support 9 tons, the power can reach 1.8 million Watts. The cables rotate the electric generator and negligibly brake the Moon's movement.

Theory of Optimal Cable from Earth to Moon

1. **Equations for an optimal cable from the Earth to the Moon**. The gravitation of the Earth, the Moon and the cable mass acts on every element of the cable. These forces create stress in the cable material. The cable mass will be minimum if the stress is constant along the cable. The stress equals the force divided by the cross-sectional area of cable.

The force active in the cable is given by:

$$F = \sigma A = F_0 + \int_{R_0}^{R} dG = F_0 + \int_{R_0}^{R} \gamma \, A dR \qquad , \qquad (7.1)$$

where

$$\gamma = \gamma_0 g_0 \left[\left(\frac{R_0}{R} \right)^2 - \frac{g_m}{g_0} \left(\frac{R_m}{D - R} \right)^2 - \frac{\omega_m^2 R}{g_0} \right], \qquad (7.2)$$

where F = force in a given cross-section area [N]; F_0 = force at Earth surface [cabin (load) weight at earth surface] [N]; dG = weight of a cable element; A = cross-section area of cable [m²]; σ = tensile strength in the cable [N/m²]; R = distance from Earth's center [m]; R_0 = radius of Earth [m] (R_0 = 6378 km); R_m - radius of Moon = 1737 km; γ = specific weight of cable [kg/m³] at radius R; γ_0 = specific weight of the cable [kg/m³] at the Earth's surface; g_0 = gravitation at R_0 [m/s²], for Earth, 9.81 m/s² ; g_m = gravitation on Moon surface [m/s²], 1.62 m/sec²; D = distance from Earth to Moon [m], D_{min} = 356,400 km, D_{max} = 406,700 km; ω_m = orbital angle speed of the Moon around Earth [rad/s] 2.662·10⁻⁶ rad/s.

Let us substitute equation (7.2) in (7.1) and differentiate to obtain:

$$dA / A = \frac{\gamma_0 g_0}{\sigma} \left[\frac{R_0}{R} - \frac{g_m}{g_0} \left(\frac{R_m}{D - R} \right)^2 - \frac{\omega_m^2 R}{g_0} \right] dR \quad . \qquad (7.3)$$

The solution of equation (7.3) is

$$a_m(R) = \frac{A}{A_0} = \exp\left[\frac{g_0 B(R)}{k} \right] \quad ; \qquad (7.4)$$

where

$$B(R) = R_0 - \frac{R_0^2}{R} - \frac{g_m R_m^2}{g_0} \left[\frac{1}{D - R} - \frac{1}{(D - R_0)} \right] - \frac{\omega_m^2}{2 g_0} \left(R^2 - R_0^2 \right) , \qquad (7.5)$$

where a_m is the relative cross-section area of Earth–Moon cable; A_0 is the cable's cross-section area at the Earth's surface [m²]; $k = \sigma/\gamma_0$, the ratio of cable tensile stress σ to cable density γ_0 [Nm/kg]; $K = k/10^7$ − the stress coefficient.

2. The mass, W [kg], of the cable is

$$W = \frac{F_0}{k} \int_{R_0}^{R} a_m dR \quad . \qquad \textbf{(7.6)}$$

3. The volume, V [m³], of the cable is

$$V = \frac{F_0}{\sigma} \int_{R_0}^{R} a_m dR . \qquad (7.7)$$

Figs. 7.2a and 7.3a represent computations of cable cross-section area and mass of a single cable for the maximum distance (400,000 km) from Earth to the Moon and for different stress coefficients K. Figs. 7.2 and 7.3 are computed for the stress coefficient K = 2–4.5. These figures show, if K = 2, the maximum cross-section cable area is more then 21 times the cross-section area at Earth (A_0 = 1). The cable area equals 19A_0 at the Moon. The cable weight for a force of 3 tons is 11,200 tons. If K = 4.5 the maximum cross-section area is 4 times more than the cross-section area near Earth and the cable

weight for the force (load) of 3 tons is decreased to 1000 tons. The Figs. 7.2 and 7.3 are computed for some very strong material available in the future. These figures show if, for example, the stress coefficient equals 15, the required cable mass for a load of 3 tons is decreased to 120 tons. For the three-cable system (main + two transport cables) this means that the system mass is 360 tons. Increasing or decreasing the load changes the cable mass proportionally.

Moon delivery work of 1 kg load is presented in Fig. 7.4.
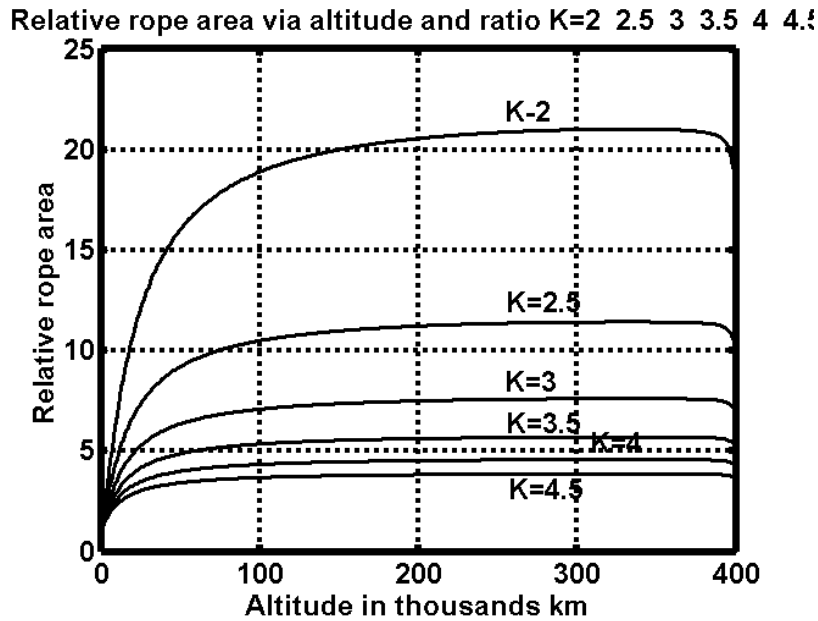

Fig. 7.2a. Relative area for a cable from Earth to Moon (up to 400,000 km) for stress coefficient $K = 2 - 4.5$.
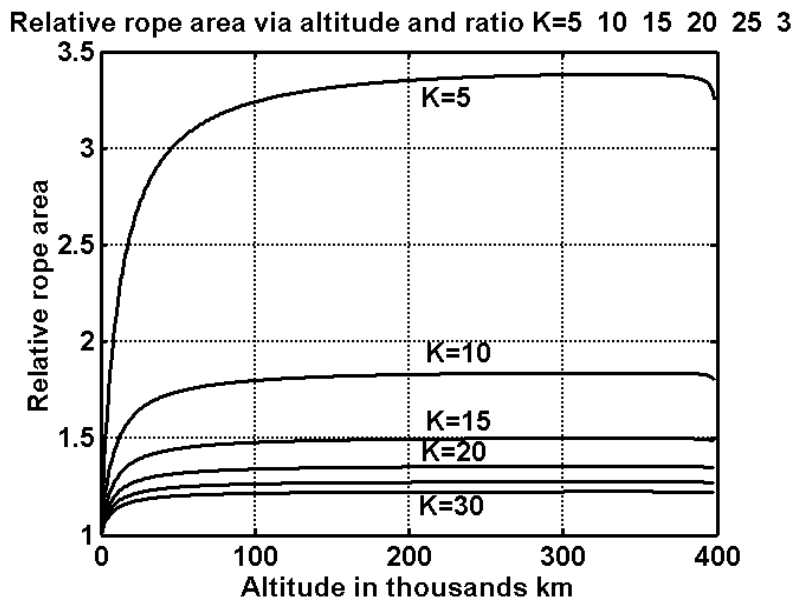

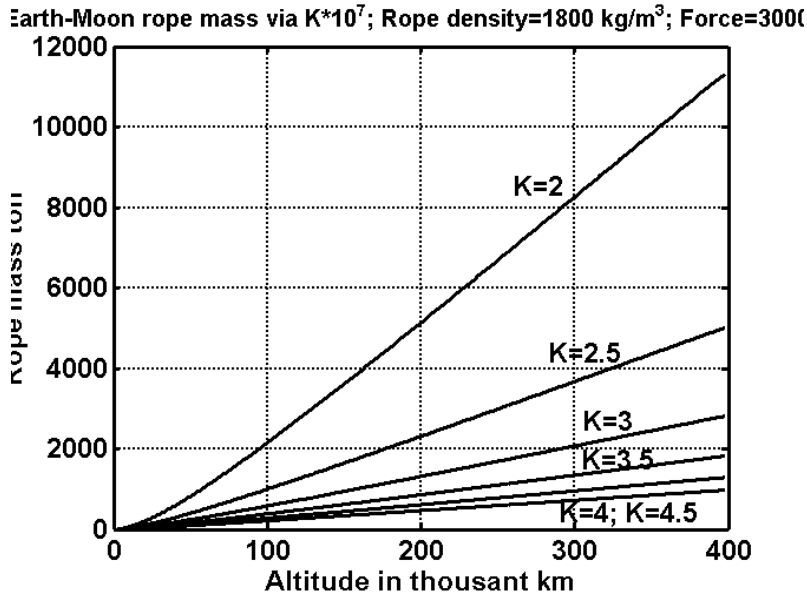**Fig. 7.2b.** Relative area for a cable from Earth to Moon (up to 400,000 km) for stress coefficient $K = 5–30$.

Earth-Moon rope mass via K*10⁷; Rope density=1800 kg/m³; Force=300(

Fig. 7.3a. The Earth–Moon cable mass [tons] versus altitude (in thousand km) for cable density 1800 kg/m³, delivery mass of 3 tons, $K = 2$–4.5.

Rope density=1800 kg/m³; Force=30000n
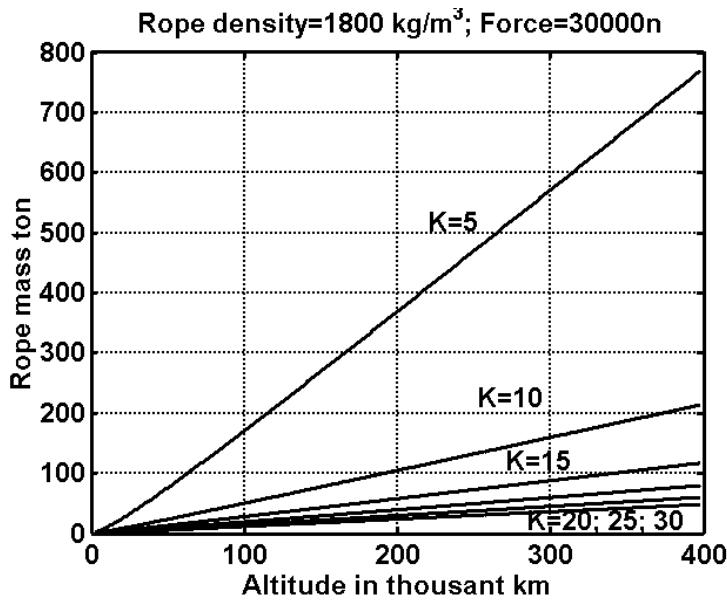
Fig. 7.3b. The Earth–Moon cable mass versus altitude (in thousand km) for cable density 1800 kg/m³, delivery mass of 3 tons, $K = 5$–30.

Fig, 7.4. (see hard copy). Moon delivery work [MJ] of 1 kg load versus altitude in thousand km.

Technical Parameters of Projects

The following are some data for estimating the characteristics of the cable system. The system has three cables: one main and two transport cables. Each transport cable can maintain a force (load) of 3 tons. This means that the cable can support two 3 ton loads, one going up and one going down. The material of the cable is assumed to have $K = 4$. The main cable has the optimal cross-sectional area for an equal stress cable. The transport cables are approximately optimal for 10 links. The main cable has a minimum cross-section area A_0 of 0.42 mm² (diameter $d = 0.73$ mm) and maximum cross-section area A_m of 1.9 mm² ($d = 1.56$ mm). The mass of the main cable would be 1300 tons. The total mass of the

main cable plus the two transport cables (for delivering a mass of 3000 kg) is about 3950 tons for the transport system shown in Fig. 7.1. If the cable can be made from nanotubes with $K = 10$, the total mass will be 665 tons, and if the cable has $K = 15$, the total cable mass would be 360 tons. The cabins that ride on the cable transport system are assumed to have a mass of 3 tons. Each would be capable of carrying a payload of either people or cargo. With suitable development, transfer speeds of 6 km/sec might be reached. This could allow a single cable system to transfer about 1000 tons of cargo per year to and from the Moon. The cabin speed is controlled by an engine located at the Earth pole drive station. If one cable is damaged the other two cables can be used to rescue people and to repair the injured cable.

Conclusion

There are a lot of problems that must be solved before the proposed Earth–Moon transport system can be built. The chief of these is producing a cheap strong cable and composite materials of appropriate strength for the rollers and transmission which can operate at high speed. Another problem is the design of connectors that would allow the payload to pass the rollers without stopping. The purpose of this work is to draw attention to the possibilities of further studies of this system, which has a great promise for future applications.

New materials could make the suggested transportation system realistic for trips between the Earth and the Moon with little expenditure of energy. The author is prepared to discusses the project details with serious organizations that have similar research and development goals. The same ideas were offered by author in patent applications 09/789,959 of 2/23/01, 09/873,985 of 06/01/01, 09/974,670 of 10/11/01, and patent US 6,494,143 of 12/17/02.

References

1. Bolonkin A.A., "Non-Rocket Earth-Moon Transport System". Paper B0.3-F3.3-0032-02 presented to 34th COSPAR Scientific Assembly, The World Space Congress 2002, 10–19 Oct 2002, Houston, Texas, USA.

2. Bolonkin A.A., "Non-Rocket Earth–Moon Transport System", *Advanced Space Research*, Vol. 31, No. 11, pp. 2485-2490, 2003.

3. Bolonkin A.A., "Non-Rocket Transport System for Space Travel", IBIS, Vol. 56, No. 7/8, 2003, pp. 237–249.

4. Bolonkin A.A., "Bolonkin's Method Movement of Vehicles and Installation for It", Patent US 6,494,143 B1, 2002.

5. Cosmo, M.L. and Lorenzini E.C. (eds.). *Tethers in Space Handbook*. 3rd ed. *Smithsonian Astrophysical Observatory*, December, 1997.

6. Smitherman D.V. Jr., "Space Elevators", NASA/CP-2000-210429, U.S. National Aeronautics and Space Administration, Washington, DC, 2000.

7. Galasso, F.S. , *Advanced Fibers and Composites*, Gordon and Branch Science Publisher, New York,1989, p.158.

8. *Carbon and High Perform Fibers Directory and Data Book*, London & New York: Chapman & Hall, 6th ed., 1995.

9. Dresselhous, M.S. *Carbon Nanotubes*, Springer, 2000.

Chapter 8
Earth–Mars Cable Transport System*
Summary

The author offers and computes a new permanent cable transport system that links a pole of the Earth with Mars orbit. This system connects Earth and Mars for 1–1.5 months every 1.7–2 years when they are located at the nearest distance and allows the transfer of people and loads to Mars and back. The system has many advantages because it uses a transport engine located on Earth, but it also requires the high strength cable made from nanotubes.   This chapter contains theory of an optimal equal stress cable, that connects the Earth and Mars orbit, as well as computed parameters of the suggested system.

Introduction

 The author has proposed a new transport system for delivering payloads and people to Mars. The author has not found an analog of similar facilities for transporting a payload into space in the literature and patents.

   The present method does not require rockets. The installation has a cable transport system and uses kinetic energy from the Earth's orbit. The suggested transport system is driven by an engine located on the Earth's surface.

   In the proposed method, a cable transport system is permanently connected from the Earth's pole to Mars orbit. This way, a space ship moved to Mars obtains its energy from the Earth's orbit (not Earth's rotation). When the ship returns to the Earth, it obtains its energy from an onboard engine or from an engine located on Earth.

   This chapter contains the theory of an optimal equal stress cable for the complex Earth–Sun–Mars gravitational field and results of computations of the project.

   The project uses artificial materials like nanotubes and whiskers that have a ratio of tensile strength to density equal 20 million meters or greater[4, 5, 6]. Theory predicts a nanotubes with specific tensile stress of 100 million meters. That will significantly improves the parameters of the suggested project.

   The author's other non-rocket closed methods are presented in References[7, 8] and in chapters of this book.

Brief Description

   The chapter contains the theory and results of computation for a special project. This project uses three cables (one main cable and two for driving loads) mass from artificial material: whiskers, nanotubes, with the specific tensile strength (ratio of tensile stress to density) $k = \sigma/\gamma = 20 \cdot 10^7$ ($K = 20$) or more. Nanotubes with the same or better parameters are available in scientific laboratories. The theoretical limit of nanotubes of SWNT type is about $k = 100 \cdot 10^7$ ($K = 100$).

   A proposed centrifugal Mars cable transport system is shown in Figs. 8.1 and 8.2. The system includes the optimal equal stress cable which has a length approximately equal to the minimum distance of the Earth to Mars orbit. The installation has a transport system with chains connected by rollers and two transport cables.
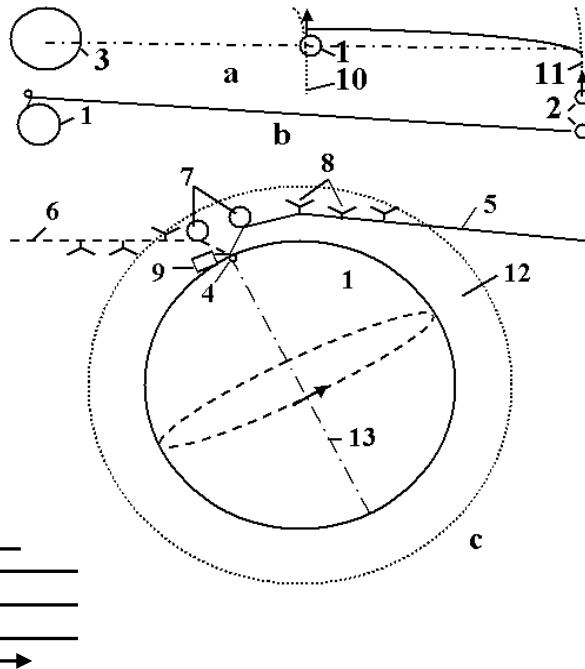
Fig. 8.1. The offered Earth–Mars orbit Transport System. a. Sun–Earth–Mars; b. Earth–Mars; c. Connection to Earth pole. Notations: 1– Earth, 2 – Mars, 3 – Sun, 4 – Earth pole, 5 – Earth–Mars cable transport system in right position, 6 – Earth–Mars cable transport system in left position, 7 – air balloon, 8 – support wing, 9 – drive station, 10 – Earth orbit, 11 – Mars orbit, 12 – Earth atmosphere, 13 – axis of Earth rotation.

Fig. 8.2. Cables of transport system. Notations: 144 – space ship, 15 – rollers, 17 – transport cable, 18 – main cable.

   The upper ends of the cables are located near Mars orbit and the lower ends of the cables are connected to the Earth's pole. They are supported in the Earth's atmosphere by air balloons (near the Pole) and winged devices at a maximum distance of up to 2800 km. The rotary speed of the cables changes from zero (at the pole) to 190 m/s (at the end of the maximum distance in the atmosphere). These winged devices can support cables when they are located within the lower atmosphere.
   The installation would have a device, that allows the length of the cables to be changed. The device would consist of a spool, motor, brake, transmission, and controller. The facility could have mechanisms for delivering people and payloads to Mars and back using the suggested transport system.
   The delivery devices include: containers (passenger cabins, space ships, etc.), cables, motors, brakes, and controllers.
   The space cabin can temporarily land on the surface of the Mars for loading and performing research. The space cabin has a small rocket engine for maneuvering and landing on the surface of Mars.
   Every two years Mars comes within a minimum distance from Earth. For about 1–1.5 months the cable transport system (CTS) can be used to deliver people and loads to Mars. The space ship moves in advance to the upper end of the CTS, then when Mars arrives, the vehicles land on its surface and the people work on for Mars 1–1.5 months; afterwards the space ships return to Earth. While living on Mars, the people can fly from one place to another with speeds of about 230 m/s (including Mars round trip at low altitude) in their space cabin (ship). Exploring using the CTS would not require rocket fuel.

Theory of Earth–Mars equal stress cable

1.   Writing the equation of equilibrium for a small element of the Earth–Mars cable

$$\sigma dA = -g_0 \gamma_0 \left(\frac{R_0}{R - R_e} \right)^2 AdR + \gamma_0 g_m \left(\frac{R_{mo}}{R_m - R} \right)^2 AdR + R\omega^2 \gamma_0 AdR - \gamma_0 g_s \left(\frac{R_s}{R} \right)^2 AdR. \quad (8.1)$$

Dividing the left and right sides of equation (8.1) by $\gamma_0 A$ and taking the integral from $(R_m - R_{mo})$ to R, the equation of the optimal equal stress cable from the Earth to Mars may be written and solved as given below

$$a = \frac{A}{A_0} = \exp \left\{ -\frac{1}{k} \left[\begin{array}{l} g_m R_{mo}^2 \left(\dfrac{1}{R_m - R} - \dfrac{1}{R_{mo}} \right) + g_o R_o^2 \left(\dfrac{1}{R - R_e} - \dfrac{1}{R_m - R_{mo} - R_e} \right) \\[2mm] + g_s R_s^2 \left(\dfrac{1}{R} - \dfrac{1}{R_m - R_{mo}} \right) + \dfrac{\omega^2}{2} \left(R^2 - (R_m - R_{mo})^2 \right) \end{array} \right] \right\} \quad (8.2)$$

2. The mass of cable is

$$W = \frac{F_0}{k} \int_{R_0}^{R} a \, dR. \quad (8.3)$$

3. The volume of cable is

$$v = \frac{F_0}{\sigma} \int_{R_0}^{R} a \, dR. \quad (8.4)$$

Here: a – relative cross-section area of cable; A – cross-section area of cable [m²]; A_o – near Mars orbit cross-section area of cable [m²]; g_o – gravitation at the planet surface R_0 [m/s²], for Earth $g_o = 9.81$ m/s²; $g_m = 3.72$ m/s² – gravitation on Mars surface; $g_s = 274$ m/s² – gravitation on Sun surface; F_o – force [N] (ship mass); $k = \sigma/symbol\ 103\ \backslash f\ "Symbol"\ \backslash s\ 10$g – ratio of cable tensile stress to density [Nm/kg]; $K = k/10^7$ – stress coefficient [million meters]; R – radius from Sun center to given cross-section of cable [m]; $R_o = 6.378 \times 10^6$ – radius of Earth [m]; $R_e = 14.95 \times 10^{10}$ – Sun–Earth distance [m]; $R_{mo} = 3.39 \times 10^6$ – radius of Mars [m]; $R_m = 22.8 \times 10^{10}$ - radius of Mars orbit [m]; $R_s = 696 \times 10^6$ – radius of Sun [m]; v – volume of the cable [m³]; W – mass of the cable [kg]; σ – cable tensile strength [N/m²]; $\omega = 2 \times 10^{-7}$ – angular speed of Earth orbit [rad/second]; γ – density of cable [kg/m³].

Figs. 8.3 to 8.5 represent the computation for the shortest distance (78 million km) from Earth to Mars.

Readers can finds the performances of current cables and a discussion of cable problem in References[4 to 8].

Project
Earth-Mars non-rocket transport system

The following are some data estimations of the Mars transport system, which provides an inexpensive payload transfer between the Earth and Mars. The system has three cables. Each cable can hold a force of 3 tons. All cables have optimal cross-sectional areas of equal stress.

Results of computation for $K = 20$–50 are presented in Figs. 8.3–8.5. If material of the cable has specific strength $k = 20 \times 10^7$ ($K = 20$), the ratio of the maximum cross-section area (near Earth) to the minimum cross-section area of the cable (near Mars orbit) is 4.4 (Fig. 8.3), at the Earth's surface this ratio equals 3.15 (Fig. 8.5). If the space cabin has a mass of 3 tons, the mass of the main cable is 34,000 tons (Fig. 8.4). The total mass of the main cable plus the two container cables (for delivering a mass of 3000 kg) equals about 110,000 tons. If one cable is damaged, two others will be used for assuring people's safety as well as for repairing the original cable.

Patent applications are 09/789,959 of 2/23/01, 09/873,985 of 06/01/01, 09/974,670 of 10/11/01, patent US 6,494,143 of 12/17/02.
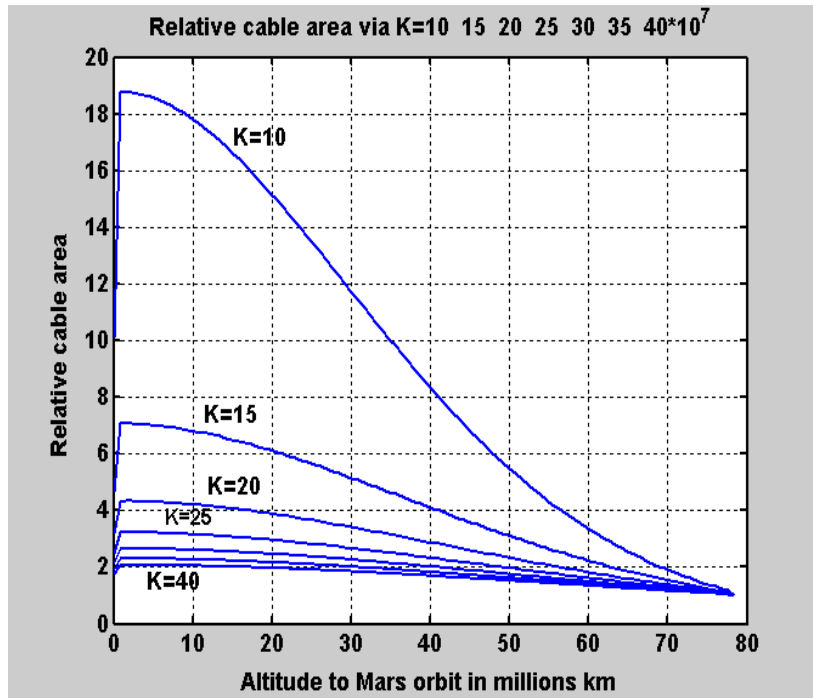
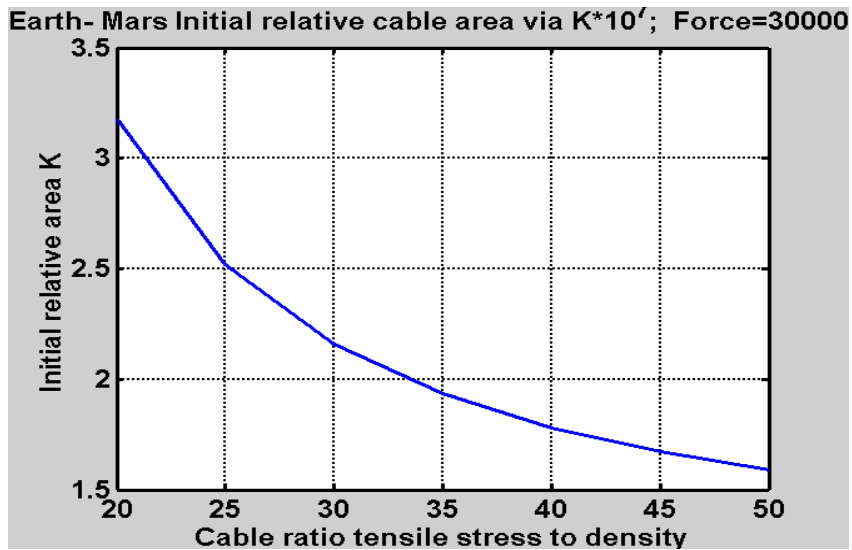**Fig. 8.3.** Relative cable area of Earth–Mars transport system via distance to Mars orbit in million kilometers.

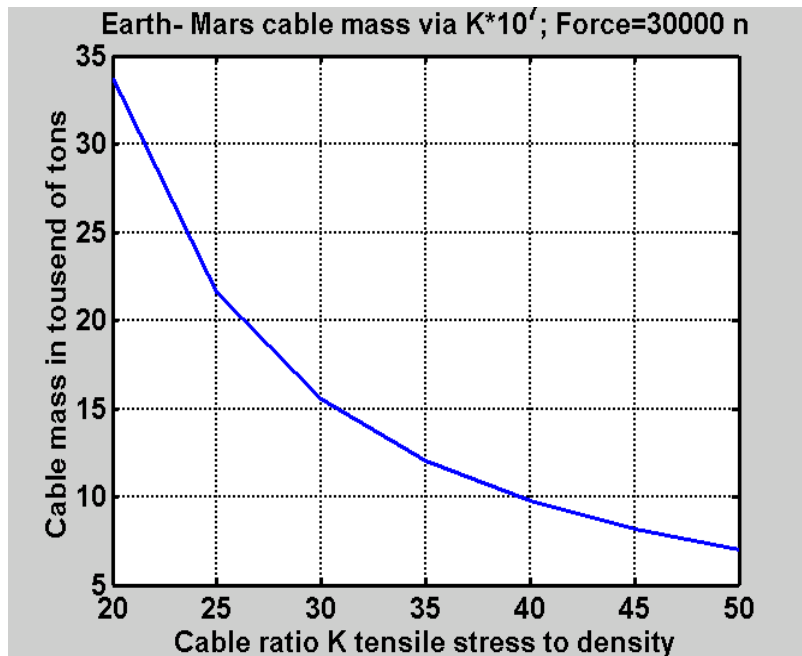**Fig. 8.4.** Earth–Mars cable mass via stress coefficient *K*.

Fig. 8.5. Earth–Mars initial (near Earth) relative cable area via the stress coefficient *K*.

Conclusion

The offered transport system is not a well-known tether system because it does not have the main attributes of a standard tether system: free rotation in space and connection two **artificial** bodies. Our system does not rotate and it is only temporarily connected to a second **natural** body. It may be compared with an aerial ropeway in mountains. However it is as different from an aerial ropeway as a current airplane is different from a children's paper airplane.

The offered transport system is not a conventional space elevator. The conventional space elevator connects the Earth's equator to a space station located on the geosynchronous Earth orbit. The offered system is connected to a **pole** of the Earth. It is impossible for space elevator, because it will not work if it is connected to the Earth's pole. The space elevator must rotate a space station using the Earth's energy. It means the Earth end of the space elevator **must** be connected to the Earth's **equaor**. Our system is rotated using movement of the Earth along the Earth's orbit around the Sun.

The offered system has a new simple mechanical **transfer** system for transferring energy from the Earth mechanical engine (located on Earth) to a load cabin, located in space. The system has a new idea – separating the cable transmission into sub-sections, which dramatically decreases the cable weight. This transport system may be applied to the space elevator and it can solve the main problem of the space elevator: how to transfer energy for movement of the load carbine. This idea can also be applied to building space towers, for cable space launchers and for transferring mechanical energy over long distancis on Earth.

New materials could make the suggested transportation system realistic for trips between the Earth and the Moon in the future with little expenditure of energy. The author is prepared to discuses the project details with serious organizations that have similar research and development goals.

References

1. Edited by M.L. Cosmo and E.C. Lorenzini. *Tethers in space handbook*. 3rd Edn. Smithsonian Astronomic Observatory, December, 1997.

2. S.W. Ziegler and M.P. Cartmell, "Using Motorized Tethers for Payload Orbital Transfer", *Journal of Spacecraft and Rockets,* Vol. 38, No 6, 2001.

3. D.V. Smitherman Jr., "Space Elevators", NASA/CP-2000-210429.

4. F.S. Galasso, *Advanced Fibers and Composite*, Gordon and Branch Science Publisher, 1989.

5. *Carbon and High Performance Fibers Directory and Data Book* , 1995, London–New York, Chapman & Hall.

6. M.S. Dresselhous, *Carbon Nanotubes*, Springer-Pergamon, NY, 1996–2000.

7. A.A. Bolonkin, "Cable Earth–Mars Transport System", Presented as paper BO.4-C3.4-0036-02 to The World Space Congress-2002, 10–19 Oct. 2002, Houston, Texas, USA.

8. A.A. Bolonkin, "Cable Earth–Mars Transport System", *Actual Problems of Aviation and Aerospace Systems.* No. 2 (16), vol.8, 2003.

Chapter 9
Kinetic Anti-Gravitator*

Summary

This Chapter describes a method and devices that provides a repulsive (repel, push, opposed to gravitation) force between given bodies. The basic concept is that a strong, heavy cable is projected upwards using a motorized wheel on the ground. The upward momentum of the cable is transferred to the apparatus by means of a pulley/roller mechanism, which sends the cable back down to the motor. The momentum transferred from the cable to the apparatus produces a push force which can suspend the apparatus in the air or lift it. There is an equal and opposite force on the motorized wheel on the ground. The push force can be great (up to tens of tons) and operate over long distances (up to hundreds of kilometers). This force produces great accelerations and velocities of given bodies (vehicles). This device is called a kinetic (mechanical) anti-gravitator (kinetic repulsator or repellor) because gravitation attracts any two bodies, whereas the offered device repels any two bodies.

  The offered method can be applied to: VTOL aircraft, non-rocket space apparatus, flyng, walking, and jumping (pogo-stick) superman (vehicles), long arm (long hand), high altitude crane, high tower (up to 200 km), and for construction of Space Elevator without rockets.

Nomenclature

b – atmospheric exp. coeff. (for example, an altitude H in the interval 0–10 km, $b \approx 1/9218$),
D – average air drag [N],
D_L – laminar air drag [N],
D_T – turbulent air drag [N],
d – cable diameter [m or mm],
F – repulsive (lift) force [N],
g – gravity, $g_o = 9.81$ m/s^2 is gravity on the Earth's surface,
H – the height of the kinetic device (top end of the cable) [m],
$k = \sigma/\gamma$ – relative cable stress [m^2/sec^2], $K = k/10^7$,
L – cable length between an Earth support and the object (load) [m],
$L_s = L^{0.8}s$ – cable surface parameter,
m, m_c – the cable mass [kg],
m_1 – mass of apparatus [kg],
m_2 – mass of a repulsive engine [kg],
n – number of the installation cables ($n = 2; 4; 8$; etc.),
P – engine power [W],
P_T – power of turbulent drag [W],
P_L – power of laminar drag [W],
R – circle radius [m],

V – cable speed [m/s],
V_s – ship speed [m/s].
V_1 – apparatus speed [m/s],
v – objective speed [m/s],
R_o = 6,378 km – Earth radius,
S – cable cross-section areas (one branch or all branches) [m^2],
s – perimeter of all cable cross-section areas [m],
α – angle of circle part [rad],
σ – cable tensile stress [N/m^2],
γ – cable density [kg/m^3],
μ – air viscosity [kg/s.m],
ρ – air density at altitude H (for example, at H = 0 km, ρ_o = 1.225 kg/m^3, μ = 1.7894·10^{-5}).

Introduction

At present, we know some methods of flight on Earth and in space. Earth atmospheric devices (aircraft, helicopters) push down the air; space apparatus pushes away a rocket gas. These methods have many disadvantages. For example, we need an atmosphere of sufficient density or rocket fuel. We cannot be immobile and suspended for a extended period of time at a given point over the surface of a planet that has gravity but no atmosphere.

The winged and liquid rocket methods of flight have reached the peak of their development. In the last 30 years there has been no increase the air speed, no wide application of VTOL aircraft, no significant decrease in space delivery cost, no common space tourism, and no non-vehicle individual flights to the atmosphere. Space launches are very expensive.

The aviation, space, and energy industries need revolutionary ideas which will significantly improve the capability of air and space vehicles.

Other than rockets, one method for reaching space is the space elevator. It is very complex, expensive and technologically impossible at the present time.

Below is a new method[1, 2, 3]. This method produces a push (repulsive, repel, opposed to gravitation) force between given bodies, for example, between the ground and a flying vehicle. The basic concept is that a strong, heavy cable is projected upwards using a motorized wheel on the ground. The upward momentum of the cable is transferred to the vehicle by means of a pulley/roller mechanism. This mechanism creates a push force and that also sends the cable back down to the motor. The momentum (push force) transferred from the cable to the vehicle can suspend it in the air or lift it. This force is equal and opposite to the force on the motorized wheel on the ground. The push (mechanical) force opposes the gravitational force between these bodies (for example, the ground and a flying vehicle). This force is created by a linear thin cable moved between the given bodies. If there is no roller and air friction and the distance between the given bodies is not changed, the suggested pusher does not require energy (except for the initial start and wheel friction). When the distance is increased, the energy is spent, when the distance is decreased, we gain energy. For some people this push force may be surprising because the bodies are connected only by the flexible thin long cable. But there are no violations of the laws of physics – we transfer a momentum between the bodies through the moving cable. When this momentum in a unit of time (force) is more than the gravity force, the bodies will move away from one other; when the momentum is less than the gravity force, the bodies will be drawn together.

The offered method makes it easy to achive a large push (repulsive, repel) force over long distances, to accelerate a vehicle in flight or keep it at a given distance and to equalize the gravity force. This chapter contains some applications of this method.

The suggested method is different from a 2000-km space launcher (cable into tube) at an altitude of 80 km offered by K. Loftstrom in, published in 2002[4]. These differences are discrtbed in the "Discussion" section.

Brief description of the installation

Some variants of the installation are shown in Figs. 9.1 to 9.5. The installation includes (see notations in Fig. 9.1 and others): a linear closed-loop cable, top and bottom rollers, any conventional engine, and a load. Details of the top roller are shown in Fig. 9.2, the bottom (lower) driver roller is shown in Fig. 9.3. The small rollers (Fig. 9.3) press on the cable and together with the large roller and engine move the cable. The possible cable cross-section areas are shown in Fig. 9.3c. Fig. 9.4 shows the anti-gravitator in a slope position.

The spool mechanisms are shown in Fig. 9.5a,b. They allow reeling and unreeling of the left and right cable branches or different speeds as well as changing the length of the closed-loop cable without stopping of the installation. The spool may be one of two variants: a mobile spool (Fig. 9.5a) or a motionless spool (Fig. 9.5b).

The installation works in the following way: the engine rotates the lower driver roller and continuously sends the closed-loop cable upwards at high speed. The cable reaches a top roller (which may be at high altitude), turns back and moves to the lower driver roller. When the cable turns back, it creates a push (repulsive, repel, reflective, centrifugal, momentum) force. This repulsive force can easily be calculated using centrifugal theory (see the theoretical section of this chapter).
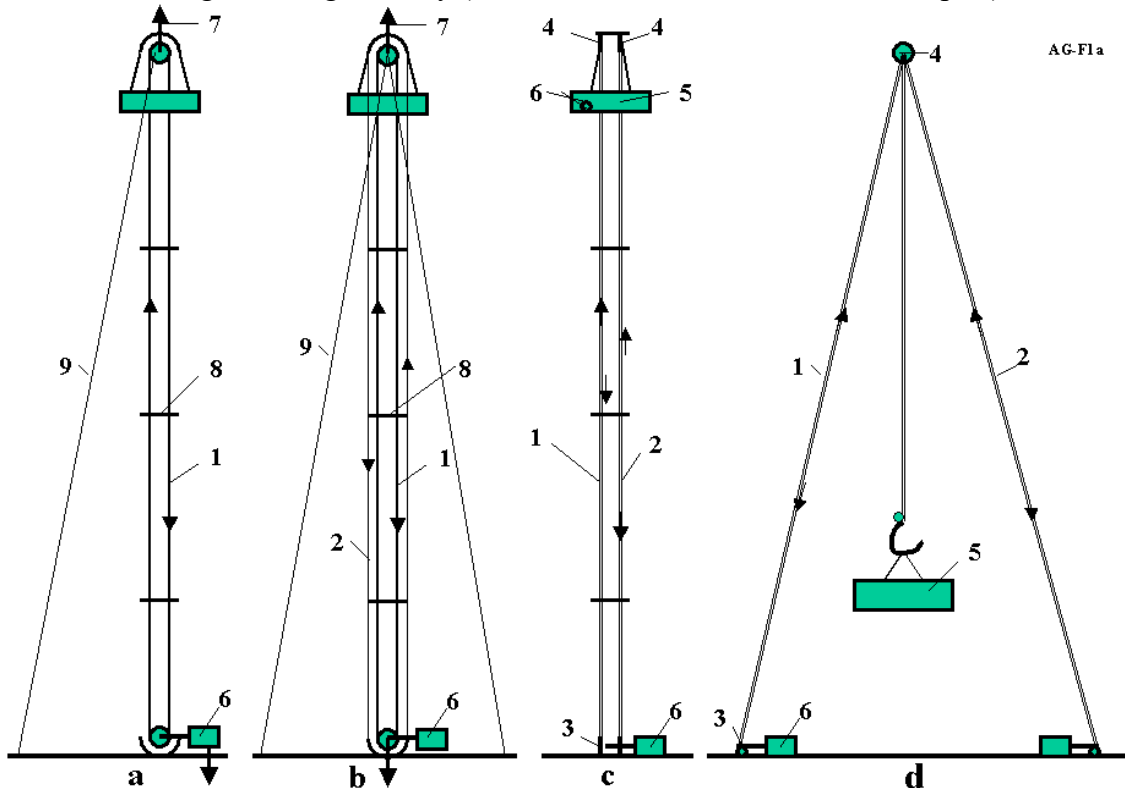
Fig. 9.1. Push devices (kinetic anti-gravitators) with closed-loop alastic cables: **a** – single cable with brace, **b** – double cables are moved in opposite directions and located in one plane, **c** – installation with four closed-loop cables in different plates and without braces, **d** – load crank with a minimum three cables. Notations are: 1– one closed-loop cable; 2 – the second closed-loop cable; 3 – lower rollers; 4 – top rollers; 5 – suspended object; 6 – engine; 7 – push (lift) force; 8 – spreader, 9 – braces.

The push force can also be calculated against the mobile cable mass using momentum or reflection theories (see the theoretical section).

The cable turns 180 degrees around pulleys. That turn produces a centrifugal force which supports or moves the load. However, Newton's laws say that for every action there is an equal and opposite reaction. In this case, the action comes from the wheel as this is what is pushing the cable and producing the net negative gravity field direction force on the cable. To do that, the wheel moves (is pressed) by the cable producing the reaction, which adds up to (similar to how the cable loads) an equal load in the positive gravity direction. This means the cable will push the wheel back toward the source of the gravity (in this case to the ground).

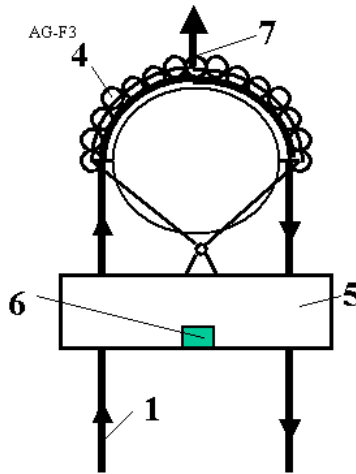**Fig. 9.2**. Top roller of kinetic anti-gravitator (Notation as in Fig. 9.1).
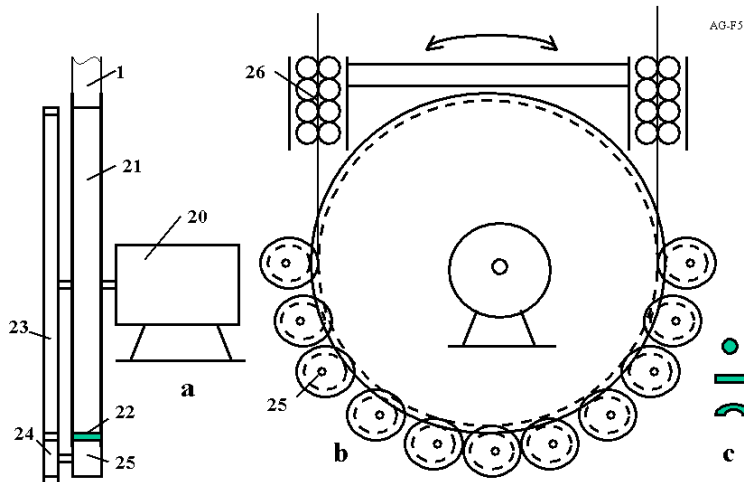
Fig. 9.3. Drive roller of kinetic anti-gravitator. Notations are: 20 – engine; 21 – drive roller; 22 (1) – flexible cable; 23 – large gear wheel; 24 – small gear wheels; 25,26 – directive rollers. **a** – side view, **b** – front view, **c** – cable cross-section.
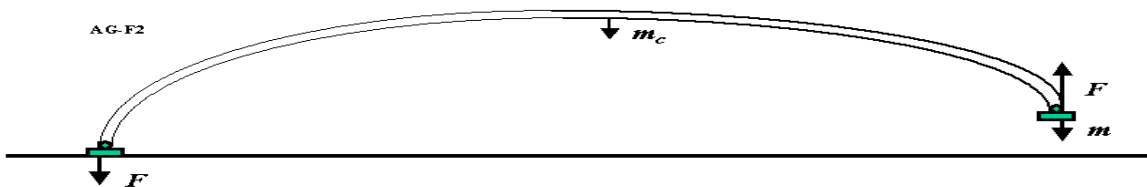
Fig. 9.4. Kinetic anti-gravitator in slope position.

The repulsive force points in a vertical direction and it must be more than the gravitational force of the cable and load. This anti-gravity force keeps the load or space station suspended on the top roller; and the load cable (or special elevator) allows the delivery of a load to the space station. The rollers and cable may have high speed and stress. They must be made from a strong (for example, composite) material. In this case, the rollers have the same permitted stress (and permitted rotary speed) as the cable. The permitted (safety assurance) speed (of the cable or roller) is the speed permitted (admitted, safety) by the maximum material strength divided by an assurance factor.

The moment of friction in the top roller can be compensated by guy lines as in Fig. 9.1a, or by the second closed-loop cable rotating in an opposed direction to the first cable (Fig.1 b,c,d) and located in one plane (Fig. 9.1a).

A low altitude (up to 10 km) pusher may have its cable made from conventional steel wire (or steel fiber). This cable has a smaller permitted maximum speed and air drag. It requires less power for rotation than a light cable made from artificial fibers (see "Applications" section in this chapter).
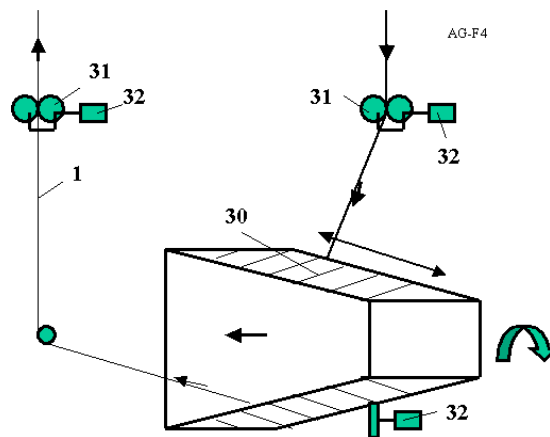
Fig. 9.5a. Revolving spool. Notation are: 30 – cable spool; 31 – directive rollers; 32 – spool engine. The left and right cables can have different speeds.
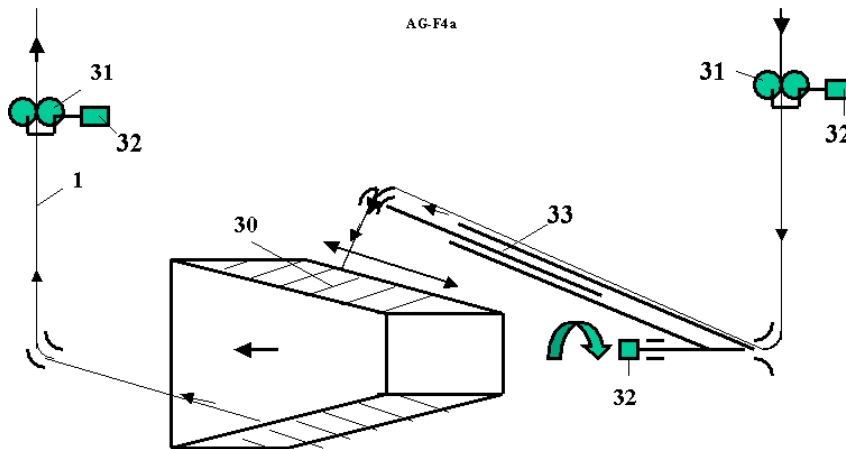
Fig. 9.5b. Motionless spool (the lever rotates around the spool). Notation are: 30 – cable spool; 31 – directive rollers, 32 – motor, 33 – revolving lever. The left and right cables can have different linear speeds.

As shown in the theoretical section, the current widely produced artificial fibers allow reaching altitudes of up to 100 km (see also Projects 1 and 2 in "Kinetic Space Towers and Launchers"[3]). If more altitude is required a multi-stage tower must be used (Fig. 2 and Project 3[3]), and very high altitude is

needed (geosynchronous orbit or more), a very strong cable made from nanotubes must be used (Project 4[3]).

The closed-loop cable can have be of variable length. This allows starting from zero altitude, increasing the load (station) altitude to a required value, and spooling the cable for repair. If we change the length of the cable (for example, using the spool) the cable will lift the load to high altitude or into space.

The devices for this action are shown in Fig. 9.5. The offered spools allow reeling and unreeling the left and right branches of the cable with different speeds to change the length of the cable.

The advantages of the proposed method are the same as for the centrifugal launcher[5]. The suggested design has approximately half the construction cost of the semi-circle launcher[5] because it uses vertical cables (not circle cables[5]). It also has approximately half the production delivery cost (up to $2–4 per kg), because it has half the air drag and fuel consumption (the straight line is 3.14 times shorter than the circle).

Experiments requested by author and cames out by Mr. Gregory Lishanski in 2002– 2003 show the revolving straight closed-loop cable is stabile in the vertical and horizontal positions.

Theory of the kinetic anti-gravitator

1. **Push force for immobile object[3].**

   a) **Repulsive (repel, push) force in space without gravitation.** We can find the push force of the kinetic anti-gravitator from centrifugal theory (Fig. 9.5c)
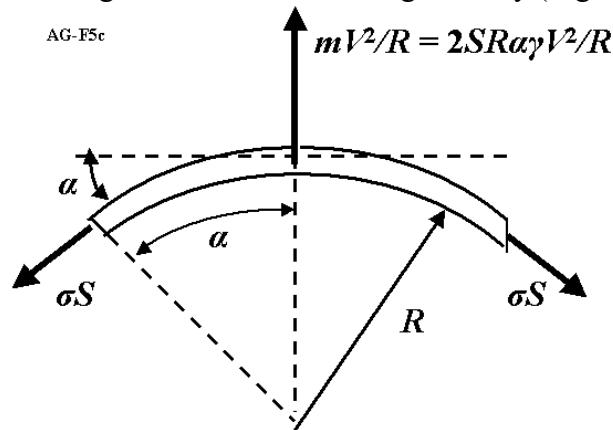
Fig. **9.5c**. Forces of the rotary circle cable.

We first take a small part of the rotary circle cable and write the equilibrium rotation for centrifugal force and tensile stress

$$\frac{2SR\alpha\gamma V^2}{R} = 2S\sigma \sin \alpha , \qquad (9.1)$$

where α = angle of the circle part [rad]. When $\alpha \to 0$ the relationship between maximum rotary speed V and tensile strength σ of a closed-loop (curved) cable is

$$V = \sqrt{\frac{\sigma}{\gamma}} = \sqrt{k} , \quad F = 2\sigma S , \qquad (9.2)\text{-}(9.3)$$

where F is the repulsive (lift) force [N], $k = \sigma/\gamma$ is to relative cable stress [m²/s²], S is the area of one branch of the cable cross section [m²]. The more convenient value of $K = 10^{-7}k$ is used for graphs. Equation (9.2) is found in the References[5] for a circle centrifugal cable launcher (chapter 3). The

computation of V versus k for intervals of $0 - 4K$ ($K = k/10^7$) is presented in the same publication (chapter 3, Fig. 3.10). For example, the cable has the cross-section area $S = 1$ mm^2, stress $\sigma = 100$ kg/mm^2. Two cables can keep a load of 200 kg at altitude.

   We can find the lift force using reflection theory (see textbooks on theoretical mechanics). Writing the momentum of the reflected mass in one second gives

$$F = mV - (-mV) = 2mV, \quad m = \gamma SV, \quad \text{or} \quad F = 2\gamma SV^2. \tag{9.4}$$

   Here m is the cable mass reflected in one second [kg/s]. If equation (9.2) is substituted into (9.4), the expression for the repulsive (lift) force $F = 2\sigma S$ will be same.

b) **Repulsive force in constant gravity field.** In constant gravity field without air drag, the repulsive force of the offered device equals the centrifugal force F minus the cable weight W

$$F_g = F - W = F - 2\gamma gSH = 2\gamma S(V^2 - gH) = 2S(\sigma - \gamma gH) = 2S\gamma(k - gH), \tag{9.5}$$

   where H is the height of the kinetic device (top end of the cable) [m].

c) **Repulsive force in variable gravity field and rotary Earth.** Below it is shown a way of finding the final equation for the force F.

$$dP = \left(g - \frac{V^2}{R}\right)dm, \quad g = g_0\left(\frac{R_0}{R}\right)^2, \quad \frac{V^2}{R} = \omega^2 R, \quad dm = \gamma SdR, \quad R = R_0 + H,$$

$$P = \int_{R_0}^{R}\left[g_0\left(\frac{R_0}{R}\right)^2 - \omega^2 R\right]\gamma SdR = g_0\left(R_0 - \frac{R_0^2}{R}\right) - \frac{\omega^2}{2}\left(R^2 - R_0^2\right), \quad or \tag{9.6}$$

$$F = 2\sigma S - 2P = 2\gamma Sk - 2P = 2\gamma S\left[k - g_0\left(R_0 - \frac{R_0^2}{R}\right) + \frac{\omega^2}{2}\left(R^2 - R_0^2\right)\right], \quad k = \frac{\sigma}{\gamma} = V^2.$$

   The minimum cable stress or a minimum cable speed of a revolving planet is

$$k_{min} = V_{min}^2 = g_0\left(R_0 - \frac{R_0^2}{R}\right) - \frac{\omega^2}{2}\left(R^2 - R_0^2\right). \tag{9.7}$$

   If $K > 5$ the height of the kinetic tower may be more than the Earth's geosynchronous orbit. For Mars $K > 1$, for Moon $K > 0.3$. The Fig. 5.10 (chapter 5) shows that the offered device with a height of 145,000 km can keep its position without cable rotation (movement), and if the device height is more than 145,000 km, the device has a useful lift force. That allows the lifting of a payload using a non-moving cable. We can stop the cable rotation and create the space elevator.

   2. Repulsive force for a mobile object. For a mobile object the repulsive force is

$$F = 2\gamma S(V \pm v)^2 \tag{9.8}$$

where v is the objective speed [m/s]. The minus "– " is taken when the cable length is increased, the plus "+" is taken when the cable length is decreased. From equation (9.8) it follows that the maximum object speed obtained from the cable cannot exceed the cable speed. Equation (9.8) is used for launching and landing of flight apparatus.

   3. Restore force. When the cable is deviated from a vertical position in the gravity field, the restore force is

$$F_r = F - \frac{gm_c}{2}. \tag{9.9}$$

   4. Air drag of the cable. The computation of cable drag is not developed. No experimental data are available air drag of a very long cable.

a) The air drag of a double **subsonic** cable can be estimated using the drag equations for plates (the Reynolds number is included):

$$D_L = 0.5 \cdot 0.664\rho^{0.5}\mu^{0.5}V^{1.5}L^{0.8}s, \quad D_T = 0.5 \cdot 0.0592\rho^{0.8}\mu^{0.2}V^{1.8}L^{0.8}s, \quad D = 0.5(D_L + D_T). \tag{9.10}$$

The cable has only one side, as opposed to a plate which has two sides, that way the multiplier 0.5 is inserted (Fig. 9.10).

Fig. 9.6. Air cable drag versus cable speed for the cable surface parameter $L_s = L^{0.8} s = 0.1 - 0.5$.
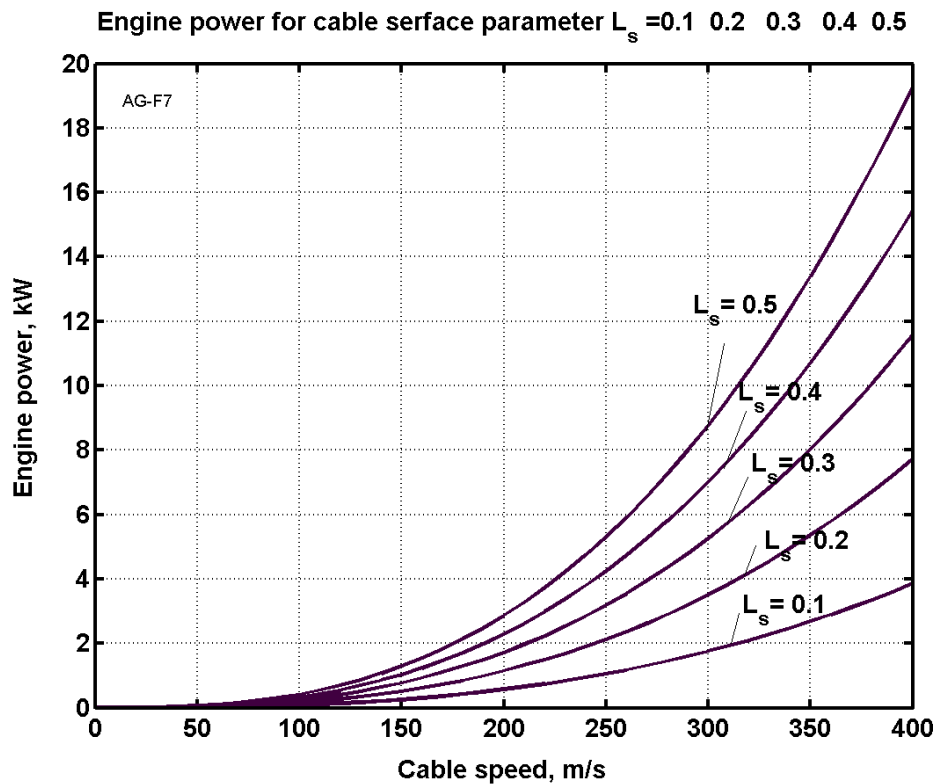
Fig. 9.7. Engine power versus cable speed for the cable surface parameter $L_s = L^{0.8} s = 0.1 - 0.5.$

The power P of cable air drag D is

$$P = DV = 0.5(D_T V + D_L V) = 0.5(P_T + P_L), \quad V = \sqrt{\sigma/\gamma} \qquad (9.11)$$

The power of turbulent drag P_T and of laminar drag P_L, respectively is

$$P_L = 0.5 \cdot 0.664 \rho^{0.5} \mu^{0.5} \left(\frac{\sigma}{\gamma}\right)^{1.25} L^{0.8} s, \quad P_T = 0.5 \cdot 0.0592 \rho^{0.8} \mu^{0.2} \left(\frac{\sigma}{\gamma}\right)^{1.4} L^{0.8} s, (9.12)$$

where the total cable perimeter s of the round cables is

$$s = 2\sqrt{\frac{\pi n F}{\sigma - \gamma g H}} \quad . \qquad (9.13)$$

Most of the engine power (80– 90%) takes the turbulent cable drag. In space there is no air, thus no air drag and we can use a very long cable. If the altitude H is small (up to 5 – 6 km), we can ignore the factor $\gamma g H$. In this case, the cable depends on the relation ($\sigma^{0.9}/\gamma^{1.4}$). As you see, a cable with low tensile stress σ and high density γ (for example, conventional steel cable) requires less power because the safe maximum cable speed is small ($V \approx 250 – 350$ m/s). However, the required cable weight increases 10– 15 times. The round and single closed-loop cable ($n = 2$) requires minimum power. The plate and semi-circle cables require more power, but they may be more suitable for a drive mechanism.

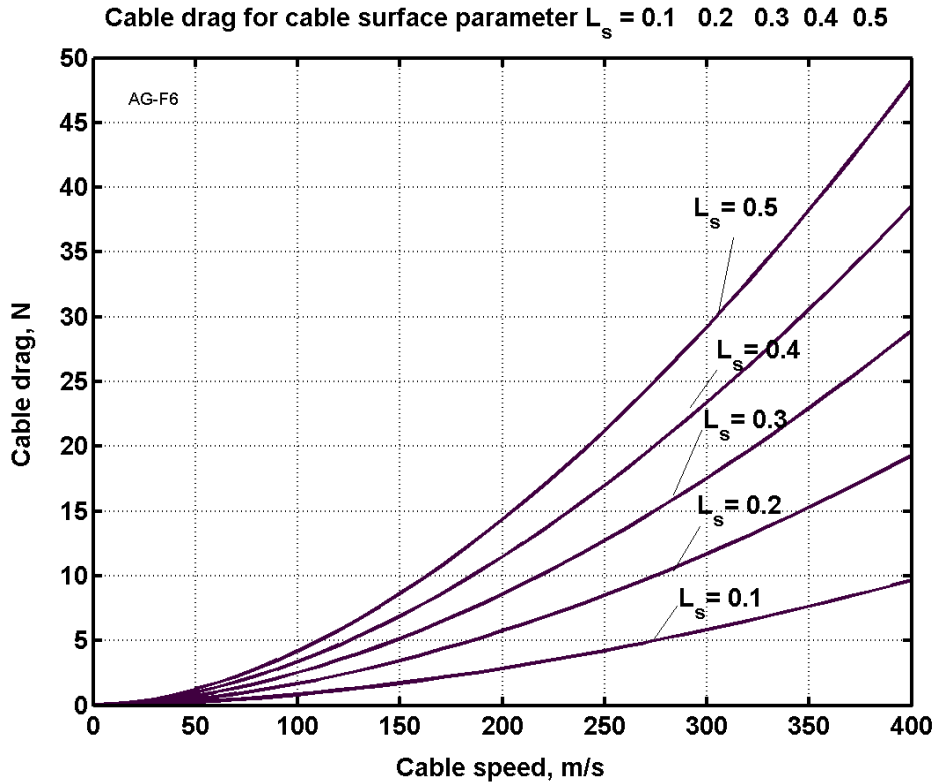**Fig. 9.8a**. Cable drag versus cable speed for the cable surface parameter $L_s = L^{0.8} s = 1$– 5.

Engine power for cable surface parameter L$_s$ =1 2 3 4 5
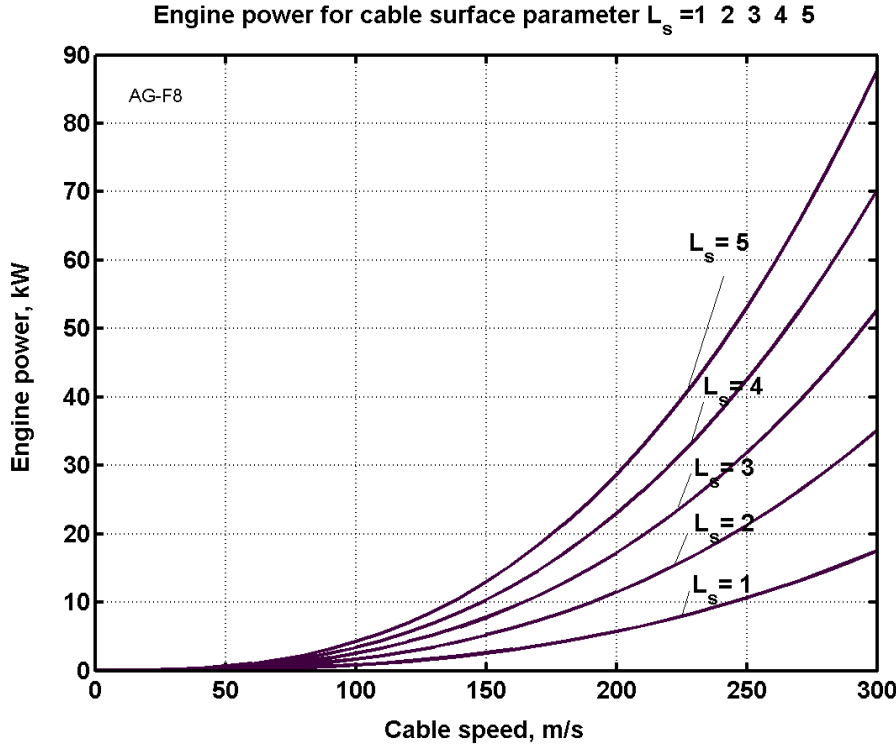
Fig. 9.8b. Engine power versus cable speed for the cable surface parameter $L_s = L^{0.8}$ $s = 1–5$.

b) Air drag of supersonic and hypersonic double cable.

Below, the equation from Anderson[6] for the computation of local air friction for a two-sided plate is given.

$$\frac{T^*}{T} = 1 + 0.032M^2 + 0.58\left(\frac{T_w}{T} - 1\right), \quad M = \frac{V}{a}, \quad \mu^* = 1.458 \times 10^6 \frac{T^{*1.5}}{T^* + 110.4},$$

$$\rho^* = \frac{\rho T}{T^*}, \quad R_e^* = \frac{\rho^* V x}{T^*}, \quad C_{f,L} = \frac{0.664}{(R_e^*)^{0.5}}, \quad C_{f,T} = \frac{0.0592}{(R_e^*)^{0.2}},$$

$$D_L = 0.5C_{f,l}\rho^*V^2S, \quad D_T = 0.5C_{f,t}\rho^*V^2S, \quad D = 0.5D_T + 0.5D_L, \qquad \qquad (9.14)$$

Where[6]: T^*, Re^*, ρ^*, μ^* are the reference (evaluated) temperature, Reynolds number, air density, and air viscosity respectively. $M = V/a$ is the Mach number, a is the speed of sound [m/s], V is cable speed [m/s], x is the length of the plate (distance from the beginning of the cable)[m], T is flow temperature [°K], T_w is body temperature [°K], $C_{f,l}$ is a local skin friction coefficient for laminar flow, $C_{f,t}$ is a local skin friction coefficient for turbulent flow. As S is the area of skin [m²] of both plate sides, it means for the cable we must take 0.5S; D is the general air drag (friction) [N]. It may be shown that the general air drag for the cable is $D = 0.5D_T + 0.5D_L$, where D_T is the turbulent drag and D_L is the laminar drag.

For a **horizontal** cable, the friction drag can be computed uding equation (9.10) where $\rho = \rho^*$, $\mu = \mu^*$.

From equation (9.14) we can derive the following equations for turbulent and laminar boundary flows of a **vertical** cable

$$D_T = \frac{0.0592s}{4}\rho_0^{0.8}\left(\frac{T}{T^*}\right)^{0.8}\mu^{0.2}V^{1.8}\int_{H_0}^{H}h^{-0.2}e^{0.8bh}dh = 0.0547d\left(\frac{T}{T^*}\right)^{0.8}\mu^{0.2}V^{1.8}\int_{H_0}^{H}h^{-0.2}e^{0.8bh}dh,$$

$$\tag{9.15}$$

$$D_L = \frac{0.664s}{4}\rho_0^{0.5}\left(\frac{T}{T^*}\right)^{0..5}\mu^{0.5}V^{1.5}\int_{H_0}^{H}h^{-0.5}e^{0.5bh}dh = 0.5766d\left(\frac{T}{T^*}\right)^{0.5}\mu^{0.5}V^{1.5}\int_{H_0}^{H}h^{-0.5}e^{0.5bh}dh,$$

where s is the cable perimeter. The laminar drag for high speed is 50–300 times less than the turbulent drag and we can ignore it.

Engine power and additional cable stress can be computed using conventional equations:

$$P = 2DV, \quad \sigma = \pm\frac{D}{S} = \pm\frac{4D}{\pi d}, \tag{9.16}$$

The factor 2 is needed because we have two branches of the cable: one moves up and the other moves down. The drag does not decrease the repulsive (lift) force because in the different branches the drag is in the opposite directions.

5. Computations of equation (9.8) are presented in Figs. 9.6 to 9.8 for low cable speeds and in Fig. 9.9 and 9.10 for high cable speeds for different value $L_s = L^{0.8}s$.

6. For space apparatus that starts from a planet with no atmosphere (asteroid), which has a mass much greater than the apparatus mass, speed is calculated using equation

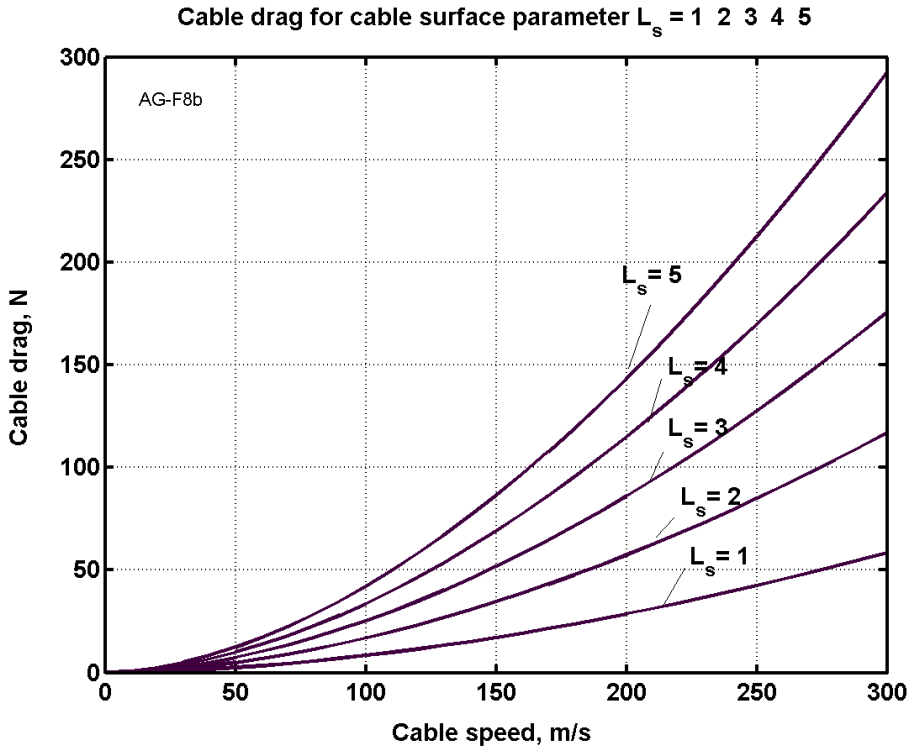$$V_1 = V\frac{m_1 + 0.5m_2}{m_1 + m_2}, \tag{9.17}$$

Fig. 9.9. Air cable drag versus cable speed for the cable surface parameter $L_s = L^{0.8}s = 50$–200.
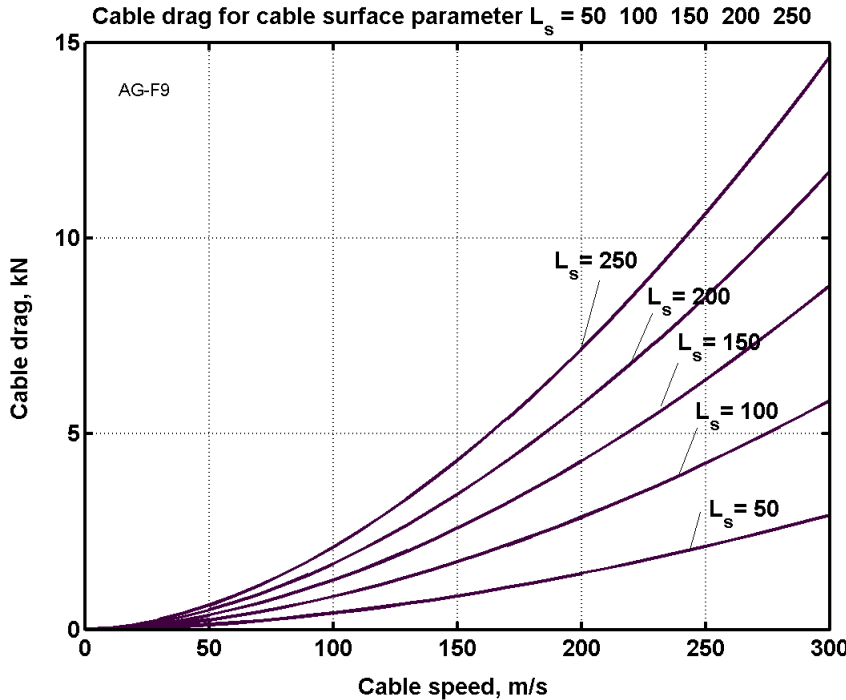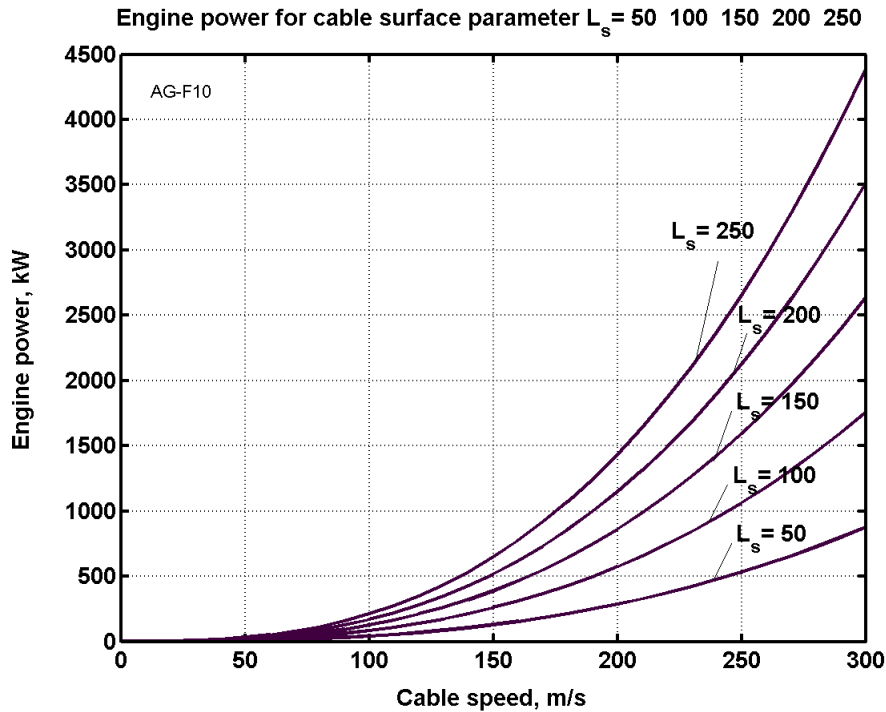
Fig. 9.10. Engine power versus cable speed for the cable surface parameter $L_s = L^{0.8} s = 50\text{–}200$.

If the space ship uses asteroid rubble (or ships garbage) to create thrust via a repulsive engine, the ship speed is (in an immovable coordinate system with the origin located in the system's center of gravity).

$$V_s = V_3 \frac{m_3}{m_1 + m_2} \ . \tag{9.18}$$

Advantages of offered method

The advantages of the proposed method are tremendous. We can fly out of the atmosphere without aircraft, helicopters, dirigibles, and rockets. The installation is very simple (only an engine and a thin cable) and very light, especially when the cable is made from the artificial fiber, a fortiori, from nanotubes. When the cable is located outside the atmosphere, it does not require power for rotation, except for a small amount of power to compensate for the friction in the rollers. We can create a big force (up to tens or hundreds of tons) and operate at long distances (tens of kilometers in the Earth's atmosphere and hundreds of kilometers in space).

The kinetic anti-gravitator may have applications in many fields of civilian and military life: flights on Earth, in space, to planets and asteroids, launching space ships, lifting loads at high altitude, problems of communication, observation, searching, and rescues. The same idea may be used to transfer mechanical energy over long distances[7], for moving aircraft in the air[8] or ground vehicles using an engine located at a large distance, for building simple air bridges over straits, canals, and mountains instead of tunnels or conventional bridges[9], and so on. Some of these problems are considered below.

Applications

Conventional steel cable has a maximum tensile stress of $\sigma = 300$ kg/mm^2 and density of $\gamma = 7900$ kg/m^3, and fiber steel cable has a tensile strength of about $\sigma = 2000$ kg/mm^2. At present, industry

widely produces cheap artificial fibers with a maximum tensile stress of σ = 500–620 kg/mm^2 and density[10,11] γ = 800–1800 kg/m^3. Whiskers have σ = 2000–8000 kg/mm^2 and density[10] γ = 2000–4000 kg/m^3, and nanotubes, created in scientific laboratories, have σ = 20,000 kg/mm^2 = $2 \cdot 10^{11}$ N/m^2 and density γ = 800 –1800 kg/m^3. Theory[11] predicts that nanotubes can have σ = 100,000 kg/mm^2 and density γ = 800 –1800 kg/m^3. We will consider a double closed-loop cable in projects below. We will also use the conventional steel cable that has confirmed (safety, permitted) tensile stress of σ = 50–100 kg/mm^2 or the conventional fibers with a maximum confirmed strength of σ = 200 kg/mm^2 and density γ = 1800 kg/m^3. This means the safety factor is 3–6 or 2.5–3.1. The use of whiskers or nanotubes dramatically improves the parameters of the kinetic anti-gravitator for long distances.

1. VTOL (Vertical Takeoff and Landing) conventional aircraft (Fig. 9.11). Let us estimate the parameters of the kinetic anti-gravitator for conventional aircraft. Assume the mass of the aircraft is M = 20 tons, the takeoff speed is less than or equal to V_m = 80 m/s (most aircraft have takeoff speeds of 50–70 m/s), safety stress of the artificial fiber cable is σ = 200 kg/mm^2 and density is γ = 1800 kg/m^3, and the start and landing acceleration is a = 3g ≈ 30 m/s^2. This acceleration is acceptable for the general population (with training, people can withstand 8g permanently and 16g for a short time). The required cable length is L = $V_m^2/2a$ = 80^2/60 = 107 m. The total cross-section area of all artificial cable is S = $Ma/(g\sigma)$ = 20000×30/(10×200) = 300 mm^2, and one branch of the four-cable system has a diameter of d = 10 mm. Cable mass is m = $SL\gamma$ = 300×10^{-6}×107×1800 = 58 kg. The cable speed is V_c = (200×10^7/1800)$^{0.5}$ = 1054 m/s [see equation (9.2)]. If the roller is made from the same composite material as the cable, they will maintain this speed. Time of acceleration is t = V/a = 80/30 = 2.7 seconds. The engine power equals the kinetic energy divided by time P = $MV^2/2t$ = 20000×80^2/2×2.7 = 23704 kW. This value is two to three times more than the power of a typical aircraft engine. However, the start engine may be located on the ground and can have any power. If we want to use an aircraft engine (for cable drive), we must decrease the start acceleration by 2–3 times or use a flywheel. In landing, this energy will return to the fly wheel because the distance between the ground and the apparatus is reduced (see the description of innovation).

2. Non-rocket space apparatus. The same results will apply for a space ship starting from an asteroid or planet without atmosphere. However, if the final speed is high, we must use equation (9.8).
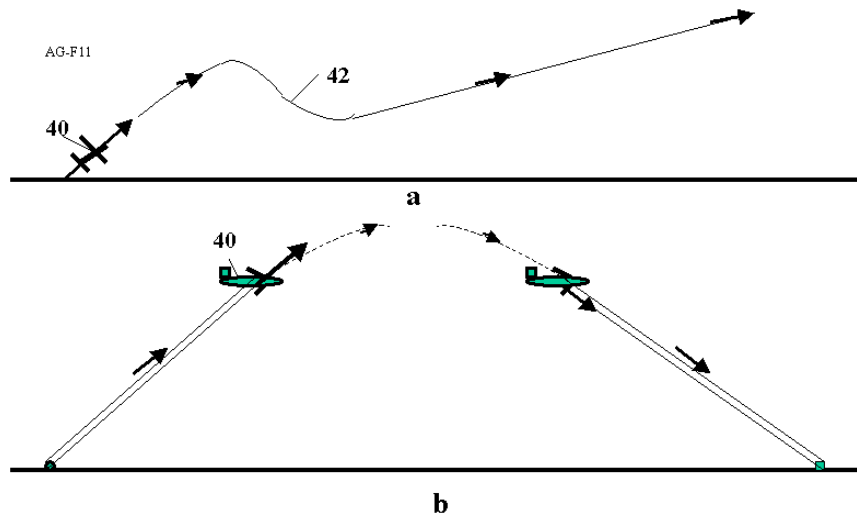

Fig. 9.11. Slope takeoff (**a**) and landing (**b**) of conventional aircraft using the kinetic anti-gravitator. Notations are: 40 – aircraft, 42 – aircraft start trajectory.

3. Flying "superman" (Fig. 9.12a). Takjng on altitude $H = 100$ m, the maximum load is $M = 200$ kg (this is enough for superman, his girl-friend, an engine and a parachute for safety). The steel cable has tensile stress $\sigma = 100$ kg/mm^2 and density $\gamma = 7900$ kg/m^3. The required total cross-section area of all cables is $S = Mg/\sigma = 2$ mm^2, cable diameter is $d = 1.6$ mm, the perimeter of the four cables is $s = 10$ mm. The cable mass is $m = SL\gamma = 2 \times 10^{-6} \times 100 \times 7800 = 1.56$ kg, and cable speed is

$V = \sqrt{\sigma/\gamma} = \sqrt{10^9/7900} = 356$ m/s. Area parameter is $L_s = L^{0.8} s = 100^{0.8} \cdot 0.01 = 0.4$. The cable drag is $D = 31$ N (Fig. 9.6 or equations (9.11) – (9.12)), and the required engine power is $P = 11$ kW (Fig. 9.7). The cable can be made from transparent fibers and in any case it will be invisible from a long distance.

4. Walking "superman" or vehicle (Fig. 9.12b). The lower rollers can be made separately and have separate controls. This allows the supermen to walk, run, and move with high speed. For example, if the previous "flying superman" described above takes one step (length 100 m) in 2 seconds, he will have a speed of 180 km/hour.
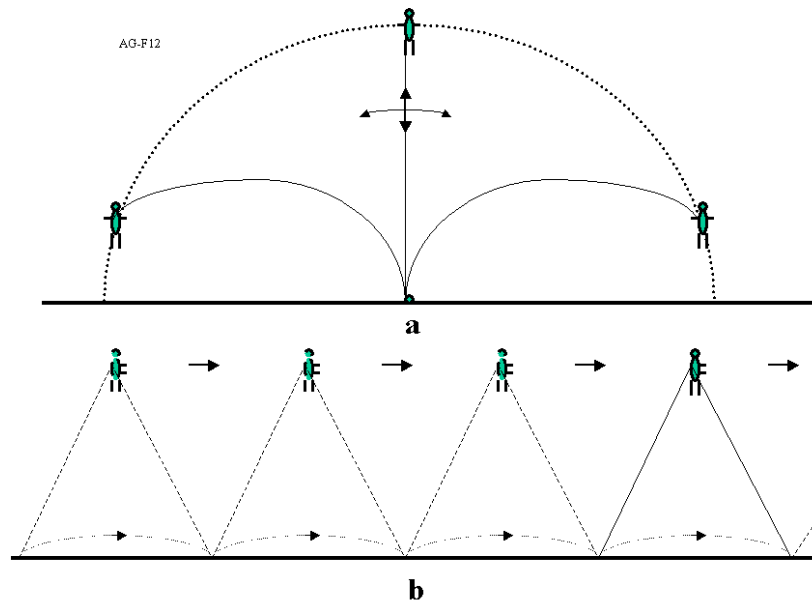
Fig. 9.12. **a)** Flying superman using the kinetic anti-gravitator. **b)** Legged (walking) superman using two kinetic anti-gravitators.

5. **Jumping (pogo-stick) "superman"** (Fig. 9.13a). Assume the short kinetic anti-gravitator gives a man of mass $M = 100$ kg the speed $V = 70$ m/s with acceleration $a = 3g = 30$ m/s^2. The cable length is $L = V^2/2a = 70^2/2 \times 30 = 82$ m. The time of acceleration $t = V/a = 70/30 = 2.33$ seconds. The total cross-section areas of all cables is $S = Ma/\sigma = 100 \times 30/200 \times 10^7 = 1.5$ mm^2, and the cable mass is $m = SL\gamma = 1.5 \times 10^{-6} \times 82 \times 1800 = 230$ g. The jump distance at an angle $\alpha = 45°$ without air drag (it is small at this speed) is $J = V^2/g = 70^2/10 = 490$ m, the altitude is $H = V^2 \sin\alpha/2g = 70^2 \sin 45°/20 = 173$ m, jump time is about 10 seconds. The required starting thrust is 300 kg, and the start (jump) power is about $P = E/t = mV^2/2t = 100 \times 70^2/2 \times 2.33 = 105$ kW, but the start energy will be restored in landing except for the air drag loss of 10–20%. If we have an energy accumulator, a permanent power of 5 –10 kW will be enough for this device.

6. Jumping vehicle. Assume the kinetic anti-gravitator gives a vehicle of mass $M = 1000$ kg the speed of $V = 200$ m/s with acceleration $a = 8g = 80$ m/s^2 (which is acceptable for military soldiers). The cable length is $L = V^2/2a = 200^2/2/80 = 250$ m. The time of acceleration $t = V/a = 2.5$ seconds. The

jump distance at an angle of 45° without air drag (it is not very much for a streamlined body) is about 4 km, the altitude is 1.4 km, and the jump time is about 20 seconds. The cross-section area of all the cables is $S = Ma/\sigma = 1000 \times 80/200/10^7 = 40$ mm^2. Cable mass is $m = SL\gamma = 40 \times 10^{-6} \cdot 250 \times 1800 = 18$ kg. The required start thrust is 8 tons, and the jump power is about $P = 8000$ kW, but the start energy will be restored in landing except for the air drag loss of 10–20%. If we have an energy accumulator, an engine with 500–800 kW power will be enough for this device. The vehicle can have a small wing (area 2 m^2) and glide from an altitude of 1.4 km for a the distance of 14–17 km to the selected place for the next jump.

7. Long arm (long hand) (Fig. 9.13b). The proposed method allows us to create a "long arm" which suspends a video camera or weapon aloft. Assume the load mass of the long hand is $M = 2$ kg and the hand has a length of 1 km. The hand uses a steel cable with $\sigma = 100$ kg/mm^2 and $\gamma = 7.9$ g/cc. Maximum speed is×

$$V = \sqrt{\sigma/\gamma} = \sqrt{10^9/7900} = 356 \text{ m/s}.$$

The cross-section area is $S = M/\sigma = 2/100 = 0.02$ mm^2, $d = 0.08$, $s = 1$ mm, and the cable mass is $m = SL\gamma = 0.02 \times 10^{-6} \times 1000 \times 7900 = 158$ g. The cross-section area parameter is $L_s = L^{0.8} s = 1000^{0.8} \cdot 0.001 = 0.25$. The cable drag is $D = 20$ N (Fig. 9.6 or equations (9.11) – (9.12)), and the required engine power $P = 6.8$ kW (Fig. 9.7). The operator (a.g. a soldier) can observe regions within a 1 km radius and immediately apply the weapon if necessary. The radius may be increased up to 10 km. If using a more powerful kinetic anti-gravitator that can hold a load of 200 kg with a net and catcher installed at the end of the cable, the operator can catch the soldier and deliver him or her to another place. This may be very useful for rescue and anti-terrorist operations.
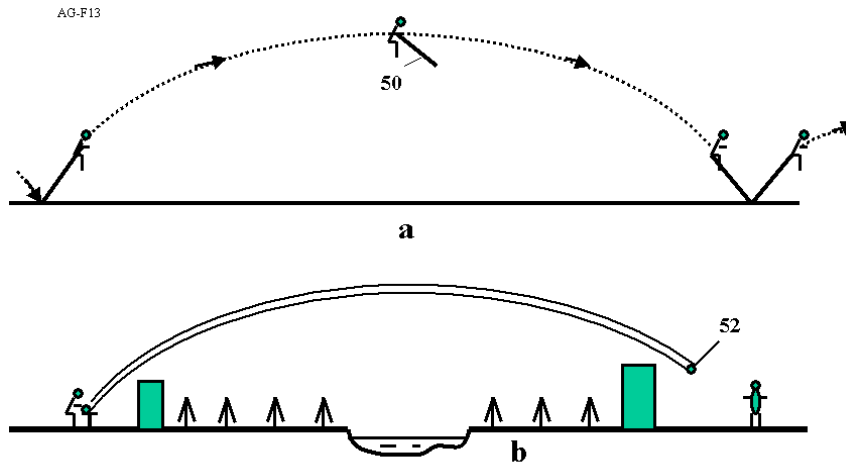
Fig. 9.13. a) "Superman" using the jump kinetic anti-gravitator (50). **b)** The super-hand (52), which allows operation at long distances of 1–10 km.

8. High altitude crane. The construction of skyscrapers needs high cranes. Consider the design of a crane of $L = H = 500$ m height using the offered method. Take the useful load as 1 ton and the steel cable as having safe tensile stress of $\sigma = 50$ kg/mm^2 and cable density of $\gamma = 7.9$ g/cc. The total cross-section cable area is (equation (9.4)) $S = F/(\sigma - \gamma gH) = 22$ mm^2. The cable mass is $m = S\gamma H = 2 \times 10^{-6} \times 500 \times 7900 = 87$ kg, and safe cable speed is $V = (\sigma \gamma)^{0.5} = 250$ m/s. If the installation has four cables of diameter $d = 2.6$ mm each, the total perimeter of the four cable is $s = 4\pi d = 33.2$ mm, the parameter $L_s = L^{0.8} s = 500^{0.8} 0.0332 = 4.8$, the cable air drag is $D = 200$ N (Fig. 9.6, equation (9.10)), and the required power to support cable rotation is $P = 50$ kW (Fig. 9.7, equation (9.12)). This is the highest (500 m) and the lightest (87 kg) crane in the world having a load capability of 1 ton.

9. High tower. Consider the design of a high tower of $L = H = 4$ km using the offered method. Take the useful load as 30 tons and the steel cable as having a safe tensile stress of $\sigma = 50$ kg/mm^2 and cable density of $\gamma = 7.9$ g/cc. The total cross-section (all branches) of the cable area is (equation (9.4)) $S = F/(\sigma - \gamma gH) = 1630$ mm^2. Cable mass is $m = S\gamma H = 51.5$ tons, and safe cable speed is $V = (\sigma/\gamma)^{0.5} = 250$ m/s. If the installation has four cables, the diameter of one cable is $d = 23$ mm, the total perimeter of the four cable is $s = 4\pi d = 0.289$ m, the parameter $L_s = L^{0.8}s = 4000^{0.8} \cdot 0.289 = 220$, the cable air drag is $D = 9500$ N, and the required power to support cable rotation is $P = 2.3$ MW. This is highest (4 km) and the lightest (52 tons) tower in the world, which has a load capability of 30 tons at the top.

Note: the computation for the same tower in[3] "Kinetic Space Towers and Launchers" with an artificial fiber cable, having a safe tensile stress of $\sigma = 200$ kg/mm^2 and density of $\gamma = 1800$ kg/m^3, gives the required speed of $V = 1000$ m/s and power $P = 11$ MW. We have changes only the cable material (from artificial fiber to steel). As a result, the required support power decreases by approximately 5 times, and the total production cost for delivery of one tourist decreases from \$3.35 to \$1.4. This happens because the required speed decreases from 1000 m/s to 250 m/sec, decreasing the required power and fuel consumption. The power depends on the third order ($V^{2.8}$, see equation (9.12)) of speed.

This shows that the parameters of the considered example are very far from optimal. On the other hand, the cable mass increases from 1.13 tons up to 51.5 tons.

10. **The construction of the Artsutanov space elevator without rockets.** The space elevator, first proposed by Y. Artsutanov in 1959, may be a promising breakthrough in space. However, the space elevator needs an equalizer weiting hundreds of tons, and thousands of tons of cable. Also, delivery using rockets into geosynchronous orbit is very expensive. When nanotubes become cheaper the offered kinetic anti-gravitator will allow the construction of the space elevator without rockets. The author shows in[3] "Kinetic Space Towers and Launchings" that if $K = \sigma\gamma/10^7 > 5$ the cable space tower (cable mast) can be up to 150,000 km hogh or more. This is enough to reach geosynchronous orbit (37,000 km).

Discussion

In 2002 Loftsrom[4] published a description of a space launcher. The offered device has the following technical and physical differences from the Loftstrom installation.

The Loftstrom installation has a the 2000-km long launch path located at an altitude of 80 km, which accelerates the space vehicle to space speed. The Loftstrom space launcher is a loop cable of complex path enclosed in an immobile tube. The cable is made from rubber-iron material and is moved using an electromagnetic linear engine. The cable is turned by electromagnets.

The idea offered in this article is the kinetic device which creates a push (repulsive, repel) force between two given bodies (for example, between a planet and the apparatus). This force supports a body at a given altitude. The body is connected to the cable by rollers that slide along the cable. The cable can be made of artificial fiber and moved by the rollers and any engine. The kinetic anti-gravitator supports any body at altitude (for example, towers) and may also be used to launch vehicles. The Loftstrom device is only a space launcher and cannot permanently support a body at altitude or towers (he did not write anything about this).

The kinetic anti-gravitator creates a permanent controlled force. If the distance between bodies does not change, the kinetic anti-gravitator requires only a small amount of energy to compensate for the friction in the rollers and air.

Conclusion

The offered method, the kinetic anti-gravitator, may be applied in many fields and may have a big future. The method does not need special technology. Current cheap and widely produced materials

such as steel or artificial fiber can be used to operate up to an altitude of 75–225 km. The kinetic anti-gravitator is simple and does not need complex equipment. If the installation is designed correctly, Lishanski's experiments show that the high speed closed-loop straight-line cable is stable in any direction including the horizontal position.

References

1. Bolonkin, A.A., 'Theory of Flight Vehicles with Control Radial Force'. Collection "*Researches of Flight Dynamics*", "Mashinostroenie" Publishers, Moscow, 1965, pp. 79–118 (in Russian).
2. Bolonkin, A.A., "Transport System for Delivery of Tourists at Altitude 140 km". IAC-02-IAA.1.3.03, 53rd International Astronautical Congress. The World Space Congress – 2002, 10–19 Oct. 2002, Houston, Texas, USA.
3. Bolonkin, A.A., "Kinetic Space Towers and Launchers", *JBIS* (*Journal of British Interplanetary Society*), Vol. 57, No 1/2, pp. 33–39, 2004.
4. Lofstrom K.H., "The Launch Loop: A Low Cost Earth-to-High-Orbit Launch System", http://www.Launchloop.com/launchloop.pdf (2002).
5. Bolonkin, A.A., "Centrifugal Keeper for Space Stations and Satellites", *Journal of the British Interplanetary Society* (*JBIS*), Vol. 56, No 9/10, pp. 314–327, 2003.
6. Anderson, J.D., *Hypersonic and High Temperature Gas Dynamics*. McGraw-Hill Book Co.
7. Bolonkin, A.A., "High Efficiency Transfer of Mechanical Energy", AIAA-2004-5660, International Energy Conversion Engineering Conference, Rhode Island, 16–19 Aug. 2004.
8. Bolonkin, A.A., "Air Cable Transport", *Journal of Aircraft*, Vol. 40, No. 4, July–August 2003.
9. Bolonkin, A.A., "Air Cable Transport and Bridges", TN 7567, International Air & Space Symposium – The Next 100 Years, 14-17 July 2003, Dayton, Ohio, USA.
10. *Carbon and High Performance Fibers*, Directory, London-NY, 1995, Chapman & Hall, 6th ed.
11. Dresselhous, M.S., *Carbon Nanotubes*, Springer, NY, 2000.
12. Bolonkin A.A., "Kinetic Anti-Gravitator", AIAA-2005-4505, 41st Propulsion Conference, 10–12 July, 2005, Tucson, Arizona, USA.

Chapter 10
Centrifugal Space Launchers*

Summary

The purpose of this chapter is to draw attention to the idea of sling rotary launchers. This idea allows the building of inexpensive new space launcher systems, to launch missiles, projectiles, and space apparatus, and to use many types of energy. This chapter describes the possibilities of this method and the conditions which influence its efficiency. Included are four projects: a non-rocket sling projectile launcher, a space sling launcher, a spaceship for launching using conventional supersonic, and a space ship using subsonic aircraft. The last two only require low-cost cable made from artificial fiber, using whiskers that are produced in industry now or increasingly perfected nanotubes that are being created in a scientific laboratories.

Nomenclature

A – general work, [J],
A_1 – acceleration work for space apparatus (s.a.),
A_2 – sling acceleration work,
A_3 – s.a. air drag work,
A_4 – sling air drag work,
A_5 – acceleration and air drag work of lever (disk). Value A_5 equals 0 for the aircraft launcher and it
    may be estimated for the lever using conventional calculations,
a – the speed of sound [m/s],
c – the relative thickness of the sling ($c = 0.07$ to 0.1),
c_L – the lift coefficient of the s.a. ($c_L = 0 – 1$),
D – the vehicle drag [N],
D_c – air drag of the sling,
$g = 9.81$ m/s^2 is the Earth's gravity,
H – the altitude [m],
ΔH – the change in altitude [m],
Δh – the additional altitude of the s.a. [m],
k – the strength coefficient [m^2/s^2],
k_1 – the aerodynamic efficiency of the s.a.,
L – the vehicle lift force [N], and
L – the vehicle range [m],
L_c – the sling lift force [N],
M – the flywheel's mass [kg],
m – mass of space apparatus [kg], or
m – the vehicle mass [kg],
n – centrifugal overload [g],
n_1 – the vertical overload of the s.a. [g],
P – the engine power [W],
R – radius of the s.a. trajectory [m],

R_0 – lever radius [m],
R_b – the range of ballistic trajectory [m],
S – cross-section sling area [m^2],
S_0 – the sling cross-section area near the lever [m^2],
$\overline{S}_0$ – the relative cross-section area near the lever [m^2],
S_c – the sling wing area. [m^2],
S_s – the sling cross-section area at the sling center of gravity [m^2],
S_w – the required area of the s.a. wing [m^2],
T – the thrust of the lead aircraft or force on the lever [N],
t – the acceleration time [seconds],
t_p – the time between launches [seconds],
Δt – the elapsed time [seconds],
V – the speed [m/s], and
V – the speed of the s.a. [m/s],
V_0 - speed of the lever end [m/s],
V_c – the average sling speed or speed of the center of gravity of the sling [m/s],
V_a – the average speed of the s.a. [m/s],
ΔV – the change in s.a. speed [m/s],
α_c – the sling attack angle [rad],
σ – sling stress [N/m^2],
σ_f – the safe stress on the flywheel [N/m^2],
γ – the density of the sling [kg/m^3],
γ_f – the density of the flywheel [kg/m^3],
ρ – the air density [kg/m^3],
θ – the trajectory angle [rad].
$\Delta\theta$ – the change in the trajectory angle [rad],
θ_a – the average trajectory angle [rad],
the subscript "$_b$" means the initial value of the ballistic trajectory.

Introduction

At present, rockets are used to carry people and payloads into space[1]. Other than rockets, one method of reaching space is the space elevator[2]. This is very complex, expensive and technologically impossible at the present time. Once industry produces low-cost nanotubes, the author has shown that the space elevator may be easily built without rockets (project 4)[3]. Also offered is a transport system for the space elevator[4]. The author has also proposed a centrifugal keeper and launcher for space stations and satellites[5], a hypersonic tube air rocket of high capacity[6,9], optimally inflated space towers of 3–100 km height[7], using asteroids as a propulsion system for space ships[8], a multi-reflection beam launcher[10], a new method of flight – a kinetic anti-gravitator[11], and has researched optimal trajectories and space cable launcher[12, 13]. Many of them are in this book.

The space elevator requires very strong nanotubes, as well as a rocket and the high technology needed for the initial development. The tube air rocket and non-rocket systems require more detailed research. The electromagnetic transport system, suggested by Minovich[14], is not realistic at the present time. This requires a vacuum underground tunnel 1530 kilometers long located at a depth of 40 kilometers. The project requires a power cooling system (because the temperature is very high at this depth), a complex electromagnetic power system, and a huge impulse of energy that is greater than the power of all of the electricity generator stations on Earth. The beam propulsion system[15] needs very

powerful lasers and magnetic sails[16] have many problems. The author is suggesting a very simple and inexpensive method and installation for launching payloads into space.

The presented work is a new space launcher system for achieving high supersonic speeds. The main difference from a conventional centrifugal launcher is the light, strong sling that dramatically increases the apparatus speed. The sling launcher can produce supersonic vehicle speed in the Earth's atmosphere and space vehicle speed in a vacuum. This method uses a strong sling (cable), a power (drive) station, conventional engines (mechanical, electrical, gas turbines), and flywheels (for energy storage) located on the ground.

A conventional high-speed aircraft may also be used in this manner to launch projectiles and space ballistic space ships.

Description of Innovative Launcher

 Ground sling launcher. The installation includes (see notations in Fig. 10.1): a tower, a lever (or disk), a sling (cable), conventional engines and flywheels (drive station). Optimally, the installation is located on a mountain (high altitude) to reduce air drag on the sling and apparatus and for a lower slope of initial trajectory angle. A winged space apparatus (space ship, missile, probe, projectile, etc.) is connected to the end of the sling.
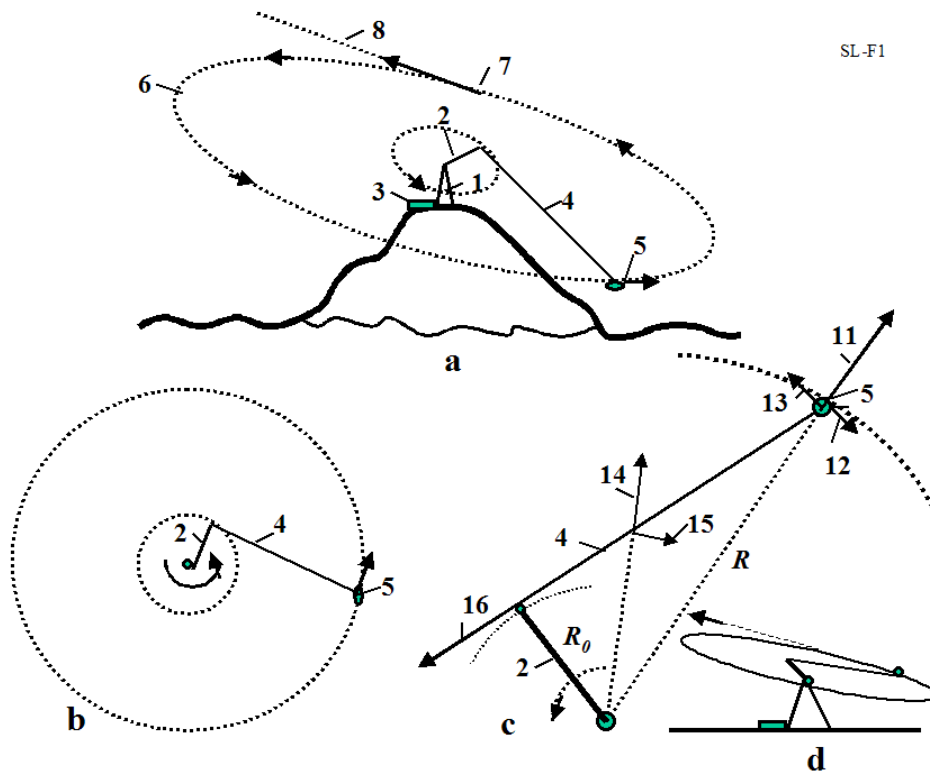
Fig. 10.1. Sling rotary launcher. a) launcher located on mountain, b) top view of installation, c) acting forces, d) side view. Notations: 1 – tower, 2 – lever or disk, 3 – engine, 4 – sling, 5 – space apparatus (s.a.), 6 – circular launch trajectory, 7 – point of disconnection, 8 – direction of launch, 11 – centrifugal force of space apparatus, 12 – drag of s.a., 13 – speed of s.a., 14 – centrifugal force of sling, 15 – drag of sling, 16 – lever force.

SL-F2

a

b

13 11

5

12

14

15

4

17

c

16

2
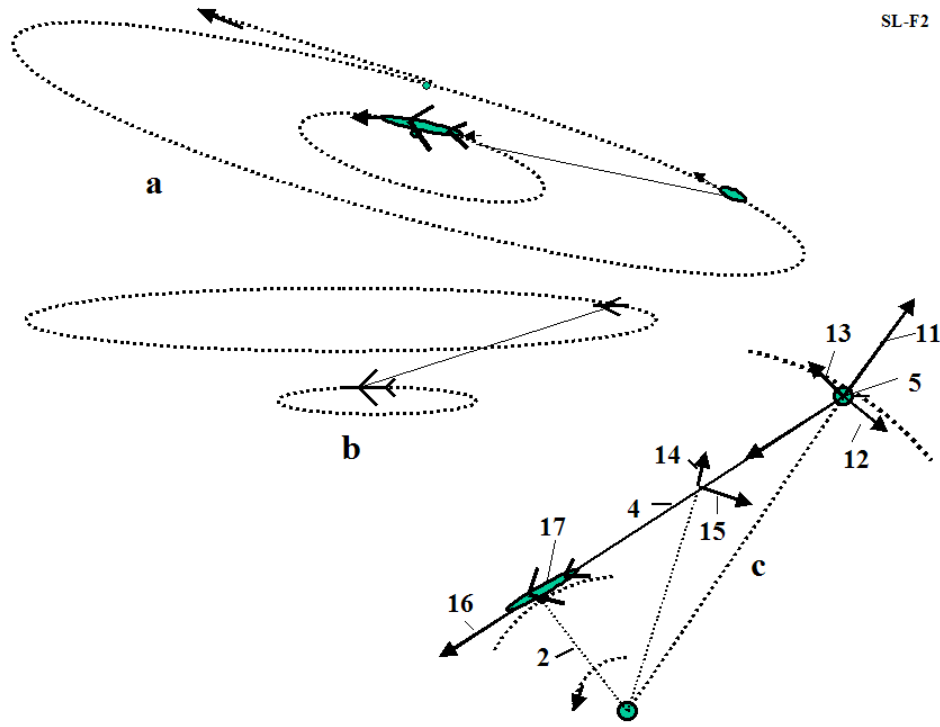
Fig. 10.2. Launching a space ship using aircraft. a) slinging slope start, b) upper start, c) installation forces.

SL-F3

T

C_C

$\alpha+\beta$ 4   5 C

D_C

α D

R_C

R_0

R

20   22

β

21   **d**

a

L

C

L_c 4   5

φ Δh

b

L_c 4 L C

5

c

Fig. 10.3. Forces acting on the sling launcher. a) top view, b) cone launching when lift force of sling equals sling weight (side view), c) cone launching when sling lift force is more than sling weight (side view), d) cross section of the sling. Notation: 20 – sharp thin sling, 21 – head protection, 22 – stabilizer of sling.
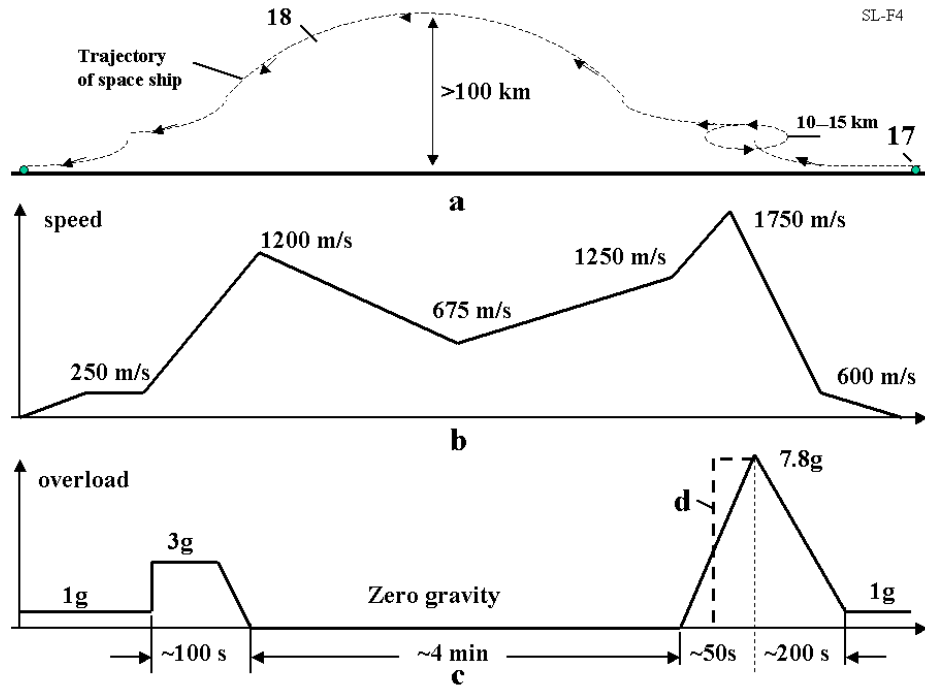
Fig. 10.4. a) Space flight trajectory. Notations: 17 – aircraft, 18 – trajectory of space ship.
b) graph of ship speed (project 3). c) graph of ship overload (project 3). d) change of overload graph in project 4.

The installation works in the following way (Fig. 10.1). The engine rotates the flywheels. When the flywheels accumulate sufficient energy, they rotate as a lever. The lever accelerates the space apparatus ("s.a."). The apparatus may be located on the lever and the sling is increased after the start. The apparatus speed increases. It is greater than the lever speed in the ratio R/R_0, where R is the radius of the apparatus trajectory circle, R_0 is the radius of the lever (or disk). When the apparatus reaches its chosen speed, the winged apparatus is disconnected from the sling at the desired point of the circle. While the winged apparatus is flying in the atmosphere, it can increase its slope and correct its trajectory. If the apparatus has a hypersonic (supersonic) form, the speed loss is small[13].

The offered launcher is different from conventional centrifugal catapults, which have a projectile in a lever. This launcher has a long sling and the projectile is in the sling. The sling increases the lever speed many tim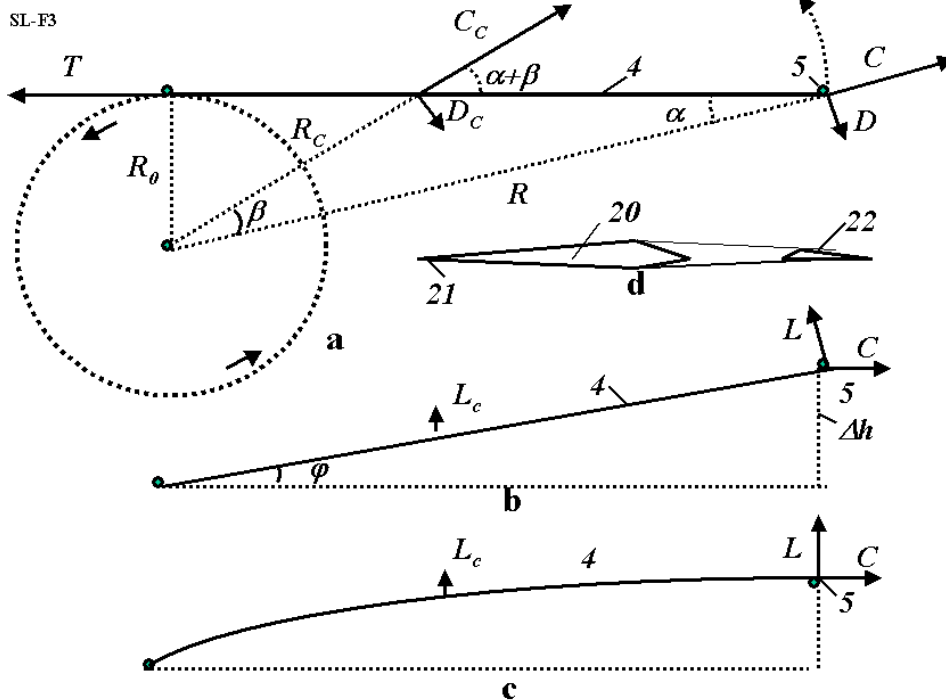es and decreases the mass of the lever. Conventional catapults made from nanotubes have a huge mass and requires gigantic energy to work. This sling is also made from nanotubes (for space speed), but its mass is small.

If the circle is parallel to the Earth's surface, the winged apparatus disconnects from the cable, converts the linear and centrifugal acceleration into vertical acceleration (while it is flying in the atmosphere) and leaves the Earth's atmosphere.

The power station houses the engine. It can be any engine, for example, a gas turbine, or an electrical or mechanical motor. The power drive station also has an energy storage system (flywheel accumulator of energy), a transmission drive train and a clutch mechanism.

The installation can be set on a slope, and launch a projectile at an angle to the horizon (Fig. 10.1).

The attained speed may be up to eight or more km/s (see project 2 below). If the planet does not have an atmosphere, a small installation (with a small lever) can give the projectile a very high speed, limited only by the power of the engine and the strength of the sling.

On the Earth's surface the launcher can be located under a special cover (or in a tube) in a vacuum.

Aircraft sling launcher. Another design of this sling launcher is presented in Figs. 10.2 to 10.4. A small spacecraft (1 – 2 tons) is connected to a large, high-speed aircraft. The aircraft flies in a circle, increasing the sling length and accelerating the ship to high speed. The attained speed depends largely on the specific strength of the sling, the maximum aircraft speed and the thrust of the aircraft. For large existing aircraft operating in the atmosphere, the launch speed may reach up 2 km/s. This is enough for the X-prize flight, reaching an altitude of up to 100 km and sufficient for a spaceship for tourists (see projects 3–4 below).

Advantages. The suggested launch cable system has advantages compared to the current rocket systems, as follows:

1. The sling launcher is many times less expensive than modern rocket launch systems. No expensive rockets are needed. Only motor and cable are required.
2. The sling launcher reduces the delivery cost by several thousand times (to as low as $5 to $10 per pound). (No rocket, cheaper fuel.)
3. The sling launcher could be constructed within one to two years. The aircraft sling launcher requires only a cable and a spaceship. Modern rocket launch systems require many years for R&D and construction.
4. The sling launcher does not require high technology and can be made by any non-industrial country.
5. Rocket fuel is expensive. The ground sling launcher can use the cheapest sources of energy, such as wind, water, or nuclear power, or the cheapest fuels such as gas, coal, peat, etc., because the engine is located on the Earth's surface. Flywheels may be used as an accumulator of energy.
6. It is not necessary to have highly qualified personnel, such as rocket specialists with high salaries.
7. The fare for space tourists would be small.
8. There is no pollution of the atmosphere from toxic rocket gas.
9. Thousands of tons of useful payloads can be launched annually.

   Shortcomings of sling space launchers:

1. The need for a very strong sling (cable), made from carbon whiskers or still-to-be manufactured long nanotubes.
2. The Earth ground sling launcher may be used only for robust loads because high centrifugal acceleration is imposed on the payload. Such payloads normally account for 70–80% of space payloads.

   Cable (sling) discussion. The experimental and industrial fibers, whiskers, and nanotubes are considered in Chapters 1–2.

   The reader can find a more complete cable discussion of cable and cable characteristics in the References[3–13, 17–20].

Theory of the Sling Launcher
Formulas for Estimation and Computation (in metric system)

1. Centrifugal force, C, cross-section area of the sling at the s.a., S, and the speed of the s.a., V, are calculated using conventional equations

$$C = \frac{V^2}{R}, \quad n = \frac{C}{g}, \quad S = \frac{mC}{\sigma}, \quad \frac{R}{R_0} = \frac{V}{V_0} \ . \tag{10.1}$$

2. Optimal relative sling cross-section area, $\overline{S}$, along radius, r is

$$\overline{S} = \exp\left\{\frac{V^2}{2k}\left[1 - \left(\frac{r}{R}\right)^2\right]\right\}, \quad S_0 = S\overline{S}, \quad \overline{S}_0 = \exp\left\{\frac{V^2}{2k}\right\}, \quad where \quad k = \frac{\sigma}{\gamma}, \tag{10.2}$$

The results of computation [equation (10.2)] are presented in Figs. 10.5 and 10.6. For low k the relative area, $\overline{S}$, is very large. For example, a conventional fiber with $k = 2 \times 10^6$ requires this parameter to be 2.72 for a speed of $V = 1410$ m/s.
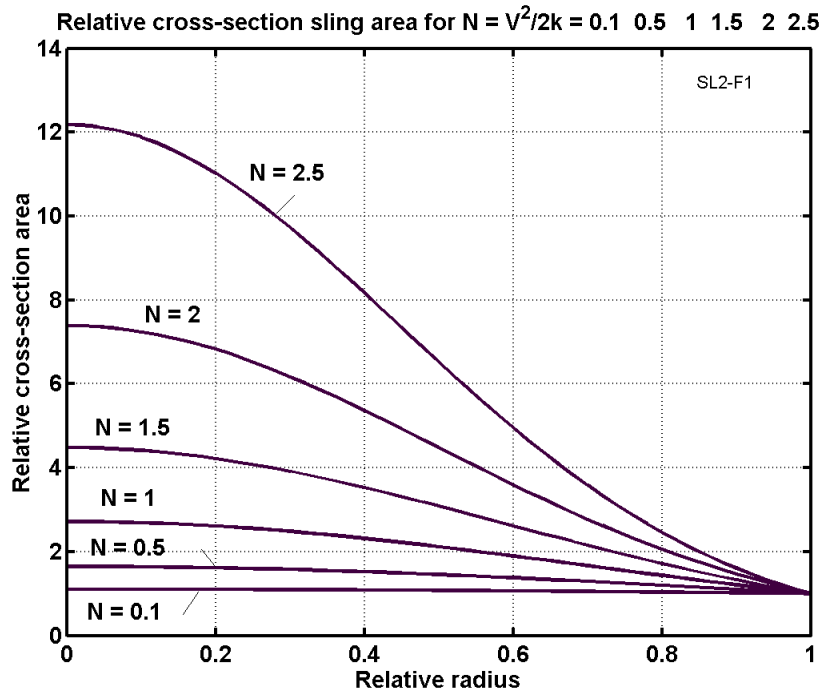

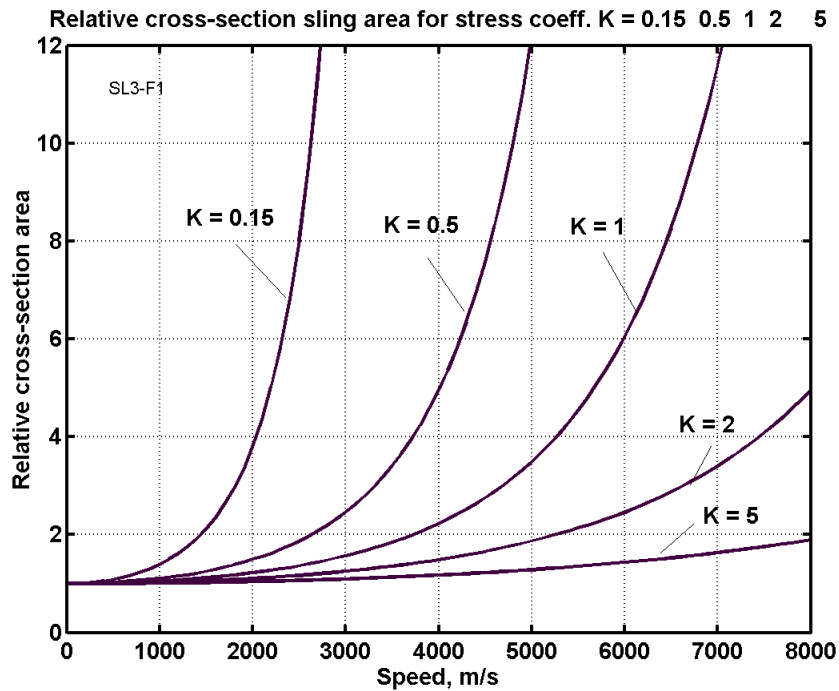Fig. 10.5. Relative cross-section area of sling for different ratio is $N = V^2/2k$ in equation (10.2).

Fig. 10.6. Relative cross-section area of sling with $\overline{S}_0$ in $r = 0$ via sling end speed and a stress coefficient $K = 10^{-7}k$ [equation (10.2)].

3. Air drag (Fig. 10.7) of space apparatus, D, and air drag of the sling, D_c, are approximated as follows:

$$D = \frac{mn_1 g}{k_1}, \quad D_c = 4c^2 \rho a V_c S_c / 2, \quad S_c = R\sqrt{\frac{S_S}{c}}, \quad L_c = 2\alpha_c \rho a V_c S_c . \qquad (10.3)$$

Additional drag forces arising from the sling lift force are small, and are ignored in this analysis.

The sling has a variable speed of from 0 to V, and a variable wing area. To simplify, we assume the average value as near the sling's center of gravity. In an effort to decrease air drag, the sling has a sharp form and is stabilized by a stabilizing tail (Fig. 10.3d). The space apparatus and sling also have a thin ceramic cover for protection against the short periods of launch heating. More exactly, the sling drag may be calculated by integration.
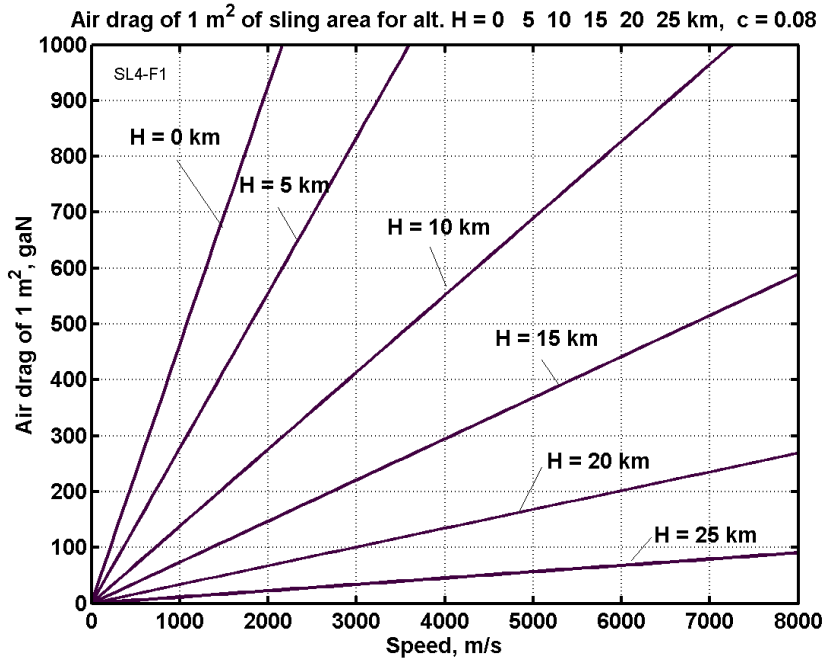
Fig. 10.7. Air drag of one square meter of wing sling (with relative profile thickness $c = 0.08$) based on speed and altitude [equation (10.3)].

1. Flight angle of cone. To decrease the sling drag, the wing apparatus and the sling have an attack angle and lift force. They climb at high altitude where the air has low density (Fig. 10.3b). The sling moves along a cone surface. The sling lift force may be more than the sling weight and then the sling will be curved at the top, as shown in Fig. 10.3c. In this case, the fastest part of the cable will be in the low-density upper atmosphere. The additional sling drag from the lift force is small and we ignore it here.

The additional altitude, Δh, of the s.a. may be found from the equation:

$$\sin \varphi \approx \varphi = \frac{\Delta h}{R} = \frac{n_1 - 1}{n} . \qquad (10.4)$$

5. In a vacuum, the ratio R / R_0 may be large. However, when the sling moves in the atmosphere, the common projection of all forces perpendicular to the sling must be greater than zero. Only in this case may the system be accelerated. This gives rise to two inequalities (the necessary *acceleration inequalities*)

$$C\sin\alpha > (g/k_1)\cos\alpha, \quad mC\sin\alpha + m_c C_c \sin(\alpha+\beta) > D\cos\alpha + D_c \cos(\alpha+\beta), \quad C_c = V_c^2 / R_c$$
$$\sin\alpha = R_0 / R, \quad \sin\beta = R_0 / R_c, \quad C_c = V_c^2 / R_c, \quad m_c = \gamma S_s L_s \qquad (10.5)$$

where C_c is the average centrifugal acceleration of the sling [m/s^2], m_c is the sling mass [kg], and L_s is the sling length [m].

6. Engine power and the necessary mass of the flywheel may be estimated by the following equations:

$$A = A_1 + A_2 + A_3 + A_4 + A_5 , \quad A_1 = \frac{mV^2}{2} , \quad A_2 = \frac{m_c V_c^2}{2} , \quad A_3 = \frac{mg}{k_1} t , \quad A_4 = \frac{D_c V_c}{4} t ,$$

$$M = \frac{2\gamma_f A}{\sigma_f} , \quad P = \frac{A}{t_p} , \quad T = \sigma S_0 = nmg\bar{S}_0 , \quad S_w = \frac{2n_1 mg}{c_L \rho a V} , \quad L = \frac{k_1 V^2}{2g} \tag{10.6}$$

The value of A_5 equals 0 for the aircraft launcher and may be estimated for the lever using conventional calculations.

7. Estimation of tourist trajectory of the space vehicle.

a) The vertically accelerated part of the trajectory. The purpose of this part of the trajectory is to increase the trajectory slope, θ, relative to the horizon. The trajectory may be computed by the following differential equations:

$$\dot{H} = V \sin\theta , \quad \dot{V} = -\frac{D}{m} - g\sin\theta , \quad \dot{\theta} = \frac{L}{mV} - \frac{g}{V}\cos\theta . \tag{10.7}$$

Changes in the trajectories parameter may be estimated using equations obtained from conventional aircraft equations (10.7)

$$\Delta t = \frac{\Delta H}{V_a \sin\theta_a} , \quad \Delta V = -g\left(\frac{n_1}{k_1} + \sin\theta_a\right)\Delta t , \quad \Delta\theta = \frac{g}{V_a}(n_1 - \cos\theta_a)\Delta t , \tag{10.8}$$

where n_1 is the vertical overload of the a.s [g].

b) The ballistic part of the space vehicle (apparatus) trajectory may be calculated by conventional equations as follows:

$$\Delta H_b = \frac{V_b^2 \sin^2\theta_b}{2g} , \quad R_b = \frac{V_b^2 \sin 2\theta_b}{g} , \quad t_b = \frac{R_b}{V_b \cos\theta_b} , \tag{10.9}$$

where the subscript "b" means the initial value of the ballistic trajectory, and R_b is the range of the ballistic trajectory.

Projects

Described below are details and estimates of four projects:

(1) Projectile launcher for long distances, using a sling made from currently available artificial fibers.

(2) Space projectile launcher, with a sling made from whiskers.

(3) Tourist flights using supersonic aircraft with a sling made from nanotubes.

(4) Tourist flights using subsonic aircraft with a sling made from whiskers.

These projects are not optimized. They only illustrate the method and rough estimations for installations for different purposes. We sometimes indicate thrust (forces) in kilograms or tons, and stress in kg/mm^2. For reader reference, 1 kg = 9.81 N ≈ 10 N (Newton), 1 ton ≈ 10^4 N, and 1 kg/mm^2 ≅ 10^7 N/m^2).

Project 1

Projectile launcher for long distances, using a sling made from existing artificial fiber (Fig. 10.1)

Assume the mass of the projectile (load) is $m = 100$ kg = 0.1 ton, the required final projectile speed is $V = 2,500$ m/s, the length of the lever (or disk radius) is $R_0 = 10$ m, the maximum lever speed is $V_0 = 800$ m/s, the safe sling stress is $\sigma = 180$ kg/mm^2, and the sling density is $\gamma = 1,800$ kg/m^3. The coefficient $k = \sigma/\gamma = 0.1 \times 10^7$. If aerodynamic efficiency is $k_1 = 6.5$, a speed of 2,500 m/s is sufficient for a projectile range of 2000 km [equation (10.6)].

The radius of the circle is $R = R_0 V/V_0 = 10 \times 2500 / 800 = 31.25$ m. Conventional gas turbines have a blade tip speed of up to 600 to 800 m/s in a high-temperature gas flow[21]. Our lever (or disk) made from current composite material can maintain a speed of 800 m/s, because the lever radius is larger and is not exposed to high temperature. These parameters are not optimal. Our purpose is only to show that the offered launcher is possible using current technology. Industry widely produces cheap artificial fiber with $\sigma = 500 – 620$ kg/mm^2. The safety coefficient is $n = 620/180 = 3.44$.

Computations. The maximum centrifugal overload of the projectile is $C = V^2 / R = 6 \times 25 \times 10^6 / 31.25 = 2 \times 10^5$ m/s$^2 = 2 \times 10^4$ g. This overload and acceleration are the same as these of a conventional cannon. Maximum centrifugal force exerted on the projectile is $F = m\,C = 10^2 \cdot 2 \cdot 10^5 = 2 \cdot 10^7$ N = 2,000 tons. The sling cross-section area near the projectile is $S = F/\sigma = 2,000 / 0.18 = 11,111$ mm$^2 = 111$ cm^2. The sling cross-section area near the lever is $\bar{S} = 23$, $S_0 = \bar{S} \cdot S = 0.255$ m^2, [equation (10.2)]. The average cross-section area is $S_a = 0.5 \cdot (0.0111 + 0.255) = 0.133$ m. If the relative sling thickness is $c = 0.1$, the average sling width is $b = (S_a./c)^{0.5} = 1.15$ m. The wing sling area is $S_k = b \cdot R = 1.15 \times 30 = 34.5$ m^2, [equation (10.3)]. Assume the sling center of gravity is at $R_c = 0.35R = 12.5$ m, $V_c = 0.35V = 875$ m/s. Sling mass is $m_c = \gamma S_a R = 1800 \times 0.133 \times 30 = 7,182$ kg = 7.2 tons. The sling centrifugal acceleration is $C_c = V_c^2 / R_c = 875^2 / 11 = 69.6 \times 10^3$ m/s^2, the sling centrifugal force is $F_c = m_c C_c = 718,2 \cdot 69.6 \cdot 10^3 = 5 \cdot 10^8$ N = 50,000 tons. For $\rho = 1.225$, $a = 330$ m/s, $k_1 = 5$, the sling air drag is $D_c = 24.5$ tons [equation (10.3)], and the projectile air drag is only $D = m/k_1 = 100/5 = 20$ kg.

The angle $\alpha \approx R_0/R = 10 / 31.25 = 0.32$ rad, and the angle $\beta \approx R_0/R_c = 10 / 11 = 0.91$ (Fig. 10.3a). The acceleration inequality (10.5) is $46140 > 24$. This is acceptable.

Assuming an acceleration time of $t = 25$ seconds, the work of acceleration and air drag of the installation are follows: projectile acceleration work $A_1 = 0.312 \times 10^9$ J, sling acceleration work $A_2 = 2.75 \times 10^9$ J, a 30 ton disk (lever) acceleration work $A_3 = 0.2 \times 10^9$ J, sling drag work $A_4 = 1.34 \times 10^9$ J, [equation (10.3)]. We neglect projectile and disk drag. The total launch energy is $A = 4.6 \times 10^9$ J. The flywheel mass is $M = 9.2$ tons. If the time between launches is $t_p = 30$ min = 1800 seconds, the required engine power is $P = A/t_p = 4.6 \times 10^9 / 1800 = 2.56$ MW. This is the power of a conventional aviation turbo engine.

Without energy recuperation, the launchers efficiency (conversion of mechanical energy into projectile speed) is 7%. With energy recuperation (kinetic energy of the sling and disk is used for flywheels support), the launcher efficiency reaches 36%.

Discussion of project 1

Compare the offered sling launcher with the big cannon (Project HARP[22]) built and tested after World War II. The cannon barrel had a diameter of 42.4 cm, and a length of up 86–126 calibers (58 m). Weight of the gun powder was 342 kg, projectile weight was 174 kg, and the projectile speed was 1,840 m/s. The range was 183 km and the altitude 50 km for a 50° angle of sight. A speed of 3,200 m/s was reached for a projectile weight of 20 kg and a length of 126 calibers. Maximum pressure was 340 MPa. The cannon cost about $10 million (1946).

The offered sling launcher installation can launch a winged projectile and has a range of up to $L = k_1 V^2 / 2g = 6.5 \times 2,500^2 / 20 = 2,031$ km[12]. Improved sling material will permit this capability. The end of the sling has a speed of about 7.6 M (Mach) for a short time (some few seconds) and may be protected by conventional methods such as the Shuttle coating (ceramic cover or other heat resistant material).

Project 2

Space projectile launcher with a sling made from whiskers (Fig. 10.1)

Using a space sling launcher with a sling made from whiskers that has a tensile strength rating of $\sigma = 3500$ kg/mm^2 and a sling density of $\gamma = 1800$ kg/m^3, the stress coefficient will be $k = \sigma/\gamma = 3.9 \times 10^7$. Assuming the mass of the projectile (load) is $m = 1,000$ kg = 1 ton, the required final projectile speed is $V = 8$ km/s, the length of the lever is $R_0 = 50$ m, the maximum lever speed is $V_0 = 800$ m/s, then the maximum radius $R = R_0 V / V_0 = 50 \times 8000 / 800 = 500$ m. Conventional gas turbines have a turbine blade tip speed of up to 600–800 m/s in high temperature gas. Our lever, made from current composite material, can withstand a speed of more than 800 m/s, because the lever (or disk) radius is larger and it is protected from high temperature. The sling material attains a speed of $V_0 = \sqrt{\sigma/\gamma} = 6.24$ km/s$^{3-13}$. The parameters used below are not optimal. Our purpose is only to estimate the offered launcher properties.

Computation. The maximal centrifugal overload of the projectile is $C = V^2 / R = 64 \times 10^6 / 500 = 128 \times 10^3$ m/s$^2 = 12.8 \times 10^3$ g. This acceleration is less than that achieved by a conventional cannon. Maximal centrifugal force around the projectile is $F = mC = 10^3 \times 128 \times 10^3 = 28 \times 10^6$ N = 12,800 tons. The sling cross-section area near the projectile is $S = F/\sigma = 12,800 / 3.5 = 3,660$ mm$^2 = 36.6$ cm^2. The sling cross-section area near the lever is $\bar{S} = 5$, $S_0 = 181$ cm^2 [equation (10.2)]. We assume the sling's center of gravity is at $R_c = 0.5R$, $V_c = 0.5V$, and $S_s \approx (S+S_0) / 2 = 109$ cm^2. The sling mass is $m_c = \gamma S_s R = 1,800 \times 0.0109 \times 500 = 9.81$ tons. Sling centrifugal acceleration is $C_c = V_c^2 / R_c = 4,000^2 / 250 = 64 \times 10^3$ m/s^2, sling centrifugal force is $F_c = m_c C_c = 9,810 \times 64 \times 10^3 = 628 \times 10^6$ N = 62,800 tons. For a sling of relative thickness $c = 0.1$, b = 33 cm, the sling wing area is $S_s = 165$ m^2 [equation (10.3)]. For $\rho = 1.225$ and $a = 330$ m/s, the sling air drag is $D_c = 54.4$ tons, for $k_1 = 5$ the projectile air drag is only $D = m/k_1 = 1,000/5 = 200$ kg. The angle $\alpha \approx R_0/R = 50 / 500 = 0.1$ rad, the angle $\beta \approx R_0 / R_c = 50 / 250 = 0.2$ (Fig. 10.3a).

The acceleration inequality (10.5) is 13880 > 53.4 which is acceptable.

Assuming an acceleration time of $t = 25$ seconds., then the work of acceleration and air drag of the installation are: projectile acceleration $A_1 = 32 \times 10^9$ J, sling acceleration $A_2 = 78.5 \times 10^9$, 100 tons disk (lever) acceleration $A_3 = 10 \times 10^9$ J, sling drag $A_4 = 133.5 \times 10^9$ J, disk drag $A_4 = 40 \times 10^9$ J [equation (10.6)]. Ignoring projectile drag, the common launch energy is $A = 300 \times 10^9$ J. The flywheel mass is $M = 30$ tons for material similar to the sling. If the time between launches is $t_p = 3$ hours = 10,800 seconds, the required engine power is $P = A / t_p = 300 \times 10^9 /10,800 = 27.8$ MW. This is the power of 2 or 3 large aviation turbo engines.

Without energy recuperation, the launcher's efficiency (transfer of mechanical energy into projectile speed) is 10%, and with energy recuperation (kinetic energy of the sling and disk is used for flywheel support), the launcher efficiency reaches 30%. Launch capability is 8 tons of payload, every day.

Economic Efficiency

Assume a cost of $100 million for the installation[23], a useful life of 20 years, and an annual maintenance cost of $2 million. If each launch has a payload of 1 ton, and there are 8 launches per day for 300 days a year, then the annual payload capacity is 2,400 tons. The launch cost for each kg of payload is $7 \times 10^6 / 2.4 \times 10^6 = \$2.9$/kg plus fuel cost. If 10,000 liters of fuel are used every day and the fuel price is $0.25 per liter, then the fuel cost is $2500 per day, resulting in a launch capability of 8,000 kg/day or $0.31 per kg. This results in a total cost of $3.2 per kg of payload. If the revenue generated is based on sales of $23.2 per kg of payload in space, then the operating profit would be about $48 million per year.

The reader may calculate using other assumptions. In every reasonable case, the cost of delivery would be hundreds of times less expensive then delivery by existing rockets. It is emphasized that the primary efforts of this article are not economical estimations, but a new concept in space launch capability.

Discussion

Currently, there are whiskers that have parameters close to those required for this project. Industrial production of nanotubes will soon allow the design of a better space sling launcher. The heating problem of the sling end may be solved by head protection, given that the heat will be imposed for only a few of seconds. The heating of the projectile and the problem of speed loss in the atmosphere are considered elsewhere[6,13]. It is shown that the speed loss is small, about 100 to 250 m/s. There is also a speed "reserve" of 460 m/s provided by the Earth's rotation if the launch is made near the equator.

Project 3

The launcher for space tourists with a sling made from nanotubes (Fig. 10.2)

Let us consider a ship which flies to an altitude of 100 km, carrying 3 people. The following is an estimation of a sling launcher installation which achieves these objectives. We will use the method depicted in Fig. 10.2, where ship acceleration is provided using a sling and a supersonic aircraft.

It is known that the average person can withstand centrifugal forces of 3 to 4g. A trained (or in good health) person can withstand up to 7 to 8g, and for short periods up to 16g. With the proposed sling launcher, we assume centrifugal forces of $n = 7.8g$, a permissible overload for trained people.

We assume that the mass of the spaceship is $m = 1,500$ kg $= 1.5$ ton. The vehicle has only a small engine and fuel for maneuverability during landing and half of its total weight is payload (10 people). It may be shown that the necessary ship speed for reaching an altitude of 100 km is $V = 1,600$ to 1,750 m/s. Assuming the speed $V = 1,750$ m/s, $n = 7.8g$.

Computation. The required radius of the circle is $R = V^2 / g\,n = 1,750^2 / 78 \approx 40$ km. Assume a sling length of $L = 35$ km. If speed of the supersonic aircraft is $V_0 = 600$ m/s, the flight radius is $R_0 = RV_0 / V = 13.8$ km. Constructing the sling from carbon nanotubes with the permitted stress of $\sigma = 9,000$ kg/mm^2, the sling density is $\gamma = 1,800$ kg/m^3. The coefficient $k = \sigma/\gamma = 10 \times 10^7$, $\overline{S} = 1.06 \cong 1$, aircraft thrust $T = F = 7.8 \times 1.5 = 11.7$ tons. The required sling cross-section area is $S = F / \sigma = 11.7 / 9 = 1.3$ mm$^2 \approx S_0$. Mass of the sling is $m_c = \gamma SL = 800 \times 1.3 \times 0^{-6} \times 3,000 = 82$ kg.

Take $c = 0.08$. Then $b = (S/c)^{0.5} = 4$ mm, $S_s \approx b\,L = 0.004 \times 35,000 = 140$ m^2. Assume the sling has the lift force and form shown in Fig. 10.2b, with convexity toward the top. The supersonic aircraft has an altitude of 15 km, the average altitude of the sling's center of gravity is $H = 25$ km (air density $\rho = 0.041$ kg/m^3) and the space ship has a altitude of 30 km (air density $\rho = 0.018$ kg/m^3). Speed of the sling's center of gravity is $V_c = 1,181$ m/s, the speed of sound at this altitude is $a = 295$ m/s. The sling drag is [equation (10.3)] $D_c = 4 \times 0.08^2 \times 0.41 \times 295 \times 1,181 \times 140 / 2 = 2.56$ tons. $R_c = R_0 + 0.5$ $(R - R_0) = 27$ km, $C_c = 51.6$ m/s^2 [equation (10.5)]. Calculating angles, $\sin\alpha = R_0 / R = 13.8 / 40 = 0.345$, $\sin\beta \approx R_0 / 2R = 0.69$. Calculating the acceleration inequality (10.6), this figure is $4.2 > 2.04$. This is acceptable. Assume we increase the sling length with speed 150 m/s. Then the time of untwisting will be $t = 35,000 / 150 = 233$ seconds ≈ 4 min. The maximum overload of 7.8 g is imposed on the passengers for only a few seconds.

On disconnection, the winged spaceship has an average vertical acceleration of $n \approx 4g$. The integration of equation (10.8) during $t = 50$ seconds for average $k_1 = 6.5$ indicates that the angle of trajectory increases from 0 to 57.3^0, the altitude increases up to 59 km, and the speed decreases to 1,250 m/s. An alternate way is to compute using equation (10.9), as a ballistic trajectory out of the atmosphere. The result is an altitude of 115 km, a range of 145 km, and a time of 215 seconds. After the ballistic part of the trajectory, the vehicle enters the atmosphere again, increases its vertical acceleration up to 3g and its trajectory angle to near 0°, flying into the atmosphere and landing. The

graphs of trajectory, flight acceleration and flight time are shown in Fig. 10.4a, b and c. The total time out of the Earth's gravitational field is about 4 minutes and the maximum altitude is 115 km (Fig. 10.4a).

Discussion

Acceptable aircraft. Data for large existent and old supersonic aircraft are shown in Table 10.1.

Table 10.1

Name	Max.weight (tons)	Max. speed (m/s)	Max. altitude (km)	Engine thrust (tons)
TU-144	195	694	18	51
Concorde	185	603	16	48
TU-160	275	600	15	68
XB-70	244	900	21	61
SR-71A	77	935	24	29
F-111A	41	738	16	11

Source: Jane's.

Conventional aircraft have the following characteristics: their empty weight is 30–40% of their total weight (or take-off weight), the fuel for long range is 30–40%, and the payload is 30–40%.

An safe vertical overload for passengers and large military aircraft (bombers) is 2.5 to 2.6g; the aerodynamic efficiency in supersonic speed is 6–7.5, the maximum thrust is about 25% of the maximum weight for an aircraft with a maximum speed of 2M (Mach number) and 35% for aircraft with a maximum speed of 3M.

For our purposes, we concede a supersonic aircraft without a payload and with only a small amount of fuel, resulting in a net weight of about half the take-off weight. In flights with speed $V = 600$ m/s and radius $R = 13.8$ km, the overload equals $V^2/gR = 2.6$ g. If the aircraft weight is 50% of its take-off weight, this means that the real aircraft overload is only $n_1 = 0.5 \cdot 2.6 = 1.3$ g.

The required additional thrust for our space vehicle increases from zero to maximum $T_{max} = ngW\bar{S} = 7.8 \times 9.81 \times 1,500 \times 1.06$ N = 12.2 tons . The required aircraft thrust for aerodynamic efficiency $k_1 = 6.8$ and aircraft weight $W_a = 195$ tons is $T = n_1 W_a / k_1 = 1.3 \times 195 / 6.8 = 37.3$ tons when the engine is in its cruise regime. The additional thrust necessary is only require for 40–50 seconds. This may be provided by a brief boost of the engine performance (take-off regime, plus injection of fuel through a jet engine nozzle). This is done at high aircraft speed. The thrust may be temporarily increased by up to 50–80%. In our case, in the cruise regime, the engines provide thrust of 195 / 6.8 = 28.7 tons. In boost regime, they provide $1.8 \times 28.7 = 51.7$ tons. The difference is 51.7–37.3 = 14.4 > 12.2 tons. This is enough. If the boost thrust provided is less, then the required thrust may be obtained by the installation of an additional outboard suspended air or rocket engine.

The end of the sling has a high speed (5.9M) for a short period and may be protected by a ceramic skin. The main technical problem is producing the necessary high-strength sling. There is as yet not commercial production of cheap, long nanotubes. A low-strength sling can not be used, because people cannot tolerate the overload (minimal radius is 40 km, for the initial speed of 1,750 m/s and the overload 7.8 g), which has a large air drag and so the acceleration inequality (10.5) is unsatisfied.

However, our parameters are not optimal and the offered space launch needs further R&D. For example, the slope circle trajectory (Fig. 10.2) improves all flight parameters.

Project 4
The launch of space tourists accelerated by subsonic aircraft with a sling made from whiskers
(See Fig. 10.2)

The previous project design has its drawbacks: it requires a sling made of nanotubes and a supersonic aircraft. Let us consider the project which uses a sling made from whiskers and a commercial subsonic aircraft. This may be realized at the present time. To reduce the sling length, we install a small rocket engine in the spaceship.

To estimate a sling installation which satisfies these conditions, we use the method depicted in Fig. 10.2, where the rocket ship acceleration is provided by the sling along with a current subsonic aircraft. Assume the weight of the spaceship is $m = 2$ tons, where 450 kg of this is a rocket fuel and 1,550 kg is space body and payload. The number of passengers is 10, including a pilot. The safe overload is $n = 7.8$ g.

The ship has a rocket engine and a small amount of fuel to increase the speed after separating from the sling and to increase the trajectory angle by one radian (57.3°). Assume the speed after the sling acceleration is $V = 1,000$ m/s.

Computation. The required radius is $R = V^2 / g\, n = 1,000^2 / 78 \approx 12.8 \approx 13$ km. Assume the sling length $L = 11$ km. If the speed of the supersonic aircraft is $V_0 = 265$ m/s ($V = 0.89$M), the flight radius is $R_0 = R V_0 / V = 3.4$ km. The aircraft overload in this flight radius is $n_1 = V^2 / g\, R_0 = 2.1$. Using a sling made from C_D whiskers with a maximum stress of $\sigma = 8,000$ kg/mm^2, the density is $\gamma = 3,500$ kg/m^3 [see Reference[17]], p.158. Assume safe stress is $\sigma = 2,000$ kg/mm^2. The coefficient $k = \sigma/\gamma = 0.572 \times 10^7$, $\overline{S} = 1.09$, maximum aircraft thrust $T = F_0 = 2 \times 7.8 \times 1.09 = 17$ tons. The centrifugal force from the aircraft is $F = m\, n\, g = 15.3$ tons. The required sling cross-section areas are $S = mn / \sigma = 2.7 \times 8 / 2 = 7.8$ mm^2, $S_0 = 1.09 \times 7.8 = 8.5$ mm^2, and $S_a = 8.15$ mm^2. The mass of the sling is $m_c = \gamma\, S_a\, L = 3,500 \times 8.15 \times 10^{-6} \times 11,000 = 385$ kg.

Assuming $c = 0.08$, that $b = (S_a /c)^{0.5} = 10$ mm, $S_s \approx bL = 0.01 \times 11,000 = 110$ m^2. Assume the sling has a lift force and form as in Fig. 10.2b with convexity to the top. The subsonic aircraft has an altitude of 12 km, the average altitude of the sling's center of gravity is $H = 15$ km (air density $\rho = 0.191$ kg/m^3) and the spaceship has an altitude of 17 km (air density $\rho = 0.142$ kg/m^3). Speed of sling's center of gravity is $V_c = 618$ m/s, and the speed of sound at this altitude is $a = 295$ m/s. The sling drag is [equation (10.3)] $D_c = 4 \times 0.08^2 \times 0.191 \times 295 \times 618 \times 110 / 2 = 4.9$ tons. $R_c = R_0 + 0.5(R - R_0) = 8.1$ km, $C_c = 1.85$ m/s^2 [equation (10.5)]. Calculating the angles, $\sin\alpha = R_0 / R = 3.4 / 12.8 = 0.27$ rad, $\sin\beta \approx R_0 / 2R = 0.54$. The inequality (10.6) is $5.2 > 4.2$, which is acceptable. Assume we increase the sling length with a speed of 100 m/s. Then the time of untwisting will be $t = 11,000 / 100 = 110$ seconds ≈ 2 minutes. The maximum overload 7.8 g will be imposed on the passengers for only a few seconds (Fig. 10.4).

After spaceship's disconnection the average vertical acceleration is $n \approx 7.8$ g. The integration of equation (10.7) during $t = 14$ seconds for an average $k_1 = 6.5$ shows that the angle of trajectory increases from 0 to 57.3° (1 rad), the altitude increases up to 19.1 km, and the speed decreases to $V_2 = 890$ m/s. During the next part of the flight, the rocket engine turns on and accelerates the space vehicle with a constant overload of 7.8 g and with a constant slope of trajectory. The changes in the trajectory parameters may be estimated by the following equations:

$$\Delta t = \frac{V_e}{ng} \ln \frac{m_e}{m} , \quad \Delta V = g\left(n - \frac{1}{k_1} - \sin \theta \right)\Delta t , \quad \Delta H = V_a \Delta t , \quad V_a = V_2 + \frac{\Delta V}{2} , \quad (10.10)$$

where $m_e = 1{,}550$ kg is the final mass of the space vehicle, k_1 is the aerodynamic efficiency of the ship, and θ is the angle of trajectory.

The result of computation are $\Delta t = 9.33$ seconds, $\Delta V = 623$ m/s, and $\Delta H = 11.2$ km. At the end of the acceleration part of the trajectory, we will have $V = 890 + 623 = 1513$ m/s, altitude $H = 15 + 4 + 11.2 = 30.2$ km, and the trajectory angle $\theta = 1$ rad $= 57.3°$.

The ballistic part of the trajectory gives [equation (10. 9)] additional altitude $H_b = 82.4$ km, ballistic distance $R_b = 212$ km, gravity zero time $t_b = 260$ seconds $= 4.3$ min. The total altitude is $H = 30.2 + 82.4 = 112.4$ km. The total time of flight with overload 7.8 g is $14 + 9.3 = 23.3$ seconds.

After the ballistic part of the trajectory, the vehicle re-enters the atmosphere, increasing vertical acceleration up to 3g or less and angle trajectory from -57° up to near 0°, flying into the atmosphere and landing. The graph of flight acceleration is shown in Fig. 10.4d. The amount of time out of gravitation is about 4 minutes. The maximum altitude is 115 km.

Discussion

Required aircraft. Data on some large existing commercial subsonic aircraft are given in table 10.2.

Table 10.2 (Source: Jane's)

Name	Max.weight (tons)	Max. speed (m/s)	Max. altitude (km)	Engine thrust (tons)
Boeing 747	397	265	14	98
Airbus	230	265	14	58

Conventional subsonic aircraft have the following characteristics: their empty weight is 30–40% of the total maximum weight (or take-off weight), fuel for a long range flight is 30–40%, and the payload is 30–40%. An safe vertical overload for passenger aircraft is 2.5 g. The aerodynamic efficiency at supersonic speed is $10 - 14$, the maximum thrust is 25% of the maximum weight for an aircraft than has a maximum speed of 0.92M. The take-off regime of the engine gives a thrust of about 50% more than the cruising regime.

For our purposes, we consider a subsonic aircraft, without a payload and only a small amount of fuel, resulting in a net weight equal to about half that of normal take-off weight. When an aircraft has a speed of $V = 265$ m/s and trajectory radius of $R_0 = 3.4$ km, the overload is $V^2 / g R_0 = 2.1$ g. If the aircraft weight is 50% of its take-off weight, this means that the true aircraft overload is only $n_1 = 0.5 \times 2.1 = 1.05$ g.

The required additional thrust for our space vehicle increases from zero to maximum $T_{max} = ngm \overline{S} =$ 7.8 × 9.81 × 2,000 × 1.09 N = 17 tons. The required aircraft with thrust for aerodynamic of efficiency $k_1 = 12$ and an aircraft weight of $W_a = 397$ tons, results in $T = n_1 W_a / k_1 = 1.05 \times 397 / 12 = 34.7$ tons in cruise regime. If the engine works in take-off regime, the additional thrust will be 0.5 × 34.7 = 17.35 tons, which is sufficient for the sling launcher. The additional thrust is necessary only for 80–110 seconds. If we use a middle-sized aircraft, this thrust may also be obtained from a brief engine boost (take-off engine regime, plus additional force generated by the injection of fuel by the jet engine nozzle applied in combat aircraft), or the installation of an additional outboard suspended air or rocket engine.

The end of the sling has a speed of 3.4M for a short time, and may be made of or protected by heat resistant material.

These parameters are not optimal, and the offered space launch needs further research.

Economic efficiency

Our projects presented here are intended for large-scale commercial implementation, with 8–9 tourists per flight and can be reused up to 1,000 times.

Let us estimate the cost of a space ticket per passenger, if the space ship takes 8 passengers.

A fully loaded long-distance Boeing 747 carries 400 passengers, for an average passenger ticket cost of $200, and a flight from New York to London takes about 8 hours. This translates to a cost of about $15,000 per hour of flight. Our flight will be about 1.5 hours, costing about $22,500. Assuming the space ship costs $3 million to build and is designed for 1,000 flights, the average depreciation cost per flight is $3,000. Assuming the maintenance cost for 1 flight is $4,500, the total cost of 1 flight would be $30,000. The net actual cost per passenger is $30,000 / 8 = $3,850. At the present time with existing rocket technology, it costs $20 million. With the proposed successful X-prize projects, the projected cost per passenger is $0.7 to $2 million.

General discussion

Project 1 describes the suggested method for delivering projectiles to a distance of up to 2000 km, using current technology and inexpensive, currently available materials. The space launcher (project 2) requires whiskers, and it may be used for non-human space payloads. The X-prize space flights (project 3) requires a sling made of nanotubes or whiskers (project 4) and, in all probability, the installation of an additional outboard air or rocket engine on a currently-existing subsonic or supersonic aircraft.

Industry now produces whiskers, and science laboratories can make nanotubes that have high tensile strength[20]. Theory indicates that these values are only 10% of the potential strength. We need to develop the means to manufacture a long, thin cable, such as the strings or threads produced from cotton or wool, from whiskers and nanotubes.

The fiber industry at the present time produces fibers which are theoretically employed in the author's concept projects. However, whiskers, and especially nanotubes, strongly improve the possibilities of this method. They increase the potential speed and decrease the cable mass and drag (rotation energy). These projects are unusual for specialists and others now, but there are advantages, and it is believed that they have good commercial potential.

A reviewer drew the author's attention to the Slingaton Launcher described by D.A. Tidman [24]. This launcher is very different from the sling launcher in this chapter. Tidman's launcher is a vacuum circle tube bulb-like form with a circle diameter up 1 km. The rocket and space ship are located inside this tube. The tube has big mass and makes oscillation like a conventional hula-hoop. This oscillation helps

to move the inside apparatus. The weaknesses of this design are its large installation mass, large required power, very big friction (huge centrifugal force presses the vehicle to the wall of the tube), problems with exit of the vehicle into atmosphere from the vacuum tube, etc.

By contrast, the sling launcher described here is very simple. It has only the lever, motor and sling and it is all located in the atmosphere.

Many people ask about heating problems when a vehicle returns into the atmosphere. They recall the heating tile defects of the "Space Shuttle" and think that this problem is very troublesome for the suggested vehicles. However, there is a big difference between a re-entry space vehicle and a launch space vehicle. The re-entry vehicle has high speed and enormous kinetic energy, which must be dispersed. It has a bulbous fuselage and wing edges, and slides along the Earth's atmosphere for a long time. The offered projectiles save energy (speed) during flight. They have sharp edges, fly in the atmosphere for a short time and have a small projected area.

References for Chapter 10

1. Space Technology and Application. International Forum (STAIF) , Albuquerque, MN, USA, 1996–1997.
2. Smitherman D.V. Jr., "Space Elevators", NASA/CP-2000-210429, 2000.
3. Bolonkin A.A., "Kinetic Space Towers and Launchers", *Journal of the British Interplanetary Society (JBIS),* Vol. 57, No 1/2 , pp. 33–39, 2004.
4. Bolonkin A.A., "Non-Rocket Transport System for Space Travel", *JBIS*, Vol. 56, No 7/8. pp. 232–254, 2003.
5. Bolonkin A.A., "Centrifugal Keeper for Space Stations and Satellites", *JBIS*, Vol. 56, No 9/10, pp. 314-327.
6. Bolonkin A.A., "Hypersonic Gas-Rocket Launcher of High Capacity", *JBIS*, Vol. 57, No 5/6, pp. 162–172.
7. Bolonkin A.A., "Optimal Inflatable Space Towers with 3–100 km Height", *JBIS*, Vol. 56, No 3/4, 87-97.
8. Bolonkin A.A., "Asteroids as Propulsion Systems of Space Ships", *JBIS,* Vol. 56, No 9/10, pp. 98–107, 2003.
9. Bolonkin A.A., "Hypersonic Gas-Rocket Launch System.", AIAA-2002-3927, 38th AIAA/ASME/ SAE/ASEE Joint Propulsion Conference and Exhibition, 7–10 July, 2002, Indianapolis, IN, USA.
10. Bolonkin A.A., "Multi-reflex Propulsion Systems for Space and Air Vehicles and Energy Transfer for Long Distance", *JBIS*, Vol. 57, No. 11/12, pp. 379–390.
11. Bolonkin A.A., "Kinetic Anti-Gravitator", AIAA-2005-4504, 41st Propulsion Conference, 10-12 July, 2005, Tucson, Arizona, USA.
12. Bolonkin A.A., "Optimal Trajectories of Air and Space Vehicles", Journal *Aircraft Engineering and Space Technology* (*AEAT*), Vol. 76, No. 2, 2004, pp. 193–214.
13. Bolonkin A.A., "Space Cable Launchers", Paper No. 8057 presented at the Symposium "The Next 100 years", Dayton, OH, USA, 14–17 July, 2003.
14. Minovich M., "Electromagnetic Transportation System for Manned Space Travel", US Patent #4,795,113, 3 January 1989.
15. Beamed Energy Propulsion. First International Symposium on Beamed Energy Propulsion. Melville, New York, 2003. American Institute of Physics.
16. Zubrin R.M., "The Use of Magnetic Sails to Escape from Low Earth Orbit", *JBIS*, No. 1, 1993, pp. 3–10.
17. Galasso F.S., *Advanced Fibers and Composites*, Gordon and Branch Scientific Publisher, 1989.
18. *Carbon and High Performance Fibers*, Directory, 1995.
19. *Concise Encyclopedia of Polymer Science and Engineering*, Ed. J.I.Kroschwitz, 1990.
20. Dresselhous M.S., *Carbon Nanotubes*, Springer, 2000.
21. Anderson J.D., *Hypersonic and High Temperature Gas Dynamics*. McGraw-Hill Book Co., 1989.
22. Bill G.V., Murphy, C.H., Paris Kanoneu – the Paris Guns and Project HARP, JFF91-1277, 1988.
23. Koell D.E., *Handbook of Cost Engineering*, TCS, Germany, 2000.
24. Tidman D.A., "Constant - Frequency Hypervelocity Slings", *Journal Propulsion and Power* (*JPP*), 2003, 0748-4658, vol. 19, No. 4, pp. 581-587.

25. Bolonkin A.A., "Sling Rotary Space Launcher", AIAA-2005-4035, 41 Propulsion Conference, 10–12 July, 2005, Tucson, Arizona, USA.

Chapter 11
Asteroids as Propulsion System of Space Ships*

Summary

Currently, rockets are used to change the trajectory of space ships and probes. Sometimes space probes use the gravity field of a planet. However, there are only nine planets in the solar system, all separated by great distances. There are tens of millions of asteroids in outer space. This chapter offers a revolutionary method for changing the trajectory of space probes. This method uses the kinetic or rotary energy of asteroids, comet nuclei, meteorites or other space bodies (small planets, natural planet satellites, space debris, etc.) to increase (to decrease) ship (probe) speed up to 1000 m/s (or more) and to achieve any new direction in outer space. The flight possibilities of space ships and probes are increased by a factor of millions.

Introduction

 At the present time, rockets are used to carry people and payloads into space[1]. Other than rockets, methods used to reach space speed include the space elevator[2], tethers[3, 4], the electromagnetic system[5], and the tube rocket[9, 10]. The space elevator is not technically feasible at the present time; it would require substantial costs for development. In particular, the space elevator concept requires extremely strong nanotubes. Tethers are very complex and would require two artificial bodies. Electromagnetic systems are also complex and expensive. The author has previously discussed several other non-rocket launch methods (see other author proposals and articles) that are potentially low cost, but which require much additional research. These include cable launchers[6–10], circle launchers[11], and inflatable towers[12].

  There are many small solid objects in the Solar System called asteroids. The vast majority are found in a swarm called the asteroid belt, located between the orbits of Mars and Jupiter at an average distance of 2.1 to 3.3 astronomical units (AU) from the Sun. Scientists know of approximately 6,000 large asteroids of a diameter of 1 kilometer or more, and of millions of small asteroids with a diameter of 3 meters or more. Ceres, Pallas, and Vesta are the three largest asteroids, with diameters of 785, 110 and 450 km (621, 378, and 336 miles), respectively. Others range all the way down to meteorite size. In 1991 the Galileo probe provided the first close-up view of the asteroid Caspra; although the Martian moons (already seen close up) may also be asteroids, captured by Mars. There are many small asteroids, meteorites, and comets outside the asteroid belt. For example, scientists know of 1,000 asteroids of diameter larger than one kilometer located near the Earth. Every day 1 ton meteorites with mass of over 8 kg fall on the Earth. The orbits of big asteroids are well known. The small asteroids (from 1 kg) may be also located and their trajectory can be determined by radio and optical devices at a distance of hundreds of kilometers.

  Radar observations enable to discern of asteroids by measuring the distribution of echo power in time delay (range) and Doppler frequency. They allow a determination of the asteroid trajectory and spin and the creation of an asteroid image.

  Most planets, such as Mars, Jupiter, Saturn, Uranus, and Neptune have many small moons that can be used for the proposed space transportation method.

  There are also the asteroids located at the stable Lagrange points of the Earth–Moon system. These bodies orbit with the same speed as Jupiter, and might be very useful for propelling spacecraft further out into the solar system. Comets may also be useful for propulsion once a substantial spacecraft speed

is obtained. It seems likely that the kinetic and rotational energy of both comets and asteroids will eventually find application in space flight.

Most asteroids consist of carbon-rich minerals, while most meteorites are composed of stony-iron.

The present idea[6-8] is to utilize the kinetic energy of asteroids, comets, meteorites, and space debris to change the trajectory and speed of space ships (probes). Any space bodies more than 10% of a ship's mass may be used, but here mainly bodies with a diameter of 2 meters (6 feet) or larger are considered. In this case the mass (20–100 tons) of the space body (asteroid) is some 10 times more than the mass of probe (1 ton, 2000 lb) and the probe mass can be disregarded.

Connection Method

The **method** includes the following main steps:
  (a) Finding an asteroid using a locator or telescope (or looking in catalog) and determining its main parameters (location, mass, speed, direction, rotation); selecting the appropriate asteroid; computing the required position of the ship with respect to the asteroid.
  (b) Correcting the ship's trajectory to obtain the required position; convergence of the ship with the asteroid.
  (c) Connecting the space apparatus (ship, station, and probe) to the space body (planet, asteroid, moon, satellite, meteorite, etc.) by a net, anchor, and a light strong rope (cable), when the ship is at the minimum distance from the asteroid.
  (d) Obtaining the necessary position for the apparatus by moving around the space body and changing the length of the connection rope.
  (e) Disconnecting the space apparatus from the space body; spooling the cable.
The equipment required to change a probe (spacecraft) trajectory includes:
  (a) A light strong cable (rope).
  (b) A device to measure the trajectory of the spacecraft with relative to the space body.
  (c) A device for spacecraft guidance and control.
  (d) A device for the connection, delivery, control, and disconnection and spooling of the rope.

Description of Utilization

The following describes the general facilities and process for a natural space body (asteroid, comet, meteorite, or small planet) with a small gravitational force to change the trajectory and speed of a space apparatus.
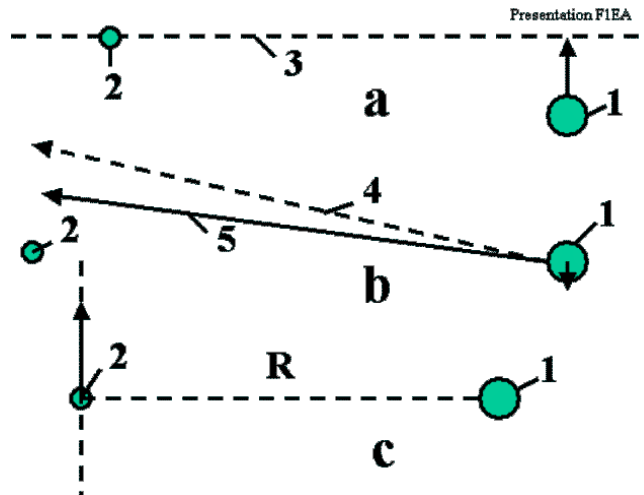

Fig. 11.1. Preparing for employment of the asteroid. Notations: 1 – space ship, 2 – asteroid, 3 – plane of maneuver. 4 – old ship direction, 5 – corrected ship direction. a) Reaching the plane of maneuver; b) Correcting the flight direction and reaching the requested radius; c) Connection to the asteroid.

Figs. 11.1a,b,c show the preparations for using a natural body to change the trajectory of the space apparatus; for example, the natural space body 2, which is moving in the same direction as the apparatus (perpendicular to the sketch, Fig. 10.1a). The ship wants to make a maneuver (change direction or speed) in plane 3 (perpendicular to the sketch), and the position of the apparatus is corrected and moved into plane 3. It is assumed that the space body has more mass than the apparatus.
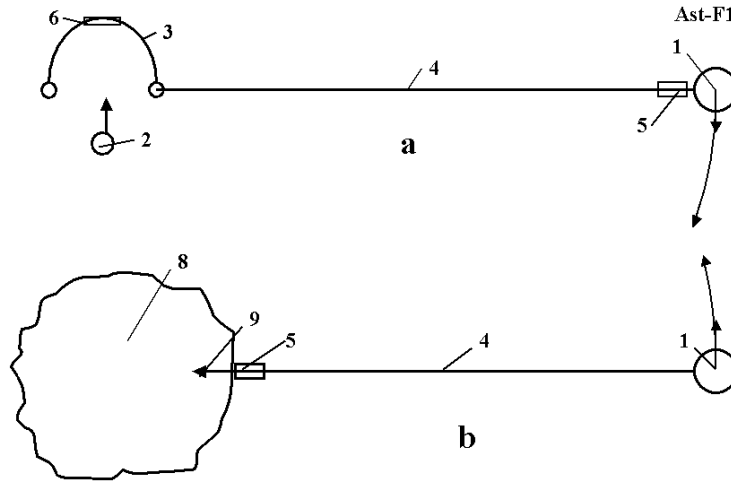

Fig. 11.2. a) Catching a small asteroid using net; b) Connection to a big asteroid using an anchor and cable. Notation: 1 – space ship, 2, 8 – asteroid, 3 – net with inflatable ring, 4 – cable (rope), 5 – load cabin, 6 – valve, 9 – anchor.
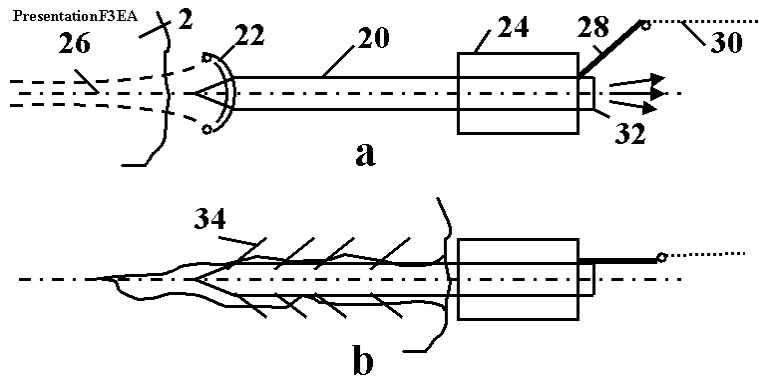

Fig. 11.3. a) Anchor (harpoon fork). Notation: 2 – asteroid, 20 – body of anchor; 22 – cumulative charge (shaped charge), 24 – rope spool, 26 – canal is made by shaped charge, 28 – rope keeper, 30 – rope, 32 – rocket impulse engine, which implants the anchor into the asteroid, 34 – anchor catchers. b) Anchor connected to the asteroid.

When the apparatus is at the shortest distance R from the space body, it connects to the space body means of the net (Fig. 11.2a) or by the anchor (Fig. 11.2b) and rope. The apparatus rotates around the common center of gravity at the angle φ with angular speed ω and linear speed ΔV (Fig. 11.4). The cardioids of additional speed and direction of the apparatus are shown in Fig. 11.4 (right side). The maximum additional velocity is $\Delta V = 2V_a$, where V_a is the relative asteroid velocity when the coordinate center is located in the apparatus.

Fig. 11.4b shows the case where the space body moves in the opposite direction to the apparatus with velocity ΔV.

Fig. 11.2a shows how a net can be used to catch a small asteroid or meteorite. The net is positioned in the trajectory of the meteorite or small asteroid, supported in an open position by the inflatable ring and connected to the space apparatus by the rope. The net catches the asteroid and transfers its kinetic energy to the space apparatus. The space apparatus changes its trajectory and speed and then disconnects from the asteroid and spools the cable. If the asteroid is large, the astronaut team can use the asteroid anchor (Figs. 11.2b, 11.3).

The astronauts use the launcher (a gun or a rocket engine) to fire the anchor (harpoon fork) into the asteroid. The anchor is connected to the rope and spool. The anchor is implanted into the asteroid and connects the space apparatus to the asteroid. The anchor contains the rope spool and a disconnect mechanism (Fig. 11.3). The space apparatus contains a spool for the rope, motor, gear transmission, brake, and controller. The apparatus may also have a container for delivering a load to the asteroid and back (Fig. 11.2b). One possible design of the space anchor is shown in Fig. 11.3. The anchor has a body, a rope, a cumulative charge (shared charge), the rocket impulse (explosive) engine, the rope spool and the rope keeper. When the anchor strikes the asteroid surface the cumulative charge burns a deep hole in the asteroid and the rocket-impulse engine hammers the anchor body into the asteroid. The anchor body pegs the catchers into the walls of the hole and the anchor's strength keeps it attached to the asteroid. When the apparatus is to be disconnected from the asteroid, a signal is given to the disconnect mechanism.
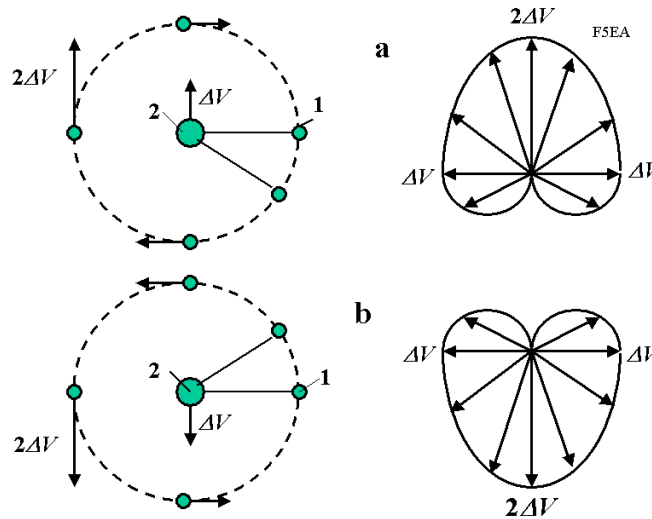

Fig. 11.4. Using the kinetic energy of an asteroid to change the space ship trajectory (speed and direction). On the right are cardioids of the additional velocity and its direction. The ship can get this velocity from the asteroid. Notations: 1 – space ship, 2 – asteroid, ΔV – difference between velocities of space ship and asteroid. a) Case when the asteroid has the same direction as the ship; b) Case when the asteroid has the opposite direction to the ship a.

If the asteroid is rotated with angular speed ω (Fig. 11.5), its rotational energy can be used for increasing the velocity and changing the trajectory of the space apparatus. The rotary asteroid spools the rope on its body. The length of the rope is decreased, but the apparatus speed is increased (see a momentum theory in physics).

The ship can change the length of the cable. When the radius decreases, the linear speed of the apparatus increases; conversely, when the radius increases the apparatus speed decreases. The apparatus can obtain energy from the asteroid by increasing the length of the rope.

The computations and estimations show the possibility of making this method a reality in a short period of time (see projects than follows).
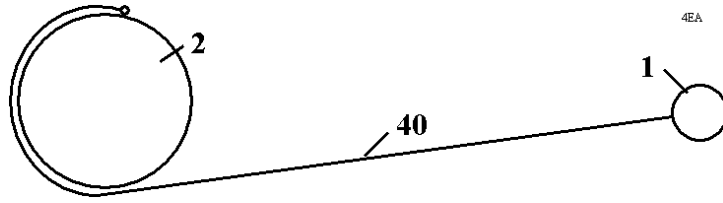
Fig. 11.5. Using the rotary energy of a rotating asteroid. Notations: 1 – space ship, 2 – asteroid, 40 – connection cable.

An abandoned space vehicle or large piece of space debris in Earth orbit can also be used to increase the speed of the new vehicle and to remove the abandoned vehicle or debris from orbit.

Theory and Computation

1. The differential equation can be found from the equilibrium of a small cable part under centrifugal force. This equation for optimal (equal stress from centrifugal force) cable is
$$da/A = (\omega^2 \gamma /\sigma)RdR \ .$$
   Its solution is the cable equal stress
$$a(R)=A/A_o=\exp(V^2/2k) = \exp(\omega^2 R^2/2k) \ . \tag{11.1}$$
   where a – relative cross-section area of cable; A – cross-section area of cable [m^2]; A_0 – initial (near probe) cross-section area of cable [m^2]; V – speed of probe or space ship about asteroid [m/s]; $k = \sigma/\gamma$ – ratio of cable tensile stress to density [Nm/kg]; $K = k/10^7$ – coefficient; R – radius from the common gravity center: asteroid + probe [m]; ω - angular speed of a probe around asteroid [rad/s]; σ – tensile strength [N/m^2]; γ – density of cable [kg/m^3];

2. Mass W [kg] of cable is
$$W = A_0\gamma \int_0^R a(r)dr = \frac{F_0}{k} \int_0^R e^{\omega^2 r^2/2k} dr \ , \tag{11.2}$$
   where r – variable [m]; F_o – force from the probe [N]

3. Relative cable mass $W_r = W/ W_s$ is
$$W_r = B(1+B), \quad B = \frac{n}{k} \int_0^{v^2/ng} \exp\left[\left(\frac{ng}{V}\right)^2 \frac{r^2}{2k}\right]dr, \tag{11.3}$$
   where the integration interval is $[0, V^2/ng]$, $n = F_o/g$ is the overload, V is the circle apparatus speed around the common center of gravity, W_s is ship (probe) mass, g is Earth gravitation [m/s^2], $g = 9.81$ m/s^2 .

4. Circular velocity of ship around asteroid
$$R = V^2/gn , \quad V = (gnR)^{0.5} \ . \tag{11.4}$$
   Computations are represented in Figs. 11.6–11.8.

5. Relative mass of cable with constant cross-section area for small speed
$$W_r = W/W_s = \gamma V^2/\sigma g = V^2/kg \ . \tag{11.5}$$

6. Finding the additional velocity the space vehicle has received from the asteroid.
   Let us take the coordinate axis along the positive direction of the asteroid speed and write the momentum and energy laws of the asteroid-apparatus system for this axis
$$m_1 V_1 + m_2 V_2 = m_1 u_1 + m_2 u_2 , \tag{11.6}$$
$$0.5m_1 V_1^2 + 0.5m_2 V_2^2 = 0.5m_1 u_1^2 + 05m_2 u_2^2 + A, \tag{11.7}$$

where m_1, V_1 are the mass and speed of the asteroid respectively before connection to apparatus; m_2, V_2 are the mass and speed of the apparatus respectively before connection to asteroid; u_1 is speed of the asteroid after disconnection from the apparatus; u_2 is speed of the apparatus after disconnection from the asteroid; A is energy (work) applied by the apparatus to change the length of the connection cable.

Let us locate beginning of the axis of at the apparatus (this means $V_2 = 0$) and apply the variable $V = V_1$ - asteroid speed around apparatus; $u = u_2$ – the additional apparatus speed; and $m = m_2/m_1$ – the relative apparatus mass.

Substitute u_1 from (11.6) into (11.7), we receive the quadratic equation about u

$$(m+1)u^2 - 2Vu + 2A/m_1m = 0 . \tag{11.8}$$

Solution of this equation is

$$u = \{V \pm [V^2 + 2A(m+1)/mm_1]^{0.5}\}/(m+1) . \tag{11.9}$$

Investigating this equation, if $A = 0$ (the apparatus does not change the length of the connection cable) and the asteroid mass is large ($m \approx 0$), the maximum additional speed of the apparatus is $u = 2V$ in the asteroid direction and $V = 0$ in the opposite direction. If $A \neq 0$, the maximum work (energy) apparatus can receive from the asteroid by increasing the connection cable length, is less than

$$A \leq mm_1V^2/2(m + 1) . \tag{11.10}$$

If the apparatus expends internal energy (decreases the length of the connection cable), the additional apparatus speed is limited only by the safe cable strength and apparatus overload. The apparatus does not lose mass to increase its speed.

If apparatus is disconnected in a direction with an angle of φ to the asteroid speed direction, the additional apparatus speed is

$$\Delta V = V(1 + \cos \varphi). \tag{11.11}$$

where V is initial speed of the asteroid around the space ship [m/s] (coordinate center is located at the space apparatus); ΔV is additional speed received by the ship from the asteroid [m/s]; φ is the angle between the old velocity vector of the asteroid and the new velocity vector of the apparatus.

The additional kinetic energy of the apparatus is then

$$E_k = 0.5m_2(\Delta V)^2. \tag{11.12}$$

7. The known formulas below may be useful:

$$V = \omega R, \; V_3R_3 = V_2R_2. \quad V_1 = R_o\left(\frac{g_0}{R}\right)^{0.5}, \quad V_2 = \sqrt{2}V_1, \quad R_g = \left(\frac{g_0R_0^2}{\omega^2}\right)^{1/3}, \tag{11.13}$$

where V_1 is the circular speed around the Earth, V_2 is the escape speed, R_o is the Earth's radius, and R_g is the radius of Earth's geosynchronous orbit.

Project

The capability to change the trajectory and speed of a space vehicle using an asteroid is shown in Fig. 11.4. The space ship could obtain a maximum additional speed equal to twice the speed difference between the space vehicle and the asteroid (speed of the asteroid around the space ship). If the length of the connection cable is changed, the speed of the space ship could change by more than double the speed difference. If the asteroid is rotating, the space ship can also obtain an additional speed increase from the rotation. The additional speed from one asteroid is also limited (for a manned ship) by the mass of the cable. For an additional speed of 1,000 m/s and $K = 0.2$, the mass of cable would equal 5% of the mass of the space apparatus. For an additional speed of 2,000 m/s, the mass of cable would equal 23% of the mass of the space apparatus. To travel to an asteroid, a connection device may be mounted onto the transport cable. The cable may be used many times.

The results of computation for different cases are shown in Figs. 11.6–11.11.

Fig. 11.6. Asteroid cable relative ratio via circle speed and coefficient $K = 0.1 – 0.4$.

Fig. 11.7. Relative cable asteroid mass via circle speed in m/s and coefficient $K = 0.1 – 0.4$.

Fig. 11.8. Cable radius in km via circle speed in m/s and overload $n = 4–16$.
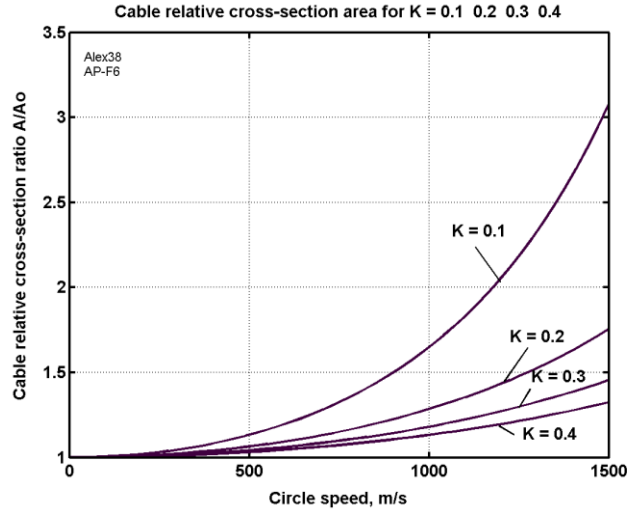
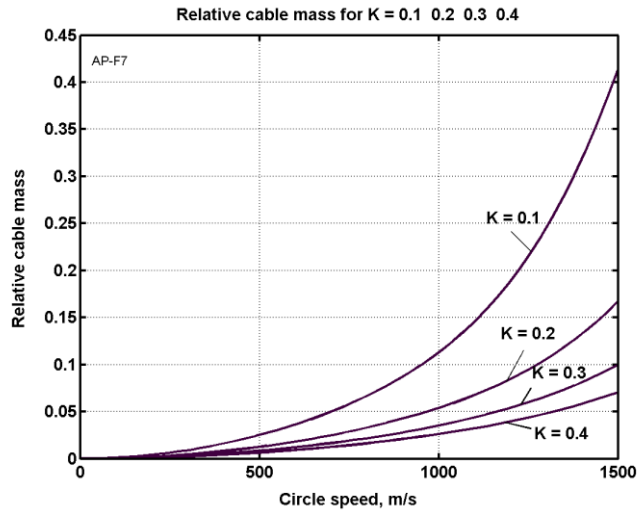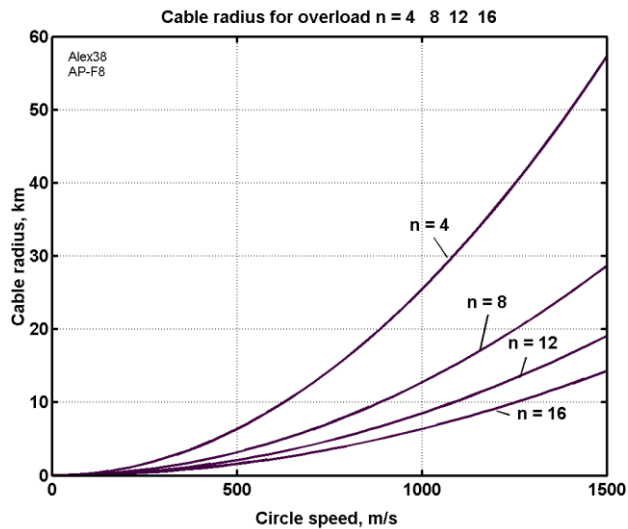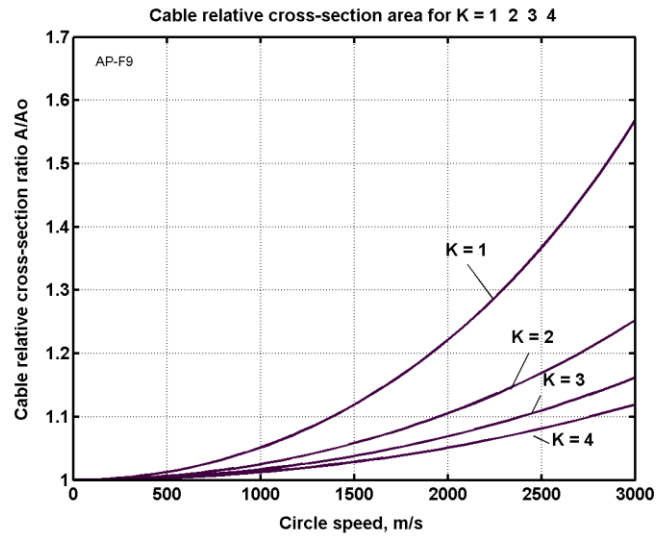**Fig. 11.9**. Asteroid cable relative ratio via circle speed and coefficient $K = 1 - 4$.
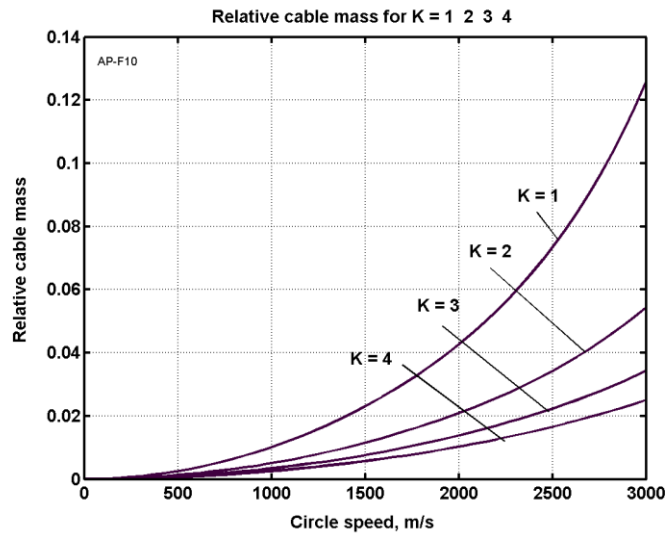
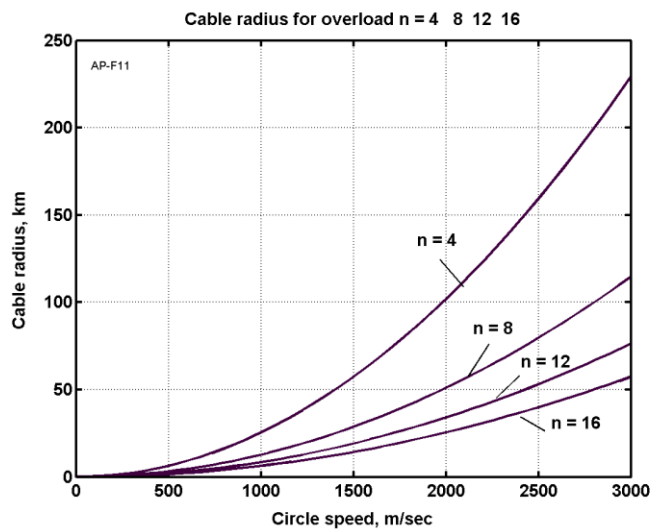**Fig. 11.10**. Relative cable asteroid mass via circle speed in m/s and coefficient $K = 1 - 4$.

Fig. 11.11. Cable radius in km via circle speed in m/s and overload n.

Discussion

If the change in the ship's speed is less than 1000 m/s, the conventional widely produced fiber (safe $K = 0.1$) can be used. The cable mass is about 8% of the ship's mass. After disconnection the cable will be spooled and can be used again. The reader can make estimations for other cases. Radio or optical devices can locate asteroids at distance of thousands of kilometers. Their speed, direction of flight and mass can be computed. The ship (probe) can make small corrections to its own trajectory to obtain the required position relative to the asteroid. All big asteroids with a diameter of more than 1 kilometer are listed in astronautic catalogs and their trajectories are well known. One thousand of them are located near the Earth. For those, we can compute in advance the intercept parameters. At the present time, long-range space apparatus uses the gravity of a planet to change its trajectory. However, the solar system has only nine planets, and they are located very far from one another. The employment of asteroids increases this possibility a million times over.

Estimation of the probability of meeting a small asteroid. It is known that every day about a ton of meteorites with a mass greater than 8 kg fall into the Earth's atmosphere. The Earth's surface area is about 512 million km^2. If the average mass of meteorites is 10 kg, then the Earth encounters 100 meteorites per day or one meteorite a day for every 5 millions km^2. If a space probe has a mass around 100 kg, a 10 kg meteorite has enough mass for it to be employed to change the direction and speed of the space probe. Ground locators can detect a 1 kg space mass at distances up to thousands of km. If the space ship can detect over a range of 1000 km, it means it can see a space body with an area of one million km^2, or about one meteorite in every 5 days. If one meteorite in ten is suitable for employment, it means every 50 days the space apparatus will meet an eligible meteorite near the Earth. The likelihood is ten times greater in the asteroid belt between Mars and Jupiter. For 6,000 big asteroids, we can compute the intercept parameters now. This number is expected to increase as more small asteroids are registered.

There are about 8,000 fragments of old rockets and space equipment near the Earth. The trajectories of these are known. They also can be used to accelerate space apparatus. In this case we will have a double benefit: to accelerate the current space apparatus and remove space garbage into the Earth's atmosphere (or into outer space). This space garbage is dangerous for current ships and the problem increases every year.

Note that the kinetic energy of space bodies may be used if the space body has a different speed or direction. It is difficult to use a tether system (for example, the last stage of a rocket and the Shuttle ship) because they have the same speed and direction.

Cable. If the required change of speed is less than 1,000 m/s, then cable from current artificial fibers can be used. In chapter 1 the reader with find a brief overview of the research information regarding the proposed experimental test fibers[19-22].

Conclusion

The availability of both current and new materials makes the suggested propulsion system and projects more realistic for a long trip to outer space with a minimum expenditure of energy[23].

References for Chapter 11

1. Space technology & Application. International Forum, 1996-1997, Albuquerque, MN, parts, 1–3.
2. D.V. Smitherman, Jr., "Space Elevators", NASA/CP-2000-210429.
3. Edited by M.L. Cosmo and E.C. Lorenzini, *Tethers in Space Handbook*. 3rd Edition. Smithsonian Astronomic Observatory, December,1997.
4. S.E. Ziegler and M.P. Cartmell, "Using Motorized Tethers for Payload Orbital Transfer", *Journal*

of Space and Rockets, Vol. 38, No. 6, 2001.

5. M.R. Palmer, "A Revolution in Access to Space Through Spinoff of SDI Technology", *IEEE Transactions on Magnetic*, Vol. 27, No 1, January 1991, p. 11–20.

6. A.A. Bolonkin, "Theory of Flight Apparatus with Control Radial Force". Collection *Researches of Flight Dynamic*, Ed. I.V. Ostoslavsky, Moscow, Mashinostroenie, 1965, pgs. 79–118 (in Russian).

7. "Asteroids as Engine of Space Ships" (Suggestions of American scientist Alexander Bolonkin), *"Weekly News"*, 28 April 1998, Israel (in Russian).

8. A.A. Bolonkin, "Employment of Asteroids for Movement of Space Ship and Probes", IAC-02-S.6.04, 53rd International Astronautical Congress, The World Space Congress – 2002, 10–19 Oct 2002, Houston, Texas, USA.

9. A.A. Bolonkin, "Hypersonic Gas-Rocket Launch System.", AIAA-2002-3927, 38th AIAA/ASME/ SAE/ASEE Joint Propulsion Conference and Exhibition, 7–10 July, 2002, Indianapolis, IN, USA.

10. A.A.Bolonkin, "Hypersonic Launch System of Capability up 500 tons per day and Delivery Cost $1 per lb", IAC-02-S.P.15. 53rd International Astronautical Congress, The World Space Congress – 2002, 10–19 Oct 2002, Houston, Texas, USA.

11. A.A.Bolonkin, "Inexpensive Cable Space Launcher of High Capability", IAC-02-V.P.07. 53rd International Astronautical Congress, The World Space Congress – 2002, 10–19 Oct 2002, Houston, Texas.

12. A.A.Bolonkin, "Non-Rocket Missile Rope Launcher", IAC-02-IAA.S.P.14. 53rd International Astronautical Congress. The World Space Congress – 2002, 10–19 Oct 2002, Houston, Texas.

13. A.A.Bolonkin, "Non-Rocket Space Rope Launcher for People", IAC-02-V.P.06. 53rd International Astronautical Congress, The World Space Congress – 2002, 10–19 Oct 2002, Houston, Texas.

14. A.A.Bolonkin, "Non-Rocket Earth-Moon Transport System", COSPAR 02-A-02226, 34th Scientific Assembly of the Committee on Space Research (COSPAR), The World Space Congress – 2002, 10-19 Oct 2002/Houston, Texas.

15. A.A.Bolonkin, "Non-Rocket Earth-Mars Transport System", COSPAR 02-A-02224. 34th Scientific Assembly of the Committee on Space Research (COSPAR), The World Space Congress – 2002, 10–19 Oct 2002, Houston, Texas.

16. A.A.Bolonkin, "Transport System for Delivery Tourists at Altitude 140 km", IAC-02-IAA.1.3.03. 53rd International Astronautical Congress. The World Space Congress – 2002, 10–19 Oct 2002, Houston, Texas.

17. A.A.Bolonkin, "Optimal Inflatable Space Towers of High Height". COSPAR 02-A-02228. 34th Scientific Assembly of the Committee on Space Research (COSPAR), The World Space Congress – 2002, 10–19 Oct 2002, Houston, Texas.

18. F.S. Galasso, *Advanced Fibers and Composite*, Gordon and Branch Scientific Publisher, 1989.

19. *Carbon and High Performance Fibers*, Directory, 1995.

20. M.S. Dresselhous, *Carbon Nanotubes*, Springer, 2000.

21. *Concise Encyclopedia of Polymer Science and Engineering*. Ed. J.I. Kroschwitz, 1990.

22. Newsletter Chim.& Rng., 8 Oct., 2001.

23. A.A. Bolonkin, "Asteroids as Propulsion Systems of Space Ships, *JBIS*, Vol. 56, No. 3/4, 2003, pp. 98–107.

The reader can find the information about asteroids in the following publications:

Dobrovolskis, A.R., *Icarus*, **88**, 24 (1990); Scotti, J.V. & Melosh, H.J., N*ature*, **365**, 733 (1993); Weissman, P., *Nature,* **320**, 242 (1986); Weidenschilling, S.J., *Nature*, **368**, 721 (1994); Sekanina, D. & Yeomans D.K., *Asronomical Journal*, **90**, 2335 (1985); Sekanine, D., *Science*, **262**, 382 (1993); Hudson, R. & Ostro, S., *Science*, **263**, 940 (1994; Ostro, S., *Rev.Mod. Phys*., **65**, 1235 (1995); Ostro, S. et al, *Nature*, **375**, 474 (1995); Hills, J. and Leonard, P., *Astrophys. J*., **109**, 401 (1995); Solem, J. and Hills, J., *Astrophys. J.*, **111**, 1382 (1996).

The Asteroid Belt

Asteroid Main-Belt Distribution
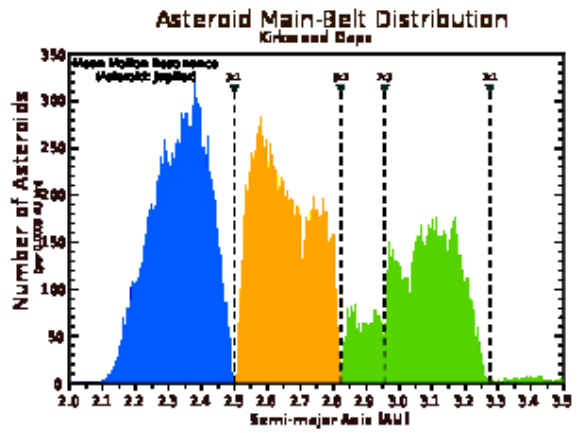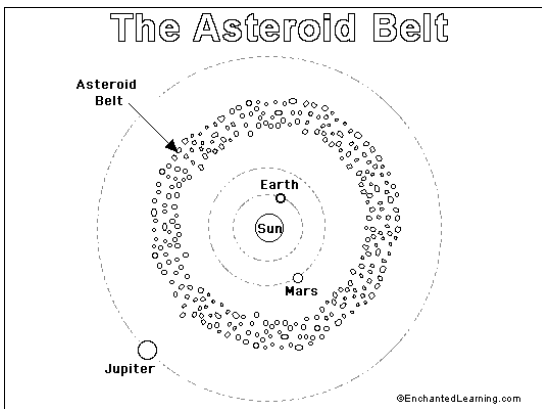
Chapter 12

Multi-reflex Propulsion Systems for Space and Air Vehicles and Energy Transfer for Long Distance*

Summary

The purpose of this chapter is to draw attention to the revolutionary idea of light multi-reflection. This idea allows the design of new engines, space and air propulsion systems, storage systems (for a beam or solar energy), transmission of energy (over millions of kilometers), creation of new weapons, etc. This method and the main innovations were offered by the author in 1983 in the former USSR. Now the author shows the immense possibilities of this idea in many fields of engineering – astronautics, aviation, energy, optics, direct conversion of light (laser beam) energy to mechanical energy (light engine), to name a few. This chapter considers the multi-reflex propulsion systems for space and air vehicles and energy transmission over long distances in space.

Introduction

   Short history. The relatively conventional way to send a spacecraft on an interstellar journey is to use the solar sail[1] or a laser sail[2]. This method is not effective because the light intensity is very low, with only one reflection. There has been a lot of research in this area and into solar sails in general. A. Kantrowitz offered the conventional method for using a laser beam for space propulsion[3]. He transferred energy using laser beam to a space vehicle, converted light energy into heat and evaporated a material, then obtained thrust from the gas pressure of this evaporated material. There is much research on this method[4]. However, it is complex, has low efficiency, has limited range (divergence of the laser beam), requires special material located on board the space ship, and requires a very powerful laser.

   In 1983 the author offered another method: that of using light beam energy, then the direct conversion of light energy into mechanical pressure (for an engine) or thrust (for launchers and propulsion systems) by multiple reflections[5].

   The author found only one work related to this topic, published in 2001[6]. However our work is very different from this. Our suggested system has several innovations which make the proposed method possible improve its parameters millions of times. The difference between our suggested system and the previous system[6] is analyzed in the "Discussion" section, below.

   The reflection of light is the most efficient method to use for a propulsion system. It gives the maximum possible specific impulse (light speed is $3 \cdot 10^8$ m/s). The system does not expend mass. However, the light intensity in full reflection is very small, about 0.6×10^{-6} kg/ kW. In 1983 the author suggested the idea of increasing the light intensity by a multi-reflex method (multiple reflection of the light beam) and he offered some innovations to dramatically decrease the losses in mirror reflection (including a cell mirror and reflection by a super–conducting material). This allows the system to make some millions of reflections and to gain some Newtons of thrust per kW of beam power. This allows for the design of many important devices (in particular, beam engines[7]) which convert light directly into mechanical energy and solve many problems in aviation, space, energy and energy transmission.

In the last years achievements in optic materials and lasers have decreased the losses from reflection. The author returned to this topic and made it his primary area of research. He solved the main problems: the design of a highly efficient reflector (cell mirror), a light lock, focusing prismatic lightweight mirrors and lenses, a laser ring, and a beam transfer over very long distances (millions of km) with only very small beam divergence, light storage, a beam amplifier, a modulator of light frequency, balloon suspension of mirrors, and so on.

Brief information about light and light devices. A short description of electromagnetic radiation can be found in the publication[7]. A conventional mirror can reflect a maximum of 98–99% of the incident light energy of some bands of light waves. This gives a maximum of 200–300 reflections which is not enough for propulsion systems and engines. Because the light pressure is so low (about $0.6 \cdot 10^{-6}$ kg/ kW), we need at least a million reflections.

There is a well-known method for increasing mirror reflection. The layers of a quarter-wave optical thickness of high and low refractive-index materials increase the reflectance. After more than 12 layers, the reflective efficiency of a dielectric mirror approaches 100%, with virtually no absorption or scattering. Maximum reflectance occurs only in a region around the design wavelength. The size of the region depends on the design of the stack of multiple dielectric coatings. Outside this region the reflectance is reduced. For example, at one-half the design wavelength it falls to the level of the uncoated substrate. The dielectric mirror is also designed for use at a specific angle of incident radiation. At other angles, the performance is reduced, and the wavelength of maximum reflectance is shifted.

Unfortunately, this dielectric mirror method is not suitable for mirrors moving relative to each other as the reflected frequency is shifted slightly, and this frequency shift accumulates over multiple reflections. Also conventional mirrors tend to reflect the beam off in some other direction if the mirrors are not kept in perfect alignment to the beam. The author's proposed cell mirror reflects the beam in the same direction which is very important for decreasing the beam divergence. The small cells provide high reflectance and small absorption.

A narrow laser beam is the most suitable for a light engine and light propulsion. There are many different types of lasers with different powers (peak power up to 10^{12} W), wavelength (0.2–700 μm), efficiency (1% up to about 95%), and pulse rate (up to some thousands of impulses per second) or continuous operations. In publications in the References the reader will find a brief description of the laser [7] or more detail[8].

At the present time we are seeing significant advances in high-power weapons-class lasers[7]. The laser power reaches 1 million watts.

For our computation the beam divergence is very important. The laser beam divergence[8] (see p. 4) is

$$\theta = \frac{2}{\sqrt{\pi}} \frac{\lambda}{D} = 1.13 \frac{\lambda}{D} ,$$
(12.1)

where θ is the angle of divergence [rad], λ is the wavelength [m], and D is an aperture diameter [m]. In particular, the diameter of the laser beam may be increased by an optical lens for reducing the beam divergence. The aperture diameter may be also increased by offered *laser ring* (Fig. 12.1). The reflex capacity may be improved by using a super conductive material[5] (this idea needs additional research).

More detailed information is in publication in the references[7–9].

Description of innovation

Multi-reflex launch installation of a space vehicle. In a multiple reflection propulsion system a set of tasks appear: how to increase a mirror's reflectivity, how to decrease the light dispersion (from mirror imperfections and non-parallel surfaces), how to decrease the beam divergence, how to inject the beam between the mirrors (while keeping the light between the mirrors for as long as possible),

how to decrease the attenuation (a mirror, prism material, etc), how to increase the beam range, and how much force the system has.

To solve of these problems, the author proposes[5], a special "cell mirror" which is very reflective and reflects light in the same direction from which it came, a *"laser ring"* which decreases the beam divergence, *"light locks"* which allows the light beam to enter but keep it from exiting, a "beam transfer*"*, a "focusing prismatic thin lens", prisms, a set of lenses, mirrors located in space, on asteroids, moons, satellites, and so on.

Cell mirrors. To achieve the maximum reflectance, reduce light absorption, and preserve beam direction the author uses special *cell mirrors* which have millions of small 45º degree prisms (1 in Fig. 12.1a,g). Cell mirror are retroreflector cells or cube corner cells. A light ray incident on a cell is returned parallel to itself after three reflections (Fig. 12.1g). In the mirror, provided the refractive index of the prism is greater than $\sqrt{2}$ ($\cong 1.414$), the light will be reflected by total internal reflection. The small losses may be only from prism (medium) attenuation, scattering, or due to small surface imperfections and Fresnel reflections at the entrance and exit faces. Fresnel reflections do not result losses when the beam is perpendicular to the entry surface. No entry losses occur where the beam is polarized in parallel of the entry surface or the entry surface has an anti-reflection coating with reflective index $n_1 = \sqrt{n_0 n_2}$. Here n_0, n_2 are reflective indexes of the vacuum and prism respectively. These cell mirrors turn a beam (light) exactly back at 180º if the beam deviation is less 5–10º from a perpendicular to the mirror surface. For incident angles greater than $\sin^{-1}(n_1/n_2)$, no light is transmitted, an effect called total internal reflection. Here n is the refractive index of the medium and the lens ($n \approx 1$–4). Total internal reflection is used for our reflector, which contains two plates (mirrors) with a set of small corner cube prisms reflecting the beam from one side (mirror) to the other side (mirror) (Fig. 12.1b,c, f). Each plate can contain millions of small (30–100 μm) prisms from highly efficient optic material used in optical cables[9]. For this purpose a superconductivity mirror[5] may also be used,

Laser ring. The small lasers are located in a round ring (Fig. 12.1c). A round set of lasers allows us to increase the aperture, resulting in a smaller divergence angle θ. The entering round beam (9 in Fig. 12.1a) has slip θ (or θ/2) to the vertical. The beam is reflected millions of times as is shown in Fig. 12.1b,c and creates a repulsive force F. This force may be very high, tens of N/kW (see the computation below) for motionless plates. In a vacuum it is limited only by the absorption (dB) of the prism material (see below) and beam divergence. For the mobile mirror (as for a launch vehicle) the wavelength increases and beam energy decreases as the mirrors move apart.

This system[5] can be applied to a space vehicle launch on a planet that has no atmosphere and small gravity (for example, the Moon; high gravity requires high beam power).

Light lock. The first design of *light lock* allows the laser beam to enter, but closes the exit of a returned ray. The beam (9 in Fig. 12.1d) of continuous laser passes through a multi-layer dielectric mirror (10 in Fig. 12.1d). The entering beam runs the full length between mirrors (Fig. 12.1b,c), reflects a million times, and enters from the other side (11 in Fig. 12.1d). For moving (separating) mirrors the wavelength is changed because the beam gives up energy to the moving mirrors (see computations
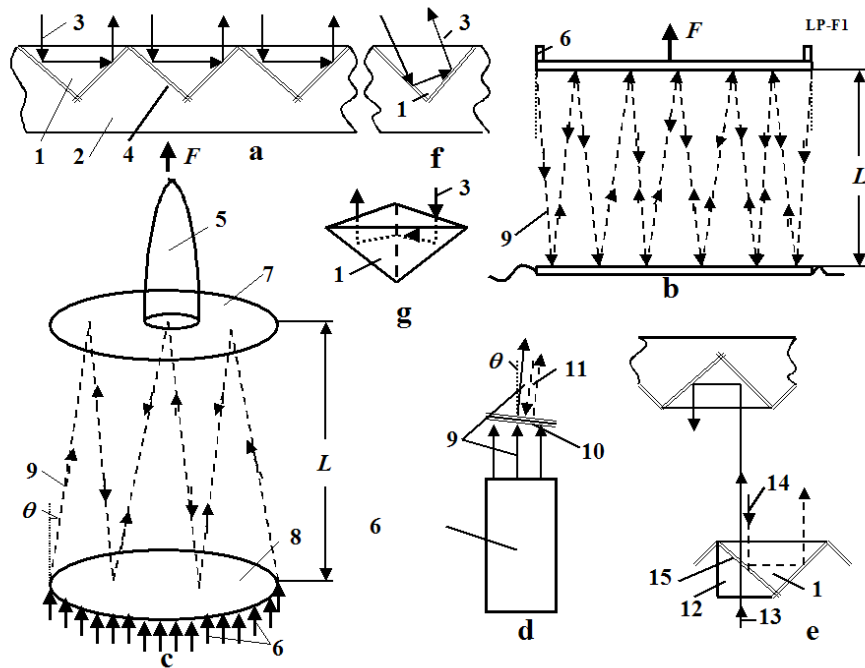
Fig. 12.1. Space launcher. Notations are: 1 – prism, 2 – mirror base, 3 – laser beam, 4 – mirror after chink (optional), 5 – space vehicle, 6 – lasers (ring set of lasers), 7 – vehicle (ship) mirror, 8 – planet mirror, 9 – laser beam, 10 – multi-layer dielectric mirror, 11 – laser beam after multi-reflection (wavelength $\lambda_{11} > \lambda_9$), 12 – additional prism, 13 – entry beam, 14 – return beam, 15 – variable chink between main and additional prisms. (a) Prism (cell, corner cube) reflector. (b) Beam multi-reflection, (c) Launching by multi-reflection, (d) The first design of the light lock, (e) The second design of the light lock, (f) Reflection in the same direction when the beam is not perpendicular to mirror surface, (g) Mirror cell (retroreflector cell or cube corner cell). A light ray incident on it is returned parallel to itself after three reflections.
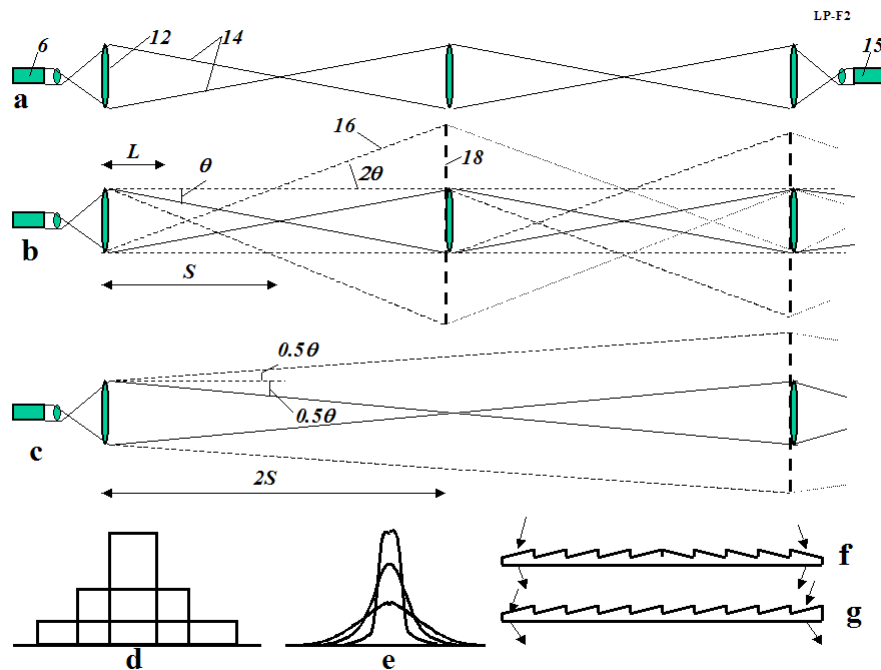

Fig. 12.2. Laser beam long-distance transfer. Notations are: 12 – lens, 14 – bounds of laser rays, 15 – light receiver, 16 – divergence ray. (a) focused beam, (b) focused beam with angle θ which has part S without

divergence, (c) focused beam with angle 0.5θ which has minimum divergence at a long distance, (d) beam with a plate wave front, (e) Gaussian beam with normal distribution of beam front, (f) Fresnel's (prism) lens, (g) lens for changing the beam direction.

. As a result the wavelength increases ($\lambda_{11} > \lambda_9$) when the distance increases, and the wavelength decreases ($\lambda_{11} < \lambda_9$) when the distance decreases. The mirror (10 in Fig. 12.1d), is designed to pass the laser beam (9 in Fig. 12.1d) and to reflect back the "used" ray (11 in Fig. 12.1d). If the beam is not reflected by the mirror (10 in Fig. 12.1d), it enters into the laser and will be reflected back by the laser's internal mirror.

The second design of the *light lock* is shown in Fig. 12.1e. This contains an additional prism 12 and an impulse laser. When laser beam 13 enters the system, the additional prism 12 is pushed into the main prism 1. While the beam runs between the mirrors, the additional prism is disconnected from the main prism and the return beam 14 cannot go back in. It travels inside the reflected mirrors with a lot of reflections if the mirrors have the right focuses. The chink, 15, between the additional and main prisms may be very small, about a light wavelength (1 micron). A piezoelectric plate can be used to move the additional prism.

A continuous or pulse laser may be used for the first light lock and a pulse laser may be used for the second lock. We compute average laser power.

The details of attenuation of light propagating through an optical material are considered in physics textbooks. To increase the number of reflections, we use a set of very small prisms and a highly efficient optical material (dB = 0.1–0.5).

Space beam transfer. Space *beam transfer* is shown in Fig. 12.2a. The first lens has a large aperture for the laser beam and focuses the beam which decreases the divergence angle θ. The other Fresnel's lens then continues to focus the beam (Fig. 12.2a).

Non-focused beam is lose intensity through diffracted rays but *beam transfer* has a special focusing lens. If the focus is located at a distance $S_1 = D/2\theta$, the beam does not have losses through up to a diffracted rays in this distance S, but after the distance S the divergence angle becomes 2θ (Fig.12.2b). If we need to transmit energy a distance L less than S (for example, in launching), this method is fine since the distance between the mirrors $L << S$ and the beam is reflected many times without loss. If we want to transfer the energy over very long distance, the method shown in Fig. 12.2c may be better. In this method the beam is focused on point at a distance $S_2 = D/\theta$. The beam has small amounts of diffraction everywhere, but the losses are smaller after a distance $1.5S_1$ than in the case of Fig. 12.2b. If an intermediate lens with a much larger diameter than the initial lens (Fig. 12.2b,c) is added midway, it is possible to decreases the beam diffraction energy losses to a very small value.

The distribution of energy in a gross section area of the beam is also important for divergence and diffraction losses. The plate front (Fig. 12.2a) of the wave and plate distribution of energy and divergence (Fig. 12.2d) are worst and give the maximum of energy losses. A normal distribution of beam energy and a Gaussian beam is better because the losses of beam energy trough diffraction are reduces at the edges (Fig. 12.2e).

Energy transfer is done in the following way. First the Fresnel's lenses (collimators) (Fig. 12.2f), Fresnel's prisms (Fig. 12.2g), and mirrors are (permanently) located in space (Fig. 12.3a). Their trajectories and the receiving space vehicle's trajectory in space are known. Through commands from Earth, a space ship or the vehicle's computer, the mirrors and lenses are turned to the required angles (angular position). A small pilot ray may be used for aiming and focusing. The required angular changes are small (for focusing and small corrections in direction) and may be made by piezoelectric controlled plates. After the pilot ray reaches the space vehicle as required, the full power beam is transmitted to the space vehicle. This beam may be used to launch vehicles from an asteroid or small mass planetary satellites (Fig, 12.1c), to change the vehicle's trajectory (Fig, 12.3b), or to increase the acceleration of the space vehicle near an asteroid (Fig. 12.3c) using the multi-reflex method (Fig. 12.3a,b,c). This beam energy may be also used by the space vehicle for its rocket engine and internal

power requirements. The distance between lenses may reach tens of millions of kilometers (see computation below, Fig. 12.13). The average distances of the nearest planets from the Sun are: Venus 108 x10^6 km, Earth 150×10^6 km, Mars 228×10^6 km. Transfer efficiency of system may be about 0.7–0.9 (see computation below).

Aviation and energy air transfer. This method may be used for the transfer of energy to air, land, sea, and ocean vehicles (Fig. 12.4). The transfer beam passes through the atmosphere only once and loses little energy. The vehicle may use light (multi-reflex) engines[5, 7]. A multi-reflex engine transfers (converges) the beam (light) energy directly into mechanical energy (rotates the propeller) with high efficiency.
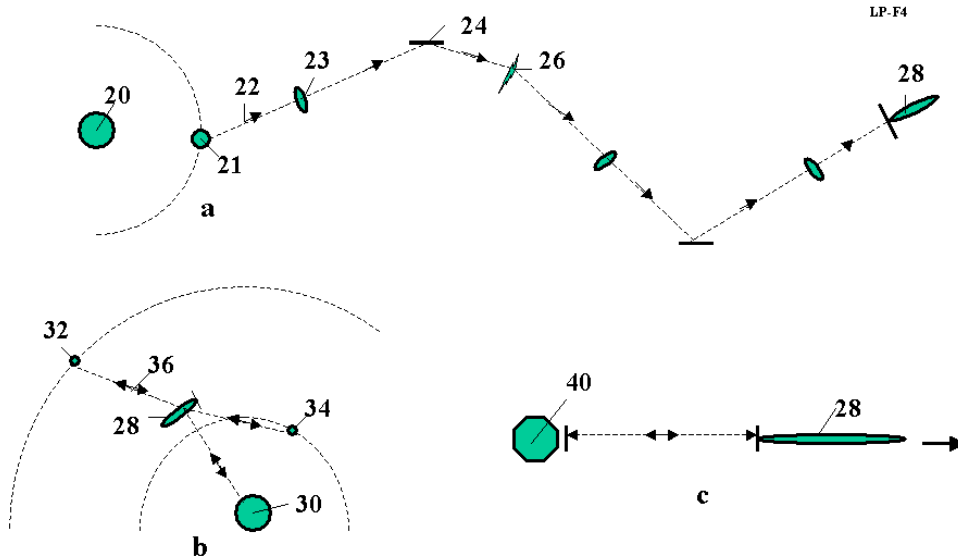

Fig. 12.3. Space energy transfer over long distance. a. Transferring thrust from Earth to space ship by laser beam, b. Using of satellites (or moons) to change the vehicle's trajectory, c. Using of asteroid for launching of ship.   Notations are: 20 – Sun, 21 – Earth, 22 – laser beam, 23 – Fresnel's lens, 24 – mirror, 26 – Fresnel's prism, 28 – Space vehicle, 30 – planet, 32, 34 – planet satellite, 36 – multi-reflection, 40 – asteroid.
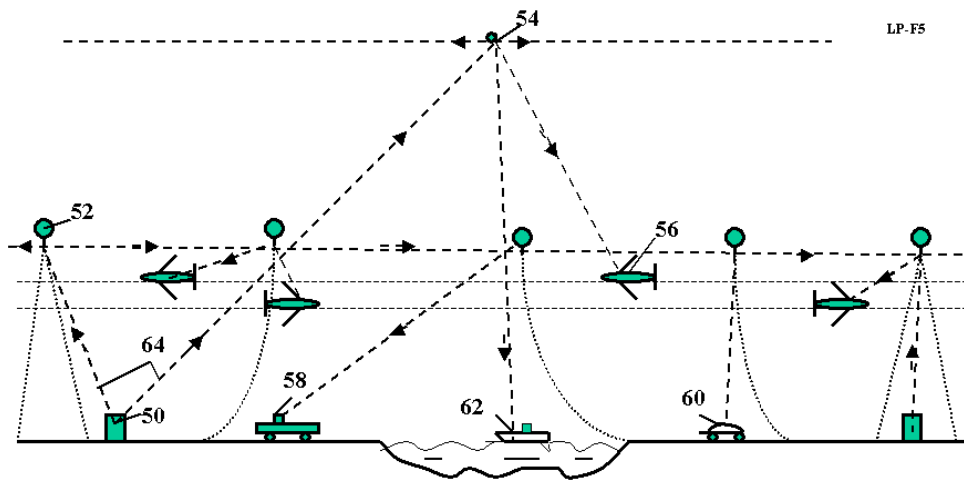
Fig. 12.4. Beam energy transfer to air, land, and sea vehicles. Notations are: 50 – beam energy station, 52 – control mirror suspended from a tethered air balloon, 54 – mirror suspended from planet satellite, 56 – aircraft, 58 – ground track, 60 – car, 62 – sea (ocean) ship, 64 – beams.

The system should include beam energy station(s), control mirrors suspended from air balloons at an altitude of 12–18 km (or on satellites), and a control system. The energy station sends the beam to the

nearest mirror. The mirror reflects it to other mirrors (or lenses, or prisms). These mirrors distribute the beam to the system's customers (aircraft, ground vehicles, river or sea ships, and so on). These customers may have light (multi-reflex) engines[5, 7] and directly convert the light (electromagnetic radiation) into mechanical work. The control system guides the energy distribution. In a clear atmosphere, the efficiency of this energy delivery system is high. It is important that the air is clean and clear at the initial, mainly vertical distance (from the energy station to the first mirror). At times of rain or smoke (from fires, etc.) a backup method should be in place, perhaps using orbiting satellite mirrors. At altitudes over 12 km the atmosphere is generaly clear.   This method allows us to delivery energy over some thousands of kilometers (see computation below, Fig. 12.14). In war time the beam may be focused and used against the enemy.

Theory (estimation) of multi-reflex launching and beam transfer

Special theory, methods and computation for this case are developed below.
   Attenuation of beam. The attenuation of light passingpropagating through an optical material is caused either by absorption or by scattering. In both absorption and scattering, the power is lost over a distance, z, from the power $N(z)$, propagating at that point. So we expect an exponential decay:
$$N(z) = N(0)\exp(-yz) . \tag{12.2}$$
   The attenuation coefficient, y, is normally expressed in dB km^{-1}, with 1 dB km^{-1} being the equivalent of 2.3×10^{-4} m^{-1}. Absorption is a material property in which the optical energy is normally converted into heat. In scattering processes, some of the optical power in the guided modes is radiated out of the material.
   Attenuation in some current and some potential very low loss materials that have been created for fiber communication has a dB value of up to $a = 0.0001$ ([7], Fig. 3 or Fig. A3.3 in this book). However, some of these materials are highly reactive chemically and are mechanically unsuitable for drawing into a fiber. Some are used as infrared light guides, none are presently used for optical communication, but may be useful for our purposes. Our mechanical property and wavelength requirements are less stringent than for optical communications. We use in our computation $a = 0.1$-0.4 dB km^{-1}. The conventional optical material widely produced by industry for optical cable has an attenuation coefficient of 2 dB km^{-1}.
   Change in beam power. The beam power will be reduced if one (or both) reflector is moved, because the wavelength changes. The total relative loss of the beam energy in one double cycle (when the light ray is moved to the reflector and back) is
$$q = 1 - (1-2\gamma)(1-2\xi)(1\pm2v)\varsigma , \tag{12.3}$$
where $v = V/c$, V is the relative speed of the mirrors [m/s], $c = 3\times10^8$ m/s is the speed of light. We take the "+" when the distance is reduces (braking) and take "– " when the distance is increased (as in launching, a useful work for light), γ is the light loss through prism attenuation, ξ is the loss (attenuation) in the medium (air) (in clean air $\xi = 0.333\times10^{-6}$ m^{-1}), v is the loss (useful work) through relative mirror (lens) movement, ς is the loss through divergence and diffraction.
   Multi-reflex light pressure. The light pressure, T, of two opposed high reflectors after a series of reflections, n, to one another is
$$T_0 = \frac{2N_0}{c} , \quad T_1 = \frac{2N_0}{c} q , \quad T_2 = \frac{2N_0}{c} q^2 , \quad T_3 = \frac{2N_0}{c} q^3 , \quad ... \quad , \quad T_{n-1} = \frac{2N_0}{c} q^n . \tag{12.4}$$
   When $q = $ const, this is a geometric series. The sum of n members of the geometric series is
$$T = \frac{2N_0}{c} \frac{q^n - 1}{q - 1} . \quad If \quad n = \infty , \quad then \quad T_\infty = \frac{2N_0}{c} \frac{1}{1-q} , \quad q < 1. \tag{12.5}$$

   Limitation of reflection number. If the reflector is moved away, the maximum number of reflections, n, is limited by cell size, l, because the wavelength, λ, is increased and that cannot be more than the cell size. This limit is

$$n \leq \frac{\ln(l/\lambda_0)}{2v},$$
(12.6)

where l is the cell width [m], λ_0 is the initial wavelength [m].

   If the reflector is moved forward to another position the wavelength is reduced, but it cannot be less than the wave length of X-rays because the material transmits the X-rays (the material lessens the reflective capability).
This limit is about $\lambda_{min} = 10$ nanometers. The maximum number of brake reflections is

$$n \leq \frac{\ln(\lambda_0/\lambda_{min})}{2v}.$$
(12.7)

Coefficient of efficiency. The efficiency coefficient, η, may be computed using the equation

$$\eta = TV/N_0,$$
(12.8)

   Focusing the beam. If the lens used in focused at a range S_1, the distance, S, without ray divergence is (Fig. 12.2b):

$$S = \frac{D}{2\theta}, \quad \theta = \frac{2}{\sqrt{\pi}}\frac{\lambda}{D}, \quad S = \frac{\sqrt{\pi}}{4}\frac{D^2}{\lambda} = 0.443\frac{D^2}{\lambda}.$$
(12.9)

   Here, D is the diameter of the lens or mirror [m]. This distance is equal to the lens focus distance for the case in Fig. 12.2b ($S_1 = S$). In the case Fig. 12.2c (transfer over very long distance), the optimal focus distance is $S_2 = 2S_1$.

   Some computations. The computation of equation (12.9) is presented in Figs. 12.5 and 12.6. As you will see, the necessary focus distance may be high.
   The values in equation (12.3) can be computed as

$$\gamma = yz = 0.00023al, \quad l = m\lambda, \quad m \geq 1, \quad \xi = 0333 \cdot 10^{-6}L,$$
(12.10)

where a is the attenuation coefficient in dB [km^{-1}] ([7], fig.3), m is initial value of the wavelength which can be located in cell size l [m].
The loss through divergence, ς, for the case in Fig. 12.2b,d is

$$\varsigma = \frac{\pi(D/2)^2}{\pi(D/2 + 2\gamma(L-S))^2}, \quad 2\gamma(L-S) = \frac{4k}{\sqrt{\pi}}\frac{\lambda(L-S)}{D}, \quad \varsigma = 1 / \left(1 + \frac{8k\lambda(L-S)}{\sqrt{\pi}D^2}\right)^2 \text{ for } L > S. (12.11)$$

   Here L is the distance between the mirrors (lenses) [m], and, k is the focus coefficient. In case in Fig. 12.2b (where the focus distance is $D/2\theta$) $k = 0$ when $L < S$ (for transfer) or $n < S/L$ (for reflection) and $k = 2$ when $L > S$, or $n > S/L$; in the case in Fig. 12.2c (S is absent, $S = 0$) $k = 0.5$ if the focus distance is D/θ; $k = 1$ if focus distance is infinity (no focusing).
   The relative beam power along its trajectory for plate power distribution as in Fig. 12.2d is

$$\overline{N} = N/N_0 = 1 \quad when \quad L \leq S_1 \quad and \quad \overline{N} = \varsigma \quad when \quad L > S_1 = D/2\theta.$$
(12.12)

   The force coefficient, A, shows how many times the initial light pressure is increased. For $L < S_1$ it is

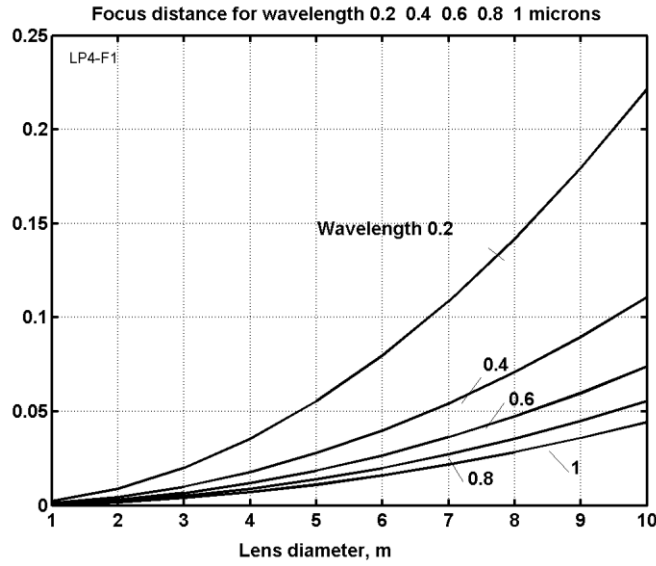$$A = \frac{q^n - 1}{q - 1}.$$
(12.13)

Fig. 12.5. Focus distances [10^6 km, million km] versus lens diameters 1–10 m and wavelength $\lambda = 0.2$–1 microns.
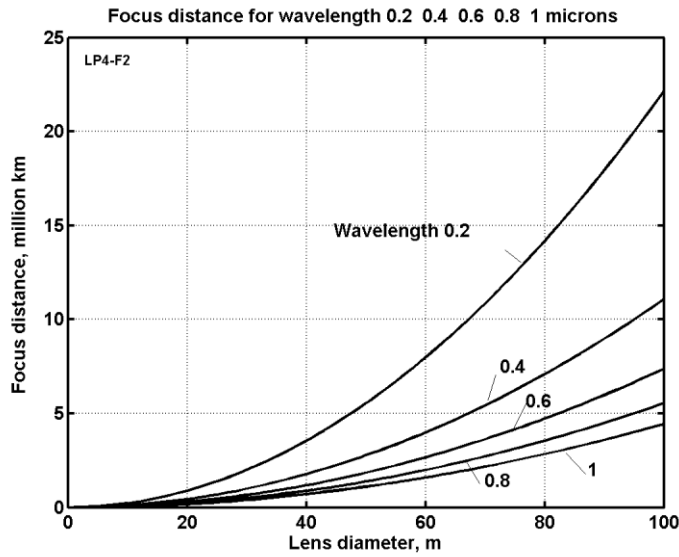

Fig. 12.6. Focus distances versus lens diameters $D = 1$–100 m and wavelength $\lambda = 0.2$–1 microns.

The multi-reflex launch of a space vehicle from a small planet with low gravity, are without an atmosphere (the Moon or an asteroid) may be computed using the following equations (for focusing Fig. 12.2b and beam distributions Fig. 12.2d):

$$T = \frac{2N_0}{c}\frac{q^{n_1}-1}{q-1} + \frac{2N_0}{c}q^{n_1}\frac{q_1^{n_2}-1}{q_1-1}, \quad n_1 = \frac{S_1}{L}, \quad n_2 = n_1 - n_3, \quad n_3 = \frac{\ln m}{2v}, \quad q = (1-2\gamma)(1-2v),$$

$$q_1 = q\varsigma, \quad \Delta V = \left(\frac{T}{M} - g\right)\Delta t, \quad V_{i+1} = V_{i_i} + \Delta V, \quad \Delta L = V_i \Delta t. \quad L_{i+1} = L_i + \Delta L, \quad t_{i+1} = t_i + \Delta t.$$

$$(12.14)$$

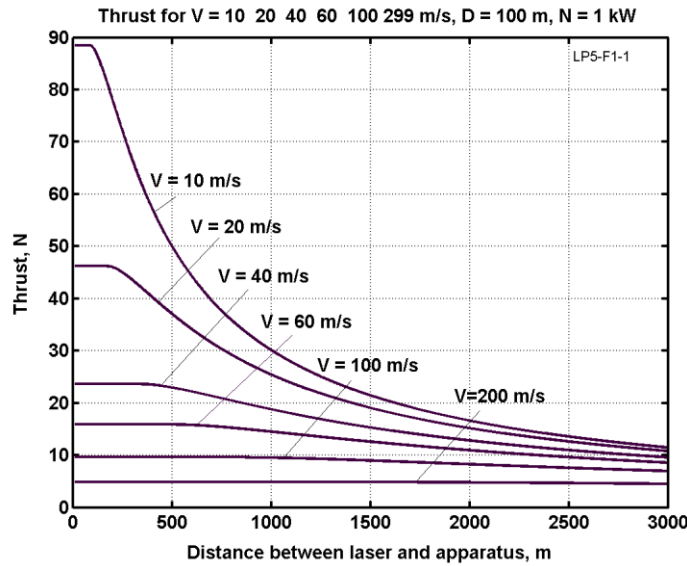Here the first element in T is the thrust when the beam runs the distance S_1 without divergence.

Thrust for V = 10 20 40 60 100 299 m/s, D = 100 m, N = 1 kW

LP5-F1-1

V = 10 m/s

V = 20 m/s

V = 40 m/s

V = 60 m/s

V = 100 m/s

V=200 m/s

Thrust, N

Distance between laser and apparatus, m

Fig. 12.7. Thrust (N) versus distance [m] for vehicle speed $V = 10$–200 m/s, attenuation coefficient $a = 0.5$ dB, cell size $m = 30$, mirror diameter $D = 100$ m, beam power $N = 1$ kW.

The second element in T is the thrust when the beam runs the distance with divergence. M is space vehicle mass [kg], g is the planet's gravity [m/s^2]. When $n_3 < n_1$, we take $n = n_3$ and compute T using equation (12.5). If $n_3 > n_1$, we compute T using equation (12.14).

Computation of thrust, T (the first part of equation (12.14)) and the efficiency coefficient, η, equation (12.8) are presented in Figs. 12.7 and 12.8.
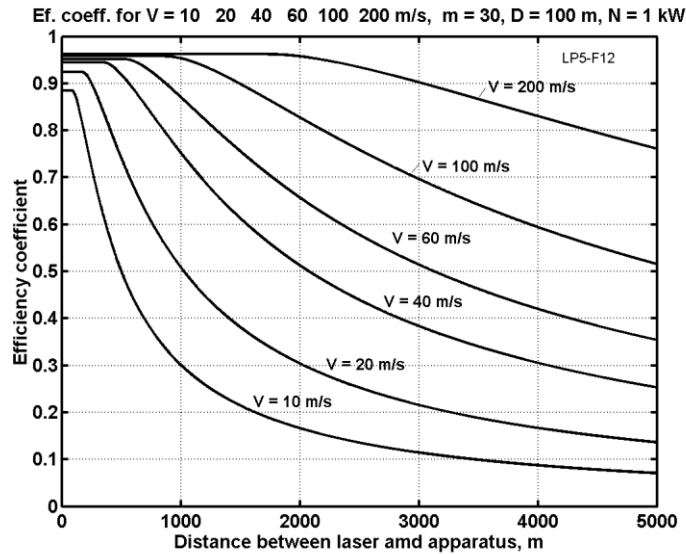
Ef. coeff. for V = 10   20   40   60 100 200 m/s, m = 30, D = 100 m, N = 1 kW

LP5-F12

V = 200 m/s

V = 100 m/s

V = 60 m/s

V = 40 m/s

V = 20 m/s

V = 10 m/s

Efficiency coefficient

Distance between laser amd apparatus, m

Fig.12.8. Efficiency coefficient versus distance [m] for vehicle speed $V = 10$–200 m/s, attenuation coefficient $a = 0.5$ dB, cell size $m = 30$, mirror diameter $D = 100$ m, beam power $N = 1$ kW.

The thrust and the efficiency coefficient decrease when the distance is above a some critical value, then a portion of the energy beam leaves the space between the mirrors through diffraction.

The computation for a vertical (the worst case) launch equation (12.14) of a space vehicle from the Earth's Moon (the Moon has gravity $g = 1.62$ m/s^2) is presented in Figs. 12.9 to 12.12 ($\lambda = 1$ micron).

The power required to launch from the Earth's Moon is quite high because, as the vehicle's speed increases, the energy transfer efficiency is reduced. In the initial launch state that efficiency starts at η

= 0.97. After acceleration (limit is 16g, g = 9.81 m/s) for a distance of $L = 2$–10 km the efficiency decreases (Fig. 12.10). The accelerating is high for only 0.1–2 seconds (16g is acceptable for trained cosmonauts). The mission designers could limit the maximum acceleration to 8g without significantly losing speed.

   The mirror diameter is large because small mirror diameters decrease the attainable speed. Starting from an asteroid or a planet's moon, that has low gravity, improves the attainable speed. Unfortunately, the multi-reflex launch from planets with an atmosphere does not wart well because the multi-reflected rays travel long distances in a gas medium and lose a lot of energy.

   Below is the equation for computing the beam power from the divergence and distance when the Gaussian beam has normal distribution (Fig. 12.2f): For case 1 (the focus is into point $2S_1$, Fig. 12.2c)

$$\overline{N}_1 = 2\psi\left[s\left(\frac{D}{D+\theta L}\right)^2 \right], \quad \theta = \frac{2}{\sqrt{\pi}}\frac{\lambda}{D}, \quad S = 0. \quad (12.15)$$

Here ψ is the probability function of normal distribution.

Fig. 12.9. Vertical launch of a space vehicle from the Earth's Moon (Moon gravity is $g = 1.62$ m/s^2). Space ship speed (m/s) versus distance (km) is computed for relative beam power $N = 5$–50 kW/kg, attenuation coefficient $a = 0.5$ dB, cell size $m = 30$, mirror diameter $D = 100$ m. Acceleration is limited to 16g (g = 9.81 m/s^2).

Fig. 12.10. Vertical launch of a space vehicle from the Earth's Moon (Moon gravity is $g = 1.62$ m/s^2). Efficiency coefficient versus distance is computed for relative beam power $N = 5$–50 kW/kg, attenuation coefficient a

= 0.5 dB, cell size m = 30, mirror diameter D = 100 m.

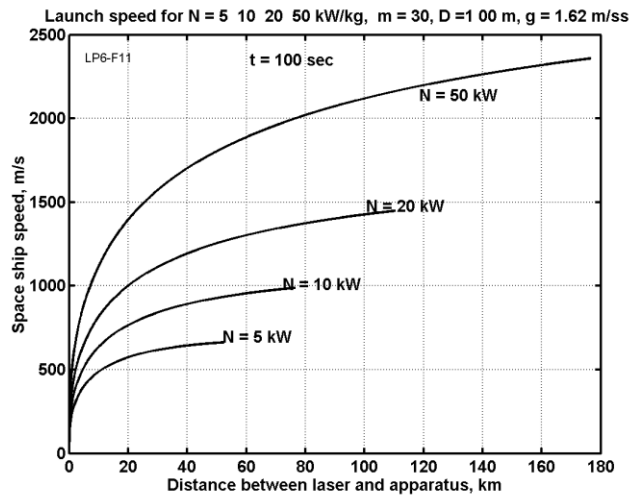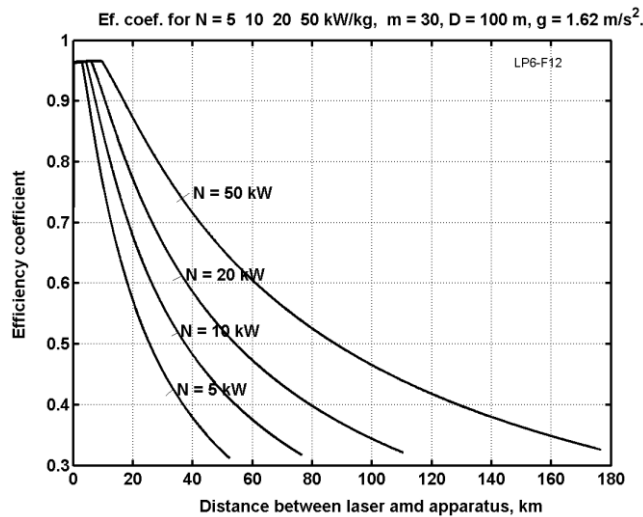**Speed for N = 5 10 20 50 kW/kg, a = 0.5 dB, m = 30, D = 100 m, g = 1.62 m/s².**
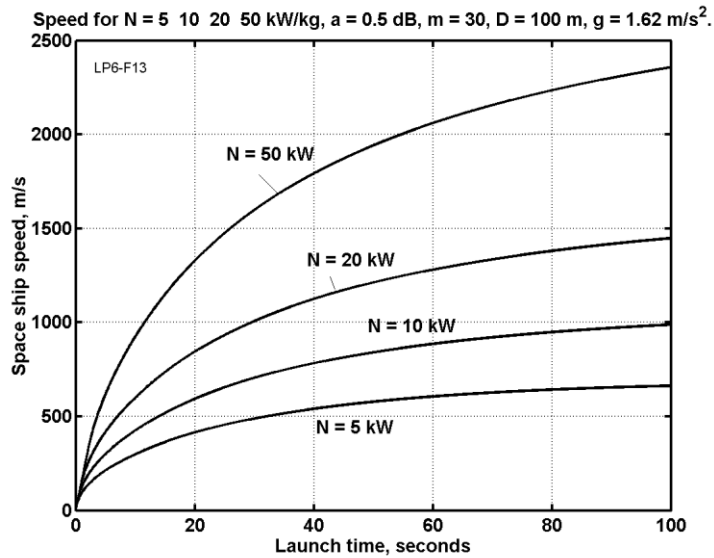

Fig. 12.11. Vertical launch of a space vehicle from the Earth's Moon (Moon gravity is g = 1.62 m/s²). Space ship speed (m/s) versus time (seconds) is computed for relative beam power N = 5–50 kW/kg, attenuation coefficient a = 0.5 dB, cell size m = 30, mirror diameter D = 100 m, λ = 1 micron.

Acceleration for N = 5 10 20 50 kW/kg, m = 30, D = 100 m, g = 1.62 m/s².

Fig. 12.12. Vertical launch of a space vehicle from the Earth's Moon (Moon gravity is g = 1.62 m/s²). Limited (<16g = 16×9.81 = 157 m/s²) acceleration is computed for relative beam power N = 5–50 kW/kg, attenuation coefficient a = 0.5 dB, cell size m = 30, mirror diameter D = 100 m, λ = 1 micron.
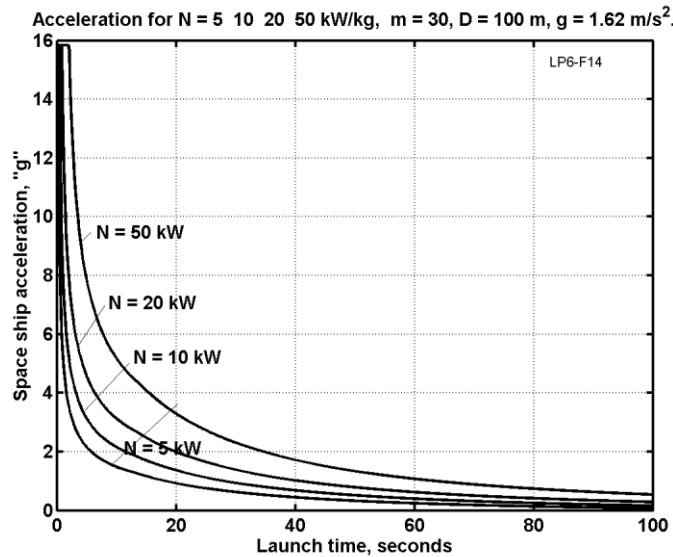
For case 2 (the focus is located at point S, Fig. 12.2b)

$$\textit{When} \quad L \le S_1, \quad \overline{N}_2 = 1. \quad \textit{When} \quad L > S_1 \quad \overline{N}_2 = 2\psi \left[s \left(\frac{D}{D + 4\theta(L - S_1)} \right)^2 \right]. \quad (12.16)$$

Here s is a relative distribution value. The results of computations for space (vacuum) are presented in Fig. 12.13. It is shown that the focused beam travels without major losses if the distance between the mirrors (for mirror diameter D = 100–200 m) is 10–18 millions kilometers, and may travel up to 100 million km with an efficiency of about 0.2. This means the focused beam can permanently transfer

(without losses) energy from the Earth to the Moon or back (a distance pf 0.4×10^6 km), and for 2–3 months (with efficiency 0.2) every two years, to Mars at a distance of $60–150 \times 10^6$ km.

For computation of the relative beam power in air at altitude H, we may use equations (12.15) and (12.16) corrected for air attenuation. That is

$$\overline{N}_{a1} = \overline{N}_1(1-b), \quad \overline{N}_{a2} = \overline{N}_2(1-b), \quad where \quad b = 0.334 \cdot 10^{-6} \frac{\rho_H}{\rho_0} L \quad . \tag{12.17}$$

Here ρ_H, ρ_o are the air density at altitudes H and $H = 0$ respectively.

The computation for an atmospheric balloon lens located at $H = 15$ km ($\rho_H/\rho_o = 0.159$) is presented in Fig. 12.14. As can be seen, the beam energy may be transferred by mirrors located on an air balloon to distances 4000 km out, with on efficiency of 0.8 . If the energy is transferred through a satellite the range is not limited and the efficiency may reach 0.98 . Any smog, mist, haze, rain, or clouds (in the region of the power station) decreases the efficiency. However, these aerosols are absent at altitudes above 12 km. We must therefore have power stations in different locations to circumvent weather phenomena.
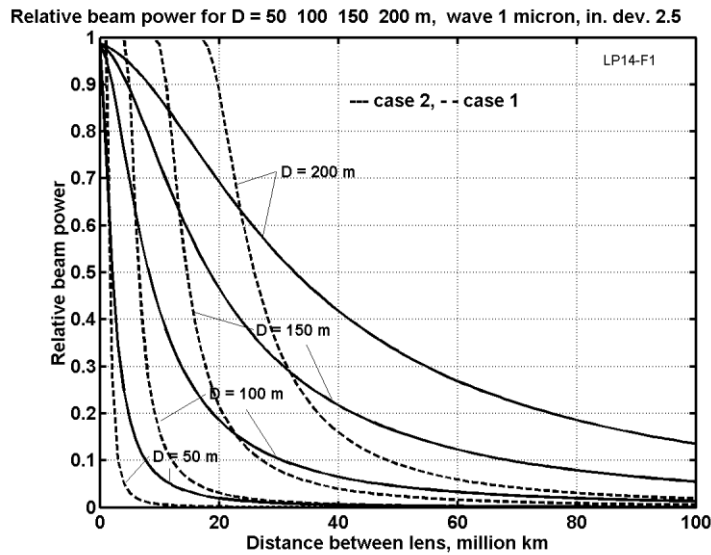

Fig. 12.13. Relative beam power of the normal (Gaussian) distribution ($s = \sigma = 2.5$) (Fig. 12.2f) in a vacuum versus distance in million kilometers between lenses for focusing at $D/2\theta$ (- - , case 1) and D/θ (-, case 2).
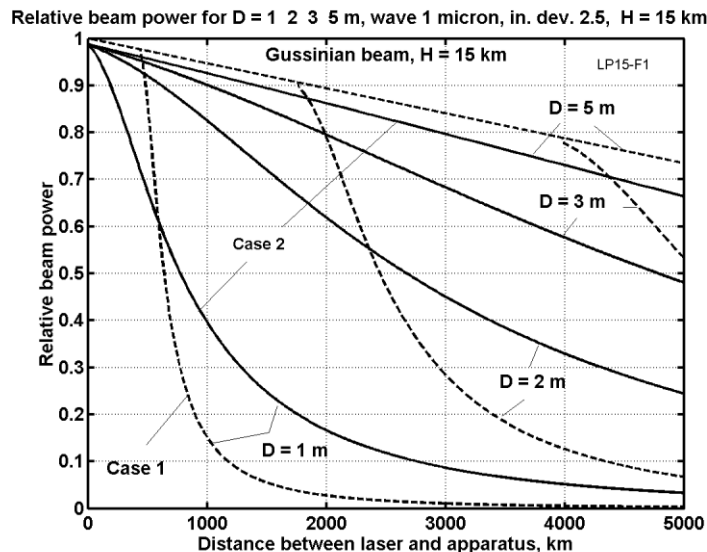
Fig. 12.14. Relative beam power of the normal (Gaussian) distribution ($s = \sigma = 2.5$) (Fig. 12.2f) in air (altitude H = 15 km) versus distance in kilometers between lenses for focusing at $D/2\theta$ (- -) and at D/θ (-).

The computed parameters are not optimal. Our purpose is to demonstrate the method of computation. Computations (Fig. 12.7 and 12.8) are made for a beam power $N_0 = 1$ kW. For beam power $N_0 = 10$, 100, 1000 kW we must multiply the force in Figs. 12.7 and 12.8 by 10, 100, and 1000 respectively.

Discussion

Comparing the "Multi-Bounce Laser-Based Sail" system[6] with the proposed method – the "Multi-Reflex Propulsion System".

1. The "Multi-Bounce Sail" uses the well known multi-layer mirror which has high reflectance only in a region around the design wavelength. Outside this region the reflectance is reduced. For example, at one-half the design wavelength it falls to that of the uncoated substrate. As shown in this work, the wavelength changes by a small amount at each reflection in the mobile mirror. This means that after enough reflections the multi-layer mirror has lost its high reflectivity. It is impossible to use the multi-layer mirror for a multi-bounce space sail that is moving. The author has proposed the innovative new cell-mirror for which the reflectivity does not depend on wavelength for wavelengths that are less then a cell length.

2. The multi-layer mirror[6] is extremely large (1 km), with extremely small thickness (1600 nm), density (10 gm/m^2) and weight (7850 kg). A very small angle of deviation at the multi-layer mirror surface (one thousandth of a degree) under beam pressure, leads to complete defocusing at a distance of some millions of kilometers. This means the mirror[6] will make only one reflection. The average mirror angle will also be changed permanently for a moving space ship.

It is impossible to exactly control (turn) the orientation of this gigantic and very thin sail.

The new cell-mirror reflects the laser beam back in exactly the same direction if the surface and sail deviation are less then 5–10 degrees. This means the mirror directoral control is not necessary on the space craft. Also, there may be imperfections in the surface film and the mirror control is not necessary.

3. The maximum reflection at multi-layer mirror is 99.95 [Reference[6]]. The reflection of the cell-mirror is $(1-0.4\cdot10^{-9})$ or 10^8 times better than the multi-layer mirror. The maximum reflection value of the multi-layer mirror is only 1000 [Reference[6]]. Value for reflections of the cell-mirror are in the millions.

4. The diameter of the multi-layer mirror is 1 km, the size of our cell mirror is 100 m.

5. The gigantic multi-layer mirror gives an acceleration of only 0.33 m/s^2. This is not enough to launch itself from Earth (Earth's gravity is 9.8 m/s^2), Mars (3.72 m/s^2) or the Moon (1.62 m/s^2). The author's cell-mirror gives an acceleration of 20 m/s^2, and its size is 100 times smaller. If we were to made cell-mirror 1 km in diameter, the capability of a space ship would be fantastic.

The author shows here only some of the advantages of one innovation (changing from the well-known multi-layer mirror to the new *cell-mirror*). There are many deficiencies of the previous system[6] which make its application virtually impossible. For example, with the multi-layer mirror the laser is located on the Earth's surface and its beam moves (from the laser to the ship and back to the laser) through the Earth's atmosphere a lot of times. The computation shows that the beam's energy will quickly be lost due to absorption and scattering by the Earth's (or Mars) atmosphere when it travels a long distance though it. In our system the beam moves through the atmosphere only once time and reflects between the Moon mirror and the space ship of all other times. This is insured by the innovation of the *light lock*.

Another deficiency of the laser-based sail system is that when the space ship is close to Earth, the sail will reflect the beam back to the laser. If the efficiency of the propulsion system were sufficient, the

laser might be damaged or destroyed. This problem is absent in the author system because it uses a "*light lock*", which closes the return path of laser beam.

The suggested *laser ring* (a set of small lasers located in a circle), *beam transfer* and *self-focused mirror* and *Fresnel's lens* decrease the beam divergence and increase the beam transfer distance. It is possible to install the cell-mirror on the Moon or on Mars and transfer a laser beam to them and then to make a space ship decelerate.

The other system[6] requires a nuclear electric power station (of several Giga Watts Power) to be built and to deliver it, and a super powerful laser on Mars.

I do not mean to criticize other small mistakes in the work[6] as, for example, the computation of multiple reflection acceleration (thrust) is not correct. The beam energy after every reflection will be decreased and the ship acceleration also will be decreased. For a large number of reflections this decrease is quite large (see the equations in this chapter).

The idea of a multiple reflection engine and cell and superconductivity mirrors was probably offered first by author in 1983[5]. But as I know, this work[6] (2001) was the first research on this topic which is important.

General discussion. The offered multi-reflex light launcher, space and air focused energy transfer system is very simple (needing only special mirrors, lenses and prisms), and it has a high efficiency. One can directly transfer the light beam into space acceleration and mechanical energy. A distant propulsion system can obtain its energy from the Earth. However, we need very powerful lasers. Sooner or later the industry will create these powerful lasers (and cell mirrors) and the ideas presented here will become possible. The research on these problems should be started now.

Multi-reflex engines[7] may be used in aviation as the energy can be transferred from the power stations on the ground to the aircraft using laser beams. The aircraft would no longer carry fuel and the engine would be lighter in weight so its load capability would double. The industry produces a one Megawatt (1000 kW) laser now. This is the right size for mid-weight aircraft (10–12 tons).

The linear light engine does not have a limit to its speed and may be used to launch space equipment and space ships in non-rockets method described in[10–29]. This method is certain also to have many military applications.

References for Chapter 12

1. R.L. Garwin, "Solar Sailing - A practical Method of Propulsion within the Solar System," *Jet Propulsion*, Vol. 28, March 1958, pp. 188–190.
2. R.L. Forward, "Pluto - The Gateway to the Stars," *Missiles and Rockets*, Vol. 10, April 1962, pp. 70–75.
3. A. Kantrowitz, "Propulsion to Orbit by Ground-Based Lasers", *Astronautics and Aeronautics*, Vol.10, pp. 74–76, May, 1972.
4. *Beamed Energy Propulsion*. First International Symposium on Beamed Energy Propulsion. Melville, New York, 2003. American Institute of Physics.
5. A.A. Bolonkin, "Light Pressure Engine". Patent (Author Certificate) # 1183421, 1985, USSR, (priority on 5 January, 1983).
6. R.A. Metzger and G. Landis, "Multi-Bounce Laser-Based Sails", Proceedings of the shape Technology and Application, Forum-2001, Albuquerque, New Mexico, 2001, AIP Conference Proceedings, Vol. 552, pe. 397 [File: STAIF 2001 B].
7. A.A. Bolonkin, "Light Multreflex Engine", *JBIS*, Vol. 57, No. 9/10, pp. 353–359.
8. P.W. Milonni, J.H. Eberly, *Lasers,* John Wiley & Sons, NY.
9. R.G. Driggers, (ed.), *Encyclopedia of Optical Engineering*., New York, Marcel Dekker, Inc.
10. A.A. Bolonkin, "Earth Accelerator for Space Ships and Missiles". *JBIS*, Vol. 56, No. 11/12, pp. 394–

404, 2003.

11. A.A. Bolonkin, "Kinetic Space Towers and Launchers", *JBIS*, Vol. 57, No. 1/2, pp. 33–39, 2004.

12. A.A. Bolonkin, "Bolonkin Anti-Gravitator", AIAA-2005-4504, 41 Propulsion Conference, 10-12 July, 2005, Tucson, Arizona, USA .

13. A.A. Bolonkin, "Air Cable Transport", *Journal of Aircraft*, Vol. 40, No. 2, March-April, 2003. Patent US 6,494,143 B1.

14. A.A. Bolonkin, "Non-Rocket Space Rope Launcher for People*"*, IAC-02-V.P.06, 53rd International Astronautical Congress. The World Space Congress – 2002, 10–19 Oct 2002, Houston, Texas, USA.

15. A.A, Bolonkin, *"*Non-Rocket Missile Rope Launcher", IAC-02-IAA.S.P.14, 53rd International Astronautical Congress. The World Space Congress – 2002, 10–19 Oct 2002/Houston, Texas, USA.

16. A.A. Bolonkin, "Optimal trajectory of air vehicles", *AEAT*, #2, 2004, pp. 193–215.

17. A.A. Bolonkin, , "Inexpensive Cable Space Launcher of High Capability", IAC-02-V.P.07, 53rd International Astronautical Congress. The World Space Congress – 2002, 10–19 Oct.   2002, Houston, Texas, USA.

18. A.A. Bolonkin, *"*Employment Asteroids for Movement of Space Ship and Probes". IAC-02-S.6.04, 53rd International Astronautical Congress. The World Space Congress – 2002, 10–19 Oct. 2002, Houston, Texas, USA.

19. A.A. Bolonkin, *"*Non-Rocket Earth-Moon Transport System", COSPAR-02 B0.3-F3.3-0032-02, 02-A-02226, 34th Scientific Assembly of the Committee on Space Research (COSPAR). The World Space Congress – 2002, 10–19 Oct 2002, Houston, Texas, USA.

20. A.A. Bolonkin, *"*Non-Rocket Earth-Mars Transport System", COSPAR-02 B0.4-C3.4-0036-02, 34th Scientific Assembly of the Committee on Space Research (COSPAR). The World Space Congress – 2002, 10–19 Oct 2002, Houston, Texas, USA.

21. A.A. Bolonkin, *"*Transport System for Delivery Tourists at Altitude 140 km". IAC-02-IAA.1.3.03, 53rd International Astronautical Congress. The World Space Congress – 2002, 10–19 Oct. 2002, Houston, Texas, USA.

22. A.A. Bolonkin, "Asteroids as Propulsion Systems of Space Ships", *JBIS*, Vol. 58, No 3/4, pp. 97–107, 2003.

23. A.A. Bolonkin, "Non-Rocket Transportation System for Space Travel", *JBIS*, Vol. 56, No 7/8, pp. 231–249, 2003.

24. A.A. Bolonkin, "Centrifugal Keeper for Space Stations and Satellites", *JBIS*, Vol. 56, No 9/10, pp. 314–327, 2003.

25. A.A. Bolonkin, "Non-Rocket Earth-Moon Transport System", *Advances in Space Research*, Vol. 31/11, pp. 2485–2490, 2003, Elsevier.

26. A.A. Bolonkin, "Earth Accelerator for Space Ships and Missiles". *JBIS*, Vol. 56, No. 11/12, pp. 394–404.

27. A.A. Bolonkin, "Kinetic Aviation", AIAA-2005-6221.

28. A.A. Bolonkin, "Long Distance Transfer of Mechanical Energy", AIAA-2004-5660.

29. A.A. Bolonkin, "Non-Rocket Transport System Earth-Mars", *Actual problems of aviation and aerospace systems*, Kazan, Russia, Vol. 8, No. 2(16), 2003.

30. A.A. Bolonkin, "Multi-Reflex Propulsion Systems for Space and Air Vehicles and Energy Transfer for Long Distance", *JBIS*, Vol. 57, No. 11/12. 2004, pp. 379–390, 2004.

Chapter 13

ELECTROSTATIC WIND PROPULSION*

Summary

A method for space flights in outer space is suggested by the author. Research is present to shows that an open high charged (100 MV/m) ball of small diameter (4–10 m) made from thin film collects solar wind (protons) from a large area (hundreds of square kilometers). The proposed propulsion system creates many Newton's of thrust, and accelerates a 100 kg space probe up to 60–100 km/s for 100–800 days. The 100 kg space apparatus offers flights into Mars orbit of about 70 days, to Jupiter about 150 days, to Saturn about 250 days, to Uranus about 450 days, to Neptune about 650 days, and to Pluto about 850 days. The author developed a theory of electrostatic wind propulsion. He has computed the amount of thrust (drag), to mass of the charged ball, and the energy needed for initial charging of the ball and discusses the ball discharging in the space environment. He also reviews apparent errors found in other articles on these topics. Computations are made for space probes with a useful mass of 100 kg.

Correspondence to: C&R, A. Bolonkin, 1310 Avenue R, #F-6, Brooklyn, NY 11229, USA, T/F 718-339-4563, aBolonkin@gmail.com , http://Bolonkin.narod.ru

Introduction
Current method of space flight

At present, we use only one main method of launch for extra-planetary flight – that is liquid or solid fuel rockets. This method is very complex, expensive, and dangerous.

The current method of flight has reached the peak of its development. In the last 30 years it has not allowed cheap delivery of loads to space, or made tourist trips to the cosmos affordable, much less individual flights to the upper atmosphere. Space flights are very expensive and not conceivable for average people. The main method used for electric energy separation is photomontage cells. Such solar cells are expensive and have a low energy storage capacity.

The aviation, space, and energy industries need revolutionary ideas which will significantly improve the capability of future air and space vehicles. The author has offered a series of new ideas [1–47] particularly in manuscripts presented to the World Space Congress(WSC)-1992, 1994 [44-47], and to WSC-2002, 10–19 October 2002, Houston, Texas, USA [4– 5, 7–13] and in his articles, patent applications [1–47, 53–57].

In this chapter a method and installations for future space flights are proposed. The method uses an open high charged ball made from thin film which collects solar wind from a large area. The offered propulsion system creates many Newton's of thrust, and accelerates a100 kg space apparatus to high speeds. This allows it, in an acceptable time of 100–800 days, to reach speeds of up to tens of km/s (50–100 km/s). A flight to Mars would take only 70days, to Jupiter about 150 days, to Saturn about 250 days, to Uranus about 450 days, to Neptune about 650 days, and to the farthest planet, Pluto, about 850 days.

History of innovation

During 1982–1983 in series of patent applications [29–41] the author offered some methods and installations for space propulsions and electric generators using solar wind. In 1987 these ideas were published in Report ESTI [42]. In 1990 the author published brief information about this topic [43] (see pp. 67–80) and in 1992–1994 he reported on further researches at the World Space Congresses-1992, 1994, 2002 [44–47]. In 2003 N. Omidi and H. Karimabadi published an article on a similar topic [48]. Differences between the ideas and results in this chapter and their work [48] are raised in the Discussion section.

Information about Solar Wind

The Sun emits plasma which is a continuous outward flow (solar Wind) of ionized solar gas through out our solar system. The solar wind contains about 90% protons and electrons and some quantities of ionized α-particles and gases. It attains speeds in the range of 300–750 km/s and has a flow density of 5×10^7– 5×10^8 protons/electrons/cm^{2}s. The observed speed rises systematically from low values a 300–400 km/s to high values of 650–700 km/s in 1 or 2 days and then returns to low values during the next 3 to 5 days (Figure 1b). Each of these high-speed streams tends to appeal at approximately 27-day intervals or to recur with the rotation period of the Sun. On days of high Sun activity the solar wind speed reaches 1000 (and more) km/s and its flow density 10^9– 10^{10} protons/electrons/cm^2, 8–70 particles in cm^3. The Sun has high activity periods some days each year.

The pressure of the solar wind is very small. For full braking it is in the interval $2.5\times10^{-10}\div6.3\times10^{-9}$ N/m^2. This value is double when the particles have full reflection. The interstellar medium also has high energy particles. Their density is about 1 particle/cm^3.The interaction of the solar wind with the Earth's magnetosphere is shown in Figure1a.

Description of the proposed Propulsion System

Offered Space Propulsion System

The suggested propulsion system is very simple. It includes a hollow ball made up of a thin, strong, film – covered conductive layer or a ball of thin net. The ball is charged by high voltage static electricity which creates a powerful electrostatic field around it. Charged particles of solar wind of like charges repel and particles with the unlike charges attract. A small proportion of them run through the ball, a larger proportion flow round the ball in hyperbolic trajectory into the opposite direction, and another proportion are deviates from their initial direction in hyperbolic curves. As a result the charged ball has drag when the ball speed is different from solar speed (Figures 2, 3). The drag also occurs when the particles and the ball have the same electrical charge. In this case the particles are repelled from the charged ball (Figure 3) and brake it. This solar wind drag provides
thrust in our proposed propulsion system. The pressure of solar wind is very small, but the offered system (a charged ball of radius 6–10 m) collects particles (protons or electrons) from a large area (an area of tens of kilometers radius for protons and hundreds of kilometers for electrons), creates a thrust of some Newton's and a 100-kg space ship reaches speeds of tens of km/s in 50–300 days (see theory and computation below and References [29, 42–47]).
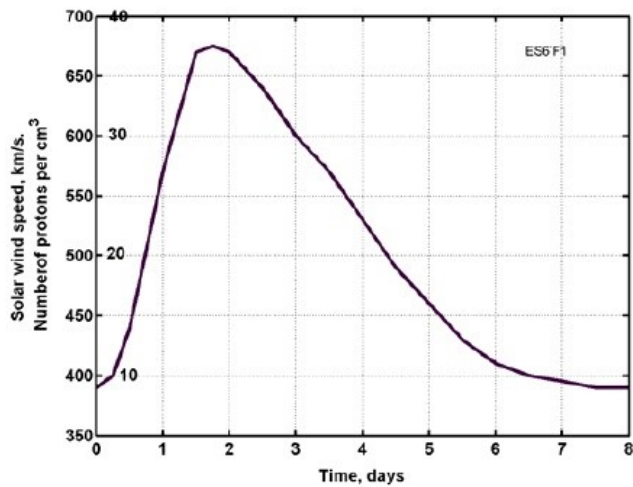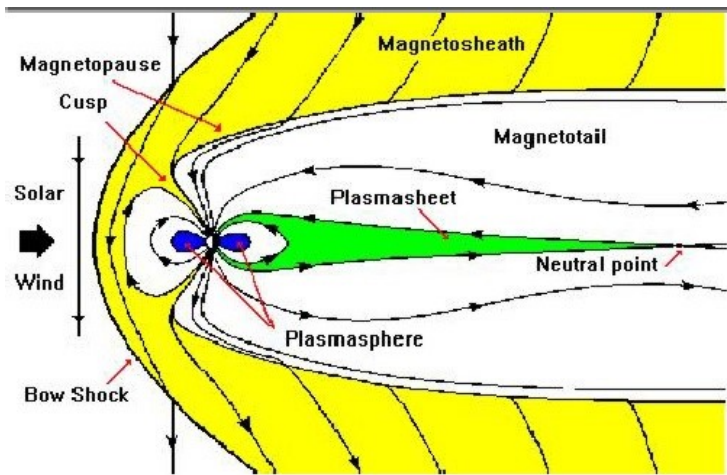
Figure 13.1a (up). Interaction of solar wind with Earth's magnetosphere.
Figure 13.1b (down). Speed and density variations of solar wind in the Earth's orbit. The speed is in km/s, the density is in protons/cm^3.
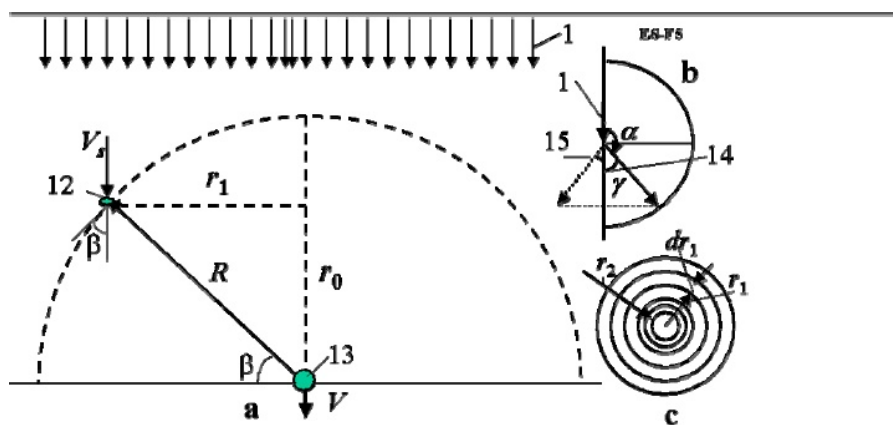
Figure 13.2. a - Interaction between solar wind and the electrostatic field of a charged ball. Notations are: 1– solar wind (protons/electrons), 12 – charged particles (protons/electrons); 13 – electrically charged ball (balloon); 14 – line of turn of angle γ of a particle that is attracted (attracted force of unlike charges); 15 – line of turn of angle of a particle that is repelled (repulsive force of like charges); R – radius of interaction or neutral

radius, r_1 – radius of integration, V_s – wind speed, V – ship speed. b –change of particle direction caused by electric ball field. c – collection area (top view).
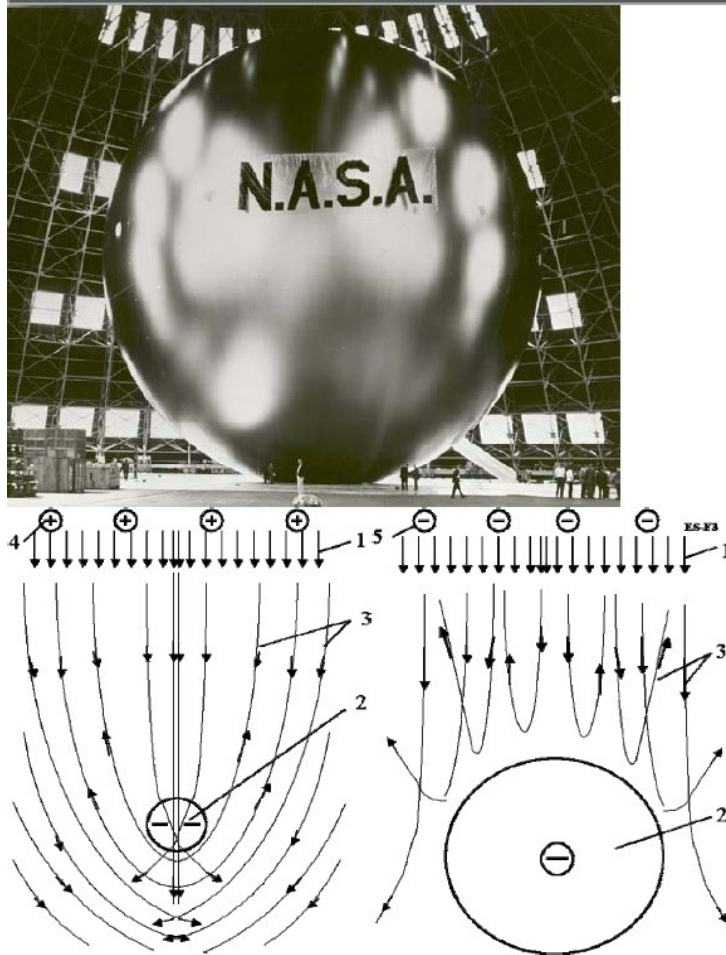

Figure 13.3b (up). A very large sphere, even of a thin film, can hold a massive charge. Here is an Echo balloon satellite of the early '60s, 30 meters (100 feet) across; note the men for scale. With suitable insulation and charge protection a very light sphere can hold enormous energies within.
Credit: NASA.http://dayton.hq.nasa.gov/IMAGES/SMALL/GPN-2002-000203.jpg.

Figure 13.3a. Hyperbolic trajectory of protons around static negative charge (or electrons around positive charge) (unlike charges). Notations are: 1 – solar wind (charged particles); 2 – hollow negatively charged ball of thin film; 3 – hyperbolic trajectory of charged particles; 4 – positively charged particles (protons). (Right). Trajectory of particles having the same charge as the ball. Notations are: 5 – negatively charged particles.

Steerability of the System and Control of Thrust

The magnitude of thrust is determined by the controlled ball charge value, and the deviation of this thrust from the direction of the Sun is controlled using one of the two methods shown in Figure 4. In the first method the inclination of a plane formed by balls in a triangle is changed by adjusting the cable length, 8, and the thrust T is deviated from the direction of the Sun (Figure 4a). In the second method the propulsion system has a cylindrical capacitor, 20 (Figure 4b,c), which accelerates the particles on one side and brakes or turns back the particles on the opposite side (for the opposite side the capacitor works as an electrostatic mirror, Figure 4c). As a result the thrust is deviates from the direction of the Sun. A collection of three balls enables the thrust to be deviated by up to 10 degrees

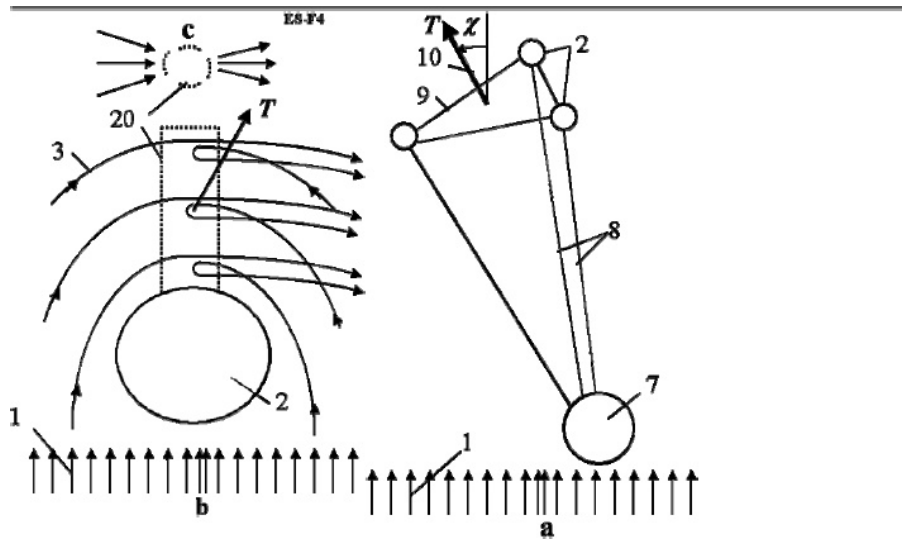(Figure 13.4a), and an additional net capacitor enables deviation of up to 20–30 degrees (Figure 13.4b).

Figure 13.4. Two methods of controlling of the thrust direction: a – control using three balls. Notations are: 7 – spaceship (probe); 8 – links (cables) connected to the space ship and the electrostatic balls. 9 –cable connection of balls; 10 – *T*– thrust of the propulsion system; b – control of thrust direction by capacitor (electrostatic mirror). c – top view of capacitor. The other notations are presented in Figure 3a.
.

Discharge of Electrostatic Ball

The solar wind has high speed at a large distance from the ball. This means the particles have a trajectory close to a hyperbolic curve in the ball's area of influence and most of them will fly again into infinity. Only a proportion of them will travel through the ball. These particles decrease its speed and can discharge the ball. However, their speed and kinetic energy are very large because they are accelerated by the high voltage of the ball's electric field (some tens or hundreds of MV). The necessary ball film is very thin (only of microns). The particles pierce through the ball. If their loss of speed is less then the solar wind speed, their trajectory will be close to a hyperbolic curve and they will fly into space. If their loss of a speed is more than the solar wind speed, their trajectory will be close to an ellipse, so they will return to the ball and after many revolutions they can discharge it if their perigee is less then the ball's radius. This discharge may be compensated using special methods.

  There are some possible methods for decreasing this discharge (Figure 5a,b,c): a) A ball made of net; b) a charged cylindrical capacitor located in front of the ball to deflect the particles from the ball; c) a capacitor located behind ball to increase the speed of the particles to hyperbolic speed (this is a particle accelerator) and to reflect the returning particles.

Problem of Blockading of the Ball Charge

  Blockading of the charge on the ball by unlike particles is the main problem with this method. The charge on the ball attracts unlike particles and repels like particles. The opposite charge particles accumulate near the ball and block its charge. As a result only the area near the ball deflects and reflects the particles. That area many times less than the area of interaction of the ball are the particles when there is no blockading. The forces are thus greatly reduces. Omidi and Karimabadi [48] apparently had not seen this and all their results seem to be wrong. There are other apparent errors in their text which affect all their other results (see Discussion section).

The author of this work proposed two models for estimation of the efficient charge area (diameter of neutral working charge). In the first model the radius of the efficient area is computed as the area where particles of like charge to the ball are absent and the density of opposite-charge (unlike) particles is the same as the solar wind. This model gives the lower limit of the efficient area. In the second model the radius of the efficient area is computed as the area where the density of unlike particles is less than the solar wind density because the unlike particles inside the efficient area have generally higher velocity than a those outside this area. The neutral area (neutral sphere) in model 2 is large than in model 1. Model 2 is better, but this problem needs more detailed research.
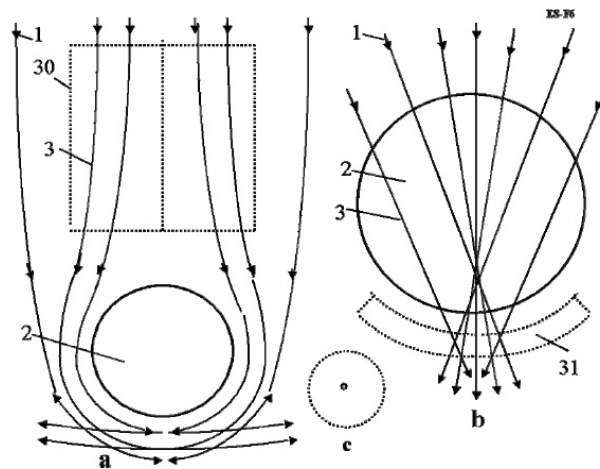

Figure 13.5. Two methods of decreasing the ball discharge: a – a charged cylindrical capacitor located in the front of the ball deflects particles from the ball; b – a capacitor located behind the ball adds speed to the particles and reflect the returned particles. c – top view of capacitor. Notations are: 30 –cylindrical capacitor, 31 – back capacitor (particles accelerator and electrostatic mirror)

The proposed system could be used as a thermonuclear propulsion system and a thermonuclear electric generator. The suggested idea may be useful in the design of thermonuclear propulsion systems and electric generators. The solar wind particles approach the ball with very high energy (hundreds   of MV). Their density near the ball axis and behind the ball may also be high. An energy of 5–15 MV is enough for a nuclear reaction. This maybe a proton–proton reaction or protons with any other matter (central electrode). In last case the cylindrical capacitor (Figure 6a) is located behind the ball. This capacitor changes the particle speed (energy) to the required value. The capacitor has a central electrode made of matter which gives a nuclear reaction (product). The products of the reaction are reflected bya parabolic electrostatic mirror in one direction. That forms the thermonuclear propulsion system. The products of nuclear reaction may be photons and the mirror may be a light reflector, in which case we have a photon propulsion system. The electrostatic mirror is made from a thin net; the light reflector is made from a thin film with a reflective layer. They do not influence the particle flow to the central electrodes because the particles have very high speed and energy. The energy of the charged particles can be converted to electrical energy by braking of the electrostatic field as the author has proposed [31–47]. These tasks need more detailed research.

Application as Interplanetary Propulsion System

The previously proposed (no-nuclear) propulsion system does not allow speeds to be reached more than the maximum speed of the solar wind – 1000 km/s. This is not enough for an interstellar trip. For an interstellar voyage the speed must be about 100,000 km/s. The thermonuclear wind propulsion system does increase propulsion capability. The space speed can be greater than the wind speed and the space ship can therefore move against the solar wind.
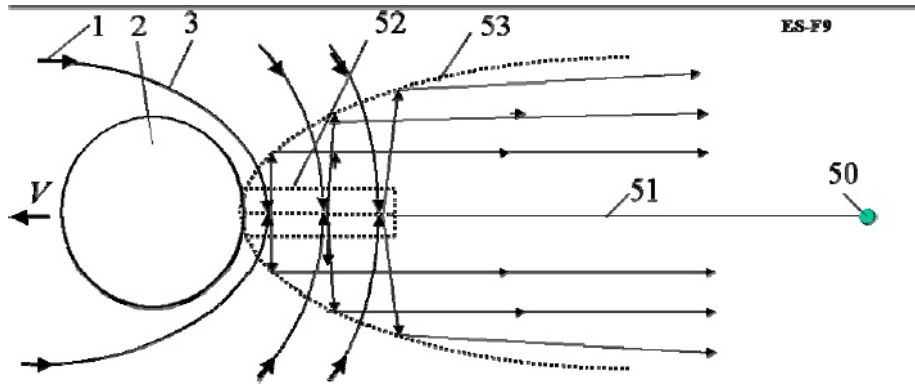
Figure 6a. Nuclear propulsion system using solar wind (or interstellar particles). Notations are: 50 –space apparatus; 51 – cable connecting the space apparatus and the ball; 52 – collector particles and thermonuclear reactor; 53 – reflector of reaction products or light photons. Other notations are the same as previous Figs.

The interstellar medium also contains high energy particles (cosmos rays) a density of about one particle per cubic centimeter. These particles can be collected from a large area by the electrostatic ball and used by the thermonuclear propulsion system. The author calls on all nuclear scientists to research these possibilities. The thermonuclear propulsion system and power thermonuclear electric generator may be easier to design for space than for the Earth because we have a natural high vacuum and a multitude of natural particles in space, and the suggested method and installation solve a major problem of thermonuclear reaction – obtaining high energy particles and collecting them in a small volume with high density.

Theory of the Solar Wind Installation. Main Estimations and Computations.

1.General Theory

Interplanetary space has a magnetic field. The motion of the charged particles in the magnetic and ball electric field is described by the Lorenz force law:

$$mdV/dt = q(E + V \times B), \qquad (13.1)$$

where m – mass of particles [kg], V – speed of particles [m/s] (vector), t – time [s], q – charge[C], E – electric intensity of charged ball field [V/m, or N/C] (vector), B – interplanetary magnetic field [T] (vector).

For a charged ball the electric intensity is $E = kQ/r^2$, where the coefficient $k \approx 9 \times 10^9$ [Nm^2/C^2], Q is ball charge [C], r is distance from the ball center [m].

The first element on the right os equation (1) is electrostatic (Coulomb's) force; the second element is Lorenz force.

The interplanetary magnetic field, B, at 1 AU (AU – Astronomical Unit, 150×10^6 km, radius of Earth orbit) is typically very small at 10 nT and makes an angle of 45° with the Sun–Earth line (i.e., the radial direction). For a typical wind speed, V_s, the second element is small ($\sim$ 4 mV/m). In a full vacuum (without space plasma) the electric intensity from 1 C of the ball at a distance of 1000 km is $\sim 10^{-2}$ V/m. Moreover, the Lorenz force does not increase the radial speed. it only deflects the particle's trajectory from the radial line. Because of that wecan ignore the Lorenz force.

The charged ball repels the like charged particles. In particular, a negatively charged ballrepels the space plasma's electrons. .

It is possible to find the minimum distance which solar wind electrons can approach a negatively charged ball. The full energy of a charged particle (or body) is the sum of the kinetic and potential electric energy. Any change of energy equals zero:

$$\frac{mV^2}{2} + E_F = 0, \quad E_F = \int_0^r F dr, \quad F = k\frac{qQ}{r^2}, \quad E_F = kqQ\left(\frac{1}{\infty} - \frac{1}{r}\right) = -\frac{kqQ}{r}, \quad \frac{mV^2}{2} - \frac{kqQ}{r} = 0, \quad (13.2)$$

Where m is the mass of a particle [kg] (mass of a proton is $m_p = 1.67 \cdot 10^{-27}$ kg, mass of an electron is $m_e = 9.11 \cdot 10{-}31$ kg); V is the speed of particle [m/s] (for solar wind $V_s = 300{-}1000$ km/s); E_p is the potential energy of a charged particle in the electric field [J]; F is the electric force, N; q is the electrical charge of a particle [C] ($q = 1.6 \times 10^{-19}$ C for electrons and protons); $k = 9 \times 10^9$ is coefficient, r is the distance from a particle to the center of the ball[m]; Q is ball charge [C].

From equation (2) the minimum distance for a solar wind electron is ($m = m_e$, $V = V_s$):

$$r_{min} = \frac{2kqQ}{mV^2} = \frac{2K}{V_s^2} = \frac{2a^2 Eq}{m_e V_s^2}, \quad where \quad K = \frac{kqQ}{m}, \quad Q = \frac{a^2 E}{k}, \quad K = \frac{a^2 Eq}{m}. \quad (13.3)$$

Where K is a coefficient; m_e is electron mass; V_s is the solar wind speed [m/s]; a is the radius of ball [m]; E is electrical intensity at the ball surface [V/m]. The maximum electrical intensity of negative charge is about $10^8 - 2 \times 10^8$ V/m in a vacuum.

For $a = 6$ m, E $= 10^8$ V/m, $V_s = 4 \times 10^5$ m/s we have $r_{min} \approx 8 \times 10^6$ km. Other values are presented in Figure 7a,b.

2. Estimation of Minimum Neutral Sphere around a Charged Ball

a) Model 1. Constant Particle Density

The charge density of the unlike space plasma particles inside a neutral sphere is equal to the density of solar wind. The minimum radius of the neutral sphere is

$$Q = \frac{4}{3}\pi R_n^3 d, \quad R_n = \sqrt{\frac{3Q}{4\pi d}} = \sqrt{\frac{3a^2 E}{4\pi kd}}, \quad d = 10^6 Nq, \quad (13.4)$$

where d is density of solar wind [C/m³]; R_n is the minimum radius of the neutral sphere [m]; N is the number of particles in cm³.

The solar wind charge density may be taken by linear interpolation from Table 1 for a distance from the Sun equals to 1 AU = 150 million km.

Computation of the minimum radius of the neutral sphere is presented in Fig. 13.8.

Table 1. Distance from Sun is 1AU

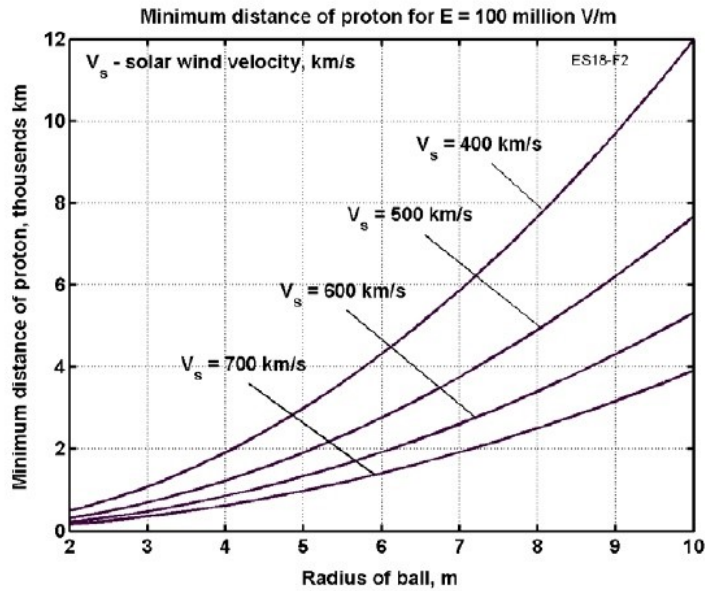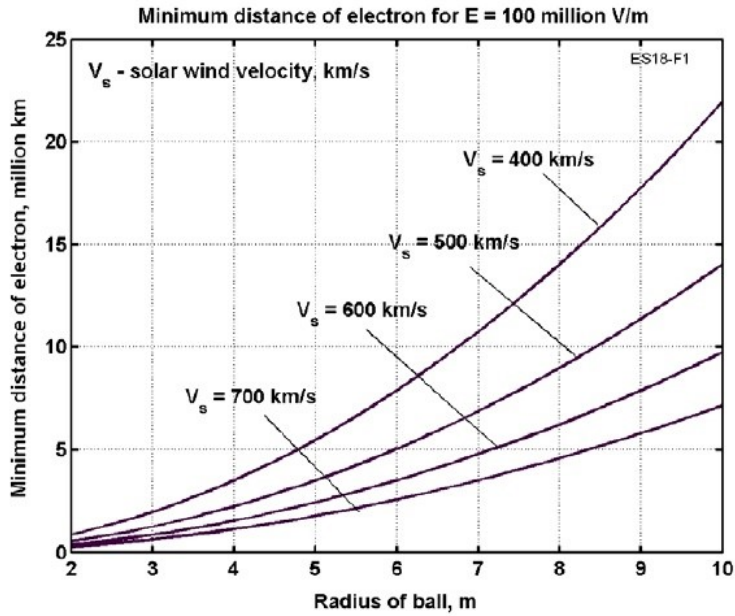| V_s , m/s	0	4×10^5	10^6
N, cm^3	0	10	70

Figure 13.7a. Minimum distance of a single electron from a negatively charged ball with electric intensity of E = 100 million volts/m.

Figure 13.7b. Minimum distance of a single proton from positively charged ball with electric intensity of E = 100 millions volts/m.
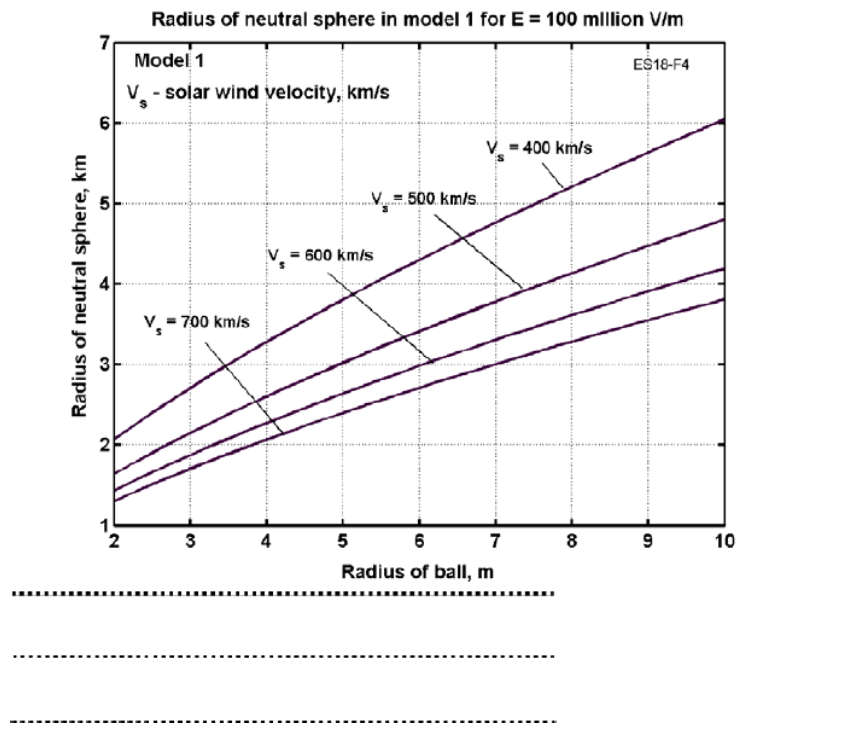
Figure 13.8. Radius of the neutral sphere in Model 1,when particle density in the sphere equals space plasma density.

b) Model 2. Variable Particle Density.

Density of the unlike particles inside the neutral sphere will be less than the density of solar wind particles because the particles are strongly accelerated by the ball charge to speed approximately the speed of light. The new density and new corrected radius can be computed in the following way:

1) The speed of protons along a ball radius is

$$V_r^2(r) = V_0^2 + 2K\left(\frac{1}{r} - \frac{1}{r_0}\right),$$ (13.5)

where $V_0 = V_s$ – proton speed at an initial radius of $R >> R_n$, and R_n is the radius of the neutral sphere.

2) Particle charge density,

$$d_p = d_{po}\frac{V_0}{V_r(r)}, \quad d_{po} = 10^6 Nq/s^2, \quad s = \frac{S}{S_0},$$ (13.6)

where S is distance from the Sun in AU; $S_0 = 1$ AU; s is relative distance from the Sun; d_{po} is density at 1 AU.

3) Charge of the neutral sphere along a sphere radius is

$$Q_r = Q - 4\pi d_{po}V_0\int_0^R \frac{r^2}{V_r(r)}dr .$$ (13.7)

4) The radius of the neutral sphere can be found from the condition $Q_r = 0$. For our estimation we will find it using the stronger condition $Q_r = 0.5Q$, and call it the efficiency radius R_e of charge q.

- 208 -

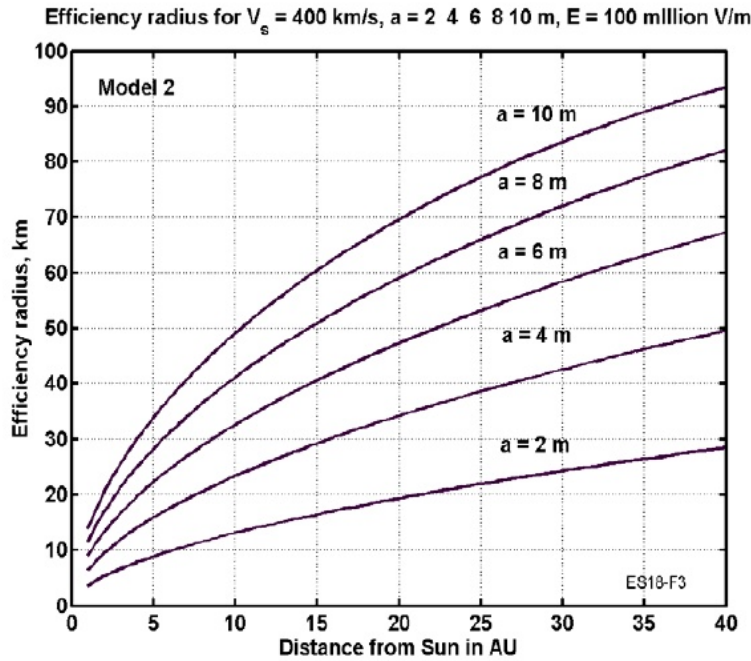Results of computation are presented in Figure 13.9.

Figure 13.9. Radius of the neutral sphere in Model 2 via distance from the Sun, when particle density is variable with radius in the neutral sphere and depends on the variable speed of accelerated particles.

As you can see the efficiency radius in Model 2 is significantly more than in Model 1.

3. Estimation of Electrostatic Sail Drag

All protons in the neutral sphere change the direction of their trajectories from $0°$ to $180°$.
The drag (thrust), D, of the electrostatic sail can be estimated by the equation

$$D = C_D 10^6 N m_p V_p^2 \pi R_e^2 / s^2, \quad V_p = V_s - V , \tag{13.8}$$

where V_p is relative speed of the probe [m/s]; C_D is the drag coefficient. If not all particles change their direction, $C_D = 0$; if all particles turn to $90°$, $C_D = 1$; if all particles turn to $180°$, $C_D = 2$. We take $C_D = 1.5$ for our computation. V is the probe speed [m/s]. When $V << V_s$, the relative speed is $V_p \approx V_s$.
Results of computation of the sail drag for $V_p \approx V_s$ using equation (8) are presented in Figure 13.10 and 13.11.
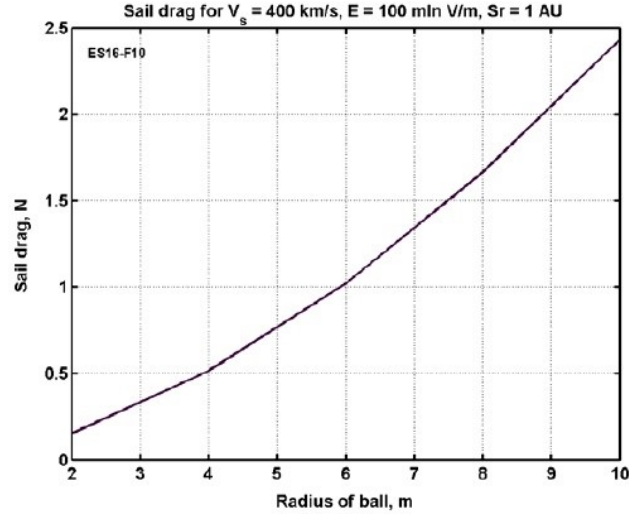
Figure 13.10. Drag of the electrostatic sail versus ball radius at the Earth's orbit (at 1 AU) for the solar wind speed 400 km/s and electrical intensity $E = 100$ million volts/meter.
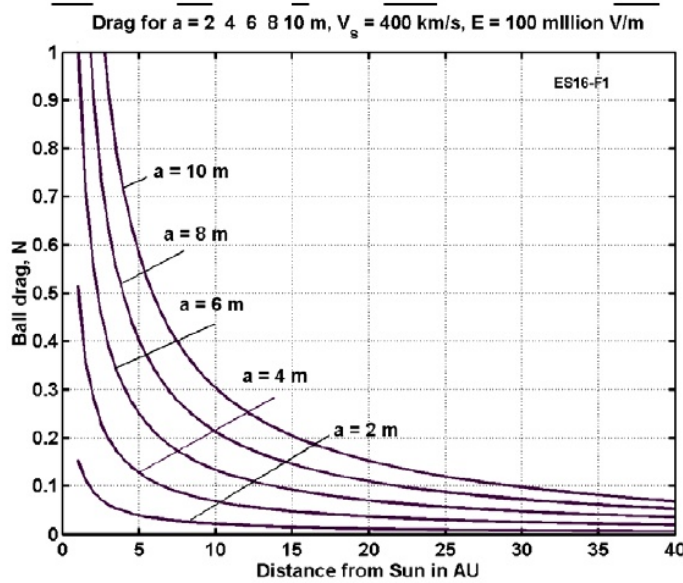
Figure 13.11. Drag of the electrostatic sail versus distance from the Sun (in AU) for ball radius $a = 2$–10m, solar wind speed 400 km/s and electrical intensity $E = 100$ million volts/meter.

4. Estimation of the Ball Stress, Cover Thickness and Ball Mass.

The ball has tensile stress from the like electric charge. We need to find the ball stress and the required thickness of the ball cover. If the ball is in a vacuum and the ball charge, Q, is constant, its ball internal force is

$$f = \frac{\partial W}{\partial a}, \quad W = \frac{Q^2}{2C}, \quad C = \frac{a}{k}, \quad k = \frac{1}{4\pi\varepsilon_0} \approx 9 \times 10^9, \quad W = \frac{kQ^2}{2a},$$

$$f = -\frac{kQ^2}{2a^2}, \quad Q = \frac{a^2 E}{k}, \quad f = -\frac{(aE)^2}{2k}.$$

(13.9)

where f is the tensile force inside the ball [N]; W is the charge energy [J]; C is the capacity of the ball as a sphere capacitor [F]; E is electrical intensity [V/m].
  The internal ball pressure is

$$p = \frac{f}{S}, \quad S = 4\pi a^2, \quad p = \frac{E^2}{8\pi k},$$
(13.10)

where p is the internal pressure [N/m²], S is the ball surface area [m²].
  The thickness of the ball cover, δ, is

$$\pi a^2 p = 2\pi a \delta \sigma, \quad \delta = \frac{ap}{2\delta}, \quad \delta = \frac{aE^2}{16\pi k\sigma},$$
(13.11)

Where δ is cover thickness [m]; σ is safe cover stress [N/m²]. The ball mass i

$$M_s = S\delta\gamma, \quad S = 4\pi a^2, \quad M_s = \frac{a^3 E^2 \gamma}{4k\sigma}.$$
(13.12)

Where M_s is the ball (sail) mass [kg]; γ is the ball cover density [kg/m³]; σ is safe stress of the ball cover [N/m²].
  Computation of the ball thickness and ball mass are presented in Figs. 13.12 and 13.13.
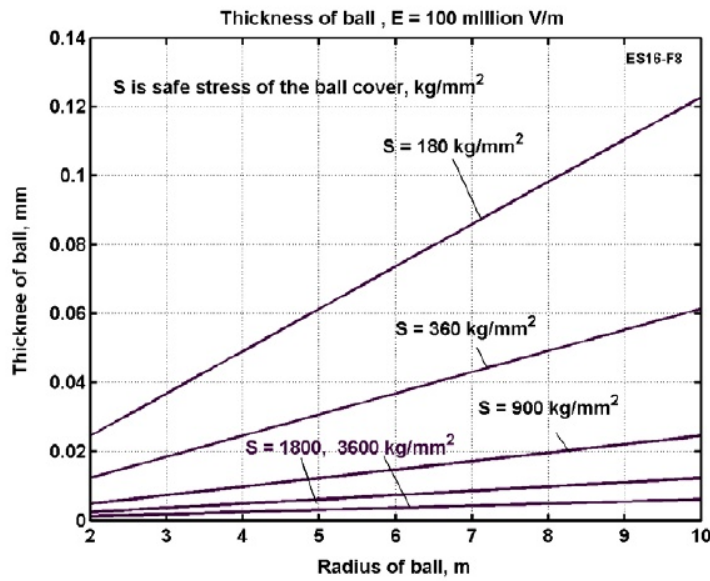
Figure 13.12. Thickness of ball cover versus ball diameter for different safe cover stress value, electrical intensity $E = 100$ million volts/m.

5. Estimation of Probe Acceleration, Speed, and Flight Time

We estimate these values only for a probe moving along the Sun's radius. The equations are

$$A_e = \frac{D(R_e)}{M + M_s}, \quad dV = \frac{D(R_e)}{(M + M_s)V} ds, \quad dt = \frac{1}{V} ds,$$
(13.13)

where A_c – probe acceleration [m/s]; D – probe drag [N]; M – probe mass [kg]; M_s – sail(ball) mass (Figure 13) [kg]; V – radial probe speed [m/s]; t – flight time [s]; s – distance from Sun [m].
  The result of computation for $a = 6$ m, $E = 10^8$ V/m, $M = 100$ kg, $\sigma = 180$ kg/mm², $\gamma = 1800$ kg/m³, $s = 1 – 40$ AU are presented in Figs. 14, 15, 16, and 17.

The ball (sail) weight increases as a cubic value and the total acceleration reaches a maximum. Figure 13.14 shows optimal ball radius for current materials.
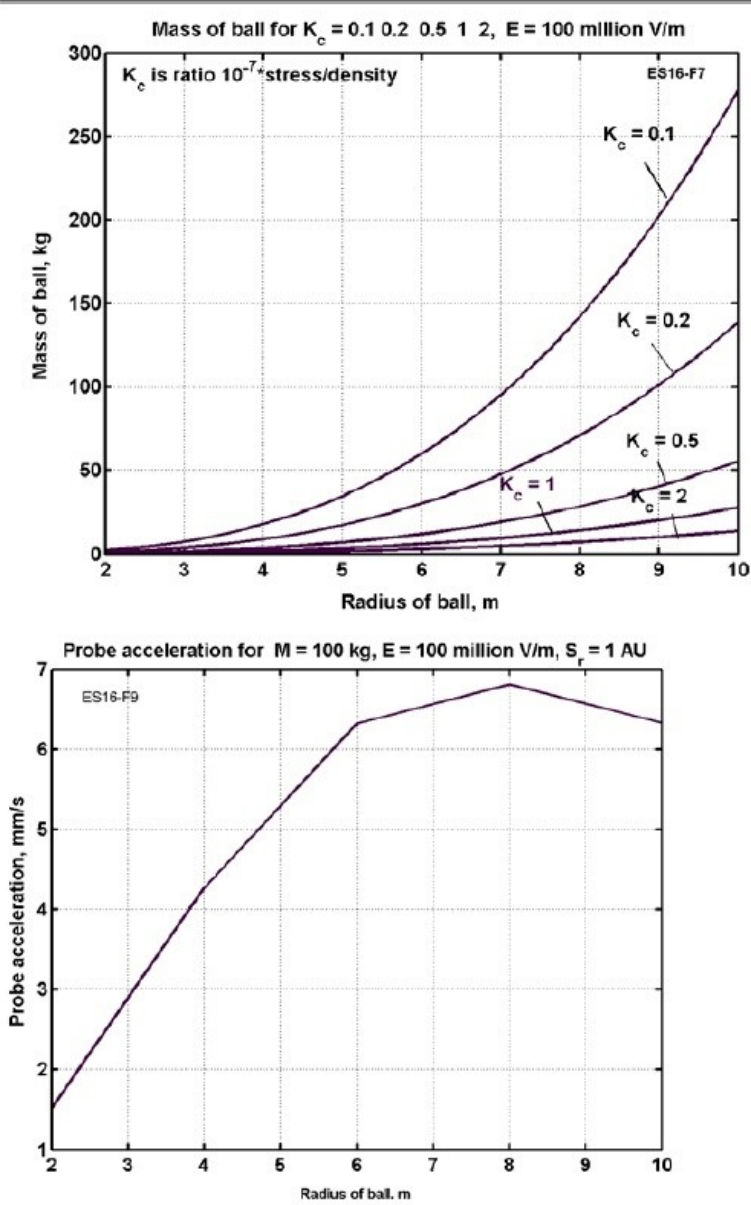
Figure 13.13 (up). Mass of ball cover versus ball diameter for different safe ratio's of stress/cover density and Electric intensity $E = 100$ million volts/m.

Figure 13,14 (down). Probe acceleration versus ball radius for useful probe mass $M = 100$ kg, and the sail weight computed for safe cover stress $\sigma = 180$ kg/mm2, cover density $\gamma = 1800$ kg/m3, electric intensity $E = 100$ million volts/meter, at a distance from the Sun of 1 AU (Earth orbit).
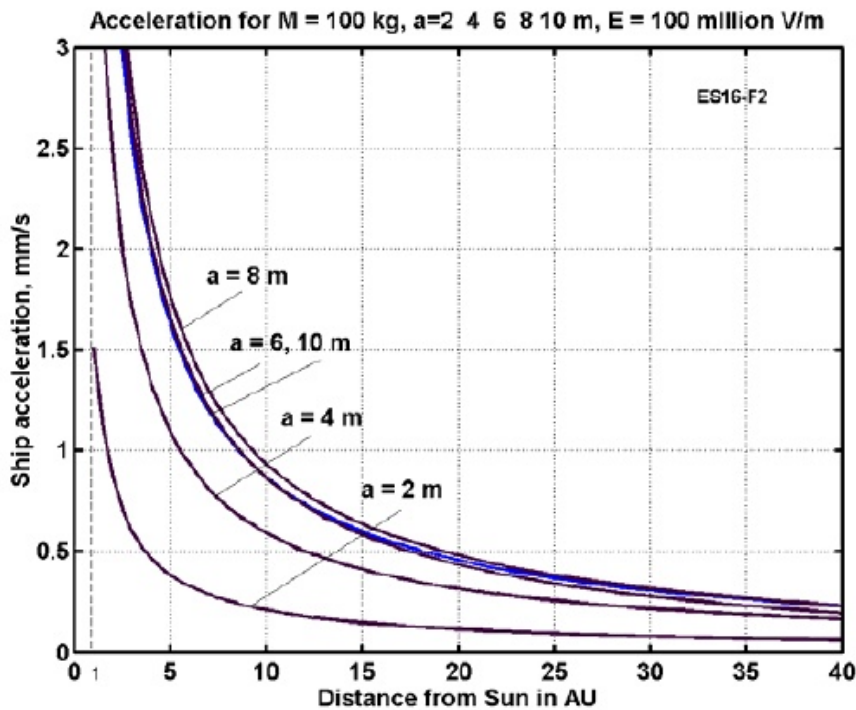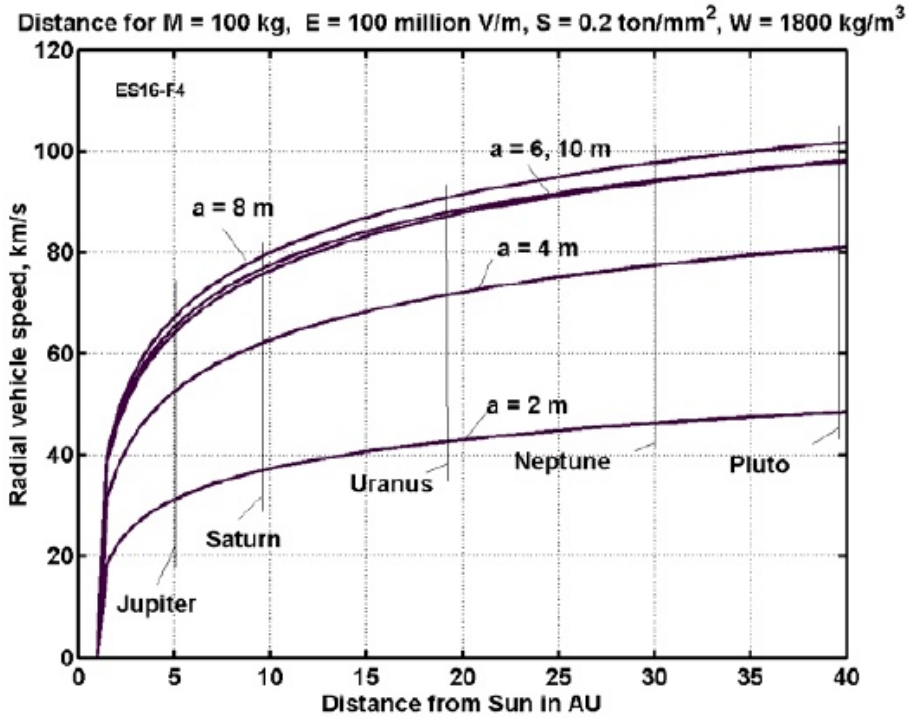
Figure 13.15 (down). Probe acceleration versus distance from the Sun and ball radius for useful probe mass $M = 100$ kg, and sail weight computed for safe cover stress $\sigma = 180$ kg/mm^2, cover density $\gamma = 1800$ kg/m^3, electric intensity $E = 100$ million volts/meter, at a distance from the Sun of $1 - 40$ AU.

Figure 13.16 (up). Probe velocity versus distance from Sun and the ball radius for useful probe mass $M = 100$ kg, and sail weight computed for safe cover stress $\sigma = S = 180$ kg/mm^2, cover density $\gamma = 1800$ kg/m^3, electrical intensity $E = 100$ million volts/meter, at a distance from Sun $1 - 40$ AU, $V_p \approx V_s$.

Figure 13.17. Probe trip time versus distance from the Sun and the ball radius for useful probe mass $M = 100$ kg, and sail weight computed for safe cover stress $\sigma = S = 180$ kg/mm^2, cover density $\gamma = 1800$ kg/m^3, electrical intensity $E = 100$ million volts/meter, at a distance from the Sun of $1 - 40$ AU, $V_p \approx V_s$.
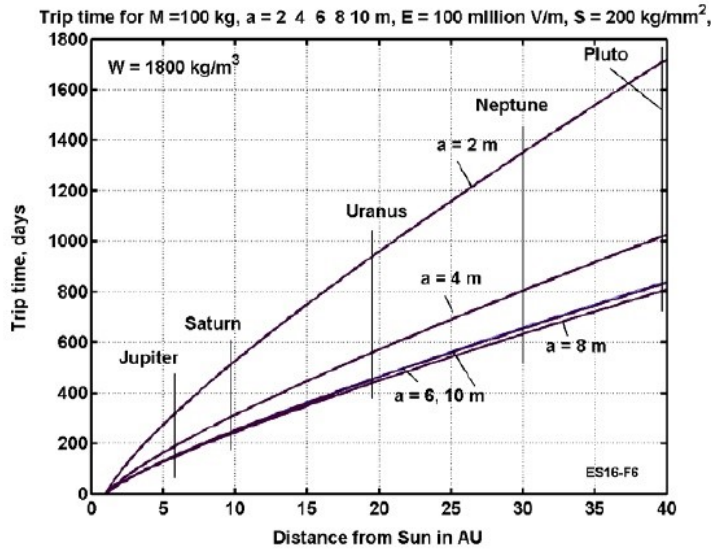
The proposed probe can reach Mars orbit in about 70 days (and reaches a speed of 50 km/s), Jupiter in about 150 days, Saturn in about 250 days, Uranus in about 450 days, Neptune in about 650 days, and the farthest planet Pluto (5800 million km) in about 850 days. The final (interstellar) speed is about 100 km/s. The parameters of the probe (spaceship) are not optimal, but may be improved.

6. Estimation of Absorption of Particles by Ball Cover

The particle (proton) track in the matter can be computed in following way (p. 953, table 44.1 [50]),

$$l = R_t /\gamma, \qquad (13.14)$$

where l is track distance of the particles [cm]; $R_t = R_t (U)$ is magnitude (from table) [g/cm^2]; γ is matter density [g/cm^3]. The magnitude of R_t depends on the kinetic energy (voltage) of the particles. For protons the values of R_t are presented in Table 2.

Table 2. Magnitude of R_t as a function of accelerated voltage $U = aE$, volts.

U, MV	100	200	300	400	500	600	700	1000	2000	3000	5000
R_t g/cm^2	10	33.3	65.8	105	149	197	248	370	910	1463	2543

The proton energy is $U = aE$. For magnitudes $a = 6$ m, $E = 10^8$ V/m, proton energy $U = 600 \times 10^6$ V and ball cover density $\gamma = 1.8$ g/cm^3 the proton track is $l = 197/1.8 = 109$ cm. The required ball cover thickness is only 230 microns (see Figure 12). All protons will run across the ball cover. However, if the losses of speed in the ball cover are less $V_s = 400$ km/s, the protons will leave a neutral sphere. In other cases, they can rotate in a neutral sphere, cross the cover thousands of times, lose their energy and discharge the ball's charge.

The safe ball cover thickness may be estimated using the following method. The solar wind proton energy is

$$E_d = \frac{m_p V_s^2}{2} \qquad (13.15)$$

For $V_s = 400 \times 10^3$ m/s the proton energy is $E_d = 4 \times 10^{-17}$ J $= 4 \times 10^{-17} \times 0.625 \times 10^{19}$ eV $= 840$ eV.

If the loss of proton energy is proportional to the cover thickness, the maximum safe cover thickness (which will not discharge the ball) will be

$$E_d = U \frac{\delta_{max}}{l} \quad or \quad \delta_{max} = \frac{E_d(V_s)l}{U}, \quad U = aE. \qquad (13.16)$$

For $a = 6$ m, $E = 10^8$ V/m the required ball cover thickness is $\delta_{max} = 1.53$ micron. For $a = 4, 10$ m $\delta_{max} = 1.22, 1.73$ microns respectively.

This magnitude is less than the ball thickness required for the charge stress (see Figure 13.12) for current cover matter. Methods of decreasing the cover discharge are offered in the description section.

For electrons the thickness of half absorption may be calculated using equation (p. 958 [50])

$$R_r = 0,095 \frac{Z}{A}(aE)^{3/2} \quad [\text{g/cm}], \quad d_{0.5} = \frac{R_s}{\gamma}, \quad [\text{cm}]. \qquad (13.17)$$

Here Z is the nuclear charge of the ball matter; A is the mass number of the ball matter.

7. Estimation of Initial Expenditure of Electrical Energy Needed to Charge the Ball

The ball must be charged with electrical energy of high voltage (millions of volts). Let us estimate the minimum energy when the charged device has 100% efficiency. This energy equals the work of moving of the ball charge to infinity, which may be computed using equation

$$W = \int_0^a F dr = \int_0^a k \frac{Q_1 Q_2}{r^2} dr = k \frac{Q_1 Q_2}{a}, \quad W = \frac{Q^2}{2C}, \quad Q = \frac{a^2 E}{k}, \quad C = \frac{a}{k}, \quad W = \frac{a^3 E^2}{2k}, \qquad (13.18)$$

where W is ball charge energy [J]; C is ball capacitance [F]; Q is ball charge [C]. The result of this computation is presented in Figure 18. As can be seen this energy not great as it is about $1 - 20$ kWh for a ball radius of $a = 5$ m and the electrical intensity is $25 - 100$ MV/m. This energy may be restored through ball discharge by emitting the charge into space using a sharp edge.
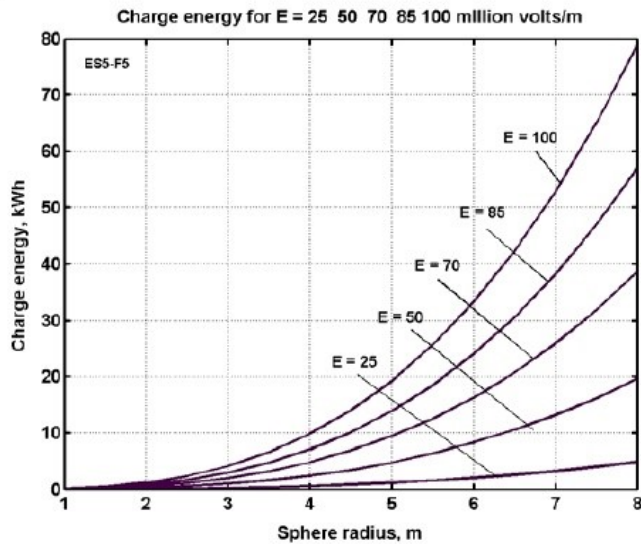

Figure 13.18. Initial expenditure of electrical energy needed to charge the space apparatus, $a = 1 - 8$ m, electrical intensity is $25–100$ MV/m and coefficient of efficiency 1.

8. Short Notes about Thermonuclear Propulsion from Solar Wind

When particles are moved toward the ball, they gain a huge amount of energy equal to the voltage (aE) of the charged ball in infinite space $U = aE$ (100 – 1000 MeV), approaching the speed of light. The particle reactions have the greatest efficiency when the particles move in opposite directions. Their energy is then more than the energy of most common thermonuclear reactions (5 – 20 MeV). The electric field of the brake capacitor can decrease this energy to the required value. The particles may be used for a proton–proton reaction (as inside the Sun), or proton–electrode, or electron–electrode thermonuclear reaction, where the central electrode is made from a suitable matter. The solar wind also contains alpha–particles and ions of other elements (up to 10%). These are accelerated to high energy and can take part in the thermonuclear reaction.

The thermonuclear reaction also needs a certain concentration of the free particles. These are concentrated in the area of the central electrode. This concentration, Q_x, can be computed. The angle of deviation of the initial (in infinity) solar wind particles is small (about 1 – 2 degrees) and the diameter of the central area (maximum concentration near the electrode) is small (possibly less than 1 mm), meaning the thermonuclear cross-section is large. The Lawson criterion is executed because the collision time is infinity. We have continuous particle flow and do not use internal apparatus energy. I call on nuclear experts to research the possibility of thermonuclear reactions in the proposed engine (and generator). This thermonuclear engine is impossible on Earth where the solar wind is blocked by the atmosphere and the Earth's magnetic field, but it is possible in extra-planetary space, in a high vacuum. It may be a way of achieving not only interplanetary trips, but also interstellar apparatus where a space-craft is accelerated to a relativistic velocity.

9. Estimation of Charging the Ball

The main innovation in the proposed idea is the open electric charge of one sign and high intensity. To obtain this open charge, it is necessary to send an opposite charge into infinite space. This is possible if we accelerate the opposed particles (protons, electrons, ions) with energy of more than aE = 100–10^3 MV (a is ball diameter [m], E is electrical intensity [MV/m]). It can be carried and using simple electrostatic accelerators or linear accelerators (electric guns). Their design for use in space is easier than for Earth because outer space has a high vacuum and a high allowable electrical intensity. For example, the allowable electrical intensity is only 3 MV/m on the ground belong the Earth's atmosphere and >100 MV/m in a space vacuum. A Van de Graff accelerator on the ground needs a special high pressure camera and special vacuum camera, but in space they are not needed. Below are data of some ground accelerators of protons (p) and electrons (e).

Electrostatic accelerators (Tandem Van de Graff, Tandem pelletron, Vivitro) accelerate particles (p, d, α , e) up to 20–35 MV, linear accelerators (p) up to 50 – 800 MeV, electron linear accelerators (e) up to 100 GeV and alter-gradient synchrotron (p, e) up to 900 GeV (p) (v. 13, p. 130 [51]).

These data show there is no significant problem in designing a high efficiency space charging gun which will move charges to infinity and create the open charged ball. The energy for this charging is not high (see Figure 18).

These and other possible problems are discussed in the next section. One of possible form of offered space propulsion used the solar wind is shown in Figure19.

Discussion

1. Possible Limitations of offered solar wind system

The above computations suggest a range of possibilities for acceleration using solar wind. The pressure of solar wind is very small but charged particles may be collected by the open charged ball from a big region. They will the give enough thrust for mobile space apparatus. They can accelerate the direct able apparatus to speeds of about 100 km/s and offer flights to far planets of the Solar system in a short time. If the thermonuclear engine (and the electric generator) is possible, thermonuclear wind propulsion will permit us to realize interstellar trips. This is a revolutionary breakthrough in interstellar space.
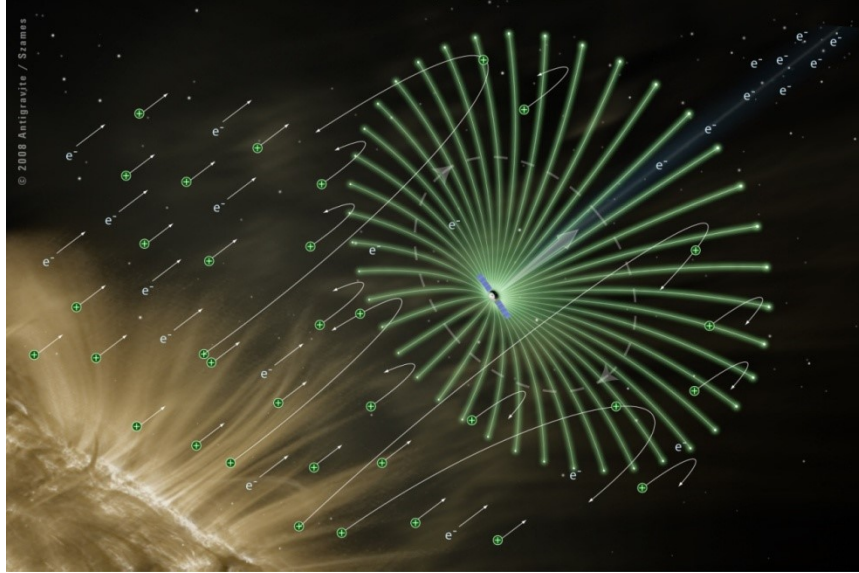

Figure 13.19. Possible form of offered propulsion used the solar wind.

What restrictions may appear in detailed researches to limit these possibilities? The author sees the following problems:

a) Discharging of the ball. The author offers some methods (Figure 5) for reducing of this discharging. Detailed computation is needed.
b) Design of an acceptable charging gun. This is a technical problem which can be solved by current technology.
c) Source of energy.
d) Research and development into the offered space thermonuclear propulsion system and power generator.

2. Comparison with Other Works about Solar Wind Propulsion System

The author suggested a series of solar wind propulsion systems and generators in 1982–1983and later [29–47]. These works included also the nuclear propulsion system and electric generators, and particle and solar wind electrostatic mirrors. In American scientific literature the author found only work published in 2003 [48]. The proposed methods, installation and results have the following differences:

a) The offered propulsion installation design is very different from work [48]. Authors of work [48] use a magnetic field; I use only an electric field. They use a conventional spherical capacitor with two skins (layers) and polarity (unlike) charges (see Figure 6 [48]). These authors wrote (p. 6): "So, from the point of EPS power consumption, it is highly desirable to keep the charge separation distance as small as possible while achieving acceleration".

In my opinion this design cannot work efficiently, because the main part of the electricfield is inside the capacitor. The authors [48] understood that when they wrote (p. 6); "one charge layer is exposed to

the solar wind electric field the other is exposed to a considerably reduced electric field."My proposed propulsion design has a single-skin ball, one type of charge (the opposite charge is expelled in infinity), and an open electric field effective over long distance. The intensity of this field is decreased as $1/r^2$. If the charges in the other system [48] are dipolar their intensity will be small and decrease as $1/r^3$. This means, the author's electric field should be stronger by thousands of times over long distance.

b) The work [48] contains only common speculation. It doesn't contain theory, initial data, detailed numerical results. The authors give only some pictures of solar wind disturbances. In Figure 3, p. 4 the apparatus speed is twice the wind speed (??). No explanation is given for this strange result.

Omidi and Karimabad [48] use the very high specific charges of up to $300 - 500$ C [0.1 –1 (and more) C/kg for full spacecraft mass]. This requires a very large spherical capacitor and very high electrical intensity which is impossible in physics. They wrote: 'this technology would initially be applied to the propulsion of micro spacecraft where charge levels of a low C would be sufficient."

My results are very different from these [48]. The authors do not show their calculation's, but say their apparatus with its propulsion can reach a speed of 64 km/s at a distance 33 AU of 5 years. This means the acceleration is 0.0004 m/s and the thrust is very small.

There are also many articles about magnetic sails using solar wind drag into a magnetic field of a gigantic superconductive ring (diameter 60–150 km). Unfortunately, no theory currently exists to allow computation of magsail drag. It is beyond the capability of current technology. The reader can find information about the space magsail in Reference [52].

Conclusion

The proposed new propulsion mechanism differs from previous concepts in very important respects; including the coupling to the protons of the solar wind using an open single-charge ball. The opposite charge is expelled into infinite space. This innovation increases the area of influence by up to hundreds of kilometers for protons and allows the acquisition of significant vehicle thrust. This thrust is enough to accelerate a heavy space craft to very high speed and permits very short flight times to far planets.

The offered revolutionary propulsion system has a simple design, which can give useful acceleration to various types of spacecraft. The offered propulsion system creates many Newtons of thrust, and can accelerate a 100 kg space probe up to 60–100 km/sec in 100–800days.

In the offered wind propulsion system the particles run away from the ball, brake and return in infinity for initial speed. These premises must be examined using more complex theories to account for the full intersection between the suggested installation and solar wind (including thermonuclear reactions). This would be a revolutionary breakthrough in interplanetary space exploration.

The author has developed the initial theory and the initial computations to show the possibility of the offered concept. He calls on scientists, engineers, space organizations, and companies to research and develop the offered perspective concepts.

References

[1] A.A. Bolonkin, "Theory of Flight Vehicles with Control Radial Force". Collection Researches of Flight Dynamics, Public house "Mashinostroenie", Moscow, 1965, pp.79–118 (in Russian).
[2] A.A. Bolonkin, "Air Cable Transport and Bridges", TN 7567, International Air &Space Symposium – The Next 100 Years, 14–17 July 2003, Dayton, Ohio, USA.
[3] A.A. Bolonkin, "Kinetic Space Towers and Launchers", JBIS (Journal of British Interplanetary Society),

Vol. 57, No 1/2, pp. 33–39, 2004.

[4] A.A. Bolonkin, "Non-Rocket Space Rope Launcher for People", IAC-02-V.P.06, 53rdInternational Astronautical Congress. The World Space Congress– 2002, 10–19 Oct2002, Houston, Texas, USA.

[5] A.A. Bolonkin, "Non-Rocket Missile Rope Launcher", IAC-02-IAA.S.P.14, 53rdInternational Astronautical Congress. The World Space Congress – 2002, 10–19 Oct2002, Houston, Texas, USA.

[6] A.A. Bolonkin, "Optimal trajectory of air vehicles". AEAT (Aircraft Engineering and Aerospace Technology), Vol. 76, No. 2, pp. 193–214, 2004 .

[7] A.A. Bolonkin, "Inexpensive Cable Space Launcher of High Capability", IAC-02-V.P.07, 53rd International Astronautical Congress. The World Space Congress – 2002, 10–19 Oct. 2002, Houston, Texas, USA.

[8] A.A. Bolonkin, "Hypersonic Launch System of Capability up 500 tons per day and Delivery Cost $1 per Lb". IAC-02-S.P.15, 53rd International Astronautical Congress. The World Space Congress – 2002, 10–19 Oct 2002, Houston, Texas, USA.

[9] A.A. Bolonkin, "Employment Asteroids for Movement of Space Ship and Probes".IAC-02-S.6.04, 53rd International Astronautical Congress. The World Space Congress– 2002, 10–19 Oct. 2002, Houston, Texas, USA.

[10] A.A. Bolonkin, A.A., "Optimal Inflatable Space Towers of High Height". COSPAR-02C1.1-0035-02, 34th Scientific Assembly of the Committee on Space Research (COSPAR). The World Space Congress – 2002, 10–19 Oct 2002, Houston, Texas, USA.

[11] A.A. Bolonkin, "Non-Rocket Earth-Moon Transport System", COSPAR-02 B0.3-F3.3-0032-02, 02-A-02226, 34th Scientific Assembly of the Committee on Space Research (COSPAR). The World Space Congress – 2002, 10–19 Oct 2002, Houston, Texas, USA.

[12] A.A. Bolonkin, "Non-Rocket Earth-Mars Transport System", COSPAR-02 B0.4-C3.4-0036-02, 34th Scientific Assembly of the Committee on Space Research (COSPAR).The World Space Congress – 2002, 10–19 Oct 2002, Houston, Texas, USA

 [13] A.A. Bolonkin, "Transport System for delivery Tourists at Altitude 140 km". IAC-02-IAA.1.3.03, 53rd International Astronautical Congress. The World Space Congress –2002, 10–19 Oct. 2002, Houston, Texas, USA.

[14] A.A. Bolonkin, "Optimal Inflatable Space Towers with 3-100 km Height", JBIS, Vol.56, pp. 87–97, 2003.

[15] A.A. Bolonkin, "Asteroids as Propulsion Systems of Space Ships", JBIS, Vol. 58, pp.97–107, 2003.

[16] A.A. Bolonkin, A.A. "Hypersonic Gas-Rocket Launch System.", AIAA-2002-3927,38th AIAA/ASME/ SAE/ASEE Joint Propulsion Conference and Exhibit, 7–10 July,2002. Indianapolis, IN, USA.

[17] A.A. Bolonkin, "Non-Rocket Transportation System for Space Travel", JBIS, Vol. 56,No 7/8, pp. 231–249, 2003.

[18] A.A. Bolonkin, A.A., "Hypersonic Space Launcher of High Capability", Actual problems of aviation and aerospace systems, Kazan, No. 1(15), vol. 8, 2003, pp. 45–58.

[19] A.A. Bolonkin, "Centrifugal Keeper for Space Stations and Satellites", JBIS, Vol. 56,pp. 314–327, 2003.

[20] A.A. Bolonkin, "Non-rocket Earth-Moon Transport System", Advances in Space Research, Vol. 31/11, pp. 2485–2490, 2003, Elsevier.

[21] A.A. Bolonkin, "Earth Accelerator for Space Ships and Missiles". JBIS, Vol. 56, pp.394–404, 2003.

[22] A.A. Bolonkin, "Air Cable Transport", Journal of Aircraft , Vol. 40, No 4, July–August2003.

[23] A.A. Bolonkin, "High Speed Catapult Aviation", AIAA-2005-6221, AIAA Atmospheric Flight Mechanic Conference, 15–18 August, 2005, USA.

[24] A.A. Bolonkin, "High Efficiency Transfer of Mechanical Energy", AIAA-2004-5660, International Energy Conversion Engineering Conference, Rhode Island, 16-19 Aug.2004.

[25] A.A. Bolonkin, "Light Multi-Reflex Engine", Journal JBIS, Vol. 57, No 9/10, pp. 353–359, 2004.

[26] A.A. Bolonkin, Multi-Reflex Propulsion System, JBIS, Vol. 57, No. 11/12, pp. 370–390, 2004.

[27] A.A. Bolonkin, "Sling Rotary Space Launchers", 41 Propulsion Conference, 10–13July, 2005, Tucson, Arizona, USA, AIAA-2005-4035.

[28] A.A. Bolonkin, "Kinetic Anti-Gravitator", 41 Propulsion Conference, 10–13 July,2005, Tucson, Arizona, USA. AIAA-2005-4504.

[29]A.A. Bolonkin, "Space Propulsion using Solar Wing and Installation for It". Russian patent application

#3635955/23 126453, 19 August, 1983 (in Russian). Russian PTO.

[30] A.A. Bolonkin, "Installation for Open Electrostatic Field". Russian patent application #3467270/21 116676, 9 July, 1982 (in Russian). Russian PTO.

[31] A.A. Bolonkin, "Getting of Electric Energy from Space and Installation for It". Russian patent application #3638699/25 126303, 19 August, 1983 (in Russian).Russian PTO.

[32] A.A. Bolonkin, "Protection from Charged Particles in Space and Installation for It". Russian patent application #3644168 136270 of 23 September 1983, (in Russian).Russian PTO

[33] A.A. Bolonkin, "Method of Transformation of Plasma Energy in Electric Current and Installation for It". Russian patent application #3647344 136681of 27 July 1983 (in Russian), Russian PTO.

[34] A.A. Bolonkin, "Method of Propulsion using Radioisotope Energy and Installation for It". Russian patent application #3601164/25 086973 of 6 June, 1983 (in Russian),Russian PTO.

[35] A.A. Bolonkin, "Transformation of Energy of Rarefaction Plasma in Electric Current and Installation for it". Russian patent application #3663911/25159775 of 23 November 1983 (in Russian). Russian PTO.

[36] A.A. Bolonkin, "Method of a Keeping of a Neutral Plasma and Installation for it". Russian patent application #3600272/25 086993 of 6 June 1983 (in Russian). Russian PTO.

[37] A.A. Bolonkin, Radioisotope Propulsion. Russian patent application #3467762/25116952 of 9 July 1982 (in Russian). Russian PTO.

[38] A.A. Bolonkin, "Radioisotope Electric Generator". Russian patent application #3469511/25 116927 of 9 July 1982 (in Russian). Russian PTO.

[39] A.A. Bolonkin, "Radioisotope Electric Generator". Russian patent application #3620051/25 108943 of 13 July 1983 (in Russian). Russian PTO.

[40] A.A. Bolonkin, "Method of Energy Transformation of Radioisotope Matter in Electricity and Installation for it". Russian patent application #3647343/25 136692 of 27 July 1983 (in Russian). Russian PTO.

[41] A.A. Bolonkin, "Method of stretching of thin film" Russian patent application#3646689/10 138085 of 28 September 1983 (in Russian). Russian PTO.

[42] A.A. Bolonkin, "New Way of Thrust and Generation of Electrical Energy in Space". Report ESTI, 1987, 109 p. (Soviet Classified Project).

[43] A.A. Bolonkin, "Aviation, Motor and Space Designs". Emerging Technology in the Soviet Union, 1990, Delphic Ass., Inc., pp. 32–80, (English).

[44] A.A. Bolonkin, "A Space Motor Using Solar Wind Energy". The World Space Congress, Washington, DC, USA, 28 Aug. – 5 Sept., 1992, IAF-0615.

[45] A.A. Bolonkin, "The Simplest Space Electric Generator and Motor with Control Energy and Thrust", 45th International Astronautical Congress, Jerusalem. Israel. Oct. 9–4,1994, IAF-94-R.1.368 .

[46] A.A. Bolonkin, "Space Electric Generator, run by Solar Wing". The World Space Congress, Washington, DC, USA, 28 Aug.–5 Sept., 1992, IAF-92-0604.

[47] A.A. Bolonkin, "Simple Space Nuclear Reactor Motors and Electric Generators Running on Radioactive Substances". The World Space Congress, Washington, DC,USA, 28 Aug. –5 Sept., 1992, IAF-92-0573.

[48] N.Omidi and H.Karimabadi, "Electrostatic Plasma Sail", AIAA 2003-5227, 2003. 39th AIAA/ASME/SAE/ASEE Joint Propulsion Conference and Exhibit 20–23 July 2003,Hurtisville, Alabama. See also this work in NIAC site http://niac.usra.edu , Omidi final report where director NIAC Mr. Cassanova awarded this work $75000.

[49] V.I. Feodosev, Base of Rocket Flight Techniques, Moscow, "Science", 1981 (in Russian).

[50] I.K. Kikoin, (ed), Directory, Tables of physic values, Moscow, Atomizdat, 1976 (in Russian).

[51] McGraw-Hill Encyclopedia of Science & Technology.

[52] L. Funaki, et. al, "Trust Production Mechanism of Magnetoplasma Sail", AIAA 2003-4292.

[53] A.A. Bolonkin, "Electrostatic Solar Wind Propulsion System", AIAA-2005-3653. 41 Propulsion Conference, 10-12 July, 2005, Tucson, Arizona, USA.

[54] A.A. Bolonkin, "Electrostatic Utilization of Asteroids for Space Flight", AIAA-2005-4032. 41 Propulsion Conference, 10–12 July, 2005, Tucson, Arizona, USA.

[55] A.A. Bolonkin, "Radioisotope Space Sail and Electric Generator", AIAA-2005-4225. 41 Propulsion Conference, 10–12 July, 2005, Tucson, Arizona, USA.

[56] A.A. Bolonkin, "Guided Solar Sail and Electric Generator", AIAA-2005-3857.41 Propulsion

Conference, 10–12 July, 2005, Tucson, Arizona, USA.

[57] A.A. Bolonkin, "Problems of Electrostatic Levitation and Artificial Gravity", AIAA-2005-4465. 41 Propulsion Conference, 10–12 July, 2005, Tucson, Arizona, USA.

[58] A.A. Bolonkin, Femtotechnology and Revolutionary Projects, Lambert, 2007, iSBN: 978-3-8473-2229-0.

[59] Bolonkin A.A., "New Concepts, Ideas, and Innovation in Aerospace, Technology and Human Science", NOVA, 2006, 502 pgs.

[60] Bolonkin A.A., "Macro-Projects: Environment and Technology ", NOVA, 2007, 536 pgs.

Chapter 14
Electrostatic Utilization of Asteroids for Space Flight*

Summary

  This chapter offers a electrostatic method for changing the trajectory of space probes. The method uses electrostatic force and the kinetic or rotary energy of asteroids, comet nuclei, meteorites or other space bodies (small planets, natural planet satellites such a moons, space debris, etc.) to increase or decrease ship/ probe speed by 1000 m/s or more and to achieve any new direction in outer space. The flight possibilities of spaceships and probes are thereby increased by a factor of millions.

Introduction

. The method includes the following main steps (Fig. 14.1):

 (a) Finding an asteroids using a locator or telescope (or looking in a catalog) an asteroid and determining its main parameters (location, mass, speed, direction, rotation); selecting the appropriate asteroid; computing the required position of the ship with respect to the asteroid.

 (b) Correcting the ship's trajectory to obtain the required position; convergence of the ship with the asteroid.

 (c) Charging the asteroid and space apparatus ball using a charge gun.

 (d) Obtaining the necessary apparatus position and speed for the apparatus by flying it around the space body and changing the charge of the apparatus and space body (asteroids).

 (e) Discharging the space apparatus and the space body.

  The equipment requires for changing a probe (spacecraft) trajectory includes:
(a) A charging gun.

(b) Devices for finding and measuring the asteroids (space bodies), and computing the trajectory of the spacecraft relative of the space body.

(c) Devices for spacecraft guidance and control.

(d) A device for discharging of the apparatus and asteroids (space body) (see Fig. 14.1).

Description of Utilization

The following describes the general facilities and process for a natural space body (asteroid, comet, meteorite, small planet), or other spaceship with a small gravitational force to change the trajectory and speed of a space probe.

   Fig. 14.2a,b,c,d. show the preparations for using a natural body for changing the trajectory of the space apparatus', for example, the natural space body 2, which moves near the space apparatus. The ship needs to make a maneuver (change direction or speed) in plane 3 (perpendicular to the sketch), and the position of the apparatus is corrected and it is moved into the required plane 3 using small rocket impulses. It is assumed that the natural elected object has more mass than the artificial apparatus, and the space body speed is close to that of the apparatus (the difference can be as much as 1000 m/s).
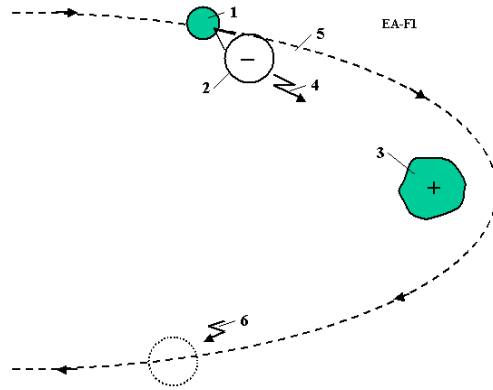
Fig. 14.1. Method of electrostatic maneuvers of the space apparatus. Notations: 1 – space apparatus, 2 – charged ball, 3 – asteroid, 4 – charged gun, 5 – new apparatus trajectory, 6 – discharging the apparatus and asteroid.
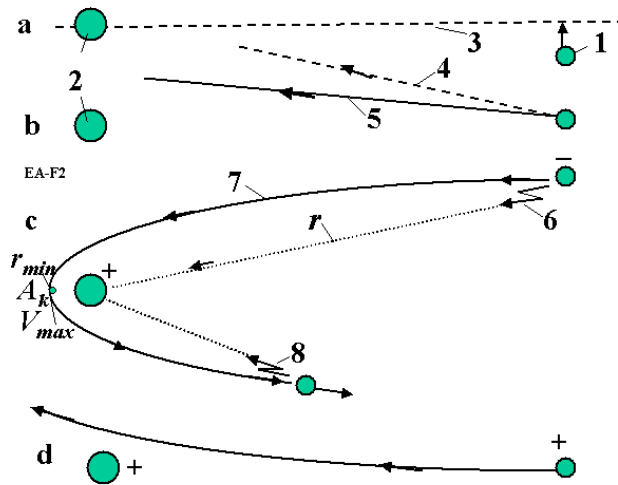

Fig. 14.2. Maneuvers of electrostatic space apparatus. a – preparing for maneuver, correcting the plane of maneuver; b – correcting the apparatus trajectory in the maneuver plane; c – charging the apparatus and asteroids, changing apparatus trajectory and velocity, discharging apparatus and asteroid; d – the case of like charges (which repel).

   Notations: 1 – space apparatus (ball); 2 – asteroid; 3 – plane of maneuver; 4 - initial apparatus trajectory; 5 – primary correction of the trajectory in the maneuver plane; 6 – charge impulse from apparatus to asteroid using charge gun; 7 – new apparatus trajectory; 8 – discharge impulse from apparatus (return part of charge energy) using sharp edge.

   In the early computed point of the trajectory the space apparatus sends the asteroid a charge which takes root on asteroid surface, electrifying it. The apparatus also is charged (with unlike or like charges). If the apparatus and asteroid have unlike charges, they will be attracted one to another (Fig. 14.2c). If they have like charges, they will repel such other (Fig. 14.2d). The electrostatic force changes the apparatus trajectory and speed. The trajectory gains a new direction with a new velocity. When the trajectory has the selected direction and speed, the apparatus is then discharged and leaves the asteroid. The charge energy returns to the apparatus. If efficiency equals 1, this energy will be less when the new

apparatus speed is more than before, equal when the speeds are same, and more when the apparatus speed is less than the previous speed.

Charging is done using a special charge gun, which accelerates charged particles (electrons or ions) to the required speed, and discharging is done using the edge of a pike. The return energy is an electric current through the pike's edge. The apparatus can also utilize the asteroid's speed and asteroid kinetic energy by mechanical connection as described herein[1-6].

An abandoned space vehicle or large piece of space debris in the Earth's orbit can also be used to increase the speed of the new vehicle and to remove the abandoned vehicle or debris from orbit (see point 5 in the Theory and Computation section).

The charging equipment may be used to land the apparatus on an asteroid (small planet) surface and to launch the apparatus from an asteroid (see point 5 in the Theory and Computation section). The apparatus ball is usually charged with negative charges because negative charges (electrons) are emitted from an open surface which does not have a high resistance electric cover, when the electrical intensity (in a vacuum) is over 100 MV/m.

Theory and Computation (in metric system)

1. The electrostatic force between charged bodies is

$$F = k\frac{Q_1 Q_2}{r^2}, \quad if \quad Q = Q_1 = Q_2, \quad F = k\frac{Q^2}{r^2}, \quad Q = \frac{a^2 E}{k}, \tag{14.1}$$

where F is the force [N]; k is a coefficient, $k = 9 \times 10^9$; Q is the charge [C]; r is the distance between the center of charges [m]; a is radius of the charged ball apparatus [m]; E is the electrical intensity at the ball's surface [volts/m] (it may be up 100–200 MV/m in the vacuum and negative charge, and is more for positive charge).

2. Computation of space apparatus trajectories. Assume the asteroid mass is many times greater than the apparatus mass and start the origin of the coordinate system at the asteroid's center of gravity. The initial apparatus position is shown in Fig. 14.3.
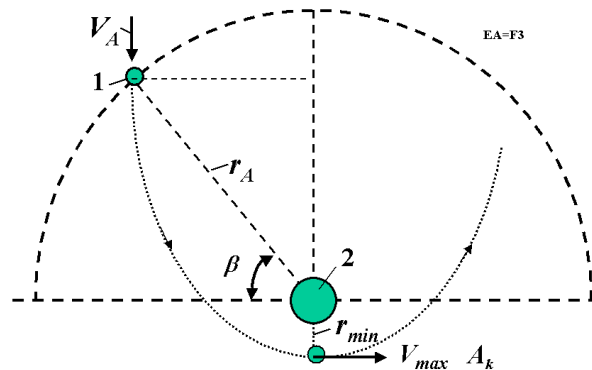
Fig. 14.3. Interaction between the charged ball apparatus and the charged asteroid. Notations are: 1 – space apparatus and electrically charged ball (balloon); 2 – asteroid; r_A – initial radius, V_A – initial apparatus speed.

We assume the charging happens instantly and the charges are constant up to point of discharge.

The equations for computation of the hyperbolic ($e > 1$) apparatus trajectory are (asteroid mass $\gg$ apparatus mass):

$$K = \frac{kqQ}{m}, \quad H = V_A^2 \mp \frac{2K}{r_A}, \quad c = r_A V_A \cos\beta, \quad e = \frac{c}{K}\sqrt{H + \frac{K^2}{c^2}}, \quad \alpha = 2\arctan\sqrt{e^2 - 1}, \ e > 1,$$

$$\gamma = \pi - \alpha, \quad V = \sqrt{H + \frac{2K}{r}}, \quad p = \frac{c^2}{K}, \quad r = \frac{p}{1 + e\cos\varphi}, \quad T = \frac{2\pi}{\sqrt{K}}\left(\frac{p}{1 - e^2}\right)^{3/2}, \quad r_{min} = \frac{p}{1 + e}, \quad (14.2)$$

$$V_{max} = \sqrt{H + \frac{2K}{r_{min}}}, \quad A_k = \frac{V_{max}^2}{p}.$$

Here: K – coefficient [constant]; m – apparatus mass [kg]; q – electrical charge of the space apparatus [C]; Q – electrical charge of the asteroid [C], which is conventionally $q = Q$; H – coefficient of apparatus energy (kinetic and electric potential) around the asteroid; V_A – relative speed of the asteroid about spaceship [m/s] at the initial radius r_A (moment of charge impulse); $V(r)$ – spaceship speed [m/s], c – momentum constant, e – eccentricity of the apparatus trajectory ($e > 1$ for a hyperbolic trajectory, $e = 1$ for parabolic trajectory, $0 < e < 1$ for an elliptical trajectory, $e = 0$ for a circle), β – the angle between V_A and perpendicular to r_A at the moment of charging (see Fig. 14.2), α – angle between the asymptotes of the hyperbolic trajectory, γ – final deviation of the hyperbolic trajectory from the initial direction [radians]; p – parameter of the hyperbolic trajectory [m]; r – variable radius-vector at the trajectory point [m]; r_{min} – minimum distance of the charge apparatus center from the asteroid [m]; V_{max} – maximum apparatus speed relative to the asteroid [m/s]; A_k – maximum centrifugal acceleration of apparatus [m/s^2].

The constant (H) may be found from the initial position (r_A) and initial speed of the apparatus (V_A) (see the second formula in (14.2)). Sign "–" is used for attraction, sign "+" is used for repelling charges.

Note than the trajectory may be circular or elliptical and the apparatus can orbit for a long time around the asteroid.

Readers can find initial formulas for gravity fields in space mechanics and physics text-books and modify them for electrical charged bodies (electric fields). Formulas in equation (14.2) are used for deviation of the charged apparatus by the electrically charged asteroid.

Computations of a typical parameter of trajectory versus parameter r_A for space apparatus of mass 100 kg are presented in Figs. 14.4 – 14.7.

3. Initial expenditure of electrical energy needed to charge of the ball. The ball must be charged with electrical energy of high voltage (millions of volts). Let us estimate the minimum energy, when charged the device has 100% efficiency. This energy is equals to the work of moving of the ball charge to infinity. This may be computed using the equation

$$W = \frac{Q^2}{2C}, \quad Q = \frac{a^2 E}{k}, \quad C = \frac{a}{k}, \quad W = \frac{a^3 E^2}{2k}, \quad (14.3)$$

where W is ball charge energy [J]; C is ball capacitance [F]; Q is ball charge [C].

The result of this computation is presented (same) in Fig. 13.18. As you can see this energy is not enormous – it is about $1 - 10$ kWh for a ball radius of $a = 2$–4 m and electrical intensity of 25–100 MV/m. This energy (equal, or less, or more) may be returned when the ball is discharged by emitting of the charge into space using a sharp edge.

The energy (work) requirement for the separation of unlike charges (apparatus – asteroid, $q = Q$) can be computed by the following equations (for efficiency equal to 1):

$$W = \int_a^{r_A} k\frac{Q^2}{r^2}dr = kQ^2\left(\frac{1}{a} - \frac{1}{r_A}\right), \quad \Delta W = \frac{mV_A^2}{2} - \frac{mV_f^2}{2}, \quad \Delta W = kQ^2\left(\frac{1}{r_A} - \frac{1}{r_f}\right), \quad (14.3)'$$

where ΔW is increment in energy [J]; V_f is apparatus speed on the moment of discharge [m/s]; r_f- is the distance to the asteroid at the moment of discharge [m]. Charging the asteroid requires less energy because it is located at a limited distance from the space apparatus. The increment ΔW may be either positive, zero, or negative.

Fig. 14.4. Maximum turn angle of trajectory, γ, versus the initial charge distance to asteroid and radius of the charged ball for electrical intensity of 100 million volts/meter, initial apparatus speed 200 m/s, and apparatus mass 100 kg, $\beta = \pi/4$.

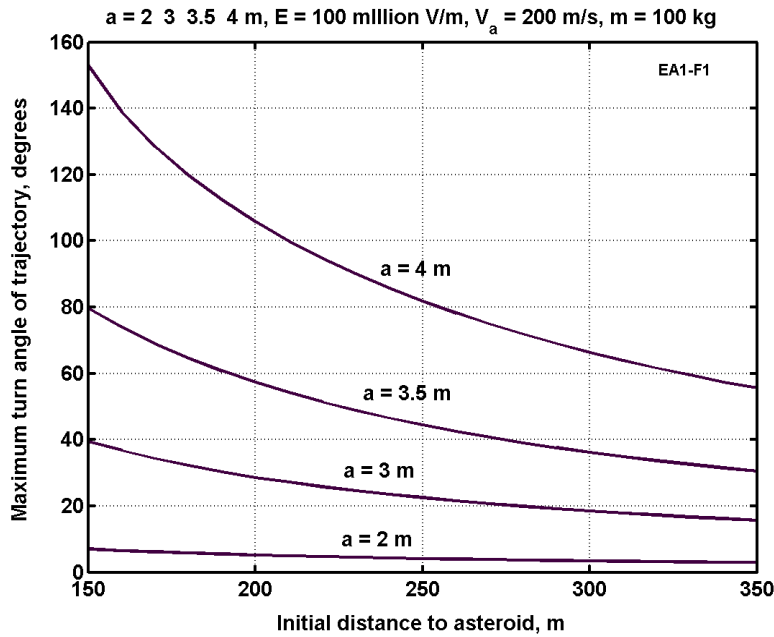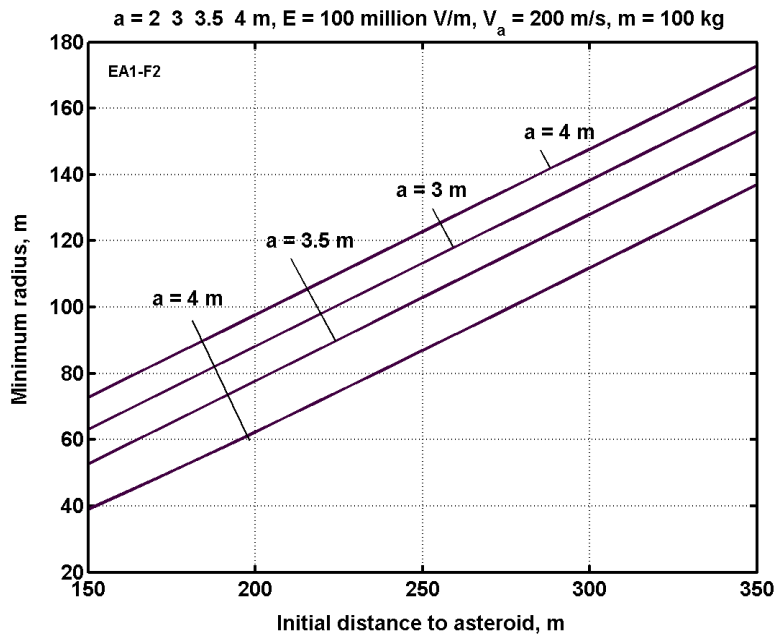Fig. 14.5. Minimum radius of trajectory versus the initial charge distance to the asteroid and radius of the charged ball for electrical intensity 100 million volts/meter, initial apparatus speed 200 m/s, and apparatus mass 100 kg, $\beta = \pi/4$.

a = 2 3 3.5 4 m, E = 100 million V/m, V_a = 200 m/s, m =100 kg

EA1-F3
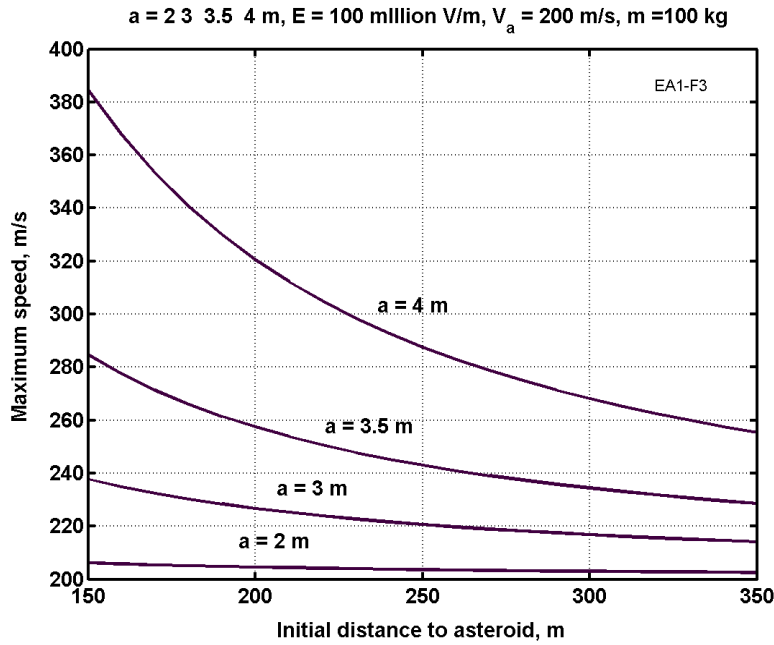
Fig. 14.6. Maximum speed of the space apparatus versus the initial charge distance to the asteroid and radius of the charged ball for electrical intensity 100 million volts/meter, initial apparatus speed 200 m/s, and apparatus mass 100 kg, $\beta = \pi/4$.

a = 2 3 3.5 4 m, E = 100 million V/m, V_a = 200 m/s, m = 100 kg

EA1-F4
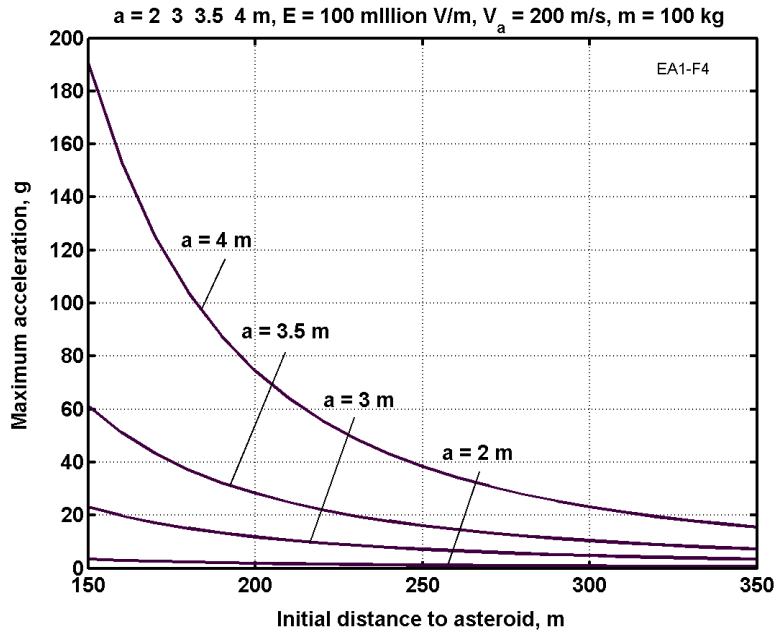
Fig. 14.7. Maximum acceleration (in g) of space apparatus versus the initial charge distance to the asteroid and radius of the charged ball for electrical intensity 100 million volts/meter, initial apparatus speed 200 m/s, and apparatus mass 100 kg, $\beta = \pi/4$.

4. The ball stress, cover thickness and ball mass. The ball has tensile stress from the like electric charges. The equations are same 13.9-13.12 of chapter 13.

The computations of the ball thickness and ball mass are presented in Figs. 13.12, 13.13.

5. Landing on and launching the space apparatus from asteroids and small planets.

If the apparatus and the asteroid have like charges, they will repel each other. This can be used to brake the apparatus for landing on the asteroid or for launching the apparatus from the asteroid surface. The change in apparatus speed can be computed using the following equations:

$$Q = \frac{a^2 E}{k}, \quad \frac{mV^2}{2} = k\frac{Q^2}{a} = \frac{a^3 E^2}{k}, \quad V = \sqrt{\frac{2a^3 E^2}{km}}, \tag{14.4}$$

where V is the initial (for braking) or final (for launching) speed of the apparatus [m/s]. Computations of braking (landing) and launch speed are presented in Fig. 14.8. The launch speed can be quite high, at up to 1600 m/s or more.

Electrical intencity E = 25 50 75 100 million V/m, App. mass M = 100 kg
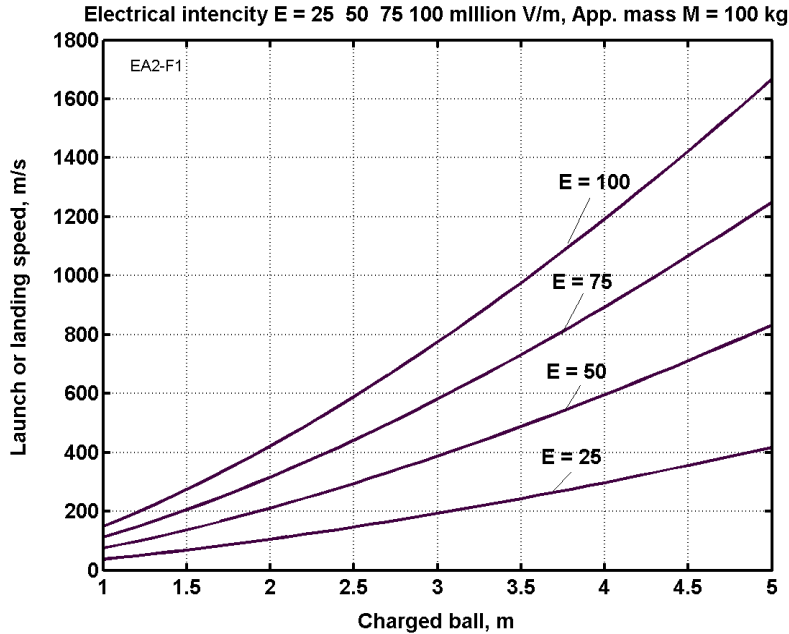

Fig. 14.8. Launch and landing (braking) speed of apparatus versus the charged ball radius and the electrical intensity (in million of volts/meter).

Project

As a project we can take the space apparatus of the mass 100 kg. All its parameters and maneuver capabilities can be estimated from the figures above.

Discussion

1. Estimation of probability of meeting a small asteroid. This problem was considered in chapter 11. Note that the kinetic energy of space bodies may be used through mechanical connections[4] if the space body has a different speed or direction. However, electrostatic apparatus can use space body that has the same direction and speed for its acceleration if the apparatus has electrical energy (through charging and discharging the space body).

2. Charging the ball. This problem was considered in chapter 13, point 9.

3. Blockading of the ball charge. Blockading of the charge on the ball and the asteroid by unlike solar wind particles may be a problem with this method. The charge on the ball attracts unlike particles and repels like particles and opposite-charge particles accumulate near the ball and block its charge. As the result the efficient area near the ball is less than electrostatic theory predicts. The area has a radius of about 7–25 km in Earth orbit. The electrostatic forces can be reduced. The method of computation for a neutral (efficient) area is offered by author elsewhere[5] (see aso chapter 13). This problem is not important for suggested method by following reasons:

1. The apparatus trajectory is usually located inside the neutral sphere.

2. The maneuvers are usually made far from the Sun where the solar wind intensity (density of space plasma) is very small.

3. The maneuvers are made quickly.

   Possible drawbacks of the method may include the mass of the charge gun, electrical energy storage, and the mass of ball because the apparatus has big centrifugal acceleration.

References

1. A.A. Bolonkin, "Theory of Flight Apparatus with Control Radial Force". Collection *Researches of Flight Dynamic*, Ed. I.V. Ostoslavsky, Moscow, Mashinostroenie, 1965, pp. 79-118 (in Russian).
2. "Asteroids as Engine of Space Ships" (Suggestion of American Scientist Alexander Bolonkin), *Weekly News*. 28 April 1998, Israel (in Russian).
3. A.A. Bolonkin, "Employment of Asteroids for Movement of Space Ship and Probes". IAC-02-S.6.04, 53rd International Astronautical Congress, The World Space Congress – 2002, 10–19 Oct 2002, Houston, Texas, USA.
4. A.A. Bolonkin, "Asteroids as Propulsion Systems of Space Ship, Journal of British Interplanetary Society (JBIS), Vol,56, No.3/4, 2003, pp.98-107.
5. A.A. Bolonkin, "Electrostatic Solar Wind Propulsion System", AIAA-2005-3653. 41 Propulsion Conference, Tucson, Arizona, USA.
6. A.A. Bolonkin, "Electrostatic Utilization of Asteroids", AIAA-2005-4032. 41 Propulsion Conference, Tucson, Arizona, USA.

Asteroid distribution

© 2014 Encyclopædia Britannica, Inc.
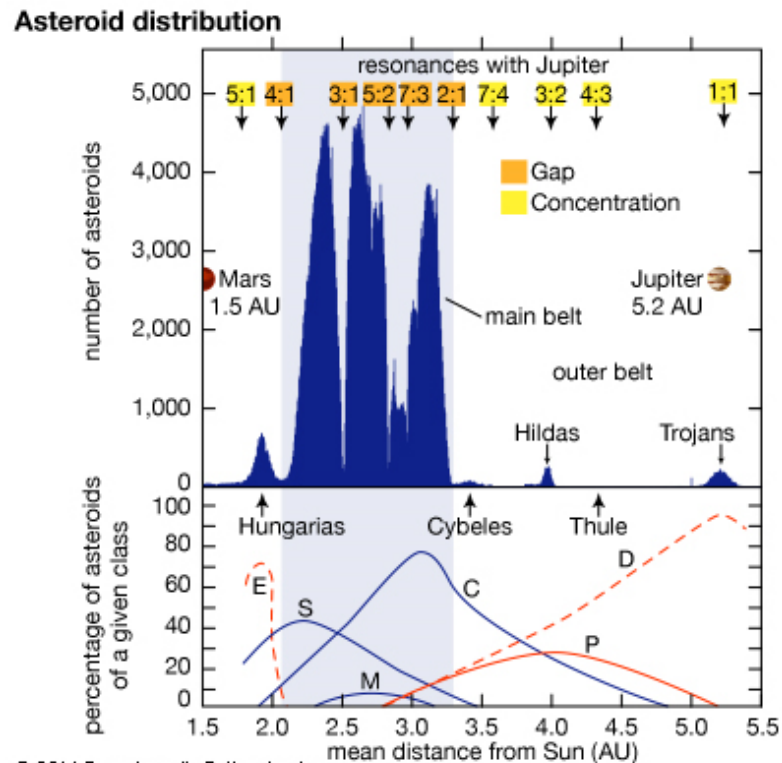
Chapter 15
Electrostatic Levitation on the Earth and Artificial Gravity for Space Ships and Asteroids*

Summary

The author offers and researches the conditions which allow people and vehicles to levitate on the Earth using the electrostatic repulsive force. He shows that by using small electrically charged balls, people and cars can take flight in the atmosphere. Also, a levitated train can attain high speeds. He has computed some projects and discusses the problems which can appear in the practical development of this method. It is also shown how this method may be used for creating artificial gravity (attraction force) into and out of space ships, space hotels, asteroids, and small planets which have little gravity.

Introduction

People have dreamed about a flying freely in the air without any apparatus for many centuries. In ancient books we can find pictures of flying angels or God sitting on clouds or in heaven. At the present time you can see the same pictures on walls in many churches.

  Physicist is know only two methods for creating repulsive force: magnetism and electrostatics. Magnetism is well studied and the use of superconductive magnets for levitating a train has been widely discussed in scientific journals, but repulsive magnets have only a short-range force. They work well for ground trains but are bad for air flight. Electrostatic flight needs powerful electric fields and powerful electric charges. The Earth's electric field is very weak and cannot be used for levitation. The main innovations presented in this chapter are methods for creating powerful static electrical fields in the atmosphere and powerful, stable electrical charges of small size which allow levitation (flight) of people, cars, and vehicles in the air. The author also shows how this method can be utilized into and out of a space ship (space hotel) or on an asteroid surface for creating artificial gravity. The author believes this method has applications in many fields of technology.

   Magnetic levitation has been widely discussed in the literature for a long time. However, there are few scientific works related to electrostatic levitation. Electrostatic charges have a high voltage and can create corona discharges, breakthrough and relaxation. The Earth's electrostatic field is very weak and useless for flight. That is why many innovators think that electrostatic forces cannot be useful for levitation.

  The author's first innovations in this field which changed this situation were offered in (1982)[1], and some practical applications were given in (1983)[2]. The idea was published in 1990 p. 79[3]. In the following presented work, these ideas and innovations are researched in more detail. Some projects are also presented to allow estimation of the parameters of the offered flight systems.

Brief description of innovation

 It is known that like electric charges repel, and unlike electric charges attract (Fig. 15.1a,b,c). A large electric charge (for example, positive) located at altitude induces the opposite (negative) electric charge at the Earth's surface (Figs. 15.1d,e,f,g) because the Earth is an electrical conductor. Between the upper and lower charges there is an electric field. If a small negative electric charge is placed in this electric

field, this charge will be repelled from the like charges (on the Earth's surface) and attracted to the upper charge (Fig. 15.1d). That is the electrostatic lift force. The majority of the lift force is determined by the Earth's charges because the small charges are conventionally located near the Earth's surface. As shown below, these small charges can be connected to a man or a car and have enough force to lift and supports them in the air.

The upper charge may be located on a column as shown in Fig. 15.1d,e,f,g or a tethered air balloon (if we want to create levitation in a small town) (Fig. 15.1e), or air tube (if we want to build a big highway), or a tube suspended on columns (Fig. 15.1f,g). In particular, the charges may be at two identically charged plates, used for a non-contact train (Fig. 15.3a).
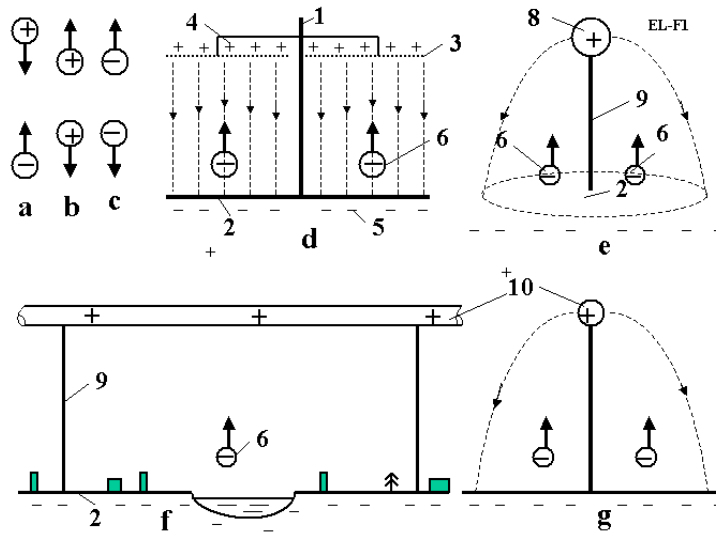
Fig. 15.1. Explanation of electrostatic levitation: a) Attraction of unlike charges; b,c) repulsion of like charges; d) Creation of the homogeneous electric field (highway); e) Electrical field from a large spherical charge ; f,g) Electrical field from a tube (highway) (side and front views). Notations are: 1, 9 – column, 2 – Earth (or other) surface charged by induction, 3 – net, 4 – upper charges, 5 – lower charges, 6 – levitation apparatus, 8 – charged air balloon, 9 – column, 10 – charged tube.

A lifting charge may use charged balls. If a thin film ball with maximum electrical intensity of below 3×10^6 V/m is used, the ball will have a radius of about 1 m (the man mass is 100 kg). For a 1 ton car, the ball will have a radius of about 3 m (see the computation below and Fig. 15.2g,h,i). If a higher electric intensity is used, the balls can be small and located underneath clothes (see below and Fig. 15.2 a,b,c).

The offered method has big advantages in comparison to conventional vehicles (Figs. 15.1 and 15.2):

1) No very expensive highways are necessary. Rivers, lakes, forests, and buildings are not obstacles for this method.
2) In given regions (Figs. 15.1 and 15.2) people (and cars) can move at high speeds (man up 70 km/hour and cars up to 200–400 km/hour) in any direction using simple equipment (small balls under their clothing and small engines (Fig. 15.2a,b,c)). They can perform vertical takeoffs and landings.
3) People can reduce their weight and move at high speed, jump a long distance, and lift heavy weights.
4) Building high altitude homes will be easier.

This method can be also used for a levitated train and artificial gravity in space ships, hotels, and asteroids (Fig. 15.3a,b).
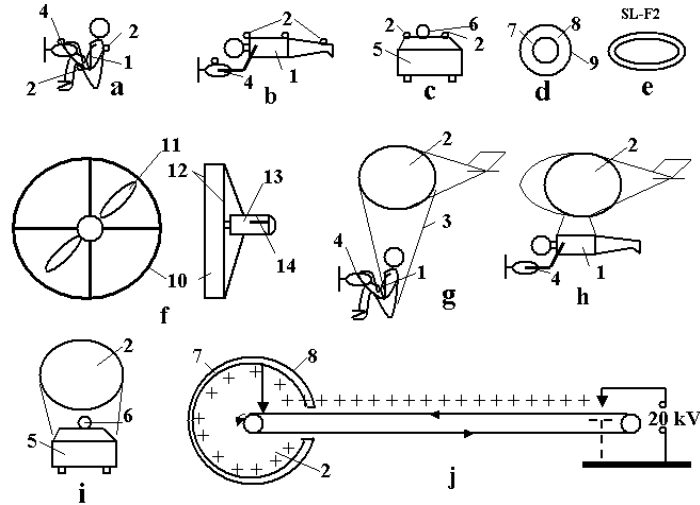
Fig. 15.2. Levitation apparatus: a,b) Single levitated man (mass up to 100 kg) using small highly charged balls 2. a) Sitting position; b) Reclining position; c) Small charged ball for levitating car; d) Small highly charged ball; e) Small highly charged cylindrical belt; f) Small air engine (forward and side views); g) Single levitated man (mass up to 100 kg) using a big non-highly charged ball which doesn't have an ionized zone (sitting position); h) The some man in a reclining position; i) Large charged ball to levitate a car which doesn't have an ionized zone; j) Installation for charging a ball using a Van de Graaff electrostatic generator (double generator potentially reaches 12 MV) in horizontal position. Notations: 1 – man; 2 – charged lifting ball; 4 – handheld air engine; 5 – car; 6 – engine (turbo-rocket or other); 7 – conducting layer; 8 – insulator (dielectric); 9 – strong cover from from artificial fibers or whiskers; 10 – lagging; 11 – air propeller; 12 – preventive nets; 13 – engine; 14 – control knobs.
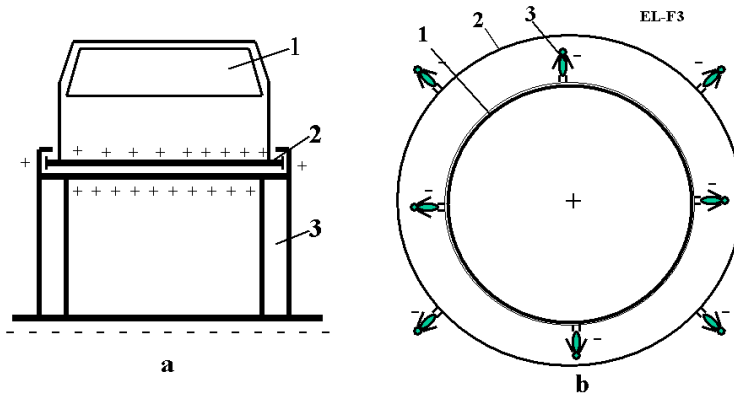
Fig. 15.3. Levitated train on Earth and artificial gravity into and on space ships and asteroids. a) Levitated train; b) Artificial gravity on a space ship. Notation: a) 1 – train; 2 – charged plates; 3 – insulated column; b) 1 – charged space body; 2 – space ship; 3 – man.

A space ship (hotel) definitely needs artificial gravity. Any slight carelessness in space can result in the cosmonaut, instruments or devices drifting away from the space ship. Presently, they are connected to the space ship by cables, but this is not comfortable for working. Science knows only two methods of producing artificial gravity and attractive forces: rotation of space ship and magnetism. Both methods are bad. The rotation creates artificial gravity only inside the space ship (hotel). Observation of space from a rotating ship is very difficult. The magnetic force is only effective over a very short distance. The magnets stick together and a person has to expend a large effort to move (it is the same as when you are moving on a floor smeared with glue).

If then is a charge inside the space ship and small unlike charges attached to object elsewhere, then will fall back to the ship if they are dropped.

The same situation occurs for cosmonauts on asteroids or small planets which have very little gravity. If you charge the asteroid and cosmonauts with unlike electric charges, the cosmonauts will return to the asteroid during any walking and jumping.

The author acknowledges that this method has problems. For example, we need a high electrical intensity if we want to use small charged balls. This problem (and others) is discussed below.

Theory of an electrostatic lift force and results of computations
(in metric system)

 a) Brief information about electric charges, electrical fields, and electric corona. Electric charge creates an electrical field. Every point this field has a vector of magnitude called electrical intensity, E, measured in volts/meter. If the unlike charges (or non-insulated electrodes under voltage) are located in an air atmosphere with a surface atmospheric pressure and the electrical intensity is less than $E_c = (3$ to $4)\times10^6$ V/m, the discharge current will be very small. If $E > E_c = 3\times10^6$ V/m and we have a closed-loop high-voltage circuit (**for non-insulated electrodes**), electric current appears. The current increases following an exponential law when the voltage is increased. In a homogeneous electric field (as between plates), the increasing voltage makes a spark (flashover, breakthrough, lighting). A non-homogeneous electric field (as between a sphere and plate or an open sphere) makes an electric **corona**. Electrons break away from the metal **negative** electrode and ionize the air. Positive ions hit the non-insulated positive electrode and knock out electrons. These unlike ions can cause a particle blockade (discharge) of the main charge. The efficiency of ionization by positive ions is much less than for electrons of the same energy. Most ionization occurs as a result of secondary electrons released at the negative electrode by positive ion bombardment. These electrons produce ionization as they move from the strong field at the electrode out into the weak field. This, however, leaves a positive-ion space charge, which slows down the incoming ions. That has the effect of diminishing the secondary electron yield. Because the positive ion mobility is low, there is a time lag before the high field conditions can be restored. For this reason the discharge is somewhat unstable.

The air contains a small amount of free electrons. These electrons can also create an electric corona around the **positive non-insulated electrode**, but under higher voltage than the negative electrode. The effect here is to enable the free electrons to ionize by collision in the high field surrounding this electrode. One electron can produce an avalanche in such a field, because each ionization event releases an additional electron, which can then could further ionization. To sustain the discharge, it is necessary to collect the positive ions and to produce the primary electrons far enough from the positive electrode to permit the avalanche to develop. The positive ions are collected at the negative electrode, and it is their low mobility that limits the current in the discharge. The primary electrons are thought to be produced by photo-ionization.

The particular characteristics of the discharge are determined by the shape of the electrodes, the polarity, the size of gap (ball), and the gas or gas mixture and its pressure. In high voltage electric lines the corona discharge that surrounds a high-potential power transmission line represents power loss and limits the maximum potential which can be used.

The offered method is very different from the conventional cases described in textbooks. The charges are **isolated** using an insulator (dielectric). They cannot emit electrons in the air. There is not a closed circuit. This method is nearer to single polarity electrets, when like charges are inserted into an insulator[5]. Electrets have typical surface charges of about $\sigma = 10^{-8}$ C/cm^2, PETP up to 1.4×10^{-7} C/cm^2 [p.17][5], and TSD with plasticized PVB up to 1.5×10^{-5} C/cm^2 [p.253][5]. This means the electrical intensity near their surface reaches ($E = 2\pi k\sigma$, $k = 9\times10^9$) 6×10^6 V/m, 80×10^6 V/m, and 8500×10^6 V/m

respectively. The charges are not blockaded and the discharge (half-life time) continues from 100 days up to several years. In humid air the electrets lose part of their properties, but in dry air they regain them.

Natural Earth radioactivity and cosmic rays create about 1.5–10.4 ions into 1 cm^3 every second (see p. 1004)[7]. These ions gradually recombine back into conventional molecules.

In a vacuum the discharge mechanism is different. In non-insulated negative metal electrodes, the electrons may be extracted from the conducting electrode by the strong electric field. The critical surface electric intensity, E_o, is about 100×10^6 V/m at the non-insulated negative electrode. This intensity is about 1000 times more at the positive electrode because the are ions very difficult to tear away from the solid material. Conducting sharp edges increase the electric intensity. That is why it is better to charge the planet or asteroid surface with positive charges. A very sharp spike allows the electrical energy of the charged ball to be regaired.

b) Size of corona (ionized sphere) and safety of a ball of electric intensity. The size of the corona may be found as a spherical area where the electrical intensity is more than safe air intensity

$$E \geq E_c, \quad \frac{kq}{R_c^2} \geq E_c, \quad q = \frac{E_a a^2}{k}, \quad R_c \leq \sqrt{\frac{kE_a a^2}{kE_c}}, \quad \bar{R}_c = \frac{R_c}{a} \leq \sqrt{\frac{E_a}{E_c}} \quad , \tag{15.1}$$

where E – electrical intensity of the charge, [V/m]; E_c – electrical intensity at the beginning of the corona, [V/m], $E_c \approx 3 \times 10^6$; E_a – electrical intensity at the ball surface, [V/m]; a – ball radius, m; R_c – radius of corona, [m]; $k = 9 \times 10^9$.

To find the safe electrical intensity, E_a, for a negatively charged ball in an insulated cover from the point of rupture (spark) into a neutral environmentthe following equation can be used:

$$U \leq U_i, \quad U = \frac{kq}{\varepsilon}\left(\frac{1}{a} - \frac{1}{a+\delta}\right), \quad U_i = \varepsilon E_i \delta, \quad \frac{kq}{\varepsilon}\left(\frac{1}{a} - \frac{1}{a+\delta}\right) \leq \varepsilon E_i \delta, \quad q = \frac{a^2 E_a}{k},$$

$$\bar{\delta} = \frac{\delta}{a} \geq \frac{E_a}{\varepsilon E_i} - 1, \quad for \quad \bar{\delta} = 0, \quad E_a \leq \varepsilon E_i \tag{15.2}$$

where U – ball voltage, [V]; U_i – safe voltage of ball insulator, [V]; E_i – safe electrical intensity of ball insulator, [V/m]; δ – thickness of the ball cover, [m]; ε – dielectric constant.

In equations (15.1) and (15.2) the last formulas are the final result.

Example: The ball is covered by Mylar with E_i = 160 MV/m, ε = 3 (see Table 15.1). Then $E_a = 3 \times 160$ = 480 MV/m, and the relative radius of the ionized sphere [equation (15.1)] is $(480/3)^{0.5}$ = 12.6. If a = 0.05 m, the real radius is R_c = 12.6×0.05 = 0.63 m.

c) For a cylindrical cable or belt. The radius of the corona (ionized cylinder) can be found using the same method:

$$E \geq E_c, \quad E = \frac{2k\tau}{R_c}, \quad \tau = \frac{aE_a}{2k}, \quad \frac{aE_a}{R_c} \geq E_c, \quad R_c \leq a\frac{E_a}{E_c}, \quad \bar{R}_c = \frac{R_c}{a} \leq \frac{E_a}{E_c} \quad , \tag{15.3}$$

where τ is the linear charge, [C/m].

To find using the same method [equation (15.2)] the safe intensity, E_a, for a negatively charged cable (belt, tube) in an insulated cover from point of rupture into a neutral environment the following equation can be used

$$U \leq U_i, \quad U = 2k\tau \ln\left(\frac{a+\delta}{a}\right), \quad U_i = \varepsilon E_i \delta, \quad 2k\tau \ln\left(\frac{a+\delta}{a}\right) \leq \varepsilon E_i \delta, \quad \tau \leq \frac{\varepsilon E_i a\delta / a}{2k\ln(1+\delta/a)},$$

$$for \quad \frac{\delta}{a} \to 0, \quad \bar{\tau} = \frac{\tau}{a} \leq \frac{\varepsilon E_i}{2k}, \quad E_a = k\frac{2\tau}{a}, \quad \frac{\tau}{a} = \frac{E_a}{2k}, \quad \frac{E_a}{2k} \leq \frac{\varepsilon E_i}{2k}, \quad E_a \leq \varepsilon E_i \tag{15.4}$$

d) Discharging by corona. Below, the author makes computations to show how the milliards (10^9 1/m^3) of charged particles influence the main charge.

If 1 m³ of air contains d like-charged (electrons or ions) particles and the charge density is constant, the charge, q, of a sphere with radius r is

$$q = \frac{4}{3}\pi r^3 ed,$$ (15.5)

where $e = 1.6\times10^{-19}$; C – charge of one particle (electron or single charged ion); d –particle density.

On the other side, the main charge, q_o, will be partially blockaded until the intensity at radius r becomes E_c. As a result the equation is

$$q_0 - q = \frac{E_c}{k}r^2, \quad \frac{4}{3}\pi edr^3 + \frac{E_c}{k}r^2 - q_0 = 0,$$ (15.6)

where $k = 9\times10^9$. The equation (15.6) has only one real root. The results of this computation are presented in Figs. 15.4 and 15.5, which show that a large density only decreases the main charge. But only experiments can show what causes this discharge to take place.
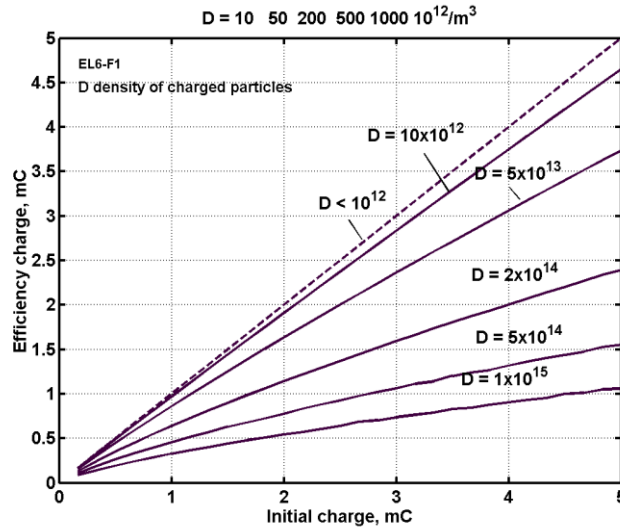

Fig. 15.4. Efficiency charge versus the main charge and density of charged particles in the environment (ionized zone).
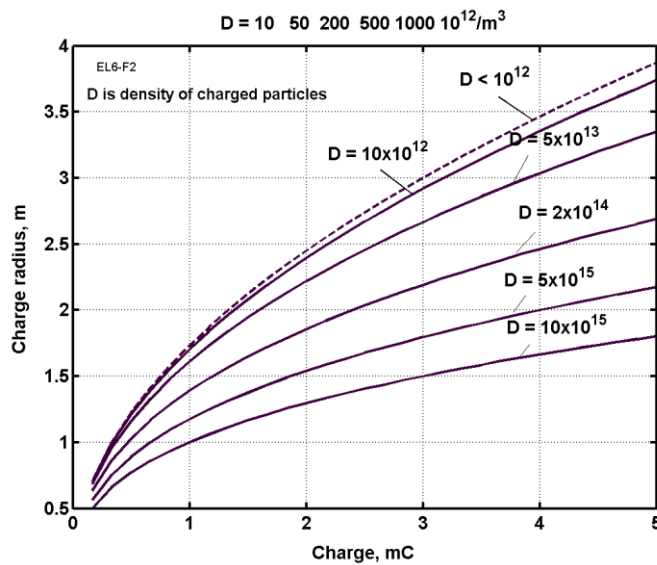

Fig. 15.5. Critical radius of main charge versus the main charge and density of charged particles in the environment (ionized zone).

e) Some data about the ball material. The properties of electrical insulation vary depending on the impurities in the material, temperature, thickness, etc. and different for the same material with a different dieletric. For example, the resistivity of fused quartz is 10^{15} Ohm.cm for $T = 20$ ºC, the resistivity of the quartz fused (from crystal) reaches about 10^{24} Ohm.cm for $T \approx 20$ ºC (see p. 231 and p. 329, fig.20.2 in publication[6]).

Below are properties of some materials recalculated in the metric system (Table 15.1).

Table 15.1. Properties of various good insulators (recalculated in metric system)

Insulator	Resistivity Ohm-m.	Dielectric strength MV/m. E_i	Dielectric constant, ε	Tensile strength kg/mm^2, $\sigma \times 10^7$N/m^2
Lexan	10^{17}–10^{19}	320–640	3	5.5
Kapton H	10^{19}–10^{20}	120–320	3	15.2
Kel-F	10^{17}–10^{19}	80–240	2–3	3.45
Mylar	10^{15}–10^{16}	160–640	3	13.8
Parylene	10^{17}–10^{20}	240–400	2–3	6.9
Polyethylene	10^{18}–5×10^{18}	40–680*	2	2.8–4.1
Poly (tetra-fluoraethylene)	10^{15}–5×10^{19}	40–280**	2	2.8–3.5
Air (1 atm, 1 mm gap)	-	4	1	0
Vacuum (1.3×10^{-3} Pa, 1 mm gap)	-	80–120	1	0

*For room temperature 500–700 MV/m.
** 400–500 MV/m.

Source: Encyclopedia of Science & Technology[9] (Vol. 6, p. 104, p. 229, p. 231).

For small balls, the tensile stress is important for reducing the weight (because like charges tear the ball). The author believes that an artificial fiber having a maximum tensile stress at 500–620 kg/mm^2 (fiber) or whiskers up to 2000 kg/mm^2 is better. These fibers can also be used to strengthen balls insulated by a dielectric (for example, as an additional cover, Fig. 15.2d).

f) The half-life of the charge.

(1) *Spherical ball*. Let us take a very complex condition; where the unlike charges are separated **only** by an insulator (charged spherical condenser):

$$Ri - U = 0, \quad U = \delta E, \quad E = \frac{kq}{\delta^2}, \quad R = \rho \frac{\delta}{4\pi a^2}, \quad U = \frac{q}{C}, \quad R\frac{dq}{dt} + \frac{a}{C} = 0, \quad \frac{dq}{q} = \frac{dt}{RC}, \quad C = \frac{a}{k},$$

$$q = q_0 \exp\left(-\frac{4\pi ak}{\rho\delta}t\right), \quad \frac{q}{q_0} = \frac{1}{2}, \quad -\frac{4\pi ak}{\rho\delta}t_h = \ln\frac{1}{2} = -0.693 \approx -0.7, \quad t_h = 0.693\frac{\rho\delta}{4\pi ka}$$

(15.7)

where: t_h – half-life time, [sec]; R – insulator resistance, [Ohm]; i – current, [A]; U – voltage, [V]; δ – thickness of insulator, [m]; E – electrical intensity, [V/m]; q – charge, [C]; t - time, [seconds]; ρ – specific resistance of insulator, [Ohm-meter, Ωm]; a – internal radius of the ball, [m]; C – capacity of the ball, [C]; $k = 9\times10^9$.

Example: Let us take typical data: $\rho = 10^{19}$ Ω-m, $k = 9\times10^9$, $\delta/a = 0.2$, then $t_h = 1.24\times10^6$ seconds = 144 days.

(2) *Half-life of cylindrical tube.* The computation is same as for tubes (1 m charged cylindrical condenser):

$$q = q_0 \exp\left(-\frac{1}{RC}t\right), \quad C = \frac{1}{k \ln(1+\delta/a)}, \quad R = \frac{\rho\delta}{2\pi a}, \quad -0.693 = -\frac{1}{RC}t_h, \quad t_h = \frac{0.693\rho\delta}{2\pi ka \ln(1+\delta/a)},$$

$$\text{for} \quad \frac{\delta}{a} \to 0, \quad t_h \approx 0.7\frac{\rho}{2\pi k}. \tag{15.8}$$

g) Rupture (breakthrough) of insulator. The breakthrough of a ball can only occur when the charge contacts an unlike charge or conducting material. The voltage between the charges must be less than $U = \delta U_r$, where U_r is the breakthrough voltage for a given insulator and δ is the thickness of the insulator. For a good insulator this is up to $U_r \approx 700$ million V/m, for thin mica it as up to $U_r = 1000$ million V/m.

h) **Levitation between flat net and ground surface** (Fig. 15.1d). This is the simplest for both utilization and computation. The top of the column contains the insulated metallic net with a high voltage (it may be a direct current electricity line). This induces the opposite charge in the Earth and powers the static electric field. The man (car) has charged balls or a balloon with like charges to the Earth's charge. These balls repel from the Earth's surface (charges) and support the man (car) in the air.

The lifting force, L, and radius, a, of a small lifting balloon with charge q can be computed by the equations:

$$L = qE_0, \quad E_a = k\frac{q}{a^2}, \quad a = \sqrt{k\frac{q}{E_a}} = \sqrt{\frac{kMg}{E_a E_0}}, \quad U = E_0 h, \tag{15.9}$$

where E_o – electrical intensity between the net and the Earth's surface [V/m]; E_a – electrical intensity at the ball's (balloon) surface from the internal ball (balloon) charge [V/m]; a – internal radius of ball (balloon) [m]; M – mass of the flight vehicle (man, car); $g = 9.81$ m/s^2 – Earth's gravity; U – voltage between the net and Earth [V]; h – altitude of the net [m].

Examples. Assume $E_o = E_a = 2.9 \times 10^6$ V/m, the man's mass is $M = 100$ kg, and the car's mass is 1000 kg. The radius of a single support balloon will be $a \approx 1.1$ m for the man and $a \approx 3.3$ m for the car, respectively. Note that this voltage is lower than the discharge voltage for a non-insulated conductor and the ionized zone is absent. We can change the single balloon to some small highly charged balls or a belt with an ionized zone.

The flying vehicles can be protected from contact with the top net by a dielectric (insulator) safety net located below the top net (Fig. 15.1d, mark 7).

i) Electrostatic levitation of a train (Fig. 15.3a). Two identically charged closed plates of area S have a repelling force L:

$$L = 2\pi k\sigma_c^2 S, \tag{15.10}$$

where σ_c is surface charge density [C/m^2].

For example, two 1 m^2 plates with identical charge $\sigma_c = 2 \times 10^{-4}$ C/m^2 will have a specific lift force of $L = 2260$ N/m^2 = 226 kgf/m^2. Conventional electrets have $\sigma_c = 10^{-4} - 1.4 \times 10^{-3}$ C/m^2 charge and can be used for a non-contact train.

j) Top tube highway. The parameters of a tube highway can be calculated by the following equations:

$$\tau = \frac{aE_a}{2k}, \quad E_0 = \frac{4k\tau}{h}, \quad \frac{E_0}{E_a} = \frac{a}{h}, \quad C_1 \approx \frac{1}{2k\ln(2h/a)}, \quad U = \frac{\tau}{C_1}, \quad W = \frac{\tau^2}{2C_1},$$

$$\text{for} \quad \tau = const \quad F_h = \frac{\partial W}{\partial h} = \frac{2k\tau^2}{h}, \quad F_a = \frac{\partial W}{\partial a} = -\frac{2k\tau^2}{a} \tag{15.11}$$

where: τ – the linear charge of 1 meter of tube [C/m]; a – radius of tube cross section [m]; E_a – electric intensity at tube surface [V/m]; E_0 – electrical intensity at the Earth's surface at a point under the tube [V/m], for other points $E = E_0\cos^3\alpha$ where α is the angle between a vertical line from the tube center and a line to a given point (electric lines are perpendicular to the Earth's surface, there is no lateral acceleration); h – altitude [m]; $k = 9\times10^9$ – coefficient [Nm²/C²]; C_1 – capacity of 1 meter of tube [C/m] [see p. 64][8]; U – voltage [V]; W – electrical energy of 1 meter of tube [J/m]; F_h – electric force of 1 meter of tube between the tube and the Earth's surface [N/m]; F_a – radial tensile force of 1 meter of tube [N/m].

The thickness and mass of the top tube (with a thin cover) are given by

$$F_a = -2\sigma\delta, \quad \delta = \frac{k\tau^2}{a\sigma}, \quad M_1 = 2\pi\gamma a\delta, \tag{5.12}$$

where σ – safe tensile stress of tube cover [N/m²]; δ – thickness of the tube cover [m]; M_1 – mass of 1 m of tube cover [kg/m]; γ – density of tube cover [kg/m³].

The lift force of the tube as an air balloon filled by helium can be computed by the equation

$$F_L = (\rho - \rho_g)\pi a^2 \overline{\rho}(h)g, \tag{15.13}$$

where $\rho = 1.225$ kg/m³ – air density; ρ_g – filling gas density (for helium $\rho_g = 0.1785$ kg/m³); a – radius of tube [m]; $\overline{\rho}(h)$ – relative air density at altitude, for $h = 0$ km the $\overline{\rho}(h) = 1$, for 1 km $\overline{\rho}(h) = 0.908$. Note that E_c decreases in proportional to the atmospheric density. Unfortunately, the attractive electric force F_h in many cases is more than the air lift force F_L.

See the example computation in project 2.

k) Spherical main ball on mast and air balloon. The parameters of charges of the main ball and spherical balloon can be calculated using the following equations

$$E_a = k\frac{q}{a^2}, \quad E_0 = k\frac{2q}{h^2}, \quad \frac{E_0}{E_a} = 2\left(\frac{a}{h}\right)^2, \quad C = \left[k\left(\frac{1}{a} - \frac{1}{2h-a}\right)\right]^{-1} \approx \frac{a}{2k}, \quad U \approx \frac{kq}{a}, \quad W = \frac{q^2}{2C},$$

$$for \quad q = const, \quad F_h = \frac{\partial W}{\partial h} = -\frac{kq^2}{4h^2} \tag{15.14}$$

where q – the charge of air balloon (sphere) [C]; a – radius of air balloon [m]; E_a – electrical intensity at the balloon's surface [V/m]; E_o – electrical intensity at the Earth's surface at a point under the balloon [V/m], for other points $E = E_0\cos^3\alpha$ where α is the angle between a vertical line from the balloon center and a line to a given point (electric lines are perpendicular to the Earth's surface, there is no lateral acceleration); h – altitude [m]; $k = 9\times10^9$ – coefficient [Nm²/C²]; C – capacity of balloon [C]; U – voltage [V]; W – electrical energy of the balloon [J]; F_h – electrical force between the balloon and the Earth's surface [N].

The thickness and mass of the top atmospheric air balloon as a spherical capacitor 1 m (with a thin cover) are

$$F_a = \frac{\partial W}{\partial a}, \quad W = \frac{q^2}{2C}, \quad c = \frac{a}{k}, \quad for \quad q = \frac{a^2 E_a}{k} = const, \quad F_a = -\frac{kq^2}{2a^2} = -\frac{(aE_a)^2}{2k},$$

$$p = -\frac{F_a}{4\pi a^2} = \frac{E_a^2}{8\pi k}, \quad \pi a^2 p = 2\pi a\delta\sigma, \quad \delta = \frac{ap}{2\sigma} = \frac{aE_a^2}{8\pi k}, \quad M_b = 4\pi a^2\gamma\delta = \frac{a^3 E_a^2\delta}{4k\sigma}, \tag{15.15}$$

where σ – safe tensile stress of the balloon cover [N/m²]; δ – thickness of the balloon cover [m]; M_b – mass of the balloon cover [kg]; γ – density of the balloon cover [kg/m³]; p – internal pressure under like charges [N/m²].

The lift force of the air balloon filled by helium can be computed using the equation

$$F_L = \frac{4}{3}(\rho - \rho_g)\pi a^3 \overline{\rho}(h)g, \tag{15.16}$$

where ρ = 1.225 kg/m³ – air density; ρ_g – filling gas density (for helium ρ_g = 0.1785 kg/m³); a – radius of balloon [m]; $\overline{\rho}(h)$ – relative air density at altitude, for $h = 0$ km the $\overline{\rho}(h) = 1$, for 1 km $\overline{\rho}(h) = 0.908$. In many cases the attracted electric force F_h is more than the air lift force F_L. See the computation in Project 3.

l) Small spherical lifting balls. Assume the electrical intensity of the main top charge is significantly more then the lifting charges. The parameters of large spherical balls with thin covers can be computed using the equations above. The parameters of small balls with thick covers can be computed using the following equations

$$L = nqE_0, \quad q = CU, \quad C = \frac{r}{k}, \quad U = aE_a, \quad q = \frac{a^2 E_a}{k}, \quad L = n\frac{a^2 E_a E_0}{k}, \quad (15.17)$$

where L – total lift force [N]; n – number of balls; E_a – electrical intensity at the ball surface from electrical charge of the ball q [C]; a – internal radius of the ball [m].

The thickness and mass of the ball (with a thick cover) are

$$p_b = \frac{E_a^2}{8\pi k}, \quad \sigma = \frac{p_b}{(R/a)^2 - 1} = \frac{E_a^2}{8\pi k[(R/a)^2 - 1]}, \quad (R/a)^2 - 1 = \frac{E_a^2}{8\pi k\sigma}, \quad M_b = \frac{4}{3}\pi\gamma a^3\left(\frac{R^3}{a^3} - 1\right), \quad (15.18)$$

where $R = a + \delta$ – external radius of ball [m]; σ – safe tensile stress of the ball material [N/m²]; δ – thickness of the ball cover [m]; M_b – mass of the ball cover [kg]; γ – density of the ball cover [kg/m³]. Results of this computation are in Figs. 15.6 to 15.9. Notice that the lifting balls have a large ratio of lift force/ball mass, about 10,000–20,000.

m) Long ($a \ll l$) cylindrical lifting belt. The maximum charge and mass of a 1 meter long cylindrical lifting belt may be computed using the following equations (from (15.11))

$$L = E_0\tau l, \quad 2\sigma\delta = F_a, \quad F_a = \frac{2k\tau^2}{a}, \quad \tau = \sqrt{\frac{a\delta\sigma}{k}}, \quad q = \tau l, \quad M_1 = 2\pi\gamma a\delta, \quad M = M_1 l, \quad E_a = k\frac{2\tau}{a},$$

$$(15.19)$$

where τ – charge of 1 meter [C/m]; a – internal radius of the belt cross-section area [m]; δ – thickness of the belt [m]; σ – safe tensile stress of the belt cover [N/m²]; q – charge of the belt [C]; l – length of the belt [m]; M – mass of the belt [kg]; E_a – electrical intensity of the belt surface [V/m]; F_a – electrostatic force in the tube [N] [see equation (15.11)]; γ – density of belt cover [kg/m³]. Computations are presented in Fig. 15.10 and 15.11. See also example computation in project 3.

n) Aerodynamics of the levitated vehicles. The drag, D, (required thrust, T) and required power of
the levitated person, car and vehicles can be computed by the following equations

$$(15.20)$$

$$T = D = C_D\frac{\rho V^2}{2}S, \quad W = \frac{VD}{\eta}, \quad a = \frac{T}{M},$$

where C_D – aerodynamic drag coefficient, for a sitting person $C_D \approx 0.5$, for a lying man $C_D \approx 0.3$, for a car $C_D \approx 0.25$, for a sphere $C_D \approx 0.1$– 0.2 (depending on the size and speed), for a dirigible $C_D \approx 0.06 – 0.1$; $\rho = 1.225$ kg/m³ – standard air density; V – speed [m/s]; S – vehicle cross section area [m²]; W – required power [W]; η – propeller coefficient of efficiency, $\eta = 0.7 – 0.8$.

For example, a flying person ($S = 0.3$ m²) has D = 5.5 N for speed $V = 10$ m/s (36 km/hour). He only needs a small motor, W = 0.073 kW.

o) Control and stability. Control is accomplished using the direction (and magnitude) of motor thrust (and variable torque) and the charging and discharging of lifting charges. The levitated vehicle will be stable in a vertical position if its center of gravity is lower than the center of levitation (lift) force. The dipole moment of the particular vehicle's design can give additional stability. Note that electric lines are vertical at the Earth's surface (Figs. 15.1d,e,f,g), which means that the lift force is vertical.

p) Flight in thunderstorms. Thunderstorms produce an electric field of about 300,000 to 1,000,000 V/m. This field can be used for levitation.

q) Charging. In the author's opinion, the easiest method of charging and maintaining the charge is by using a Van de Graaff electrostatic generator (Fig. 15.2j). Any other high voltage generation devices can also be used.
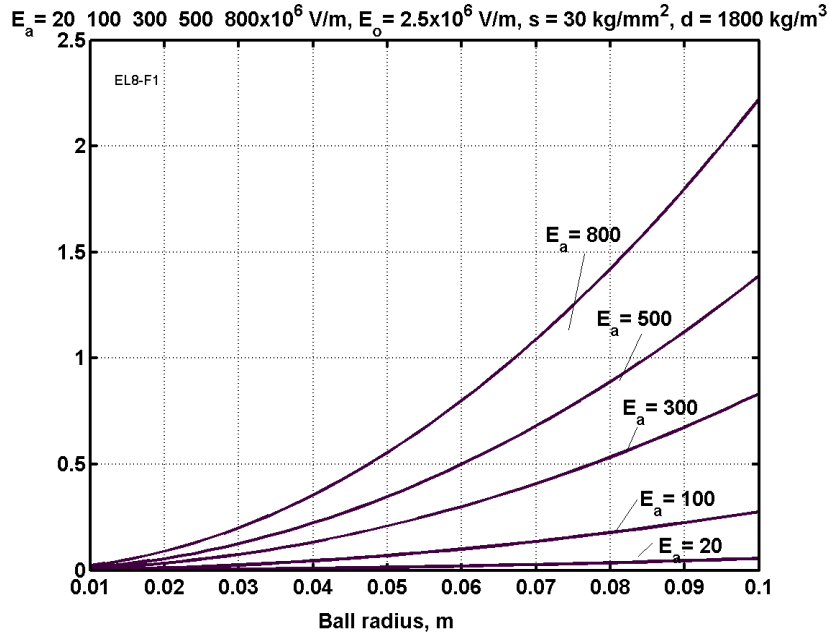

Fig. 15.6. Electrostatic lift force (kN) of small lifting ball versus radius of ball for the electrical intensity of the ball's surface $E_a = (20–800) \times 10^6$ V/m, general electrical intensity $E_o = 2,5 \times 10^6$ V/m, safe tensile stress of the ball cover 30 kg/mm^2, specific density of the ball cover 1800 kg/m^3.
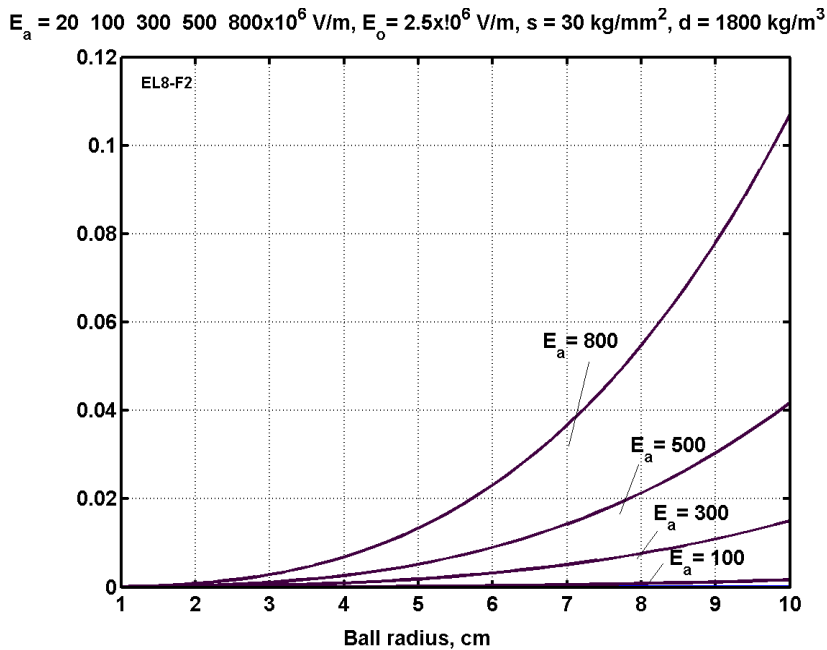

Fig. 15.7. Mass (kg) of small lifting ball versus radius of ball for the electrical intensity of the ball's surface $E_a = (100–800) \times 10^6$ V/m, general electrical intensity $E_o = 2.5 \times 10^6$ V/m, safe tensile stress of the ball cover 30 kg/mm^2, specific density of the ball cover 1800 kg/m^3.
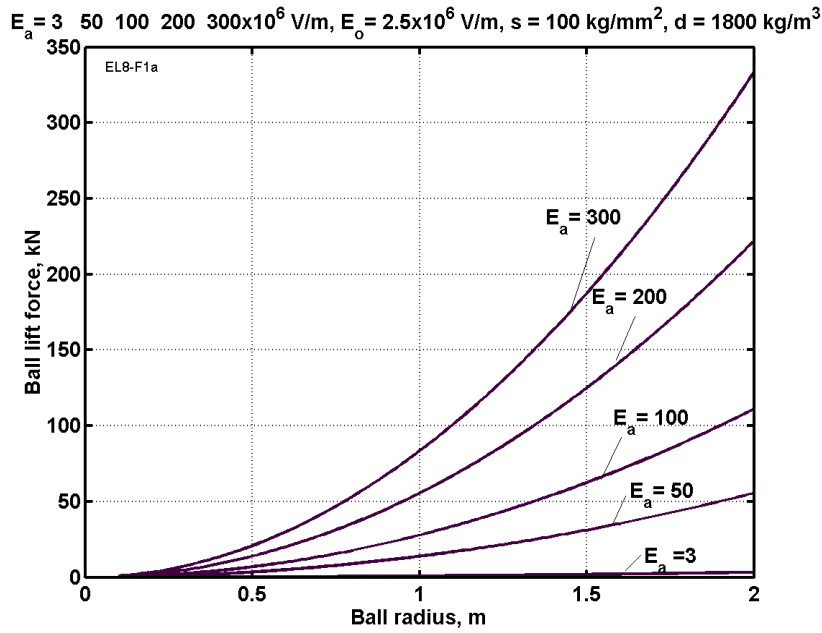
Fig. 15.8. Electrostatic lift force (kN) of the lifting ball versus radius of ball for the electrical intensity of the ball's surface $E_a = (3–300) \times 10^6$ V/m, general electrical intensity $E_o = 2.5 \times 10^6$ V/m, safe tensile stress of the ball cover 100 kg/mm², specific density of the ball cover 1800 kg/m³.
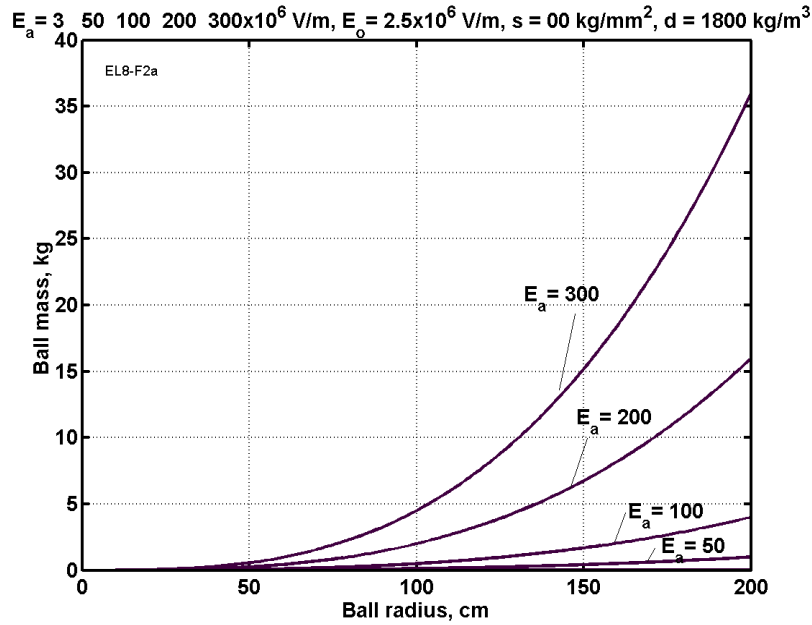

Fig. 15.9. Mass (kg) of the lifting ball versus radius of ball for the electrical intensity of the ball's surface $E_a = (3–300) \times 10^6$ V/m, general electrical intensity $E_o = 2.5 \times 10^6$ V/m, safe tensile stress of the ball cover 100 kg/mm², specific density of the ball cover 1800 kg/m³.
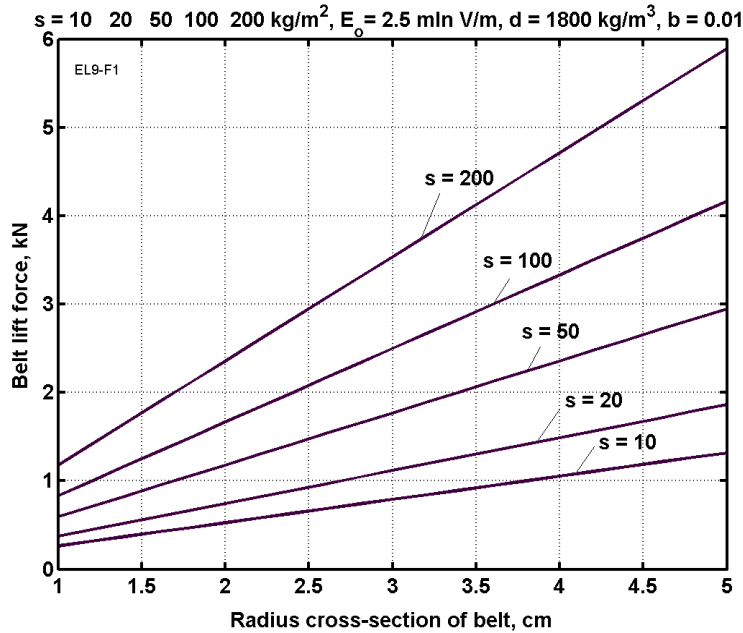
Fig. 15.10. Electrostatic lift force (kN) of a 1 m small lifting belt via radius of ball cross-section area for general electrical intensity $E_o = 2.5 \times 10^6$ V/m, safe tensile stress of the ball cover 10–200 kg/mm², $\sigma = (10–200) \times 10^7$ N/m², density of ball cover $\gamma = 1800$ kg/m³.
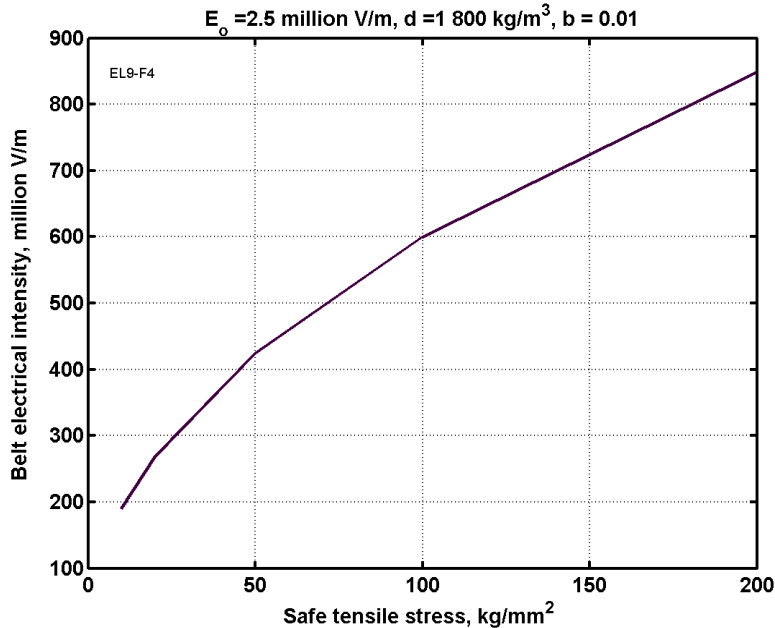
Fig. 15.11. Belt electrical intensity via safe tensile stress for general electrical intensity $E_o = 2.5 \times 10^6$ V/m, safe tensile stress of the ball cover 10–200 kg/mm², $\sigma = (10–200) \times 10^7$ N/m²; γ – specific density of ball cover 1800 kg/m³, relative thickness of belt cover, $\delta = 0.01 \times a$.

r) Safety. It is not known exactly how static fields of electrical intensity affect a human body. People in an electric field of about 300,000 to 1,000,000 V/m during a thunderstorm or under high voltage electrical lines feel normal. The inside space of a conventional car with a metal body (or conductive paint) does not have an electric field. The Museum of the Massachusetts Institute of Technology (MIT) shows people inside metal shells, under high voltage, and surrownded by lightning. People can wear clothes armored by conductive filaments as a defense against the electric field.

s) Charged ball as an accumulator of energy. The energy required to charge a ball (accumulate at in the ball) can be calculated by the following equations

$$W = \frac{1}{2}\frac{q^2}{C}, \quad C = \frac{a}{R}, \quad E_a = k\frac{q}{a^2}, \quad q = \frac{a^2 E_a}{k}, \quad W = \frac{1}{2}\frac{a^3 E_a^2}{k}, \tag{15.21}$$

where W is energy [J].

The ball mass at safe stress levels with repelling charges can be calculated using equation (15.17)

$$\left[\left(\frac{R}{a}\right)^2 - 1\right] = \frac{E_a^2}{8\pi k\sigma}, \quad \left(\frac{R}{a}\right) = \sqrt{\frac{E_a^2}{8\pi k\sigma} + 1}, \quad M = \frac{4\pi\gamma a^3}{3}\left[\left(\frac{R}{a}\right)^3 - 1\right], \quad \frac{W}{M} = \frac{3E_a^2}{8\pi\gamma k\left[(R/a)^3 - 1\right]}, \tag{15.22}$$

where M – mass [kg]; σ – safe tensile stress of the ball cover [N/m²]; γ – specific density of the ball cover [kg/m³]; $R = a + \delta$ – external radius of the ball [m].

The accumulated relative energy for $\sigma = 200$ kg/mm² may be close to conventional powder and last a lot langer than electrical energy in a typical condenser. This electrical energy can be reclaimed (by using a sharp spike) or used for launching or accelerating space vehicles if we take two like charges (balls) and allow them to repel each other. This method of transforming electrical energy into thrust may be more useful than the thrust from a conventional electric space engine because one can create a big thrust by utilizing space masses (asteroids).

Projects

Let us estimate the main parameters for some offered applications. Most people understand the magnitudes and properties of applications better than theoretical reasoning and equations. The suggested application parameters are not optimal, but our purpose is to show the method can be utilized by current technology.

1. Levitation Highway (Fig.15.1d).

The height of the top net is 20 m. The electrical intensity is $E_o = 2.5 \times 10^6$ V $< E_c = (3-4) \times 10^6$ V. The voltage between the top net and the ground is $U = 50 \times 10^6$ V. The width of each side of the road is 20 m. We first find the size of the lifting ball for the man (100 kg), car (1000 kg), or track (10,000 kg). Here R_c is the radius of the ionized zone [m]:

1) Flying man (mass $M = 100$ kg, $\varepsilon = 3$, $E_i = 200 \times 10^6$ V/m, g ≈ 10 m/s²)

$$E_a \leq \varepsilon E_i = 3 \times 200 \times 10^6, \quad a = \sqrt{\frac{kMg}{E_0 E_a}} = \sqrt{\frac{9 \times 10^9 \times 100 \times 10}{2,5 \times 10^6 \times 6 \times 10^8}} \approx 0.08 \, m, \quad R_c = \sqrt{\frac{E_a}{E_c}} \approx 1 \, m.$$

Notice that the radius of a single ball supporting the man is only 8 cm, or the man can use two balls $a = 5$–6 cm., R_c=0.75 m (or even more smaller balls). If the man uses a 1 m cylindrical belt, the radius of the belt cross-section area is 1.1 cm, $\sigma = 100$ kg/mm², $E_a = 600 \times 10^6$ V/m (Figs. 15.10 and 15.11). The belt may be more comfortable for some people.

2) With the same calculation you can find that a car of mass $M = 1000$ kg will be levitated using a single charged ball $a = 23$ cm, $R_c = 3.2$ m (or two balls with $a = 16$ cm. $R_c = 2.3$ m).

3) A truck of mass $M = 10,000$ kg will be levitated using a single charged ball $a = 70$ cm, $R_c = 10$ m (or two balls with $a = 0.5$ m. $R_c = 7$ m).

2. Levitating tube highway

Assume the levitation highway has the design of Fig.15.1f,g where the top net is changed to a tube. Take the data $E_o = 2.5 \times 10^6$ V $< E_c = (3-4) \times 10^6$ V, $E_a = 2 \times 10^8$ V/m, $h = 20$ m. This means the electrical intensity, E_o, at ground level is the same as in the previous case. The required radius, a, of the top tube is

$$\frac{a}{h} = \frac{E_0}{2E_a} = 0.00625, \quad a = 0.00624h = 0.125 \, m, \quad R_c = a\frac{E_a}{E_0} = 10 \, m \, .$$

The diameter of the top tube is 0.25 m, the top ionized zone has a radius of 10 m.

3. Charged ball located on a high mast or tower

Assume there is a mast (tower) 500 m high with a ball of radius $a = 32$ m at its top charged up to $E_a = 3 \times 10^8$ V/m. The charge is

$$q = \frac{a^2 E_a}{k} = 34 \, C, \quad E_0 = k\frac{2q}{h^2} = 2.45 \times 10^6 \, V/m \quad .$$

This electrical intensity at ground level means that within a radius of approximately 1 km, people, cars and other loads can levitate.

4. Levitation in low cumulonimbus and thunderstorm clouds

In these clouds the electrical intensity at ground level is about $E_o = 3 \times 10^5 - 10^6$ V/m. A person can take more (or more highly charged) balls and levitate.

5. Artificial gravity on space ship's or asteroids

Assume the space ship is a sphere with an inner radius at $a = 10$ m and external radius of 13 m. We can create the electrical intensity $E_o = 2.5 \times 10^6$ V/m without an ionized zone. The electrical charge is $q = a^2 E_o/k = 2.8 \times 10^{-2}$ C. For a man weighing 100 kg (g = 10 m/s², force $F = 1000$ N), it is sufficient to have a charge of $q = F/E_o = 4 \times 10^{-4}$ C and small ball with $a = 0.1$ m and $E_a = qk/a^2 = 3.6 \times 10^8$ V/m. In outer space at the ship's surface, the artificial gravity will be $(10/13)^2 = 0.6 = 60\%$[10] of g.

6. Charged ball as an accumulator of energy and rocket engine

The computations show the relative W/M energy calculated from safe tensile stress does not depend on E_a. A ball cover with a tensile stress of $\sigma = 200$ kg/mm² reaches 2.2 MJ/kg. This is close to the energy of conventional powder (3 MJ/kg). If whiskers or nanotubes are used the relative electrical storage energy will be close to than of liquid rocket fuel.

Two like charged balls repel one another and can give significant acceleration for a space vehicle, VTOL aircraft, or weapon.

Discussion

Electrostatic levitation could create a revolution in transportation, building, entertainment, aviation, space flights, and the energy industry.

The offered method needs development and testing. The experimental procedure it is not expensive. We just need a ball with a thin internal conducting layer, a dielectric cover, and high voltage charging equipment. This experiment can be carried out in any high voltage electric laboratory. The proposed levitation theory is based on proven electrostatic theory. There may be problems may be with

discharging, blockage of the charge by the ionized zone, breakdown, and half-life of the discharge, but careful choice of suitable electrical materials and electric intensity may be also to solve them. Most of these problems do not occur in a vacuum.

Another problem is the affects of the strong electrostatic field on a living organism. Only experiments using animals can solve this. In any case, there are protection methods – conducting clothes or vehicle is (from metal or conducting paint) which offer a defense against the electric field.

Other related ideas from the author are shown in the References[10–13].

References

1. Bolonkin, A.A., Installation for creating open electrostatic field, Patent applications #3467270/21 116676, 9 July 1982. USSR Patent office.
2. Bolonkin, A.A., (Electrostatic) method for tensing of films. Patent application #3646689/10 138085, 28 September 1983. USSR Patent office.
3. Bolonkin, A.A., "Aviation, Motor, and Space Design", Collection *Emerging Technology in the Soviet Union*, pp.32-80, Delphic Ass., 1990. USA.
4. Shortley, G., Williams, D., *Elements of Physics*, 5th Edn., Prentice-Hall, Inc., New Jersey, USA.
5. Kestelman, V.N., Pinchuk, L.S., Goldale, V.A., *Electrets in Engineering, Fundamentals and Applications*. Klumer Academic Publisher, 2000.
6. Kikoin, I.K., (ed.), *Tables of physical values, Directory*, Atomisdat, Moscow, 1976 (in Russian).
7. Koshkin, N.I., Shirkevich, M.G., *Directory of Elementary Physics*, Nauka, Moscow, 1982 (in Russian).
8. Kalashnikov, C.K., *Electricity*, Nauka, Moscow, 1985 (in Russian).
9. *McGraw-Hill Encyclopedia of Science & Technology*.
10. Bolonkin, A.A., "Electrostatic Utilization of Asteroids for Space Flight", AiAA-2005-4032. 41 Joint Propulsion Conferences, 10–13 July, 2005, Tucson, Arizona, USA.
11. Bolonkin A.A., "Electrostatic Solar Wind Propulsion System", AIAA-2005-4225. 41 Joint Propulsion Conferences, 10-13 July, 2005, Tucson, Arizona, USA.
12. Bolonkin, A.A., "Kinetic Anti-Gravitator", AIAA-2005-4505, 41 Joint Propulsion Conferences, 10-13 July, 2005, Tucson, Arizona.
13. Bolonkin, A.A., "Sling Rotary Space Launcher", AIAA-2005-4035, 41 Joint Propulsion Conferences, 10-13 July, 2005, Tucson, Arizona.

Chapter 16
Guided Solar Sail and Energy Generator*

Summary

A solar sail is a large thin film mirror that uses solar energy for propulsion. The author proposed innovations and a new design of Solar sail in 1985[1]. This innovation allows (main advantages only): 1. An easily controlled amount and direction of thrust without turning a gigantic sail; 2) Utilization of the solar sail as a power generator (for example, electricity generator); 3) Use of the solar sail for long-distance communication systems.

Description of method and innovations
Introduction

Solar sails are composed of large flat smooth sheets of very thin film, supported by ultra-lightweight structures. The side of the film which faces the sun is coated with a highly reflective material so that the resulting product is a huge mirror, typically about the size of a football field (see Fig. 16.1). The force generated by the sun shining on this surface is about equal to the weight of a letter sent via first class mail. Even though this is a very tiny force, it is perpetual, and over days, weeks, and months, this snail-paced acceleration results in the achievement of velocities large enough to overtake and pass the Voyagers and Pioneers that are now speeding away through the outer reaches of our solar system.

Fig. 16.1. **Artist's conception of a solar sail**

NASA has a program in place to develop solar sail technology to a point where it can be used to implement important space exploration missions. There are a number of missions on the NASA strategic roadmap that require this type of propellantless propulsion to achieve their objectives. There

are other classes of missions that are greatly enhanced by solar sails because these vehicles are inexpensive to construct and can deliver such high performance propulsion.

There are important applications for solar sails beyond the science missions that NASA has planned. The National Oceanic and Atmospheric Administration (NOAA) needs this technology to create a new class of space and earth weather monitoring stations that can provide greater coverage of the earth and provide better advance warning of the solar storms that sometimes plague communications and electrical power grids. There are also a number of military missions in earth orbit that can be enabled by low cost sailcraft.

Solar sailing is a method of converting light energy from the sun into a source of propulsion for spacecraft. In essence, a solar sail is a giant mirror that reflects sunlight in order to transfer the momentum from light particles (photons) to the object one is interested in propelling. Since the phrase "solar sails" is often confused with "solar cells", which is a technology for converting solar light into electrical energy, we will use the term "light sail" for the purpose of this discussion.

Solar radiation pressure = 9.12 $\mu N/m^2$

The light sail material must be as thin and lightweight as possible. Conventional light sail film has comprised 5 micron thick aluminized mylar or kapton with a thin film aluminum layer (approximately 100 nm thick) deposited on one side to form a mirror surface with 90% reflectivity.

For 5 micron thick mylar, which has an areal density of 7 g/m^2, the acceleration would be 1.2 mm/s^2. This acceleration results in a daily velocity increase of about 100 m/s, a velocity which is useful for maneuvering around the solar system. Although mylar is inexpensive and readily available in 0.5 micron thickness, it is not ideal sail film material because it is easily degraded by the sun's ultraviolet radiation. The other key contender, kapton, can withstand ultraviolet radiation but isn't available in layers much thinner than 8 μm, with a resulting area density of 12 grams per square meter.

A solar sail is a spacecraft with a large, lightweight mirror attached to it that moves by being pushed by light reflecting off the mirror instead of using rockets. The light to push a sail can come from the Sun or large lasers we could build. Satellites in orbit around the Earth can survive for many years without any maintenance while using only a small amount of rocket propellant to hold their positions. Solar sails can be made to survive in space for many years as well. But, because solar sails use sunlight that never runs out like rocket propellant, during those years the sail can move around as much as you want it to, such as from the Earth to Mars and back, possibly several times if the sail remains in good condition. A similarly equipped rocket would either be ridiculously huge because it has to carry the fuel for each trip, or would need to be refueled regularly.

Sunlight exerts a very gentle force. The power of sunlight in space at the Earth's distance from the Sun is between 1.3–1.4 kilowatts per square meter. When you divide 1.4 kilowatts by the speed of light, about 300 million meters per second, the result is very small. A square mirror of side 1 kilometer would only receive about 9 newtons.

Light pressure is $P = E/c$ if the light is absorbed (black surface) and $P = 2E/c$ if the light is reflected (mirror). Here E is light energy, $c = 3\times10^8$ m/s is light speed.

There are three major designs used for light sail construction (Fig. 16.2):

- Three axis stabilized sails which require booms to support the sail material.
- Heliogyro sails, which are bladed like a helicopter and must be rotated for stability.
- Disk sails which must be controlled by moving the center of mass relative to the center of pressure.

Fig. 16.2. Design of light sail

A practical sail places great demands on our physical construction capabilities. The sail must be as large as possible so that it can collect enough light to gain a useful thrust. At the same time it must be as light weight as possible. This implies an extremally thin sail film with minimal mass. Finally, it must be durable enough to with stand a wide range of temperature changes, charged particles, and micrometeoroid hazards. A laser beam may be used for moving the solar sail[3-11].

Description of innovation and their advantages

The proposedd innovation of a solar sail[1] is presented in Fig. 16.3. Theory developed in author publication[2] may be useful for flight analysis. The solar sail contains: a space ship, 1, a spherical reflector, 2, a mirror, 5, and additional devices to support spherical reflector, control the thrust direction, and convert the light energy into electricity and additional thrust.
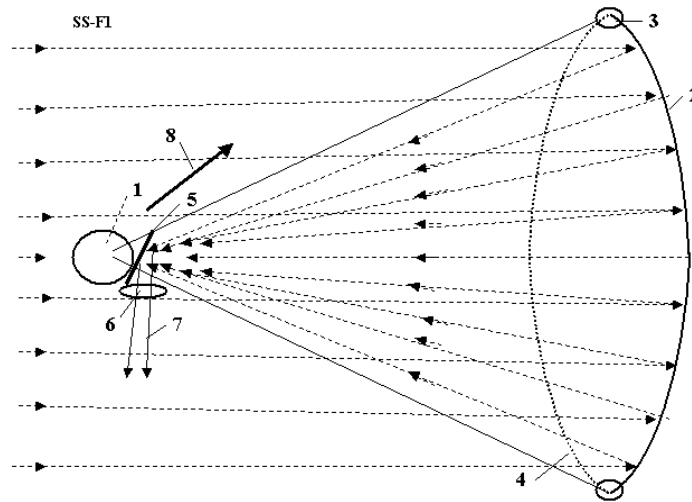

Fig. 16.3. proposed guided solar sail and electricity generator. Notations are: 1 – space ship; 2 – thin film reflector; 3 – inflatable (or electrically charged) toroid which support the reflector in an open (unfolded)

position; 4 – transparent thin film or light charged net which support the spherical form of the reflector; 5 – control mirror, which guides thrust direction; 6 – lens or trap for communication; 7 – reflected beam (located at the center of the ship's mass). 8 – direction of thrust.

The suggested propulsion system works in the following way. The reflector, 2, focuses the sunlight into the control ship mirror, 5, located at the spaceship's center of mass. We are able to change the position of this mirror, send the focused beam in the right direction and achieve the necessary thrust direction without turning the space sail because the space sail is large, turning it is very complex problem, but this problem is avaided in the suggested design.

If we direct the solar beam into the ship, we can convert the huge solar energy into any other sort of energy, for example, into electricity using a conventional method (solar cell or heat machine). A reflector of 100×100 m^2 produces 14,000 kW energy at 1 AU. The developed ion thrusters are very efficient and have a high specific impulse, but they need a great amount of energy. We have this energy in the proposed sail and can increase the thrust over time.

The offered system can be also used for long distance communication by sending a focused beam is to the Earth and transmitting the necessary information.

The author has also proposed a method using surface tension of a solar sail and a solar mirror[10].

The suggested revolutionary propulsion system uses current technology and may be produced in the near future but needs detailed research and computation.

Further development

Initial attempts to improve sail acceleration failed to take future development into account because they focused only on developing the lowest density film material possible. For example, researchers anticipate a 25 times improvement over the baseline mylar design described above by removing the plastic substrate and leaving the 100 nm Al layer. Reducing the aluminum thickness from 100 nm to 4 or 5 nm would yield another factor of 12, resulting in a net 300 times increase in sail acceleration. The trade off, of course, is that the reflectivity goes down for such a thin metal film thereby driving one to use longer wavelengths such as microwaves. Perforating the aluminum metal sail pushes this number somewhere between 500 times and 5000 times. More recently, nanotubes, a meshwork of interlocking carbon fibers which can provide stiff, but extremely lightweight support for the sail coating, are being explored. Since carbon is relatively impervious to solar-radiation damage and has a higher melting point than aluminum, nanotubes are thought to have high potential for providing a significant breakthrough for light sail development; potentially yielding factors of 10,000 to 100,000 in Earth orbit acceleration. One concept, gray sails, tries to turn the tables on the heating problem by moving to within 3 solar radii to heat the sail up to 2000 degrees centigrade. The radiating heat would then act as a propellant as the spacecraft passes through the perihelion and arcs away from the Sun.

References

1. A.A.Bolonkin, "Solar Sail Engine for Spaceships". Patent (Author sertificate # 1262870), priority since 10 January 1985, USSR Patent Office.
2. A.A. Bolonkin, "Theory of Flight Vehicles with Control Radial Force". Collection *Researches of Flight Dynamics*, Mashinostroenie, Moscow, 1965, pp. 79–118 (in Russian).

3. K.E. Tsiolkovskiy, *Extensions of Man Into Outer Space*, 1921, See also K. E. Tsiolkovskiy, *Symposium on Jet Propulsion*, No. 2, United Scientific and Technical Presses (NIT), 1936 (in Russian).

4. R.L. Forward, "Roundtrip Interstellar Travel Using Laser-Pushed Lightsails", *Journal of Spacecraft* Vol. 21, pp. 187–195, 1984.

5. A. Marx, "Interstellar Vehicle Propelled by Terrestrial Laser Beam", *Nature*. pp. 22–23, July 1966.

6. D. Spieth and R. Zubrin, "Ultra-Thin Solar Sails for Interstellar Travel: Phase I Final Report", by Pioneer Astronautics, Inc., Lakewood, CA., published December 1999.

7. K. Tsander, "From a Scientific Heritage", NASA TTF-541, 1967 (quoting a 1924 report by the author).

8. B. Mallove and G. Matloff, *The Starflight Handbook*: *A Pioneer's Guide to Interstellar Travel*, John Wiley & Sons, Inc, New York, 1989.

9. L.Funaki, et. al, "Thrust Production Mechanism of Magnetoplasma Sail", AIAA 2003-4292.

10. A.A. Bolonkin, "Method of stretching of thin film". Russian patent application #3646689/10 138085, 28 September 1983 (in Russian), Russian PTO.

11. A.A. Bolonkin, "Guided Solar Sail and Electric Generator", AIAA-2005-3857, 41st Propulsion

Conference, 10-12 July, 2005, Tucson, Arizona, USA.
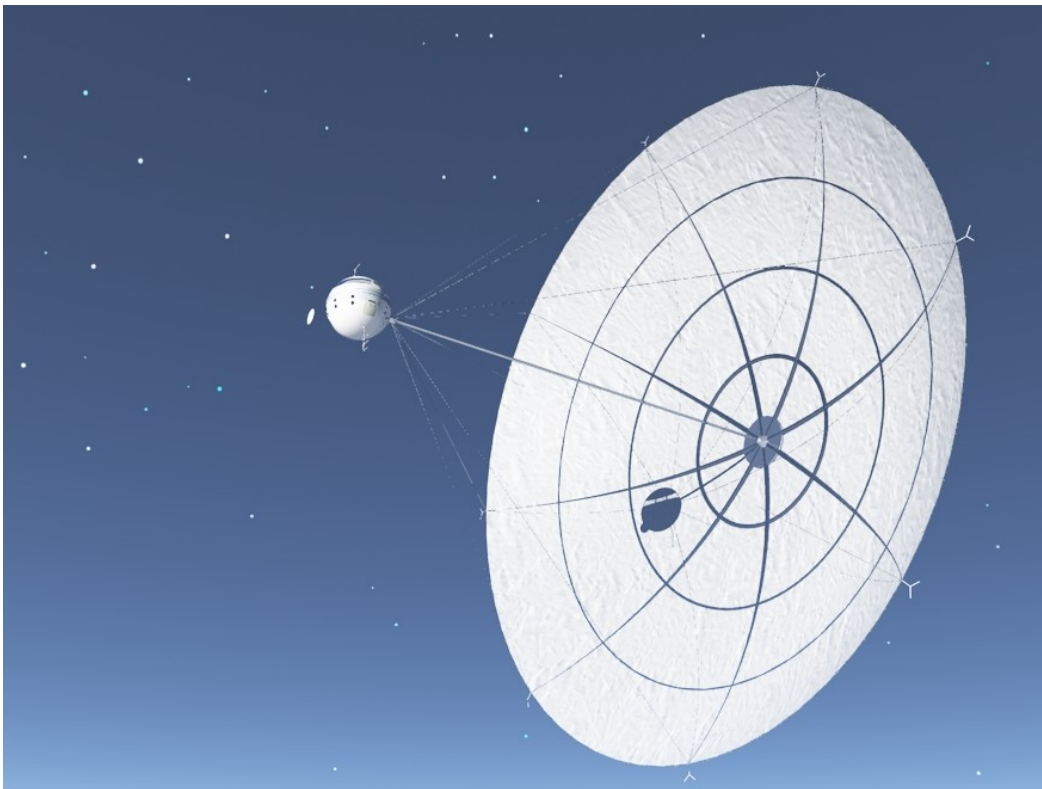
Chapter 17
Radioisotope Space Sail and Electro-Generator*

Summary

Radioisotope sail is a thin film of an alpha particle emitting radioisotope deposited on the back of a plastic sail that can provide useful quantities of both propulsion and electrical power to a deep space vehicle. The momentum kick of the emitted alpha particles provides radioisotope sail thrust levels per square meter comparable to that of a solar sail at one astronautical unity (1 AU). The electrical power generated per 1 square m is comparable to that obtained from solar cells at 1 AU. Radioisotope sail systems will maintain these propulsion and power levels at distances from the Sun where solar powered systems are ineffective.

  The propulsion and power levels available from this simple and reliable high-energy-density system would be useful for supplying propulsion and electrical power to a robotic deep space mission to the Oort Cloud or beyond, or to a robotic interstellar flyby or rendezvous probe after its arrival at the target star.

----

* Detailed work was presented by the author as AIAA-2005-4225 at the 41st Propulsion Conference, 10–12 July, 2005, Tucson, Arizona, USA.

Description of method and innovations
Brief history of innovation

  The idea of using a radioisotope recoil propulsion as it is shown in Fig.17.1a is very old[15].
The author has proposed many innovations in method is using radioisotope space sail and electric generators in patent applications[1–13] in 1983 and in paper IAF 92-0573 presented to the World Space Congress in 1992[14]. The work[16] written in 1995 summarized the knowledge for the conventional case in Fig. 17.1a. Bolonkin innovations decrease the weight of traditional radioisotope sail (RadSail, RS, IsoSail) by 2–4 times; increase the thrust by 2–3 times, and the electric power by 2 times and allows control of thrust and thrust direction without needing to turn the large RadSail.

   Our innovation allows us to reach a probe speed of more then 2000 km/s, so the design may be used for interstellar probes.

  This method allows nuclear waste and unnecessary nuclear bombs to be used for producing the radioisotope material.

  The offered method is realistic at the present time, has a high possibility to being successful, and is much cheaper for deep missions than other currently proposed method.

General information about the isotope sail

There are a number of radioactive elements that emit particles at a high velocity. It is conceptually possible to utilize these high velocity particles to provide rocket thrust for a space vehicle. Usually, the concepts involve placing a thin layer of the radioactive material on the back of a metal or plastic film substrate, producing a radioisotope sail. The particles emitted in the forward direction would be absorbed by the substrate, while the particles emitted in the backward direction would produce thrust on the vehicle.

Since the emitted particles also carry electric charge, they generate a current flow as they leave, which can be harnessed to provide electric power to the vehicle.

A short list of isotopes with a decay lifetime and alpha particle energy of interest for deep space propulsion and power is given in Table 17.1.

Table 17.1. Some alpha particle radioisotopes

Element	Mass Number	Atomic Number	Lifetime Half-life	(yr) 1/e	α Energy (MeV)	Specific density
	A	Z				
Polonium	208	84	2.9	4.2	5.12	9.4
Polonium	209	84	103	149	4.88	9.4
Thorium	228	90	1.9	2.8	5.42	11.7
Uranium	232	92	72	104	5.32	19.1
Plutonium	236	94	2.8	4.1	5.77	19.1
Plutonium	238	94	86	124	5.50	19.8

Charged particles, such as alpha particles, have a finite stopping range in materials, which depends upon the charge, mass, and energy of the alpha particle, the density of the stopping material, and, to a slight degree, on the mass number A of the stopping material. The range of all the alpha particles is within a few percent of the average. As a result, for a conventional radioisotope sail (see Fig. 17.1a), a substrate of stopping material with thickness a little greater than the average alpha-particle range will stop all alpha particles. The range for 5 MeV alpha particles in hydrogen-containing materials like water and plastic is 50 µm. In heavy metals, the range is 200 µm/ρ, where ρ is the specific density. For polonium, with $\rho = 9.4$, the range is 20 µm. For plutonium, with $\rho = 19.8$, the range is 10 µm.

For propulsion, the radioisotope should be deposited as a thin metal film on the back of a space sail substrate made of plastic. If made 50 µm thick, the plastic substrate will stop all the alpha particles going in the forward direction. Then, if the radioisotope film is made thin, most of the alpha particles emitted in the backward direction will exit the thin metal film and produce a reaction thrust on the sail. For example, if the film of polonium is made 10 µm thick, then a large percentage of the rearward-emitted alpha particles will emerge from the surface of the film with most of their energy. A square meter of such a sail would consist of 50 gm/m^2 of plastic substrate with 94 gm/m^2 of polonium deposited on it.

The conventional IsoSail allows (theoretically) reaching a velocity of 200 km/s. Our innovation allows us to reach more the 1000 km/s. This design may be used for interstellar probes.

Description of new method, installation and innovation

The old RadSail has a substrate layer (base about 50 µm thick) and a thin 10 µm film of a 5 MeV alpha-particle-emitting radioisotope (Fig. 17.1a). The substrate layer (sail base) absorbs the high energy particles.

The innovations and their advantages are follows (Fig. 17.1b):

1) The sail base, 1, is thin, and particles pass across it. Both sides of the base contain horizontal condenser nets, 10–11, and vertical nets, 12. These nets create the electric fields. The lower electric field turns the lower particles back (to an upward), and this doubles (at least) the sail thrust. The top electric field also turns the side particles to an upward direction and accelerates them. As a result the

efficiency coefficient is increases from the theoretical level (up to 25%) for conventional isotope sails by a minimum of 2–3 times and can potentially reach 90%.
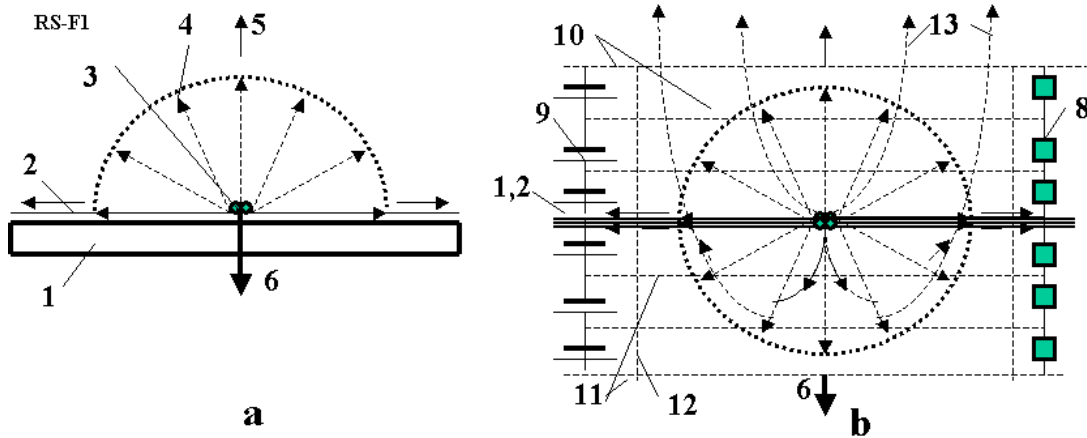

Fig. 17.1. a) Conventional radioisotope sail; b) suggested (innovated) radioisotope sail. Notations are: 1 – substrate (base of sail), 2 – isotope layer, 3 – isotope atom, 4 – alpha particles, 5 – direction of 1/6 particle flow, 6 – thrust, 8 – electric loading, 9 – initial charging, 10, 11, 12 – condenser nets, 13 – particle trajectory.
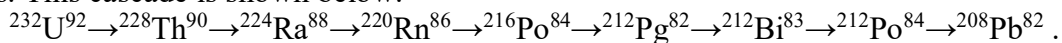
2) We can control the amount of thrust and the thrust direction. By changing the electric tension (voltage) of our fields (horizontal nets), we can change the thrust up to zero. By changing the electric tension of the vertical nets, we can change the thrust direction without turning the sail. This is the important innovation because the large size of the isotope sail makes turning it a very complex problem.

3) The suggested isotope sail may work as an electricity generator (as well as a propulsion system). By decreasing the electrical tension of the electric field, a proportion of the charged particles will be adsorbed by the net and produce electricity.

4) The sail base (base film) has a thickness of 2–10 μm (not 50–100 μm as conventional isotope sail). The net is made of wire of 2–10 μm and has cells 5–10 cm or a film thickness of 1–2 μm (for an electricity generator). That means the weigh of the proposed sail will be 2–5 times less than the conventional isotope sail.

Improvements to the radioisotope sail

The way to improve the performance of the IsoSail is to choose an initial radioisotope, that has a decay chain with a large number of alpha particles 1–14. For example, $^{232}U^{92}$ emits in turn a 5.32 MeV $^{4}\alpha^2$ with a 1/e lifetime of 104 years to become $^{228}Th^{90}$, and that emits a 5.42 MeV $^{4}\alpha^2$ after a 1/e lifetime of 2.8 years to become $^{224}Ra^{88}$, which emits a 5.68 MeV $^{4}\alpha^2$ after 5 days to become $^{220}Rn^{86}$. This radon emits a 6.78 MeV $^{4}\alpha^2$ after 80 s and becomes $^{212}Pb^{82}$. The $^{212}Pb^{82}$ then emits a 0.34 Mev electron after 15 hr and changes to $^{212}Pb^{83}$, which emits a 2.25 Mev electron after 85 min to become $^{212}Pb^{84}$, then this emits a 8.78 MeV $^{4}\alpha^2$ after 0.4 μs to become $^{206}Pb^{82}$, which is finally stable. Thus $^{232}U^{92}$ would be a good choice for a mission with a lifetime much longer than 2.8 years but less than 104 years. This cascade is shown below.

$$^{232}U^{92} \rightarrow {}^{228}Th^{90} \rightarrow {}^{224}Ra^{88} \rightarrow {}^{220}Rn^{86} \rightarrow {}^{216}Po^{84} \rightarrow {}^{212}Pg^{82} \rightarrow {}^{212}Bi^{83} \rightarrow {}^{212}Po^{84} \rightarrow {}^{208}Pb^{82}.$$

The total increment in velocity in the old design after six cascades reaches 210 km/s. In my new design the final speed is 10 times more. This is large enough to be useful for exploration of comet bodies and brown dwarfs outside the solar system, to divert the propulsion of an interstellar flyby probe

to allow it to maneuver close to a planet observed on the way into the target system, and for propulsion within an extra-solar planetary system after completing a rendezvous mission at the target star using some other method to stop, such as a magnetic sail drag brake.

Possibility of electric power

The emission of charged particles from a radioisotope sail produces a current flow outward from the vehicle. In conventional designs the current per unit area is carried by the escaping half of the alpha particles (each with charge $2e = 3.2 \times 10^{-19}$ C) emitted by a sail. The maximum power of $^{208}Po^{84}$ per unit area available from a power source sail, given the full potential of 5 MV, is 1600 W/m^2 . For comparison, a solar cell array with an efficiency of 14% would provide 200 W/m^2 of electric power at 1 AU. If no propulsion, only electric power, is desired from the radioisotope sail, the electric power generated can be increased by a factor of two by decreasing the thickness of the plastic substrate and radioisotope film so that nearly all the alpha particles can escape from both sides of the sail. That case is our design.

  Heating. An area of concern is the waste heat generated by the radioisotope material. If we assume that half of the alpha particles deposit their energy in the sail (conventional design), the thermal power deposited per unit area by a 10 μm layer of polonium is 850 W/m^2. This is less than from the Sun (1400 W/m^2), so heating should not be a significant problem once the sail is unfurled.

  Our design of IsoSail has twice as much efficiency and does not have this problem.

Equation for computation of conventional IsoSail

The mass M of a given amount of radioactive isotope decays exponentially with time according to the well-known relation from the physics of isotopes:

$$M(t) = M_0 e^{-\frac{t}{\tau}}, \qquad (17.1)$$

where M_0 is the mass of the mass of the initial quantity of radioisotope and τ is the 1/e lifetime, t is time. The "halflife" is the time t_h when $\exp(-t_h/\tau) = 1/2$. The halflife t_h is $\ln(2) = 0.693$ of the 1/e lifetime τ .

$$t_h = 0.693\tau.$$

  Conventionally scientists choase as a typical example the radioisotope $^{208}P_0^{84}$ with an 1/e lifetime of 4.2 years and specific density of 9.4 . The number per second dn/dt of alpha particles emitted from a given mass M is given by the equation:

$$\frac{dn}{dt} = \frac{N_A M}{A\tau}, \quad \text{[alphas/kg·s]} \qquad (17.2)$$

where n is the number of alpha particles, $N_A = 6.02 \times 10^{26}$ [atoms/kg-mole] is Avogadro's number. For the radioisotope matter with a mass number of $A = 208$ kg/kg-mole and an 1/e lifetime of $\tau = 4.2$ this magnitude is $dn/dt = 2.2 \times 10^{16} M$ [alphas/kg·s] .

  The velocity V of an alpha particle is

$$v = \left(\frac{2E}{m}\right)^{1/2} . \qquad (17.3)$$

  For a mass of $m = 4$, a unit of atom mass (amu) $= 6.64 \times 10^{-27}$ kg emitted at an energy of $E = 5.12$ *MeV* $= 8.2 \times 10^{-13}$ J, this value is: $v = 16,000$ km/s $= 16$ mM/s $= 0.05c$, where $c = 300$ Mm/s is the speed of light. The speed of particles is equivalent specific impulse of $I_{sp} = 1,600,000$ sec.

The thrust T per unit area B of a conventional IsoSail is estimated by the equation:

$$\frac{T}{B} = \frac{1}{4B}\frac{dn}{dt}mV \text{ , for polonium } \quad \frac{T}{B} = 5.7 \times 10^{-4}\frac{M}{B} \quad \text{[N/kg] or } T/B = 5.3 \times 10^{-5} \text{ [N/m}^2\text{]}, \qquad (17.4)$$

where the coefficient ¼ shows that only ¼ of full thrust used in conventional IsoSail.

For the proposed IsoSail this coefficient is about 1/2 or more.

For comparison the solar light pressure thrust at 1 AU for full reflection is

$$\frac{T}{B} = 2\frac{S}{c} \approx 9.3 \times 10^{-6} \quad [\text{N/m}^2], \tag{17.5}$$

where $S = 1,400$ W/m^2 is the solar light flux at 1 AU. This shows that the IsoSail has thrust in 5.7 times greater than the solar sail. Unfortunately, the mass of the conventional Isosail is also much greater then the solar sail at distance from the Sun equals 1 AU. However, the IsoSail produces useful thrust at great distances from the Sun.

The maximum sail velocity of a conventional IsoSail is estimated using the momentum equation:

$$V = \frac{v\,m}{M - m}. \tag{17.6}$$

For example, if $M = 208$ amu, $m = 4$ amu, $v = 16,000$ km/s, this velocity is about 300 km/s. In reality the conventional IsoSail can reach only ¼ of this velocity or less. The maximum is up 30 km/s.

The net impulse given by the cascade is approximately estimated by equation (from (17.1),(17.2),(17.4)):

$$I_t = \int_0^t T dt = \frac{m V_t N_A M_0}{4A}\left(1 - e^{-\frac{t}{\tau}}\right), \tag{17.7}$$

where V_t is the average particle velocity. If the sail mass makes up most of the space vehicle, the conventional sail consists of a 50 μm thick layer of plastic sail with a mass of 50 g/m^2, and a 5 μm thick layer of $^{232}\text{U}^{92}$ with a density of 19.8 g/cc and a mass of 100 g/m^2, then the velocity increment after a $1/e$ lifetime of $\tau = 104$ years is $\Delta V = 210$ km/s.

For proposed IsoSail ΔV is in about 3–5 times more (thrust is double, weight is less).

Electric power of conventional IsoSail. The current I per unit area carried by particles (each with a charge of $2e = 3.2 \times 10^{-19}$ C) emitted by a conventional IsoSail with area B and mass M is:

$$\frac{I}{B} = \frac{1}{2B}(2e)\frac{dn}{dt}. \tag{17.8}$$

For isotope $^{208}\text{Po}^{84}$ this magnitude is 3.5 M/B mA/kg = 0.33 mA/m^2.

The maximum power, P, per unit area available from a power source conventional sail power souce with area B and radioisotope mass M is:

$$\frac{P}{B} = \frac{IE}{B}. \tag{17.9}$$

For $E = 5$ MV this value is $P/B = 17,500 M/B$ W/m^2 = 1600 W/m^2. For comparison, a solar cell array with an efficiency of 14% would provide 200 W/m^2 of electrical power at 1 AU.

In reality that value is arrived at because the conventional IsoSail has very low coefficient of efficiency (10–15%). For the proposed IsoSail this power is increased by a factor of two. The efficiency of the offered device can reach 70–85% for a multilayer IsoSail, which has a some condenser nets.

Heating a conventional IsoSail. In a conventional IsoSail half of the alpha particles deposit their energy in the sail and the thermal power P_t deposited per unit area B is:

$$\frac{P_t}{B} = \frac{1}{2}\frac{dn}{dt}\frac{E}{B}. \tag{17.11}$$

For a 10 μm layer of polonium $P_t/B = 9 M/B$ kW/kg = 850 W/m^2. That is less than from the Sun (1400 W/m^2), so heating should not be a significant problem. This problem does not apply to the proposed IsoSail because its efficiency is high and the amount of heating is small.

Conclusion

The IsoSail concept can potentially provide useful amounts of propulsion and electrical power in

robotic deep space and interstellar missions. Whether the actual performance ultimately achievable would justify the immense problems of coping with the technical difficulties of fabricating, deploying, and using this new technology with its extremely hazardous material that is 'hot' in both the thermal and nuclear sense, is a question to be answered by further studies. The IsoSail (especially the offered IsoSail) needs in more detailed research and development.

This method allows nuclear waste and unnecessary nuclear bombs for be used to produce the radioisotope material.

References

1. A.A. Bolonkin, Radioisotope Propulsion, Russian patent application #3467762/25 116952, 9 July 1982 (in Russian), Russian PTO.

2. A.A. Bolonkin, Radioisotope Electric Generator, Russian patent application #3469511/25 116927, 9 July 1982 (in Russian). Russian PTO.

3. A.A. Bolonkin, Radioisotope Electric Generator, Russian patent application #3620051/25 108943, 13 July 1983 (in Russian), Russian PTO.

4. A.A. Bolonkin, Method of Propulsion using Radioisotope Energy and Installation for It, Russian patent application #3601164/25 086973, 6 June 1983 (in Russian), Russian PTO.

5. A.A. Bolonkin, Method of Energy Transformation of Radioisotope Matter in Electricity and Installation for it, Russian patent application #3647343/25 136692, 27 July 1983 (in Russian), Russian PTO.

6. A.A. Bolonkin, Space Propulsion using Solar Wind and Installation for It, Russian patent application #3635955/23 126453, 19 August 1983 (in Russian), Russian PTO.

7. A.A. Bolonkin, Installation for Open Electrostatic Field. Russian patent application #3467270/21 116676, 9 July 1982 (in Russian), Russian PTO.

8. A.A. Bolonkin, Getting of Electric Energy from Space and Installation for It, Russian patent application #3638699/25 126303, 19 August 1983 (in Russian), Russian PTO.

9. A.A. Bolonkin, Protection from Charged Particles in Space and Installation for It, Russian patent application #3644168 136270, 23 September 1983, (in Russian), Russian PTO/

10. A.A. Bolonkin, Method of Transformation of Plasma Energy in Electric Current and Installation for It, Russian patent application #3647344 136681, 27 July 1983 (in Russian), Russian PTO.

11. A.A. Bolonkin, Transformation of Energy of Rarefaction Plasma in Electric Current and Installation for it, Russian patent application #3663911/25 159775, 23 November 1983 (in Russian), Russian PTO.

12. A.A.Bolonkin, Method of a Keeping of a Neutral Plasma and Installation for it, Russian patent application #3600272/25 086993, 6 June 1983 (in Russian), Russian PTO.

13. A.A.Bolonkin, Method of stretching of thin film. Russian patent application #3646689/10 138085, 28 September 1983 (in Russian), Russian PTO.

14. A.A. Bolonkin, Simple Space Nuclear Reactive Motors and Electric Generators Running on Radioactive Substances, The World Space Congress – Jerusalem, 1992. IAF Preprint 92-0573.

15. A. Berman, *Physical Principles of Aeronautics*, New York, 1961, p. 252–254.

16. R.L. Forward, "Radioisotope Sails for Deep Space Propulsion and Electric Power", AIAA 95-2596.

17. Dwight E. Gray, *American Institute of Physics Handbook*, McGraw-Hill, New York.

18. A.A. Bolonkin, "Radioisotope Space Sail and Electric Generator", AIAA-2005-4225, 41st Propulsion Conference, 10–12 July, 2005, Tucson, Arizona, USA.

Chapter 18
Electrostatic Solar Sail

Summary

The solar sail has become well-known after much discussion in the scientific literature as a thin continuous plastic film, covered by sunlight-reflecting appliquéd aluminum. Earlier, there were attempts to launch and operate solar sails in near-Earth space and there are experimental projects planned for long powered space voyages. However, as currently envisioned, the solar sail has essential disadvantages. Solar light pressure in space is very low and consequently the solar sail has to be very large in area. Also it is difficult to unfold and unfurl the solar sail in space. In addition it is necessary to have a rigid framework to support the thin material. Such frameworks usually have great mass and, therefore, the spacecraft's acceleration is small.

  Here, the author proposes to discard standard solar sail technology (continuous plastic aluminum-coated film) with the intention instead of using millions of small, very thin aluminum charged plates and to release these plates from a spacecraft, instigated by an electrostatic field. Using this new technology, the solar sail composed of millions of plates can be made gigantic area but have very low mass. The acceleration of this new kind of solar sail may be as much as 300 times that achieves by an ordinary solar sail. The electrostatic solar sail can even reach a speed of about 300 km/s (in a special maneuver up to 600–800 km/sec). The electrostatic solar sail may be used to move a large spaceship or to act as an artificial Moon illuminating a huge region of the Earth's surface.

Introduction

The description of solar sail is in chapter 16. Solar radiation pressure equals 9.12 µN/m² at distance 1 AU from the Sun.

No solar sails have been successfully deployed as primary propulsion systems, but research into this technology is continuing. On 9 August , 2004 the Japanese ISAS successfully deployed two prototype solar sails in low Earth orbit. A clover-shped sail was deployed at 122 km altitude and a fan-shaped type sail at 169 km. Both sails used 7.5 micrometer thick film.

  A joint private project between the Planetary Society, Cosmos Studios and the Russian Academy of Science launched Cosmos 1, the first solar sail spaceship, on 21 June, 2005. The rocket was supposed to push the 124 kg spacecraft into 800 km orbit where it was intended to unfurl the 15 meter sails (with a total area of 600 m²). Unfortunately, the launch was unsuccesful. A suborbital prototype test by the group also did not succeed in 2001 because of rocket failure.

Brief description of the innovations

A conventional solar sail is a dielectric thin film (thickness 5 mkm = 5000 nm) with an aluminum layer 100 nm thick, and it has 90% reflectivity. The weight of one square meter is 5–7 g/m². If it accelerates by itself the maximum acceleration is about 1 mm/s². However, the gigantic thin film needs a rigid structure to support the very thin film in an unfolded position and to anable it to be contrilled. This rigid structure has a large weight, so it is very difficult to launch and to unfurl the structure in space. All attempts to do this (for example, to unfurl the inflatable radio-antennas in space) have failed.

The author proposes to use small thin charged aluminium plates (petals) supported by a central electrostatic ball and rotated around the ball (Fig. 18.1). They rotate also around their own axis and main thin a direction perpendicular to the solar rays. The diameter of the plate-petals is small, about 1 mm or less, and, it is not a necessity to use the dialectric film. The aluminium film may be very thin because the individual petal size is small.
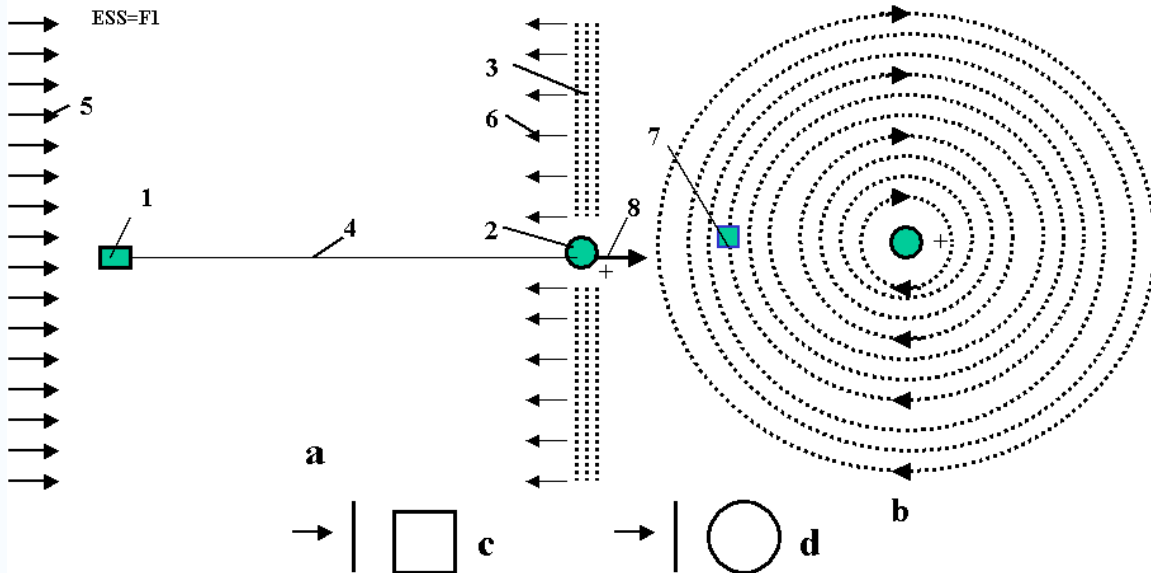

Fig. 18.1. The proposed electrostatic solar sail. **a**. Side view; **b.** Front view; **c.** Side and front views of square petal; **d.** Side and front views of round petal. Notation: 1 – spaceship, 2 – charged ball, 3 – charged plate-petals, 4 – cable connecting the ship and the ball, 5 – solar rays, 6 – reflected rays, 7 – charged petals, 8 – thrust (drag).

The electrostatic sail can be controlled by changing charge on the ball (diameter of the mirror) and by the positioning of an additional charged ball, 9 (Fig. 18.2), which turns the mirror.
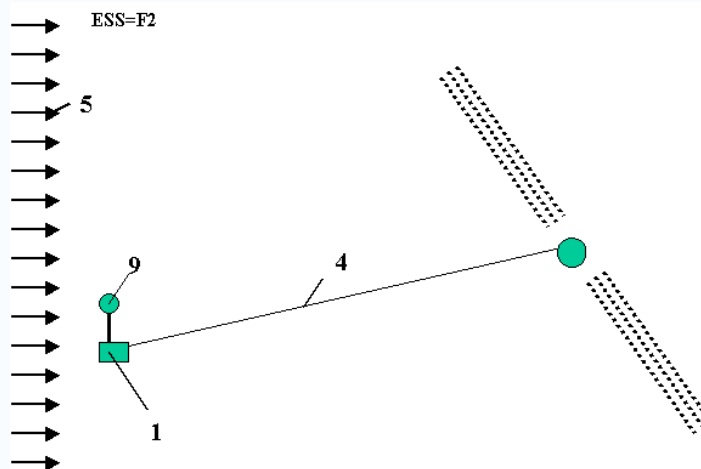

Fig. 18.2. Guidance and control of the electrostatic solar sail. Notation: 9 – charged ball for control. All other notations are the same as Fig. 18.1.

The unfurling of the sail may be done using a rotated charged head 10 (Fig. 18.3). The head is detached from the apparatus in the radius of sail, and is rotated around it's axis (parallel to the solar

rays) and around the ball. The head emits the negativity charged petals. The speed of the petals may be controlled by the head charge (voltage). The same charge stretches the petals[3] and repels them from the others. The sail can be collected back by the head, through the head changing the opposite charge.
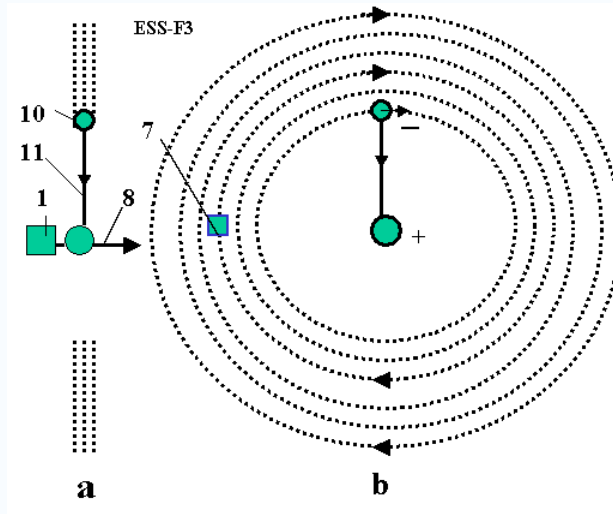

Fig. 18.3. Unfurling of the electrostatic solar sail. Notation: 10 – rotating mobile charged head connected by a variable cable to the central ball, 11 – variable cable connecting the head and the ball. All other notations are same as Fig. 18.1.

The proposed solar sail has many unique advantages in comparison with the conventional solar sail or a space mirror:

1. The proposed sail (made only of film) is easier to use (has less mass) in 50–100 times because of the absence of a support substrate (dielectric film of 5000 nm thickness) and the aluminum film used can be of minimum thickness (6–15 nm, not 100 nm).
2. A rigid support structure giving a large additional mass is unnecessary.
3. The size of the reflected mirror is not limited and may be more than 1 km. This means the proposed sail can accelerate a large spaceship with a mass of 1 ton or more.
4. There are no big problems with the unfurling and collection of the sail.
5. The electrostatic sail may be collected (furled) to the head.

Theory of estimation and computation

1. The sail. The spectrum of solar radiation is presented in Fig. 19.1[1]. If we want to use the most energy, the sail must reflect or absorb all waves having the wavelength less than $\lambda = 1$–2 μm (mkm). The amount of light that can pass capability through metal depends on its thickness[2]:

$$I = I_0 \exp(-4\pi nkd / \lambda), \quad d = -\frac{\lambda \ln(I / I_0)}{4\pi nk}, \tag{18.1}$$

where I – light intensity after passing through metal film, I_0 – initial light intensity, I/I_0 – coefficient of clarity, n – refraction coefficient, k – absorption coefficient, d – metal thickness [m], λ – wavelength [m].

The refraction and absorption coefficients of aluminum are equal (see Reference[2], p. 639):

for $\lambda = 0.5$ μm, coefficient $n = 0.5$, $k = 9.18$, $nk = 4.59$; $\lambda/nk = 0.109 \times 10^{-6}$;

for $\lambda = 5$ μm, coefficient $n = 6.7$, $k = 5.61$, $nk = 37.59$; $\lambda/nk = 0.133 \times 10^{-6}$,

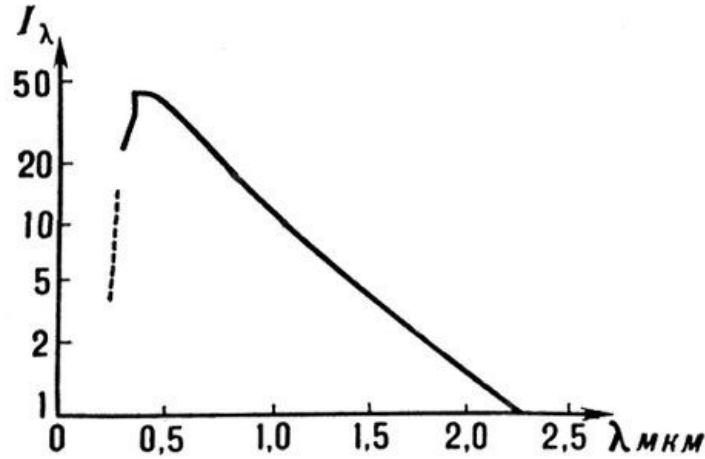**Fig. 18.4.** Spectrum of solar radiation. λ is the wavelength [0–2.5 μm], I_λ is the energy density.

For other values the product nk can be found using linear interpolation: $\lambda = 1$ μm, $nk = 8.26$; $\lambda = 2$ μm, $nk = 15.59$.

The computation of the metal film thickness versus the coefficient of clarity I/I_0 is presented in Fig. 18.5.
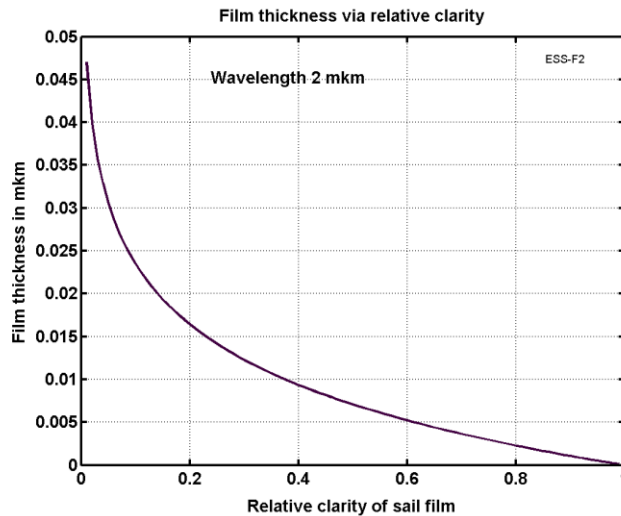

Fig. 18.5. The sail film thickness via clarity coefficient I/I_0 for the wavelength $\lambda = 2$ μm.

The weight of the sail is computed using the equation:

$$W = \rho Sd , \qquad\qquad (18.2)$$

where W – sail weight (mass) [kg], $\rho = 2700$ kg/m³ is the density of aluminum, S – sail area [m²], d – sail (aluminum) thickness [m].

The mass of a 1 m² sail of thickness $d = 10$ nm is $W = 2700{\times}10^{-8} = 0.027$ g/m². Compared with 5–7 g/m² for the conventional sail this is 185–260 times less. Clarity correction makes this value 110–150 times less.

The acceleration, a, of a spaceship with a sail can be computed using the equation:

$$a = \frac{P_0 S(1 - I/I_0)}{M - W} = \frac{P_0 S(1 - I/I_0)}{M - \dfrac{\lambda \rho S \ln(I/I_0)}{4\pi nk}}, \tag{18.3}$$

where P_0 is light pressure [N], M is useful mass (of the ship without sail) [kg]. If we take solar radiation pressure for 88% reflection at 1 AU, it is about $P_0 = 8 \times 10^{-6}$ [N/m²]. This works out at 8 N for a sail with a radius of 564 m (area 10^6 m²). The mass of our sail is 27 kg, the mass of a conventional sail (without the support structures) is 5 tons. However, the unbiased comparison is of sail acceleration for $M = 0$.

The result of computation for equation (18.3) are presented in Fig. 18.6. As you can see, the acceleration of the proposed sail reaches as much as $a \approx 0.3$ m/s² $= 300$ mm/s². In comparison, acceleration of the conventional solar sail without a useful load is 1 mm/s². If our sail spacecraft has an additional useful mass (the ship, the ball, and other devices) of 100 kg, the acceleration is 45 mm/s²; for a useful mass of 500 kg, the acceleration is 13 mm/s².
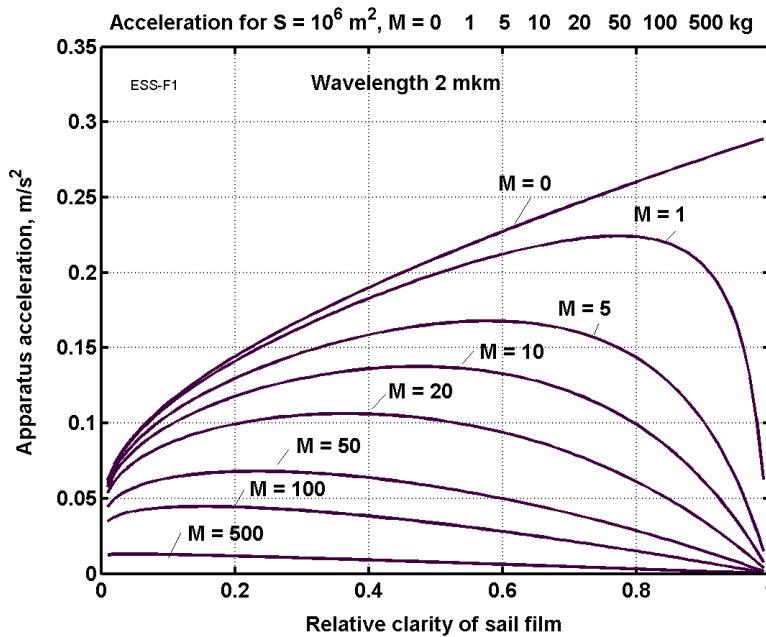

Fig. 18.6. Apparatus acceleration via relative clarity of sail film and additional apparatus mass.

The maximum speed of a solar-sail spacecraft can be estimated using the equation:

$$dV = adt, \quad dt = \frac{s}{V}, \quad a = a_0 \left(\frac{s_0}{s}\right)^2, \quad VdV = a_0 \left(\frac{s_0}{s}\right)^2 ds, \quad V^2 = 2a_0 s_0^2 \left(\frac{1}{s_0} - \frac{1}{s}\right), \tag{18.4}$$

where V is the apparatus speed [m/s], a is acceleration [m/s²], t is time [seconds], a_0 is acceleration at distance 1 AU (astronautic unit, for an Earth orbit of radius $s_0 = 15 \times 10^{10}$ m), s is distance from the Sun [m].

If $s \gg s_0$, the maximum apparatus speed is

$$V_{max} = \sqrt{2a_0 s_0} . \tag{18.5}$$

The proposed solar sail without a load reaches a maximum speed of 295 km/s $\approx$ 300 km/s whereas the conventional sail without a load reaches only 55 km/s. With a load of 100 kg the new sail reaches a speed of 116 km/s. If the apparatus makes a maneuver and starts at $s_0 = 30$ million km from the Sun ($a = 25a_0$) the maximum speed reaches 660 km/s.

We can find the tangent speed of the petals (aluminum plates) around the charged ball from the following equations:

$$F = k\frac{qQ}{r^2} = \frac{mv^2}{r}, \quad q = \frac{Q}{N}, \quad m = \frac{\rho S d}{N}, \quad v = Q\sqrt{\frac{k}{\rho S r d}}, \tag{18.6}$$

where F – the electrostatic force between the central ball and the petal [N], $k = 9\times10^9$ – electrostatic coefficient, q – charge of a petal [C], Q – charge of the ball [C], r – distance between the petal and the center of ball [m], m – mass of a petal [kg], v – tangent speed of a petal (around the ball) [m/s], N – number of petals.

If $\rho = 2700$ kg/m³ (for aluminum), $S = 10^6$ m² , $r = 600$ m, $d = 10^{-8}$ m, then $v = 745Q$. For $Q = 0.01$ C the speed $v = 7.45$ m/s.

2. Initial expenditure of electrical energy to charge of the ball. The ball has to be charged with electrical energy of high voltage (millions of volts). Let us estimate the minimum energy, when the charged device has 100% efficiency. This energy equals the work done to move of the ball charge to infinity. It can be computed using the equation

$$W_b = \frac{Q^2}{2C}, \quad Q = \frac{a^2 E}{k}, \quad C = \frac{a}{k}, \quad W_b = \frac{a^3 E^2}{2k}, \tag{18.7}$$

where W_b – ball charge energy [J]; C – ball capacitance [F]; Q – ball charge [C]; a – radius of ball [m]; E – electric intensity [V/m].

For our charge $Q = 0.01$C and electrical intensity (safe for a vacuum) $E = 10^8$ V/m the required ball radius is $a = 0.95$ m ≈ 1 m [equation (18.7)], the required charge energy is $W_b = 0.154$ kWh [equation (18.7)]. This energy is not great, and it may be returned when the ball discharged by emitting the charge into space using a sharp edge.

3. The ball stress, cover thickness and ball mass. The ball has tensile stress from the like electric charge. We can find the ball stress and the necessary thickness of the ball cover. If the ball is in a vacuum and the ball charge, Q, is constant, the internal force within the ball is

$$f = \frac{\partial W_b}{\partial a}, \quad W_b = \frac{Q^2}{2C}, \quad C = \frac{a}{k}, \quad k = \frac{1}{4\pi\varepsilon_0} = 9\times10^9, \quad W_b = \frac{kQ^2}{2a},$$

$$f = -\frac{kQ^2}{2a^2}, \quad Q = \frac{a^2 E}{k}, \quad f = -\frac{(aE)^2}{2k}, \tag{18.8–18.9}$$

where f is the ball's internal tensile force [N]; W_b is the charge energy [J]; C is the capacity of the ball as a spherical capacitor [F]; E is electric intensity [V/m].
The internal pressure of the ball is then

$$p = \frac{f}{S_b}, \quad S_b = 4\pi a^2, \quad p = \frac{E^2}{8\pi k}, \tag{18.10}$$

where p is internal pressure [N/m²], S_b is ball surface area [m²].

The thickness of a ball cover is

$$\pi a^2 p = 2\pi a \delta \sigma, \quad \delta = \frac{ap}{2\sigma}, \quad \delta = \frac{aE^2}{16\pi k\sigma}, \tag{18.11}$$

where δ is the cover thickness [m]; σ is the safe cover stress [N/m²].

The ball mass is then

$$M_s = S_b \delta \gamma, \quad S_b = 4\pi a^2, \quad M_s = \frac{a^3 E^2 \gamma}{4k\sigma}, \tag{18.12}$$

where M_s – ball (sail) mass [kg]; γ – ball cover density [kg/m³]; σ – safe stress level of the ball cover [N/m²].

For our case where $a = 1$ m, $E = 10^8$ V/m, $\gamma = 1800$ kg/m^3, $\sigma = 10^9$ N/m^2, the mass of the ball is $M_s = 0.5$ kg [equation (18.12)].

4. Technology. The thin plate-petals can be produced by electrolytic or vapor precipitation.

5. Artificial Moon. The proposed idea may be used to construct on artificial Moon when the light pressure equals the Earth's gravity and a gigantic electrostatic mirror illuminates the Earth's surface.

Other electrostatic applications are offered in the References[4-9].

References

1. "Dispersion of light", *Big Soviet Encyclopedia* Moscow (in Russian).
2. Kikoin I.K., *Tables of physical values* (directory). Moscow, 1975 (in Russian),
3. Bolonkin, A.A., Method of Stretching of Thin Film. Russian patent application #3646689/10 138085. 28 September 1983 (in Russian), Russian PTO.
4. Bolonkin, A.A., "Electrostatic Utilization of Asteroids for Space Flight", 41 Propulsion conference, 10–12 July, 2005, Tucson, Arizona, USA, AIAA-2005-3857.
5. Bolonkin, A.A., Electrostatic Solar Wind Propulsion, 41 Propulsion conference, 10–12 July, 2005, Tucson, Arizona, USA, AIAA-2005-3653.
6. Bolonkin, A.A., "Guided Solar Sail and Electric Generator", 41 Propulsion conference, 10–12 July, 2005, Tucson, Arizona, USA, AIAA-2005-3857.
7. Bolonkin A.A., "Electrostatic Levitation and Artificial Gravity", 41 Propulsion conference, 10-12 July, 2005, Tucson, Arizona, USA, AIAA-2005-3365.
8. Bolonkin, A.A., "Radioisotope Space Sail and Electric Generator", 41 Propulsion conference, 10-12 July, 2005, Tucson, Arizona, USA, AIAA-2
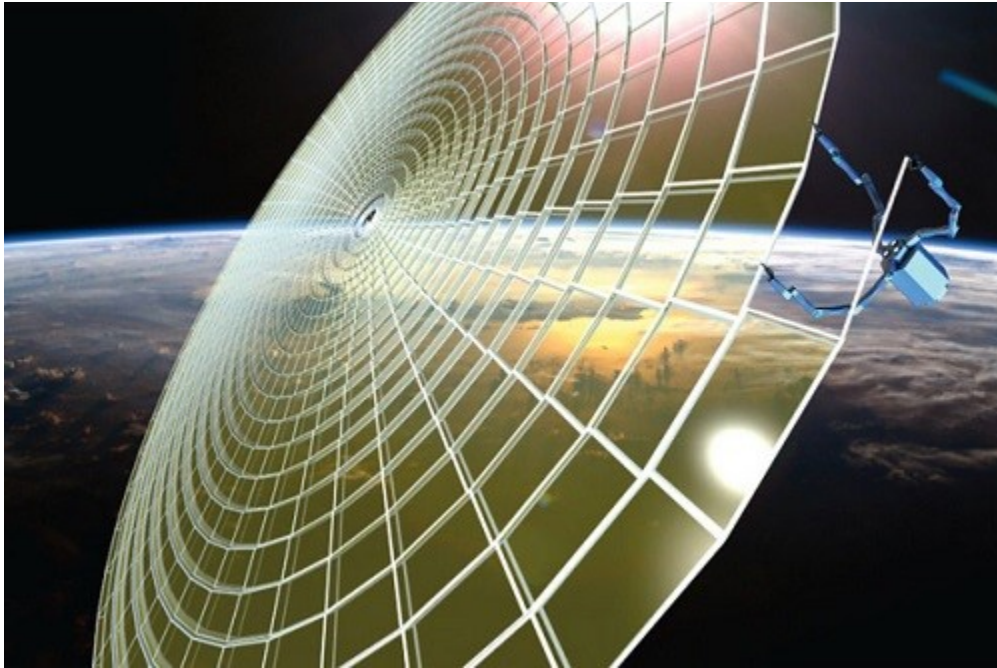
Chapter 19
Utilization of Space
Summary

This chapter describes some new ideas[1-23] which may be useful for utilization in space: (1) recombination propulsion, (2) a space mirror, (3) electronic sail, (4) astronauts in space without space suits, and (5) an electrostatic space radiator.

Recombination Space Jet Propulsion Engine
Summary

There are four known ionized layers in the Earth's atmosphere, located at an altitude of 85–400 km. Here the concentration of ions reaches millions of particles in 1 cubic centimeter. In the inter-planetary medium the concentration of ion reaches $10–10^3$ particles in 1 cm^3 and in interstellar space it is about 1–10 in 1 cm^3. As a result there is interaction between solar radiation in the Earth's atmosphere, solar wind, and galactic radiation.

About 90% these particles are protons and electrons. The particle density is low and they can exist for a long time before they come into collision with each other. However, if we increase the density of the particles in an engine, they collide with one another, recombine, warm up, leave the propulsion system with high speed, and create thrust.

The energy of recombination is significantly more than the heat capability of conventional fuel and the specific impulse of the propulsion system is high.

The author proposes collecting and concentrating charged particles from a large area using a magnetic field. Space ships, space apparatus, and satellites would then not need fuel and could be accelerated or fly to infinity. This may be a revolution in aerospace.

Description of method and innovation

Introduction

The Earth's Atmosphere. The present atmosphere of the Earth is probably not its original form. Our current atmosphere is what chemists would call an *oxidizing atmosphere*, while the original atmosphere was what chemists would call a *reducing atmosphere*. In particular, it probably did not contain oxygen.

Composition of the atmosphere. The original atmosphere may have been similar to the composition of the solar nebula and close to the present composition of the gas giant planets, though this depends on the details of how the planets condensed from the solar nebula. That atmosphere was lost into space, and replaced by compounds given out as gases from the crust or (in some more recent theories) much of the atmosphere may have come instead from the impacts of comets and other planets similary rich in volatile materials.

The oxygen so characteristic of our atmosphere was almost all produced by plants (cyanobacteria or, more colloquially, blue-green algae). Thus, the present composition of the atmosphere is 79% nitrogen, 20% oxygen, and 1% other gases.

Layers of the atmosphere. The atmosphere of the Earth may be divided into several distinct layers, as the Fig.19.1 indicates. The *troposphere* is where all the weather takes place; it is the region of rising and falling packets of air. The air pressure at the top of the troposphere is only 10% of that at sea level

(0.1 atmospheres). There is a thin buffer zone between the troposphere and the next layer called the *tropopause*.

 Above the troposphere is the *stratosphere*, where air flow is mostly horizontal.

 Above the stratosphere is the mesosphere and above that is the *ionosphere* (or *thermosphere*), where many atoms are ionized (gain or lose electrons so they have a net electrical charge). The ionosphere is very thin, but it is where aurora takes place, and it is also responsible for absorbing the most energetic photons from the Sun, and for reflecting radio waves, thereby making long-distance radio communication possible.
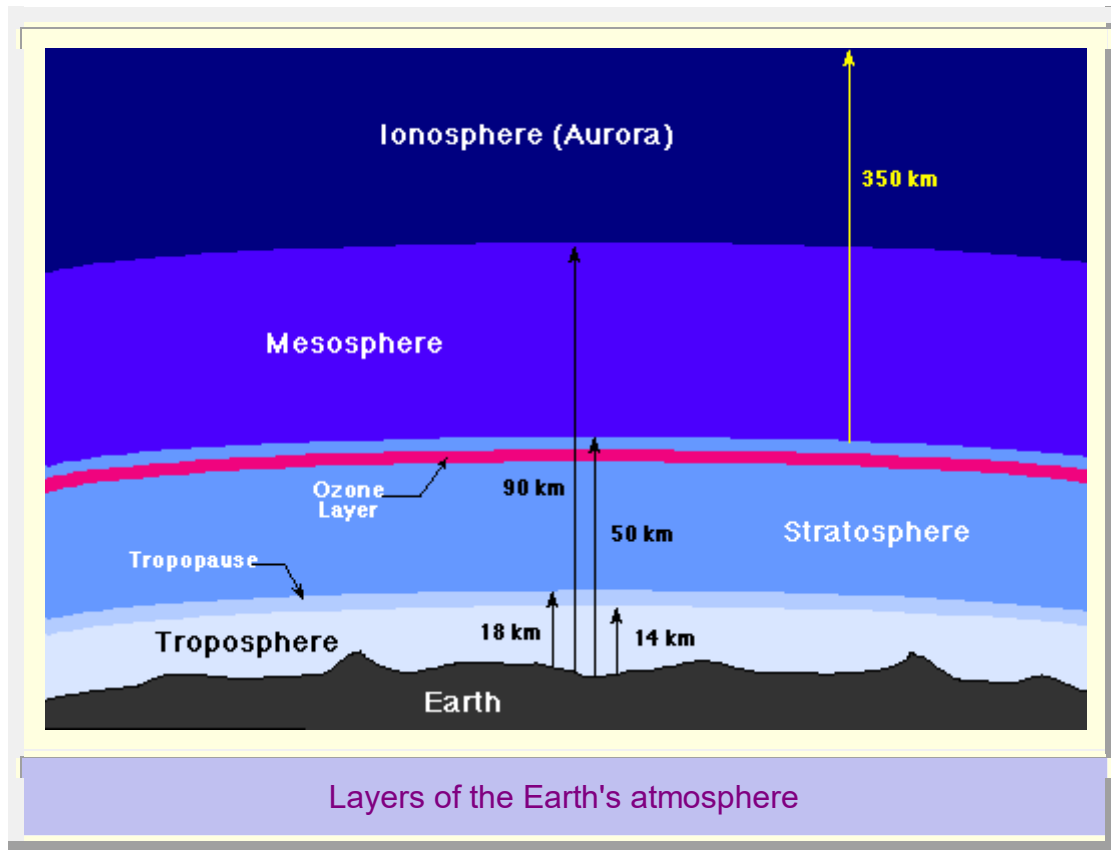

Fig. 19.1. Layers of the Earth's atmosphere.

The structure of the ionosphere is strongly influenced by the charged particle wind from the Sun (solar wind), which is in turn governed by the level of solar activity. One measure of the structure of the ionosphere is the free electron density, which is an indicator of the degree of ionization. There are electron density contour maps of the ionosphere available for months in 1957 to the present. As an example, comparison of the simulations of the monthly variation of the ionosphere for the year 1990 shows this was a period of high solar activity with many sunspots, and that 1996 was a period of low solar activity with few sunspots.

 The ionosphere can be further broken down into the D, E and F regions. This breakdown is based on what wavelength of solar radiation is absorbed in that region most frequently, or on what level of radiation is needed to photodissociate the molecules found in these individual regions.

 The D region is the lowest in altitude, at though it absorbs the most energetic radiation, hard x-rays. The D region has no have a definite starting and stopping point, but includes the ionization that occurs below about 90 km (or ionization that occurs below the E region).

 The E region peaks at about 105 km. It absorbs soft x-rays.

The F region starts around 105 km and reaches a maximum at about 600 km. It is the highest of all of the regions. Extreme ultra-violet radiation (EUV) is absorbed there.
On a more practical note, the D and E regions (the lower parts of the ionosphere), reflect standard AM radio waves back to Earth. Radio waves with shorter lengths are reflected by the higher F region. Visible light, radar, television and FM wavelengths are all too short to be reflected by the ionosphere, so these types of global communication are made possible by satellite transmissions.

Description of innovation

In the recombination propulsion engine contains a tube with an intake and a nozzle, and a solenoid (Fig. 19.1).
The solenoid may be conventional or superconductive. It produces a powerful magnetic field, which collects charged particles. If the density of the charged particles is sufficient (the distance the particles travel is less than the tube length) the particles came into contact with each other and recombine.

The energy of recombination (ionization and dissociation atoms and molecules) is:

Ionization:

Atom	(Symbol)	Level from 1 to top (eV)
Proton	H	13.6
Nitrogen	N	14.54–666.83
Oxygen	O	13.6–871.12

Dissociation

Hydrogen $H + H = H_2$ 4.48

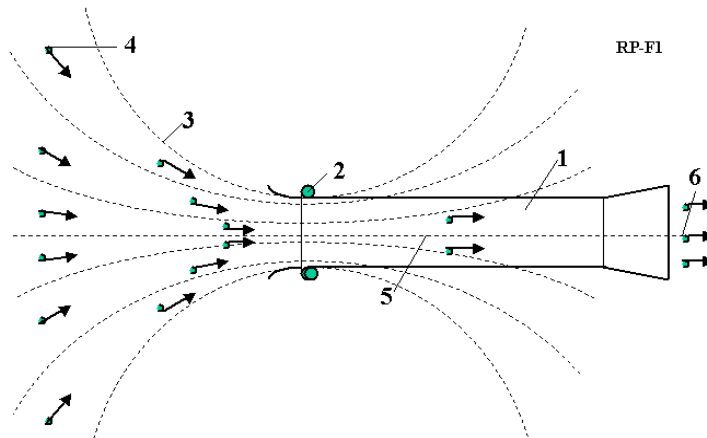---

Fig. 19.1. Recombination space jet propulsion engine (actuator of magnetic field). Notations are: 1 – engine, 2 – solenoid, 3 – magnetic lines, 4 – charged particles, 5 – recombination zone, 6 – exit.

This minimum energy is more than the energy of the most efficient chemical reaction, $H_2 + O = H_2O$, by hundreds of times. This means the specific impulse of the recombination engine will be very high. The heating of engine walls will be small, however, because the density of the particle gas is low. Using this proposed method, we do not need to expend fuel and can achieve a large acceleration of a space vehicle, or support the satellite at altitude for an infinite amount of time.

Idea's are needed in research and development of this method.

2. Utilization of the High Altitude Mirror for Lighting in Local Earth Areas

Summary

A space mirror is a large thin film space reflector. It may be used for lifting, heating of local Earth areas, and controlling weather on Earth. The author proposes an innovation and new design of space mirror, which allows the mirror to be located on the Moon or in high altitude orbits. The main advantages of these innovations are: (1) the Moon moves slowly around the Earth (its period is 29 days) and mirror control is easy, (2) the Moon is located outside Earth's shadow and the mirror can illuminate any town on Earth in full night in any area, for example, a region where there has been a disaster such as a tsunami, earthquake, etc, (3) the proposed mirror can be used to heat polar towns and control the weather, (4) the mirror is easy to maintain and repair, especially if we have an astronaut station on the Moon, (5) controlling the angle and focus of the proposed mirror is easy, (6) and the mirror may be used to support solar sail propulsion systems for space apparatus.

This innovation of a revolutionary solar mirror needs future research and computations.

Description of method and innovations
Introduction

Short history. The space mirror that reflects the Sun's rays onto the nightside of our planet is one of the impressive space projects. In 1993, the spaceship "Progress M-15" placed into orbit a 20-meter film mirror (the project "Znamya 2"). The mirror unfurled and produced a light spot that was equal in strength approximately to one full moon. A huge plash of sunlight glanced over a cloud-covered Europe to be seen only by astronomers on the top of the Alps.

The project "Znamya 2.5" stood head and shoulders above its predecessor. The mirror was expected to be perceived on the Earth as 5 to 10 full moons and it formed a trace of about 7 km in diameter which could be controlled by fixing it on one spot for a long time. The space mirror was a slightly concave membrane of 25 m in diameter made of thin film with a mirror surface, which was attached around the periphery of the station. The membrane was expected to unfold and to be held unfolded by centrifugal forces (Fig. 19.3). However, the project was a failure. Soon after deployment started, the membrane caught on the antenna. The spaceship Progress M-40 was taken out of orbit and buried in the ocean.

The Russian Space Agency announced a plan to launching in the spring 2005 a space mirror of tennis-court size. It was to be made from 2 μm film and weigh 2 kg. Its solar beam (trace) would have a diameter of 5 km (RIA "News" of 13 January 2005).

Current design of space mirror. A space mirror is composed of large flat smooth sheets of very thin film, supported by ultra-lightweight structures. The side of the film which faces the Sun is coated with a highly reflective material so that the resulting product is a huge mirror, typically about the size of a football field. The solar mirror is a method of using light energy from the Sun to illuminate the Earth at night. There are also a number of military missions in Earth orbit. The light mirror material must be as thin and lightweight as possible. Conventional light sail film has comprised 5 micron thick aluminized mylar or kapton with a thin film aluminum layer (approximately 100 nm thick) deposited on one side to form a mirror surface with 90% reflectivity.

For 5 micron thick mylar, the area density is 7 g/m^2. Although mylar is inexpensive and readily available in 0.5 micron thickness, it is not the ideal mirror film material because it is easily degraded by the Sun's ultraviolet radiation. The other key contender, kapton, can withstand ultraviolet radiation but

is not available in layers much thinner than 8 μm, with a resulting a real density of 12 grams per square meter.
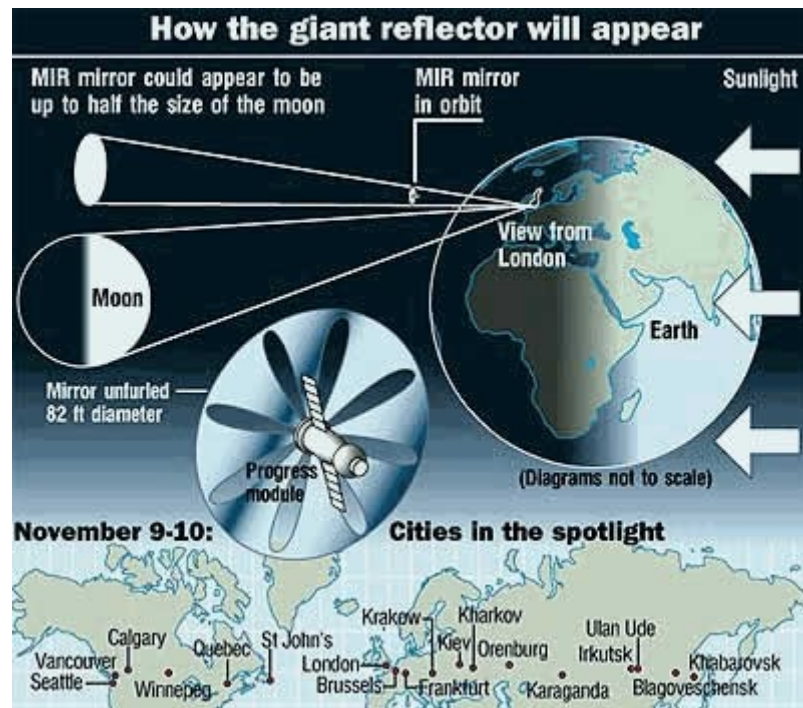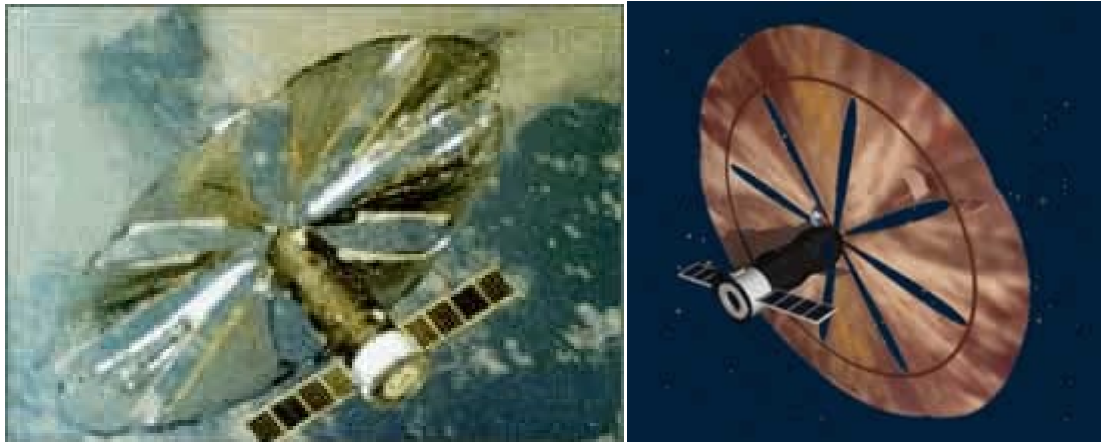
Figs. 19.3. Images of project "Znamya 2.5".

A *solar mirror* is a satellite with a large, lightweight reflector attached to it. Satellites in orbit around the Earth can survive for many years without any maintenance while using only a small amount of rocket propellant to hold their positions. Solar mirrors can be made to survive in space for many years as well.

    Standard lighting (luxs):
----
1. Sun in cloudless noon at a middle latitude   100,000
2. Cloudy day   1000
3. Necessary for reading   30–50
4. Full Moon   0.2

5. Starlight on a moonless night   0.0003

The last above table shows a sun beam at 1×1 km can illuminate an area of 2000-3300 km^2 at night with sufficient light for reading. The sun mirror of 100×100 m can illuminate 22–33 km^2. The average area of a small town is $2 \times 2 = 4$ km^2, a medium size town is $3 \times 3 = 9$ km^2 and a city $10 \times 10 = 100$ km^2. Two 100×100 m mirror are enough to illuminate a city 5×5 km as much as on a cloudy day. The power of a 1 km^2 solar beam is about 1.4 million kW, which is enough to heat a small polar town covered by thin film. We could thus save vast amounts energy in illumination and heating. By concentrating sun beams from several mirrors or focusing a beam from one large mirror on a given point (the center of a hurricane or tornado), we could influence the Earth's weather.

Unfortunately, the conventional (altitude up to 1000 km) space mirror has a lot of imperfections which limit its application (see Fig. 19.4):

1) A satellite has a high speed (8 km/s) and is located for only a short time over a given Earth area (a few minutes).
2) Satellites observe only a narrow Earth zone.
3) The satellite's high speed means a quick turn of the mirror is required to illuminate a given point (town). This is very difficult because the mirror has a large size and very thin structures, and does not allow a large angle of acceleration. It also requires a very complex control devices and a lot of fuel.
4) The satellite has orbit located in the ecliptic (equator) plate. This means it is difficult to light the polar zones, which are more in need of indirect lighting at night or additional solar heating.

These imperfections are absent from the proposed new space mirror system. It can illuminate a given point for a long time and it is easy to operate. Some of these innovations are described below.

Description of innovations and their advantages

The proposed space system for lighting, heating and weather control is presented in Fig. 19.4. The detailed design is presented in Fig. 19.5. The mirror is made from a double thin film and installed on inflatable controlled columns made from thin film. The mirror has controls for this a film tension, mirror focus, and angle (all are inventions). The system includes a set of controlled mirrors.
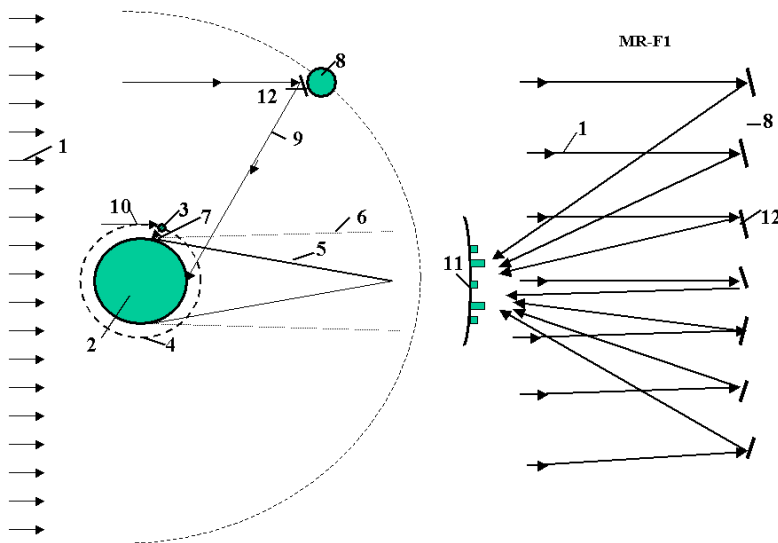
Fig. 19.1. Solar mirror located in conventional orbit. Notations are: 1 – Solar light; 2 – Earth; 3 – conventional mirror satellite; 4 – conventional mirror orbit (altitude about 200 km); 5 –Earth shadow; 6 – Earth semi-shadow; 7 – small Earth region which can be illuminated; 8 – satellite; 9 – reflected solar beam; 10 – solar beam of conventional mirror; 11 - Earth town; 12 – mirror in high altitude.

If we send the solar beam into a special Earth station, we can convert the huge amount of solar energy into any other form of energy, for example, into electricity using a conventional method (solar cell or heat machine). The 100×100 m² reflector produces 12,000 kW energy at the Earth's surface. The proposed system can be also used for long distance communication. The focused beam is directed at far distant space apparatus and can transmit information.

The set of focused mirrors may be used as an outer propulsion system for solar sail apparatus.

The suggested revolutionary system is achievable using current technology and could be produced in the near future but needs in detailed research and computation.
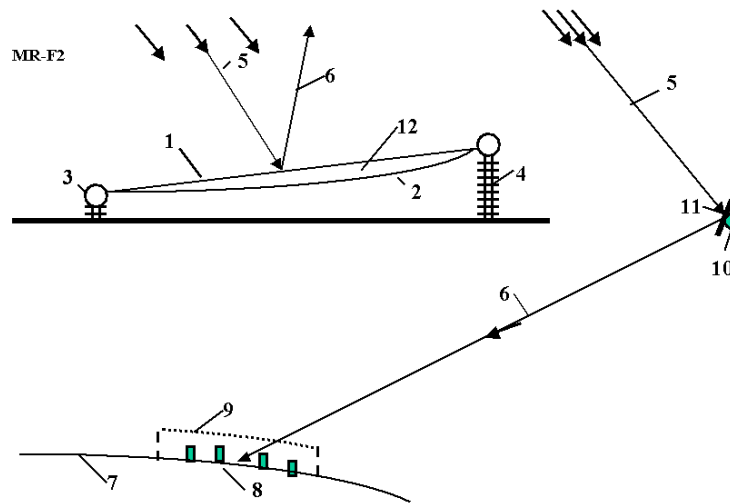

Fig. 19.5. Guided mirror on the Moon and heating a town at night. Notations are: 1, 2 – double thin film mirror; 3 – toroid ring to support and the mirror surface tension; 4 – inflatable column for controlling the mirror angle; 5 – solar beam; 6 – reflected beam; 7 – Earth; 8 – town; 9 – thin transparent film protecting the town from cold air; 10 – satellite; 11 – mirror.

3. Electronic Sail
Summary
A solar sail reflects solar light and can be a used as propulsion system, as described in Chapter 16. It needs thin film of a very large area. This section proposes a new way of creating a reflecting surface of large area using an electronic method. This method needs research and development but it may be easier and more efficient than the film method.

Brief description of innovation

The proposed electronic sail has a positive charge, 1 (see Fig. 19.6). The free electrons, 2, are injected into space around the positive charge so they rotate around the center of the charge and form a thin disk in a plane perpendicular to the direction of the Sun light. If the concentration of electrons is sufficient, they will reflect the solar light like a mirror and produce thrust.

   This electronic sail may be an electrostatic solar wind sail, as described in Chapter 13, if the central charge is positive. The solar wind electrons became concentrated around it and the mass of electrons reflects the solar light. Thrust from the solar wind is small because the electron mass is about 2000 times less than the proton mass, but the solar light pressure is thousands of times greater than solar wind (protons) pressure. The offered installation may also be used as a space mirror to illuminate the Earth's surface.   This idea needs further research.
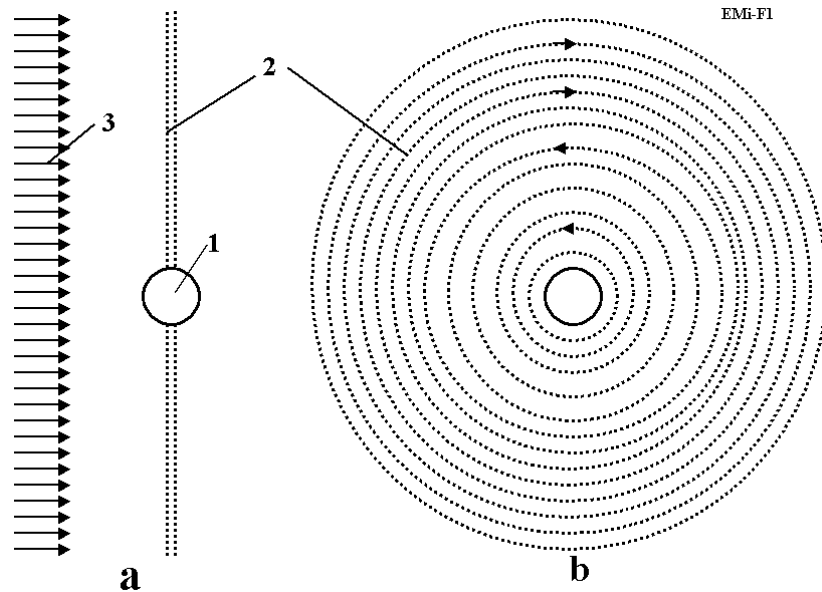

Fig. 19.6. Electronic solar sail. a – side view, b – front view. Notations are: 1 – positive charge, 2 – electronic disk, 3 – solar light.

4. In outer Space without a Space Suit?

Summary

The proposed system would enable a person to be in outer space without a space suit.

Brief Description of Innovation

   A space suit is a very complex and expensive device (Fig. 19.7). Its function is to support the person's life, but it makes an astronaut immobile and slow, prevents him or her working, creates discomfort, does not allows eating in space, has a toilet, etc. Astronaut need a space ship or special space home located not far from away where they can undress for eating, toiler, and rest.
   Why do we need a special space suit in outer space? There is only one reason – we need an oxygen atmosphere for breathing, respiration. Human evolution created lungs which aerates the blood with oxygen and remove carbon dioxide. However we can also do that using artificial apparatus. For example, doctors, performing surgery on someone's heart or lugs connect the patient to a heart–lung machine that acts in place of the patent's lungs or heart.
   We can design a small device which will aerate the blood with oxygen and remove the carbon dioxide. If a tube from the main lung arteries could be connected to this device, we could turn on (off) the artificial breathing at any time and enablethe person to breathe in a vacuum (on an asteroid or planet without atmosphere) in a bad or poisonous atmosphere, or under water, for a long time. In space we can use a conventional Earth suit to protect us against solar light. This idea may be investigated
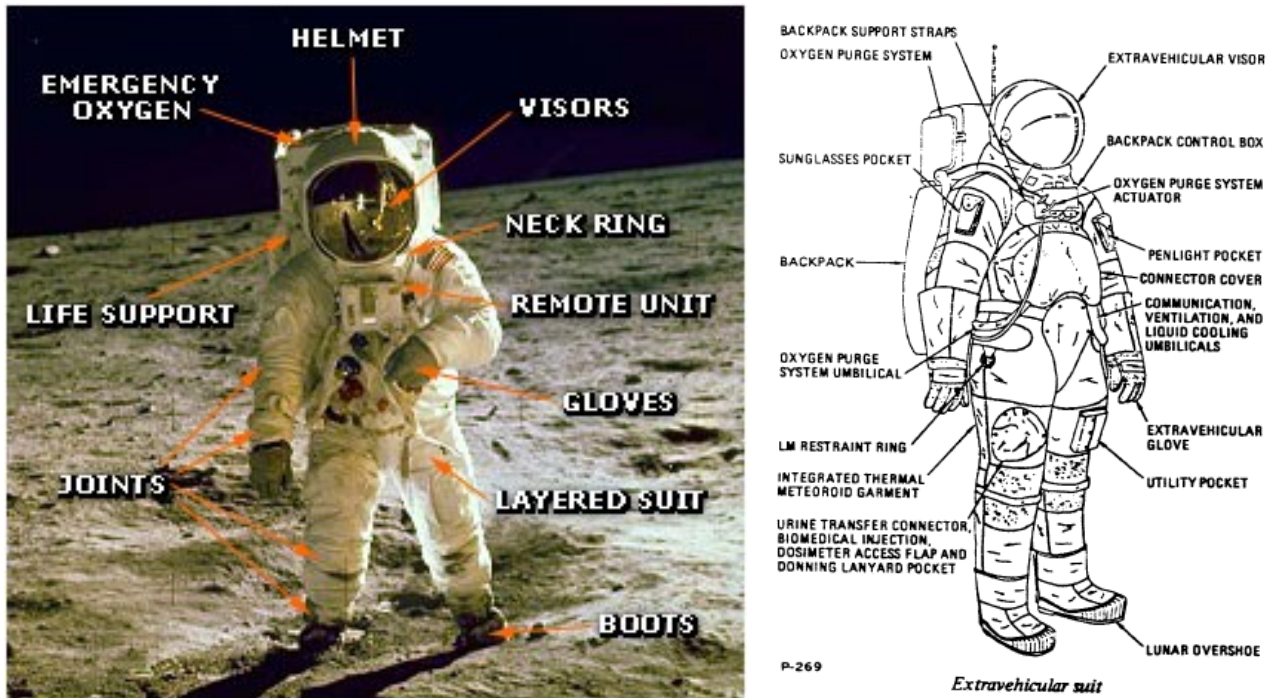
animals on Earth.

Fig. 19.7. a. Astronaut in a space suit. b. Diagram showing component parts of a space suit.

5. Electrostatic Space Radiator

A large space ship needs a vast amount of energy. For example, we can travel to far planets in a space ship with a nuclear reactor. However, its powerful electricity generator or engine requires a very large radiator to remove the surplus heat. The coefficient of efficiency of any heat machine is about 30–60%.

This means that about a half the heat gained from the reactor has to be removed thought radiation. Computation shows the heat radiator needs to have a size and weight many time greater than the space ship.

The author proposers an electrostatic radiator which has small weight and can cool a refrigerant very quickly. This is shown in Fig. 19.8.
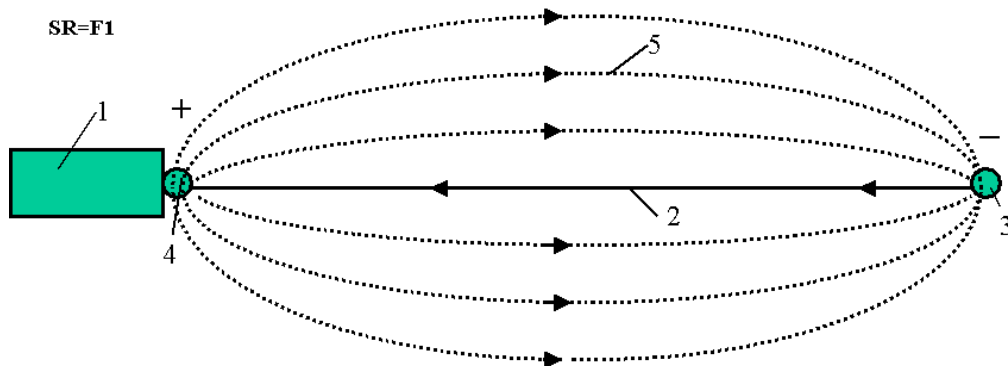

Fig. 19.8. Electrostatic radiator, Notation are: 1 – space ship, 2 – tube, 3, 4 – electrode, 5 – trajectory of drops.

The radiator works in the following way. The refrigerant is charged and sprays from one electrode and

retracts from the opposite electrode. The small drops of refrigerant have a very large surface area and emit (radiate) heat very quickly.

These and others ideas are in References[1–23].

References

1. A.A. Bolonkin, Solar Sail Engine for Spaceships, Patent (Author certificate # 1262870), priority since 10 January 1985, USSR Patent Office.

13. A,A, Bolonkin, Space Propulsion using Solar Wing and Installation for It, Russian patent application #3635955/23 126453, 19 August, 1983 (in Russian). Russian PTO.

14. A.A. Bolonkin, Installation for Open Electrostatic Field. Russian patent application #3467270/21 116676, 9 July, 1982 (in Russian), Russian PTO.

15. A.A.Bolonkin, Getting Electric Energy from Space and Installation for It, Russian patent application #3638699/25 126303, 19 August 1983 (in Russian), Russian PTO.

16. A.A.Bolonkin, Protection from Charged Particles in Space and Installation for It, Russian patent application #3644168 136270, 23 September 1983 (in Russian), Russian PTO.

17. A.A. Bolonkin, Method of Transformation of Plasma Energy in Electric Current and Installation for It, Russian patent application #3647344 136681, 27 July 1983 (in Russian), Russian PTO.

18. A.A. Bolonkin, Method of Propulsion using Radioisotope Energy and Installation for It, Russian patent application #3601164/25 086973, 6 June, 1983 (in Russian), Russian PTO.

19. A.A. Bolonkin, Transformation of Energy of Rarefaction Plasma in Electric Current and Installation for it, Russian patent application #3663911/25 159775, 23 November 1983 (in Russian), Russian PTO.

20. A.A. Bolonkin, Method of a Keeping of a Neutral Plasma and Installation for it, Russian patent application #3600272/25 086993, 6 June 1983 (in Russian), Russian PTO.

21. A.A. Bolonkin, Radioisotope Propulsion, Russian patent application #3467762/25 116952, 9 July 1982 (in Russian), Russian PTO.

22. A.A.Bolonkin, Radioisotope Electric Generator, Russian patent application #3469511/25 116927, 9 July 1982 (in Russian), Russian PTO.

23. A.A. Bolonkin, Radioisotope Electric Generator, Russian patent application #3620051/25 108943, 13 July 1983 (in Russian), Russian PTO.

24. A.A. Bolonkin, Method of Energy Transformation of Radioisotope Matter in Electricity and Installation for it, Russian patent application #3647343/25 136692, 27 July 1983 (in Russian). Russian PTO.

25. A.A. Bolonkin, Method of stretching of Thin Film, Russian patent application #3646689/10 138085, 28 September 1983 (in Russian), Russian PTO.

26. A.A. Bolonkin, "New Way of Thrust and Generation of Electrical Energy in Space". Report ESTI, 1987, (Soviet Classified Project).

27. A.A. Bolonkin, "Aviation, Motor and Space Designs". Collection *Emerging Technology in the Soviet Union*, 1990, Delphic Ass., Inc., USA, pp. 32–80.

28. A.A. Bolonkin, "A Space Motor Using Solar Wind Energy". The World Space Congress, Washington, DC, USA, 28 Aug. – 5 Sept., 1992, IAF-0615.

29. A.A. Bolonkin, "The Simplest Space Electric Generator and Motor with Control Energy and Thrust", 45th International Astronautical Congress, Jerusalem, Israel, 9–14 Oct., 1994, IAF-94-R.1.368

30. A.A. Bolonkin, "Space Electric Generator, Run by Solar Wing". The World Space Congress, Washington, DC, USA, 28 Aug. –5 Sept. 1992, IAF-92-0604.

31. A.A. Bolonkin, " A Simple Space Nuclear Reactor Motors and Electric Generators Running on Radioactive Substances", The World Space Congress, Washington, DC, USA, 28 Aug. –5 Sept. 1992, IAF-92-0573.

32. A.A. Bolonkin, , "Theory of Flight Vehicles with Control Radial Force". Collection *Researches of Flight Dynamics*, Mashinostroenie publisher, Moscow, 1965, pp. 79–118 (in Russian).

33. Internet site http://Bolonkin.narod.ru.

34. Internet site http://NASA-NIAC.narod.ru .

Attachments

Non-conventional and non-rocket flight on Earth
Attachment 1

Air Cable Transport and Bridges*
Summary

Currently aircraft are used to move payloads and passengers from one place to other. This method is expensive, because aircraft use expensive fuel and have high capital costs. The author proposes a new method for less expensive delivery of payloads and people from one city to another (similar to airlines), or across streams, rivers, canyons, and mountains. This method uses a closed-loop cable path with a propulsion system located on the ground. The system can utilize any inexpensive energy source and air vehicles or cheaper winged containers without expensive electronic equipment. This method is particularly effective for providing an air bridge across straits, or mountains, or for gas lines. It is cheaper by hundreds of times than conventional long bridges, tunnels, and gas lines.

  The author develops the theory and provides computations for two projects: airline travel from New York to Washington and New York to Paris, and air bridges such as across the Straits of Gibraltar, the English Channel, Bering Straits (Russia–America), Sakhalin–Asia, Russia–Japan, etc. Calculations are also provided for one gas line project. The proposed systems can also transfer large amounts of mechanical energy from one place to another (about 3 to 10 million watts) with high efficiency.

Introduction

Currently, aircraft, cars, trucks, trains, and ships are used to move payloads from one place to another. This method is expensive and requires good highway systems and expensive vehicles, which limits the feasibility of delivering many types of freight. Aircraft use expensive fuel and have high capital costs. The author offers a new, revolutionary method and installations for cheaper delivery of payloads and people (1) from one place to another, (2) across streams, rivers, canyons, etc., (3) accelerating vehicles to a desired velocity, and (4) cheaper vehicles which do not require their own engine. The method uses a closed-loop cable path with the propulsion system located on the ground; the concept includes airlines. The proposed system is unique with no references found for similar systems in the literature or patents.

  At the present time, all vehicles (cars, trucks, buses, trains, aircraft, airships, dirigibles, sea ships) use engines located on the vehicle. Their engines require expensive fuel (for example, gasoline). The vehicle must carry both the engine and the fuel, which reduces the payload capacity. For example, for

aircraft flying long distances the fuel weight may reach 30 to 40% of the takeoff weight, and the engine weight is about 10% of the full weight of the vehicle. As a result the payload is decreased to only 10–20% of the vehicle takeoff weight.

The proposed method maximizes the payload (no engine, no fuel in the vehicle), allows use of the cheapest form of energy (such as liquid fuel, natural gas, wind, or hydro-power stations) and cheaper vehicles.

The basic idea is simple (see Fig. A1.1): to connect the vehicle to an engine located on the ground using a strong light cable. Loss of flexibility is not a large problem, because heavily traveled routes for civilian airlines are fixed. The problems appear when we want to cover a long distance (from one mile up to hundreds or thousands of miles) across a stream, river, sea, ocean, or heavily congested area, especially when suspending the cable in the air at high altitudes (5–11 km). For highways, the connection and disconnection of the vehicle (auto, car, truck, bus) at required locations along the route of a permanently moving cable is also a problem. For city transport systems (large numbers of routes and stops), the changing of lines and directions, and the organization of the delivery of a huge flow of different vehicles to many points also must be addressed.

These main problems are solved in the proposed innovation[1-3].

The important feature of this invention is the possibility of using existing aircraft and autos (trucks, or buses) for the suggested system after connection–disconnection devices are added to them.

Computations show a strong and light cable (rope) for long-distance movement (delivery, transportation) system (some hundreds or thousands of miles) is required. Currently, industry is producing cheap fibers which have the required properties. We also have fibers, whiskers, and experimental nanotubes, that have the required properties for application to the proposed ideas.

For distances of over 100 kilometers the light, strong, cable (rope) requires a ratio of tensile strength/specific weight, of more than 200 km.

The objective of this innovation is to provide cheap delivery of payloads and people from one place to another. This may include airlines from one city to another, bridge delivery over a stream, river (flying bridge), ferry-boats, a ground highway, a city transportation system or gas line.

Moreover the suggested transportation system can transfer large amounts of mechanical energy from one place to another on Earth (about 3 to 10 Millions watt) with high efficiency.

Other applications that use these ideas are presented in the References[4–12].

Short Description of Installation

An example of an installation is shown in Fig. A1.1a (side view). This is an airline, an air bridge over a sea strait, stream, or channel, for example, the Straits of Gibraltar (16 km). The installation includes the terminals (departure and arrival), a light, strong closed-loop (main) cable (rope, chain) over the surface, strait, mountain, or water (in both directions), winged containers (winged cabins) for payloads and people, a wing support devices (suspension, support system). The Fig. A1.1b shows the upper (top) view of this installation.

Fig. A1.1c shows the terminals (departure and arrival ports). The departure terminal (port) has a starting (acceleration) station (system), a takeoff runway, on arrival (braking) station (system), a starting (acceleration) closed-loop cable (rope), starting rollers, starting engine (engine of the starting system), starting connection–disconnection sliding device (connected to a starting cable and to the winged container), main connection–disconnection sliding devices (connected to the main cable and to the winged container), landing runway, platform for arriving winged containers (unloading station), platform for departing winged containers (loading station). The terminals also have rollers for the main cable and an engine (drive) station for the main cable. The engine (drive) station includes engines,

storage of energy (energy storage system) (for example, inertial flywheel), transmission, clutches, brake, control system, and an energy transfer system.
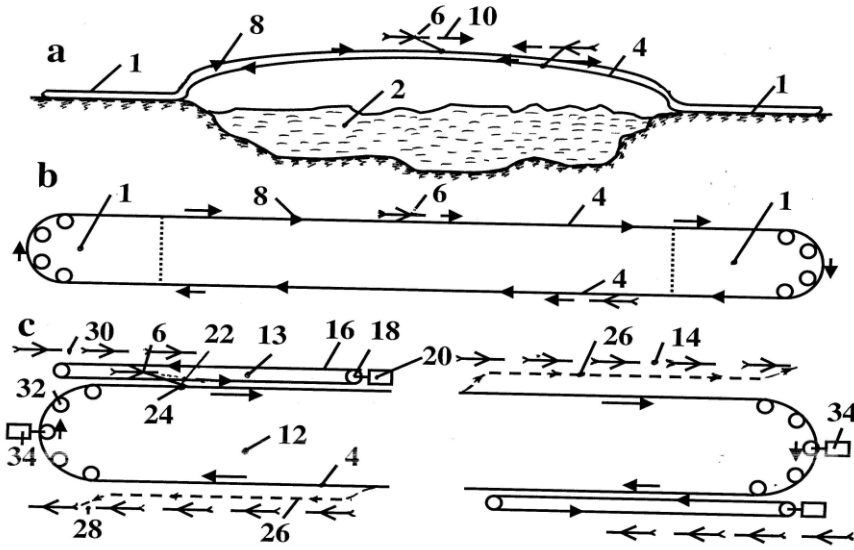

Fig.1a,b,c.

Fig. A1.1 a. Airline or bridge (side view).Notations: 1 – terminal; 2 – Earth's surface, strait, river, mountain, canyon, etc.; 4 – main closed-loop cable (loop, rope, chain) of the transport system; 6 – winged container (cabin); 8 – support devices (support wings); 10 – direction of a winged container motion. **b.** Air line or bridge (top view). **c.** Terminals. Notations: 12 – departure (starting) port (terminal); 13 – acceleration station; 14 – braking station of an arrival port; 16 – closed-loop cable (loop, rope) of acceleration station; 18 – rollers; 20 – drive system (station); 22 – connection–disconnection device to an acceleration cable; 24 – connection–disconnection device to the main transport cable; 26 – landing (braking) runway for the winged container; 28 – delivery (arrival) (unloading) port; 30 – departure (loading) port; 32 – rollers of the main cable; 34 – engines of the main cable.

This installation works the following way (Fig. A1.1c). The acceleration engine moves the closed-loop starting cable (rope, chain) and the main engine moves the primary closed-loop main cable. When payload (cars, trucks) and people arrive at the port, they are loaded onto the platform and rolled to the winged containers. The winged container is connected to the starting cable via the connection device and the starting engine system accelerates the container to a velocity on which the wing can keep the container in the air. At the end of the takeoff segment of the flight, the container is disconnected from the starting cable and transferred on to the main cable. The container flies over the surface (strait, water) and lands at the arrival port. Here it is disconnected from the main cable, and brakes on the landing runway. It moves to the arrival platform, where it is unloaded, and moved to the departure platform for the next loading and flight. Delivery in the opposite direction is the same.

Fig. A1.2 shows the support wings at the main transport cable. Fig. A1.3a,b shows the support system using columns or air balloons.

In a ground (highway) system, then the cars and trucks can connect to the moving cable and travel without using fuel or polluting the environment.
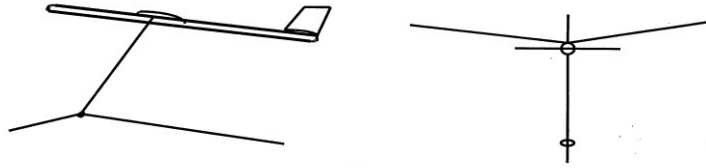
Fig.2.

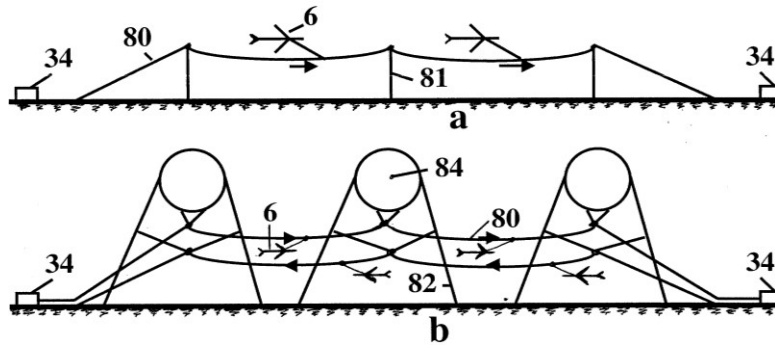**Fig. A1.2.** Support wings of main transport cable.

Fig. A1.3. a. Column support system of the main transport cable. 80 – main transport cable; 81– column.
b. Air balloon support system. 82 – balloon cable tether; 84 – balloon.

Advantages

The suggested movement system has large advantages in comparison with the current systems of airlines, bridges, underground tunnels, and delivery by conventional cars and trucks.

Airlines

1. Aircraft are very expensive. The suggested Airlines system does not use conventional aircraft. It use a cheap winged container or cabin, without engines and expensive electronic equipment for navigation and communication.
2. Aviation fuel is expensive. The proposed airline system can use any sort of energy such as wind, water, or nuclear power or fuels such as natural gas, coal, peat, etc., because the engine is located on the Earth's surface. The cheapest energy can be used. The old airplanes (without their engines and electronic equipment) may be used as winged containers.
3. It is not necessary to have highly qualified personnel such as pilots with their high salaries.
4. The fare for the flight will be much lower.
5. Terrorists cannot use this system to damage important structures.

Bridge or underground tunnel

1. The suggested air bridge is cheaper than a conventional long bridge, or especially an underground (underwater) tunnel, by hundreds of times (for long bridges, by thousands of times). The cost decreases from some billions of dollars to some tens of millions of dollars.
2. An air bridge can be made in a few months, whereas a conventional bridge or tunnel requires years for construction.

3. The cost of an air bridge does not increase as its length increases (only the length of the cable increases). The cost of a conventional bridge or tunnel increases more quickly as its length increases.
4. The air bridge can be built in places where it is impossible to build a bridge or tunnel by modern technology (for example, across the Bering Straits between the continents of Asia and North America (between Russia and the USA).
5. The transit time (time of delivery) is reduced significantly.
6. The toll fee for using an air bridge will be lower and/or decrease more rapidly due to lower overall construction costs.

Surface transport (movement) system

1. Very simple and cheap vehicles can be used for passenger and payload transportation by the suggested transportation system. It may be a simple (no engine) box or platform with wheels, a roller board or roller skates. It can also be a conventional car, bus, or truck. The vehicle only need to have (or be equipped with) the sliding connection device.
2. The system does not pollute the environment on highways nor, especially, in large cities.
3. The system does not use expensive liquid fuels (gasoline or diesel). It may use wind, water or any cheap form of energy.
4. Delivery can be made without a conventional vehicle (for example, people on roller skates).
5. It can use as vehicles cars, buses, trucks, trains, and ships, and can utilize old vehicles, with their engines turned off to prolong the life of the old vehicle, whose engines may be outdated.
6. It reduces traffic accidents because the vehicles move sequentially and cannot pass one another.

Air gas line

1. The suggested air gas line is cheaper than a conventional ground gas pipeline by hundreds of times. The cost falls from some billions of dollars to some tens of millions of dollars.
2. An air gas line can be made in a few months whereas a conventional ground pipeline requires several years for building.
3. There is no damage to the environment.
4. It has very high load capability. The line can delivery gaseous, liquid, and solid payloads.
5. It has impossible to steal the gas when the pipeline runs across the territory of a third country.
6. It is easy to change the direction (the route) of the line, for example when a conflict arises with a country whose territory is used (crossed) by the gas line.

Formulas for Estimation and Computation (in metric system)

 The following formulas have been developed or used by the author. They allow you to calculate different variants.
1. The cross-section area and weight of a starting (acceleration) cable of constant cross-section area can be found from equation (balance, equilibrium) inertia force to cable stress

$$S = mng/(\delta - ng\gamma L), \quad W = SL\gamma, \tag{A1.1}$$

where: S – cross-section area of cable area [m^2]; m – mass of apparatus [kg]; n – overload; δ – tensile stress [N/m^2]; γ – specific density [kg/m^3]; L – distance between power stations [m]; W – cable weight [kg]; $g = 9.81$ m/s^2.
2. Cross-section area S_o and weight W_o of a transportation cable supported by wings are

$$S_o = (D + m/K_1)/(\sigma - \gamma L/K_2) \ , \tag{A1.2}$$
$$W_o = S_o\gamma L \tag{A1.3}$$

where : K_1 – ratio of lift force to drag force of the winged container ($K_1 = 10$–17), K_2 – ratio of lift force to drag force of the support cable wing, D – drag of cable. The cable drag is small. Results of computation for $D = 0$ presented in Figs. A1.4 and A1.5.
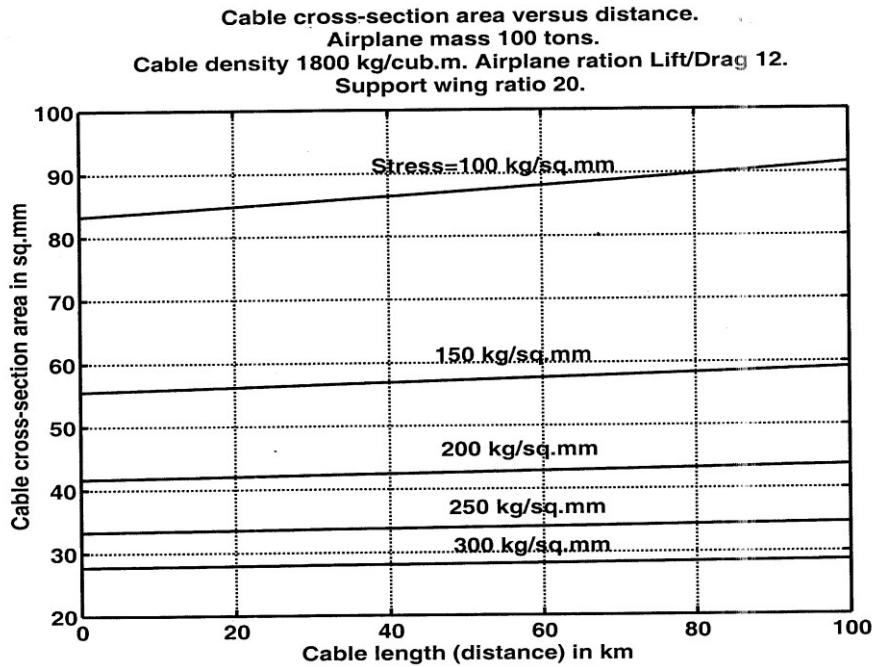

Fig. A1.4. Cable cross-section area versus distance 0–100 km for safe tensile stress 100–300 kg/mm². Airplane mass is 100 tons. Cable specific density is 1800 kg/m³. Airplane ratio of lift/drag is 12. Support wing ratio of lift/drag is 20. Cable drag is 0.

Fig. A1.5. Cable mass versus distance 0–100 km for cable tensile stress 100–300 kg/mm². Airplane mass is 100 tons. Cable specific density is 1800 kg/m³. Airplane ration of lift/drag is 12. Support wing ratio of lift/drag is 20. Cable drag is 0.
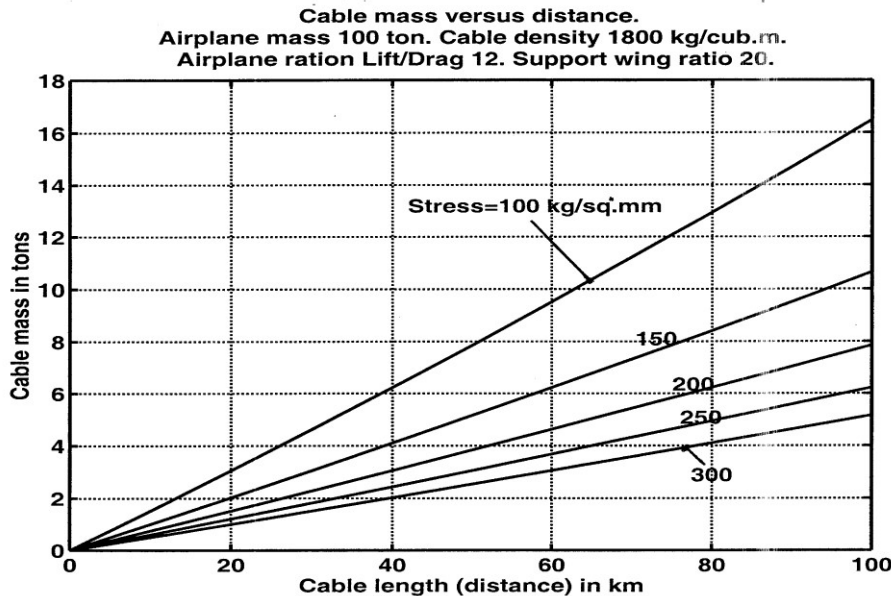
Equation (A1.2) gives a maximum cable distance L supported by wings

$$L = KK_2 , \qquad\qquad\qquad (A1.4)$$

where $K = 10^{-7}\sigma/\gamma$ is the stress coefficient. Results of the computation are presented in Fig. A1.6. The other methods of cable support (balloons or columns) do not have this restriction. They may be computed using equations (A1.2) – (A1.3) if $K_2 = \infty$.
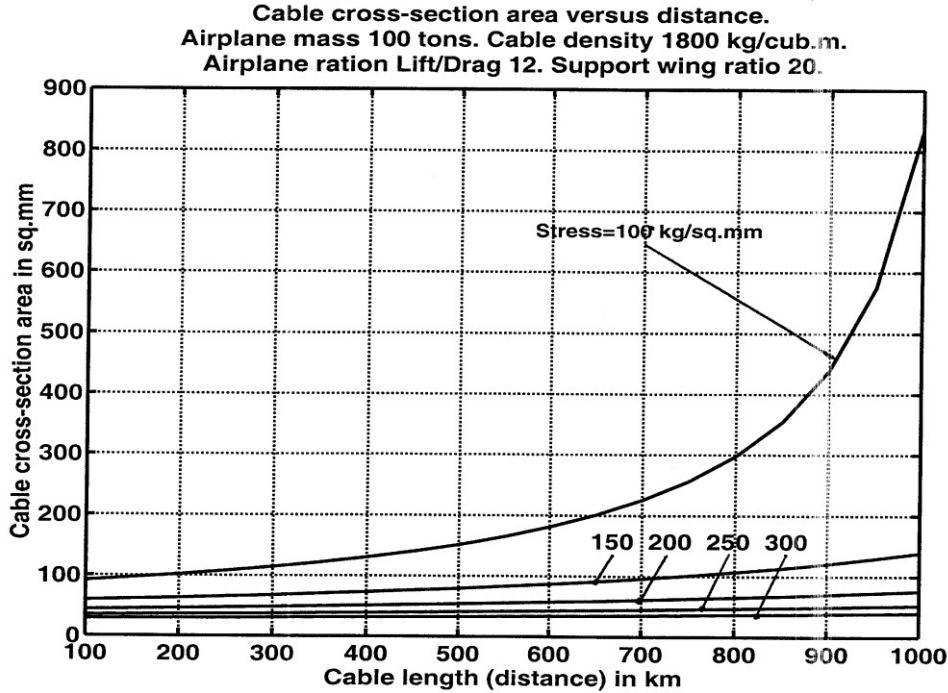
Cable cross-section area versus distance.
Airplane mass 100 tons. Cable density 1800 kg/cub.m.
Airplane ration Lift/Drag 12. Support wing ratio 20.

Fig. A1.6. Cable cross-section area versus distance 100–1000 km for tensile stress 100–300 kg/mm². Airplane mass is 100 tons. Cable specific density is 1800 kg/m³. Airplane ratio of lift/drag is 12. Support wing ratio of lift/drag is 20. Cable drag is 0.

3. Energy, E, stored by the rotary flywheel per 1 kg cable [joules/kg] can be found from the known equation of the kinetic energy

$$E = 2\delta/\gamma . \tag{A1.4}$$

4. Estimation of cable friction due to air. This estimation is difficult because there are no experimental data for air friction of an infinitey thin cable. Let us use the well-known equation for air friction (drag) of a flat plate. This friction (drag) may be turbulent or laminar. Their values are different. The plate has two sides, which means for the cable, the drag value must be halved. For subsonic speed and a flat plate the equations for turbulent and laminar drags are

$$D_T = 0.0573\rho^{0.8}\mu^{0.2} V^{1.8}L^{0.8}d , \tag{A1.6}$$
$$D_L = 1.04\rho^{0.5}\mu^{0.5} V^{1.5}L^{0.5}d . \tag{A1.7}$$

Where: D_T is turbulent drag, D_L is laminar drag; ρ, μ are air density and air viscosity respectively; $\rho = 1.225$ kg/m³, $\mu = 1.79/10^5$ kg/s.m at altitude 0 km and $\rho = 0.5258$ kg/m³, $\mu = 1.527/10^5$ kg/s.m at altitude 8 km; V is speed [m/s], L is length of plate (distance between drive station) [m], d is diameter of the cable [m]. It is postulated that the cable surface has a half-laminar boundary layer because a small side wind will blow away the turbulent layer and restore the laminar flow.

$$D = 0.5(D_T + D_L) , \tag{A1.8}$$

where D is air drag (friction) [N].
Results of these computations are given in Figs. A1.7 to A1.10.

Cable mass versus distance. Airplane mass 100 ton.
Cable density 1800 kg/cub.m. Airplane ration Lift/Drag 12.
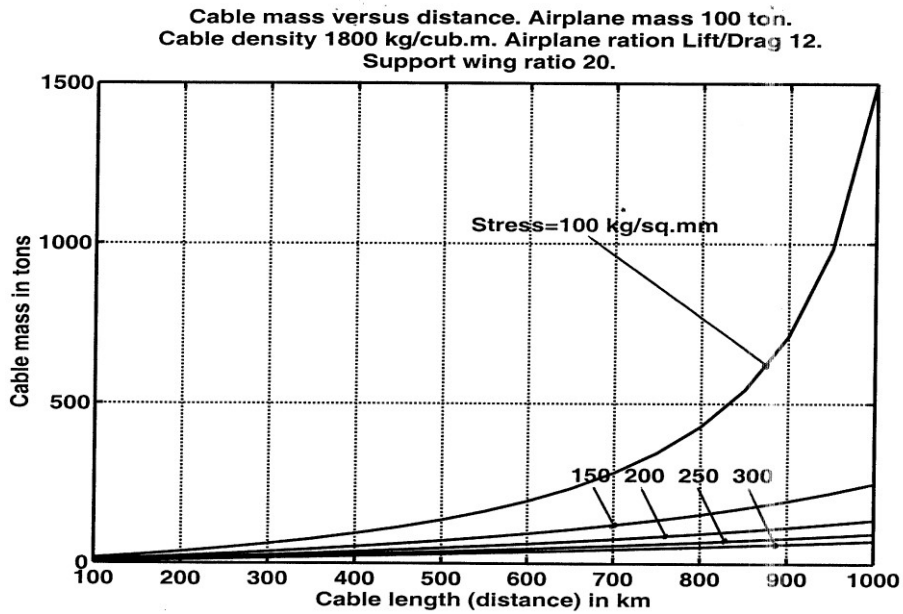**Support wing ratio 20.**

Fig. A1.7. Cable mass versus distance 100–1000 km for cable tensile stress 100–300 kg/mm². Airplane mass is 100 tons. Cable specific density is 1800 kg/m³. Airplane ratio of lift/drag is 12. Support wing ratio of lift/drag is 20. Cable drag is 0.
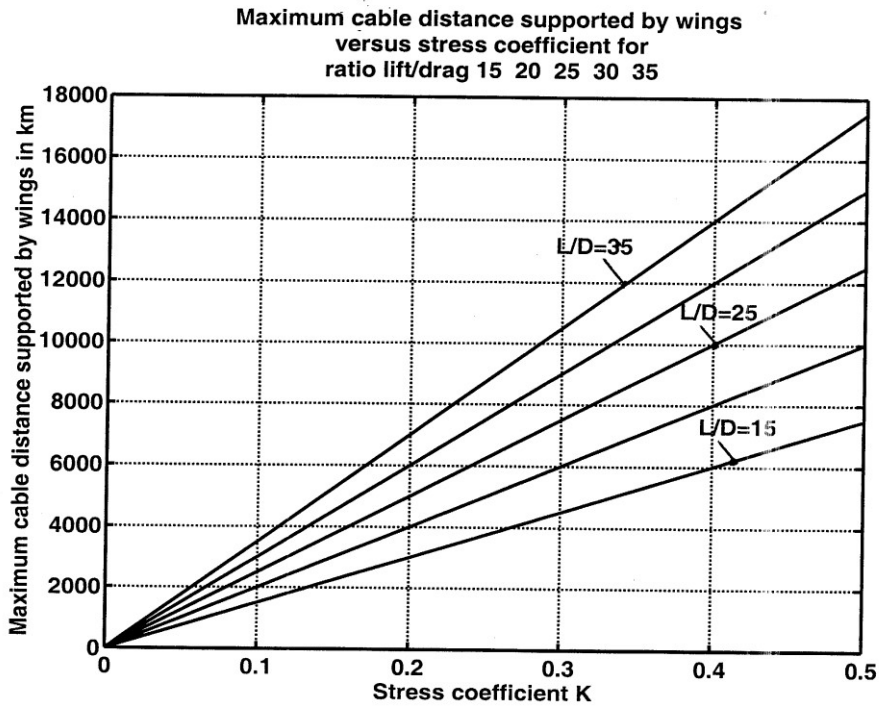
Maximum cable distance supported by wings
versus stress coefficient for
ratio lift/drag 15 20 25 30 35

Fig. A1.8. Maximum cable distance supported by wings versus stress coefficient for lift/drag ratio 15, 20, 25, 30, 35.

Cable air drag versus speed and cable diameter 0.2 0.4 0.6 0.8 1 cm.
Length 100 km. Altitude 4 km

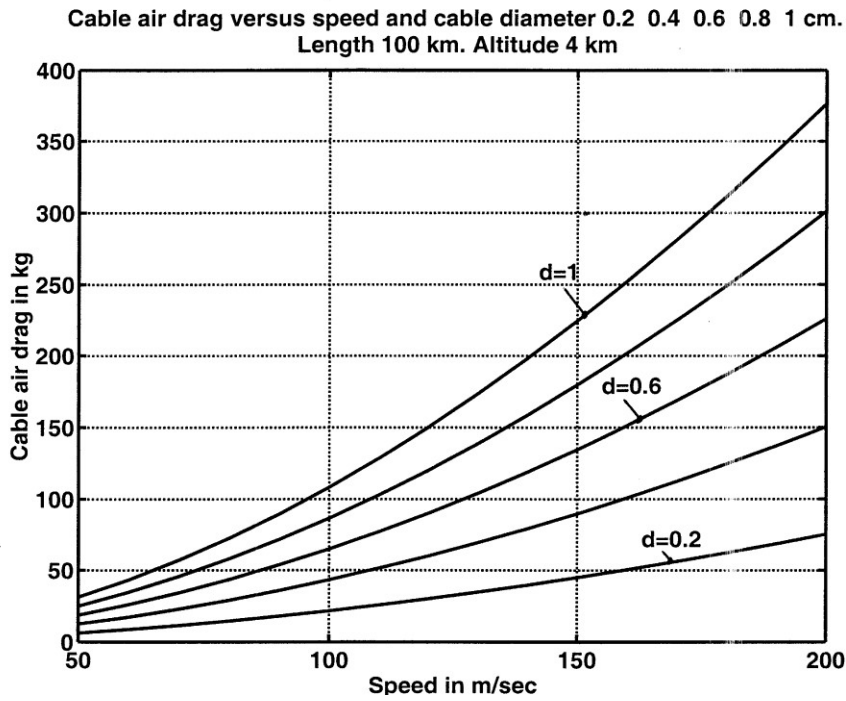**Fig. A1.9.** Cable air drag versus speed for cable diameter 0.2, 0.4, 0.6, 0.8, 1 cm. Cable length is 100 km. Altitude is 4 km.

Cable air drag versus speed
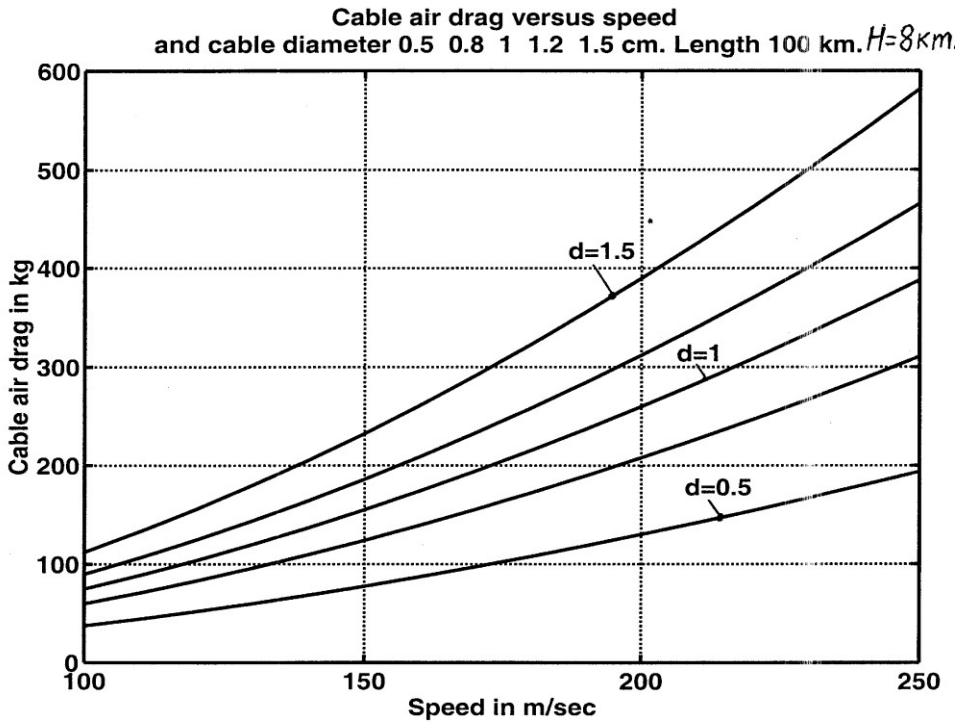**and cable diameter 0.5 0.8 1 1.2 1.5 cm. Length 100 km.** *H=8km.*

Fig. A1.10. Cable air drag versus speed for cable diameter 0.5, 0.8, 1, 1.2, 1.5 cm. Cable length is 100 km. Altitude is 8 km.

Cable problems

The cable problem were discussed in Chapter 1. They are same for all projects in other chapters.

Below, the author provides a brief overview of recent research information regarding the proposed experimental (tested) fibers.

Data which can be used for computation

Let us consider the following experimental and industrial fibers, whiskers, and tubes (see chapters 1):

1. Experimental nanotube CNT (carbon nanotube) has a tensile strength of 200 Giga-Pascals (20,000 kg/mm^2), Young's modulus is over 1 Tera Pascal, specific density $\gamma = 1800$ kg/m^3 (1.8 g/cc) (year 2000).

   For a safety margin $n = 2.4$, $\sigma = 8300$ kg/mm$^2 = 8.3 \times 10^{10}$ N/m^2, and $\gamma = 1800$ kg/m^3, $(\sigma/\gamma) = 46 \times 10^6$. SWNTs have a density of 0.8 g/cc, MWNTs have a density of 1.8 g/cc. Unfortunately, nanotubes are very expensive at the present time (2002).

   C_D whiskers have $\sigma = 8000$ kg/mm^2 and $\gamma = 3500$ kg/m^3 (1989). The computations assume $\sigma = 7000$ kg/mm^2, $\gamma = 3500$ kg/m^3, and $\sigma/\gamma = 20 \times 10^6$.

2. Industrial fibers have $\sigma = 500$–620 kg/mm^2, $\gamma = 1800$ kg/m^3, and $\sigma/\gamma = (2,78 - 0.334) \cdot 10^6$.

Projects

Below readers could find some examples of projects which utilize the suggest ideas.

Project 1: Air line from New York to Washington (340 km)

Let us take one winged cabin (container) with a weight of 100 tons. The payload is 2/3 of the full weight (66 tons ≈ 660 passengers). The flight time at a speed of 200 m/s is 28.3 min ≈ 30 min, or about 100 flights per day (in both directions). The total (maximum) number of passengers is 66,000 or 6,600 tons of payload per day. Assuming an aerodynamic efficiency of 16 (ratio of lift/drag), the required thrust is 100/16 = 6.2 tons. We assume a thrust of 10 tons for one direction (including cable drag and drag of the support devices). For safe cable tensile strength $\sigma = 250$ kg/mm^2, the required cable cross sectional area is 40 mm^2, the cable diameter is 7.2 mm, and the cable weight is 24.5 tons for a cable density of 1.8 g/cc. The air drag of a cable at an altitude of 7 km is 1.08 tons.

Estimation of drag for the support flight devices assumes the aerodynamic efficiency equals 25. Then the support device drag will be 24.5/25 = 1 ton. The total drag is 6.2 + 1.08 + 1= 8.28 tons, which is less than the 10 tons of thrust available. The required power is $V \cdot T = 200 \times 10,000 \times 10 = 20$ MW or 40 MW for both directions. This equals the power of four 10,000 KW turbo-jet engines.

The winged container has a wing area of 170 m^2 and a wingspan of 42 m
.

Production cost of one passenger delivered

Assume the cost of the installation is $20 million dollars and it has a service life of 20 years. The system requires 40 employees with an average salary of $50K per year, the fuel cost is $0.25 per liter. The depreciation is $2750 per day, the salary is $5500 per day, and the fuel cost is $64750 per day. Assuming 66,000 passengers daily, we find that the delivery production cost is less than $1 per passenger (64750/66000). If this cost is divided by a loading coefficient of 0.75, the delivery cost is $1.3 per passenger. This is less than a subway fare in New York ($2, 2005). If a flight fare of $4.99 is charged, the profit is $173K per day or $63 million per year. You can live in New York and work in Washington DC. The flight takes about 30 minutes, which is less than the average transit time of the NY subway.

Project 2: Airline from New York to Paris (6200 km)

Assume a flight speed of $V = 250$ m/s, an altitude of $H = 11$ km, and a cable is supported by winged devices. The New York to Paris flight time is $(6,200,000/250) \approx 7$ hours.

   Let us take three winged cabins (containers) for one route, which move simultaneously in one direction. Each cabin has a weight of 100 tons (the payload is 66 tons) and has an aerodynamic efficiency of 16 (ratio of lift/drag). The required cable thrust is about $6.2 \times 3 = 18.6 \approx 20$ tons for one direction or 40 tons for both directions. There are 10 flights per day in one direction and 10 flights in the return direction. The total load capability is (6600×2) 13,200 passengers in both direction per day or 1320 tons of payload.

   Assume the cable is manufactured from whiskers, C_D, with a tensile strength of $\sigma = 8000$ kg/mm^2 and density of 3.5 g/cc. Using a typical safety coefficient (safe margin) of 2.4, the safe tensile strength is $\sigma = 3300$ kg/mm^2, the cable cross-sectional area of 12.1 mm^2, and cable diameter is 4 mm for a thrust of 40 tons in one direction. The cable weight is 262.6 tons (for 6200 km), and the cable drag is 3.3 tons (half the boundary layer is turbulent and half is laminar). If the aerodynamic efficiency of the support devices is 25, their additional drag is (262.6/25) 10.5 tons. The total drag is $(18.6 + 3.3 + 10.5) = 32.4$ tons, which is less then the assumed thrust of 40 tons.

   The winged cabin is the same as the New York–Washington DC project. If the support device supports 10 km of cable (424 kg), the required wing area equals 0.743 m^2, with a wing span of 3.3 m.

   The required power is $P = 4,000,000 \times 250 = 100$ MW for one end; that is 10 turbo-jet engines with 10,000 KW of power each.

Economical Estimation.

   The system installation cost is \$30 million with a service lifetime of 10 years. Employee costs assume 100 men with an average salary of \$50K per year, and fuel cost is \$0.25 per liter.

   Assuming a depreciation of \$8.24K per day, salaries of \$13.74K per day, and fuel costs of \$324K per day; if the average load equals 75% of the maximum load, the number of passengers is 9150 per day. The operational cost of the delivery of one passenger is \$38 per person or \$0.38 per kg. If the fare is \$120, the profit is $80 \times 9150 = \$732$K per day $= \$266.5$ million per year.

   More than 90% of this cost is fuel; if aviation fuel is not required, a lower cost fuel (for example natural gas) can reduce operational costs in proportion to the reduced cost of the fuel.

Project 3: Air Bridge

There are a lot of islands in the world, located close to one another or located close to a continent, which have large transportation flows. For example:

1. Straits of Gibraltar (16 km); connects Europe with Africa.
2. English Channel (40km); connects England with Europe.
3. Sicily and Italy (5 km).
4. The Dardanelles (2 to 5 km).
5. Various Japanese Islands.
6. Taiwan with mainland China (25 km).
7. Bering Straits (100 km) (Russia and America).
8. Sakhalin-Asia (20 km) (Russia).

   An estimation of the main parameters for a Gibraltar air bridge (16 km) are presented, this estimation is similar for the English Channel or the other bridges listed above.

The main parameters are computed for the following daily load flow (same in both directions):
1. 1000 cars, the weight of each is 1 ton, total is 1000 tons.
2. 1000 trucks, the weight of each is 10 tons, total is 10,000 tons.
3. 10,000 people, the weight of each is 100 kg, the total is 1000 tons.

The total daily load flow in one direction is 12,000 tons, for a total load flow of 24,000 tons. Let us assume the average payload of a winged container is 2/3 of its maximum payload capability. The total payload capability of the winged container is 300 tons, thus the average payload is 200 tons for one container. Then we will need (12000/200) = 60 flights per day in each direction.

Let us assume a flight (cable) speed of 100 m/s (speeds up 250 m/s can be used). The flight takes (16000/100) 160 seconds (about 3 minutes) in one direction; the English Channel transit time (40 km) will be 7 min with a speed of 100 m/s and 3 min with a speed of 250 m/s.

If the loading of the winged container takes 25 minutes, one wing container can make 50 flights per day. For 120 flights we will need 3 winged containers.

Estimates for the cables assume they are manufactured from fibers which have a tensile strength of σ = 620 kg/mm^2 and density of 1.8 g/cc (for example, QC-8805). Let use a safety coefficient of 2.4, then the safe σ = 250 kg/mm^2. Let us use an aerodynamic efficiency (ratio of lift/drag) of 12 (current airplanes are up to 17, and gliders up 40). Then the drag of the container is (300/12) 25 tons. This is increased to 30 tons (we assume about 2–3% cable air drag plus 1–2% drag from the flight support devices). The cross-sectional area of the cable is (30000/250) 120 mm^2, and the cable diameter is d = 12.4 mm. The weight of two cable branches (32 km) is 6912kg $\approx$ 7 tons. It the aerodynamic efficiency of the flight support devices equals 20–30 the additional drag will be 7000/20 = 350 kg or 350/30000 = 0.012 = 1.2% of the total thrust.

The required energy impulse is N = 300000N × 100m/sec = 30 MW over a 160 seconds period. If we use an inertial accumulator of energy and the flight frequency is 12 min, we will need an engine with a steady state power output of N = 30×160/12×60 = 6670 kW; this is equivalent to one turbo engine. The weight of the inertial accumulator of energy (constructed from fibers) is 30×160/0.75 = 6400 kg = 6.4 tons.

Estimations of acceleration system requirements assume an acceleration for take-off and landing of a = 0.5g = 5 m/s^2. Takeoff and landing distance is $L = V^2/2a$ = 10000/10 = 1000 m = 1 km. The thrust required for acceleration is $T = Wa/g$ = 300×5/10 = 150 tons. The cable has a cross-sectional area of (150000/250) 600 mm^2, a diameter of 28 mm^2, and a weight of 4320 kg.

Estimation of the support flight devices assumes that one device supports 1 km of cable. The weight of 1 km of cable with a cross-sectional area of 120 mm^2 is 216 kg. If the lift coefficient is 1, the necessary wing area is 0.42 m^2, resulting in a wing size of 2×0.2 m.

Data on the flight container assume the wing area is 480 m^2, the wing span is 80 m (80x6 m), the size of the container is 10x5x86 m, the useful area of the floor is 500 m^2, and the useful volume is 2500 m^3.

For the suggested bridge we need only 11.4 tons of cable, 3 winged containers, a 6700 KW engine, an inertial accumulator of energy with a disk weight of 6.4 tons, and two simple ports with 1 km of runway length. The bridge system would cost 10–30 million dollars and require 6 months for construction. The English Channel tunnel costs some billions of dollars, construction took many years, and delivery transit time is more than 0.5 hour. If the tunnel is damaged, the repair will be very expensive and take a long time.

Economic Estimation

Let us assume the cost of the air bridge is 15 million dollars (winged containers, engines, flywheels, and departure and arrival stations) and has a service life of 15 years (depreciation is $1 million per

year) . Employee costs assume 80 people with an average salary of $50K per year (maintenance is $5 millions per year, $14K per day), and fuel costs of $0.25 per liter ($10,850 per day). The total load flow is 24,000 tons per day. The direct operating costs will be less then $2 per ton ($2 per car). If the toll charge for using the bridge is $5 from 1 car (1 ton), the profit will be $13 million per year.

Project 4: Ground vehicles (e.g., Auto Highway)

Assume a closed-loop ground cable section with a length of 100 km in one direction. The cable is made of fibers with an safe tensile strength of $\sigma = 250$ kg/mm^2 and a density of 1.8 g/cc. Also assume 1000 cars, weighing 1 ton each, connected to the line in one direction. Using an average friction coefficient of 0.05 requires a cable thrust of (1000×0.05) 50 tons. The cable cross-sectional area is (50,000/250) 200 mm^2, the cable diameter is 16 mm, and the cable weight (200 km) is 72 tons.
 It may be shown that roller friction (ball bearing), and air friction (speed 30 m/s) will account for less than 3% of the total thrust.

   The energy required to move of 1000 tons at a speed of 30 m/s (108 km/hour or about 70 miles/hour) is (500,000×30) 15 MgW at each end of the section (the total is 30 MgW), (three turbo engines of 10,000 KW each are required for the two ends). This system may be used for highways or as an internal city system.

Project 5: Gas line of the 2000 km (1250 miles) and Capability of carring 20 billion cubic meters per year

   There is a big demand for gas pipelines, for example, in the connection of Alaska to the USA or Russia to Europe. A ground-based gas (oil) pipeline is very expensive, requires years for building, and damages the environment. Often   they cross the territory of other country, which may steal gas or oil or to capture the pipeline.

Technical data

Assume that a gas balloon (airship, dirigible) has a volume of 10^4 m^3 (diameter 11.3 m, length 115 m) (the balloon can have wings). The line has length 2000 km, speed 35 m/s, and balloons are connected every 500 m. The delivery time is 19 hours (delivery time by pipeline is 3–5 times more, oil line is 30–50 times more).
  It is then easy to calculate than the transit capability of this gas line is about 20 billion cubic meter per year.
  The line contains 4000 balloons and one middle drive station. The cable has an safe tensile strength of 200 kg/mm^2, the cross-section area of the cable is 150 mm^2, its diameter is 14 mm, and the cable weight is 1080 tons.
  The total balloon drag is 60 tons, the total cable drag is 1.3 tons. The total power of 3 engines is 18,000 kW (which is the power of three aviation gas turbines). The density of natural gas is 0.72 kg/cub.m, the density of air is 1.225 kg/m^3, and the payload lift force of each balloon is about 3–4 tons.

Economical Estimation

The balloon area is 3140 m^2, and its weight is 500 kg. Assume 1 m^2 a balloon film (cover) costs $0.15, then balloons will cost is about $2000 each. The total cost of 4000 balloons is then $8 millions. If 1 kg cable costs $1, the cable cost is about $1 million. Let us include two engines (gas turbines) and departure and arrival ports. The total installation cost is $15 million and its lifetime is 15 years. The depreciation is $1 million per year.

Taking a maintenance cost $2 million per year, and gasoline cost of $0.25 per liter, the fuel cost is $30K per day or $10 millions per year. The total annual expense is $13 million per year. Some 77% of this expense is the cost of the fuel (gasoline for driving).

The production delivery cost of 1000 m^3 of gas is $0.7 per 1000 cubic meter for a distance of up to 2000 km (1250 miles). If the fee for the delivery of 1000 m^3 gas is $1, the profit is $18.6 million per year. We can reduce the production delivery cost if we use the wind energy.

Additional possibility

Every balloon can lift 2–3 tons of useful loads. This means we can deliver about 15,000 tons of payload (for example, oil) per day in one direction.

Conclusion

The proposed method and installation for transportation are significantly cheaper than the current methods of flying traditional airlines, are constructing bridges, tunnels, and gas pipelines. This system would dramatically reduce the price of flights on conventional airlines; the cost and time of construction of long bridges, or tunnels; and put into practice huge projects such as connections between Europe and Africa across Gibraltar, Russia and America across the Bering Straits, Russia-Japanese across Sakhalin, Taiwan with mainland Chine, and so on. It would reduce the cost and construction time of gas pipelines too, and save the environment.

The author has detailed solutions for many problems which seem difficult using current technology. He is prepared to discuses the project details with serious organizations that have similar research and development goals.

Patent US 6,494,143 B1. Patent applications are 09/974,670; 09/873,985; 09/789,959; 09/978,507 (2001). The closed ideas are in References[4–12].

References

1. A.A. Bolonkin, "Air Cable Transport", *Journal of Aircraft*, Vol. 40, No. 2, July-August 2003, pp. 265–269.
2. A.A. Bolonkin, "Bolonkin's Method Movement of Vehicles and Installation for It", US Patent 6,494,143 B1, Priority is on 28 June 2001.
3. A.A. Bolonkin, "Air Cable Transport and Bridges", TN 7567, International Air & Space Symposium – The Next 100 Years, 14-17 July 2002, Dayton, Ohio, USA.
4. A.A. Bolonkin, "Non-Rocket Missile Rope Launcher", IAC-02-IAA.S.P.14, 53rd International Astronautical Congress, The World Space Congress – 2002, 10–19 Oct 2002, Houston, Texas, USA.
5. A.A. Bolonkin, "Inexpensive Cable Space Launcher of High Capability", IAC-02-V.P.07, 53rd International Astronautical Congress, The World Space Congress – 2002, 10–19 Oct.   2002. Houston, Texas, USA.
6. A.A. Bolonkin, "Employment Asteroids for Movement of Space Ship and Probes". IAC-02-S.6.04, 53rd International Astronautical Congress. The World Space Congress – 2002, 10–19 Oct. 2002, Houston, Texas, USA.
7. A.A. Bolonkin, "Non-Rocket Space Rope Launcher for People", IAC-02-V.P.06, 53rd International Astronautical Congress, The World Space Congress – 2002, 10–19 Oct 2002, Houston, Texas, USA.

8. A.A. Bolonkin, "Non-Rocket Earth-Moon Transport System", COSPAR-02 B0.3-F3.3-0032-02, 02-A-02226, 34th Scientific Assembly of the Committee on Space Research (COSPAR). The World Space Congress – 2002, 10–19 Oct 2002, Houston, Texas, USA.

9. A.A. Bolonkin, "Non-Rocket Earth–Mars Transport System", COSPAR-02 B0.4-C3.4-0036-02, 34th Scientific Assembly of the Committee on Space Research (COSPAR), The World Space Congress – 2002, 10–19 Oct 2002, Houston, Texas, USA.

10. A.A. Bolonkin, "Transport System for delivery Tourists at Altitude 140 km", IAC-02-IAA.1.3.03, 53rd International Astronautical Congress, The World Space Congress – 2002, 10–19 Oct. 2002, Houston, Texas, USA.

11. A.A. Bolonkin, "Asteroids as Propulsion Systems of Space Ships", *JBIS*, Vol. 58, pp. 97–107, 2003.

12. A.A. Bolonkin, "Kinetic Anti-Gravitator", AIAA-2005-4505, 41 Propulsion Conference, 10–12 July, 2005, Tucson, Arizona, USA.
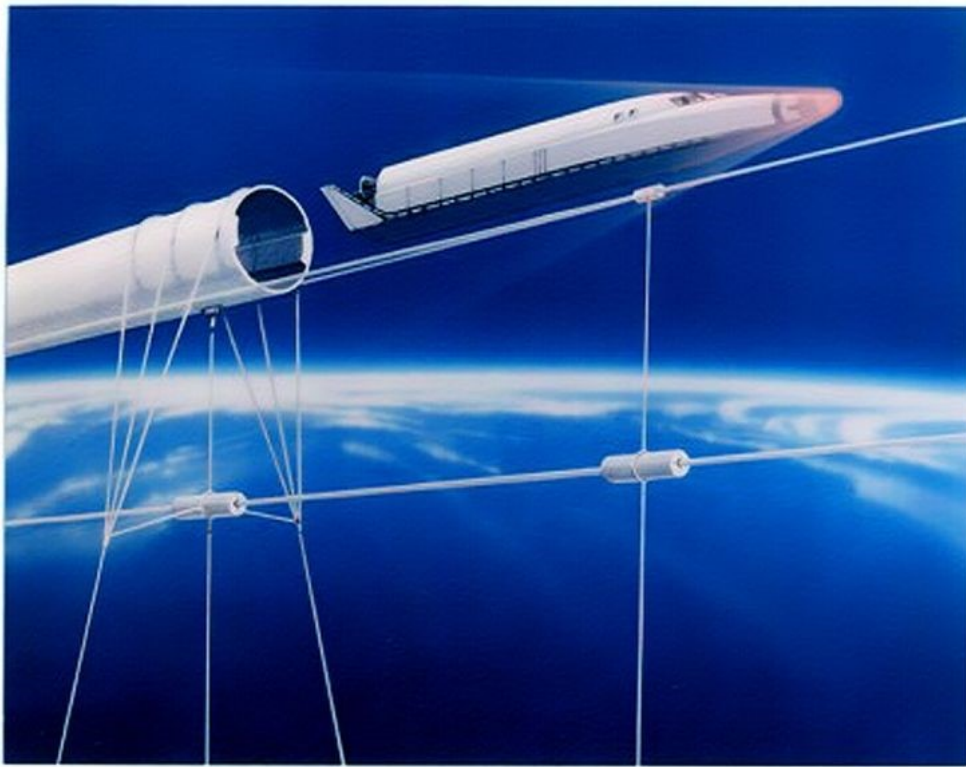
Attachment 2
High Speed Catapult Aviation*

Summary

The current passenger-transport aviation systems have reached the peak of their development. In the last 30 years there has been no increase in speed or redactions in trip costs. The aviation industry needs a revolutionary idea, which allows jumps in speed and delivery capability, and dramatic drops in trip price. The author offers a new idea in aviation in which flight time practically does not depend on distance (it is the same for lines from New York to Washington as from New York to Paris), and vehicle load capability doubles and which has a drive engine that is located on the ground and can use any cheap source of energy.

----

*See detailed manuscript AIAA-2005-6221, Atmospheric Flight Mechanic Conference – 2005, 15–18 August, USA.

Introduction

Current takeoff mass of a long distance aircraft is made up of approximately 1/3 aircraft body, 1/3 fuel, and 1/3 payload. The aircraft engine needs expensive aviation fuel. The passenger-transport aircraft cannot exceed the speed of sound. The "Concorde" history shows that the conventional passenger supersonic aircraft is unprofitable. The hypersonic aircraft, which is under development by the USA, will be more unprofitable as a passenger long distance aircraft because it will use very expensive hydrogen fuel, it is very complex and it has a high production cost. The hypersonic engine problems have not been solved in spite of spending tens of millions dollars in research and testing. Aviation needs new ideas which increase speed, and load capability, and reduce a delivery cost. Some of these ideas have been published by the current author [1–7].

  The author's idea is the acceleration of a flight vehicle (non-engine aircraft) to high speed using a cable engine located on the ground. The vehicle will then use its kinetic energy for flight. The computation shows that a kinetic aircraft accelerated to subsonic speed of 270–300 m/s can for 60–80 km until its speed decreases to a landing speed of 50–60 m/s. This is far enough for suburban transport or for air bridges across the Straits of Gibraltar, English Channel, Bering Straits (Russia–America), Sakhalin–Asia, Russia–Japan, etc. For acceleration to this speed at a rate this is acceptable to passengers (3g) the runway length must be 1.5 km (current runways for large aircraft are 1.5–3 km long). For the long-distance flight (6000–8000 km), the air vehicle must be accelerated to a speed of 4–4.5 km/s. For acceleration of no more than 3g the required runway length would then be 290–340 km. It is constructed using the methods described in References[5,7]. Rather than being a conventional runway, it is an air cable acceleration system[5–7] for the acceleration of space vehicles and it is located in atmosphere.

Brief description of the innovation

This system for kinetic vehicles includes (Fig. A2.1) a chain made of closed-loop cables and drive stations. A subsonic system (Fig. A2.1b) may be located on the surface or underground, a high speed

(up to hypersonic speed) system (Fig. A2.1a) is located above ground[5-7]. The chain is supported in the air by flight devices [1-7] or by columns with rollers. Drive stations have engines located on the ground and work on any cheap energy.

   The system works in the following way. The subsonic aircraft starts from a conventional aerodrome, and is accelerated (with 3g) up to a speed of 270–300 m/s (Mach number 0.9) by the drive station on the runway which is 1200–1500 m long (Fig. A2.1b). The aircraft takes off, flies (50–70 km, Figs. A2.1c, A2.2), gradually loses speed and increases its attack angle. When the speed drops so it is close to landing speed, the aircraft lands.

   The high speed aircraft also starts from a conventional aerodrome, lifts off the ground at take off and is accelerated up to a speed of 1000–5000 m/s in air by the ground drive stations. The acceleration distance (with 3g) may be 13–400 km (depending on the final speed, see Figs. A2.4, A2.5). This is not a problem because acceleration is made in the air (Fig. A2.1a).
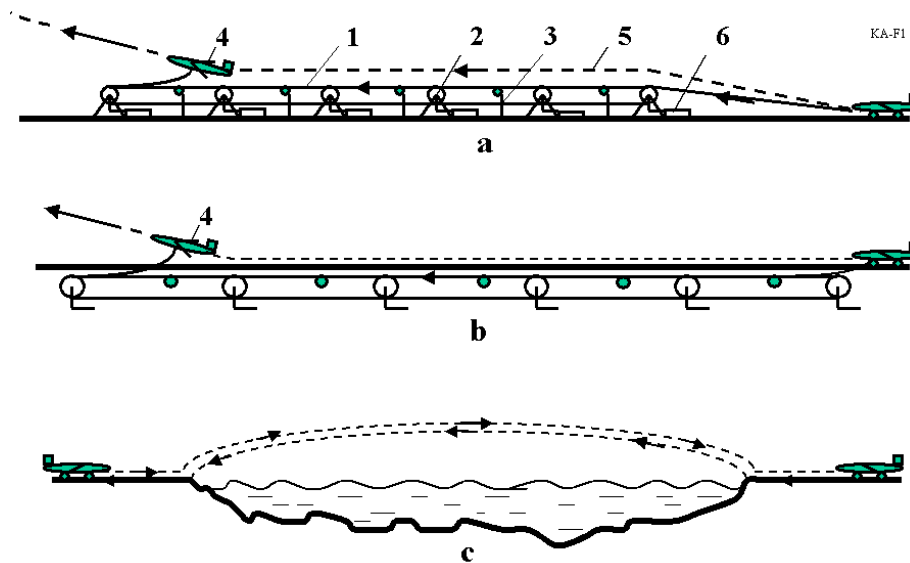

Fig. A2.1. Drive system for acceleration of kinetic aircraft. (a) Hypersonic and supersonic aircraft. (b) Subsonic aircraft. Notation: 1 – chain of closed-loop cables; 2 – drive stations; 3 – support column with roller; 4 – flight vehicle; 5 – trajectory of flight vehicle; 6 – engine of drive station. (c) Kinetic subsonic aircraft as an air bridge across a stream.

   The range of the high speed aircraft may reach 200–8,000 km (see Fig. A2.3). The aircraft can make a full circle and return to its base (see Figs. A2.8 and A2.9). The flight data are significantly improved if the vehicle has variable wing area or variable swept wings[5]. Other similar ideas and useful points for kinetic aviation are presented in References[5-7]. The flight altitude does not its influence range because the energy spent in climbing will be returned in gliding.

Theory of kinetic vehicles and a general estimation of flight data
(in metric system)

1. The maximum range, R, of kinetic air vehicles is ubtained from the kinetic energy of theoretical mechanics. It is equals

$$d\left(\frac{mV^2}{2}\right) = \frac{mg}{K} dR, \quad g = g_0 - \frac{V^2}{R_0}, \quad R = -\frac{KR_0}{2g_0} \ln \frac{g_0 - V_1^2/R_0}{g_0 - V_0^2/R_0}, \quad R \approx \frac{K}{2g}\left(V_1^2 - V_0^2\right), \quad (A2.1)$$

where R is range [m]; $R_0 = 6,378 \cdot 10^6$ is the Earth's radius [m]; K is the average aerodynamic efficiency ($K = 10$–20 for subsonic air vehicles and $K = 5$–8 for supersonic air vehicles. For example: the subsonic Boeing-747 has maximum $K = 16$, the supersonic "Concorde" has maximum $K = 7,5$, supersonic aircraft XB-70 and YF-12 have $K = 7$, and Boeing 2707-300 has $K = 7.8$); $g_o = 9.81$ m/s^2 is gravity; V_1 is initial (after acceleration) speed [m/s]; $V_0 < V_1$ is final (near landing) speed [m/s] ($V_0 = 50$–60 m/s); V is variable speed, $V_0 < V < V_1$ [m/s]. For estimation $V = 0.5(V_1 + V_0)$; $mg/K = D$ is air drag [N]; m is vehicle mass [kg]. For $V < 2000$ m/s, variable gravity $g \approx g_o$. Last equation in (A2.1) is obtained from the first equation using integration.

   Results of computations for subsonic ($V < 300$ m/s, $M < 0.9$, M is Mach number) and supersonic vehicles are presented in Figs. A2.2 and A2.3. The range of a subsonic vehicle is 45–90 km for $V_1 = 300$ m/s; the range of a supersonic vehicle can reach 4000–8200 km for $V_1 = 4500$ m/s.
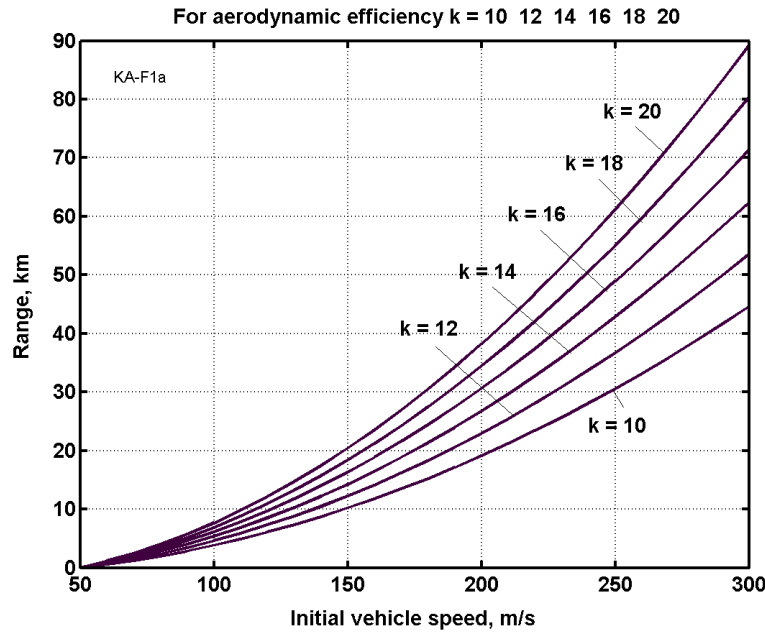

Fig. A2.2. Range of the subsonic kinetic aircraft versus initial speed for different aerodynamic efficiency $K = 10$ 12 14 16 18 20.

2. Maximum acceleration distance can be calculated using the equation

$$S = \frac{V_1^2}{2gn},$$ (A2.2)

where n is overload, g. Results of computations for subsonic and supersonic aircraft are presented in

Figs. A2.4 and A2.5.

   Acceleration (3g) distance is 1500 m for a speed of 300 m/s for the subsonic vehicle and 340 km for a speed of 4.5 km/s for the supersonic vehicle.

3. Average speed and flight time are

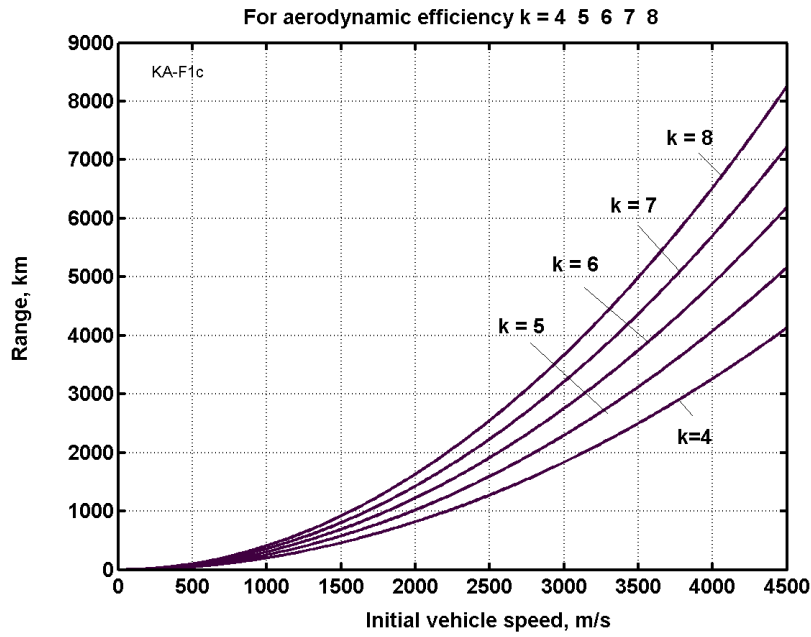$$V_a = \frac{V_1 + V_0}{2}, \quad T = \frac{R}{V_a}.$$ (A2.3)

For aerodynamic efficiency k = 4 5 6 7 8

Fig. A2.3. Range of the supersonic kinetic aircraft versus initial speed for different aerodynamic efficiency $K = 4\ 5\ 6\ 7\ 8$.

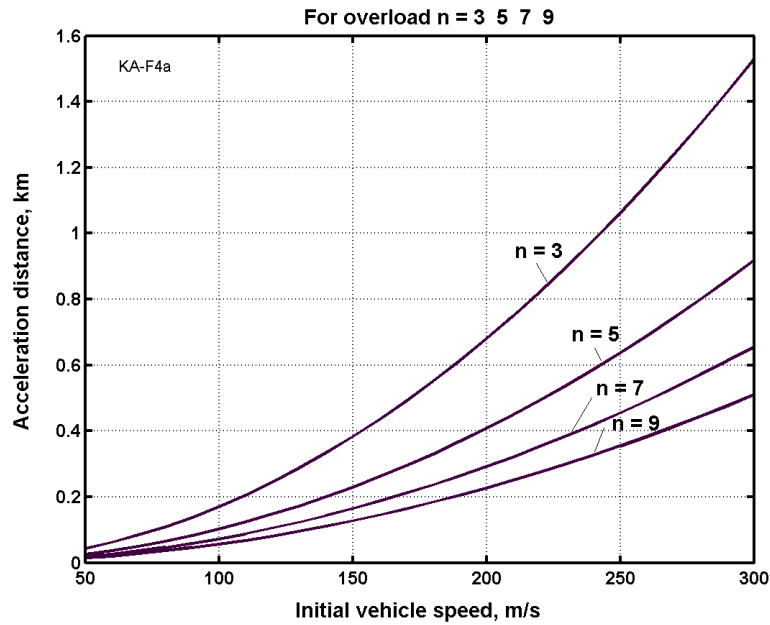**For overload n = 3 5 7 9**

Fig. A2.4. Acceleration distance of subsonic kinetic aircraft versus initial speed and different overloads.

For overload n = 3 4 5 7 9
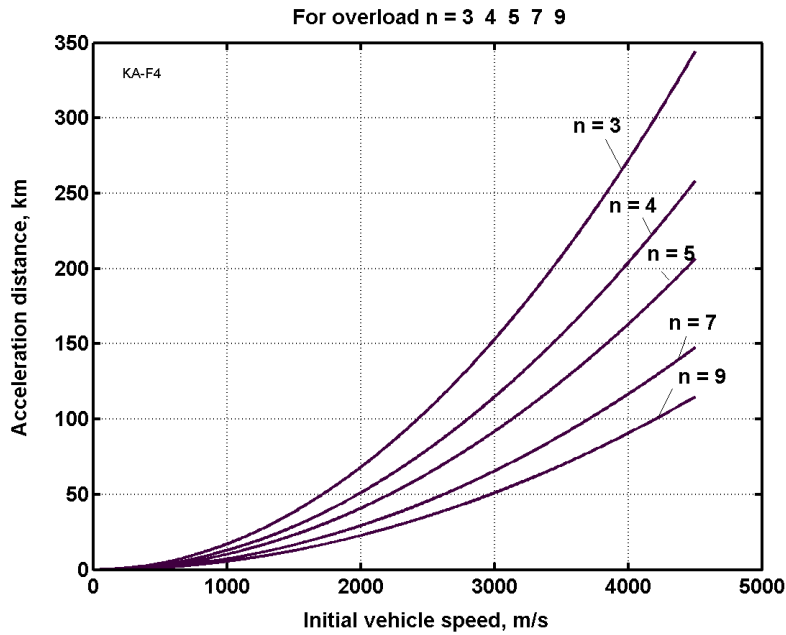

Fig. A2.5 . Acceleration distance of supersonic kinetic aircraft versus initial speed and different overload.

For aerodynamic efficiency k = 4 5 6 7 8

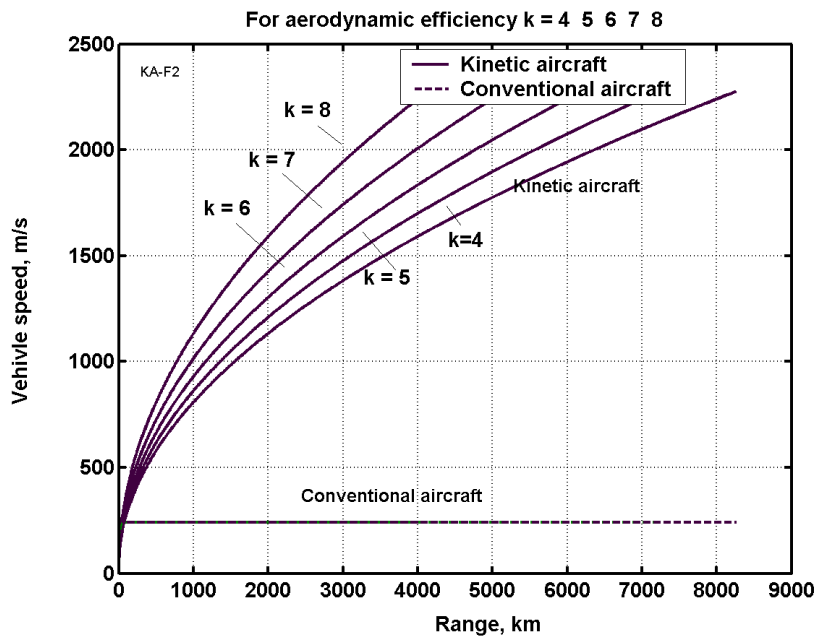Fig. A2.6 . Average speed of the kinetic and conventional aircraft versus range for different aerodynamic efficiency $K = 4\ 5\ 6\ 7\ 8$.

The results of computation are presented in Figs. A2.6 and A2.7. The subsonic vehicle has an average speed 1.5 times greater than conventional aircraft (because the kinetic vehicle has high subsonic speed of the beginning), and the average speed of the supersonic (hypersonic) vehicle is more than 6–9 times that of a conventional subsonic vehicle. The flight time is less for both cases.

4. The trajectory of horizontal turn can be found from the following differential equations

$$\dot{V} = -\frac{gn}{K}, \quad \dot{\varphi} = \frac{L_1}{mV} = \frac{g\sqrt{n^2-1}}{V}, \quad \dot{x} = V\cos\varphi, \quad \dot{y} = V\sin\varphi, \quad or$$

$$\tag{A2.4}$$

$$V = V_1 - \frac{gn}{K}t > V_0, \quad \varphi = -\frac{K\sqrt{n^2-1}}{n}\ln\left(1 - \frac{gn}{K}t\right), \quad \dot{x} = V\cos\varphi, \quad \dot{y} = V\sin\varphi,$$

where L_1 is the projection of the vehicle lift force to a horizontal plane (vertical overload is: t is time [seconds]; φ is turn angle [rad].

Results of computations for different overloads are presented in Fig. A2.8 and A2.9. They show that the vehicle can turn back and return to its original aerodrome (for example a bomber after a flight into enemy territory).
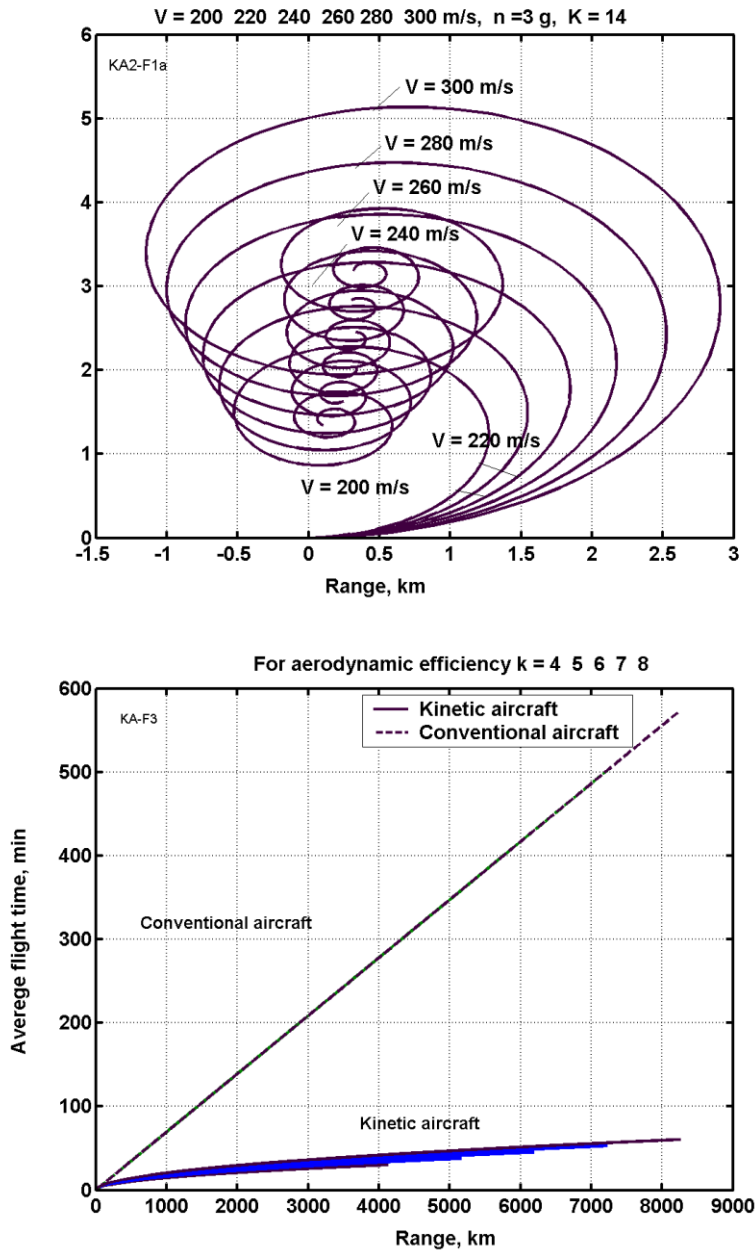

Fig. A2.7. Average flight time of the kinetic and conventional aircraft versus range.

Fig. A2.8. Horizontal deviation versus range of the subsonic kinetic vehicle for initial speed $V = 200$ 220 240 260 280 300 m/s, horizontal overload $n = 3g$, aerodynamic efficiency $K = 14$.
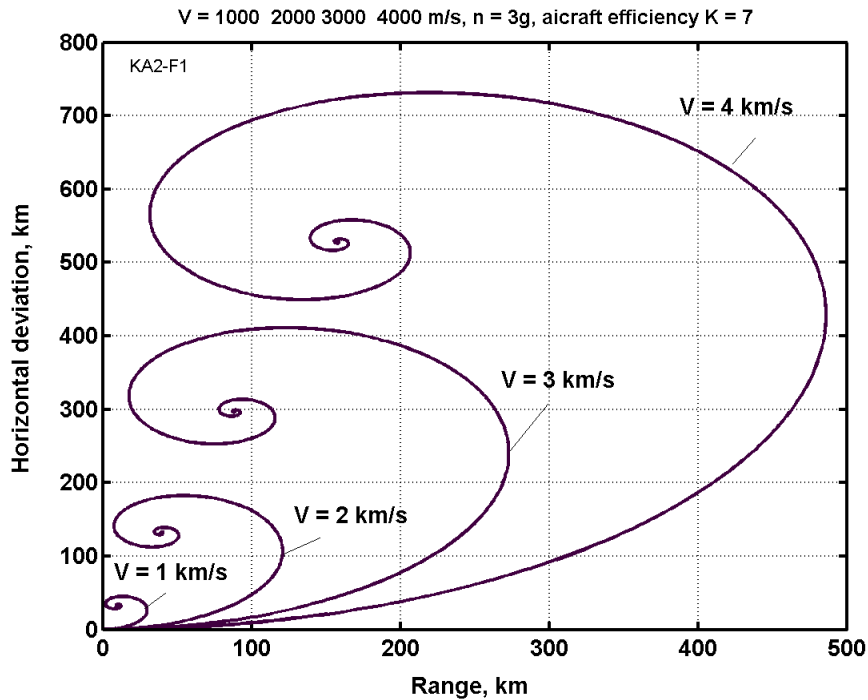
V = 1000 2000 3000 4000 m/s, n = 3g, aicraft efficiency K = 7

Fig. A2.9. Horizontal deviation versus range of the supersonic kinetic vehicle for $V = 1\ 2\ 3\ 4$ km/s, horizontal overload $n = 3$g, aerodynamic efficiency $K = 7$.

Advantages

The offered method has the following advantages:
1. The load capability of kinetic aircraft increases as a factor of two (no fuel or engine in the aircraft).
2. The kinetic aircraft is significantly cheaper than conventional aircraft (no aviation engine which is very expensive and has limited resources).
3. The engine located on the ground can work on cheaper fuel, for example natural gas, gasoline, diesel fuel, electricity.
4. The average speed for long-distance travel is increased by 6–9 times (see Fig. A2.6).
5. The maximum flight time is about 55 min for a distance at 8000 km (see Fig. A2.7).
6. The flight production cost is dramatically reduced.
7. One installation can have a very large capability and can serve many airlines, for example, most airlines from USA to Europe (New York to London, Paris, Berlin, Madrid, Brussels, etc). The load capability is also increased greatly.
8. The installation can be used to launch of satellites and probes (some projects currently offered use conventional airplanes but they have a maximum speed of only 270 m/s).
9. The installation can be used for space tourism and flights along high altitude ballistic trajectories.

Project

Assume the mass of the space vehicle is $m = 15$ tons (100 passengers and 4 members of crew); the acceleration is $a = 3g$ (this acceleration is acceptable for conventional people). The range is approximately 7200 km (see Fig. A3.3 or calculate using $R \approx KV^2/2g$ for a final acceleration speed of 4.5 km/s and $K = 7$, g = 9.81 m/s^2.

The request acceleration distance is $S = 340$ km. The time of horizontal acceleration is $t = (2S/a)^{0.5} =$ 150 seconds = 2.5 minutes. Assuming it uses the artificial cheap fiber ($\sigma = 600$ kg/mm^2) widely produced by current industry, an safe tensile strength of the vehicle cable is $\sigma = 180$ kg/mm^2 (the safety factor is 600/180 = 3.33), density $\gamma = 1800$ kg/m^3 ($K_1 = 180/1800 = 0.1$). Then the cross-section area of the vehicle cable around the vehicle will be $S_1 = 3m/\sigma = 250$ mm^2, and the cable diameter is $d = 18$ mm. Let us assume that the drive stations are located every 10 km [21]. It therefore needs 34 drive stations. The mass of the cable is $M = 1.5 S_1 \gamma L_d = 6750$ kg. Here $L_d = 10$ km is the distance between drive stations. A directive cable[21] and a variable cross-section area of the main cable are included in the coefficient 1.5.

The energy required for acceleration of the aircraft and the cable is $E = (m+M)V^2/2$. This is about 220 Giga joules (1 Giga joules = 10^9 J) if $V = 4.5$ km/s. The drag of the aircraft and cable is about $D = 3$ tons, which means $E = DL = 3 \cdot 10^4 \cdot 390{,}000 = 11.7$ Giga joules. If the launches are made every 0.1 hours the engines must have a total power of about $P = E/t = 231.7 \cdot 10^9/6/60 = 643{,}600$ kW distributed between the 34 drive stations (which is 18,900 kW each). If the engine efficiency is $\eta = 0.3$ the fuel consumption will be $F = E/\varepsilon/\eta = 232 \cdot 10^9/\varepsilon/0.3 = 18.4$ tons per flight. Here $\varepsilon = 42 \cdot 10^6$ [J/kg] is the energy capability of diesel fuel. This means that 184 kg of fuel is used for each passenger.

If tensile strength is $\sigma = 180$ kg/mm$^2 = 1.8 \cdot 10^9$ N/m^2, $\gamma = 1800$ kg/m^3, then the total weight of the flywheels (as storage energy) will be about $M_w = 2E\gamma/\sigma = 2 \cdot 232 \cdot 10^9 \cdot 1800/1.8 \cdot 10^9 = 835$ tons or 835/34 = 25.6 tons for each drive station (see more details in Reference[7]).

Economical efficiency

Assume a cost of 500 million dollars for the installation (see publication[7]), a lifetime of 20 years, and an annual maintenance cost of 5 million dollars. If 100 passengers are launched on every flight, there are 10 flights every hour for 350 days a year and the load coefficient is 0.75, then $N =$ 100×10×24×350×0.75 = 6,300,000 passengers will be launched per year (one installation can serve many lines, for example, New York to London, Paris, Berlin. Rome, etc). The launch cost per passenger is $30,000,000/6,300,000 = \$4.76 plus fuel cost. If 184 kg of fuel is used for 1 passenger and the liquid fuel price is \$0.25 per kg, then the cost is \$46 for liquid fuel. The total production cost will be about \$53/person for liquid fuel. If the ticket costs \$153, then the profit will be about 630 millions dollars per year. It significantly reduses the fuel cost if the aircraft uses a cheap natural gas as fuel for the drive station engines. The flight from the USA to Europe will be cheaper and take less time than it does now. The efficiency will be improved when the aircraft can take 200 and more passengers. The number of require aircraft decreases by 6–9 times because each hypersonic aircraft has very high speed.

In Table A2.1 the reader will find the approximate costs of the different form of energy converted to mechanical energy.

Table A2.1. Cost of mechanical energy for different fuels.

No	Fuel	Price $/kg	Energy J/kg	Price of 10^6 J $	Conv. coeff.	Cost of mech. energy $/$10^6$ J
1.	Liquid	0.3	$43 \cdot 10^6$	0.007	0.3	0.0233
2.	Natural gas	0.2	$45 \cdot 10^6$	0.0044	0.3	0.0147
3.	Coal	0.035	$22 \cdot 10^6$	0.0016	0.3	0.0053
4.	Electricity	0.06 kWh	-	0.0167	0.95	0.0176

Issue: Internet, Cost of fuel, July 2003.

Fuel prices change with time, but in any case the cost of delivery will be some times less than delivery by conventional aircraft. Critics must remember that main content of this article is not economic estimations, but the new idea for aviation and space apparatus.

Discussion of Problems

1. Cable problem. At present the current industry produces cheap artificial fiber with a tensile stress up σ = 500–620 kg/mm^2 and density γ = 970–1800 kg/m^3 (see Chapters 1–2). This is enough for the subsonic, supersonic, and even the hypersonic systems (see [1–7]). A hypersonic system with this cable requires a drive station every 10 km. When the industry produces cheap whiskers or nanotubes the distance between the drive stations can be increased up to 100 km and the system parameters will be significantly improved.
2. Vehicle heating. The proposed hypersonic vehicle will have heating from compressed air. The space ship "Shuttle" and warheads of ballistic rockets have the same problem and in more difficult form because they have greater maximum speed (about 8 km/s). The heat flow increases by more than a third power of speed as $V^{3.15}$. This problem is successfully solved by a demountable terminal cover on "Shuttle" and on warheads. The same solution may apply in the proposed kinetic vehicle (KV). The other solution is cooling, but that needs additional research. The nose and the leading edges of the wing of supersonic (speed less the $4M$) kinetic vehicles can be made from heat-resistant material. If the speed is more then 4M, the hypersonic vehicle may need to have a cooling system. However, this problem is not as difficult for kinetic vehicles as it is for the space Shuttle. The problems of the "Shuttle" and the KV are different. The "Shuttle" has much greater speed (about 8000 m/s) and kinetic energy, and has to reduce this speed and energy by air drag. For this the "Shuttle" has an obtuse nose and leading edges of the wings. The KV must conserve its speed and energy for the long flight. The KV has a sharp nose and leading edges of the wings. The maximum speed of a hypersonic KV is two times less, which means the heat flow will be approximately 5 times less than the "Shuttle". This problem can be solved by a light knockout ceramic cover (as on the "Shuttle") or a cooling system. If it uses water for cooling, the vapor can be used for additional thrust. Lithium as a cooler has 5 times the capability of water, 0.9 kg of lithium is enough to cooling a 5-ton projectile launched from the ground at a speed of 8 km/s. However, this method needs more research and computation.
3. High aerodynamic efficiency. The KV can be more efficient than a conventional hypersonic aircraft with an engine because it does not have the air intake needed for air breathing engines. The permanent high aerodynamic efficiency can be preserved by having variable wing area and variable swept wing. The optimal trajectory is as follows: after acceleration the hypersonic vehicle has a high vertical acceleration (3g), reaches its optimal (high) altitude, and flies along the optimal trajectory (see Attn. 4 of this book). After this the KV glides to the air port. On arrival the KV brakes and lands.
4. Maneuverability in a landing. This problem can be solved by conventional methods – air brakes and a small engine.
   Some other ideas the reader finds in of the author can be found in the References [5–7].

References

1. A.A. Bolonkin, "High Speed Catapult Aviation", AIAA-2005-6221, Atmospheric Flight Mechanic Conference – 2005. 15–18 August, USA.

2. A.A. Bolonkin, "Air Cable Transport", *Journal of Aircraft*, Vol. 40, No. 2, July-August 2003, pp. 265–269.

3. A.A. Bolonkin, "Bolonkin's Method Movement of Vehicles and Installation for It", US Patent 6,494,143 B1, Priority is on 28 June 2001.

4. A.A. Bolonkin, "Air Cable Transport and Bridges", TN 7567, International Air & Space Symposium – The Next 100 Years, 14-17 July 2002, Dayton, Ohio, USA

5. A.A. Bolonkin, "Non-Rocket Missile Rope Launcher", IAC-02-IAA.S.P.14, 53rd International Astronautical Congress, The World Space Congress – 2002, 10–19 Oct 2002, Houston, Texas, USA.

6. A.A. Bolonkin, "Inexpensive Cable Space Launcher of High Capability", IAC-02-V.P.07, 53rd International Astronautical Congress, The World Space Congress – 2002, 10–19 Oct.   2002. Houston, Texas, USA.

7. A.A. Bolonkin, "Non-Rocket Space Rope Launcher for People", IAC-02-V.P.06, 53rd International Astronautical Congress, The World Space Congress – 2002, 10–19 Oct 2002, Houston, Texas, USA.

8. Koell D.E., Handbook of Cost Engineering, TCS, Germany, 2000.
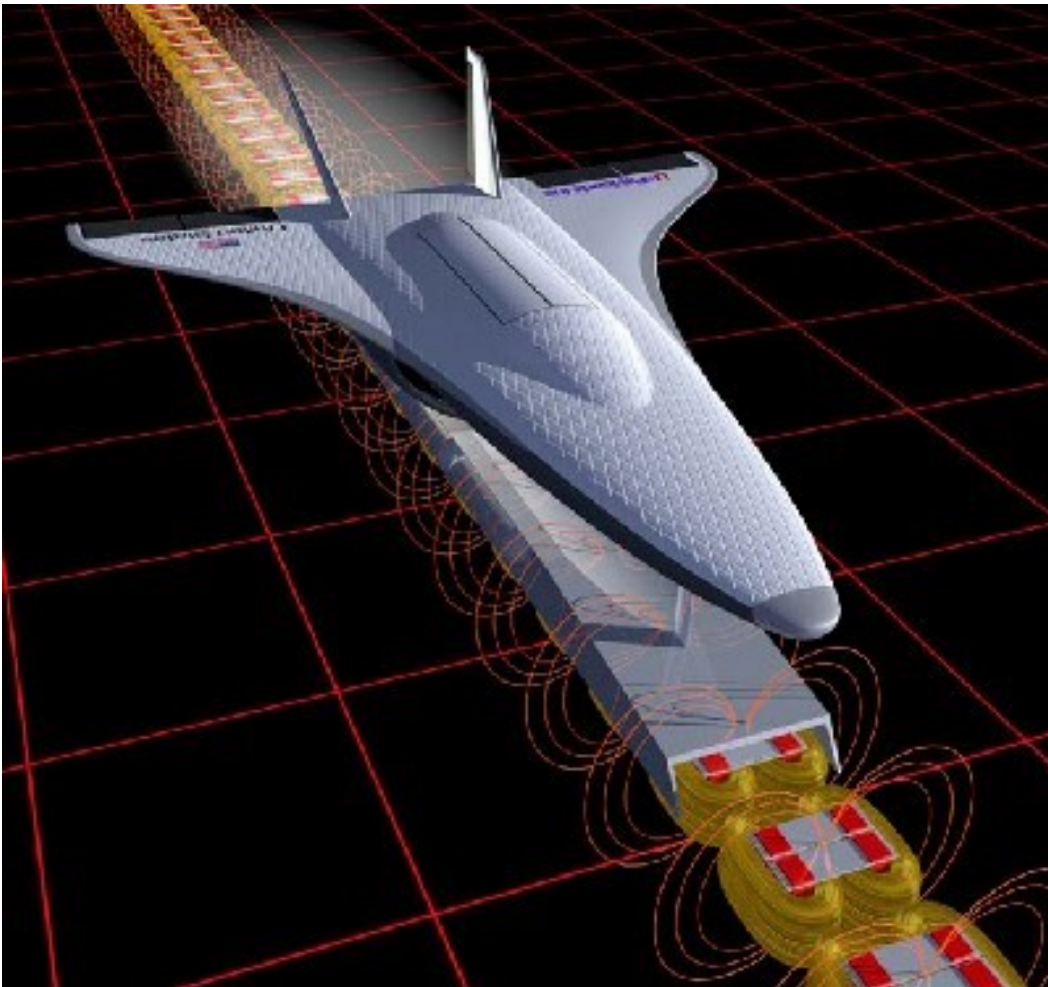
Attachment 3

Light Multi-Reflex Engine*

Summary

The purpose of this attachment is to draw attention to the revolutionary idea of multi-reflection. The method and its main innovations were offered by the author in 1983 in the former USSR. Now the author is showing the huge possibilities of this idea in many fields such as space, aviation, energy, energy transmission, beam amplification, light transformation and so on. This chapter considers the direct transfer of light beam energy to mechanical energy and back.

Introduction
Short history.

In 1972 Kantrowitz draw attention to the use of a laser beam for a space propulsion system[1]. He proposed using the conventional method: to transfer energy by laser beam to space apparatus, to convert light energy into heat and evaporate matter, and to gain thrust from evaporated matter. There is a lot of research on this method [2]. However, it is complex, not very efficient, has limited range (divergence of the laser beam), requires special matter located on board the space ship, and requires a very powerful laser.

   In 1983 the author offered another method of using beam (light) energy: the direct conversion of light energy into mechanical pressure (for engines) or thrust (for launchers and propulsion systems) using multiple reflection[3].

   The directing away or reflecting of light is the most efficient method for a propulsion system. It gives the maximum possible specific impulse (a speed of 3×10^8 m/s). The system does not expend mass, which is important for space ships, because launching mass into space is very expensive (at the present time it costs about \$20,000–\$50,000 /kg). However, light pressure is very low at about 0.3×10^{-6} kg/kW (solar light pressure without reflection is about 0.2×10^{-6} kg/m^2). In 1983 the author proposed the idea of increasing the light pressure using multi-reflex method and offered some innovations which dramatically reduce the loss of mirror reflection. This enables the system to make millions of reflections and to gain several Newtons of the thrust per kW of beam power. It allows the design of many important devices (in particular, engines) which transfer light directly into mechanical energy and solve many problems in aviation, space, energy and energy transmission.

   The advances in optical materials and lasers in the recent years have reduced the loss from reflection. The author returned to this topic and carried out the primary research. He solved the main problems that arise in research: the design of a the very highly efficient reflector, a light lock, self-focusing lightweight mirrors and lenses, a beam transferor for very long distances (millions of km) without beam divergence, light storage, a beam amplifier, etc. As with any new innovation it appears many additional problems will need to be addressed in the research and development. However, the solution of these problems promises a revolution in many technical fields. The author wants to draw the attention of researchers and engineers to these innovative ideas.

Brief information about light and used light devices

The optical diapason of electromagnetic radiation is approximately from a few nanometers to 1 cm. Visible light is approximately located in the interval 400 to 700 nm (1 nm is 10^{-9} m). Ultraviolet radiation has a shorter range than visible light while the range of infrared rays is longer than visible light. The diapason of microwave radio waves is a higher than the optical diapason, and X-rays have a smaller optical diapason.

A conventional mirror can reflect a maximum of 98–99% of the light energy of some light waves are can give a maximum of 200–300 reflections. This is not enough, because the light pressure is very small at only about $0.6{\cdot}10^{-6}$ kg/ kW (for high reflection). For technical applications it is necessary to have a minimum of a million reflections.

This method is not suitable for our purpose (see chapter 12). The wavelength is considerable changed for a mobile reflector (rotary disk). A conventional mirror reflects the beam in another direction if the mirror plate is not perpendicular to the beam.

A narrow laser beam is the most suitable for a light engine. There are many different types of lasers with different powers (peak power up to 10^{12} W), wavelength (0.2 to 700 μm), efficiency (from 1% up to about 95%), and impulse (up to some thousands of impulses per second) or continuous operations. A gas laser may be suitable for our purpose. Many molecular gases, such as hydrogen cyanide, carbon monoxide, and carbon dioxide, can provide laser action. Carbon dioxide lasers can be operated at a number of wavelengths near 10 μm on various vibrational–rotational spectral lines of the molecule. They can be relatively efficient, up to about 30%, and have been made large enough to give continuous power outputs exceeding tens of thousands of watts.

At the present time we have seen significant advances in high-power weapons-class lasers. The Missile Defense Agency/USAF Airborne Laser (ABL) program is rapidly developing a six-module chemical oxygen-iodine laser (COIL) to go at the heart of the weapon. Preparations are under way at the System Integration Laboratory for a moth-balled 747-200 converted into a ground test platform, for first testing of the megawatt-class COIL flight hardware. The laser mirror is larger than 1.5 m in diameter.

The Air Force Research laboratory (AFRL) has contracted with Northrop Grumman Space Technologies and Raytheon to develop a high-power solid-state 25-kW laser.

The laser beam divergence is

$$\theta = \frac{2}{\sqrt{\pi}}\frac{\lambda}{D} = 1.13\frac{\lambda}{D} \; , \qquad\qquad (A3.1)$$

where θ is the angle of divergence [rad], λ is the wavelength [m], and D is the aperture diameter [m]. Diffraction theory gives the coefficient in (A3.1) as 1.22 .

Solar light has a radiation spectrum approximately in the interval λ = 0.4 to 2.2 μm and maximum energy when λ = 0.5 μm. The divergence of solar light is about 0.005 radians.

More detailed information is given in the References[1–10,15].

Description of innovation

To achieve maximum reflectance, degree 45° prisms (Fig. A3.1a) are used. For incident angles greater than $\sin^{-1}(n_1/n_2)$, no light is transmitted. Here n is the refractive index ($n \approx 1$ to 4). Instead the light is totally reflected back into the incident medium. This effect is called total internal reflection. Total internal reflection is used in the proposed reflector. Our reflector contains two plates than have a set of small prisms reflecting a beam from one prism to another prism (Fig. A3.1b). Every plate can contain millions of small (30 to 100 μm) prisms. (An optical cable has a diameter of 2–10 microns). The entering beam, 3, is reflected millions of times as shown in Fig. A3.1c,d (see path 2) and creates a

repulsive force F. This force may be very high at thousands of N/kW (see computation below) for motionless plates. It is limited only by the absorption (dB) of the prism material (see below).

   The prisms and their cells can have a slope (Fig. A3.2a) and located on a rotor outer surface and a stator inner surface (Fig. A3.2b) or plates (Fig. A3.2a). This system can be applied to rotary or linear engines. Two questions arise: how the beam enters this cell (without the possibility of leaving the cell) and how much force the system has. The prism material attenuates the light energy and reduce the beam power (wave amplitude).

   To solve of the first problem the author offers a *"light lock"* which allows the light beam to enter but closes the exit (Fig. A3.1b). Fig. A3.1 shows three designs of *light lock*s.
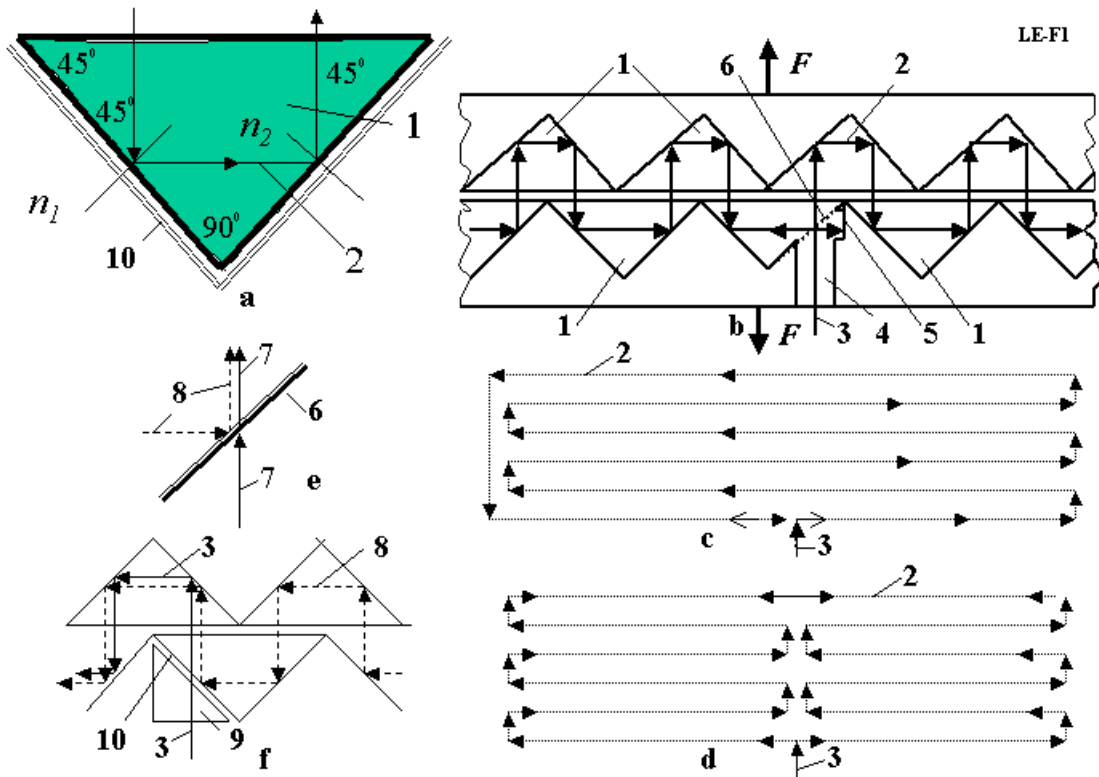

Fig. A3.1. Multi-reflection system: a) Prism with full internal reflection: 1 – prism, 2 – path of a light beam, 10 – gap between the prism and the body of the plate, rotor, stator (it may be filled with a matter (cover) which has $n_1 < n_2$, n – reflective index; b) Passage of the beam a through series of prisms: 3 – entering beam, 4 – entrance canal, 5 – mirror (light lock version 1); 6 – light lock (version 2) (multi-layer mirror) , F – repulsive force; c) The first version of the beam path through the reflected cells; d) The second version of the beam path through the reflected cells; e) Light lock (version 2): 6 – multi layer mirror, 7 – entering beam, 8 – final path of beam ($\lambda_8 \neq \lambda_7$); f) Light lock (version 3): 9 – additional prism, 10 – variable gap between main prism 1 and additional prism 9.

   The first light lock is shown in Fig. A3.1b. The beam inters through a narrow beam canal, 4. The entering beam runs the full path, 2 (Fig. A3.1b,c,d), is reflected in millions of cells, and travels up to enter the cell from the other side. Here the beam is partially reflected back into the system by mirror 5, and partially reflected back to way it came in a straight line. With mobile plates part of the beam is reflected back to the laser and the laser mirror returns it into the system. This part of the beam is s_1/s_2, where s_1 is the width of the beam canal and s_2 is the length of a prism hypotenuse.

The second light lock is shown in Fig. A3.1e. This has a mirror, 6, with a multi-layer coating. This coating lets the entering beam, 3, 7, passes but reflectes the internal beam, 8. This is possible because the wavelengths of beams 7 and 8 are different ($\lambda_8 \neq \lambda_7$) in the mobile plates.

The third light lock is shown in Fig. A3.1f. It contains an additional prism, 9, and is used as an impulse laser. When the laser beam 3 enters into the system, the prism, 9, is pressed against the main prism, 1.As the beam travels along path 2, the additional prism, 9, is disconnected from prism 1 and the beam, 3, can only travel inside the reflected system while it expends all its energy. The gap, 10, may be very small, about a light wavelength (1 micron). A piezoelectric plate can be used for this purpose.

The detailed attenuation of light propagating through optical matter is considered in the next section. To increase the number of reflection we use a set of very small prisms and current high efficiency optical matter. A pulsed or continuous laser may be used. We compute an average laser power.
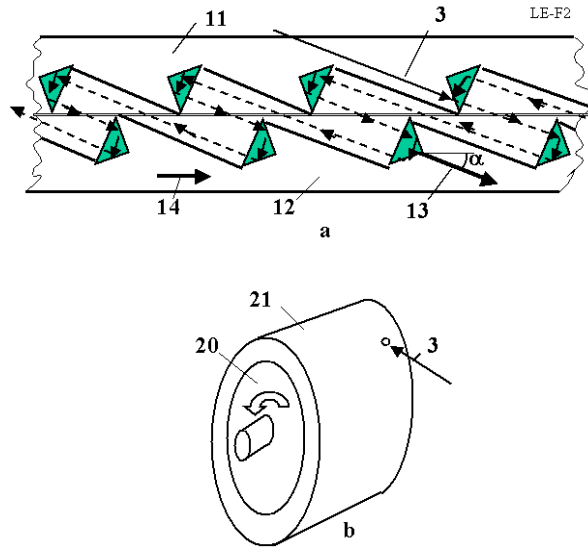

Fig. A3.2. Sloping reflective cells and light engine: a) 11 – stator (motionless), 12 – mobile rotor, 13 – local force (of single cell), 14 – direction of rotor movement; b) Light engine: 20 – rotor, 21 – stator.

Theory of the multi-reflex engine

The attenuation of light propagating through optical matter is caused either by absorption or by scattering. In both absorption and scattering, the power lost over a distance, z, and the power $N(z)$, propagating at that point is given by an exponential decay:

$$N(z) = N(0)\exp(-\gamma z) .\qquad\qquad\qquad (A3.2)$$

The attenuation coefficient, γ, is normally expressed in dB km^{-1}, with 1 dB km^{-1} being the equivalent of 2.3×10^{-4} m^{-1}. Absorption is a material property in which the optical energy is normally converted into heat. In scattering processes, some of the optical power in the guided modes is radiated out of the material.

Attenuation of some current and some potential future very low loss materials created for fiber communication is presented in Fig. A3.3. However, some of these materials are highly reactive chemically and are mechanically unsuitable for drawing into fibers. Some are used as infrared light guides. None is presently used for optical communication but may be used for our purposes. Our mechanical property and wavelength requirements are less than in optical communication. However, we use in our computation conventional values of 0.1 to 0.4 dB. Clean air has $\xi = 0.333 \times 10^{-6}$ m^{-1}. The

conventional optical matter widely produced currently in industry has an attenuation coefficient equal to 2 dB.
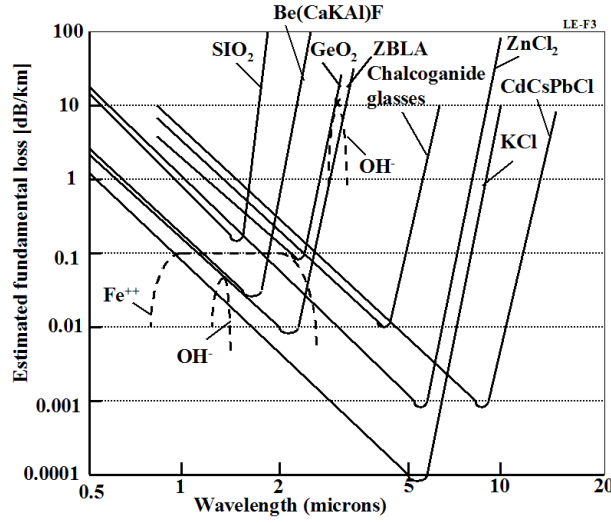

Fig. A3.3. Estimation of basic attenuation of some possible very low loss materials.

The beam power will be reduced if one (or both) reflector is moved, because the wavelength is increased. The total loss of beam energy in one double cycle (as the light beam is moved to the reflector and back) is

$$q = (1-2\gamma)(1-2\xi)(1\pm2v), \tag{A3.3}$$

where $v = V/c$, V is relative speed of cells [m/s], $c = 3\times10^8$ m/s is light speed. We take the "+" when the distance is reduced (braking) and take "– " when the distance is increased (useful work by light).

The light pressure, T, of two opposed high reflectors after a series of reflections, n, to one another is

$$T_0 = \frac{2N_0}{c}, \quad T_1 = \frac{2N_0}{c}q, \quad T_2 = \frac{2N_0}{c}q^2, \quad T_3 = \frac{2N_0}{c}q^3, \quad \dots \quad , \quad T_{n-1} = \frac{2N_0}{c}q^n, \tag{A3.4}$$

This is a geometric series. The sum of n members of the geometric series is

$$T = \frac{2N_0}{c}\frac{q^n-1}{q-1}. \quad If \quad n=\infty \quad then \quad T_\infty = \frac{2N_0}{c}\frac{1}{1-q}, \quad q<1. \tag{A3.5}$$

If the reflector is moved away, the maximum number of reflections, n, is limited by the cell size, l, because the wavelength is increased and that cannot be more than the cell size. This limit is

$$n \le \frac{\ln(l/\lambda_0)}{2v}, \tag{A3.6}$$

where l is cell width [m], λ_o is the initial wavelength [m].

If the reflector is moved forward to another position, the wave length is reduced, but it cannot be less than the wave length of X-rays because the material transmits X-rays (the material lowers the reflective capability).

This limit is about $\lambda_{min} = 10$ nanometers. The maximum number of brake reflections is

$$n \le \frac{\ln(\lambda_0/\lambda_{min})}{2v}. \tag{A3.7}$$

The force of the engine with slope, α, cells (Fig. A3.2) and engine coefficient efficiency, η, may be computed by the equation

$$T = \frac{2N_0}{c}\frac{q^n-1}{q-1}\cos\alpha, \quad \eta = \frac{TV}{N_0}. \tag{A3.7'}$$

The values in equation (A3.3) can be computed using

$$\gamma = 0.00023al, \quad l = m\lambda, \quad m \geq 1, \quad \xi = 0333 \cdot 10^{-6} l_c, \quad l_c = \frac{l + \delta}{\tan \alpha}, \qquad (A3.8)$$

where a is the attenuation coefficient in dB [km] (see Fig. A3.3), m is the initial number of wavelengths which can be located in cell size l, l_c is the length of a cell [m], and δ is the gap between engine disks [m].

The engine rotor force coefficient, A, shows how many times the initial light pressure is increased. It is

$$A = \frac{q^n - 1}{q - 1} . \qquad (A3.9)$$

The results of computations are presented in Figs. A3.4 to A3.8. The computed parameters are not optimal. Our purpose is to demonstrate the method of computation.

Fig. A3.4 shows the maximum pressure that can be created by a 1 kW beam in the cell design of Fig. A3.1b for a motionless disk ($V = 0$, $a = 0.1$ dB, $m = 30$, $N_0 = 1$ kW, $\lambda = 0.1$ to 1 μm). This pressure reaches a high force of 5000 N for the wavelength of 1 micron. This high pressure may be used, for example, for moving a heavy device a micron distance, for loudspeaker devices, or for frequency modulation of laser beams by mechanical energy, etc.

Fig. A3.5 presents the number of reflections for disk speed $V = 200$ m/s, $a = 0.2$ dB, $m = 10$ to 300. This number reaches 4 million double reflections (one from each mirror).
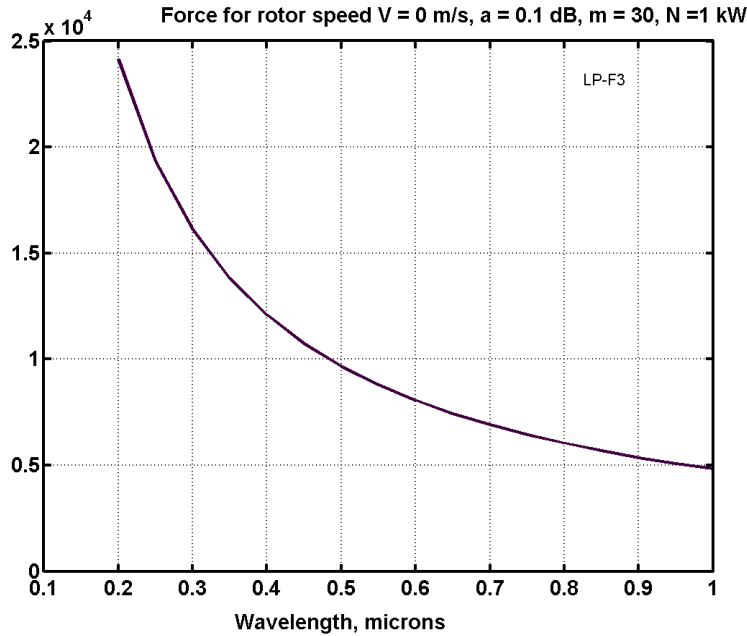

Fig. A3.4. Repulsive force, T [N], of motionless plates ($V = 0$ m/s) for infinite reflections, attenuation coefficient $a = 0.1$ dB, cell size $m = 30$, beam power $N_0 = 1$ kW and different wavelengths.

Fig. A3.6 presents the transmission efficiency coefficient of light energy, η_t, converted into mechanical energy for $V = 200$ m/s, $a = 0.2$ dB, $\lambda = 0.2, 0.5, 0.7, 1, 2$ μm, $m = 10$ to 300. The efficiency of the proposed light engine is very high and reaches 98%–99% if $m > 50$ (equation (A3.7)).

Fig. A3.7 presents the force on the rotary disk of the light engine for different speeds $V = 20$ to 500 m/s, $a = 0.1$ dB, $m = 30$, $P = 1$ kW. This force changes from 50 N through 2 N.

Fig. A3.8 presents the efficiency coefficient for a rotary engine for the data in Fig. A3.7, when the engine works in a vacuum (-) and in air (- -). The gap between disks is 0.1 mm. This coefficient reaches

more than 0.96 and only considers the transformation loss without mechanical friction. The mechanical friction is conventional for turbines and it is small.

All computations are made for a beam power of $N_0 = 1$ kW. For beam powers $N_0 = 10, 100, 1000$ kW we must multiply the forces in Fig. A3.7 by 10, 100, 1000 respectively.

We can ignore the loss from the sides of the cells because this is small if the beam divergence is small and the lateral side of the cells has the full reflection cover (as in the light cable).
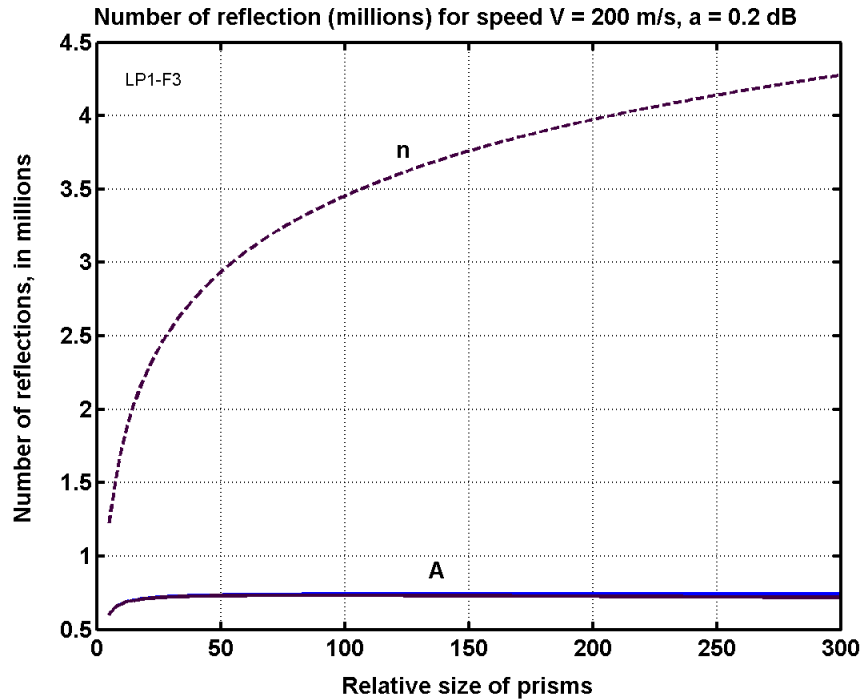
Fig. A3.5. Force coefficient, A (equation (A3.9)) and number of reflections n (equation (A3.6)) for rotor speed V = 200 m/s, a = 0.2 dB, and relative size of prisms m = 10–300.
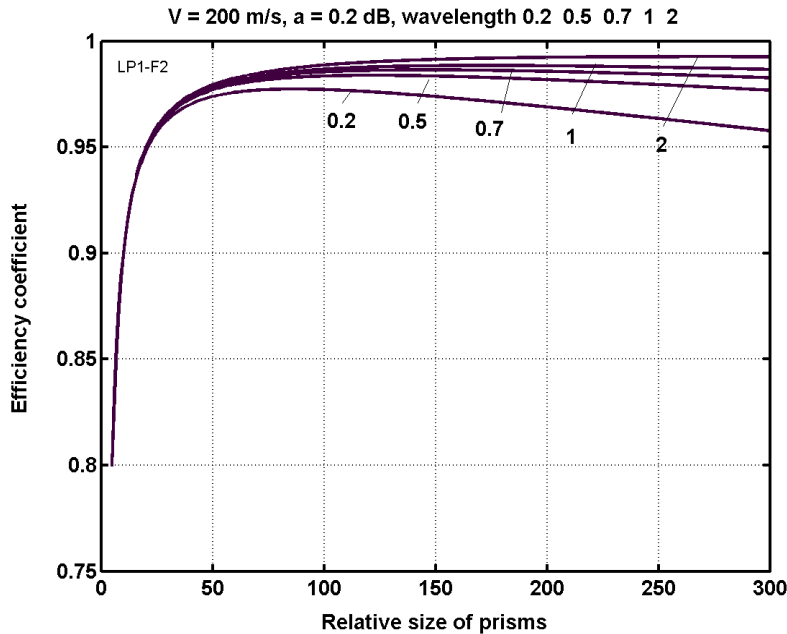

Fig. A3.6. Efficiency coefficient (equation (A3.7)) for rotor speed V = 200 m/s, a = 0.2, wavelength λ = 0.2 to 2 microns, relative size of prisms m = 10 to 300.
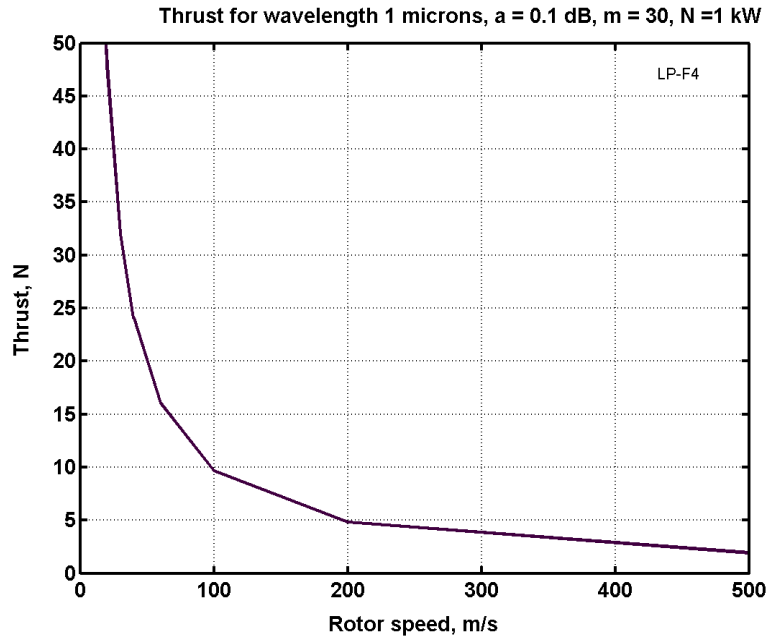
Thrust for wavelength 1 microns, a = 0.1 dB, m = 30, N =1 kW

Fig. A3.7. Thrust (force) (equation (A3.7)) versus the rotor speed (*V* = 20 to 500 m/s) for wavelength *λ* = 1μm, *a* = 0.1 dB, *m* = 30, beam power N_0 = 1 kW.

Ef. coef. for V=100 200 300 400 500 m/s, (in air "--"), a = 0.5 dB, m = 30, N = 1 kW
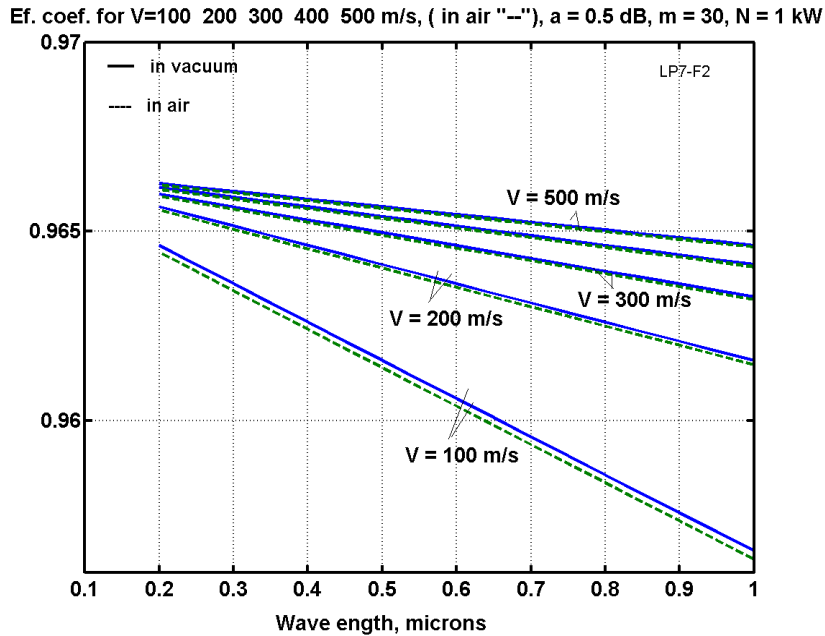

Fig. A3.8. Efficiency coefficient (equation (A3.7)) versus wavelength *λ* = 0.2 to 1 μm, *a* = 0.5 dB, *m* = 30, N_0= 1 kW, and rotor speed *V* = 100 to 500 m/s. The broken lines - - show the computations with air attenuation.

Discussion

The proposed multi-reflex light engine is very simple (only two disks), has a small size, a very high ratio of power/weight, and is efficient. One can directly convert the beam light into mechanical energy.

   This engine may be applied in aviation because the energy can be transferred from an earth surface station to an aircraft by the laser beam. The aircraft does not need to carry fuel and has a more

lightweight engine, so its load capability doubles as a result. Industry can produce a 1 Megawatt (1000 kW) laser now. This is enough for middle-range aircraft with a weight of 10 to 12 tons[10].

The linear light engine does not have a speed limit and one may be used to launch space equipment and space ships[11–13]. This method may be also used in the design of new efficient weapons[14].

The intensity of solar light on a clear day is about 1 kW/m^2. If we can convert this light into mechanical energy, the mechanical energy can be converted into electrical energy. The efficiency of this process may be higher and cheaper than the efficiency of expensive commercial solar cells (10–12% efficient).

This text is published in Reference[15, 16].

References for Attachment 3

1. A. Kantrowitz, "Propulsion to Orbit by Ground-Based Lasers", *Astronautics and Aeronautics*, 10, pp. 74-76, May 1972.
2. *"Beamed Energy Propulsion. First International Symposium on Beamed Energy Propulsion"*, American Institute of Physics, Melville, New York, 2003.
3. A.A. Bolonkin, "Light Pressure Engine", Patent (Author Certificate) *# 1183421*, 1985, USSR, (priority on 5 January 1983).
4. R.G. Driggers (Ed.), *Encyclopedia of Optical Engineering*, Marcel Dekker, Inc., New York, 2003.
5. "*Handbook of Optics*", 2nd edn., McGraw-Hill, Inc., 2000.
6. *Military Standardization Handbook. Optical Design,* No. 141, 1962.
7. P.W. Milonni, and J.H. Eberly, "*Lasers*", John Wiley & Sons., NY, 1988.
8. D.C. O'Shea, *Elements of Modern Optical Design*, John Wiley and Sons, NY, 1985.
9. A.W. Snyder, *Optical Waveguide Theory*, Chapman and Hall, NY–London, 1983.
10. A.A. Bolonkin, "Multi-reflex Propulsion Systems for Space and Air Vehicles and Energy Transfer for Long Distance", *JBIS*, Vol. 57, No 11/12, pp, 379–300, 2004,.
11. A.A. Bolonkin, "Kinetic Space Towers and Launchers", *JBIS*, Vol. 57, No 1/2, pp. 33-39, 2004.
12. A.A. Bolonkin, "Hypersonic Launch System of Capability up 500 tons per day and Delivery Cost $1 per Lb", IAC-02-S.P.15, 53rd International Astronautical Congress – The World Space Congress, Houston, Texas, USA, 10–19 Oct 2002.
13. A.A. Bolonkin, "Earth Accelerator for Space Ships and Missiles", *JBIS*, Vol. 56, No 11/12, pp. 394-404, 2003.
14. A.A. Bolonkin, "Air Cable Transport", *Journal of Aircraft*, Vol. 40, No 2, March-April, 2003.
15. A.A. Bolonkin, "Light Multi-Reflex Engine", *JBIS*, vol.57, No 9/10, pp. 353–359, 2004.
16. A.A. Bolonkin, Patent US 6,494,143 B1, USA.

Attachment 4
Optimal Trajectories of Air and Space Vehicles*
Summary

The author has developed a theory on optimal trajectories for air vehicles with variable wing areas and with conventional wings. He applied a new theory of singular optimal solutions and obtained in many cases the optimal flight. The wing drag of a variable area wing does not depend on air speed and air density. At first glance the results may seem strange, however, this is the case and this chapter will show how the new theory may be used. The equations that follow enable computations of the optimal control and optimal trajectories of subsonic aircraft with pistons, jets, and rocket engines, supersonic aircraft, winged bombs with and without engines, hypersonic warheads, and missiles with wings.

The main idea of the research is to use the vehicle's kinetic energy to increase the range of missiles and projectiles.

The author shows that the range of a ballistic warhead can be increased 3–4 times if an optimal wing is added to it, especially a wing with variable area. If we do not need increased range, the warhead mass can be increased. The range of large gun shells can also be increased 3–9 times. The range of an aircraft may be improved by 3–15% or more.

The results can be used for the design of aircraft, missiles, flying bombs and shells for large guns.

Nomenclature (in metric system)

a – the speed of sound, m/s,

a_1, b_1, a_2, b_2 – coefficients of exponential atmosphere,

C_L – lift coefficient,

C_D – drag coefficient,

C_{Do} – drag coefficient for $C_L = 0$,

C_{DW} – wave wing drag coefficient when $\alpha = 0$,

C_{Db} – body drag coefficient,

c – relative thickness of a wing,

c_b – relative thickness of a body,

c_1 – relative thickness of a vehicle body,

c_s – fuel consumption, kg/s/ kg thrust,

$\overline{D}$ – drag of vehicle, N,

D – drag of vehicle without α, N,

D_{0W} – wave wing drag when $\alpha = 0$, N,

D_{0b} – drag of a vehicle body, N,

H – Hamiltonian,

h – altitude, m,

$K = C_L/C_D$ – the wing efficiency coefficient,

k_1, k_2, k_3 – vehicle average aerodynamic efficiencies for sub-distances 1, 2, 3 respectively,

L – range,

$M = V/a$ – Mach number,

m – mass of vehicle, kg,

$p = m/S$ – load on a square meter of wing,

$q = \rho V^2/2$ – a dynamic air pressure,

R – aircraft range or R = distance from flight vehicle to Earth center; $R = R_o + h$, where $R_o = 6378$ km is Earth radius,

t– time,

$T = V_e \beta$ – thrust, N,

V – vehicle speed, m/s,

V_e – speed of throw back mass (air for propeller engine, jet for jet and rocket engine), m/s,

S – wing area, m^2,

s – length of trajectory,

T – engine thrust, N,

Y – lift force, N,

α – wing attack angle,

β – fuel consumption,

θ – angle between the vehicle velocity and the horizon,

ω – thrust angle between thrust and velocity,

ω_E – Earth angle speed,

φ_E – lesser angle between the Earth's Polar axis and a perpendicular to a flight plate,

ρ – air density. kg/m^3.

Introduction

The topic of the optimal flight of air vehicles is very important. There are numerous articles and books about the optimal trajectories of rockets, missiles, and aircraft. The classical research of this topic is by Miele[1]. Unfortunately, the optimal theory of this problem is very complex. In most cases, the researchers obtained complex equations, that allow one to compute a single optimal trajectory for a given aircraft and for given conditions, but the structure of optimal flight is not clear and simple formulas of optimal control (which depend only on flight conditions) are absent.

The author's new theory of singular optimal solutions, developed earlier[2–14], does not contain unknown coefficients or variables as previous theories have. He found that the optimal flight path depends only on the flight conditions and the addition of certain variable wing structures.

In conclusion, the author applies his solution to ballistic missiles, warheads, flying bombs, large gun shells, and subsonic, supersonic, and hypersonic aircraft with rocket, turbo-jet, and propeller engines. He shows that the range of these air vehicles can be increased 3–9 times.

1. General equations

Let us consider the movement of an air vehicle given the following conditions: (1) The vehicle moves in a plane containing the Earth's center. (2) The vehicle design allows the wing area to be changed (this will prove important in the remainder of this chapter). (3) We ignore the centrifugal force from the Earth's rotation (it is less then 1%). (4) Earth has a curvature.

Then the equations for flying vehicle (in a system of coordinates where the center of the system is located at the center of gravity of the flying vehicle, the x-axis is in the direction of flight, the y-axis is perpendicular to the x- axis, Fig. A4.1) are
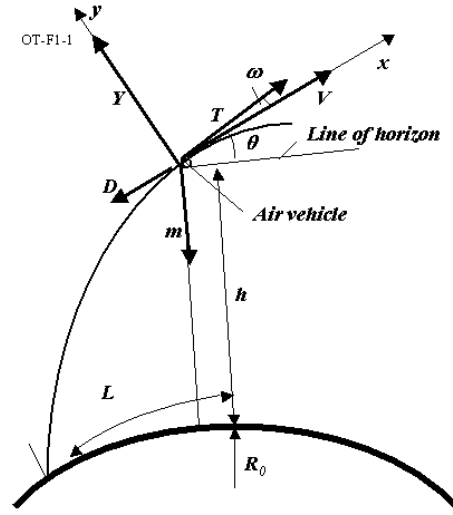
Fig. A4.1 Vehicle forces and coordinate system.

$$\frac{dL}{dt} = V\cos\theta \quad,$$

$$\frac{dh}{dt} = V\sin\theta \quad,$$

(A4.1)–(A4.2)

$$\frac{dV}{dt} = \frac{T(h,V,\beta)\cos\omega - \overline{D}(\alpha,V,h)}{m} - g\sin\theta \,,$$

$$\frac{d\theta}{dt} = \frac{T(h,V,\beta)\sin\omega + Y(\alpha,V,h)}{mV} - \frac{g}{V}\cos\theta + \frac{V\cos\theta}{R} + 2\omega_E\cos\varphi_E \,, \qquad (A4.3) - (A4.5)$$

$$\frac{dm}{dt} = -\beta \quad.$$

All values are in the metric system and all angles are taken to be in radians.

Flight with a small change of vehicle mass and flight path angle

Most air vehicles fly at an angle θ in the range $\pm15°$ ($\theta = \pm 0.2618$ rad), with the engine located along the velocity vector. This means

$$\sin\theta = \theta, \qquad \cos\theta = 1 \,, \qquad \omega = 0 \,, \qquad \text{(A4.6) – (A4.8)}$$

because $\sin15° = 0.25882$, $\cos15° = 0.9659$.

Let as substitute (A4.6) – (A4.8) into (A4.1) – (A4.5)

$$\frac{dL}{dt} = V \quad,$$

$$\frac{dh}{dt} = V\theta \quad,$$

(A4.9) – (A4.10)

$$\frac{dV}{dt} = \frac{T(h,V) - \overline{D}(\alpha,V,h)}{m} - g\theta \,,$$

$$\frac{d\theta}{dt} = \frac{Y(\alpha,V,h)}{mV} - \frac{g}{V} + \frac{V}{R} + 2\omega_E\cos\varphi_E \,,$$

(A4.11) – (A4.12)

$$\frac{dm}{dt} = -\beta \quad , \tag{A4.13}$$

where

$$|\theta| \le \theta_{\max} . \tag{A4.14}$$

Many air vehicles fly with a low angular speed of $d\theta/dt$. The change of mass is also low in flight. This means $m = $ const, $dm/dt \cong 0$.

$$d\theta/dt \approx 0, \ dm/dt = 0 . \tag{A4.15} – (A4.16}$$

Let us take a new independent variable $s = $ length of trajectory

$$dt = ds/V, \tag{A4.17}$$

and substitute (A4.14)-(A4.17) in (A4.9)-(A4.13). Then system (A4.9)-(A4.13) takes the form

$$\frac{dL}{ds} = 1 ,$$

$$\frac{dh}{ds} = \theta ,$$

$$\frac{dV}{ds} = \frac{T(h,V) - \overline{D}(\alpha,V,h)}{mV} - \frac{g}{V}\theta , \tag{A4.18} – (A4.21)$$

$$0 = \frac{Y(\alpha,V,h)}{mV} - \frac{g}{V} + \frac{V}{R} + 2\omega_E \cos\varphi_E .$$

Let us re-write equation (A4.21) in the form

$$Y(\alpha,V,h) - mg + \frac{mV^2}{R} + 2mV\omega_E \cos\varphi_E = 0 . \tag{A4.22}$$

If we ignore the last element, equation (A4.22) takes the form

$$Y(\alpha,V,h) - mg + \frac{mV^2}{R} = 0 . \tag{A4.22'}$$

If V is not very large ($V <$ 3 km/s), the two last elements in equation (A4.21) are small and they may be ignored. Equations (A4.22) and (A4.22)' can be used for deleting α from $\overline{D}$.

Note the new drag without α is

$$D=D(h,V). \tag{A4.23}$$

If we substitute α from (A4.22) into equation (A4.20) the equation system take the form

$$\frac{dL}{ds} = 1 ,$$

$$\frac{dh}{ds} = \theta , \tag{A4.24} – (A4.26}$$

$$\frac{dV}{ds} = \frac{T(h,V) - D(V,h)}{mV} - \frac{g}{V}\theta ,$$

Here the variable θ is new control limited by

$$|\theta| \le \theta_{\max} . \tag{A4.27}$$

Statement of the problem

Consider the problem: finding the maximum range of an air vehicle described by equations (A4.24) – (A4.26) for the limitation (A4.27). This problem may be solved using conventional methods. However, it is a non-linear problem but contains the linear control, which means the problem has a singular solution. To find this singular solution, we will use methods developed previously[2, 4].

Write the Hamiltonian

$$H = 1 + \lambda_1 \theta + \lambda_2 \frac{1}{V}\left(\frac{T-D}{m} - g\theta\right) , \tag{A4.28}$$

where $\lambda_1(s)$, $\lambda_2(s)$ are unknown multipliers. Application of the conventional method gives

$$\dot{\lambda}_1 = -\frac{\partial H}{\partial h} = -\lambda_2 \frac{1}{V}\left(\frac{T_h' - D_h'}{m}\right) ,$$

$$\dot{\lambda}_2 = -\frac{\partial H}{\partial V} = -\lambda_2\left[-\frac{1}{V^2}\left(\frac{T-D}{m} - g\theta\right) + \frac{1}{V}\left(\frac{T_V' - D_V'}{m}\right)\right] , \tag{A24.29)-(A4.31}$$

$$\theta = \max_\theta H = \theta_{max} sign\left[\lambda_1 - \lambda_2 \frac{g}{V}\right] .$$

Where D_h', D_v', T_h', T_v' denote the first partial derivatives of D, T by h, V respectively.

The last equation shows that the control θ can have only two values $\pm\theta_{max}$. We consider the singular case when

$$A = \lambda_1 - \lambda_2 \frac{g}{V} \equiv 0 . \tag{A4.32}$$

This equation has two unknown variables λ_1 and λ_2 and does not contain information about the control θ.   Let us to differentiate equation (A4.32) for the independent variable s. After substitution the equations (A4.26), (A4.29), (A4.30), and (A4.32) into the result of differentiation , we obtain the relation for $\lambda_1 \neq 0$, $\lambda_2 \neq 0$

$$V(T_h' - D_h') = g(T_V' - D_V') \tag{A4.33}$$

This equation does not contain θ either, but it contains the important relation between the variables V and h on the optimal trajectory.

If we have the formulas (or graphs)

$$D = D(h,V), \tag{A5.34}$$
$$T = T(h,V), \tag{A4.35}$$

we could find the relation

$$h = h(V) \tag{A4.36}$$

and the optimal trajectory for a given air vehicle.

This also gives important information about the structure of the optimal solution. Investigation of equation (A4.33) shows that the equation has one solution in each of the subsonic, supersonic, and hypersonic fields. The equation can have two solutions for a transonic field.

This means the optimal trajectory in most cases has three parts (see Fig. A4.2):

a) When climbing and in flight a vehicle moves from the initial point A with the angle $\pm\theta_{max}$ up to the optimal curve (A4.36), then continues along the optimal curve (A4.36) and moves with at an angle $\pm\theta_{max}$ to point B.

b) When descending and in flight (Fig. A4.3) a vehicle moves from the initial point A with the angle $\pm\theta_{max}$ (up or down) to the optimal curve (A4.36), then continues down the optimal curve (A4.36), and moves at an angle $\pm\theta_{max}$ (up or down) to the point B.
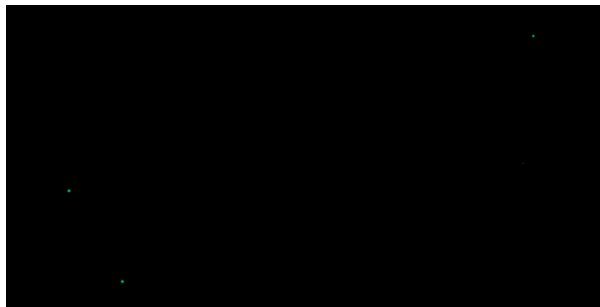
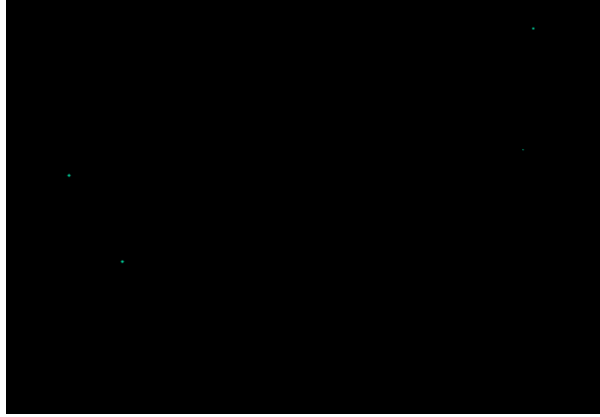**Fig. A4.2.**. Optimal trajectory for air vehicle climb and flight.

Fig. A4.3. Optimal trajectory for air vehicle descent and flight.

The selection of direction (up or down, with θ_{max} or $-\theta_{max}$ respectively) depends only on the position of the initial and end points A and B.

For air vehicles with rocket engines $T = $ const, equation (A4.33) has a very simple form

$$VD'_h = gD'_V \ . \tag{A4.37}$$

The same form (same curve) also applies for a ballistic warhead, which does not have engine thrust (after its short initial burn) $(T = 0)$.

If we want to find an equation for the control θ, we continue to differentiate equation (A4.33) with the independent variable s, and substitute into the equations (A4.25), (A4.26), (A4.29), (A4.30), (A4.32), and (A4.33). We obtain the relation for θ if $\lambda_1 \neq 0$, $\lambda_2 \neq 0$

$$\theta = \frac{B_1(T - D)}{mV\left(B_1 \dfrac{g}{V} - B_2\right)} \ , \tag{A4.38}$$

where

$$\begin{aligned}
B_1 &= (T'_h - D'_h) + V(T''_{hV} - D''_{hV}) - g(T''_{VV} - D''_{VV}) \ , \\
B_2 &= V(T''_{hh} - D''_{hh}) - g(T''_{hV} - D''_{hV}) \ .
\end{aligned} \tag{A4.39)–(A4.40}$$

Here signs in form D''_{hV} are the second partial derivates D for h, V.

$$D''_{hV} = \frac{\partial^2 D}{\partial h \partial V} \ . \tag{A4.41}$$

If the thrust does not depend on h, V $(T = $ const) or no engine $(T = 0)$, the equation for θ becames simpler

$$\theta = \frac{[(gD''_{VV} - D'_h) - VD''_{hV}](T - D)}{m[g(gD''_{VV} - D'_h) + V^2 D''_{hh}]} \ . \tag{A4.42}$$

In accordance with other publications[2–8] (e,g, equation (4.2)[4]) the necessary condition for optimal trajectory is

$$-(-1)^k \frac{\partial}{\partial \theta}\left[\frac{d^{2k}}{ds^{2k}}\left(\frac{\partial H}{\partial \theta}\right)\right] \geq 0 . \tag{A4.43}$$

where $k = 1$.

To obtain results for different forms of the drags and thrusts, we must take formulas (or graphs) for subsonic, transonic, supersonic, or hypersonic speed, and specific formulas for the thrust

and substitute them in the equation (A4.33) and (A4.38). Consider two cases: subsonic and hypersonic speeds.

Subsonic speed ($V < 270$ m/s) and different engines.

Lift, drag, and derivative equations for subsonic speed are

$$L = mg = \varsigma \alpha \frac{\rho V^2}{2} S, \quad \overline{D} = C_D \frac{\rho V^2}{2} S, \quad C_D = C_{Do} + \varepsilon \alpha^2, \quad D = \left[C_{Do} + \varepsilon\left(\frac{2mg}{\varsigma \rho V^2 S}\right)^2\right]\frac{\rho V^2}{2} S,$$

$$\tag{A4.44}$$

$$\rho = a_1 e^{-h/b_1}, \quad \frac{\partial D}{\partial V} = \left[C_{Do} - \varepsilon\left(\frac{2mg}{\varsigma \rho V^2 S}\right)^2\right]\rho V S, \quad \frac{\partial D}{\partial h} = -\frac{1}{b_1}\left[C_{Do} - \varepsilon\left(\frac{2mg}{\varsigma \rho V^2 S}\right)^2\right]\frac{\rho V^2}{2} S,$$

where $\varsigma = \frac{6.24\lambda}{\lambda + 2}$, $\varepsilon = \frac{\varsigma^2}{\pi\lambda}$, magnitude $\varepsilon \approx \varsigma^2/\pi\lambda$ is an induced drag coefficient, $\lambda = l^2/S$, l is a wing span.

It is known in conventional aerodynamics that the coefficient of flight efficiency k is

$$k = \frac{C_L}{C_D} = \frac{\varsigma \alpha}{C_{Do} + \varepsilon \alpha^2}, \quad from \quad \max_\alpha k \quad we \ obtain \quad \alpha_{opt} = \sqrt{\frac{C_{Do}}{\varepsilon}}, \quad k_{max} = \frac{\varsigma}{2\sqrt{\varepsilon C_{Do}}} . \tag{A4.45}$$

a) Aircraft with rocket engine. For this aircraft the thrust T is constant or 0. Equation (A4.33) has form (A4.37). Find the partial derivatives

$$T'_V = 0, \quad T'_h = 0 . \tag{A4.46}$$

Substituting (A4.44) to (A4.46) in (A4.37) we obtain the relation between air density ρ, altitude h, and aircraft speed V:

$$\rho = \frac{2gp}{\varsigma V^2}\sqrt{\frac{\varepsilon}{C_{Do}}}, \quad p = \frac{m}{S}, \quad h = b_1 \ln\frac{a_1}{\rho} , \tag{A4.47}$$

where $p = m/S$ is the load on a square meter of wing. For a diapason of $h = 0$–11 km the coefficients $a_1 = 1.225$, $b_1 = 9086$.

Results of this computation are presented in Fig. A4.4.

b) Aircraft with turbo-jet engine. The thrust for this engine is

$$T = T_0 \frac{\rho}{\rho_0}, \quad T'_h = -\frac{T}{b_1}, \quad T'_V = 0 . \tag{A4.48}$$

Substitute (A4.48) in (A4.33). We obtain

$$V\left(-\frac{T}{b_1} - D'_h\right) = -gD'_V \quad or \quad T = \frac{b_1}{V}\left(gD'_V - VD'_h\right), \tag{A4.48'}$$

and substituting (A4.44) and (A4.48) in (A4.33), we obtain

$$\frac{1}{p}\left(\frac{V^2}{2b_1} + g\right)\left[C_{Do} - \varepsilon\left(\frac{2pg}{\varsigma \rho V^2}\right)^2\right] = \frac{\overline{T}_0}{b_1 \rho_0}, \quad where \quad \overline{T}_0 = \frac{T_0}{m} . \tag{A4.49}$$

We can then find ρ, h from (A4.49)

$$\rho = \frac{2pg\sqrt{\varepsilon}}{\varsigma V^2 \sqrt{A_2}}, \quad where \quad A_2 = C_{Do} - \frac{2p\bar{T}_0}{\rho_0(V^2 + 2b_1 g)} \quad \bar{T}_0 = \frac{T_0}{m}, \quad h = b_1 \ln\frac{a_1}{\rho}. \quad (A4.50)$$

Results of computation for the different p, $T = 0.8$ N/kg, $a_1 = 1.225$, $b_1 = 9086$ are presented in Fig. A4.5.
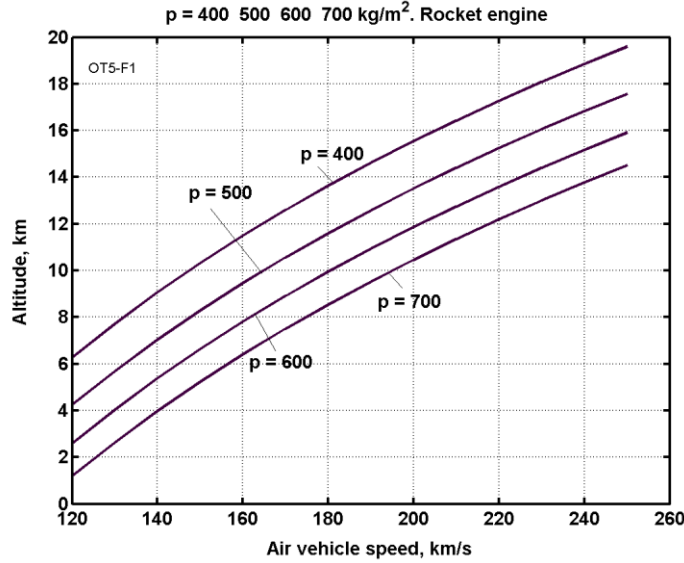

Fig. A4.4. Air vehicle altitude versus speed for wing load $p = 400, 500, 600, 700$ kg/m^2 and a rocket engine.
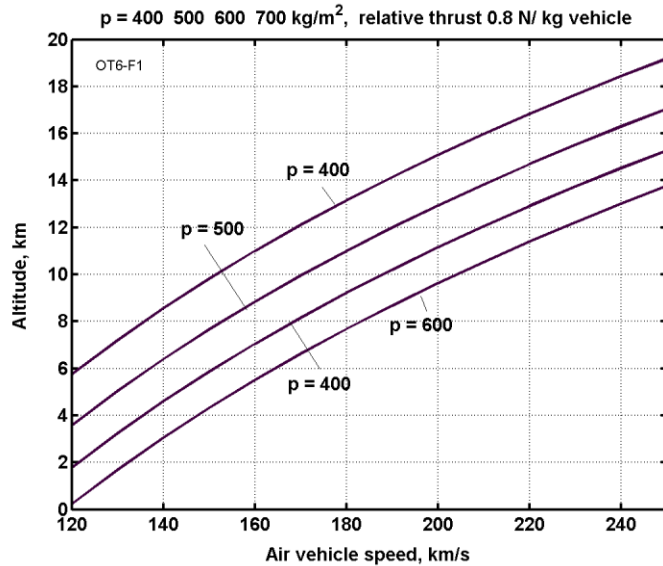

Fig. A4.5. Air vehicle altitude versus speed for wing load $p = 400, 500, 600, 700$ kg/m^2, turbo-jet engine, and relative thrust 0.8 N/kg vehicle.

c) **Piston and turbo engines with propeller.** All current propeller engines have propellers with variable pitch. The propeller coefficient efficiency, η, approximately is constant. The thrust of this engine is

$$T = \frac{N_0}{V}\frac{\rho}{\rho_0}, \quad T_V' = -\frac{T}{V}, \quad T_h' = -\frac{T}{b_1}, \quad (A4.51)$$

where $N_0 = N_e \eta$, N_e is engine power at $h = 0$.

Substituting (A4.44) in (A4.33). We obtain the equation for thrust

$$V\left(\frac{T}{b_1} + D_h'\right) = g\left(\frac{T}{V} + D_V'\right) \quad or \quad T = \frac{b_1 V (g D_V' - V D_h')}{V^2 - g b_1} . \tag{A4.51'}$$

Substitute (A4.44) and (A4.51) in (A4.33). We obtain

$$\frac{V}{p}\left(\frac{V^2}{b_1} - g\right)\left[C_{Do} - \varepsilon\left(\frac{2pg}{\rho V^2}\right)^2\right] = \frac{\overline{N}_0}{\rho_0}\left(\frac{g}{V^2} - \frac{1}{b_1}\right), \quad where \quad \overline{N}_0 = \frac{N_0}{m}, \quad p = \frac{m}{S}. \tag{A4.52}$$

We can then find ρ, h from (A4.52)

$$\rho = \frac{2pg\sqrt{\varepsilon}}{\varsigma V^2 \sqrt{A_3}}, \quad where \quad A_3 = C_{Do} + \frac{p\overline{N}_0}{\rho_0 V^3}, \quad h = b_1 \ln\frac{a_1}{\rho}. \tag{A4.53}$$

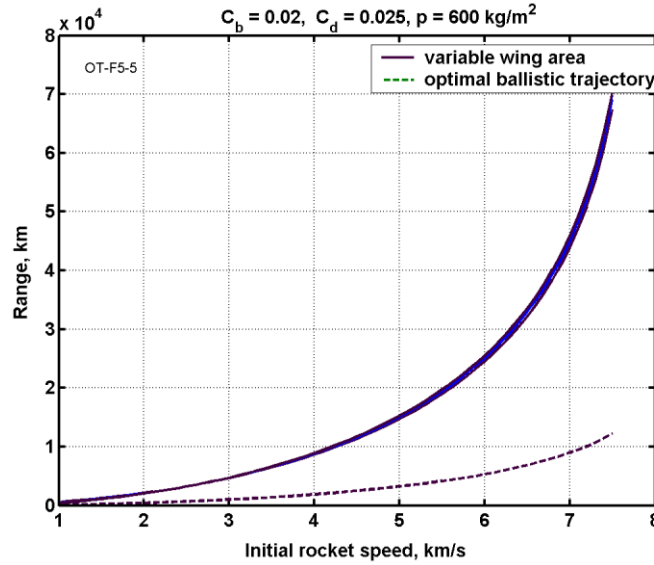Results of computation for $C_{Do} = 0.025$, $\lambda = 10$, for different values of p, N are presented in Fig. A4.6.

Fig. A4.6. Air vehicle range versus speed for wing load $p = 250, 300, 350, 400$ kg/m², piston (propeller) engine, and relative engine power 100 W/kg vehicle.

Hypersonic speed (1 km/s $< V <$ 7 km/s).

The lift and drag forces in hypersonic flight are approximately (see (A4.22)')

$$L(\alpha, V, h) = mg - \frac{mV^2}{R} = \varsigma\alpha\frac{a\rho V}{2}S, \quad \overline{D} = (C_{DW} + \varepsilon\alpha^2)\frac{a\rho V}{2}S + C_{Db}\frac{a\rho V}{2}S_b,$$

$$\alpha = \frac{2p(g - V^2/R)}{\varsigma\rho a V}, \quad D = \left[C_{DW}\frac{a\rho V}{2} + \frac{2\varepsilon}{\rho a V}\left(\frac{m(g - V^2/R)}{\varsigma S}\right)^2\right]S + C_{Db}\frac{a\rho V}{2}S_b, \tag{A4.54}$$

$$or \quad \frac{D}{m} = \left[C_{DW}\frac{q}{p} + \frac{\varepsilon p}{q}\left(\frac{g - V^2/R}{\varsigma}\right)^2\right] + C_{Db}\frac{q}{p_b}, \quad q = \frac{\rho a V}{2} .$$

Note

$$D_{0W} = C_{DW} \frac{\rho a V}{2} S, \quad D_{0b} = C_{Db} \frac{\rho a V}{2} S_b, \quad C_{DW} = 4c, \quad C_{Db} = 2c_b, \quad \rho = a_2 e^{-\frac{h-11000}{b_2}}, \quad (A4.55)$$

The derivatives of D by V, h are

$$D_V' = \frac{D_{0W}}{V} + \frac{D_{0b}}{V} - \frac{2\varepsilon m p}{\varsigma^2 \rho a}\left(g - \frac{V^2}{R}\right)\left(\frac{3}{R} + \frac{g}{V^2}\right),$$

$$D_h' = D_\rho' \rho_h' = -\frac{1}{b_2}\left(D_{0W} + D_{0b} - \frac{2\varepsilon m p (g - V^2/R)^2}{\varsigma^2 \rho a V}\right)$$

$$(A4.56)$$

a) **Rocket engine or hypersonic glider.** The derivatives from $T = const$ and $T = 0$ are

$$T_V' = 0, \quad T_h' = 0. \tag{A4.57}$$

Substituting (A4.55) in (A4.56), and expressions (A4.56) and (A4.57) in (A4.37) to find ρ, h, we obtain for $h > 11,000$ m

$$\rho = \frac{2p\sqrt{\varepsilon}}{\varsigma a}\sqrt{A_4}, \quad A_4 = \frac{\left(g - \frac{V^2}{R}\right)\left[g\left(\frac{3}{R} + \frac{g}{V^2}\right) + \frac{1}{b_2}\left(g - \frac{V^2}{R}\right)\right]}{\left(\frac{V^2}{b_2} + g\right)\left[C_{DW} + C_{Db}\left(\frac{S_b}{S}\right)\right]}, \quad h = 11000 + b_2 \ln\frac{a_2}{\rho},$$

$$(A4.58)$$

where $a_2 = 0.365$, $b_2 = 6997$ are coefficients of the exponent atmosphere for the stratosphere at 11 to 60 km.

If we ignore the small term $g\left(\frac{3}{R} + \frac{g}{V^2}\right)$ for $M > 3$ in (A4.58), the equations take the form

$$\rho = \frac{2p(g - V^2/R)\sqrt{\varepsilon}}{\varsigma a}\sqrt{A_5}, \quad A_5 = \frac{1}{C_{Do}(V^2 + gb_2)}, \quad where \quad C_{Do} = C_{0W} + C_{Db}\left(\frac{S_b}{S}\right),$$

where $C_{DW} \approx 4c$. If we ignore the term gb_2 (for $M > 3$), then

$$\rho = \frac{2p(g - V^2/R)}{\varsigma a V}\sqrt{\frac{\varepsilon}{C_{Do}}}. \tag{A4.59}$$

In the limit as $R \to \infty$ in (2-54), we find

$$\rho = \frac{2pg}{\varsigma a V}\sqrt{\frac{\varepsilon}{C_{Do}}}. \tag{A4.59'}$$

Here $\sqrt{C_{Do}/\varepsilon} = \alpha_{opt}$ is an optimal (maximum C_L/C_D) wing attack angle of the horizontal flight. Results of the computation in (A4.58) are presented in Fig. A4.7.
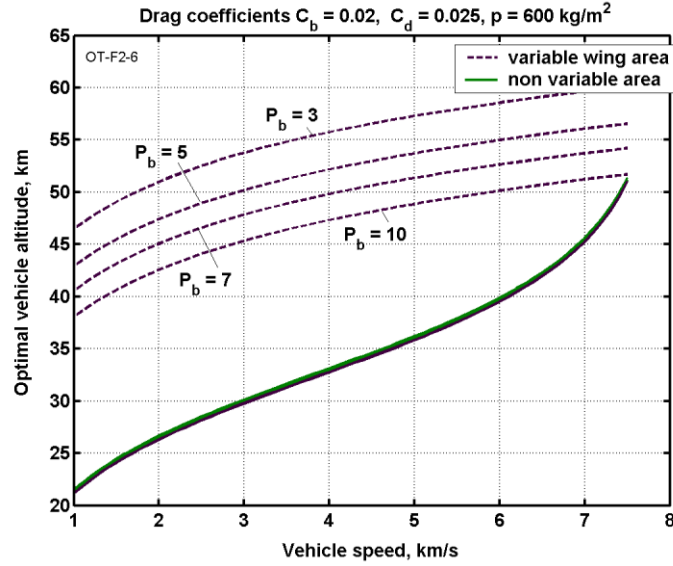
Fig. A4.7. Optimal vehicle altitude versus speed for specific body load P_b = 3, 5, 7, 10 ton/m², body drag coefficient C_b = 0.02, wing drag coefficient C_d = 0.025, wing load p = 600 kg/m².

b) **Ramjet engine.** The thrust of the jet engine is approximately ($M < 4$)

$$T = \xi \frac{\rho}{\rho_2} V^2, \quad T_V' = \frac{2T}{V}, \quad T_h' = -\frac{T}{b_2}, \qquad (A4.60)$$

where ξ is a numerical coefficient, ρ_2 is the air density at the lower end of the selected atmospheric diapason (in our case 11 km).

Substituting (A4.60) and (A4.56) in our main equation (A4.33), by repeat reasoning we can obtain the equation for the given engine

$$\rho = \frac{2p\sqrt{\varepsilon}}{\varsigma a}\sqrt{A_6}, \quad A_6 = \frac{\left(g - V^2/g\right)\left[g\left(\frac{3}{R} + \frac{g}{V^2}\right) + \frac{1}{b_2}\left(g - V^2/R\right)\right]}{\left[C_{DW} + C_{Db}\left(\frac{S_b}{S}\right)\right]\left[\left(\frac{V^2}{b_2} + g\right) - \frac{2\overline{T}_0 p}{a\rho_0}\left(\frac{V}{b_2} - \frac{2g}{V}\right)\right]}, \quad \overline{T} = \frac{T_0}{m}, \quad (A4.61)$$

where T_0 is taken at the lower end of the exponent atmospheric diapason (in our case 11 km). The curve of air density versus altitude h is computed similarly to (A4.58).

Optimal wing area

The lift force and drag of any wing may be written as

$$Y = mg = Y(\alpha, q, S), \quad D = D(\alpha^2, q, S). \qquad (A4.62)$$

Substituting (A4.62) in (A4.28) and finding the minimum H versus S, we obtain the equation

$$D + \overline{D}_\alpha' \alpha_S' S = 0, \quad \text{or} \quad D + D_S' S = 0, \qquad (A4.63)$$

where α is the value found from the first equation (A4.62). Equation (A4.63) is the general equation for the optimal wing area and optimal specific load $p = m/S$ on a wing area.

a) **Subsonic speed**. Lift force and drag of the subsonic wing are

$$Y = mg = \varsigma \alpha q S \quad \text{or} \quad \alpha = \frac{mg}{\varsigma q S}, \quad \overline{D} = \left(C_{Do} + \varepsilon\alpha^2\right)qS \quad D = C_{DW}qS + \varepsilon\left(\frac{mg}{\varsigma}\right)^2\frac{1}{qS}, \qquad (A4.62)'$$

where $q = \rho V^2/2$ is a dynamic air pressure for subsonic speed.

Substituting the last equation in (A4.62) into the first equation in (A4.63), we obtain the optimal specific load on the wing area

$$p_{opt} = \frac{\varsigma q}{g} \sqrt{\frac{C_{DW}}{\varepsilon}} \ . \tag{A4.63'}$$

Substituting α from (A4.62)' into the last equation in (A4.62)' and dividing both sides by vehicle mass m, we obtain

$$\frac{D}{m} = \left[C_{DW} \frac{1}{p} + \varepsilon \left(\frac{g}{\varsigma q} \right)^2 p \right] q \ . \tag{A4.64}$$

Here D/m is specific drag (drag per unit weight for the vehicle). Substituting (A4.63)' into (A4.64). We abtain the minimum drag for a variable wing

$$\min\left(\frac{D}{m}\right) = 2 \frac{g}{\varsigma} \sqrt{\varepsilon C_{DW}} \ , \tag{A4.64'}$$

where the term on the right is wing drag for the lift of one unit of weight for the vehicle. We discover the important fact than the **optimal** wing drag of a variable wing **does not depend** on air speed, it depends **only** on the geometry of the wing. This may look wrong, but consider the following example. Wing drag is $D = mg/K$, where $K = C_L/C_D$ is the wing efficiency coefficient. The value D/m does not depend on speed.

If the air vehicle has a body, the minimum drag is

$$\min\left(\frac{D}{m}\right) = 2 \frac{g}{\varsigma} \sqrt{\varepsilon C_{DW}} + C_{Db} \frac{q}{p_b}, \quad q = \frac{\rho V^2}{2} \ . \tag{A4.65}$$

Full vehicle drag depends on speed because the body drag depends on V.
Substituting the (A4.63)' term for α into (A4.62)', we obtain the optimal attack angle

$$\alpha_{opt} = \sqrt{\frac{C_{DW}}{\varepsilon}} \ . \tag{A4.66}$$

This is the angle of optimal efficiency, but C_{DW} is the wing drag coefficient **only** when $\alpha = 0$ (not the full vehicle as in conventional aerodynamics). The coefficient of flight efficiency

$$k = \frac{g}{D/m} \quad or \quad k_{max} = \frac{g}{\min(D/m)} \ . \tag{A4.67}$$

b) Hypersonic speed. The equations of wing lift force and wing air drag for hypersonic speed are as follows:

$$Y = \varsigma \alpha q S = m\left(g - \frac{V^2}{R} \right), \quad or \quad \alpha = \frac{p(g - V^2/R)}{\varsigma q}, \quad \overline{D} = \left(C_{DW} + \varepsilon \alpha^2 \right) q S, \quad q = \frac{\rho a V}{2} \ . \tag{A4.68}$$

Substituting α from (A4.68) into $\overline{D}$, we obtain

$$D = \left[C_{DW} + \varepsilon \left(\frac{m(g - V^2/R)}{\varsigma q S} \right)^2 \right] q S \ . \tag{A4.68'}$$

Substituting the wing load $p = m/S$ into (A4.68)', we obtain

$$\frac{D}{m} = \left[C_{DW} \frac{1}{p} + \varepsilon \left(\frac{g - V^2/R}{\xi q} \right)^2 p \right] q \ . \tag{A4.69}$$

To find the minimum the air drag D for p, we take the derivatives and set them equal to zero, then we obtain

$$p_{opt} = \frac{\varsigma q}{(g - V^2/R)} \sqrt{\frac{C_{DW}}{\varepsilon}} \ . \tag{A4.70}$$

Substituting (A4.70) into (A4.69), we find the minimum wing drag

$$\min\left(\frac{D}{m}\right)_w = \frac{2}{\varsigma}\left(g - \frac{V^2}{R}\right)\sqrt{\varepsilon C_{DW}} .$$

The sum of the minimum vehicle drag plus body drag is

$$\min\left(\frac{D}{m}\right) = \frac{2}{\varsigma}\left(g - \frac{V^2}{R}\right)\sqrt{\varepsilon C_{DW}} + C_{Db}\frac{q}{p_b}, \quad q = \frac{\rho a V}{2}, \quad p_b = \frac{m}{S_b} . \tag{A4.71}$$

Substituting (A4.70) into the term for α in (A4.65), we find the optimal attack angle of a vehicle without a body

$$\alpha_{opt} = \sqrt{C_{DW}/\varepsilon} . \tag{A4.72}$$

The coefficient of flight efficiency $k = Y/D$ is

$$k = \frac{g - V^2/R}{D/m}, \quad k_{max} = \frac{g - V^2/R}{\min(D/m)} .$$

For hypersonic speed the coefficients are approximately

$$\varsigma = 4, \quad \varepsilon = 2, \quad C_{DW} = 4c^2, \quad C_{Db} = 2c_1^2, \quad C_L = \varsigma\alpha, \quad C_{Do} = C_{DW} + C_{Db} . \tag{A4.73}$$

In numerical computation the angle θ can be found from (A4.25) as $\theta = \Delta h/\Delta R_g$.
For the rocket engine or gliding flight we find the following relation: when S is optimum (variable), the partial derivatives from (A4.71) are

$$D_V' = -\frac{4V}{\varsigma R}\sqrt{\varepsilon C_{DW}} + C_{Db}\frac{\rho a}{2p_b}, \quad D_h' = -\frac{C_{Db}\rho a V}{2b_2 p_b} .$$

Substituting these into (A4.37), we find the relationship between speed, altitude, and optimal wing load for a hypersonic vehicle with a rocket engine and **variable** optimal wing:

$$\rho = \frac{8gp_b V\sqrt{\varepsilon C_{DW}}}{\varsigma a C_{Db} R(g + V^2/b_2)}, \quad h = 11000 + b_2\ln\frac{a_2}{\rho} . \tag{A4.74}$$

For $\zeta = 4$, $\varepsilon = 2$ equation (A4.73)' has the form

$$\rho = \frac{2gp_b V\sqrt{2C_{DW}}}{C_{Db} a R(g + V^2/b_2)}, \quad h = 11000 + b_2\ln\frac{a_2}{\rho}, \tag{A4.74'}$$

Results of computation using (A4.74)' for $\zeta = 4$, $\varepsilon = 2$, $a_2 = 0.365$, $b_2 = 6997$ and different p_b are presented in Fig. A4.7 (dashed lines). As you see, the variable area wing saves kinetic energy, because its curve is located over an invariable (fixed) wing. This is advantageous only at orbital speed (7.9 km/s) because no lift force is necessary.

Estimation of flight range

Air and space vehicles without thrust

The aircraft range can be found from equation (A4.26)

$$R_a = \int_{V_1}^{V_2}\frac{mVdV}{T - D - mg\theta}, \quad V_1 > V_2 \quad or \quad R_a = \int_{V_2}^{V_1}\frac{VdV}{D/m + g\theta}, \quad if \quad T = 0. \tag{A4.75}$$

Consider a missile with the *optimal variable wing* in a descent trajectory with thrust $T = 0$.
a) Make the simplest estimation using equations for kinetic energy from classical mechanics. Separate the flight into two stages: hypersonic and subsonic. If we have the ratio of vehicle efficiency

$k_1 = C_L / C_D$, $k_2 = C_L / C_D$, where k_1, k_2 are the ratios of flight efficiency for the hypersonic and subsonic stages respectively, we find the following equations for a range in each region:

$$\frac{m}{2}\left(V_1^2 - V_2^2\right) = \frac{m(g - V^2 / R)}{k_1}R_1, \quad R_1 = \frac{k_1\left(V_1^2 - V_2^2\right)}{2(g - V^2 / R)}, \quad R_2 = k_2 h, \quad R_a = R_1 + R_2,$$

Or more exactly

$$d\left(\frac{mV^2}{2}\right) = \frac{m(g - V^2 / R)}{k_1}dR_1, \quad R_1 = -\frac{k_1 R}{2}\ln\left(\frac{g - V_2^2 / R}{g - V_1^2 / R}\right), \tag{A4.76}$$

where R_1 is the hypersonic part of the range, R_2 is the subsonic part of the range, V_1 is the initial (maximum) vehicle hypersonic speed, V_2 is a final hypersonic speed, and h is the altitude at the initial stage of the subsonic part of the trajectory.

b) To be more precise. Assume in (A4.75) $\rho = const$ (taking average air density).

1. For the **hypersonic** part of the trajectory: substitute (A4.71) into (A4.76). We then have

$$R_{1H} = \int_{V_1}^{V_2} \frac{VdV}{aV^2 + bV + c}, \quad or \quad R_{1H} = \int_{V_1}^{V_2} \frac{VdV}{X}, \quad where \quad X = aV^2 + bV + c,$$

$$a = \frac{2\sqrt{\varepsilon C_{DW}}}{\xi R}, \quad b = -C_{Db}\frac{\rho a}{2p_b}, \quad c = \frac{T}{m} - \frac{2g}{\varsigma} - g\theta, \quad \Delta = 4ac - b^2, \tag{A4.77}$$

$$R_{1H} = \left[\frac{1}{2a}\ln X - \frac{b}{2a}\int\frac{dV}{X}\right]_{V_1}^{V_2}, \quad \int\frac{dV}{X} = \frac{2}{\sqrt{\Delta}}\arg\tan\frac{2aV + b}{\sqrt{\Delta}} \quad for \quad \Delta \geq 0,$$

$$\int\frac{dV}{X} = -\frac{2}{\sqrt{-\Delta}}\arg\tanh\frac{2aV + b}{\sqrt{-\Delta}} = \frac{1}{\sqrt{-\Delta}}\ln\frac{2aV + b - \sqrt{-\Delta}}{2aV + b + \sqrt{-\Delta}} \quad for \quad \Delta \leq 0.$$

2. For the **subsonic** part of the trajectory: substitute (A4.65) into (A4.75). We then have

$$R_{1S} = -\frac{1}{2C_2}\ln\left|\frac{C_1 - C_2 V_2^2}{C_1 - C_2 V_1^2}\right|, \tag{A4.78}$$

where the values for C_1, C_2 are

$$C_1 = \frac{T}{m} - g\left(\frac{2\sqrt{\varepsilon C_{DW}}}{a\varsigma} + \theta\right), \quad C_2 = C_{Db}\frac{\rho}{2p_b}. \tag{A4.79}$$

The trajectory (without the rocket part of the trajectory) is

$$R_1 = R_{1H} + R_{1S} \quad or \quad R_g = R_{1H} + R_{1S} + R_2. \tag{A4.80}$$

where $R_2 = k_2 h$ computed for altitude h at the end of the kinetic part of the subsonic trajectory.

3. The **ballistic** trajectory of a wingless missile without atmosphere drag is

$$h = \frac{gt^2}{2}, \quad t = \sqrt{\frac{2h}{g}}, \quad R_b = V_1 t = V_1\sqrt{\frac{2h}{g}}, \quad V_i = \sqrt{V_1^2 + V_y^2}, \quad V_y^2 = 2h(g - V^2 / R), \tag{A4.81}$$

where h is the initial altitude, V_1 is the initial horizontal speed of the wingless missile at altitude h, V_y is initial (shot) vertical speed at $h = 0$, V_i is the full initial (shot) speed at $h = 0$.

For the hypersonic interval $5 < V < 7.5$ km/s, we can use the more exact equation

$$R_b = V_1\sqrt{\frac{2h}{(g - V_1^2 / R)}}, \tag{A4.82}$$

where $R = 6378$ km is the radius of Earth. The full range of a ballistic rocket plus the range of a winged missile is

$$R_f = R_b + R_a + R_g, \tag{A4.83}$$

where $R_g = kh$ is the vehicles gliding range from the final altitude h_2 (see Fig. A4.11) with aerodynamic efficiency k.

The classical method finding of the optimal shot ballistic range for spherical Earth without atmosphere is

$$R_b = 2R\beta_{opt}, \quad \tan\beta_{opt} = \frac{v_A}{2\sqrt{1-v_A}}, \quad v_A = \frac{V_A^2}{V_c^2}, \tag{A4.84}$$

where β_{opt} is the optimal shot angle, V_A is the shot projectile speed, and V_c is an orbital speed for a circular orbit at a given altitude.

4. **Cannon projectile**. We divide the distance into three sub-distances: 1) $1.2M < M$, 2) $0.9M < M < 1.2M$, 3) $0 < M < 0.9M$. The range of the wing cannon projectile may be estimated using the equation

$$R = \frac{k_1}{2g}(V_1^2 - V_2^2) + \frac{k_2}{2g}(V_2^2 - V_3^2) + \frac{k_3}{2g}(V_3^2 - V_0^2), \quad where \quad 0 < V_0 < V_3 < V_2 < V_1, \tag{A4.85}$$

where k_1, k_2, k_3 are the average aerodynamic efficiencies for sub-distances 1, 2, 3 respectively. Conventionally, these coefficients have the following values: subsonic $k_3 = 8$–15, near sonic $k_2 = 2$–3, supersonic and hypersonic $k_1 = 4$–9. If $V > 600$ m/s, the first term in (A4.85) has the greatest value and we can use the more simple equation for range estimation:

$$R = \frac{k_1}{2g}V_1^2. \tag{A4.84'}$$

At the top of its trajectory, a modern projectile can have an additional impulse from small rocket engines. Their weight is 10–15% of the full mass of the projectile and increases the maximum range by 7–14 km. In this case we must substitute $V = V_1 + dV$ into (A4.84)', where dV is the additional impulse (150–270 m/s).

Subsonic aircraft with thrust. Horizontal flight

The optimal climb and descent of a subsonic aircraft with a constant mass and fixed wing is described by equations (A4.50) and (A4.47). Any given point in a climb curve may be used for horizontal flight (with different efficiency). We consider in more detail the horizontal flight when the aircraft mass decreases because the fuel is spent. This consumption may reach 40% of the initial aircraft mass. The optimal horizontal flight range may be computed in the following way:

$$dR = Vdt, \quad dt = \frac{dm}{c_sT} = \frac{gdm}{c_sD}, \quad dR = \frac{gV}{c_sD(m)}dm, \quad R = \frac{gV}{c_s}\int_{m_k}^{m}\frac{dm}{D(m)}, \tag{A4.86}$$

where m is fuel mass, c_s is fuel consumption, kg/s/ kg thrust.

a) For a **fixed wing**, we have (from (A4.44))

$$D = C_{Do}qS + \frac{\varepsilon}{qS}\left(\frac{g}{\varsigma}\right)^2 m^2, \quad where \quad C_{Do} = C_{Dw} + C_{Db}\left(\frac{S_b}{S}\right), \quad q = \frac{\rho V^2}{2}. \tag{A.87}$$

Substituting (A4.87) into (A4.86), we obtain

$$R = \frac{gV}{c_s\sqrt{C_1 C_2}}\arg\tan\frac{\sqrt{C_1/C_2}\,(m-m_k)}{1+(C_1/C_2)mm_k}, \quad where \quad C_1 = \frac{\varepsilon}{qS}\left(\frac{g}{\varsigma}\right)^2, \quad C_2 = C_{Do}qS. \quad (A4.88)$$

b) For a **variable wing** we have (from (A4.65)

$$R = \frac{gV}{c_s C_1}\ln\frac{C_1 m - C_2}{C_1 m_k - C_2}, \quad where \quad C_1 = 2\frac{g}{\varsigma}\sqrt{\varepsilon C_{DW}}, \quad C_2 = C_{Db}qS_b, \quad \rho = \rho_0 e^{-h/b_1}. \quad (A4.89)$$

Results of the computation are presented in Fig. A4.8. The aircraft have the following parameters: C_{DW} = 0.02; C_{Db} = 0.08; b_1 = 9086; S = 120 m²; m = 100 tons, m_k = 80 tons, c_s = 0.00019 kg/s/kg thrust; wing ratio λ = 10.

As you see, the specific fuel consumption does not depend on speed and altitude, a good aircraft design reaches the maximum range only at one point, in one flight regime: when the aircraft flies at the maximum speed possible for the critical Mach number, at the maximum altitude possible for that engine. The deviation from this point decreases in the range in 5–10–15 percent or more. The variable wing increases efficiency of the other regime, which that approximately reduces the losses by a half.

The coefficient of flight efficiency may be computed using equation $k = g/(D/m)$, where the values

$$\frac{D}{m} = C_{DW}\frac{q}{p} + \frac{\varepsilon p}{q}\left(\frac{g}{\varsigma}\right)^2 + C_{Db}\frac{q}{p_b}, \quad \left(\frac{D}{m}\right)_1 = 2\frac{g}{\varsigma}\sqrt{\varepsilon C_{DW}} + C_{Db}\frac{q}{p_b}, \quad (A4.90)$$

apply for fixed and variable wings respectively. Results of computation are presented in Fig. A4.9. The curve of the variable wing is the round curve of the fixed wing.
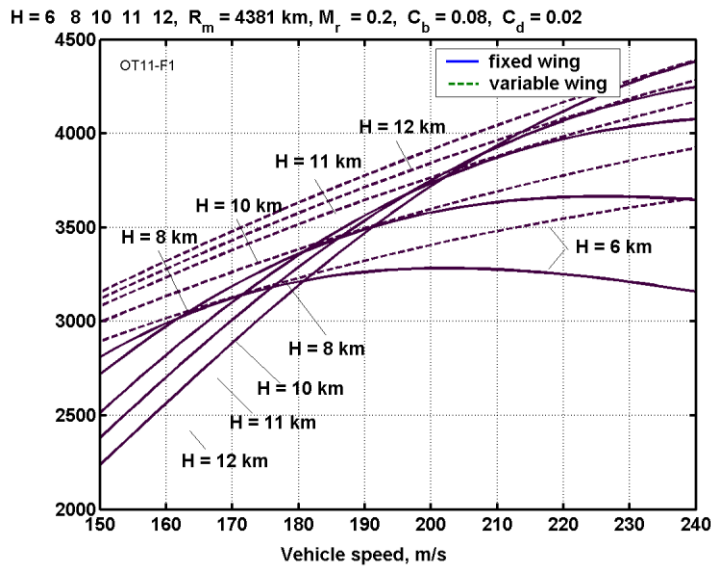

Fig. A4.8. Aircraft range for altitude H = 6, 8, 10, 11, 12 km; maximum range R_m = 4361 km; relative fuel mass M_r = 0.2; body drag coefficient C_b = 0.08; wing drag coefficient C_d = 0.02.
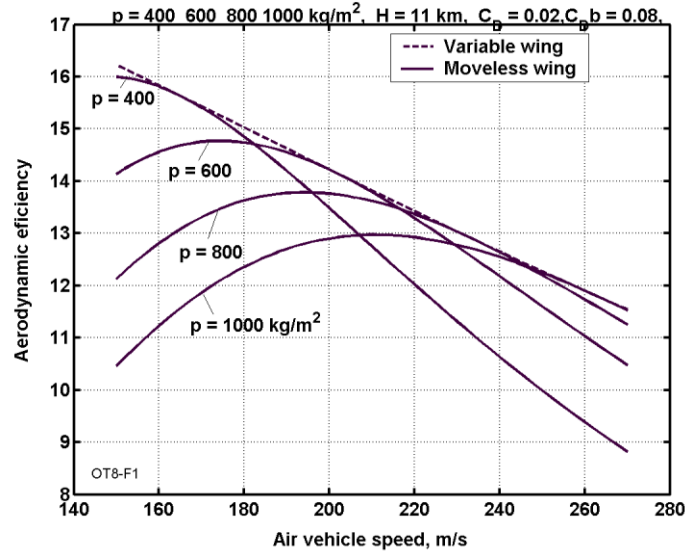
Fig. A4.9. Aerodynamic efficiency of non-variable and variable wings for wing load $p = 400, 600,$ 800, 1000 kg/m², wing drag $C_D = 0.02$, body drag $C_{Db} = 0.08$, wing ratio 10.

Optimal engine control for constant flight pass angle

Let us to consider equations (A4.1) – (A4.5) for a constant angle of trajectory, $\theta = $ const. Substituting $\theta = $ constant, thrust $T = V_e\beta$, and a new independent variable $s = Vt$ (where s is the length of the trajectory) into the equation system (A4.1) – (A4.5). We obtain the following equations

$$\frac{dL}{ds} = \cos\theta \quad ,$$

$$\frac{dh}{ds} = \sin\theta \quad ,$$

$$\frac{dV}{ds} = \frac{V_e(h,V)\beta - \overline{D}(\alpha,V,h)}{mV} - \frac{g}{V}\sin\theta \, , \qquad\qquad (A4.91) - (A4.96)$$

$$\frac{dm}{ds} = -\frac{1}{V}\beta \quad ,$$

$$Y(\alpha,V,h) - gm\cos\theta + \frac{mV^2}{R} + 2mV\omega_E\cos\varphi_E = 0 \, ,$$

$$0 \leq \beta \leq \beta_{max} \quad .$$

Equation (A4.95) is used to substitute for α in equation (A4.93) and for a change of air drag
$$\overline{D}(\alpha,V,h) = D(V, h). \qquad\qquad (A4.97)$$

We find a non-linear system with a linear fuel control β. This means the system can have a singular solution.

Solution

Consider the maximum range for vehicles described by equation (A4.91) – (A4.96).
Let us write the Hamiltonian H

$$H = \cos\theta + \lambda_1 \sin\theta + \lambda_2\left[\frac{V_e(h,V)\beta - D(V,h)}{mV} - \frac{g}{V}\sin\theta\right] - \lambda_3 \frac{1}{V}\beta \, , \qquad\qquad (A4.98)$$

where $\lambda_1(s), \lambda_2(s), \lambda_3(s)$ are unknown multipliers. Application of conventional methods gives

$$\dot{\lambda}_2 = -\frac{\partial H}{\partial V} = -\lambda_2 \left[\left(-\frac{1}{V^2} \right) \left(\frac{V_e \beta - D(V,h)}{m} - g \sin \theta \right) - \frac{D'_V}{mV} \right] - \lambda_3 \frac{1}{V^2} \beta \quad,$$

$$\dot{\lambda}_3 = -\frac{\partial H}{\partial m} = \lambda_2 \frac{V_e \beta - D}{m^2 V}, \qquad\qquad (A4.99) - (A4.101)$$

$$\beta = \max_\beta H = \beta_{max} sign \left[\lambda_2 V_e - \lambda_3 m \right] \quad.$$

Where D'_V is the first partial derivate of D by V.

The last equation shows that the fuel control β can have only two values, $\pm\beta_{max}$. We consider the singular case when

$$A = \lambda_2 V_e - \lambda_3 m \equiv 0. \qquad\qquad (A4.102)$$

This equation has two unknown variables, λ_2 and λ_3, and does not contain information about fuel control β.

The first two equations (A4.91) – (A4.92) do not depend on variabls and can be integrated

$$L = s \cos\theta, \qquad\qquad (A4.103)$$
$$H = s \sin\theta. \qquad\qquad (A4.104)$$

In accordance with the References[2] let us differentiate equation (A4.102) by the independent variable s. After substitution into equations (A4.93) – (A4.95), (A4.97), (A4.99), (A4.100), (A4.102), and (A4.104) we obtain the relation for $\lambda_2 \neq 0$, $\lambda_3 \neq 0$:

$$\dot{A} = VD - mVD'_m + V_e(-D - mg \sin \theta + VD'_V) - VV'_{e,V}(D - mg \sin \theta) + mV^2 V'_{e,s} = 0. \qquad (A4.105)$$

This equation also does not contain β, however it does contain an important relation between variables m, h and V, on an optimal trajectory. This is a 3-dimentional surface. If we know

$$D = D(h,V), \qquad\qquad (A4.106)$$
$$V_e = V_e(h,V), \qquad\qquad (A4.107)$$

The mass of our apparatus m, and its altitude h, we can find the optimal flight speed. This means we can calculate the necessary thrust and the fuel consumption for every point m, h, V (Fig. A4.10).

If we want to find an equation for the fuel control β, we continue to differentiate equation (A4.105) to find the independent variable s and substitute in equations (A4.91) – (A4.104). If we calculate the relation for β, if $\lambda_2 \neq 0$, $\lambda_3 \neq 0$, V_e = const, then

$$\beta = \frac{\dot{A}'_V (D + mg \sin \theta) - mV\dot{A}'_s}{V_e \dot{A}'_V - m\dot{A}'_m}, \qquad\qquad (A4.108)$$

where

$$\dot{A}'_V = \frac{\partial}{\partial V} \left(\frac{dA}{ds} \right), \quad \dot{A}'_s = \frac{\partial}{\partial s} \left(\frac{dA}{ds} \right). \qquad\qquad (A4.109)$$

The necessary condition of the optimal trajectory as it is shown in the References[2–8] (see for example, equation (4.2)[4]) is

$$-(-1)^k \frac{\partial}{\partial \theta} \left[\frac{d^{2k}}{ds^{2k}} \left(\frac{\partial H}{\partial s} \right) \right] \geq 0. \qquad\qquad (A4.110)$$

where $k = 1$.

If the flight is horizontal ($\theta = 0$), the expression (A4.108) is very simply

$$\beta = \frac{D}{V_e} . \qquad\qquad (A4.111)$$

This means the thrust equals the drag, a fact that is well known in aerodynamic science.
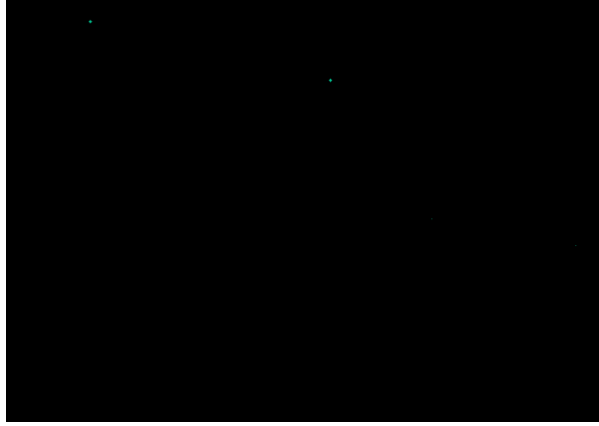
Fig. A4.10. Optimal fuel consumption of flight vehicles.

To obtain the specific equations for different forms of drag and thrust, we must take formulas (or graphs) for subsonic, transonic, supersonic and hypersonic speed for thrust and substitute them into the equations (A4.105) and (A4.108).

Simultaneous optimization of the path angle and fuel consumption

Consider the case where the path angle and the fuel consumption are simultaneously optimized.
In this case the general equations (A4.1) – (A4.5) have the form:

$$\frac{dL}{ds} = 1 ,$$

$$\frac{dh}{ds} = \theta ,$$

$$\frac{dV}{ds} = \frac{V_e(h,V)\beta - D(m,V,h)}{mV} - \frac{g}{V}\theta ,$$

(A4.112) – (A4.116)

$$\frac{dm}{ds} = -\frac{1}{V}\beta ,$$

$$Y(\alpha, V.h) = mg + \frac{mV^2}{R} + 2mV\omega_E \cos\varphi_E .$$

Let us write the Hamiltonian

$$H = 1 + \lambda_1\theta + \lambda_2\left(\frac{V_e(h,V)\beta - D(m,V,h)}{mV} - \frac{g}{V}\theta\right) - \lambda_3\frac{1}{V}\beta .$$

(A4.117)

The necessary conditions of optima give

$$A = \frac{\partial H}{\partial \theta} = V\lambda_1 - g\lambda_2 = 0 ,$$

(A4.118) – (A4.119)

$$B = \frac{\partial H}{\partial \beta} = V_e\lambda_2 - m\lambda_3 = 0 ,$$

The lambda equations are

$$\dot{\lambda}_1 = -\frac{\partial H}{\partial h} = -\lambda_2 \frac{V'_{e,h}\beta - D'_h}{mV} \ ,$$

$$\dot{\lambda}_2 = -\frac{\partial H}{\partial V} = -\lambda_2 \left[\frac{(V'_{e,V}\beta - D'_V)V - (V_e\beta - D)}{mV^2} + \frac{g}{V^2}\theta \right] - \lambda_3 \frac{1}{V^2}\beta \ , \quad (A4.120)-(A4.122)$$

$$\dot{\lambda}_3 = -\frac{\partial H}{\partial m} = \lambda_2 \frac{V_e\beta - D + mD'_m}{m^2 V} \ .$$

If we differentiate A (A4.118), from $dA/ds = 0$, we find the optimal fuel consumption

$$\beta = \frac{gVD'_V - V^2 D'_h}{g(V_e + V'_{e,V}V) - V'_{e,h}V^2} \ . \quad (A4.123)$$

Then we differentiate B (A4.119), from $dB/ds = 0$ we find the optimal path angle

$$\theta = \frac{V'_{e,V}D - V_e D'_V - V_e D/V - D + mD'_m}{m(g + V'_{e,h}V - V'_{e,V}g)} \ . \quad (A4.124)$$

We have used the conventional forms for the partial derivatives in (A4.120)–(A4.124) as in the earlier sections of the chapter (see for example (A4.51)).

If we know from analytical formulas or graphical functions Ve, D, Y we can find the optimal trajectory of the air vehicle.

In the general case, this trajectory includes four parts:
1. Moving between limitations θ and β.
2. Moving between one limitation θ or β and one optimal control β or θ.
3. Moving simultaneously with both optimal controls θ and β.
4. Moving at a given point along one limitation and/or both limitations.

Application to aircraft, rocket missiles, and cannon projectiles

A) Application to rocket vehicles and missiles.

Let us apply the previous results to typical current middle- and long-distance rockets with warheads. We will show: if the warhead has wings and uses the optimal trajectory, the range of the warhead (or its useful load) is increased dramatically in most cases. We will compute the optimal trajectories for a rocket-launched warhead at a particular altitude (20–60 km) and speed (1–7.5 km/s). Point B is located on the curve (A4.58) for a fixed wing and on curve (A4.73)' for a variable wing (Fig. A4.11). Further, the winged warhead flies (descends) along the optimal trajectory BD (Fig. A4.58) according to equations (A4.58) (fixed wing) or equations (A4.73)' (variable wing) respectively. When the speed is reduced by a small amount (for example, 1 km/s) (point D in Fig. A4.11), the winged warhead glides (distance DE in Fig. A4.11).
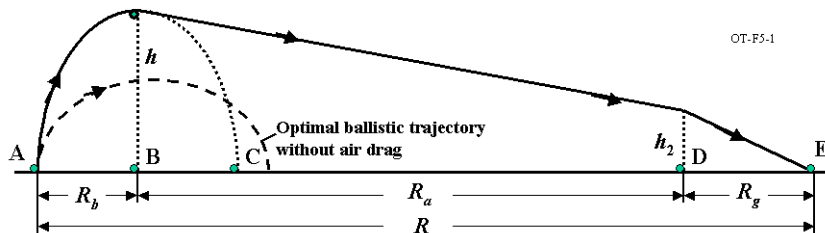

Fig. A4.11. Trajectory of flying vehicles.

The following equations are used for computation:

1. ***The optimal trajectory for a fixed wing space vehicle.***
   a) Equation (A4.58) is used to calculate $h = h(V)$ to find the optimal trajectory of a warhead with a non- variable fixed wing in the speed interval $1 < V < 7.5$ km/s. The result is presented in Fig. A4.7.
   b) Equation (A4.54) gives the magnitude (D/m).
   c) The equation (A4.75) in the form

   $$\Delta R_a = \frac{V\Delta V}{(D/m)+g\theta}, \quad R_a = \Sigma \Delta R_a, \quad \theta = -\frac{\Delta h}{\Delta R_a}, \quad k = \frac{g - V_0^2 / R}{D/m}, \quad R_g = h_0 k, \qquad (A4.125)$$

   is used for computation in the intervals R_a, R_g (Fig. A4.11). Here R_g is the range of a gliding vehicle.

   d) Equation (A4.75) is used to calculate R_b in the launch interval AB (Fig. A4.11).
   e) The full range, R, of a warhead with a fixed wing and the full ballistic warhead range, R_w, are
   $$R = R_b + R_a + R_g, \quad R_w = 2R_b. \qquad (A4.126)$$

   f) Equation (A4.84) is used to calculate the optimal **ballistic** trajectory of a shot without air drag (a vehicle **without** wings). The range of this trajectory, as it is known, may be significantly more than the range in the atmosphere.
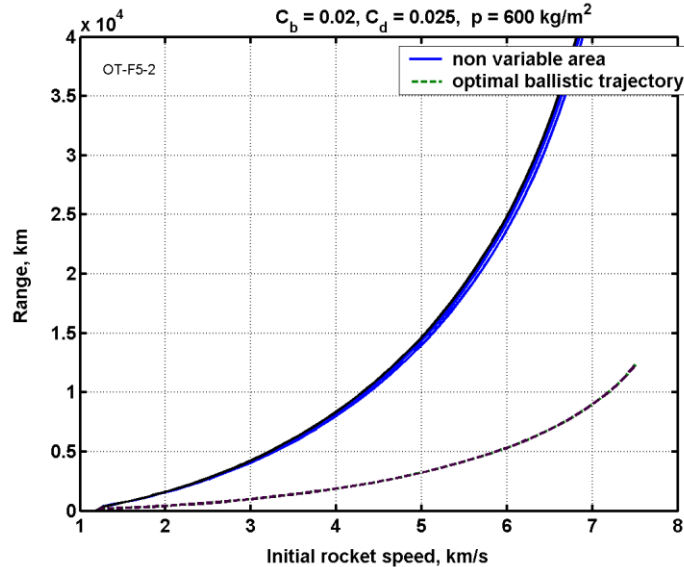   g)

Fig. A4.12. Range of NON-VARIABLE wing vehicle for body drag coefficient $C_b = 0.02$, wing drag coefficient $C_d = 0.025$, wing load $p = 600$ kg/m².

The results are presented in Fig. A4.12. Computation of the relative range (for different p_b) using the formula

$$R_r = \frac{R_f}{R_b} \qquad (A4.127)$$

is presented in Fig. A4.12. The optimal range of the winged vehicle is approximately 4.5 times that of the ideal ballistic rocket computed without air drag. In the atmosphere this difference will be significantly more.
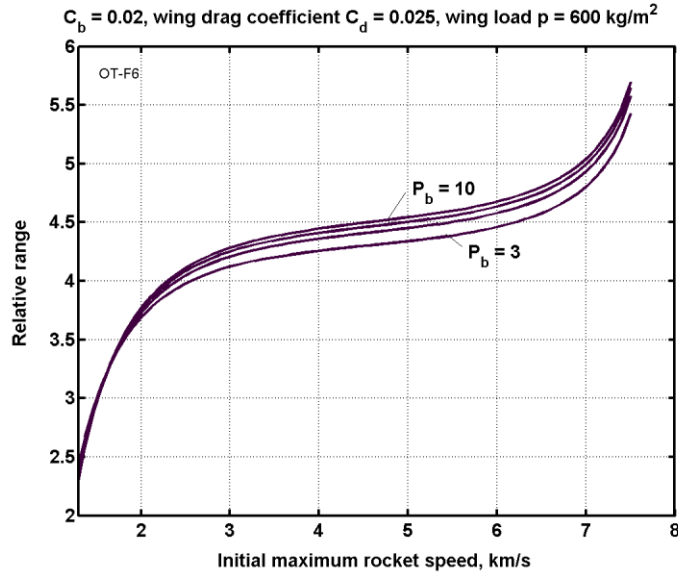
Fig. A4.12. The relative range of a **non**-variable wing vehicle for the body drag coefficient $C_b = 0.02$, wing drag coefficient $C_d = 0.025$, wing load $p = 600$ kg/m², body load $P_b = 3–10$ ton/m².

2. *Rockets, missiles and space vehicles with* variable *wings*

The computation is the same. For computing ρ, h, D/m we can use equations (A4.73)' and (A4.71) respectively. The results for different body loads are presented in Fig. A4.7. The optimal trajectories of vehicles with variable wing areas have less slope. This means the vehicle loses less energy when it moves. It travels above the optimal trajectory of a vehicle with fixed wings, which means it needs a lot more time (10–20) and more wing area than a fixed wing space vehicle (Fig. A4.14). The computation of the optimal variable wing area is presented in Fig. A4.15. The relative range (equation (A4.127)) is presented in Fig. A4.16.
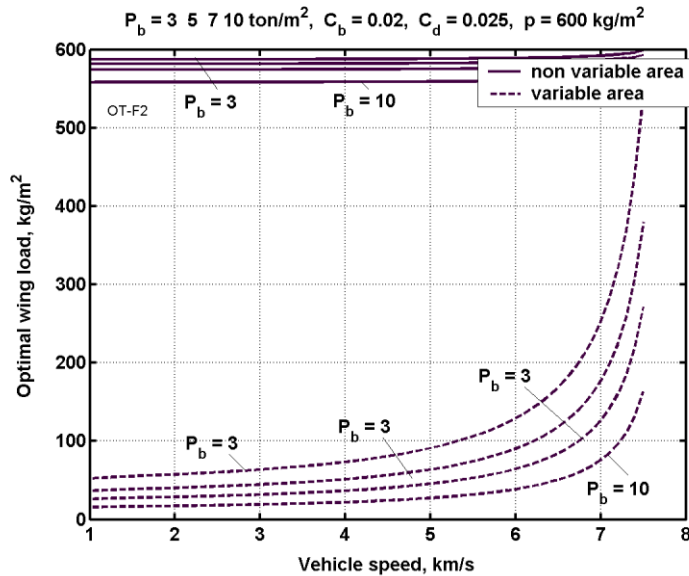

Fig. A4.14. Optimal wing load versus speed for specific body load $P_b = 3, 5, 7, 10$ ton/m², body drag coefficient $C_b = 0.02$, wing drag coefficient $C_d = 0.025$, wing load $p = 600$ kg/m².
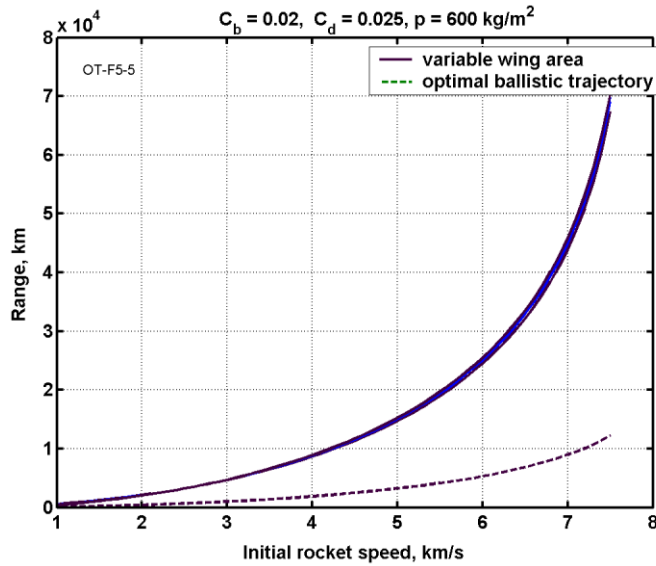
Fig. A4.15. Range of a variable wing vehicle for the body drag coefficient $C_b = 0.02$, the wing drag coefficient $C_d = 0.025$, the wing load $p = 600$ kg/m^2.
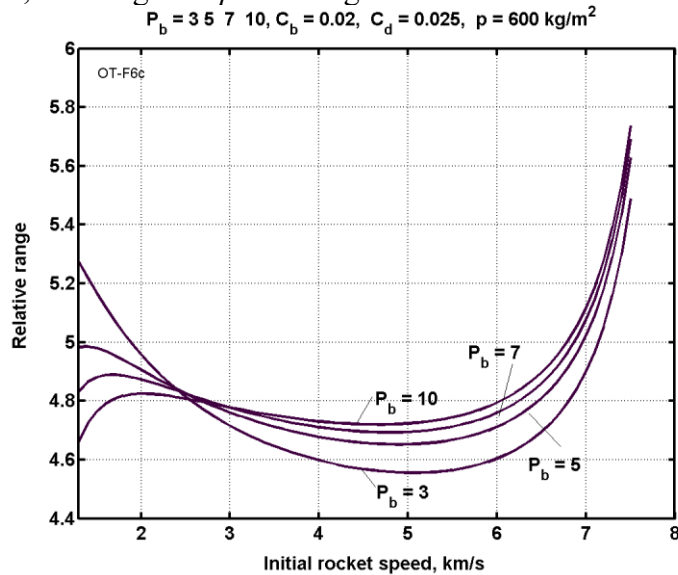

Fig. A4.16. Relative range of variable wing vehicle for the body drag coefficient $C_b = 0.02$, the wing drag coefficient $C_d = 0.025$, the wing load $p = 600$ kg/m^2, the body load $P_b = 3$–10 ton/m^2.

The aerodynamic efficiency of vehicles with fixed (for different p_b bodies) and optimal variable wings computed using equations (A4.125) and (A4.67) respectively is presented in Fig. A4.12. The difference between vehicles with fixed and variable wings reaches 0.2–0.6 . The slope of the trajectory to horizontal is small (Fig. A4.18).

The range of the **fixed** wing vehicle computed using equation (A4.125) is presented in Fig. A4.12. The range of the **variable** wing vehicle computed using equation (A4.126) is presented in Fig. A4.15. The curve is practically the same (see Figs. A4.12 and A4.15).

3. ***Increasing the rocket payload for the same range.*** If we do not need to increase the range, the winged vehicle can be used to increase the payload, or to save rocket fuel. We can change the mass of the fuel or the payload. The additional payload may be estimated by the following equation

$$\mu = 1 - e^{-\frac{\Delta V}{V_e}}, \tag{A4.128}$$

where $\mu = m/m_b$ is relative mass (the ratio of rocket mass of the winged vehicle to the ballistic rocket), $\Delta V = V_b - V$ is the difference between the optimal ballistic rocket speed (equation (A4.84)) and the rocket with a winged vehicle (equation (A4.126)) for given range (see Fig. A4.12). Results of computation are presented in Fig. A4.19. The mass of the rocket with a winged vehicle may be only 20–35% of the optimal ballistic rocket flown without air drag.

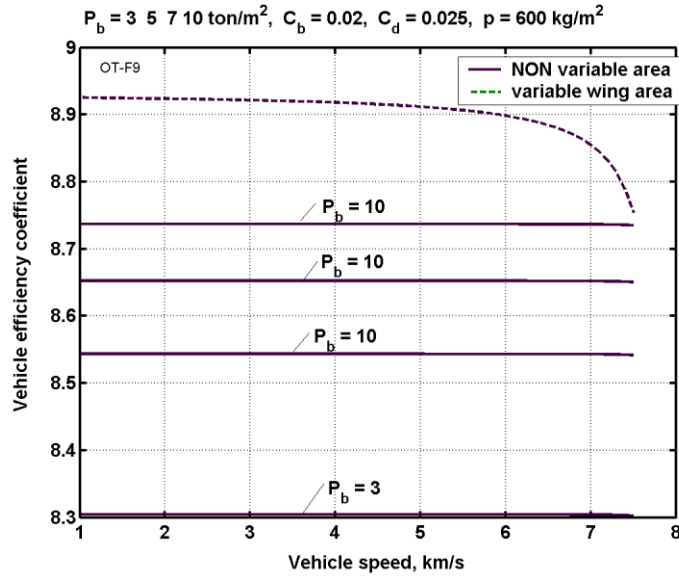**Fig. A4.17**. Vehicle efficiency coefficient versus speed for specific body load $P_b = 3, 5, 7, 10$ ton/m², body drag coefficient $C_b = 0.02$, wing drag coefficient $C_d = 0.025$, wing load $p = 600$ kg/m².
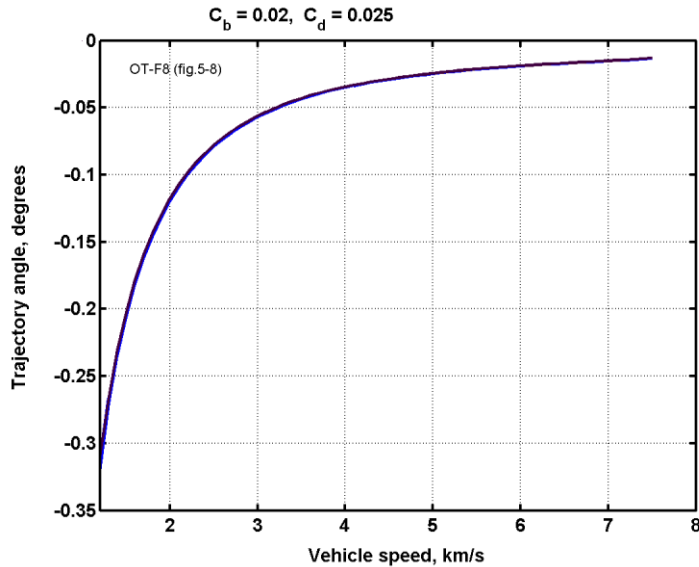

Fig. A4.18. Trajectory angle versus speed for body drag coefficient $C_b = 0.02$, wing drag coefficient $C_d = 0.025$.
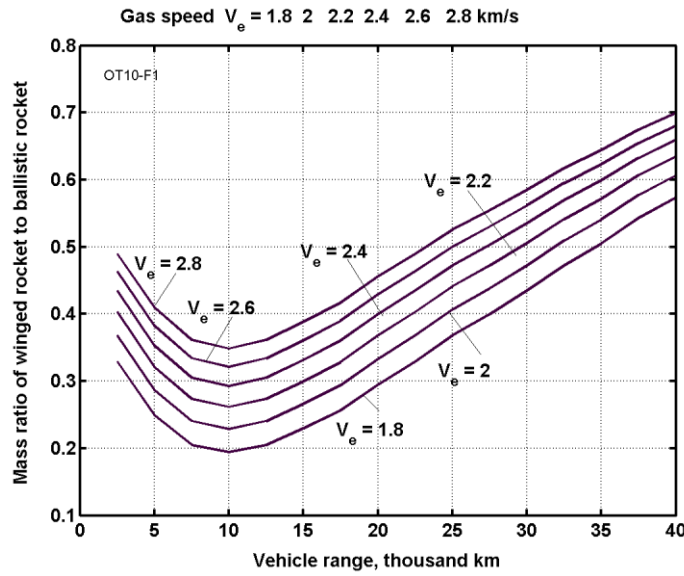
Fig. A4.19. Ratio of mass of winged rocket to ballistic rocket for specific engine run-out gas speed V_e = 1.8, 2, 2.2, 2.4, 2.6 and 2.8 km/s.

Conclusion: The winged air-space vehicle has a range that is greater by a minimum of 4.5–5 times than an optimal shot ballistic space vehicle. The variable wing improves the aerodynamic efficiency by 3–10% and also improves the range. An optimal variable wing requires a large wing area. If you do not need to increase the range, you may instead increase payload.

B) Application to cannon wing projectiles

Properties of a typical current cannons are shown in Table A4.1.

Table A4.1. Properties of current typical Cannons.

Name	caliber, mm	Nozzle speed, m/s	Mass of projectile, kg	Range, km	RAP, km
M107	175	509–912	67	15–33	
SD-203	203	960	110	37.5	
2S19	155	810	43.6	24.7	
2S1	122	690–740	21.6	-	
S-23	180	-	-	30.4	43.8
2A36	152	-	-	17.1	24
D-20	152	600–670	43.5–48.8	20	

Issue: Jane's

The computations using equation (A4.84)' for different k and RAP with $dV = 270$ m/s are presented in Figs. A4.20 and A4.21.
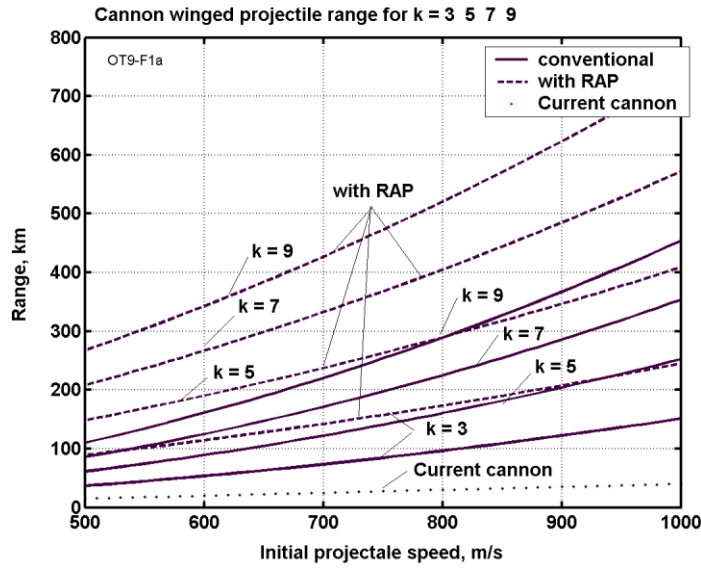
Fig. A4.20. Cannon winged projectile range for average aerodynamic efficiency k = 3, 5, 7, 9.
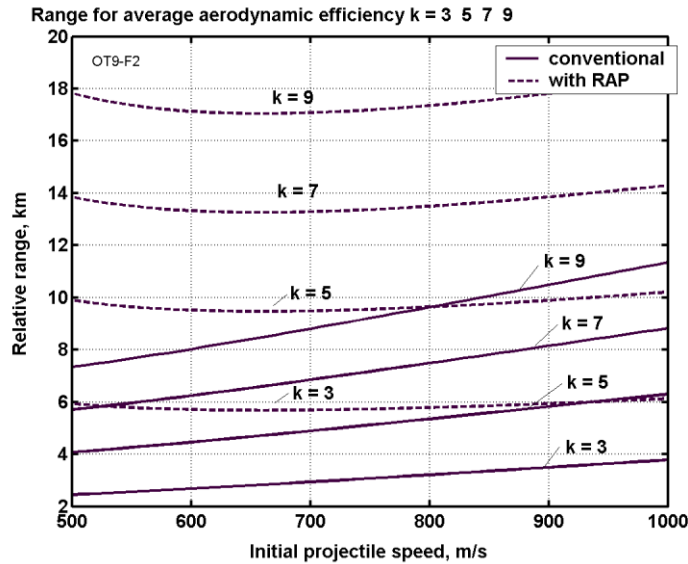

Fig. A4.21. Cannon winged projectile relative range for average aerodynamic efficiency k = 3, 5, 7, 9.

Conclusion. As you see (Figs. A4.20, A4.21), the winged projectile increase its range 3–9 times (from 35 up to 360 km, k = 9). The projectile with RAP increases its range 5–14 (from 40 up to 620 km, k = 9) . Winged shells have another important advantage: they do not need to rotate. We can use a barrel with a smooth internal channel. This allows for an increase in projectile nozzle speed of up to 2 km/s and in shell range of up to 1000 km (k = 5).

C) Application to current aircraft.

We can use equations (A4.88) and (A4.89) for computations for typical passenger airplanes (Figs. A4.22, A4.23, A4.24, and A4.8), where all values are divided by the maximum range R_m = 4381 km (for a fuel mass that is 20% of to vehicle mass) at a speed of V = 240 m/s, and altitude H = 12 km. The speed is limited by the critical Mach number ($V < M$ = 0.82), and the altitude is limited by the engine trust, when engine stability is such that it works in a cruise regime. Fig. A4.22 shows the typical long-range trajectory of aircraft.

Conclusion: The best flight regime for a given air vehicle (closed to Boeing 737) is altitude $H = 12$ km, speed $V = 240$ m/s, specific fuel consumption $Cs = 0.00019$ kg fuel/s/kg thrust. Any deviation from this flight regime significantly reduces the maximum range (by up to 10–50%). The vehicle with a variable wing area loses 50% less range than a vehicle with a fixed wing.
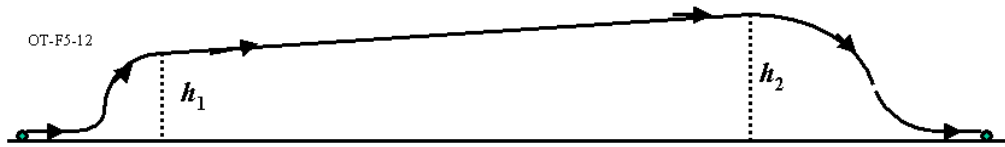
Fig. A4.22. Optimal trajectory of aircraft.

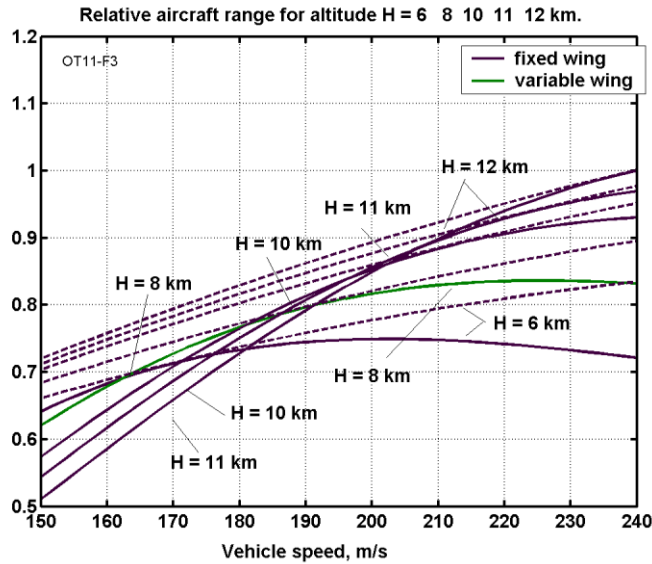**Fig. A4.23.** Relative aircraft range for altitude $H = 6, 8, 10, 11$ and 12 km, maximum range $R_m = 4381$ km, relative fuel mass $M_r = 0.2$, body drag coefficient $C_b = 0.08$, wing drag coefficient $C_d = 0.02$.
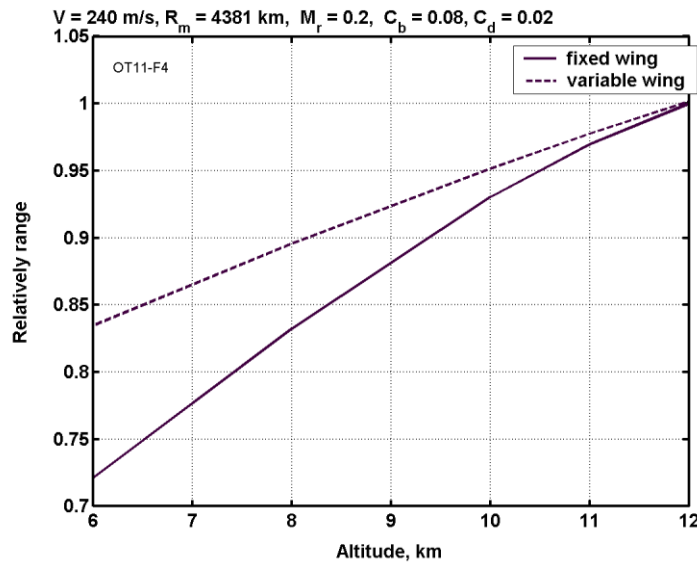

Fig. A4.23. Relative aircraft range for speed $V = 240$ m/s, maximum range $R_m = 4381$ km, relative fuel mass $M_r = 0.2$, body drag coefficient $C_b = 0.08$, wing drag coefficient $C_d = 0.02$.

General discussion and conclusion

a) The current space missiles were designed 30–40 years ago. In the past we did not have navigation satellites that allowed one to locate a missile (warhead) as close as 1 m to a target. Missile designers used inertial navigation systems for ballistic trajectories only. At the present time, we have a satellite navigation system and cheap devices, that enable aircraft, sea ships, cars, vehicles, and people to be located. If we exchange the conventional warhead for a warhead with a simple fixed wing with having a control and navigation system, we can increase the range of our old rockets 4.5–5 times (Fig. A4.13) or significantly increase the useful warhead weight (Fig. A4.19). We can also notably improve the precision of our aiming.

b) Current artillery projectiles for big guns and cannons were created many years ago. The designers assumed that the observer could see an aim point and correct the artillery. Now we have a satellite navigation system that allows one to determine the exact coordinates of targets and we have cheap and light navigation and control devices that can be placed in the cannon projectiles. If we replace our cannon ballistic projectiles with projectiles with a fixed wing, and a control and navigation system, we increase the range 3–9 times (from 35 km up to 360 km, see Fig. A4.20, A4.21). We can use a smooth barrel to increase the nozzle shell speed up to 2000 m/s and range up to 1000 km. These systems can guide the **winged** projectiles and significantly improving their aim. We can reach this result because we use all the **kinetic** energy of the projectile. A conventional projectile cannot remain in the atmosphere and drops at a very high speed. Most of its kinetic energy is wasted. In our case 70–85% of the projectile's kinetic energy is used for support of the moving projectile. This way the projectile range increases 3–9 times or more.

a) All aircraft are designed for only one optimal flight regime (speed, altitude, and fuel consumption). Any deviation from this regime decreases the aircraft range. For aircraft like to the Boeing 747 this regime is: altitude $H = 12$ km, speed $V = 240$ m/s, specific fuel consumption $Cs = 0.00019$ kgf/s/kg thrust. If the speed is reduced from 240 m/s to 200 m/s, the range decreases by 15% (Fig. A4.23). Application of the variable wing area reduces this loss from 15% to 10%. If the aircraft reduces its altitude from 12 km to 9 km, it loses 12% of its maximum range (Fig. A4.24). If it has a variable wing area, it loses only 7.5% of its maximum range. Civil air vehicles are forced to deviate from the optimal conditions by weather or a given flight air corridor. Military air vehicles sometimes have to make a very large deviation from the optimal conditions (for example, when they fly at low altitude, below the enemy radar system). A variable wing area may be very useful for them because it decreases the loss by approximately 50%, improves supersonic flight and taking off and landing lengths.

The author offers some fixed and variable wing designs for air vehicles (Fig. A4.25). Variants **a, b, c,** and **f** are for missiles and warheads, variants **d,** and **e** are for shells.

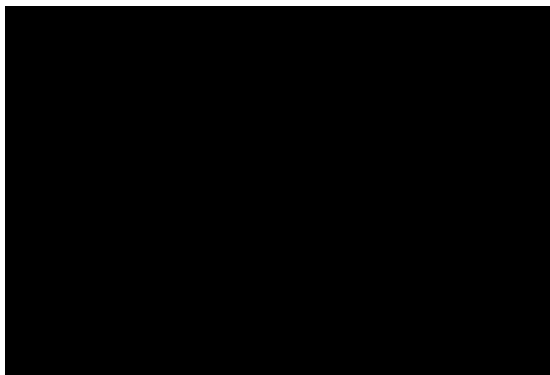**Fig. A4.25.** Possible variants of variable wing designs: **a, b, c,** and **f** for aircraft; **d** and **e** for gun projectiles.

References for Attachment 4

1. A. Miele, "General Variable Theory of the Flight Paths of Rocket-Powered Aircraft, Missile and Satellite Carries", *Astronautica acta*, Vol. 4, pp. 256–288, 1958.

2. A.A. Bolonkin, "Special Extrema in Optimal Control Problems", Akademiya Nauk, Izvestia, *Theknicheskaya Kibernetika*, No. 2, March–April, 1969, pp. 187–198. See also English translation in *Eng. Cybernetics*, No. 2, March–April 1969, pp. 170–183.

3. A.A. Bolonkin, *New Methods of Optimization and their Application*, Moscow, Bauman Technical University, 1972, (in Russian).

4. A.A. Bolonkin, "A New Approach to Finding a Global Optimum", *New Americans Collected Scientific Report*s, Vol. 1, 1991, The Bnai Zion Scientists Division, New York.

5. A.A. Bolonkin, "Optimization of Trajectory of Multistage Flight Vehicles", in collection *Researches of Flight Dynamics*, Masinobilding, Moscow, 1965, pp. 20–78 (in Russian).

6. A.A. Bolonkin, N.S. Khot, "Method for Finding a Global Minimum", AIAA/NASA/USAF/SSMO Symposium on Multidisciplinary Analysis and Optimization, Panama City, Florida, USA, 7–9 Sept. 1994.

7. A.A. Bolonkin, "Solution Methods for Boundary-Value Problems of Optimal Control Theory". 1973. Consultants Bureau, a division of Plenum Publishing Corporation, NY. Translation from *Prikladnaya Mekhanika*, Vol. 7, No 6, 1971, p. 639–650 (English).

8. A.A. Bolonkin, "Solution General Linear Optimal Problem with One Control". Journal "*Pricladnaya Mechanica*", Vol. 4, No 4, 1968, pps. 111–122, Moscow (in Russian).

9. A.A. Bolonkin, N. Khot, "Optimal Structural Control Design", IAF-94-1.4.206, 45th Congress of the International Astronautical Federation, World Space Congress-1994, 9–14 October, 1994, Jerusalem, Israel.

10. A. A. Bolonkin, N. S. Khot, "Optimal Bounded Control Design for Vibration Suppression", *Acta Astronautica*, Vol. 38, No. 10, pp. 803–813, 1996.

11. A.A. Bolonkin, D. Jeffcoat, "Optimal Thrust Angle of Aircraft", 2002, see Attachment 6.

12. A.A. Bolonkin, R. Sierakowski, "Design of Optimal Regulators", 2nd AIAA "Unmanned Unlimited" Systems, Technologies, and Operations – Aerospace, Land, and sea Conference and Workshop & Exhibit, San Diego, California, 15-18 Sep 2003, AIAA-2003-6638.

13. A.A. Bolonkin, Optimal Trajectories of Air and Space Vehicles", *Aircraft Engineering and Aerospace Technology*, Vol.78, No.2, 2004, pp.192–214.

14. Bolonkin's site: http://Bolonkin.narod.ru .
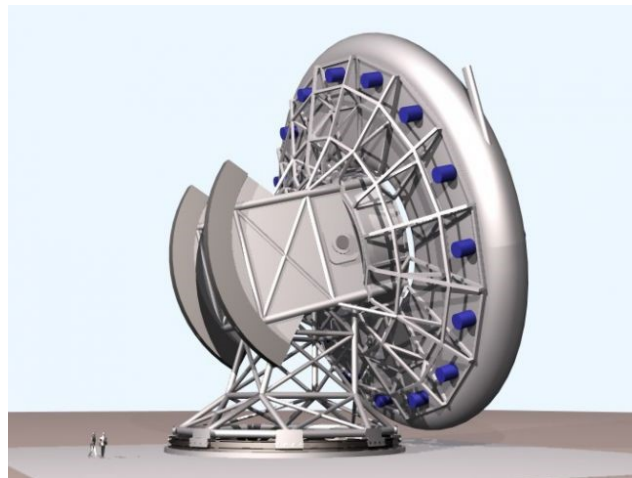
Attachment 5
High Efficiency Transfer of Mechanical Energy

Summary

At present, high-voltage electric lines are used for power transfer. This method is expensive and requires complex devices. The author proposes a new method of power transfer (mechanical cable transmission) for long distances in the air. This method does not require electricity transmission lines, high voltage equipment, large cost, or very much time for construction. It has high efficiency and is cheaper by hundreds of times. In space and on planets without atmosphere this method may be used in very long distance.

Introduction

At the current time, turbo, thermo, hydro, and wind power stations produce mechanical energy. This energy is converted into low-voltage electricity by electric generators, then the low-voltage electricity is converted into high-voltage electricity, transferred over middle or long distances, converted back into low-voltage electricity and distributed among customers. Many customers' devices convert the electricity back into mechanical energy (for example, machines, pumps, locomotives, electric motors, etc.). Short electricity lines have length 20–120 km , voltage 110,000 V, and transfer power 35–50 MW, middle-length electricity lines have length 200–300 km, voltage 330,000 V, and transfer power 300–400 MW, long electricity lines have length 800–1500 km, voltage up to 0.75 MV, and transfer up to 1.8–2.5 GW, and very long electricity lines have length up to 2000 km, voltage 1.15 MV, and transfer 4–6 GW. The coefficient of efficiency of the transferor is 85-92%. All of the lines are very expensive (tens and hundreds millions of dollars) because they require a lot of expensive, clean, electric copper (wire), a lot of masts, ground to be found for to put them in, and a long construction time. Terrorists can easily damage the masts and deprive a large region of energy, and capability to work. The detail researches were published in References[1–4].

Description of innovation

The transfer system includes (Fig. A5.1): mechanical stations for transmission and reception, and air transmission, supported by winged devices. The transmitter station may be turbo, hydro, or wind powered. The reception station may include an electric generator, flywheels as accumulators of energy, an electric and/or mechanical distribution network. Transmission involves a long closed-loop cable made from strong artificial fiber, with the winged devices connected to the cable by rope. The cable is located in the air, and is supported by the winged devices. The cable may be located at high altitude, where the air has low density and low air friction. The cross-section of the cable can be round or

rectangular (flat) (Fig. A5.1). The round form has less air drag, the flat form is better for the drive mechanism.

The energy transferor works in the following way. The transmitter pulls one branch of the closed-loop cable, and rotates the cable and the electricity generator (or wheel) at the reception station.

The cable can be installed by an aircraft (for example, a C-130) or by a helicopter in windy weather, and the winged devices (or small balloons) can keep the cable in the air until the aircraft finishes the flight and the cable is connected in a loop and begins to rotate and support itself. The winged devices have controls that allow the altitude and cable stress to be changed. There is wind virtually all the time at high altitude. You can see clouds moving at altitude in spite of the fact that there is no wind on the ground.
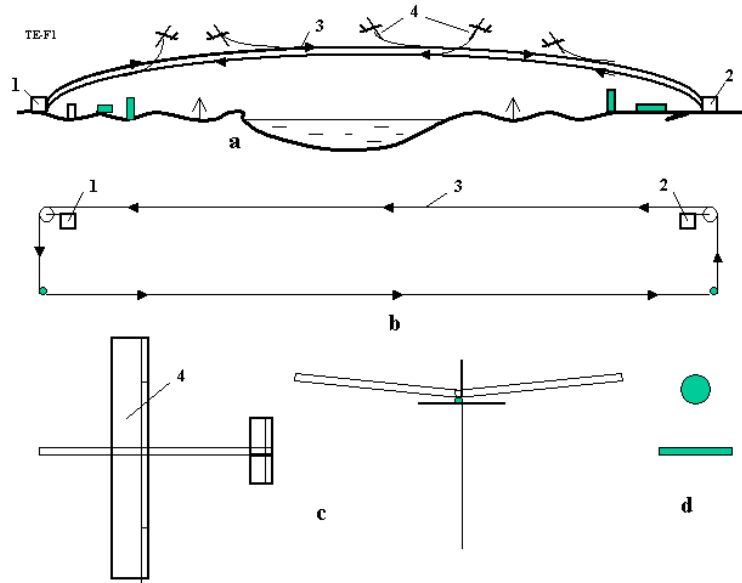
Fig. A5.1. Transferor of mechanical energy. Notations are: 1 – transmission station, 2 – reception station, 3 – closed-loop mobile cable, 4 – supporting winged device. **a** – transfer system (side view), **b** – transfer system (top view), **c** – supporting winged device, **d** – cross-section of the cable.

Theory of Air Energy Transfer
(in metric system)

1. Maximum transfer energy, *E*, is

$$E = TV = 0.24\pi d^2 \sigma V,$$ (A5.1)

where $T = 0.24\pi d^2 \sigma$ is thrust [N], *V is* cable speed [m/s], *d* is cable diameter [m], σ is cable tensile stress [N/m^2].

Results of computations for current fibers, whiskers, and nanotubes are presented in Figs. A5.2, A5.4, A5.6.

As you see a large amount of energy (up to 200 MW) can be transferred over a distance of up to 150 km using a fiber cable of diameter 10–25 mm, up to 1.8 GW over a distance of 1000 km using a whisker cable of diameter 15–30 mm, and up to 25 GW over a distance of more than 7000 km (for example from continent to continent, the USA to Europe) using nanotubes cable. With more power systems then one can transfer more energy over longer distance.

2. The air drag of a double cable can be computed by the following equations (Reynolds number is included):

$$D_L = 2.08\rho^{0.5}\mu^{0.5}V^{1.5}L^{0.8}d, \quad D_T = 0.2292\rho^{0.8}\mu^{0.2}V^{1.8}L^{0.8}d, \quad D_S = m/k,$$

$$m = 0.5\pi d^2 L\gamma, \quad D = 0.5(D_L + D_T) + D_S,$$

(A5.2)

where D_L is laminar air drag [N], D_T is turbulent air drag [N], D_S is drag of wing support devices [N], D is average air drag [N] (it is impossible to show, but full drag equals half the sum of laminar and turbulent drag), ρ is air density at a given average altitude H (for example, for $H = 10$ km, $\rho = 0.4125$, $\mu = 1.458 \cdot 10^{-5}$), μ is air viscosity [kg/s·m], L are cable length between the transfer and reception station [m], m is mass of half the cable [kg], γ is density of the cable [kg/m³], k is the aerodynamic coefficient ($k = 20$–30 in our case).

3. Efficiency coefficient of transfer, η, is

$$\eta = 1 - \frac{D}{T},$$

(A5.3)

Results of computations for current fibers, whiskers, and nanotubes are presented in Figs. A5.3, A5.5, A5.7.

The transfer efficiency ($\eta = 88$–94.5) is the same as or better than efficiency of current electricity lines
.

Fig. A5.2. Transfer energy versus cable speed for cable diameter $d = 10$–25 mm, cable stress 200 kg/mm², cable length $L = 150$ km, average cable altitude $H = 10$ km, aerodynamic efficiency of winged support devices $k = 25$.

cable stress 200 kg/mm^2, cable length L = 150 km, av. altitude H = 10 km.
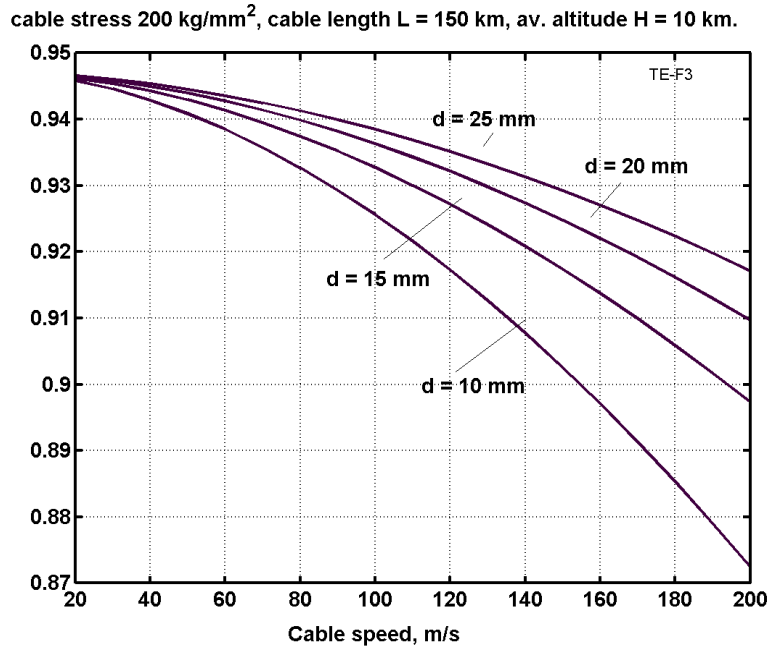
Fig. A5.3. Electrical efficiency coefficient versus cable speed for cable diameter d = 10–25 mm, cable stress 200 kg/mm^2, cable length L = 150 km, average cable altitude H = 10 km, aerodynamic efficiency of winged support devices k = 25.

cable stress 1000 kg/mm^2, cable length L = 1000 km, altitude H = 10 km.
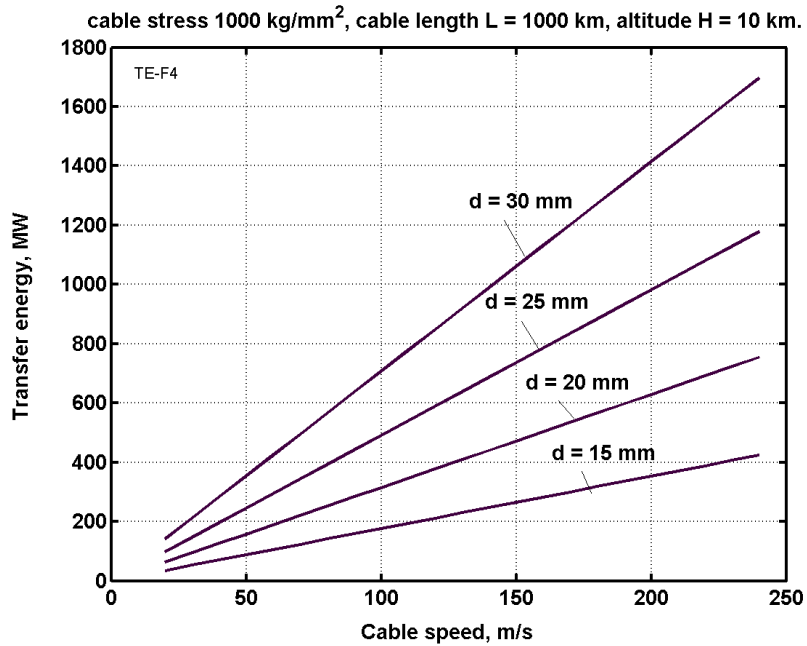
Fig. A5.4. Transfer energy versus cable speed for cable diameter d = 15–30 mm, cable stress 1000 kg/mm^2, cable length L = 1000 km, average cable altitude H = 10 km, aerodynamic efficiency of winged support devices k = 25.

Cable stress 1000 kg/mm², cable length L =1 000 km, altitude H = 10 km.
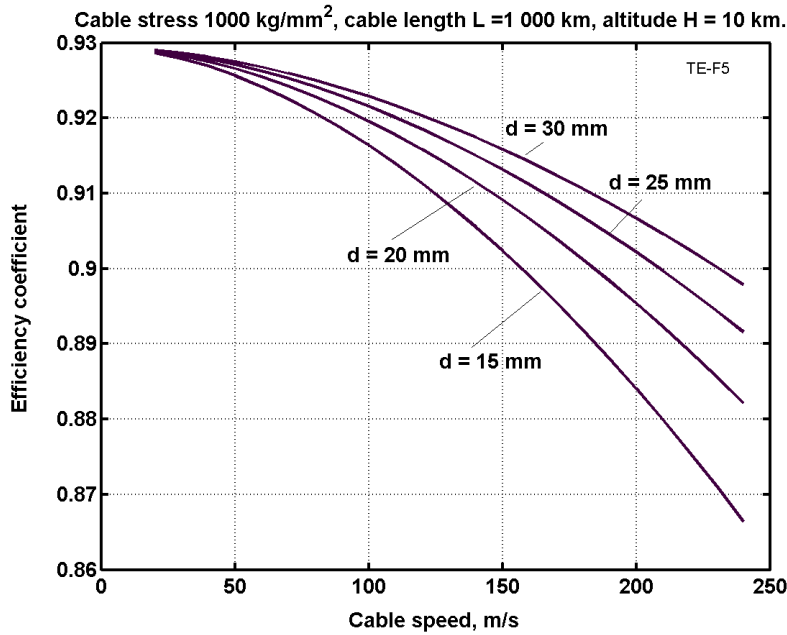
Fig. A5.5. Electric efficiency coefficient versus cable speed for cable diameter $d = 15$–30 mm, cable stress 1000 kg/mm², cable length $L = 1000$ km, average cable altitude $H = 10$ km, aerodynamic efficiency of winged support devices $k = 25$.

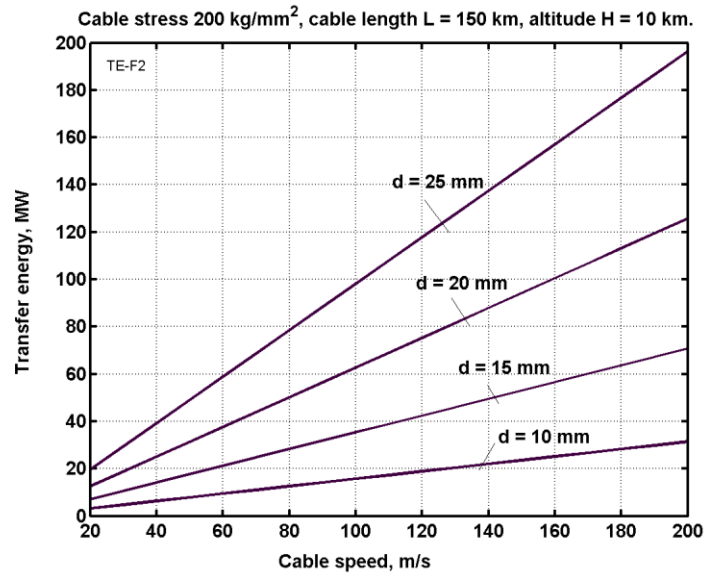**Cable stress 6000 kg/mm², L = 7000 km, altitude H = 10 l**

Fig.A5.6. Transfer energy versus cable speed for cable diameter $d = 25$–40 mm, cable stress 6000 kg/mm², cable length $L = 7000$ km, average cable altitude $H = 10$ km, aerodynamic efficiency of winged support devices $k = 25$.
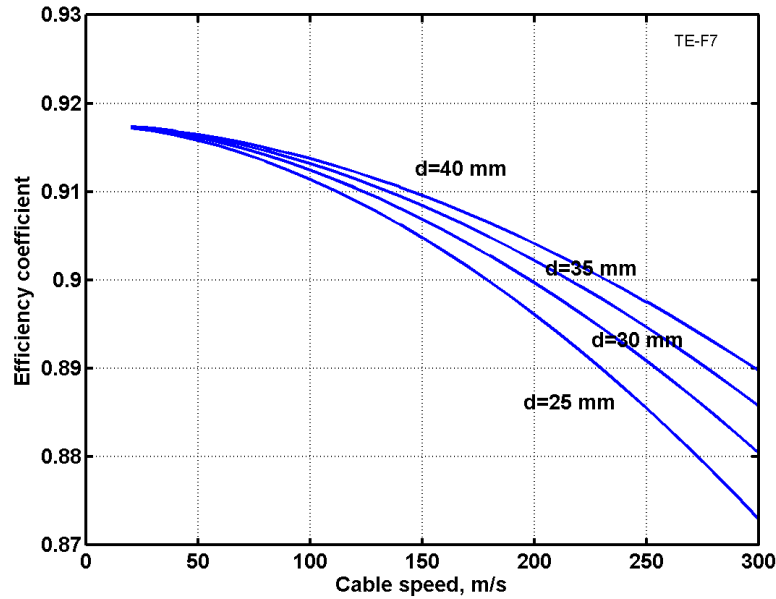
Fig. A5.7. Electric efficiency coefficient versus cable speed for cable diameter $d = 25–40$ mm, cable stress 6000 kg/mm², cable length $L = 7000$ km, average cable altitude $H = 10$ km, aerodynamic efficiency of winged support devices $k = 25$.

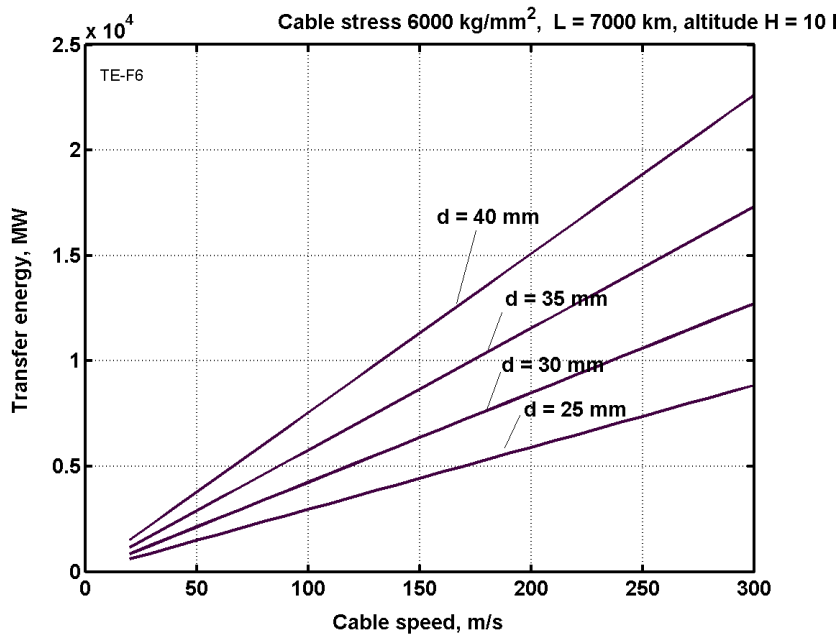**4.** Maximum energy storage using a 1 kg flywheel from artificial fiber, whisker, or nanotubes is

$$E_S = \frac{\sigma}{2\gamma}, \qquad (A5.4)$$

where γ is wheel tread density [kg/m³].

5. Minimum energy needed to support the cable in the air when there is no transfer of energy.

$$E_{min} = D(V_{min})V_{min} . \qquad (A5.5)$$

This energy may be estimated using Figs. A5.2, A5.4, and A5.6 if they continue at low cable speed.

Discussion

Cable problem (see also Chapters 1, 2). At present, industry produces cheap artificial fibers with a tensile stress of up $\sigma = 500–620$ kg/mm² and density $\gamma = 970–1800$ kg/m³. This is enough for a distance up 150–300 km. The coefficient of efficiency is about 87%. However, if the cable made the whiskers (for example, C_D with maximum $\sigma = 8000$ kg/mm², the range increases by 1000–2000 km (Figs. A5.4 and A5.5).

The nanotubes created in scientific laboratores promise a revolution in space, aviation, machine-building, and transferring of energy. They increase the transfer distance by up to 7000–10000 or more, kilometers, in air (in space, without limit). They allow a transfer distance of up to 20,000 km throgh space with high cable speed when the cable is supported by centrifugal force.

Building problems. This problem may be solved by transport aeroplanes or helicopters as described in the description of the innovation.

Air traffic problems. Commercial passenger aircraft fly in special air corridors in most cases. The energy lines (winged support devices) will be visible in daytime and can have red lights at night. They can be located at high altitudes (14–15 km), over the conventional aircraft routes. High altitude only improves the parameters.

The proposedd design of the air transfer power lines is not optimal. My purpose is to show the new method and its possibilities.

The offered method may seen strange to electrical engineers. However, this method can have a big future. The author has more detailed research and can take part in design and testing an experimental installation.

Advantages of proposed method

The proposed mid-length energy transferor has large advantages in comparison with equivalent electricity lines.

1) The cable transferor is cheaper than equivalent (equal power) electricity line by tens or hundreds of times (no masts, expensive copper wires, ground costs, high-voltage substations, no additional electricity generator, transformers, etc.). Artificial fibers are cheap and widely produced by current industry, and current fibers may be used for short and mid-length (up to 300 km) lines.
2) Construction time is reduced from months to days (only line is installed).
3) We can transfer a high energy more than current electric lines.
4) We can transfer a huge amount of energy over a very long distance (7000–1000 km), from continent to continent (for example, from the USA to Europe and back) with high efficiency (more than electrical line efficiency).
5) The cable transferor can be used for delivery of a payload (for example, mail).
6) The cable transferor can be used as high altitude communication antenna for radio, TV, and telephone.
7) Nanotubes have an electrical conductivity close to copper and the proposed transferor can be used to deliver electricity and communications.
8) Terrorists cannot damage the line.

Defect:
1) If no is energy being transferred it is necessary to expend a small amount of energy for cable rotation (for support in the air if there is no wind).

References

1. Bolonkin, A.A., "Inexpensive Cable Space Launcher of High Capability", IAC-02-V.P.07, 53rd International Astronautical Congress. The World Space Congress – 2002, 10–19 Oct., 2002/Houston, Texas, USA.
2. A.A. Bolonkin, "Transmission of Mechanical Energy to Long Distance", The International Energy Conversion Engineering Conference at Providence, RI, 16–19 August, 2004, as Paper AIAA-2004- 5660.
3. A.A. Bolonkin, "Air Transfer of Mechanical Energy", *Actual Problems of Aviation and Aerospace Systems*, Vol. 10, No 1 (19) 2005, pp. 102–110.
4. A.A.Bolonkin, "Non-Rocket Transportation System for Space Travel", *JBIS*, Vol. 56, No 7/8, pp. 231–249, 2003.

Attachment 6
Optimal Aircraft Thrust Angles*
By Alexander Bolonkin* and David Jeffcoat**(2003)

Summary

The optimal angle for an aircraft's thrust vector is derived from first principles. Two equations are shown to encompass six different flight regimes. The main result for takeoff and landing is that the optimal thrust angle in radians approximately equals the coefficient of rolling friction. For climb, cruise, turn and descent, the optimal thrust angle equals the arctangent of the ratio of the drag coefficient to the lift coefficient. The second result differs from the well-known result that optimal thrust angle equals the arctangent of the partial derivative of drag with respect to lift. The authors discuss this difference.

Nomenclature

B – artificial function, $B = \lambda dx/dt – H$,
C_D – drag coefficient,
C_L – lift coefficient,
D – drag,
d – takeoff or landing distance,
E – aircraft efficiency, C_L/C_D ,
F – fuel consumption,
f – performance function,
g – n-dimensional vector constraint function,
g_0 – acceleration due to gravity,
H – Hamiltonian, $–f + \lambda g$,
h – altitude,
I – performance index,
L – lift force,
M – aircraft mass ,
OTA – optimal thrust angle,
q – dynamic pressure, $\rho V^2 / 2$,
R – range,
S – wing area,
t – time,
T – thrust or time of flight,
T_f – friction force,
u – m-dimensional control vector,
V – aircraft speed,
W – aircraft weight,
w_f – specific fuel consumption,
x – n-dimensional state vector,
λ – n-dimensional Lagrange multiplier,
γ – thrust angle,

μ – friction coefficient,
ψ – specific function,
ϕ – roll angle

Introduction

Aircraft designers must determine the angle of the thrust vector relative to the main horizontal flight direction. When this angle is positive (up from the horizontal plane), an additional lift force is generated, but at the expense of horizontal thrust. In this chapter, the optimal thrust angle is derived, using both classical methods and an alternative optimization method developed by the first author.[1,2] Many methods of deflecting the nozzle exhaust stream of rocket engines to provide thrust vector control have been investigated, including jet vanes, gimbaled or swiveled nozzles, and extendable nozzle deflectors.[3,4,5,6] Jet vanes have been widely applied for the control of solid rocket engines and for early liquid-rocket engines, including the German V-2 missile.[7] Reference[8] presents metrics for assessing the performance of fighter aircraft implementing thrust vector control.

References[3] and[9] are most closely related to this paper. Gilyard and Bolonkin[3] use numerical calculations to search for the optimal thrust angle, whereas in this chapter the focus is theoretical, rather than numerical. Miele[9] presents a basic theory for analyzing the optimum flight paths of rocket-powered vehicles. Miele simultaneously optimizes the time history of lift, thrust modulus and thrust direction, and states that the optimal thrust angle equals the arctangent of the partial derivative of drag with respect to lift. In this chapter, we provide theory and formulas for the OTA for six primary flight regimes of any aircraft type. The formulas provided are accurate for stable flight conditions, but may be sub-optimal during high dynamic maneuvers. The six flight regimes are listed below, each with one or more optimization objectives.

1. Takeoff, to minimize takeoff distance.
2. Climb, to minimize fuel consumption.
3. Cruise, to minimize fuel consumption or to maximize range.
4. Turn, to minimize fuel consumption or to minimize turn time.
5. Descent, to minimize fuel consumption or to maximize range.
6. Landing, to minimize landing distance.

General Methodology

Consider the problem of minimizing a performance index I, where

$$I = \int_0^T f(t,x,u)dt \qquad (A6.1)$$

We wish to minimize I with respect to x and u, subject to the dynamic constraint

$$\dot{x} = g(t,x,u) \qquad (A6.2)$$

We assume an initial condition, $x(0)$, is known. Following the approach described in Reference[1], we define an artificial function

$$B = f - \frac{\partial \psi}{\partial x} g(t,x,u) - \frac{\partial \psi}{\partial t} \qquad (A6.3)$$

In particular, the function ψ may be defined by

$$\psi = \lambda(t) \cdot x \qquad (A6.4)$$

If we find

$$\min_{x,u} B = \min_{x,u}[f(t,x,u) - \lambda(t)g(t,x,u) - \dot{\lambda}(t)x] \qquad (A6.5)$$

then the values of x and u that minimize B, subject to the constraint given in equation (A6.2), are optimal control and state vectors for the problem stated in equation (A6.1).

We can also solve this problem by a classical method[10] using the Hamiltonian for this problem, which is given by

$$H(t,x,u,\lambda) = -f(t,x,u) + \lambda(t) \cdot g(t,x,u),$$ (A6.6)

and

$$\dot{\lambda} = -\frac{\partial H}{\partial x}$$

The values of u which maximize the Hamiltonian, subject to the constraint in (A6.2), are optimal control vectors for (A6.1). That is,

$$\overline{H} = \max_u H(t,x,u,\lambda)$$ (A6.7)

When the process does not change with time, we have a more straightforward problem:
Minimize a performance index I, defined by

$$I = \int_0^T f(x,u)dt$$ (A6.8)

with respect to x and u, subject to the dynamic constraint

$$\dot{x} = g_i(x,u), \quad \text{for } i = 1,2, \ldots, n$$ (A6.9)

$$H(t,x,u,\lambda) = -f(x,u) + \lambda(t)g(x,u)$$ (A6.10)

$$\overline{H} = \max_u H(t,x,u,\lambda), \qquad \overline{u} = u(t,x)$$ (A6.11)

The parameter λ is an n-dimensional unknown Lagrange multiplier and $\overline{u}$ is the optimal control. Equations (A6.4) through (A6.6) give the system of equations

$$\frac{\partial B}{\partial u_j} = \frac{\partial H}{\partial u_j} = 0 , \quad j = 1,2, \ldots, m; \quad \frac{\partial B}{\partial x_i} = \dot{\lambda}_i(t) + \frac{\partial H}{\partial x_i} = 0 , \quad i = 1,2, \ldots, n \quad (A6.12)$$

These equations are equivalent to conventional principle of maximum[10]

$$\dot{\lambda}_i(t) = -\frac{\partial H}{\partial x_i} , \quad i = 1,2,\ldots, n; \qquad \frac{\partial H}{\partial u_j} = 0 , \quad j = 1,2,\ldots,m.$$ (A6.13)

These equations, together with equation (A6.2), allow us to find an extreme of the Hamiltonian H, which is optimal if the appropriate second-order sufficient conditions for optimality are satisfied.

Optimal Thrust Angle for Takeoff and Landing

For takeoff, the performance index is the takeoff distance, described by

$$d = \int_0^T V dt.$$ (A6.14)

The aircraft speed serves as the performance function. The dynamic constraint on acceleration is given by as illustrated in Fig. A6.1.

$$\dot{V} = \frac{1}{M}(T\cos\gamma - D - T_f)$$ (A6.15)

The friction force is given by

$$T_f = \mu \cdot (W \cdot g_0 - L - T\sin\gamma)$$ (A6.16)

We know from aerodynamics and trigonometry that

$$L = C_L qS, \quad D = C_D qS, \quad \sin\gamma = \sqrt{1 - \cos^2\gamma}$$ (A6.17)

We consider only the positive root, but the result is the same for the negative root.

To simplify subsequent calculations, make the substitution

$$u = \cos\gamma \tag{A6.18}$$

so that

$$\sin\gamma = \sqrt{1-u^2} \tag{A6.19}$$
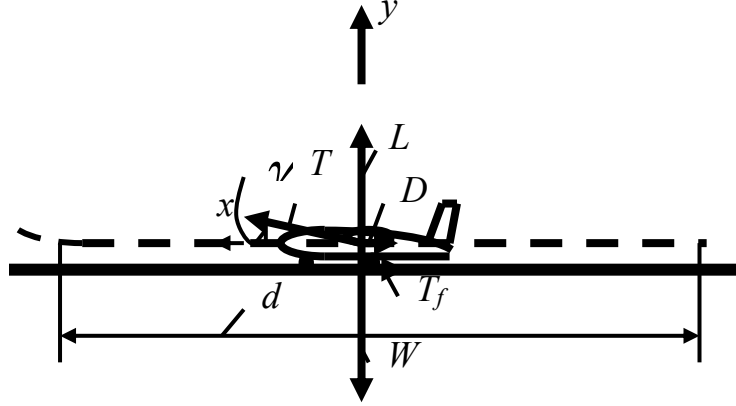
Fig. A6.1. Takeoff

Substituting equations (A6.16) – (A6.19) into (A6.15) yields

$$\dot{V} = \frac{1}{M}[T \cdot u - D - \mu \cdot (W \cdot g_0 - L - T \cdot \sqrt{1-u^2})] \tag{A6.20}$$

which leads to function B or the Hamiltonian H

$$B = f + \dot{\lambda}(t) \cdot V + \lambda(t) \cdot \dot{V} = V + \dot{\lambda}(t) \cdot V + \lambda(t) \cdot \frac{1}{M}[T \cdot u - D - \mu \cdot (W \cdot g_0 - L - T\sqrt{1-u^2})]$$

$$= \dot{\lambda}(t) \cdot V + H, \tag{A6.21}$$

where $\qquad H = V + \lambda(t)\frac{1}{M}[T \cdot u - D - \mu \cdot (W \cdot g_0 - L - T\sqrt{1-u^2})] \tag{A6.22}$

To find the minimum of B over all admissible u, the necessary condition is that the partial derivative is equal to zero, that is,

$$\frac{\partial B}{\partial u} = 0 \tag{A6.23}$$

or

$$\frac{\partial B}{\partial u} = \frac{\lambda(t) \cdot T}{M}\left[1 - \frac{\mu \cdot u}{\sqrt{1-u^2}}\right] = 0 \tag{A6.24}$$

If M, T, and $\lambda \neq 0$, then from equation (A6.24), it must be true that

$$\mu \cdot u = \sqrt{1-u^2} \tag{A6.25}$$

or

$$\mu^2 \cdot u^2 = 1 - u^2 \tag{A6.26}$$

so that the final result from (A6.26) is

$$u = \pm\frac{1}{\sqrt{1+\mu^2}} \tag{A6.27}$$

Returning to the original notation, we have the thrust angle as a function of the coefficient of friction,

$$\cos\gamma = \pm\frac{1}{\sqrt{1+\mu^2}} \qquad \text{or} \qquad \gamma = \cos^{-1}\left(\frac{\pm 1}{\sqrt{1+\mu^2}}\right) \quad \text{radians}. \qquad (A6.28)$$

We can use the trigonometric identity

$$\cos\gamma = \frac{1}{\sqrt{1+\tan^2\gamma}} \qquad (A6.29)$$

to get our final result,

$$\tan\gamma = \pm\mu \qquad (A6.30)$$

or, for small μ, say μ < 0.2, we have the design rule-of-thumb that

$$\gamma = \pm\mu \qquad (A6.31)$$

where γ is in radians.

   The sign of γ depends on our goal, minimization or maximization of the function, as well as the sign of λ and T in equation (A6.24). Clearly, the thrust must have a forward direction for aircraft takeoff, and the angle γ must be positive. Similarly, for landing, the thrust must have a backward direction to brake the airplane, and the angle γ must be negative, pushing the airplane to the ground, as illustrated in Fig. A6.2.
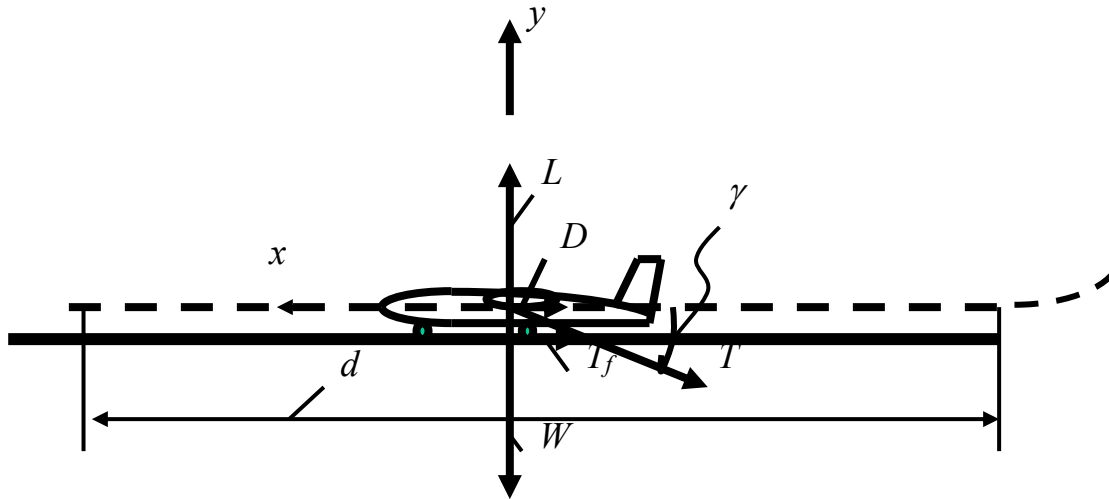
Fig. A6.2. Landing

The angles for takeoff and landing are different, because the coefficients of rolling friction are different for takeoff and landing. For takeoff, the friction coefficient is small (μ is approximately 0.01–0.05); for landing, the coefficient is larger (μ is approximately 0.3–0.4). The direction of thrust is also different for takeoff ($\gamma \cong +1$ to $+3$ degrees) than for landing ($\gamma \cong -16$ to -22 degrees). For takeoff, the thrust has a forward direction; for landing the thrust has a backward direction. As a design "rule-of-thumb," we can say that the OTA in radians is equal to the coefficient of rolling friction for takeoff, and the OTA is within 5% of the coefficient of rolling friction for landing. The expression $\tan\gamma = \mu$ is exact for any rolling friction coefficient.

The optimal angles for takeoff and landing are shown in Figs. A6.3 and A6.4, respectively.

The optimal thrust angle for airplane take-off
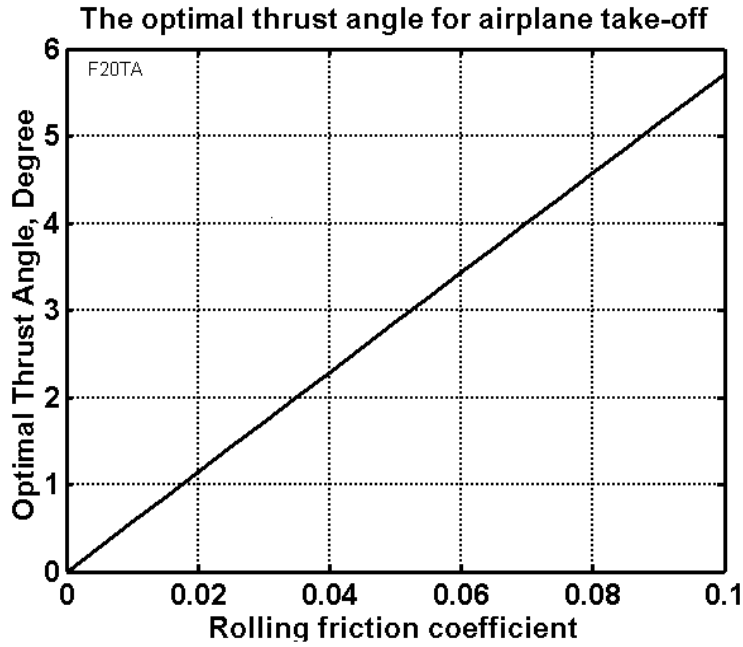
Fig. A6.3. Optima for takeoff

The optimal thrust angle for airplane landing
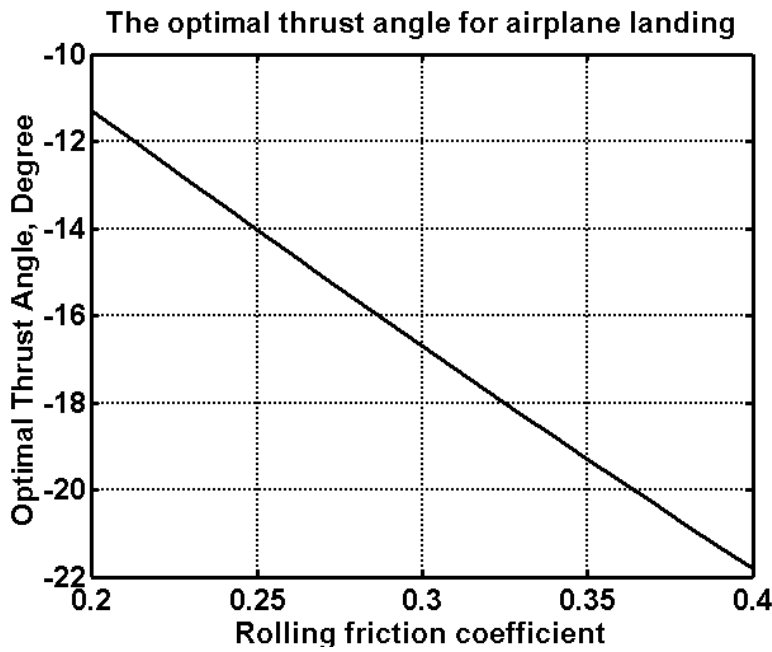
Fig. A6.4. Optimal thrust angle for landing

Optimal Angle of Thrust Vector in Horizontal Flight (Cruise Regime)

Assume that speed, altitude, and direction of flight are constant during horizontal flight time, and that we wish to maximize range, R, of the aircraft over the time interval $[0,T]$. Then

$$R = \int_0^T V dt \qquad (A6.32)$$

The equilibrium equations of motion (Fig. A6.5) are

$$T\cos\gamma - D = 0, \qquad (A6.33)$$

$$L - W \cdot g_0 + T \sin \gamma = 0 \qquad \text{(A6.34)}$$
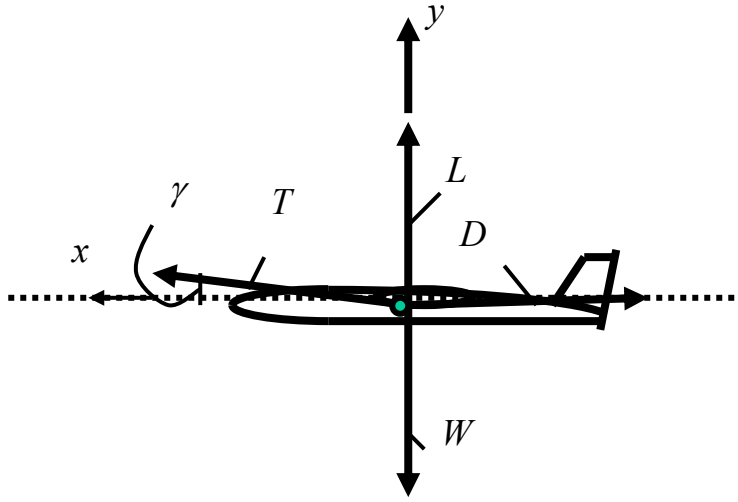
Fig. A6.5 Horizontal flight

Using the notation

$$E = \frac{L}{D} = \frac{C_L}{C_D}, \qquad u = \cos\gamma, \qquad \text{and } \sin\gamma = \sqrt{1 - u^2} = 0, \qquad \text{(A6.35)}$$

we can substitute D and u from (A6.35) and L from (A6.34) into (A6.33) to obtain

$$T \cdot u - \frac{W \cdot g_0}{E} + \frac{T}{E}\sqrt{1 - u^2} = 0 \qquad \text{(A6.36)}$$

Next, compose the Hamiltonian function H, as in equation (A6.10)

$$H = -V + \lambda \cdot \left(T \cdot u - \frac{W \cdot g_0}{E} + \frac{T}{E}\sqrt{1 - u^2}\right) \qquad \text{(A6.37)}$$

And find the maximum of this function

$$\frac{\partial H}{\partial u} = \lambda \cdot T \left[1 - \frac{u}{E\sqrt{1 - u^2}}\right] = 0 \qquad \text{(A6.38)}$$

If we take values for λ and T such that $\lambda \cdot T \neq 0$, we find that

$$u = E\sqrt{1 - u^2} \qquad \text{(A6.39)}$$

or

$$u^2 = E^2\left(1 - u^2\right) \qquad \text{(A6.40)}$$

From (A6.40), it follows that

$$u = \pm \frac{E}{\sqrt{1 + E^2}} \qquad \text{(A6.41)}$$

or

$$\cos\gamma = \pm \frac{E}{\sqrt{1 + E^2}} \qquad \text{or} \qquad \gamma = \arccos\left(\pm \frac{E}{\sqrt{1 + E^2}}\right) \qquad \text{(A6.42)}$$

Note that γ in degrees given by $\gamma° = 180 \cdot \gamma / \pi$. \qquad \text{(A6.43)}

From physical conditions, it is evident that angle γ is positive. For fighter aircraft, aerodynamic efficiency, E, ranges from 2 to 10. For transport or passenger aircraft, efficiency ratios vary from 10 to 20. Using the trigonometric identify in (A6.29), we obtain a final result

$$\tan\gamma = \frac{1}{E} \qquad \text{or} \qquad \tan\gamma = \frac{C_D}{C_L} \qquad (A6.44)$$

For small γ, say $\gamma < 0.2$ radians, we have the design rule-of-thumb that

$$\gamma \cong \frac{C_D}{C_L} \qquad (A6.45)$$

The OTA for the cruise regime is shown in Fig. A6.6 for aerodynamic efficiencies ranging from 2 to 10, typical of fighter aircraft.
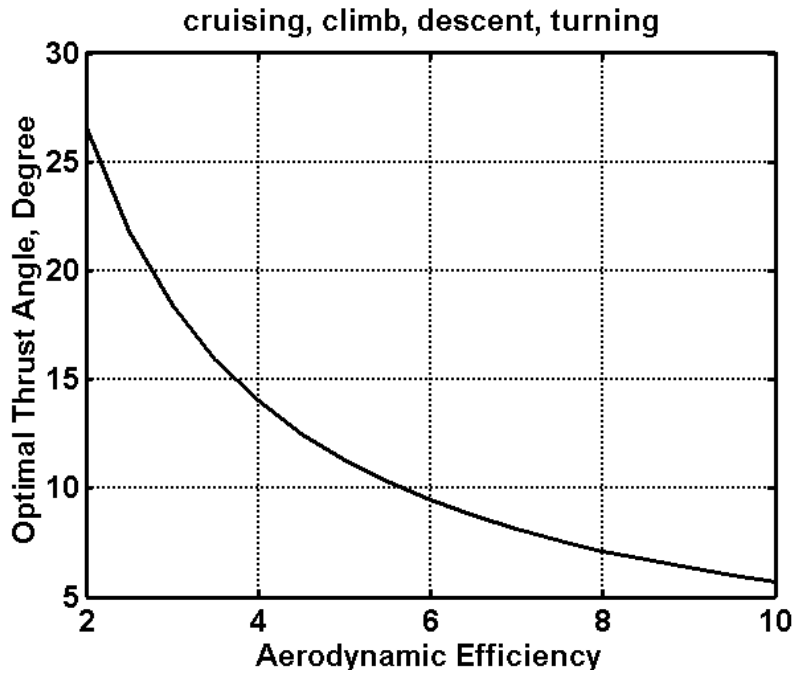
Fig. A6.6. Optimal thrust angle for cruise regime

So far, we have used as the performance index the maximum range of the aircraft. The results are the same if we minimize fuel consumption,

$$F = \int_0^T w_f \cdot dt \qquad (A6.46)$$

Or minimize time

$$T = \int_0^T dt \ . \qquad (A6.47)$$

Climb and Descent Regime

Let us take as the performance index the range or altitude,

$$R = \int_0^T V dt \qquad \text{or} \qquad h = \int_0^T V \sin\theta dt \ . \qquad (A6.48)$$

Then the equilibrium equations are

$$T \cos \gamma - D - W \cdot g_0 \sin \theta = 0 \tag{A6.49}$$

$$L + T \sin \gamma - W \cdot g_0 \cos \theta = 0 \tag{A6.50}$$

where θ is the angle between the trajectory and the horizon. Using the notation

$$E = \frac{L}{D} = \frac{C_L}{C_D}, \qquad \cos \gamma = u, \qquad \sin \gamma = \sqrt{1 - u^2}. \tag{A6.51}$$

and substituting equations (A6.50) and (A6.51) into equation (A6.49), we have

$$Tu - \frac{W \cdot g_0 \cos \theta}{E} + \frac{T}{E} \sqrt{1 - u^2} - W \sin \theta = 0 \tag{A6.52}$$

And

$$H = V + \lambda [Tu - \frac{W \cdot g_0 \cos \theta}{E} + \frac{T}{E} \sqrt{1 - u^2} - W \cdot g_0 \sin \theta] \qquad (A6.53)$$
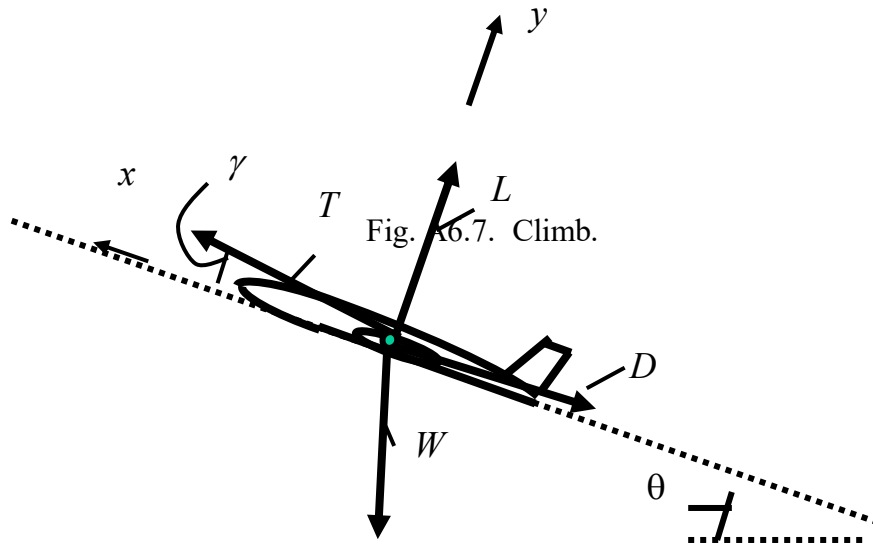
Fig. A6.7. Climb.

Fig. A6.7 illustrates the climb regime.

The necessary condition for an extreme is

$$\frac{\partial H}{\partial u} = 0 \tag{A6.54}$$

or

$$\frac{\partial H}{\partial u} = \lambda T \left(1 - \frac{u}{E\sqrt{1 - u^2}} \right) = 0 \tag{A6.55}$$

That is the same as equation (A6.38), which means that the final equation for the optimal angle of thrust vector in climb and descent will be equal to the equation for a cruise regime.

$$\cos \gamma = \pm \frac{E}{\sqrt{1 + E^2}} \qquad \text{or } \tan \gamma = \frac{1}{E} = \frac{C_D}{C_L} \qquad \text{or } \gamma \approx \frac{C_D}{C_L} \tag{A6.56}$$

From physical conditions, it is evident that angle γ is positive. The aerodynamic efficiencies are different for climb, descent, and cruise, so that the optimal thrust vector angle will be different, but the equations

for the calculation are the same. Again, note that we can use trigonometric equalities to derive the more concise expression, cot γ = E, which is exact for any aerodynamic efficiency ratio. The results are the same whether time or fuel consumption is used for the performance index.

Turning of airplane

Consider now the turning of an airplane in one plane, with a constant roll angle ϕ.
Our performance index can be distance, minimum time of turn, or fuel consumption.

$$R = \int_0^T V dt, \qquad T = \int_0^T dt, \qquad F = \int_0^T w_f dt \qquad (A6.57)$$

The equations of motion are

$$T \cos - D = 0 \qquad (A6.58)$$
$$L + T \sin \gamma - W \cdot g_0 \cos \phi = 0 \qquad (A6.59)$$

Using the notation

$$E = \frac{L}{D} = \frac{C_L}{C_D}; \qquad \cos \gamma = u; \qquad \sin \gamma = \sqrt{1 - u^2} \qquad (A6.60)$$

and substituting (A6.59) and (A6.60) into (A6.58), we obtain

$$T \cdot u - \frac{W \cdot g_0 \cos \phi}{E} + \frac{T \sqrt{1 - u^2}}{E} = 0 \qquad (A6.61)$$

and

$$H = V + \lambda \left[Tu - \frac{W \cdot g_0 \cos \phi}{E} + \frac{T}{E} \sqrt{1 - u^2} \right] \qquad (A6.62)$$

The necessary condition for an extreme is

$$\frac{\partial H}{\partial u} = 0 \quad \text{or} \quad \frac{\partial H}{\partial u} = \lambda T \left(1 - \frac{u}{E \sqrt{1 - u^2}} \right) = 0 \qquad (A6.63)$$

Equation (A6.63) is equivalent to equation (A6.38), which means the final equation for the optimal angle of thrust vector in a roll is equal to the equation for a cruise regime

$$\cos \gamma = \pm \frac{E}{\sqrt{1 + E^2}} \quad \text{or} \quad \tan \gamma = \frac{1}{E} = \frac{C_D}{C_L} \quad \text{or} \quad \gamma \approx \frac{C_D}{C_L} \qquad (A6.64)$$

From physical conditions, it is evident that angle γ is positive.

Discussion

The problem of determining an OTA is also discussed in Reference[9], in which the OTA for rocket-powered aircraft is given by

$$\omega = \arctan \frac{\partial D}{\partial L} \qquad (A6.65)$$

where ω is equivalent to our angle γ. In the particular case of a parabolic polar drag coefficient of the form $C_D = C_{D_0}(M) + K(M)C_L^2$, where M is the Mach number, K is the induced drag factor, and C_{D_0} is the zero-lift drag coefficient, equation (A6.65) leads to

$$\omega = \arctan(2KC_L). \qquad (A6.66)$$

Equations (A6.44) and (A6.66) give very different results (Fig. A6.8). For example, when there is no lift force ($C_L = 0$), equation (A6.44) gives $\gamma = 90°$, meaning that the optimal thrust angle is strictly vertical (perpendicular to the desired trajectory), while equation (A6.66) gives $\omega = 0$, corresponding to a horizontal thrust. Conversely, when the lift force is maximum, equation (A6.65) gives $\omega = 90°$. We also

see in Fig. A6.8 that as the lift force (C_L) decreases after passing through its maximum point, equation (A6.65) yields an optimal thrust angle greater than 90°, producing a reverse thrust force. So, we conclude that equations (A6.65) and (A.66) do not adequately model the OTA near extreme points.
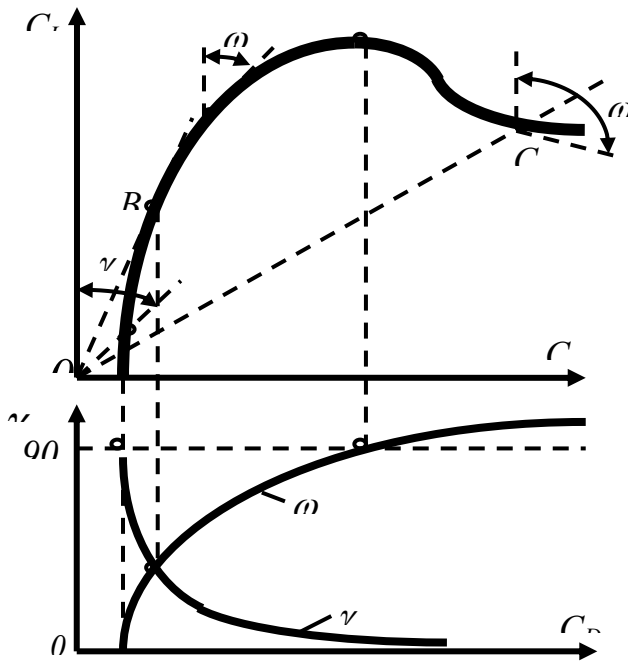
Fig. A6. 8. Comparison of γ and ω.

The angle γ produced by equation (A6.44) also has better trend characteristics, starting at 90° when $C_L = 0$, then decreasing as the lift force is increasing and positive. The angle ω starts at zero when $C_L = 0$, then increases as the aerodynamic lift force increases. Equation (A6.44) and (A6.65) do produce the same result at one point, when the efficiency coefficient, $E = C_L / C_D$ is maximized. Equation (A6.65) was derived for an optimal angle of attack, and the result is valid at the point of optimal aircraft lift. Equation (A6.44) is more general, and may be used at any polar coordinate in any of the four flight regimes: climb, cruise, turn or descent.

Conclusions

In this application, we derived two simple equations for the optimal thrust angle of an aircraft. One equation is valid for takeoff and landing, the other for climb, cruise, turn, and descent. During takeoff, the OTA is positive, decreases as the coefficient of rolling friction decreases, and is essentially equal to the friction coefficient. During landing, the OTA is negative, increases as the coefficient of rolling friction increases, and is within 5% of the value of the friction coefficient. The simple expression tan OTA = μ provides an exact result for the OTA as a function of the rolling friction coefficient.

In the climb, cruise, turn or descent flight regimes, the OTA depends only on the coefficient of aerodynamic efficiency. Here we observe an inverse proportion: the greater the coefficient of aerodynamic efficiency, the smaller the OTA. The OTA is positive in all flight regimes, with the possible exception of air braking, which is not addressed in this research. As in the cases of takeoff and landing, we have a simple expression, tan OTA = 1 / E, relating the optimal thrust angle to a single parameter, the aerodynamic efficiency. The equations for OTA developed in this attachment were also shown to have more intuitive trends and better behavior at extreme points than the Miele equations.

References

1. Bolonkin, Alexander, "A New Approach to Finding a Global Optimum," *New American's Collected Scientific Reports*, Vol. 1, The Bnai Zion Soviet–American Scientists Division, 1990.
2. Bolonkin, Alexander, "New Methods of Optimization and their Application," Bauman Technical University, Moscow, 1972 (in Russian).
3. Gilyard, Glenn and Bolonkin, Alexander, "Optimal Pitch Thrust-Vector Angle and Benefits for all Flight Regimes, NASA-TM-2000-209021, March 2000.
4. Gal-Or, Benjamin, "Thrust Vectoring for Flight Control and Safety: A Review," *International Journal of Turbo and Jet Engines*, Vol. 11, 1994, pp. 119–136.
5. Gerren, Donna S., "Design, Analysis, and Control of a Large Transport Aircraft Utilizing Selective Engine Thrust as a Backup System for the Primary Flight Control," NASA-CR-186035, September 1995.
6. Mangold, P., and Wedekind, G, "Inflight Thrust Vectoring: A Further Degree of Freedom in the Aerodynamic/Flight Mechanical Design of Modern Fighter Aircraft," *AGARD, Aerodynamics of Combat Aircraft Controls and of Ground Effects*, April 1990.
7. Koelle, Heinz Hermann, (Ed.), *Handbook of Astronautical Engineering*, McGraw-Hill, 1961, pp. 19–38.
8. Kutschera, Antony, and Render Peter M., "Performance Assessment of Thrust Vector Controlled Post Stall Manoeuvrable Fighter Aircraft Using Minimal Input Data," AIAA Paper 99-4020, 1999.
9. Miele, Angelo, "General Variational Theory of the Flight Paths of Rocket-Powered Aircraft, Missiles and Satellite Carriers," *Astronautica acta*, Vol. 4, New York: Pergamon Press, 1958, pp. 272–273.
10. Pontryagin, L.S., Boltyanskii V.G., Gamkrelidze R.V., and Mischenko E.F., *The Mathematical Theory of Optimal Processes*. New York: Interscience Publishers, Inc., 1962, pp. 17–20.

Appendix 1
Summary

Here there are values useful for calculations and estimations of aerospace projects.

1. System of Mechanical and Electrical Units

The following table contains the delivered metric mechanical and the electromagnetic SI units that have been introduced in this text, expressed in terms of the fundamental units *meter*, *kilogram*, *second*, and *ampere*. From these expressions the *dimensions* of the physical quantities involved can be readily determined.

Length……. 1 meter = 1 m
Mass………..1 kilogram = 1 kg
Time………..1 second = 1 s
Electric current…..1 ampere = 1 A

Force…….1 newton = 1 N = 1 kg·m/s^2
Pressure…..1 N/m2 = 1 kg/m·s^2
Energy…..1 joule = 1 J =1 N/m = 1 kg·m^2/s^2
Power……1 watt = 1 W =1 J/s = 1 kg·m^2/s^3

Rotational inertia……………1 kilogram·meter^2 = 1 kg·m^2
Torque………………………..1 meter·newton = 1 kg·m^2/s^2
Electric charge………………..1 coulomb = 1 C = 1 A·s
Electric intensity……………...1 N/C = 1 V/m = 1 kg·m/s^3·A

Electric potential……………...1 volt = 1 V = 1 J/C = 1 kg·m^2/s^3·A
Electric resistance……………..1 ohm =1 Ω =1 V/A = 1 kg·m^2/s^3·A^2
Capacitance…………………..1 farad = 1 F =1 C/V = 1 C2/J = 1 s^4·A^2/kg·m^2
Inductance………………………1 henry = 1 H =1 J/A2 = 1 Ω·s = 1 kg·m^2/s^2·A^2

Magnetic flux…………………..1 webwer = 1 Wb = 1 J/A = 1 V.s = 1 kg·m^2/s^2·A
Magnetic intensity…………….1 tesla = 1 Wb/m2 =1 V.s/m2 =1 kg/s^2·A
Reluctance……………………..1 ampera-turn/weber = 1 A/Wb =1 s^2·A^2/kg·m^2
Magnetizing force……………..1 ampere-turn/meter = 1 A/m
Kelvin is fundamental unit of temperature
Candela is fundamental power-like unit of photometry

Fundamental Physical Constants
Standard gravitational acceleration……. 9.806 65 m/s^2
Standard atmosphere (atm)……………..101 325 N/m^2
Thermochemical kilocalorie…………….4184 J
Speed of light in vacuum (c) ………… 2.997 935×10^8 m/s
Electronic charge (e) …………………..1.60210×10^{-19} C
Avogadro constant (N_A) ……………... 6.0225×10^{26}/kmol
Faraday constant (F) …………………..9.6487×10^7 C/kmol
Universal gas constant (R) …………….8314 J/kmol
Gravitational constant (G) ……………..6.67×10^{-11} N·m^2/kg^2
Boltzmann constant (k) …………………1.3895×10^{-23} J/K

Stefan-Boltzmann Constant (σ)............5.670×10^{-8} W/K^4·m^2
Rest energy of one atomic mass unit......931.48 MeV
Electron-volt (eV)..........................1.60210×10^{-19} J
Rest masses of particles

	(u)	(kg)	(MeV)
Electron	5.485 97×10^{-4}	9.1091×10^{-31}	0.511 006
Proton	1.002 2766	1.672 52×10^{-27}	938.26
α-particles	4.001 553	6.6441×10^{-27}	3727.3

Astronomical Data

Space body	Distance from sun (10^6 km)			Period of Revolution (d)	Mean radius (km)	Mass 10^{24} kg	Mean density Mg/m^3	Gravity on surf. m/s^2	Orbital speed km/s
	Mean	Aphelilion	Perithelion						
Sun	--	--	--	--	696 000	--	1.41	274	--
Mercury	57.9	69.8	46.0	88.0	2 420	3.167	5.46	3.72	48.8
Venus	108.1	109.0	107.5	224.7	6 261	4.870	4.96	8.69	35.0
Earth	149.5	152.1	147.1	365.2	6 371	5.975	5.52	9.78	29.8
Mars	227.8	249.2	206.6	687.0	3 389	0..639	4.12	3.72	24.2
Jupiter	777.8	815.9	740.7	4 333	69 900	1900	1.33	23.01	13.0
Saturn	1426	1508	1348	10 760	57 500	568.8	0.71	9.14	9.65
Uranus	2868	3007	2737	30 690	23 700	86.9	1.56	9.67	6.78
Neptune	4494	4537	4459	60 100	21 500	102.9	2.47	15.0	5.42
Pluto	5908	7370	4450	90 740	2 900	5.37	5.50	8.0	4.75
Moon	0.384 from Earth			27.322	1 737	0.0735	3.34	1.62	1.02

Density of gases at normal pressure and temperature 0 ºC in kg/m^3
Air   1.293
Hydrogen   0.08988
Helium   0.1785

Parameters of Earth atmosphere (relative density and temperature)

H km	ρ/ρ_o	T ºK	H km	ρ/ρ_o	T ºK	H km	ρ/ρ_o	T ºK	H km	ρ/ρ_o	T ºK
0	0	288.2	5	0.601	255.6	20	0.0725	216.7	50	0.000375	274
1	0.908	281.6	7	0.482	242,6	25	0.0332	216.7	60	0.000271	253.4
2	0.822	275.1	10	0,338	223.1	30	0.0146	230.4	100	0.32×10^{-6}	208.2
3	0.742	268.6	12	0.255	216.7	35	0.00676	244.0	200	0.295×10^{-9}	1227
4	0.669	262.1	15	0.159	216.7	40	0.00327	257.7	300	0.273×10^{-10}	1358

Specific impulse of liquid fuel (nozzle 100:0.1, seconds):
Oxygen – kerosene   372
Oxygen – hydrogen 463
 Specific impulse of solid fuel (nozzle 40:0.1, seconds): 228–341.

Heat of combustion (MJ/kg):

Benzene	44	Mazut	30–41	Natural gases	42–47	Firewood	30
Diesel fuel	43	Spirit	27.2	Hydrogen	120	Peat	8 –11
Kerosene	43	Bituminous coal	21–24	Acetylene	48	gunpowder	3

General References

Some books and articles by A. Bolonkin are published on line: http://www.scribd.com, http://www.archive.org ,
http://arxiv.org (45), http://viXra.org, http://intellectualarchive.com (28), http://AIAA.org (41) and in Bolonkin's WEB
http://Bolonkin.narod.ru/p65.htm, http://www.lulu.com . Search: "Bolonkin".
 Third List of publication: http://www.scribd.com/doc/173336338/Publications-by-Bolonkin-30-September-2013,
http://viXra.org/abs/1310.0022

[1]   Bolonkin A.A., (1958a). Design of Hydro-Aircraft with Underwater Wing. *Report of Aircraft State Construction Bureau named Antonov*, Kiev, Ukraine, 1959 (in Russian), 120 p.

[2]   Bolonkin A.A., (1959a). Investigation of Aircraft AN-12 in Take-off. *Report of Aircraft State Construction Bureau named Antonov*, Kiev, Ukraine, 1959 (in Russian), 60 p.

[3]   Bolonkin A.A., (1959b). Research of Optimal Parameters of VTOL Aircraft, *Report of Aircraft State Construction Bureau named Antonov*, Kiev, 1959 (in Russian), Part 1 40 p., part 2 35 p.

[4]   Bolonkin A.A., (1959c). Research of Optimal Parameters of High Altitude Aircraft. *Report of Aircraft State Construction Bureau named Antonov*, Kiev, Ukraine, 1959 (in Russian), 60 p.

[5]   Bolonkin A.A., (1959d). Computation of High Thrust Aircraft with unsteady polar. *Report of Aircraft State Construction Bureau named Antonov*, Kiev, Ukraine, 1959 (in Russian), 50 p.

[6]   Bolonkin A.A., (1960a). Method of Estimation the Control of Aircraft Interface. *Presiding of Kiev High Engineering Aviation Military School* (KVIAVU), Kiev, Ukraine, Issue #72, 1960.

[7]   Bolonkin A.A., (1962a), *Theory of Flight Models*, Moscow, Association of Army, Air Force, and NAVY, 328p. 1962, (in Russian).

[8]   Bolonkin A.A., (1964a). Optimization of parameters of variation problems (Ukrainian. Russian and English summaries). *Dopoviti Akad. Nauk Ukrain. RSR,* 1964, #5, p. 580-582. Math.Rev. #6352.

[9]   Bolonkin A.A., (1964b)The calculus of variations and a functional equation of Bellman, and an interpretation of Langrange's undetermined multipliers. (Ukrainian. Russian and English summaries). *Dopovidi Akad. Nauk Ukrain., RSR* 1964, #10, p. 1290-1293. M.R. #5136.

[10]   Bolonkin A.A., (1964c). The extension principle and the Jacobi condition of the variation calculus. (Ukrainian. Russian and English summaries). *Dopovidi Akad. Nauk Ukrain. RSR* 1964. #7. p. 849-853. M.R. #5117.

[11]   Bolonkin, A.A., (1965a), "Theory of Flight Vehicles with Control Radial Force". Collection *Researches of Flight Dynamics*, Mashinostroenie Publisher, Moscow, pp. 79–118, 1965, (in Russian). Intern.Aerospace Abstract A66-23338# (Eng).

[12]   Bolonkin A.A., (1965b), Investigation of the Take off Dynamics of a VTOL Aircraft. Collection *Researches of Flight Dynamics*. Moscow, Mashinostroenie Publisher, 1965, pp. 119-147 (in Russian). International Aerospace Abstract A66-23339# (English).

[13]   Bolonkin A.A., (1965c), Optimization of Trajectories of Multistage Rockets. Collection *Researches of Flight Dynamics*. Moscow, 1965, p. 20-78 (in Russian). International Aerospace Abstract A66-23337# (English).

[14]   Bolonkin A.A., (1965d). A method for the solution of optimal problems (Russian). Collection *Complex Systems Control*, pp.34-67. Naukova Dumka, Kiev, 1965. M.R. #5535.

[15]   Bolonkin A.A., (1965e). Special, Sliding, and Impulse Regimes in Problems of Flight Dynamics (Russian). Collection *Complex Systems Control*, pp.68-90. Naukova Dumka, Kiev, 1965. M.R. #5535.

[16]   Bolonkin A.A., (1966a). Boundary-value problems of Optimal Control. Military *Aviation Engeenering Academy (VVIA) named Zhukovskii*, Issue #1131, 1966, p. 103-128. (Russian).

[17]   Bolonkin A.A., (1967a). Special extreme, *Report presented to Symposium of Applied Mathematics*, Gorkii, USSR, 1967. (Russian).

[18] Bolonkin A.A., (1968a). Impulse solution in control problems. (Russian). *Izv. Sibirsk. Otdel. Akad. Nayk USSR*, 1968, No. 13, p. 63-68. M.R. 7568. (Russian).

[19] Bolonkin A.A., (1968b). Solution of Problem the Linear Optimal Control with one Control, *Journal "Prikladnaya Mechanica"*, Vol. 4, #4, 1968, p.111-121. (Russian).

[20] Bolonkin A.A., (1969a). Solution of discrete problems of optimal control on the basis of a general minimum principle (Russian. English summary). *Vycisl. Prikl. Mat. (Kiev) Vyp. 7 (1969)*, 121-132. Mathematical Review 771.

[21] Bolonkin A.A., (1969b), Special extreme in optimal control. Akademia Nauk USSR, Izvestiya. Tekhnicheskaya Kibernetika, No 2, Mar-Apr.,1969, p.187-198. See also *English translation in* Engineering Cybernetics, # 2, Mar- Apr.1969, p.170-183, (English).

[22] Bolonkin A.A., (1970a). A certain method of solving optimal problems. *Izv. Sibirsk. Otdel. Akad. Nauk SSSR*. 1970, no.8, p. 86-92. M.R. #6163.

[23] Bolonkin A.A., (1970b). A certain approach to the solution of optimal problems. (Russian. English summary). *Vycisl. Prikl. Mat.* (Kiev). Vyp. 12 (1970), p. 123-133. M.R. #7940.

[24] Bolonkin A.A., (1971a), *Solution Methods for boundary-value problems of Optimal Control Theory.* Translated from Prikladnaya Mekhanika, Vol. 7, No 6, 1971, p. 639-650, (in English).

[25] Bolonkin A.A., (1971b). Solution of Optimal Problems. *Collection "Mathematical Problems of Production Control"*, Moscow State University (MGU), Issue #3, 1971, p. 55-67.

[26] Bolonkin, A.A., (1972a), *New Methods of Optimization and their Applications*, Moscow Highest Technology University named Bauman, 1972, p.220 (in Russian).

[27] Bolonkin, A.A., (1982a), *Installation for Open Electrostatic Field*, Russian patent application #3467270/21 116676, 9 July, 1982 (in Russian), Russian PTO.

[28] Bolonkin, A.A., (1982b), *Radioisotope Propulsion*. Russian patent application #3467762/25 116952, 9 July 1982 (in Russian), Russian PTO.

[29] Bolonkin, A.A., (1982c), *Radioisotope Electric Generator*. Russian patent application #3469511/25 116927. 9 July 1982 (in Russian), Russian PTO.

[30] Bolonkin, A.A., (1983a), *Space Propulsion Using Solar Wing and Installation for It*, Russian patent application #3635955/23 126453, 19 August, 1983 (in Russian), Russian PTO.

[31] Bolonkin, A.A., (1983b), Getting of Electric Energy from Space and Installation for It, Russian patent application #3638699/25 126303, 19 August, 1983 (in Russian), Russian PTO.

[32] Bolonkin, A.A., (1983c), *Protection from Charged Particles in Space and Installation for It*, Russian patent application #3644168 136270, 23 September 1983, (in Russian), Russian PTO.

[33] Bolonkin, A. A., (1983d), *Method of Transformation of Plasma Energy in Electric Current and Installation for It*. Russian patent application #3647344 136681 of 27 July 1983 (in Russian), Russian PTO.

[34] Bolonkin, A. A., (1983e), *Method of Propulsion using Radioisotope Energy and Installation for It*. of Plasma Energy in Electric Current and Installation for it. Russian patent application #3601164/25 086973 of 6 June, 1983 (in Russian), Russian PTO.

[35] Bolonkin, A. A.,(1983f), *Transformation of Energy of Rarefaction Plasma in Electric Current and Installation for it*. Russian patent application #3663911/25 159775, 23 November 1983 (in Russian), Russian PTO.

[36] Bolonkin, A. A., (1983g), *Method of a Keeping of a Neutral Plasma and Installation for it*. Russian patent application #3600272/25 086993, 6 June 1983 (in Russian), Russian PTO.

[37] Bolonkin, A.A.,(1983h), *Radioisotope Electric Generator*. Russian patent application #3620051/25 108943, 13 July 1983 (in Russian), Russian PTO.

[38] Bolonkin, A.A., (1983i), *Method of Energy Transformation of Radioisotope Matter in Electricity and Installation for it*. Russian patent application #3647343/25 136692, 27 July 1983 (in Russian), Russian PTO.

[39] Bolonkin, A.A., (1983j). *Method of stretching of thin film. Russian patent application* #3646689/10 138085, 28 September 1983 (in Russian), Russian PTO.

[40] Bolonkin A.A., (1984a). Method Solution of Optimal Problem, Collection "*Research of Computer and Control System*", Irkutsk, USSR, 1984, pp.94-98. (in Russian).

[41] Bolonkin A.A., (1987a). Method of Deformation of Extreme. Collection "*Methods and Programs of Optimal Problems in Networks*", Irkutsk State University and West Siberian Technological Institute, 1987, (in Russian).

[42] Bolonkin A.A., (1987b). Method for Solution of Optimal Problems having equalities and non-equalities limitations. Collection "*Methods and Programs of Optimal Problems in Networks*", Irkutsk State University and West Siberian Technological Institute, 1987, (in Russian).

[43] Bolonkin A.A., (1988a). Application of the Deformation Method to Optimization Problems on any Set" (in Russian), Collection "*Design of Micro-processors*", Irkutsk (USSR), 1988 9 p.

[44] Bolonkin A.A., (1988b). Deformation Method in Control Problems" (in Russian), Collection "*Design of Micro-processors*", Irkutsk (USSR), 1988 10 p.

[45] Bolonkin, A.A., (1990a). "Aviation, Motor and Space Designs", Collection *Emerging Technology in the Soviet Union*, 1990, Delphic Ass., Inc., pp.32–80 (English).

[46] Bolonkin, A.A., (1991a), *The Development of Soviet Rocket Engines*, 1991, Delphic Ass.Inc.,122 p. Washington, (in English).

[47] Bolonkin, A.A., (1991b), New Approach to Finding a Global Optimum. *New American's Collected Scientific Reports.* Vol. 1, 1991, The Bnai Zion Scientists Division., New York.

[48] Bolonkin, A.A., (1992a), "*A Space Motor Using Solar Wind Energy (Magnetic Particle Sail)*". The World Space Congress, Washington, DC, USA, 28 Aug. – 5 Sept., 1992, IAF-0615.

[49] Bolonkin, A.A., (1992b), "*Space Electric Generator, run by Solar Wing*". The World Space Congress, Washington, DC, USA, 28 Aug. –5 Sept. 1992, IAF-92-0604.

[50] Bolonkin, A.A., (1992c), "*Simple Space Nuclear Reactor Motors and Electric Generators Running on Radioactive Substances*", The World Space Congress, Washington, DC, USA, 28 Aug. – 5 Sept., 1992, IAF-92-0573.

[51] Bolonkin A.A., The *Twenty - First Century: The advent of the non-biological civilization.* http://Bolonkin.narod.ru .

[52] Bolonkin, A.A. (1994a), "*The Simplest Space Electric Generator and Motor with Control Energy and Thrust*", 45th International Astronautical Congress, Jerusalem, Israel, 9–14 Oct., 1994, IAF-94-R.1.368.

[53] Bolonkin A.A., Khot N., (1994b), *Optimal Structural and Control Design. 45th International Actronautical Congress.* Jerusalem, Israel. October 9-14, 1994, IAF-94-I.4.206.

[54] Bolonkin A.A., (1994c), *Method for Finding a Global Min*imum, AIAA/NASA/USAF/SSMO Symposium on Multi-disciplinary Analysis and Optimization, Panama City, Florida, USA, Sept. 7-9, 1994.

[55] Bolonkin A.A., Khot N., (1995a), Design and Optimal Control in Smart Structures. Conference "*Mathematics and Control in Smart Structures*", 26 Feb.-3 March 1995, San Diego, CA, USA.

[56] Bolonkin A.A., Khot N., (1995b), *Optimum Structural Vibration Control with Bounds on Control Forces*, 1995 ASME Design Technical Conference, 15th Biennial Conference on Vibration and Noise, September 17-21,1995, Boston, MA, USA.

[57] Bolonkin A.A., (1995c), *Twenty - First Century - the beginning of human immortality*. http://Bolonkin.narod.ru .

[58] Bolonkin A.A., Khot N., (1996a), *Optimal Bounded Control Design for Vibration Suppression. Acta Astronautics,* Vol.38, No. 10, pp803-813, 1996.

[59] Bolonkin A.A., Khot N., (1996b), *Minimum Weight of Control Devices with Bounded LQG Control.* The World Space Congress -96, June 1-6, 1996, Albuquerque, MN, USA.

[60] Bolonkin A.A., Khot N., (1996c), *Design of Smart Structures with Bounded Controls, Smart Structures and Materials,* Feb. 25-29,1996,San-Diego, CA.

[61] Bolonkin A.A., Khot N., (1997a), Design of Structure control System using Bounded LQG, *Eng.Opt.*, 1997, Vol. 29, pp. 347-358.

[62] Bolonkin A.A., (1997b). *Eccentric internal combustion engine*. Patent application US PTO 08/892,665 of 07/14/97.

[63] Bolonkin A.A., (1998a). *Inflatable flight vehicles*. Patent application US PTO 09/271,700 of 1/26/98.

[64] Bolonkin A.A., (1998b). *Inflatable flight vehicles*. Patent application US PTO 09/271,700 of 1/26/98.

[65] Bolonkin A.A., (1999a). *Method of space launch and hypersonic launch system*. Patent application US PTO 09/344,235 of 6/25/99.

[66] Bolonkin, A.A. (1999b), A High Efficiency Fuselage propeller ("Fusefan") for Subsonic Aircraft, !999 World Aviation Congress, AIAA, #1999-01-5569.

[67] Bolonkin A.A., Gilyard G.B., (1999c), Estimated Benefits of Variable-Geometry Wing Camber Control for Transport Aircraft. *NASA Center for AeroSpace Information (CASI), NASA/TM-1999-206586; H-2368; NAS 1.15:206586 , 19991001; October 1999*

[68] Bolonkin A.A., (1999d). The twenty-first century: the advent of the non-biological civilization and the future of the human race, *Journal "Kybernetes"*, Vol. 28, No.3, 1999, pp. 325-334, MCB University Press, 0368-492 (English).

[69] Bolonkin A.A., (1999e). *Science, Soul, Heaven and Supreme Mind*, http://Bolonkin.narod.ru (Russian, English).

[70] Bolonkin A.A., (1999d). *Breakthrough in Immortality*. http://Bolonkin.narod.ru (Russian, English).

[71] Bolonkin A.A., (1999d). *Human Immortality and Electronic Civilization*. Electronic book, 1999. WEB: http://Bolonkin.narod.ru, http://Bolonkin.narod.ru/p101.htm (English), http://Bolonkin.narod.ru/p100.htm (Russian).

[72] Bolonkin A.A., Gilyard G.B., (2000a), *Optimal Pitch Thrust-Vector Angle and Benefits for all Flight Regimes, NASA Center for AeroSpace Information (CASI), NASA/TM-2000-209021; NAS 1.15:209021; H-2402 , 20000301; March 2000*.

[73] Bolonkin A.A., (2001a). *Method and Installation for Space Trip*. Patent application US PTO 09/789,959 of 2/23/01.

[74] Bolonkin A.A., (2001b). *Method and Installation for Space Launch*. Patent application US PTO 09/873,985 of 6/04/01.

[75] Bolonkin A.A., (2001c). "*Method Transportation of Vehicles and Installations for It*". Patent application US PTO 09/893,060 of 6/28/01. Patent US 6,434,143 B1 of 12/17/02.

[76] Bolonkin A.A., (2001d). *Method and Installation for getting of Energy*. Patent application US PTO 09/945,497 of 9/06/01.

[77] A.A. Bolonkin, (2001e). "*Method for Gas and Payload Transportation at Long Distance and Installations for It*", Patent Application USPTO # 09/978,507 of 10/18/01.

[78] Bolonkin A.A., (2001f). Cable Launcher. Patent application US PTO 09/974,670 of 10/11/01.

[79] Bolonkin, A.A., (2002a), "*Non-Rocket Space Rope Launcher for People*", IAC-02-V.P.06, 53rd International Astronautical Congress, The World Space Congress – 2002, 10–19 Oct 2002, Houston, Texas, USA.

[80] Bolonkin, A.A,(2002b), "*Non-Rocket Missile Rope Launcher*", IAC-02-IAA.S.P.14, 53rd International Astronautical Congress, The World Space Congress – 2002, 10–19 Oct 2002, Houston, Texas, USA.

[81] Bolonkin, A.A.,(2002c), "*Inexpensive Cable Space Launcher of High Capability*", IAC-02-V.P.07, 53rd International Astronautical Congress, The World Space Congress – 2002, 10–19 Oct 2002, Houston, Texas, USA.

[82] Bolonkin, A.A.,(2002d), "*Hypersonic Launch System of Capability up 500 tons per day and Delivery Cost $1 per Lb*". IAC-02-S.P.15, 53rd International Astronautical Congress, The World Space Congress – 2002, 10–19 Oct 2002, Houston, Texas, USA.

[83] Bolonkin, A.A.,(2002e), "*Employment Asteroids for Movement of Space Ship and Probes*". IAC-02-S.6.04, 53rd International Astronautical Congress, The World Space Congress – 2002, 10–19 Oct 2002, Houston, Texas, USA.

[84]   Bolonkin, A.A., (2002f), "*Optimal Inflatable Space Towers of High Height*". COSPAR-02 C1.1-0035-02, 34th Scientific Assembly of the Committee on Space Research (COSPAR), The World Space Congress – 2002, 10–19 Oct 2002, Houston, Texas, USA.

[85]   Bolonkin, A.A., (2002g), "*Non-Rocket Earth-Moon Transport System*", COSPAR-02 B0.3-F3.3-0032-02, 02-A-02226, 34th Scientific Assembly of the Committee on Space Research (COSPAR), The World Space Congress – 2002, 10–19 Oct 2002, Houston, Texas, USA.

[86]   Bolonkin, A. A.,(2002h) "*Non-Rocket Earth-Mars Transport System*", COSPAR-02 B0.4-C3.4-0036-02, 34th Scientific Assembly of the Committee on Space Research (COSPAR), The World Space Congress – 2002, 10–19 Oct 2002, Houston, Texas, USA.

[87]   Bolonkin, A.A.,(2002i). "*Transport System for Delivery Tourists at Altitude 140* km". IAC-02-IAA.1.3.03, 53rd International Astronautical Congress, The World Space Congress – 2002, 10-19 Oct. 2002, Houston, Texas, USA.

[88]   Bolonkin, A.A., (2002j), "*Hypersonic Gas-Rocket Launch System*." AIAA-2002-3927, 38th AIAA/ASME/SAE/ASEE Joint Propulsion Conference and Exhibit, 7–10 July 2002. Indianapolis, IN, USA.

[89]   Bolonkin A.A., Cloutier D., (2002k). Search, Observation, and Attack Problems, *Technical Report* AFRL-MN-EG-TR-2003-1717, 21p. 2002.

[90]   Bolonkin, A.A., (2003a), "Air Cable Transport", *Journal of Aircraft*, Vol. 40, No. 2, March–April 2003.

[91]   Bolonkin, A.A., (2003b),"Optimal Inflatable Space Towers with 3-100 km Height", *JBIS*, Vol. 56, No 3/4, pp. 87–97, 2003.

[92]   Bolonkin, A.A.,(2003c), "Asteroids as Propulsion Systems of Space Ships", *JBIS*, Vol. 56, No 3/4, pp. 97–107, 2003.

[93]   Bolonkin A.A., (2003d), "Non-Rocket Transportation System for Space Travel", *JBIS*, Vol. 56, No 7/8, pp. 231–249, 2003.

[94]   Bolonkin A.A., (2003e), "Hypersonic Space Launcher of High Capability", *Actual problems of aviation and aerospace systems*, Kazan, No. 1(15), Vol. 8, 2003, pp. 45–58. Kazan Aviation Institute.

[95]   Bolonkin A.A., (2003f), "Centrifugal Keeper for Space Stations and Satellites", *JBIS*, Vol. 56, No 9/10, pp. 314–327, 2003.

[96]   Bolonkin A.A., (2003g), "Non-Rocket Earth-Moon Transport System", *Advances in Space Research*, Vol. 31/11, pp. 2485–2490, 2003, Elsevier. London.

[97]   Bolonkin A.A., (2003h), "Earth Accelerator for Space Ships and Missiles". *JBIS*, Vol. 56, No. 11/12, 2003, pp. 394–404.

[98]   Bolonkin A.A., (2003i), "Air Cable Transport and Bridges", TN 7567, International Air and Space Symposium – The Next 100 Years, 14–17 July 2003, Dayton, Ohio, USA.

[99]   Bolonkin, A.A., (2003j), "Air Cable Transport System", *Journal of Aircraft*, Vol. 40, No. 2, March-April 2003, pp. 265-269.

[100] Bolonkin A.A., Sierakowski R., (2003k). *Design of Optimal Regulators*. The manuscript is accepted as paper AIAA-2003-6638 by 2nd AIAA "Unmanned Unlimited" Systems, Technologies, and Operations- Aerospace, Land, and See Conference and Workshop and Exhibit, San Diego, California, USA, 15-18 Sep 2003. http://arxiv.org , search "Bolonkin".

[101] Bolonkin A.A., Murphy R., (2003-l). Geometry-Based Feasibility Constraints for Single Pursuer Multiple Evader Problems, 2nd AIAA "Unmanned Unlimited" Systems, Technologies, and Operations – Aerospace, Land, and sea Conference and Workshop and Exhibit, San Diego, California, 15-18 Sep 2003, AIAA-2003-6638.

[102] Bolonkin A.A.,(2004a), "Kinetic Space Towers and Launchers ', *JBIS*, Vol. 57, No 1/2, pp. 33–39, 2004.

[103] Bolonkin A.A.,(2004b), "Optimal trajectory of air vehicles", *Aircraft Engineering and Space Technology*, Vol. 76, No. 2, 2004, pp. 193–214.

[104] Bolonkin A.A., (2004c), "*Long Distance Transfer of Mechanical Energy*", International Energy Conversion Engineering Conference at Providence RI, Aug. 16–19, 2004, AIAA-2004-5660.

[105] Bolonkin, A.A., (2004d), "Light Multi-Reflex Engine", *Journal JBIS*, Vol. 57, No 9/10, pp. 353–359, 2004.

[106] Bolonkin, A.A., (2004e), "Optimal trajectory of air and space vehicles", *AEAT*, No 2, pp. 193–214, 2004.

[107] Bolonkin, A.A.,(2004f), "Hypersonic Gas-Rocket Launcher of High Capacity", *Journal JBIS*, Vol. 57, No 5/6, pp. 167–172, 2004.

[108] Bolonkin, A.A., (2004g), "High Efficiency Transfer of Mechanical Energy". International Energy Conversion Engineering Conference at Providence RI, USA. 16–19 August, 2004, AIAA-2004-5660.

[109] Bolonkin, A.A., (2004h), "Multi-Reflex Propulsion System for Space and Air Vehicles", *JBIS*, Vol. 57, No 11/12, 2004, pp. 379–390.

[110] Bolonkin A.A., (2004i), Utilization of Wind Energy at High Altitude, AIAA-2004-5705, AIAA-2004-5756, International Energy Conversion Engineering Conference at Providence., RI, Aug.16-19. 2004. USA. http://arxiv.org .

[111] Bolonkin A., Cloutier D., (2004j). *Search and Attack Strategies*, AIAA Conference Guidance, Navigation, and Control, Rhide Island, 16-19 August, 2004, Tr. #20201.

[112] Bolonkin A., Cloutier D., (2004k). Search for Enemy Targets, *Technica. Report* AFRL-MN-EG-TR-2003-1716, June 2002. 49 p.

[113] Bolonkin A.A., (2004k)Twenty-first century – the beginning of human immortality, *Journal "Kybernetes"*, Vol. 33, No.9/10, 2004, pp. 1535-1542, Emerald Press, www.emeraldinsight.com/ISSN 0368-492X.htm (English).

[114] Bolonkin A.A.,(2005a) "*High Speed Catapult Aviation*", AIAA-2005-6221, Atmospheric Flight Mechanic Conference – 2005, 15–18 August, 2005, USA.

[115] Bolonkin A.A., (2005b), "*Kinetic Anti–Gravitator*", AIAA-2005-4504, 41 Propulsion Conference, 10–12 July 2005, Tucson, Arizona, USA.

[116] Bolonkin, A.A., (2005c), "*Electrostatic Solar Wind Propulsion System*", AIAA-2005-3857, 41 Propulsion Conference, 10–13 July 2005, Tucson, Arizona, USA.

[117] Bolonkin, A.A., (2005d), "*Sling Rotary Space Launcher*", AIAA-2005-4035, 41 Propulsion Conference, 10–13 July 2005, Tucson, Arizona, USA.

[118] Bolonkin A.A., (2005e), "*Electrostatic Utilization Asteroids for Space Flight*", 41 Propulsion conference, 10–12 July 2005, Tucson, Arizona, USA, AIAA-2005-3857.

[119] Bolonkin A.A., (2005f), "*Guided Solar Sail and Electric Generator*", 41 Propulsion conference, 10–12 July, 2005, Tucson, Arizona, USA, AIAA-2005-3857.

[120] Bolonkin A.A., (2005g), "*Problems of Levitation and Artificial Gravity*", 41 Propulsion conference, 10–12 July 2005, Tucson, Arizona, USA, AIAA-2005-3365.

[121] Bolonkin A.A., (2005h), "*Radioisotope Sail and Electric Generator*", 41 Propulsion conference, 10–12 July, 2005, Tucson, Arizona, USA, AIAA-2005-3653.

[122] Bolonkin A.A., Murphy R., (2005i). Geometry-Based Parametric Modeling for Single Pursuer Multiple Evader Problems. Journal JGCD, v.28, #1, 2005

[123] Bolonkin A.A. (2006a), Book "*Non-Rocket Space Launch and Flight*", Elsevier, London, 2006, 488 ps. Contents is in http://Bolonkin.narod.ru/p65.htm .

[124] Book contains more 20 new revolutionary author's concepts and ideas.

[125] Bolonkin A.A., (2006b), *Beam Space Propulsion*, AIAA-2006-7492, Conference Space-2006, 18-21 Sept;, 2006, San Jose, CA, USA. http://arxiv.org , search "Bolonkin".

[126] Bolonkin A.A., (2006c), *Electrostatic AB-Ramjet Space Propulsion*, AIAA/AAS Astrodynamics Specialist Conference, 21-24 August 2006, USA. AIAA-2006-6173. Journal "Aircraft Engineering and Aerospace Technology", Vol.79, #1, 2007. http://arxiv.org , search "Bolonkin".

[127] Bolonkin A.A., (2006d), Electrostatic Linear Engine, AIAA-2006-5229, 42nd Joint Propulsion Conference, 9-12 June 2006, Sacramento, USA. *Journal "Aircraft Engineering and Aerospace Technology*", Vol.78, #6, 2006, pp.502-508.

[128] Bolonkin A.A., (2006e), *High-Speed Solar Sail*, AIAA-2006-4806, 42nd Joint Propulsion Conference, 9-12 June 2006, Sacramento, USA. http://arxiv.org , search "Bolonkin".

[129] Bolonkin A.A., (2006f), *A New Method of Atmospheric Reentry for Space Shuttle*, AIAA-2006-6985, MAO Conference, 6-9 Sept. 2006, USA. http://arxiv.org , search "Bolonkin".

[130] Bolonkin A.A., (2006g), *Suspended Air Surveillance System*, AIAA-2006-6511, AFM Conference, 21-29 Aug. 2006, Keystone, USA. http://arxiv.org , search "Bolonkin".

[131] Bolonkin A.A., (2006h), Optimal Solid Space Tower, AIAA-2006-7717. ATIO Conference, 25-27 Sept. 2006, Wichita, Kansas, USA. http://arxiv.org , search "Bolonkin".

[132] Bolonkin A.A., (2006i), *Theory of Space Magnetic Sail Some Common Mistakes and Electrostatic MagSail.* Presented as paper AIAA-2006-8148 to 14-th Space Planes and Hypersonic System Conference, 6-9 November 2006, Australia. http://arxiv.org , search "Bolonkin".

[133] Bolonkin A.A., (2006j) *Micro -Thermonuclear AB-Reactors for Aerospace*. Presented as paper AIAA-2006-8104 in 14th Space Plane and Hypersonic Systems Conference, 6-8 November, 2006, USA. http://arxiv.org , search "Bolonkin".

[134] Bolonkin A., Cathcart R., (2006k). *A Low-Cost Natural Gas/Freshwater Aerial Pipeline.* http://arxiv.org, search "Bolonkin".

[135] Bolonkin A.A., (2006 l) *Cheap Textile Dam Protection of Seaport Cities against Hurricane Storm Surge Waves, Tsunamis, and Other Weather-Related Floods*. http://arxiv.org , search "Bolonkin".

[136] Bolonkin A., Cathcart R., (2006m). *The Java-Sumatra Aerial Mega-Tramway*, http://arxiv.org.

[137] Bolonkin A., Cathcart R., (2006n). *Inflatable Evergreen Polar Zone Dome* (EPZD) Settlements. http://arxiv.org , search "Bolonkin".

[138] Bolonkin, A.A. and R.B. Cathcart, (2006) "A Cable Space Transportation System at the Earth's Poles to Support Exploitation of the Moon", *Journal of the British Interplanetary Society* 59: 375-380.

[139] Bolonkin A., (2006o). *Control of Regional and Global Weather*. http://arxiv.org , search "Bolonkin".

[140] Bolonkin A., Cathcart R., (2006p). *Antarctica: A Southern Hemisphere Windpower Station?* http://arxiv.org , search "Bolonkin".

[141] Bolonkin A.A., (2006q). *AB Levitator and Electricity Storage*. http://arxiv.org , search "Bolonkin".

[142] Bolonkin A.A. (2006r). *Simplest AB-Thermonuclear Space Propulsion and Electric Generator*. http://arxiv.org , search "Bolonkin".

[143] Bolonkin A.A., (2006s). Wireless Transfer of Electricity in Outer Space. http://arxiv.org , search "Bolonkin".

[144] Bolonkin A.A., (2006t). Electrostatic AB-Ramjet space propulsion for interplanetary flight, *AEAT*, vol. 79, No. 1, 2007, pp. 3 - 16.

[145] Bolonkin A.A., (2006u). *Method of Recording and Saving of Human Soul for Human Immortality and Installation for it*. Patent application US PTO 11613380 of 12/20/06.

[146] Bolonkin, A.A. and R.B. Cathcart (2006v), "Inflatable 'Evergreen' dome settlements for Earth's Polar Regions", *Clean Technologies and Environmental Policy* DOI 10.1007/s10098-006-0073-4.

[147] Cathcart R., Bolonkin A., (2006w), *The Golden Gate Textile Barrier: Preserving California Bay of San Francisco from a Rising North Pacific Ocean*. http://arxiv.org. Search: "Bolonkin".

[148] Cathcart R., Bolonkin A., (2006x), *Ocean Terracing*, http://arxiv.org . Search: "Bolonkin".

[149] Book (2006),: *Macro-Engineering - A challenge for the future*. Collection of articles. Eds. V. Badescu, R. Cathcart and R. Schuiling, Springer, 2006. (Collection contains two Bolonkin's articles: Space Towers; Cable Anti-Gravitator, Electrostatic Levitation and Artificial Gravity).

[150] Bolonkin A.A., (2007a). AB Levitrons and their Applications to Earth's Motionless Satellites, http://arxiv.ru , search: Bolonkin.

[151] Bolonkin A.A., (2007b). Passenger life-saving in a badly damaged aircraft scenario, AIAA-2007-5844, http://arxiv.ru , search: Bolonkin.

[152] Bolonkin A.A., (2007c). Optimal Electrostatic Space Tower (Mast, New Space Elevator), AIAA-2007-6201, http://arxiv.ru , search: Bolonkin.

[153]. Bolonkin A.A., (2007d). Electrostatic Space Climber, AIAA-2007-5838, http://arxiv.ru , search: Bolonkin.

[154] Bolonkin A.A., (2007e). Inflatable Dome for Moon, Mars, Asteroids and Satellites, AIAA-2007-6262, http://arxiv.ru , search: Bolonkin.

[155] Bolonkin A.A., (2007f). Human Immortality and Electronic Civilization, 3-rd Edition, Lulu, 2007, 66 pgs., (Enflish and Russian), http://www.lulu.com search "Bolonkin".

[156] Bolonkin A.A., (2007g). Memories of Soviet Political Prisoner, Lulu, 2007, 66 pgs., (Enflish and Russian), http://www.lulu.com search "Bolonkin". English is translated from same Russian book, New your, 1991.

[157] Calasso F.E., (1989), *Advanced Fibers and Composite*, Gordon and Branch Scientific Publisher, New York, 1989.

[158] *Carbon and High Performance Fibers*, (1995), Directory, NY 1995, Chapman and Hall, 6th ed., New York.

[159] *Concise Encyclopedia of Polymer Science and Engineering*, (1990), Ed. J. I. Kroschwitz, 1990. New York.

[160] Clarke A.C.: *Fountains of Paradise*, Harcourt Brace Jovanovich, New York, 1978.

[161] Dresselhous, M.S.,(2000), *Carbon Nanotubes*, Springer, New York, 2001.

[162] Fedorov V.D., (1981), *Basis of Rocket Flight*, Moscow, Nauka.(Russian).

[163] *Handbook of Physical Quantities*, Ed. Igor S. Grigoriev, 1997, CRC Press, USA.

[164] Harris, J.T. (1973), *Advanced Material and Assembly Methods for Inflatable Structures*. AIAA, Paper No. 73-448.

[165] Johnson A., *Space Research: Organizing for Economical Efficiency*. Presented as paper AIAA-2006-7224 in Conference "Space-2006", 19-21 September 2006, San Diego, California, USA.

[166] Johnson A., Space research: problems of efficiency. *Journal "Actual Problems of Aviation and Aerospace System"*, No.1, 2007. http://www.kcn.ru/tat_en/science/ans /journals/rasj_cnt/07_1_10.html

[167] Kikoin I.K., (1976), *Table of Physical Magnitudes*, Moscow, Atomic Publish House.(Russian).

[168] Landis G.A., (2004), Interstellar Flight by Particle Beam, *Acta Astronautica*, Vol. 55, pp.931 - 934.

[169] Landis G., (2000). "Dielectric Films for Solar- and Laser-pushed Lightsails," *AIP Conference Proceedings Volume 50*4, pp. 989-992; Space Technology and Applications International Forum (STAIF-2000), Jan. 30 - Feb. 3, Albuquerque NM.

[170] Landis Geoffrey A., Cafarelli Craig, (1999). The Tsiolkovski Tower Re-Examined, *JBIS*, Vol. 32, pp. 176 -180, 1999.

[171] Landis, Geoffrey A. and Cafarelli, Craig, (1995), "The Tsiolkovski Tower," paper IAF-95-V.4.07, 46th International Astronautics Federation Congress, Oslo Norway, 2-6 Oct. 1995. There is also an errata to this paper, which was published in JBIS: Landis, Geoffrey A., (2005),"Correction," *Journal of the British Interplanetary Society*, Vol. 58, p. 58.

[172] Landis, Geoffrey A., (1998), "*Compression Structures for Earth Launch*," paper AIAA-98-3737, 24th AIAA/ASME/SAE/ASEE Joint Propulsion Conf., July 13-15, Cleveland OH.

[173] Nishikawa K., Wakatani M., *Plasma Physics*, Spring, 2000.

[174] Omidi N. and Karimabadi H., (2003), "*Electrostatic Plasma Sail*", AIAA 2003-5227, 2003. 39th AIAA/ASME/SAE/ASEE Joint Propulsion Conference and Exhibit 20-23 July 2003, Hurtisville, Alabama. Contains a principal scientific mistakes.

[175] Regan F.J., Anandakrishnan S.M., *Dynamics of Atmospheric Re-Entry*, AIAA, 1993

[176] Shortley G., Williams D., *Elements of Physics*, Prentice-Hall, Inc., Englewood Cliffs, New Jersey, 1971, USA.

[177] Smitherman D.V., Jr., Space Elevators, NASA/CP-2000-210429, 2000.

[178] Tsiolkovski K.E.: "Speculations about Earth and Sky on Vesta," Moscow, Izd-vo AN SSSR, 1959; Grezi o zemle I nebe (in Russian), Academy of Sciences, U.S.S.R., Moscow, p.35, 1999.

Russian Works

[179] Tsiolkovski, K.E. (1959),"*Speculations about Earth and Sky on Vesta*", Moscow, Izd-vo AN SSSR, 1959; Grezi o zemle i nebe (in Russian), Academy of Sciences, USSR., Moscow, p. 35, 1999.

[180] Mayboroda A., Zero Gravity on Earth, "*Yuniy Tehnik*" ("Young Technician"), No. 10, October 1988, Moscow (in Russian).

[181] Pokrovskii G.I., (1964), *Space Tower*, TM, ("Technology for Youth"), No. 10, (in Russian).

[182] Poliakov G., (1977), *Space Necklace of Earth*, TM, ("Technology for Youth"), No. 4, (in Russian).

[183] Yunitskii A., (1982), "*General Planetary Transport System*", "TM" ("Technology for Youth"), No. 6,) (in Russian). (see last four Russian works in: http://www.ipu.ru/stran/bod/ing/sovet2.htm, Pictures: http://www.ipu.ru/stran/bod/ing /sovet_ris.htm)

NIAC Reports

[184] http://auditing-science.narod.ru or http://www.geocities.com/auditing.science/

[185] Christensen C., "Ultralight Solar Sail for Interstellar Travel", http://NASA-NIAC.narod.ru

[186] Hose S. D., "Antimatter Drive Sail for Deep Space Missions", http://NASA-NIAC.narod.ru

[187] Landis G. A., "Advanced Solar and Laser Pushed Lightsail Concepts", http://NASA-NIAC.narod.ru

[188] Miller D. W., "Electromagnetic Formation Flight", http://NASA-NIAC.narod.ru

[189] Zubrin, R., "The Magnetic Sail". http://NASA-NIAC.narod.ru .

[190] About NIAC: GO TO: http://auditing-science.narod.ru   or http://www.geocities.com/auditing.science/ , http://NASA-NIAC.narod.ru .

Some Popular Bolonkin's Publications and Publications about his Ideas

[191] Personal site: Bolonkin A.A., http://Bolonkin.narod.ru

[192] Bibliography (about the author and discussing his ideas) publication in Russian press and Internet in 1994 - 2004 (http://www.km.ru , http://pravda.ru , http://n-t.ru , ets. Search: Bolonkin).

[193] Bolonkin A.A., Our children may be a last people generation, *Literary newspaper*, 10/11/95, #41 (5572), Moscow, Russia (Russian).

[194] Bolonkin A.A., Stop the Earth. I step off. *People Newspaper*, Sept.,1995. Minsk, Belorussia (Russian).

[195] Bolonkin A.A., End of Humanity, but not End of World. *New Russian Word*, 3/6/96, p.14, New York, USA (Russian).

[196] Bolonkin A.A., *Natural Human Purpose is to be God*. http://Bolonkin.narod.ru (Russian).

[197] Bolonkin A.A., *American and Russian Science*.(English). http://Bolonkin.narod.ru.

[198] Bolonkin A.A., Locate the God into Computer-Internet Network (in Russian). http://Bolonkin.narod.ru.

[199] Blekherman A., *Short biography of Dr. A. Bolonkin*. (English, Russian) http://Bolonkin.narod.ru

[200] Dr.Sci. M. Krinker, World Space Congress-2002 (about 9 Bolonkin's scientific works presented to Congress). http://Bolonkin.narod.ru (Russian).

[201] Ruduyk B., New ideas of Dr. Bolonkin, *Newspaper "Fact",* Ukraine (in Ukraine). http://Bolonkin.narod.ru.

[202] Kurolenko N., Electronic Society, *News paper "Kievskie Vedomosti*", C. Kiev, Ukraine, 27 May, 2002. http://Bolonkin.narod.ru.

[203] Bay E., Our soul is only set our knowledge (about ideas of A. Bolonkin). *Newspaper "Literary Newspaper".* 10 July, 2002. Moscow (in Russian).

[204] Golovkov A., Time for thinking, Magazime *"Ogonek",* 1988, Moscow, Russia (in Russian). http://Bolonkin.narod.ru .

[205] Levin V., "*Take-off and Landing*" (article from magazine "Vestnik" about Bolonkin. 1992)(Russian).

[206] Bolonkin A.A., Peculiarities of Soviet and American Sciences. (Russian). http://Bolonkin.narod.ru

[207] Bolonkin A.A., Memoirs of Soviet Political Prisoner (English). http://Bolonkin.narod.ru.

[208] http://wikipedia.org search "Bolonkin", http://Coogle.com search "Bolonkin'.

[209] Getmansky Igor, Price of Immortality, Moscow, EKCMO, 2003, 480 pgs.,(Fantasy, in Russian).

Launch and Flight in Outer Space without Rockets (v.2). Alexander A. Bolonkin

Alexander A. Bolonkin was born in the former USSR. He holds doctoral degree in aviation engineering from Moscow Aviation Institute and a post-doctoral degree in aerospace engineering from Leningrad Polytechnic University. He has held the positions of senior engineer in the Antonov Aircraft Design Company and Chairman of the Reliability Department in the Clushko Rocket Design Company. He has also lectured at the Moscow Aviation Universities. Following his arrival in the United States in 1988, he lectured at the New Jersey Institute of Technology and worked as a Senior Scientist at NASA and the US Air Force

Research Laboratories.
Bolonkin is the author of more than 250 scientific articles and books and has 17 inventions to his credit.

This is the first extensive study of alternative propulsion systems, as appropriate for launch, aerodynamics/space flight and trajectory correction in space. Each system of propulsion is described with comparative discussion of advantages and disadvantages quantitative calculation and estimations of system parameters, and examples of potential project application.

This book will be of particular interest to postgraduates, researchers, and engineers in aerospace science and propulsion technology, and will also be important reading for astronomers engaged in mission design policy-makers in governments and space agencies, and research and development managers in the aerospace industry.

Topics include:
* Space Elevators
* Tethers systems
* Solar and solar wind sails
* Cable Transport systems
* Centrifugal Launcher
* Gas Tube Hypersonic Launcher
* Extraction of kinetic energy from asteroids
* Electrostatic propulsion systems
* Kinetic propulsion system
* Beam propulsion systems
* Radioisotope Space Sail and Electric Generator